

HIGH-VOLTAGE ENGINEERING

5e



M S Naidu | V Kamaraju



High-Voltage Engineering

About the Authors



M S Naidu was Professor in the Department of High-Voltage Engineering, Indian Institute of Science, Bangalore. A PhD from the University of Liverpool, he served as a visiting scientist at the High-Voltage Laboratory of the Eindhoven University of Technology, Netherlands. He had also given lectures at many high-voltage laboratories in West Germany, Switzerland and France.

Professor Naidu was a Chartered Engineer, a Fellow of the Institution Of Engineers (India) and also a Fellow of the National Academy of Engineering. His research interests included gaseous insulation, circuit-breaker arcs, pollution under HVDC, etc. He published many research papers and authored *Advances in High Voltage Breakdown and Arc Interruption in SF6 and Vacuum* (Pergamon Press, 1981). Recently, a book on *Gas Insulated Substations* that had been authored by him, was published in 2008. Professor Naidu passed away in February 2002.



V Kamaraju obtained his PhD in High-Voltage Engineering from the Indian Institute of Science, Bangalore. He was formerly a Professor and Principal at the JNTU College of Engineering, Kakinada, Andhra Pradesh. He was a visiting professor at Middle East Technical University, Gaziantep, Turkey, during 1981-82.

Professor Kamaraju is a Chartered Engineer and a Fellow of the Institution of Engineers (India). He has published many research papers and has been a consultant to various industries and to the Andhra Pradesh State Electricity Board. He has published *Electrical Distribution Systems and Linear Systems: Analysis and Applications* during 2006-2008 and *High Voltage Direct Current Transmission* in 2011, all by McGrawHill Education (India). He received the *Best Teacher* award from Government of Andhra Pradesh, India, in 2001. At present, he is Professor in the Department of Electrical Engineering at Mahavir Institute of Science and Technology, Hyderabad, Andhra Pradesh, India.

Professor Kamaraju has done extensive research in the areas of liquid and solid dielectrics, composite insulation and partial discharges.

High-Voltage Engineering

(Late) M S Naidu

Formerly, *Professor in Department of High Voltage Engineering Indian Institute of Science,
Bangalore*

V Kamaraju

Formerly, *Principal and Professor of Electrical Engineering JNT University College of
Engineering Kakinada, Andhra Pradesh*



McGraw Hill Education (India) Private Limited

NEW DELHI

McGraw Hill Education Offices

New Delhi New York St Louis San Francisco Auckland Bogotá Caracas
Kuala Lumpur Lisbon London Madrid Mexico City Milan Montreal
San Juan Santiago Singapore Sydney Tokyo Toronto

Published by McGraw Hill Education (India) Private Limited
P-24, Green Park Extension, New Delhi 110 016

High-Voltage Engineering, 5e

Copyright © 2013, 2009, 2004, 1993, 1982 by McGraw Hill Education (India) Private Limited.

No part of this publication may be reproduced or distributed in any form or by any means, electronic, mechanical, photocopying, recording, or otherwise or stored in a database or retrieval system without the prior written permission of the publishers. The program listings (if any) may be entered, stored and executed in a computer system, but they may not be reproduced for publication.

This edition can be exported from India only by the publishers,
McGraw Hill Education (India) Private Limited.

Print Book:
ISBN-13: 978-1-25-906289-6
ISBN-10: 1-25-906289-9

Ebook Book:
ISBN-13: 978-93-392-0318-4
ISBN-10: 93-392-0318-6

Vice President and Managing Director: *Ajay Shukla*

Head—Higher Education (Publishing and Marketing): *Vibha Mahajan*
Publishing Manager (SEM & Tech. Ed.): *Shalini Jha*
Editorial Executive: *Koyel Ghosh*

Manager—Production Systems: *Satinder S Baveja*
Assistant Manager—Editorial Services: *Sohini Mukherjee*
Senior Production Executive: *Suhaib Ali*

Assistant General Manager (Marketing)—Higher Education: *Vijay Sarathi*
Senior Product Specialist: *Tina Jajoriya*
Senior Graphic Designer—Cover: *Meenu Raghav*

General Manager—Production: *Rajender P Ghansela*
Manager—Production: *Reji Kumar*

Information contained in this work has been obtained by McGraw Hill Education (India), from sources believed to be reliable. However, neither McGraw Hill Education (India) nor its authors guarantee the accuracy or completeness of any information published herein, and neither McGraw Hill Education (India) nor its authors shall be responsible for any errors, omissions, or damages arising out of use of this information. This work is published with the understanding that McGraw Hill Education (India) and its authors are supplying information but are not attempting to render engineering or other professional services. If such services are required, the assistance of an appropriate professional should be sought.

Typeset at Tej Composers, WZ 391, Madipur, New Delhi 110 063 and printed at Magic International Pvt. Ltd., Plot No. 26E, Sector-31 (INDUSTRIAL), Site-IV, Greater Noida - 201306

Cover Printer: Magic International Pvt. Ltd.

DZZYYRCORCYLX

**To
Our Children**

*May their world be filled with
understanding, love and peace*

Preface

Overview

The demand for the generation and transmission of large amounts of electric power today, necessitates transmission at extra-high voltages. In developed countries like the USA, power transmission voltages have reached 765 kV to 1100 kV, and 1500 kV systems are also being built. In our country, 750 kV ac power systems have already come into operation, and in another 10 years' time, every state is expected to be linked by a National Power Grid operating at 750 kV to 1100 kV.

Target Audience

In the current industrial scenario, a practicing electrical engineer or a student of electrical engineering is expected to possess knowledge of high-voltage techniques and should have sufficient background in high-voltage engineering. Unfortunately, at present, very few textbooks in high-voltage engineering are available, compared to those in other areas of electrical engineering. Even among these, no single book has covered the entire range of topics in high-voltage engineering in depth and presented the material in a lucid manner. Therefore, an attempt has been made in this book, to bring together different topics in high-voltage engineering to serve as a single-semester course for final-year undergraduate students or postgraduate students studying Electrical Engineering, Electronics Engineering, and Applied Physics.

This book is also intended to serve power engineers in the industry who are involved in the design and development of electrical equipment as well as engineers in the electricity supply and utility establishments. It provides all the latest information on insulating materials, breakdown phenomena, overvoltage, and testing techniques. It is useful for self-study by engineers in the field of electricity utilities and design, development testing of electrical apparatus, transmission line hardware, particle acceleration, etc.

About the Book

The material in this book has been organized into five sections, namely

- (i) insulating materials and their applications in electrical and electronic engineering,
- (ii) breakdown phenomena in insulating materials—solids, liquids, and gases,
- (iii) generation and measurement of high dc, ac, and impulse voltages and currents,
- (iv) overvoltage phenomena in electrical power transmission systems and insulation coordination, and
- (v) high-voltage testing techniques, testing of apparatus and equipment, and planning of high-voltage laboratories.

Much of the information on these topics has been drawn from standard textbooks and reference books and have been simplified and reorganized to suit the needs of the students and graduate engineers. Many research publications have also been referred to, and relevant standard specifications have been quoted to help the reader gain easy access to the original references.

Salient Features

- Includes latest industry inputs on HV Construction Kits
- HVDC Systems and Testing expanded to cover the updates in technology, such as

- Surge Arresters for EHV systems
- HVDC Divider for HVDC Transmission Systems
- Testing of HVDC valves and systems
- Dedicated chapter on *Design, Planning and Layout of High-Voltage Laboratories*
- Pedagogy enhanced and revised to suit examination requirements:
 - 47 Worked Examples
 - 14 Short-Answer Questions
 - 140 Review Questions
 - 34 Problems
 - 199 Multiple-Choice Questions

Chapter Organization

The text is organized in 11 concise chapters.

Chapter 1 introduces the basic concepts of high-voltage engineering and includes numerical methods for electric field computations (viz., FEM, CSM, BEM techniques)

Chapter 2 is on conduction and breakdown in gases and has been revised to include the basics of collisions processes; breakdown phenomenon in SF₆ and SF₆—air mixtures. This chapter also has a completely revised section on Paschen's Law with supporting problems.

Chapter 3 is on conduction and breakdown in liquid dielectrics and contains information on the recent developments in liquid insulents.

Chapters 4 and **5** are on breakdown in solid dielectrics and applications of insulating materials respectively, and incorporate the latest solid insulating materials and their applications in electric power apparatus.

Chapter 6 discusses the generation of high voltages and currents, while **Chapter 7** deals with measurement of high voltages and currents. This chapter also explains electric field (E) measurements, field intensity meters, impulse test and measuring systems.

Chapter 8 is on overvoltage phenomenon and insulation coordination in electric power systems. Over voltages and testing of Gas Insulated Substation (GIS) has been added in this edition (**chapters 5** and **8**).

Chapter 9 discusses non-destructive testing of materials and electric apparatus, and **Chapter 10** is on high-voltage testing of electric apparatus.

Finally, **Chapter 11** is on design, planning and layout of high-voltage laboratories. It also includes the recent developments in HV testing laboratories and includes a brief description of the UHV laboratory, CPRI, Hyderabad. Details of high-voltage laboratories across the world have also been made up-to-date. (**Table 11.6**).

Further testing of HVDC Valves and equipment is added in the present edition.

This edition offers almost 100 fresh problems in different sets such as multiple-choice questions, review questions, solved and unsolved problems to help students in self-study and understanding. Updates in the text have been made wherever necessary.

Online Learning Centre

The text is accompanied by an exhaustive Online Learning Centre which can be accessed at <http://www.mhhe.com/hve5>

It contains the following material:

For Students

- Interactive Quiz
- Useful Web links for further reading

For Instructors

- Solution Manual (for selected problems)
- PowerPoint Slides with figures from text

Acknowledgements

First, the authors wish to express their gratitude to all the reviewers who took out time to review the book.

The authors acknowledge, with thanks, for the permission given by

- Central Power Research Institute, UHV Laboratory, Hyderabad, to refer to the details of their institute
- Ms Emile Haefely and Co. Ltd., Switzerland, to include the photographs of their equipment
- MWB HV TEST SYSTEMS, Bangalore

The authors express their sincere gratitude to the Director, Indian Institute of Science, Bangalore, and Vice Chancellor, Jawaharlal Nehru Technological University, Hyderabad, for their constant encouragement.

It is hoped that students, readers, academicians and engineers will continue to favor and patronize the book.

Feedback

Suggestions for further improvement of the book are welcome and every effort will be made to incorporate them in the next edition.

(Late) M S Naidu and V Kamaraju

Publisher's Note

Do you have any further request or a suggestion? We are always open to new ideas (the best ones come from you!). You may send your comments to tmh.elefeedback@gmail.com

Piracy-related issues may also be reported!

Contents

Preface

1. Introduction

- [1.1 Electric Field Stresses](#)
- [1.2 Gas/Vacuum as Insulator](#)
- [1.3 Liquid Dielectrics](#)
- [1.4 Solids and Composites](#)
- [1.5 Estimation and Control of Electric Stress](#)
- [1.6 Numerical Methods for Electric Field Computation](#)
- [1.7 Surge Voltages, their Distribution, and Control](#)

[Key Terms](#)

[Multiple-Choice Questions](#)

[Review Questions](#)

[Short Questions](#)

[References](#)

2. Conduction and Breakdown in Gases

- [2.1 Gases as Insulating Media](#)
- [2.2 Collision Processes](#)
- [2.3 Ionization Processes](#)
- [2.4 Townsend's Current Growth Equation](#)
- [2.5 Current Growth in the Presence of Secondary Processes](#)
- [2.6 Townsend's Criterion for Breakdown](#)
- [2.7 Experimental Determination of Coefficients \$\alpha\$ and \$\gamma\$](#)
- [2.8 Break down in Electro negative Gases](#)
- [2.9 Time Lags for Breakdown](#)
- [2.10 Streamer Theory of Breakdown in Gases](#)
- [2.11 Paschen's Law](#)
- [2.12 Breakdown in Non-Uniform Fields and Corona Discharges](#)
- [2.13 Post-Breakdown Phenomena and Applications](#)
- [2.14 Practical Considerations in using Gases and Gas Mixtures for Insulation Purposes](#)
- [2.15 Vacuum Insulation](#)

[Key Terms](#)

[Worked Examples](#)

[Multiple Choice Questions](#)

[Review Questions](#)

[Problems](#)

[References](#)

3. Conduction and Breakdown in Liquid Dielectrics

- [3.1 Liquids as Insulators](#)
- [3.2 Pure Liquids and Commercial Liquids](#)

[3.3 Conduction and Breakdown in Pure Liquids](#)

[3.4 Conduction and Breakdown in Commercial Liquids](#)

[3.5 Testing of Insulating Oils \(Fluids\): Transformer Fluids](#)

[3.6 Conclusions](#)

[Key Terms](#)

[Worked Examples](#)

[Multiple-Choice Questions](#)

[Review Questions](#)

[References](#)

4. Breakdown in Solid Dielectrics

[4.1 Introduction](#)

[4.2 Intrinsic Breakdown](#)

[4.3 Electromechanical Breakdown](#)

[4.4 Thermal Breakdown](#)

[4.5 Breakdown of Solid Dielectrics in Practice](#)

[4.6 Breakdown in Composite Dielectrics](#)

[4.7 Solid Dielectrics used in Practice](#)

[Key Terms](#)

[Worked Examples](#)

[Multiple-Choice Questions](#)

[Review Questions](#)

[References](#)

5. Applications of Insulating Materials

[5.1 Introduction](#)

[5.2 Applications in Power Transformers](#)

[5.3 Applications in Rotating Machines](#)

[5.4 Applications in Circuit Breakers](#)

[5.5 Applications in Cables](#)

[5.6 Applications in Power Capacitors](#)

[5.7 Applications in High-Voltage Bushings](#)

[5.8 Applications in Fractional Horse Power Motors](#)

[Key Terms](#)

[Multiple-Choice Questions](#)

[Review Questions](#)

[References](#)

6. Generation of High Voltages and Currents

[6.1 Generation of High Direct-Current Voltages](#)

[6.2 Generation of High Alternating Voltages](#)

[6.3 Generation of Impulse Voltages](#)

[6.4 Generation of Impulse Currents](#)

[6.5 Tripping and Control of Impulse Generators](#)

[Key Terms](#)

[Worked Examples](#)

[Multiple-Choice Questions](#)

[Review Questions](#)

[Problems](#)

[References](#)

7. Measurement of High Voltages and Currents

[7.1 Measurement of High Direct-Current Voltages](#)

[7.2 Measurement of High AC and Impulse Voltages](#)

[7.3 Measurement of High Currents—Direct, Alternating and Impulse](#)

[7.4 Cathode-Ray Oscillographs for Impulse Voltage and Current Measurements](#)

[Key Terms](#)

[Worked Examples](#)

[Multiple-Choice Questions](#)

[Review Questions](#)

[Problems](#)

[References](#)

8. Overvoltage Phenomenon and Insulation Coordination in Electric Power Systems

[8.1 Natural Causes for Over voltages—Lightning Phenomenon](#)

[8.2 Overvoltage due to Switching Surges, System Faults and other Abnormal Conditions](#)

[8.3 Principles of Insulation Coordination on High-Voltage and Extra High-Voltage Power Systems](#)

[Key Terms](#)

[Worked Examples](#)

[Multiple-Choice Questions](#)

[Review Questions](#)

[Problems](#)

[References](#)

9. Non-Destructive Testing of Materials and Electrical Apparatus

[9.1 Introduction](#)

[9.2 Measurement of Direct Current Resistivity](#)

[9.3 Measurement of Dielectric Constant and Loss Factor](#)

[9.4 Partial Discharge Measurements](#)

[Key Terms](#)

[Worked Examples](#)

[Multiple-Choice Questions](#)

[Review Questions](#)

[References](#)

10. High-Voltage Testing of Electrical Apparatus

[10.1 Testing of Insulators and Bushings](#)

[10.2 Testing of Isolators and Circuit Breakers](#)

[10.3 Testing of Cables](#)

[10.4 Testing of Transformers](#)

[10.5 Testing of Surge Arresters](#)

[10.6 Radio Interference Measurements](#)

[10.7 Testing of HVDC Valves and Equipment](#)

[Key Terms](#)

[Multiple-Choice Questions](#)

[Review Questions](#)

[References](#)

1. Design, Planning and Layout of High-Voltage Laboratories

[11.1 Introduction](#)

[11.2 Test Facilities Provided in High-Voltage Laboratories](#)

[11.3 Activities and Studies in High-Voltage and UHV Laboratories](#)

[11.4 Classification of High-Voltage Laboratories](#)

[11.5 Size and Ratings of Large Size High-Voltage Laboratories](#)

[11.6 Grounding of Impulse Testing Laboratories](#)

[Key Terms](#)

[Multiple-Choice Questions](#)

[Review Questions](#)

[Problems](#)

[References](#)

Appendix : Important Formulae

Author Index

Subject Index

Visual Preview

CHAPTER

1

Introduction

In modern times, high voltages are used for a wide variety of applications covering the power systems, industry, and research laboratories. Such applications have become essential to sustain modern civilization. High voltages are applied in laboratories in nuclear research, in particle accelerators, and Van de Graaff generators. For transmission of large blocks of power over long distances, high voltages are indispensable. Also, voltages up to 100 kV are used in electrostatic precipitators, in automobile ignition coils, etc. X-ray equipment for medical and industrial applications also use high voltages. Modern high-voltage test laboratories employ voltages up to 6 MV or more. The diverse conditions under which a high-voltage apparatus is used necessitate careful design of its insulation and the electrostatic field profiles. The principal media of insulation used are gases, vacuum, solid, and liquid, or a combi-

Chapter Introduction provides a quick look into the concepts that will be discussed in the chapter.

WORKED EXAMPLES

Example 4.1 A solid specimen of dielectric has a dielectric constant of 4.2, and $\tan \delta = 0.001$ at a frequency of 50 Hz. If it is subjected to an alternating field of 50 kV/cm, calculate the heat generated in the specimen due to the dielectric loss.

Solution Dielectric heat loss at any electric stress E [Eq. (4.5)]

$$= \frac{E^2 f \epsilon_r \tan \delta}{1.8 \times 10^{12}} \text{ W/cm}^3$$

For the specimen under study, the heat loss will be

$$= \frac{50 \times 50 \times 10^6 \times 50 \times 4.2 \times .001}{1.8 \times 10^{12}}$$
$$= 0.291 \text{ mW/cm}^3$$

Every chapter contains several worked out Examples which guide the student in understanding the concepts and working out the exercise problems.

Visual Preview

TABLES

Table 3.1 Dielectric properties of some liquid dielectrics

Property	Insulating oil	Cable oil	Capacitor oil	PFEP oil	Silicone oils
Breakdown strength at 20°C on 2.5 mm standard sphere gap	15 kV/mm	30 kV/mm	20 kV/mm	> 15 kV/mm	30-40 kV/mm
Relative permittivity (50 Hz)	2.2-2.3	2.3-2.6	2.1	2.7	2-75
Tan δ (50 Hz) (1 kHz)	0.001	0.002	0.25×10^{-4}	0.1×10^{-4}	10^{-4}
Resistivity (ohm-cm)	10^{12} - 10^{13}	10^{12} - 10^{13}	10^{12} - 10^{14}	$> 10^{14}$	3×10^{14}
Specific gravity at 20°C	0.89	0.93	0.88-0.89	0.96-0.97	1.0-1.1
Viscosity at 20°C (cS)	30	30	50	80	10-1000
Acid value (mg/gm of KOH)	Nil	Nil	Nil	< 0.05	Nil
Refractive index	1.4820	1.4700	1.4740	1.4555	1.5000-1.6000
Saponification (mg of KOH/gm of oil)	0.01	0.01	0.01		< 0.01
Thermal expansion (20-100°C)	$7 \times 10^{-4}/^{\circ}\text{C}$	$7 \times 10^{-4}/^{\circ}\text{C}$	$7 \times 10^{-4}/^{\circ}\text{C}$	0.00075	$5 \times 10^{-4}/^{\circ}\text{C}$
Max. permissible water content (in ppm)	50	50	50	200	< 30 (negligible)

Wherever necessary, Tables provide accurate and extensive information on the topic discussed.

FIGURES



Fig. 4.2 Breakdown channels in perspex between point-plane electrodes. Radius of point 0.01 in, thickness 0.19 in. Total number of impulses 190. Number of channels produced 16; (n) point indicates end of nth channel. Radii of arcs increase in units of 10^{-2} in.

Source: R. Cooper, *International Journal of Elec. Engg. Education*, vol. 1, 241 (1963)

Well-labelled illustrations give a clear understanding of the concepts.

Visual Preview

M
C
Q
S

W
I
T
H

A
N
S.

MULTIPLE-CHOICE QUESTIONS

1. A small high-voltage laboratory usually will have
 - (a) ac, dc test sources with ratings less than 100 kV, 10 kVA/kW and impulse of voltage 400 kV, 5 kJ
 - (b) ac, dc test sources of 500 kV, 100 kVA/kW, and impulse of 1 MV, 10 kJ
 - (c) ac voltage sources of 300 kV, 10 kVA, and impulse voltage of 1 MV, 15 kJ
 - (d) ac, dc sources only
2. Test sources required for testing power apparatus of 220 kV, 3-phase ac system are
 - (a) 500 kV ac, 1 MV impulse
 - (b) 800 kV impulse
 - (c) 300 kV ac, 500 kV impulse
 - (d) 250 kVA, 500 kV impulse.
3. The kVA rating of a testing transformer unit intended for test voltage and test object capacitance 'C' (pF)
 - (a) $\omega C V^2$
 - (b) $\omega C V^2 \times 10^{-9}$
 - (c) $\omega C^2 V^2 \times 10^9$
 - (d) $\omega C V^2 \times 10^{-6}$
4. The rating of an impulse voltage generator with generator capacitance C_g and voltage rating V with n stages is (kJ)
 - (a) $0.5 C_g V^2$
 - (b) $(n/2) (C_g V^2)$
 - (c) $\frac{(C_g V^2)}{2n}$
 - (d) $\frac{(C_g V^2)}{2n^2}$

Multiple choice questions help the student gain a quick overview of the important topics in the chapter. Answers are also provided at the end.

REVIEW QUESTIONS

1. Explain with diagrams, different types of rectifier circuits for producing high dc voltages.
2. What are the special features of high-voltage rectifier valves? How is proper voltage division between the valves ensured, if a number of tubes are used in series?
3. Why is a Cockcroft-Walton circuit preferred for voltage multiplier circuits? Explain its working with a schematic diagram.

PROBLEMS

1. An impulse generator has 12 capacitors of $0.12 \mu\text{F}$, and 200 kV rating. The wave-front and wave-tail resistances are 1.25 k Ω and 4 k Ω respectively. If the load capacitance including that of the test object is 1000 pF, find the wave-front and wave-tail times and the peak voltage of impulse wave produced.
2. An 8-stage impulse generator has $1.2 \mu\text{F}$ capacitors rated for 167 kV. What is its maximum discharge energy? If it has to produce a $1/50 \mu\text{s}$ waveform across a load capacitor of 15,000 pF, find the values of the wave front and wave tail resistances.
3. Calculate the peak current and waveshape of the output current of the following generator. Total capacitance of the generator is 53 μF . The charging voltage is 200 kV. The circuit inductance is 1.47 mH, and the dynamic resistance of the test object is 0.051 ohms.

Review questions and problems help students hone their problem-solving skills.

Q
U
E
S
T
I
O
N
S

Visual Preview

REFERENCES

REFERENCES

1. Bewley, L.V., *Travelling Waves on Transmission Systems*, Dover Publications Inc., New York (1963).
2. Lewis, W.W., *Protection of Transmission Lines and Systems against Lightning*, Dover Publications, Inc. New York (1965).
3. *Transmission and Distribution Reference Book*, Westinghouse Electric Corporation and Oxford University Press, New Delhi (1962).
4. Marshall, J.L., *Lightning Protection*, John Wiley and Sons, New York (1973).
5. Diesendorf, W., *Insulation Coordination in H.V. Electric Power Systems*, Butterworths, London (1974).
6. Begamudre, R.D., E.H.V., *A.C. Transmission Engineering*, Wiley Eastern, New Delhi (1986).
7. Golde, R.H., *Lightning*, Vol. 1 and 2, Academic Press, London (1977).
8. Black, R.M. and E.H. Reynolds, "Ionization and irradiation effects in high voltage dielectric materials", *Journal of Institute of Engineers*, London, **112**, 1226 (1965).
9. Bell, E., *et al.*, "Lightning investigations on 220 kV systems", *Tr. AIEE*, **150**, 1101 (1931).
10. Muller Hiller Brand, *et al.*, "Lightning counter measurements", *Proc. IEE*, **112**, 203 (1965).

Extensive list of References helps in selecting books for further study.

Appendix

Important Formulae

Field enhancement factor

$$f = \frac{E_{\max}}{E_{\text{avg}}}$$

Townsend current growth equation

$$I = I_0 \exp(\alpha d)$$

Current growth in presence of secondary processes

$$I = \frac{I_0 \exp(\alpha d)}{1 - \gamma [\exp(\alpha d) - 1]}$$

Appendix at the end lists important Formulae and Symbols.

A P P E N D I X

CHAPTER

1

Introduction

In modern times, high voltages are used for a wide variety of applications covering the power systems, industry, and research laboratories. Such applications have become essential to sustain modern civilization. High voltages are applied in laboratories in nuclear research, in particle accelerators, and Van de Graaff generators. For transmission of large bulks of power over long distances, high voltages are indispensable. Also, voltages up to 100 kV are used in electrostatic precipitators, in automobile ignition coils, etc. X-ray equipment for medical and industrial applications also use high voltages. Modern high-voltage test laboratories employ voltages up to 6 MV or more. The diverse conditions under which a high-voltage apparatus is used necessitate careful design of its insulation and the electrostatic field profiles. The principal media of insulation used are gases, vacuum, solid, and liquid, or a combination of these. For achieving reliability and economy, a knowledge of the causes of deterioration is essential, and the tendency to increase the voltage stress for optimum design calls for judicious selection of insulation in relation to the dielectric strength, corona discharges, and other relevant factors. In this chapter, some of the general principles used in high-voltage technology are discussed.

1.1 ELECTRIC FIELD STRESSES

Like in mechanical designs where the criterion for design depends on the mechanical strength of the materials and the stresses that are generated during their operation, in high-voltage applications, the dielectric strength of insulating materials and the electric field stresses developed in them when subjected to high voltages are the important factors in high-voltage systems. In a high-voltage apparatus, the important materials used are conductors and insulators. While the conductors carry the current, the insulators prevent the flow of currents in undesired paths. The electric stress to which an insulating material is subjected to is numerically equal to the voltage gradient, and is equal to the electric field intensity,

$$\mathbf{E} = -\nabla\phi \quad (1.1)$$

where \mathbf{E} is the electric field intensity, ϕ is the applied potential, and ∇ (read del) operator is defined as

$$\nabla \equiv a_x \frac{\partial}{\partial x} + a_y \frac{\partial}{\partial y} + a_z \frac{\partial}{\partial z}$$

where a_x , a_y , and a_z are components of position vector $\mathbf{r} = a_x \mathbf{X} + a_y \mathbf{Y} + a_z \mathbf{Z}$.

As already mentioned, the most important material used in a high-voltage apparatus is the insulation. The dielectric strength of an insulating material can be defined as the maximum dielectric stress which the material can withstand. It can also be defined as the voltage at which the current starts increasing to very high values unless controlled by the external impedance of the circuit. The electric breakdown strength of insulating materials depends on a variety of parameters, such as pressure, temperature, humidity, field configurations, nature of applied voltage, imperfections in dielectric materials, material of electrodes, and surface conditions of electrodes, etc. An understanding of the failure of the insulation will be possible by the study of the possible mechanisms by which the failure can occur.

The most common cause of insulation failure is the presence of discharges either within the voids in the insulation or over the surface of the insulation. The probability of failure will be greatly reduced if such discharges could be eliminated at the normal working voltage. Then, failure can occur as a result of thermal or electrochemical deterioration of the insulation.

1.2 GAS/VACUUM AS INSULATOR

Air at atmospheric pressure is the most common gaseous insulation. The breakdown of air is of considerable practical importance to the design engineers of power transmission lines and power apparatus. Breakdown occurs in gases due to the process of collisional ionization. Electrons get multiplied in an exponential manner, and if the applied voltage is sufficiently large, breakdown occurs. In some gases, free electrons are removed by attachment to neutral gas molecules; the breakdown strength of such gases is substantially large. An example of such a gas, with larger dielectric strength, is sulphur hexafluoride (SF_6).

High-pressure gas provides a flexible and reliable medium for high-voltage insulation. Using gases at high pressures, field gradients up to 25 MV/m have been realized. Nitrogen (N_2) was the gas first used at high pressures because of its inertness and chemical stability, but its dielectric strength is the same as that of air. Other important insulating gases are carbon dioxide (CO_2), dichlorodifluoromethane (CCl_2F_2) (popularly known as freon), and sulphur hexafluoride (SF_6). The breakdown voltage at higher pressures in gases shows an increasing dependence on the nature and smoothness of the electrode material. It is relevant to point out that, of the gases examined to date, SF_6 has probably the most attractive over all other gases due to its better dielectric and arc-quenching properties for gas insulated high-voltage systems.

However, in recent years pure SF_6 gas has been found to be a green house gas causing environmental hazards and therefore research efforts are presently focussed on finding a replacement gas or gas mixture which is environmentally friendly. Pure nitrogen, air and SF_6/N_2 mixtures show good potential to replace SF_6 gas in high voltage apparatus. In the next few years, SF_6/N_2 , SF_6 gas has to be replaced by a new gas and lot of research is being done to find such a gas.

Ideally, vacuum is the best insulator with field strengths up to 10^7 V/cm, limited only by emissions from the electrode surfaces. This decreases to less than 10^5 V/cm for gaps of several centimetres. Under high vacuum conditions, where the pressures are below 10^{-4} torr^{*}, the breakdown cannot occur due to collisional processes like in gases, and hence the breakdown strength is quite high. Vacuum insulation is used in particle accelerators, X-ray and field emission tubes, electron microscopes, capacitors, and circuit breakers.

1.3 LIQUID DIELECTRICS

Liquids are used in high-voltage equipment to serve the dual purpose of insulation and heat dissipation. They have the advantage that a puncture path is self-healing. Temporary failures due to overvoltage are reinsulated quickly by liquid flow to the affected area. However, the products of the discharges may deposit on solid insulation supports and may lead to surface breakdown over these solid supports.

Highly purified liquids have dielectric strengths as high as 1 MV/cm. Under actual service conditions, the breakdown strength reduces considerably due to the presence of impurities. The breakdown mechanism in the case of very pure liquids is the same as the gas breakdown, but in commercial liquids, the breakdown mechanisms are significantly altered by the presence of the solid impurities and dissolved gases.

Petroleum oils are the most common insulating liquids. However, fluoro-carbons, silicones, and organic esters, including castor oil, are used in significant quantities. A number of considerations enter into the selection of any dielectric liquid. The important electrical properties of the liquid include the dielectric strength, conductivity, flash point, gas content, viscosity, dielectric constant, dissipation factor, stability, etc. Because of their low dissipation factor and other excellent characteristics, polybutanes are being increasingly used in the electrical industry. However, in 1970s it was found that Askarels which more extensively used, exhibit health hazards and therefore most countries have legally banned their production and use. Many new liquids have since been developed which have no adverse environmental hazards. These include silicone oils, synthetic and fluorinated hydrocarbons.

In practical applications, liquids are normally used at voltage stresses of about 50-60 kV/cm when the equipment is continuously operated. On the other hand, in applications like high-voltage bushings, where the liquid only fills up the voids in the solid dielectric, it can be used at stresses as high as 100–200 kV/cm.

1.4 SOLIDS AND COMPOSITES

1.4.1 Solid Dielectrics

A good solid dielectric should have some of the properties mentioned earlier for gases and liquids and it should also possess good mechanical and bonding strengths. Many organic and inorganic materials are used for high-voltage insulation purposes. Widely used inorganic materials are ceramics and glass. The most widely used organic materials are thermosetting epoxy resins such as polyvinyl chloride (PVC), polyethylene (PE) or cross-linked polyethylene (XLPE). Kraft paper, natural rubber, silicon rubber and polypropylene rubber are some of the other materials widely used as insulants in electrical equipment.

If the solid insulating material is truly homogeneous and is free from imperfections, its breakdown stress will be as high as 10 MV/cm. This is the 'intrinsic breakdown strength', and can be obtained only under carefully controlled laboratory conditions. However, in practice, the breakdown fields obtained are very much lower than this value. The breakdown occurs due to many mechanisms. In general, the breakdown occurs over the surface than in the solid itself, and the surface insulation failure is the most frequent cause of trouble in practice.

1.4.2 Composites

In many engineering applications, more than one type of insulations are used together, mainly in parallel, giving rise to composite insulation systems. Examples of such systems are solid/gas insulation (transmission line insulators), solid/vacuum insulation and solid/liquid composite insulation systems (transformer winding insulation, oil impregnated paper and oil impregnated metallised plastic film etc).

In the application of composites, it is important to make sure that both the components of the composite should be chemically stable and will not react with each other under the application of combined thermal, mechanical and electrical stresses over the expected life of the equipment. They should also have nearly equal dielectric constants. Further, the liquid insulant should not absorb any impurities from the solid, which may adversely affect its resistivity, dielectric strength, loss factor and other properties of the liquid dielectric.

It is the intensity of the electric field that determines the onset of breakdown and the rate of increase of current before breakdown. Therefore, it is very essential that the electric stress should be properly estimated and its distribution known in a high-voltage apparatus. Special care should be exercised in eliminating the stress in the regions where it is expected to be maximum, such as in the presence of sharp points.

1.5 ESTIMATION AND CONTROL OF ELECTRIC STRESS

The electric field distribution is usually governed by the *Poisson's equation*:

$$\nabla^2 \phi = -\frac{\rho}{\epsilon_0} \quad (1.2)$$

where ϕ is the potential at a given point, ρ is the space charge density in the region, and ϵ_0 is the electric permittivity of free space (vacuum). However, in most of the high voltage apparatus, space charges are not normally present, and hence the potential distribution is governed by the *Laplace's equation*:

$$\nabla^2 \phi = 0 \quad (1.3)$$

In [Eqs \(1.2\)](#) and [\(1.3\)](#), the operator ∇^2 is called the *Laplacian* and is a vector with properties

$$\nabla \cdot \nabla = \nabla^2 = \frac{\partial^2}{\partial x^2} + \frac{\partial^2}{\partial y^2} + \frac{\partial^2}{\partial z^2}$$

There are many methods available for determining the potential distribution. The most commonly used methods are the

- (i) electrolytic tank method, and
- (ii) numerical methods.

The potential distribution can also be calculated directly. However, this is very difficult except for simple geometries. In many practical cases, with a good understanding of the problem is possible by using some simple rules to plot the field lines and equipotentials. The important rules are

- (i) the equipotentials cut the field lines at right angles,
- (ii) when the equipotentials and field lines are drawn to form curvilinear squares, the density of the field lines is an indication of the electric stress in a given region, and
- (iii) in any region, the maximum electric field is given by dv/dx , where dv is the voltage difference between two successive equipotentials, dx apart.

Considerable amount of labour and time can be saved by properly choosing the planes of symmetry and shaping the electrodes accordingly. Once the voltage distribution of a given geometry is established, it is easy to refashion or redesign the electrodes to minimize the stresses so that the onset of corona is prevented. This is a case normally encountered in high voltage electrodes of the bushings, standard capacitors, etc. When two dielectrics of widely different permittivities are in series, the electric stress is very much higher in the medium of lower permittivity. Considering a solid insulation in a gas medium, the stress in the gas becomes ϵ_r times that in the solid dielectric, where ϵ_r is the relative permittivity of the solid dielectric. This enhanced stress occurs at the electrode edges and one method of overcoming this is to increase the electrode diameter. Other methods of stress control are shown in [Fig. 1.1](#).

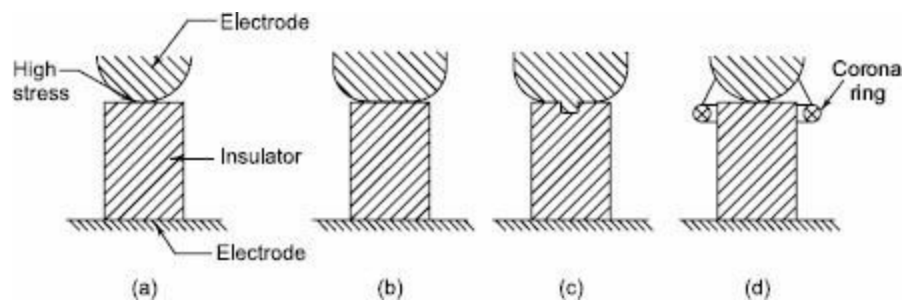


Fig. 1.1 *Control of stress at an electrode edge*

In the design of high-voltage apparatus, the electric field intensities have to be controlled, otherwise higher stresses will trigger or accelerate the ageing of the insulation leading to its failure. Over the years, many methods for controlling and optimizing electric fields to get the most economical designs have been developed. Electric field control methods form an important component of the overall design of equipment.

1.5.1 Electric Field

A brief review of the concepts of electric fields is presented, as it is essential for high voltage engineers to have a knowledge of the field intensities in various media under electric stresses. It also helps in choosing proper electrode configurations and economical dimensioning of the insulation, such that highly stressed regions are not formed and reliable operation of the equipment results in its anticipated life.

The field intensity \mathbf{E} at any location in an electrostatic field is the ratio of the force on an infinitely small charge at that location to the charge itself as the charge decreases to zero. The force \mathbf{F} on any charge q at that point in the field is given by

$$\mathbf{F} = q \mathbf{E} \quad (1.4)$$

The electric flux density \mathbf{D} associated with the field intensity \mathbf{E} is

$$\mathbf{D} = \varepsilon \mathbf{E} \quad (1.5)$$

where ε is the permittivity of the medium in which the electric field exists. The work done on a charge when moved in an electric field is defined as the potential. The potential φ is equal to

$$\varphi = - \int_l \mathbf{E} \cdot d\mathbf{l} \quad (1.6)$$

where l is the path through which the charge is moved.

Several relationships between the various quantities in the electric field can be summarized as follows:

$$\mathbf{D} = \varepsilon \mathbf{E}$$

$$\varphi = - \int_l \mathbf{E} \cdot d\mathbf{l} \text{ (or } \mathbf{E} = -\nabla \varphi)$$
$$\mathbf{E} = \frac{\mathbf{F}}{q} \quad (1.7)$$

$$\iint_s \mathbf{E} \cdot d\mathbf{S} = \frac{q}{\varepsilon_0} \text{ (Gauss theorem)} \quad (1.8)$$

$$\nabla \cdot \mathbf{D} = \rho \text{ (Charge density)} \quad (1.9)$$

$$\nabla^2 \varphi = -\frac{\rho}{\varepsilon_0} \text{ (Poisson's equation)} \quad (1.10)$$

$$\nabla^2 \varphi = 0 \text{ (Laplace's equation)} \quad (1.11)$$

where \mathbf{F} is the force exerted on a charge q in the electric field \mathbf{E} , and \mathbf{S} is the closed surface containing charge q .

1.5.2 Uniform and Non-Uniform Electric Fields

In general, the electric field between any two electrodes can be either uniform and non-uniform. In a uniform field gap, the average field E is the same throughout the field region, whereas in a non-uniform field gap, E is different at different points of the field region.

Uniform or approximately uniform field distributions exist between two infinite parallel plates or two spheres of equal diameters when the gap distance is less than the diameter of the sphere. Spherical electrodes are frequently used for high-voltage measurements and for triggering in impulse voltage generation circuits. Sometimes, parallel plates of finite size are used to simulate uniform electric fields, when gap separation is much smaller than plate size.

In the absence of space charges, the average field E in a non-uniform field gap is maximum at the surface of the conductor which has the smallest radius of curvature. It has the minimum field E at the conductor having the large radius of curvature. In this case, the field is not only non-uniform but also asymmetrical. Most of the practical high-voltage components used in electric power systems normally have non-uniform and asymmetrical field distribution.

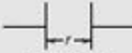

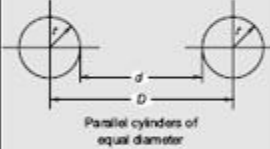
1.5.3 Estimation of Electric Field in Some Geometric Boundaries

It has been shown that the maximum electric field E_m in a given electric field configuration is of importance. The mean electric field over a distance d between two conductors with a potential difference of V_{12} is

$$E_{av} = \frac{V_{12}}{d} \quad (1.12)$$

In field configurations of non-uniform fields, the maximum electric field E_m is always higher than the average value. For some common field configurations, the maximum value of E_m and the field enhancement factor f given by E_m/E_{av} are presented in [Table 1.1](#).

Table 1.1 Some geometrical configurations and the field factors

Geometrical configuration	Maximum electric field E_m	Field enhancement factor $f = E_m/E_{av}$
 Parallel plates	$\frac{V}{d}$	1.0
 Concentric cylinders	$\frac{V}{r \ln \frac{R}{r}}$	$\frac{(R-r)}{r \ln \frac{R}{r}}$
Figure same as above Concentric spheres	$\frac{VR}{r(R-r)}$	$\frac{R}{r}$
 Parallel cylinders of equal diameter	$\frac{V\sqrt{D^2-4r^2}}{2r(D-r) \cosh^{-1}(D/2r)}$ $= \frac{V}{2r} \ln \frac{d}{r}$	$f = \frac{\left(\frac{d}{r}+1\right) + \sqrt{\left(\frac{d}{r}+1\right)^2 + 8}}{4}$
Equal spheres with dimensions as above	$\approx \frac{V}{2r}, \text{ if } d \gg r$	$\approx \frac{d}{2r}, \text{ if } d \gg r$
	For other configurations like sphere-plane and cylinder-plane f is approximately given by	
	$f = 0.94 \frac{d}{r} = 0.8$ (sphere-plane)	
	$f = 0.25 \frac{d}{r} + 1.0$ (cylinder-plane)	

Many electric conductors are normally either plane, cylindrical, or spherical in shape or can be approximated to these shapes. In other situations the conductors may be approximated into spheroidal, elliptical, toroidal and other geometrical shapes, and thus estimation of E_m can be made.

1.6 NUMERICAL METHODS FOR ELECTRIC FIELD COMPUTATION

1.6.1 Introduction

In recent years, several numerical methods for solving partial differential equations which include Laplace's and Poisson's equations have become available. There are inherent difficulties in solving these equations for two or three dimensional fields with complex boundary conditions, or for insulating materials with different permittivities and/or conductivities.

Proper design of any high-voltage apparatus requires a complete knowledge of the electric field distribution. For a simple physical system with some symmetry, it is possible to find an analytical solution. However, in many cases, the physical systems are very complex and therefore in such cases, numerical methods are employed for the calculation of electric fields. Essentially, three types of numerical methods are commonly employed in high voltage engineering applications. They are: Finite Element Method (FEM), Charge Simulation Method (CSM) and Surface Charge Simulation Method (SSM) or Boundary Element Method (BEM). The first method is generally classified as domain method and the last two are categorized as boundary methods.

The principal task in the computation of electric field is to solve the Poisson's equation [Eq. \(1.10\)](#). In case of space charge-free fields the equation reduces to Laplace's equation [Eq. \(1.11\)](#). Personal computers have the required computational power to solve these problems. However, computing times and the amount of memory to achieve the desired accuracy still play a dominant role. Further, another important aspect for the acceptance of a method is the ease with which it can be used to describe the problem. A brief description of each of these methods is given in the following sections.

1.6.2 Finite Element Method (FEM)

Finite Element Method is widely used in the numerical solution of electric field problems, and became very popular. In contrast to other numerical methods, FEM is a very general method and therefore is a versatile tool for solving wide range of electric field problems.

The finite element analysis of any problem involves basically four steps:

(a) Finite Element Discretization

To start with, the whole problem domain is ficticiously divided into small areas/ volumes called *elements* (see Fig. 1.2). The potential, which is unknown throughout the problem domain, is approximated in each of these elements in terms of the potential at their vertices called *nodes*. As a result of this the potential function will be unknown only at the nodes. Normally, a certain class of polynomials, is used for the interpolation of the potential inside each element in terms of their nodal values. The coefficients of this interpolation function are then expressed in terms of the unknown nodal potentials. As a result of this, the interpolation can be directly carried out in terms of the nodal values. The associated algebraic functions are called *shape functions*. The elements derive their names through their shape, i.e. bar elements in one dimension (1D), triangular and quadrilateral elements in 2D, and tetrahedron and hexahedron elements for 3D problems.

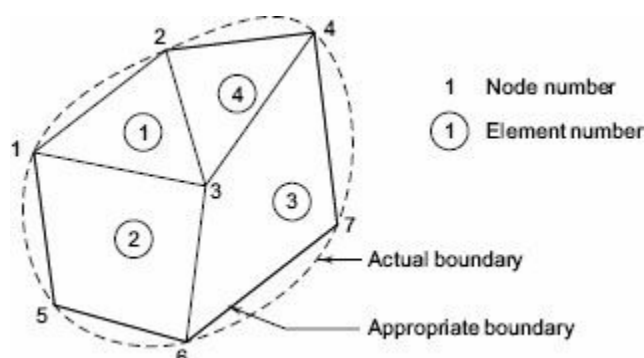


Fig. 1.2 A typical finite element subdivision of an irregular domain

(b) Governing Equations

The potential V_e within an element is first approximated and then interrelated to the potential distributions in various elements such that the potential is continuous across inter-element boundaries. The approximate solution for the whole region then becomes

$$V(x, y) = \sum_{e=1}^N V_e(x, y) \quad (1.13)$$

where N is the number of elements into which the solution region is divided.

The most common form of approximation for the voltage V within an element is a polynomial approximation

$$V_e(x, y) = a + bx + cy \quad (1.14)$$

For the triangular element, and for the quadrilateral element the equation becomes

$$V_e(x, y) = a + bx + cy + dxy \quad (1.15)$$

The potential V_e in general is not zero within the element e but it is zero outside the element in view of the fact that the quadrilateral elements are non-confirming elements (see [Fig. 1.2](#)).

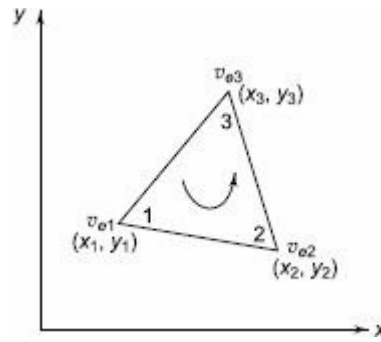


Fig. 1.3 Typical triangular element; the local node numbering 1–2–3 must proceed counterclockwise as indicated by the arrow

Consider a typical triangular element shown in [Fig. 1.3](#). The potentials V_{e1} , V_{e2} and V_{e3} at nodes 1, 2, and 3 are obtained from [Eq. \(1.14\)](#), as

$$\begin{bmatrix} V_{e1} \\ V_{e2} \\ V_{e3} \end{bmatrix} = \begin{bmatrix} 1 & x_1 & y_1 \\ 1 & x_2 & y_2 \\ 1 & x_3 & y_3 \end{bmatrix} \begin{bmatrix} a \\ b \\ c \end{bmatrix} \quad (1.16)$$

the coefficients a , b , and c are determined from the above equation as

$$\begin{bmatrix} a \\ b \\ c \end{bmatrix} = \begin{bmatrix} 1 & x_1 & y_1 \\ 1 & x_2 & y_2 \\ 1 & x_3 & y_3 \end{bmatrix}^{-1} \begin{bmatrix} V_{e1} \\ V_{e2} \\ V_{e3} \end{bmatrix} \quad (1.17)$$

Substituting this equation in [Eq. \(1.15\)](#), we get

$$V_e = [1 \ x \ y] \frac{1}{2A} \begin{bmatrix} (x_2 y_3 - x_3 y_2) & (x_3 y_1 - x_1 y_3) & (x_1 y_2 - x_2 y_1) \\ (y_2 - y_3) & (y_3 - y_1) & (y_1 - y_2) \\ (x_3 - x_2) & (x_1 - x_3) & (x_2 - x_1) \end{bmatrix} \begin{bmatrix} V_{e1} \\ V_{e2} \\ V_{e3} \end{bmatrix}$$

or,

$$V_e = \sum_{i=1}^N \alpha_i(x, y) V_{ei} \quad (1.18)$$

where,

$$\alpha_1 = (1/2 A) [(x_2 y_3 - x_3 y_2) + (y_2 - y_3)x + (x_3 - x_2)y] \quad (1.19a)$$

$$\alpha_2 = (1/2 A) [(x_3 y_1 - x_1 y_3) + (y_3 - y_1)x + (x_1 - x_3)y] \quad (1.19b)$$

$$\alpha_3 = (1/2 A) [(x_1 y_2 - x_2 y_1) + (y_1 - y_2)x + (x_2 - x_1)y] \quad (1.19c)$$

and A is the area of the element e , that is,

$$2A = \begin{bmatrix} 1 & x_1 & y_1 \\ 1 & x_2 & y_2 \\ 1 & x_3 & y_3 \end{bmatrix}$$

$$= (x_1y_2 - x_2y_1) + (x_3y_1 - x_1y_3) + (x_2y_3 - x_3y_2)$$

or

$$A = 1/2 [(x_2 - x_1)(y_3 - y_1) - (x_3 - x_1)(y_2 - y_1)] \quad (1.20)$$

The value of A is positive if the nodes are numbered counterclockwise (starting from any node) as shown by the arrow in [Fig. 1.3](#). It may be noted that [Eq. \(1.18\)](#) gives the potential at any point (x, y) within the element provided that the potentials at the vertices are known. These are called the element shape functions. They have the following properties:

$$\alpha_i(x, y) = \begin{cases} 1 & i = j \\ 0 & i \neq j \end{cases} \quad (1.21a)$$

$$V_e = \sum_{i=1}^3 \alpha_i(x, y) = 1 \quad (1.21b)$$

The energy per unit length associated with the element e is given by the following equation:

$$W_e = 1/2 \epsilon [V_e]^T [C^{(e)}] [V_e] \quad (1.22)$$

where, T denotes the transpose of the matrix

$$[V_e] = \begin{bmatrix} V_{e1} \\ V_{e2} \\ V_{e3} \end{bmatrix} \quad (1.23)$$

and

$$[C^{(e)}] = \begin{bmatrix} C_{11}^{(e)} & C_{12}^{(e)} & C_{13}^{(e)} \\ C_{21}^{(e)} & C_{22}^{(e)} & C_{23}^{(e)} \\ C_{31}^{(e)} & C_{32}^{(e)} & C_{33}^{(e)} \end{bmatrix} \quad (1.24)$$

The matrix given above is normally called *element coefficient matrix*. The matrix element $C_{ij}^{(e)}$ of the coefficient matrix is considered the coupling between nodes i and j .

(c) Assembling of All Elements

Having considered a typical element, the next stage is to assemble all such elements in the solution region. The energy associated with all the elements will then be

$$W_e = \sum_{e=1}^N W_e = 1/2 \epsilon [V]^T [C] [V] \quad (1.25)$$

where

$$[V] = \begin{bmatrix} V_1 \\ V_2 \\ \vdots \\ V_n \end{bmatrix} \quad (1.26)$$

and, n is the number of nodes, N is number of elements and $[C]$ is called the global coefficient matrix which is the sum of the individual coefficient matrices.

(d) Solving the Resulting Equations

It can be shown that the Laplace's (and Poisson's) equation is satisfied when the total energy in the solution region is minimum. Thus, we require that the partial derivatives of W with respect to each nodal value of the potential is zero, i.e.

$$\begin{aligned} \delta W / \delta V_1 &= \delta W / \delta V_2 = \dots = \delta W / \delta V_n = 0 \\ \delta W / \delta V_k &= 0 \text{ if } k = 1, 2, \dots, n. \end{aligned} \quad (1.27)$$

or,

In general, $\delta W / \delta V_k = 0$ leads to

$$0 = \sum_{e=1}^n V_e C_{ek} \quad (1.28)$$

where, n is the number of nodes in the mesh. By writing the above [Eq. \(1.28\)](#) for all the nodes, $k = 1, 2, \dots, n$, we obtain a set of simultaneous equations from which the solution for $V_1, V_2 \dots V_n$ can be found. This can be done either by using the *Iteration Method* or the *Band Matrix Method*.

Now, for solving the nodal unknowns, one cannot resort directly to the governing partial differential equations, as a piecewise approximation has been made to the unknown potential. Therefore, alternative approaches have to be sought. One such classical approach is the *calculus of variation*. This approach is based on the fact that potential will distribute in the domain such that the associated energy will reach extreme values. Based on this approach, Euler has showed that the potential function that satisfies the above criteria will be the solution of corresponding governing equation. In FEM, with the approximated potential function, extremization of the energy function is sought with respect to each of the unknown nodal potential. This process leads to a set of linear algebraic equations. In this matrix form, these equations form normally a symmetric sparse matrix, which is then solved for the nodal potentials.

Within the individual elements the unknown potential function is approximated by the shape functions of lower order depending on the type of element. An approximate solution of the exact potential is then given in the form of an expression whose terms are the products of the shape function and the unknown nodal potentials. It can be shown that the solution of the differential equation describing the problem corresponds to minimization of the field energy. This leads to a system of algebraic equations the solution for which under the corresponding boundary conditions gives the required nodal potentials. Thus, this procedure results in a potential distribution in the form of discrete potential value at the nodal points of the FEM mesh. The related field strengths at the centres of all elements are then obtained from the potential gradient. The values of the field thus obtained are dependent on the distance between the centres of the elements and the electrode surface, and thus on the sizes of the elements.

1.6.3 Charge Simulation Method (CSM)

Charge Simulation Method (CSM) belongs to the family of integral methods for calculation of electric fields. There are two variations of this method: CSM with discrete charges and CSM with area charges.

CSM with discrete charges is based on the principle that the real surface charges on the surface of electrodes or dielectric interfaces are replaced by a system of point and line charges located outside the field domain. The position and the type of simulation charges are to be determined first and then the magnitudes of the charges are calculated so that their combined effect satisfies the boundary conditions. After determining these magnitudes by using the method of solving a system of linear equations, it is to be verified whether the systems of simulation charges fulfill the boundary conditions between the location points with sufficient accuracy. Then the voltage and field strength at any point within the field domain can be calculated analytically by the superposition of simple potential and gradient functions.

(a) Basic Principle of CSM

When the conductor is excited by an applied voltage, charges appear on the surface of the conductor. These charges produce an electric field outside the conductor, while at the same time maintains the conductor at equipotential. Similarly, when a dielectric is excited by an external field, it gets polarized, i.e. the charged particles of the molecules of the dielectric get shifted from their neutral state to produce a volume of dipoles. In essence, it is possible to replace this volume polarization by the charged surface. CSM employs this physical description and attempts to simulate the above-mentioned continuous charge distribution by a set of discrete charges kept just outside the computational domain. The values of these discrete charges are then evaluated by forcing the specified voltages at some selected points called *contour points* on the surface of the conductor and by forcing the material interface conditions at some selected points on the dielectric interface.

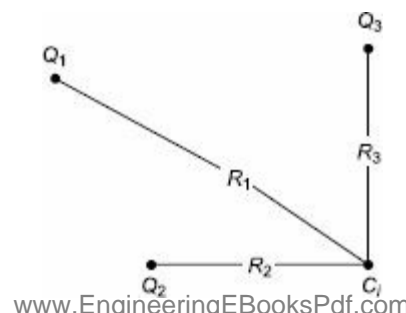
It is required that at any of these contour points on the electrode, the potential resulting from the superposition of the charges is equal to the electrode potential ϕ .

Thus

$$\phi_i = \sum_{j=1}^N P_{ij} Q_j \quad (1.29)$$

where, P_{ij} are the potential coefficients which can be evaluated analytically for many types of charges by solving Laplace's or Poisson's equation. For example, in [Fig. 1.4](#) which shows three point charges Q_1 , Q_2 and Q_3 in free space, the potential ϕ_i at point C_i will be

$$\begin{aligned} \phi_i &= Q_1/(4\pi\epsilon_0 R_1) + Q_2/(4\pi\epsilon_0 R_2) + Q_3/(4\pi\epsilon_0 R_3) \\ &= P_{i1}Q_1 + P_{i2}Q_2 + P_{i3}Q_3 \end{aligned} \quad (1.30)$$



Thus, once the types of charges and their locations are defined, it is possible to relate φ_{ij} and Q_j quantitatively at any boundary point. In CSM, the simulation charges are placed outside the space where the field solution is desired (or inside any equipotential surface such as metal electrodes). If the boundary point C_i is located on the surface of a conductor, then φ_i at this contour point will be equal to the conductor potential φ . When this procedure is applied to m contour points, it leads to the following system of m linear equations for n unknown charges.

$$\begin{bmatrix} P_{11} & P_{12} & \dots & P_{1n} \\ P_{21} & P_{22} & \dots & P_{2n} \\ \vdots & \vdots & \ddots & \vdots \\ P_{m1} & P_{m2} & \dots & P_{mn} \end{bmatrix} \begin{bmatrix} Q_1 \\ Q_2 \\ \vdots \\ Q_n \end{bmatrix} = \begin{bmatrix} \varphi_1 \\ \varphi_2 \\ \vdots \\ \varphi_m \end{bmatrix} \quad (1.31)$$

This equation is the basis of the CSM as discussed below.

(b) Use of CSM for a Single Dielectric Medium

If there are N conductors with known potentials in a single dielectric medium, then, for the calculation of field, the actual charges on the surfaces of these conductors are replaced by n_c fictitious charges placed inside or outside the conductors. The types and positions of these charges are assumed. In order to determine their magnitudes, n_b contour points are selected on the surfaces of the conductors, at known or fixed potentials and it is required that at any of these contour points the potential resulting from superposition of all the simulation charges is equal to the known conductor potential. The number of contour points is selected equal to the number of fictitious charges, i.e. $n_b = n_c = n$. Therefore, the charges are determined from

$$[P]_{n,n} [Q]_n = [\varphi]_n \quad (1.32)$$

where, $[P]$ = potential coefficient matrix, $[Q]$ = column vector of values of unknown charges, and $[\varphi]$ = potential of the boundary points.

After solving [Eq. \(1.32\)](#) to determine the magnitudes of simulation charges, it is necessary to check whether the set of calculated charges produces the actual boundary conditions everywhere on the electrode surfaces. It is possible that the potential at any point other than the contour points can be different from the actual conductor potential. Thus, [Eq. \(1.29\)](#) is solved at a number of *check points* located on the electrodes where potentials are known to determine the simulation accuracy. If simulation does not meet the accuracy criterion, calculations are repeated by changing either the number or the location or the types of simulation charges and the locations of contour points.

Once adequate charge system has been determined, the potential and field at any point outside the electrodes can also be calculated.

(c) CSM for a Multi-Dielectric Medium

The field computations for a multi-dielectric system are more complicated than for a single dielectric. This is due to the fact that, under the influence of applied voltage, the dipoles are re-aligned in a dielectric, and this re-alignment has the effect of producing a net surface charge on the dielectric. Thus, in addition to the electrodes, each dielectric-dielectric interface needs to be simulated by the discrete charges. In the simple example of [Fig. 1.5](#), charges 1 to 3 are used to simulate the electrode

while charges 4 to 7 are used to simulate the dielectric boundary. Contour points 1 to 3 are selected on the electrode surface whereas only two contour points (i.e. 4 and 5) are selected on the dielectric boundary. In order to determine the simulation charges, a system of equations is formulated by imposing the following boundary conditions:

- at each electrode boundary, potential must be equal to the known conductor potential, and
- at each dielectric boundary, potential and normal component of the flux density must be same, when viewed from either side of the boundary.

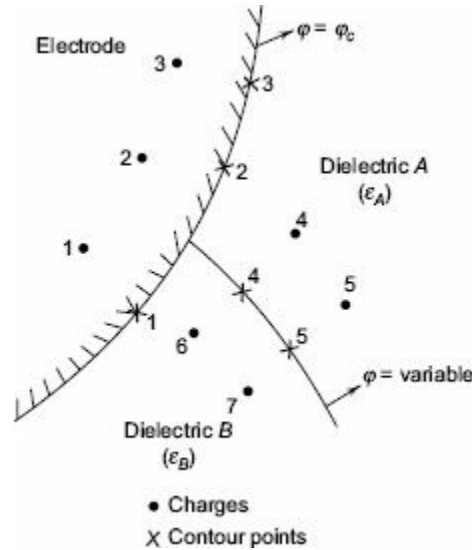


Fig. 1.5 Simulation of multi-dielectric boundary

In formulating the equations at a given contour point, the charges which lie in the same dielectric as the contour point are ignored. For example, the potential at control point 1 is calculated by the superposition of charges 1 to 5. Similarly, the potential or field intensity at contour point 5 when viewed from the side of the dielectric A will be due to the superposition of charges 1 to 3 and 6 and 7. Thus, when the first boundary condition is applied to contour points 1 to 3, (i.e. $i = 1$ to 3) the following equations are obtained.

$$\sum_{j=1}^5 P_{ij} Q_j = \varphi_c \quad (i = 1) \quad (1.33)$$

$$\sum_{j=1}^3 P_{ij} Q_j + \sum_{j=6}^7 P_{ij} Q_j = \varphi_c \quad (i = 2, 3) \quad (1.34)$$

When the second boundary condition is applied for potential and the flux density at $i = 4$ to 5, the following equations are obtained:

$$\sum_{j=4}^5 P_{ij} Q_j + \sum_{j=6}^7 P_{ij} Q_j = 0 \quad (1.35)$$

$$(\epsilon_A - \epsilon_B) \sum_{j=1}^3 f_{ij} Q_j + \epsilon_A \sum_{j=6}^7 f_{ij} Q_j - \epsilon_B \sum_{j=4}^5 f_{ij} Q_j = 0 \quad (1.36)$$

for $i = 4, 5$, where, f_{ij} are the field coefficients in a direction which is normal to the dielectric boundary at the respective contour point. The above equations are solved to determine the unknown

charges. The accuracy of simulation of multidielectric boundaries deteriorates when the dielectric boundary has a complex profile.

The error in the CSM depends upon the type, number as well as the locations of the simulation charges, the locations of contour points and the complexities of the profile of the electrodes and the dielectrics.

1.6.4 Boundary Element Method (BEM)

Though the charge simulation method is known for its accuracy and speed, it is not very efficient in case of multi-dielectric problems and very thin electrodes, which are often used to control and get the electric field strength in condenser bushings, transformers, etc. Such problems can be solved using the *Surface Charge Simulation Method (SSM)* which is also called *Boundary Element Method (BEM)*.

In many cases, electrodes and insulators used in high-voltage equipment consist of cylinders, spheres, cones, and plane electrodes. Therefore, it is necessary to consider elements having these shapes to achieve a realistic field simulation by using variable charge distribution on these surfaces. The elements are combined in computer code and used for the calculation of complex geometries wherever possible. Curved triangles are employed only at those positions where the above elements cannot be used. This method requires a large number of elements, normally more than 2000, independent of the surface shape and therefore leads to a very large number of system equations.

(a) Principle of BEM

BEM, in principle, is very similar to CSM with area elements. Like in CSM, the BEM uses area charge elements to replace the real charges. However, BEM does not require that the system components should have axial symmetry. The discretization of the real charges is generally carried out by boundary elements having three or four nodes, which use linear shape functions to approximate the internal charge distribution. If the outer surface geometry is not covered, then suitable intermediate points can be added. Boundary elements having pre-determined shapes like cylinders, cones, spheres and toroids are available. The evaluation of the resulting potential functions of the boundary elements is done by numerical integration.

(b) Basic Formulation of BEM

Boundary element formulation calls for the scalar electric potential due to surface charge density, which is written as

$$\varphi(\xi) = 1/(2\alpha\pi\epsilon_0) \int_{\gamma} \rho_s(x) \Phi^l(\xi, x) dP(x) \quad (1.37)$$

where, φ^l denotes the fundamental solution of the potential problem, $\alpha = 1$ or 2 for two or three-dimensional problems respectively, and $\rho_s(x)$ denotes the surface charge density. [Equation \(1.37\)](#) is the basic equation for the source formulation of the BEM. This equation can be solved using the standard point allocation procedure for discretized image charges that lie within the conducted boundaries. The allocation approach has been recognized as *charge simulation*. The electric field is then given

$$\varphi(\xi) = 1/(2\alpha\pi\epsilon_0) \int_{\gamma} \rho_s(x) \nabla \Phi^l(\xi, x); dP(x) \quad (1.38)$$

The resulting system of equations obtained using the source formulation will again be asymmetric. By solving this system of equations, the unknown values of the charge density can be found. Once the charge distribution is known, potential and electric field values can be calculated throughout the domain using [Eqs \(1.37\)](#) and [\(1.38\)](#) given above.

1.6.5 Relative Advantages and Disadvantages of the Various Numerical Methods

For computing the electric fields, various methods have been used, viz. Finite Element Method, Charge Simulation Method and Boundary Element Method. Each of these methods has its own advantages for solving a particular problem.

Finite Element Method is a very general method and has been used for solving a variety of problems. Any non-linearity/inhomogeneity can be modelled and the solution will be available on the entire surface of the domain. Material interface conditions are automatically satisfied. However, it needs a powerful graphic user interface for processing.

Open geometry does not pose any problem with the *Charge Simulation Method* since the surface of the conductor is the only one that is discretized. In addition, as the solution satisfies the Laplace's/Poisson's equation, it will be very smooth, and always gives a small but dense matrix and therefore can be easily handled using personal computers. However, due to the application of superposition principle, nonlinearities and non-homogeneity cannot be modelled using this method.

On the other hand, a unique feature of *Boundary Element Method* is that the electric fields are proportional to the charge densities on an enclosed electrode which is simulated by real charges. This direct field derivation is based on a well known Gauss's area integral. Although BEM is sufficiently developed for use in two-dimensional axi-symmetric problems, some difficulties still exist. They are, the programming complexity and the need for large amount of computational time to execute an improper integral.

Of the above methods, the choice of a particular method depends on the specific problem on hand. In general, the construction of Finite Element model requires considerable effort, since the entire field region should be meshed, while the Charge Simulation and Boundary Element Methods require only the outer surface of the electrode and the outer layer of the dielectric to be meshed. In practice, an important difference between the various numerical methods is that the Finite Element Method can be used only with fields which are bounded while the Charge Simulation method and the Boundary Element Methods also deal with unbounded fields.

A comparison of the accuracies of using the various computational methods shows a good agreement between the results of BEM and CSM, for two-dimensional problems a discrepancy is about 1% while in the 3-D case it is about 2%. On the other hand, discrepancies between BEM and FEM are 2% in the case of 2D calculations and 3% in the case of 3D problems.

For FEM applications, there are a few commercially available software packages like ANSYS (Ansoft Corporation Inc.) and NISA (Engineering Mechanics Research Centre). However, the electric field computations based on other methods like CSM and BEM generally require programmes to be developed individually by the user. For these methods general packages of computer software like coloumb 2D, 3D etc are available.

1.6.6 Conclusion

As described above, various numerical methods for the calculation of electric fields have already been established as reliable tools for high-voltage engineers. However, efforts are still being continued to provide better accuracy and to solve more complicated problems. Now a days, the maximum number of unknowns available in various methods has remarkably increased with the availability of large computational capacity.

The various numerical methods have been described only briefly. For further study, two review papers (References 13 and 14) and more papers dealing with the principles and applications of these methods for field calculations are added in References 15-29.

1.7 SURGE VOLTAGES, THEIR DISTRIBUTION, AND CONTROL

The design of power apparatus particularly at high voltages is governed by their transient behaviour. The transient high voltages or surge voltages originate in power systems due to lightning and switching operations. The effect of the surge voltages is severe in all power apparatuses. The response of a power apparatus to the impulse or surge voltage depends on the capacitances between the coils of windings and between the different phase windings of the multi-phase machines. The transient voltage distribution in the windings as a whole are generally very non-uniform and are complicated by travelling-wave voltage oscillations set up within the windings. In the actual design of an apparatus, it is, of course, necessary to consider the maximum voltage differences occurring, in each region, at any instant of time after the application of an impulse, and to take into account their durations especially when they are less than one microsecond.

An experimental assessment of the dielectric strength of insulation against the power frequency voltages and surge voltages, on samples of basic materials, on less complex assemblies, or on complete equipment must involve high-voltage testing. Since the design of an electrical apparatus is based on the dielectric strength, the design cannot be completely relied upon, unless experimentally tested. High-voltage testing is done by generating the voltages and measuring them in a laboratory.

When high-voltage testing is done on component parts, elaborate insulation assemblies, and complete full-scale prototype apparatus (called development testing), it is possible to build up a considerable stock of design information; although expensive, such data can be very useful. However, such data can never really be complete to cover all future designs and necessitates use of large factors of safety. A different approach to the problem is the exact calculation of dielectric strength of any insulation arrangement. In an ideal design each part of the dielectric would be uniformly stressed at the maximum value which it will safely withstand. Such an ideal condition is impossible to achieve in practice, for dielectrics of different electrical strengths, due to the practical limitations of construction. Nevertheless, it provides information on stress concentration factors—the ratios of maximum local voltage gradients to the mean value in the adjacent regions of relatively uniform stress. A survey of typical power apparatus designs suggests that factors ranging from 2 to 5 can occur in practice; when this factor is high, considerable quantities of insulation must be used. Generally, improvements can be effected in the following ways:

- (i) By shaping the conductors to reduce stress concentrations
- (ii) By insertion of higher dielectric strength insulation at high stress points
- (iii) By selection of materials of appropriate permittivities to obtain more uniform voltage gradients

The properties of different insulating media and their applications are presented in [chapters 2, 3, 4, and 5](#). The generation and measurement of high-voltages and currents are discussed in [chapters 6 and 7](#), and high-voltage test methods and the design of high-voltage laboratories are detailed in [chapters 9, 10, and 11](#). The various aspects of insulation co-ordination in high-voltage power systems are discussed in [Chapter 8](#).

- Electric Field Stresses
- Insulators: Gases and Vacuum, Liquids, Solids, and Composites
- Estimation of Electric Field

- Numerical Computation of Electric Field
- FEM
- CSM and BEM
- Field Enhancement Factor
- Surge Voltage Distribution and Control

MULTIPLE-CHOICE QUESTIONS

1. Average electrical field is the magnitude of electrical field
 - (a) at midpoint between conductors
 - (b) ratio of potential difference to the distance between the conductors
 - (c) at surface of the lower potential electrode
 - (d) ratio of potential difference to half the distance between the conductors.
2. An experimental method for computing the field distribution is
 - (a) solution of Laplace equation
 - (a) electrolytic tank method
 - (c) digital simulation (d) field intensity method.
3. Field enhancement factor is the ratio of
 - (a) maximum field to average field
 - (b) rms value of electric field to average value
 - (c) potential difference to radius of the conductor
 - (d) electric field at surface of the hv conductor to electric field at ground conductor.
4. A numerical method to determine electric field in a multi-conductor geometry is
 - (a) electrolytic tank method
 - (b) resistance analog method
 - (c) finite element method
 - (d) Laplace equation method
5. Most suitable numerical method to solve electrostatic field problems is
 - (a) Laplace equation method
 - (b) charge simulation method
 - (c) finite difference method
 - (d) resistance analog method
6. Open geometry does not pose any problem with
 - (a) boundary element method
 - (b) charge simulation method
 - (c) finite difference method
 - (d) resistance analog method
7. A unique feature of the Boundary Element Method is that
 - (a) it can be used for electric fields which are uniform only
 - (b) it can be used only with bounded fields
 - (c) electric field are proportional to the charge densities on an enclosed electrode which is simulated by real charges
 - (d) none of the above.
8. Finite Element Method can be used only with
 - (a) fields which are bounded

- (b) fields which are unbounded
- (c) fields which are both bounded and unbounded
- (d) when high accuracy is not required.

9. A comparison of the accuracies of various computational methods shows a good agreement between the results of
- (a) FEM and FDM
 - (b) CSM and BEM
 - (c) FEM and CSM
 - (d) BEM and FEM.
10. The accuracies obtained with the numerical computation of electric fields is usually (a) $< 1\%$ (b) 2 to 5% (c) 5 to 10% (d) can be very high.

Answers to Multiple-Choice Questions

- | | | | | | |
|--------|--------|--------|---------|--------|--------|
| 1. (b) | 2. (b) | 3. (a) | 4. (c) | 5. (b) | 6. (b) |
| 7. (c) | 8. (a) | 9. (d) | 10. (b) | | |

REVIEW QUESTIONS

1. What are the different dielectric materials according to their physical nature?
2. How is the Electric Stress/Electric Field Intensity controlled?
3. Define field factor. How does it vary in simple geometries?
4. Discuss the different numerical methods available for estimation of electric field distribution in dielectric media.
5. What is “Finite Element Method”? Give the outline of this method for solving the field problems.
6. Discuss briefly the “Charge Simulation Method” for solving Field Problems and estimation of potential distribution.
7. What is “Boundary Element Method”? How does it differ from Charge Simulation Method?
8. Discuss the relative advantages and disadvantages of different numerical methods for solution of field problems.
9. What are surge voltages and how are they distributed in the windings of a power apparatus like a transformer winding?
10. What is meant by control of transient or impulse voltages? Why is this necessary?

SHORT-ANSWER QUESTIONS

1. The best insulation among all insulating materials available is _____.
2. The most commonly used liquid as insulating medium is _____.
3. The new insulating liquids that have been used in recent years are _____.
4. A composite insulation is a combination of _____.
5. Impurities in insulating materials reduce _____.
6. For parallel cylindrical configuration, the field enhance factor is given by _____.
7. What is the governing equation for the electrical potential V for triangular elements in FEM?
8. What is governing equation for potential V for quadrilateral elements in FEM?
9. What is the principle of charge simulation method?
10. How is BEM different from CSM?

11. When is CSM or BEM most effective?

Answers to Short-Answer Questions

1. Vacuum
2. Mineral Oil
3. polybutanes and synthetic fluorinated hydrocarbon oils
4. Solid-gas or Solid-liquid insulation
5. breakdown strength
6. $V(x, y) = a + bx + cy$
7. $V(x, y) = a + bx + cy + dxy$
8. The given field configuration is simulated by either discrete charges like point or line charge or with a continuous charge distribution.
9. The simulated charge in BEM method is the charge distribution at the surface such as at the electrode surface or around the axis.
10. When the field configuration is two-dimensional and has axial symmetry.

REFERENCES

1. Alston, L.L., *High Voltage Technology*, Oxford University Press, Oxford (1967).
2. Seely, S., *Electromagnetic Fields*, McGraw-Hill, New York (1960).
3. Kuffel E., Zaengl, W.S. and Kuffel, J., *High Voltage Engineering Fundamentals*, (2nd edition), Butterworths Heinemann (2000).
4. Popovic, B.D., *Introductory Engineering Electromagnetics*, Addison-Wesley (1971).
5. Chari, M.V.K. and Silvester, P.P., *Finite Elements in Electrical and Magnetic Field Problems*, Wiley-Interscience Publication, John Wiley and Sons, New York (1980).
6. Silvester, P.P. and Ferrari, R.L., *Finite Elements for Electrical Engineers*, Cambridge University Press (1983).
7. Binns, K.J. and Lawrenson, P.J., *Analysis and Computation of Electric and Magnetic Field Problems*, (2nd edition), Pergamon Press (1973).
8. Zienkiewicz, O.C., *The Finite Element Method in Engineering Science*, McGraw-Hill, London (1977).
9. Anderson, O.W., "Finite Element Solution of Complex Potential Electric Fields". *IEEE Transaction on power apparatus and systems*, **97**, 1156–1166 (1977).
10. Singer, H., Steinbirglar, H. and Weiss, P., "A Charge Simulation Method for the Calculation of H.V. Fields", *IEEE Transactions on PAS*, **93** 1660–1668 (1974).
11. Malik, N.H., "A Review of Charge Simulation Method and its Applications", *IEEE Transactions on Electrical Insulation*, **EI-24** No. 13–20 (1989).
12. Brebbia, C.A., Telles, J.C.F. and Wrobel, L.C., *Boundary Element Techniques*, Springer-Verlag (1984).
13. Takuma, T., "Recent developments in calculation of electric and magnetic fields related to high voltage engineering", *Key Note Speech, Proc. of 12th Int. Symp. on High Voltage Engineering*, Bangalore, India (20–24 August, 2001).
14. Takuma, T. and Kawamoto, T., "Recent developments in electric field calculation", *IEEE Trans. on Magnetics*, **33**, No. 2, pp. 1155–1160 (1997).
15. Singer, H., "Computation of optimized electrode geometries", 3rd, *Int. Symp. on High Voltage*

Engineering (ISH), Paper No. 11.06 (1979).

16. Trinitis, C., "Field optimization of three dimensional high voltage equipment", *11th ISH, London, Paper No. 2.75. P6 (1999).*
17. Anderson, O.W., "Finite element solution for complex potential electric fields", *IEEE Trans. on Power Apparatus and systems*, **86**, pp. 1156–1161 (1977).
18. Ryan, H.M., "Electric Field of a Rod-Plane Spark gap", *IEE Proceedings*, 117, pp. 283 (1970).
19. Abou Seada, M.S. and Nasser, E., "Digital Computer Calculation of the Electric Potential and Field of a Rod gap", *IEEE Proceedings*. **56**, pp. 813–818 (1988).
20. Anderson, O.W., "Laplacian Electrostatic field calculation by Finite elements with automatic grid generation", *IEEE Trans. On Power Apparatus and Systems*, **PAS-92**, No. 5, pp. 1485–1493 (1973).
21. Miri, A.M., Riegel, N.A. and Kuhner, A., "Finite Element Models for the Computation of the Transient Potential and Field Distribution in the Winding System of High Voltage Power Transformers," *11th ISH, London, Paper No. 2.39.S4 (1999).*
22. Iravani, M.R. and Raghuvver, M.R., "Accurate field solution in the entire interelectrode space of a rod-plane gap using optimized charge simulation", *IEEE Trans. Electrical Insulation*, 17, No. 4, pp. 333–337 (1982).
23. Yializis, Kuffel, E. and Alexander, P.N., "An Optimized Charge Simulation Method for the Calculation of High Voltage Fields", *IEEE Trans. on Power Apparatus and Systems*, **PAS-97**, pp. 2434–2440 (1978).
24. Steinbigler, H., "Combined Application of Finite Element Method and Charge Simulation Method for the Computation of Electric Fields", *3rd International Symposium on High Voltage Engineering, Milan, Paper No. 11.11. August, 1979.*
25. Malik, N.H. and Al-Arainy, A., "Charge simulation modeling of three-core belted cables", *IEEE Trans. Electrical Insulation*, **20**, No. 3, pp. 499–503 (1985).
26. Kato, S., "An Estimation Method for the Electric Field Error of Charge Simulation Method", *3rd International Symposium on High Voltage Engineering, Milan, Paper No. 11.09. August, 1979.*
27. Gutfleish, F., Singer, H., Forger, K. and Gomollon, J.A., "Calculations of HV Fields by Means of the Boundary Element Method", *IEEE Transactions on PWRD* **9**, pp. 734–749 (1994).
28. Chakravorti, S. and Mukherjee, P.K., "Power frequency and impulse field calculation around an HV insulator with uniform and non-uniform surface pollution", *IEEE Trans. on Electrical Insulation, EI-28*, pp. 43–53 (1993).
29. de Kock, N., Mendik, M., Andjelic, Z. and Blaszczyk, A., "Application of the 3D Boundary Element Method in the Design of EHV GIS Components", *IEEE Elec. Ins. Mag.*, **14**, No. 3, pp. 17–22 (1998).

* torr = 1 mm of Hg.

CHAPTER

2

Conduction and Breakdown in Gases

2.1 GASES AS INSULATING MEDIA

The simplest and the most commonly found dielectrics are gases. Most of the electrical apparatus use air as the insulating medium, and in a few cases other gases such as nitrogen (N_2), carbon dioxide (CO_2), freon (CCl_2F_2), and sulphur hexafluoride (SF_6) are also used.

Various phenomena occur in gaseous dielectrics when a voltage is applied. When the applied voltage is low, small currents flow between the electrodes and the insulation retains its electrical properties. On the other hand, if the applied voltages are large, the current flowing through the insulation increases very sharply, and an electrical breakdown occurs. A strongly conducting spark formed during breakdown practically produces a short-circuit between the electrodes. The maximum voltage applied to the insulation at the moment of breakdown is called the breakdown voltage. In order to understand the breakdown phenomenon in gases, a study of the electrical properties of gases and the processes by which high currents are produced in gases is essential.

The electrical discharges in gases are of two types, i.e., (i) non-sustaining discharges, and (ii) self-sustaining types. The breakdown in a gas, called spark breakdown is the transition of a non-sustaining discharge into a self-sustaining discharge. The build-up of high currents in a breakdown is due to the process known as ionization in which electrons and ions are created from neutral atoms or molecules, and their migration to the anode and cathode respectively leads to high currents. At present, two types of theories, viz., (i) Townsend theory, and (ii) Streamer theory are known which explain the mechanism for breakdown under different conditions. The various physical conditions of gases, namely, pressure, temperature, electrode field configuration, nature of electrode surfaces, and the availability of initial conducting particles are known to govern the ionization processes.

2.2 COLLISION PROCESSES

2.2.1 Types of Collision

An electrical discharge is normally created from unionised gas by collision processes. These processes are mainly gas processes which occur due to the collision between the charged particles and gas atoms or molecules. These are of the following two types.

(a) Elastic Collisions Elastic collisions are collisions which when occur, no change takes place in the internal energy of the particles but only their kinetic energy gets redistributed. These collisions do not occur in practice. When electrons collide with gas molecules, a single electron traces a zig-zag path during its travel. But in between the collisions it is accelerated by the electric field. Since electrons are very light in weight, they transfer only a part of their kinetic energy to the much heavier ions or gas molecules with which they collide. This results in very little loss of energy by the electrons and therefore, electrons gain very high energies and travel at a much higher speed than the ions. Therefore in all electrical discharges electrons play a leading role.

(b) Inelastic Collisions Inelastic collisions, on the other hand, are those in which internal changes in energy take place within an atom or a molecule at the expense of the total kinetic energy of the colliding particle. The collision often results in a change in the structure of the atom. Thus, all collisions that occur in practice are inelastic collisions. For example ionisation, attachment, excitation, recombination are inelastic collisions.

2.2.2 Mobility of Ions and Electrons

When an ion moves through a gas under the influence of a static uniform electric field, it gains energy from the field between collisions and loses energy during collisions. Electric force on an electron/ion of charge e is eE , with the resulting acceleration being eE/m . When the energy gained by the ions from the electric field is small compared with the thermal energy, the drift velocity in the field direction W_i is proportional to the electrical field intensity E and may be expressed as follows:

$$W_i = \mu_i E \quad (2.1)$$

where μ_i is called the mobility of ions. The mobility is mainly a characteristic of the gas through which the ion moves. At normal temperatures and pressures the mobility μ is of the order of several $\text{cm}^2/\text{volt-sec}$.

However, the concept of ionic mobility cannot be directly applied to electrons because of their extremely low mass. Any externally applied electric field will cause the electrons to gain energies much higher than their mean thermal energy. So the electron drift velocity, which has been defined as the average velocity, with which the centre of mass of the electron swarm moves in the direction of the field, is not a simple function of E/p , but is determined from the energy distribution function. From the kinetic theory the electron drift velocity W_e is given in microscopic terms as follows:

$$W_e = \frac{1}{3} \frac{Ee}{mc^2} \frac{d}{dc} (lc^2) \quad (2.2)$$

where l is an equivalent mean free path of an electron with speed c .

2.2.3 Diffusion Coefficient

When particles possessing energy, which is exhibited as a random motion, are distributed unevenly throughout a space, then they tend to redistribute themselves uniformly throughout the space. This process is known as diffusion and the rate at which this occurrence is governed by the diffusion passing through unit area in unit time perpendicular to the concentration gradient and for unit concentration gradient. In three dimensions this may be written as

$$\frac{\partial n}{\partial t} = D \nabla^2 n \quad (2.3)$$

where n is the concentration of particles and D is coefficient of Diffusion.

Kinetic theory gives D in microscopic terms as follows:

$$D = 1/3 (lc) \quad (2.4)$$

where l is the mean free path and c the random velocity, the average being taken over c .

In electrical discharges, whenever there is a non-uniform concentration of charges there will be migration of these charges from regions of higher concentration to regions of lower concentration. This process is called diffusion and this causes a de-ionizing effect in the regions of lower concentration. The presence of walls confining a given volume increases the de-ionization effect since charged particles lose their charge on hitting the wall. Both diffusion and mobility result in mass motion described by a drift velocity caused either by unbalanced collision forces (concentration gradient) or by the electric field itself.

2.2.4 Electron Energy Distributions

For the development of a complete theory giving the relationship between the data concerning single collisions of electrons with gas molecules, and the experimentally obtained average properties of discharges, a knowledge of the electron energy distribution functions is essential. The most widely used distribution functions are the Maxwellian and Druyesteynian distributions which apply specifically to elastic conditions.

The Maxwellian distribution has been found to apply where there is thermal equilibrium between the electrons and molecules.

The distribution takes the form

$$F(\epsilon) = C_1 \epsilon^{0.5} \exp(-1.5 \epsilon/\bar{\epsilon}) \quad (2.5)$$

where C_1 is the constant and e is the mean energy.

Druyesteynian distribution applies when the electron or ion energy is much greater than the thermal energy and is therefore expected to be more of application in townsend discharges. This distribution takes the form

$$F(\epsilon) = C_2 \epsilon^{0.5} \exp(-0.55 \epsilon^2/\bar{\epsilon}^{-2}) \quad (2.6)$$

where C_2 is another constant.

2.2.5 Collision Cross Section

Collision cross section is defined as the area of contact between two particles during a collision, in other words, the total area of impact. This area of contact is different for each type of collision. For example, the area of impact is more for ionization while for an excitation it is less. For simultaneously occurring processes such as ionization, excitation, charge transfer, chemical reactions, etc., the effective cross section is obtained by simple addition of all the cross sections. If q_t is the total cross section, and if q_i , q_e , q_c ... etc., are the cross sections for ionization, excitation, charge transfer, etc, respectively, then

$$q_t = q_i + q_e + q_c + \dots$$

Thus the use of collision cross sections instead of mean free paths has often proved to be advantageous. The collision cross section is also expressed in terms of the probability of a collision to take place, i.e.,

$$P = nq \tag{2.7}$$

which is the reciprocal of the mean free path.

2.2.6 The Mean Free Path (λ)

The mean free path is defined as the average distance between collisions. When a discharge occurs large number of collisions occur between the electrons and the gas molecules. Depending on the initial energy of the colliding electron, the distance between the two collisions vary. The average of this is the mean free path. The free path is a random quantity and its mean value depends upon the concentration of particles or the density of the gas.

The mean free path can be expressed as

$$\lambda = k/p \text{ cm} \quad (2.8)$$

where k is a constant and p is the gas pressure in microns.

The value of k for nitrogen is 5. From this equation it is seen that at a pressure of 1 torr, λ is 5×10^{-3} cm. If the pressure is 10^{-6} torr, then $\lambda = 5 \times 10^{+3}$ cm. From this it is seen that mean free path is very large at very low pressures and is very small at high pressures.

2.3 IONIZATION PROCESSES

A gas in its normal state is almost a perfect insulator. However, when a high-voltage is applied between the two electrodes immersed in a gaseous medium, the gas becomes a conductor and an electrical breakdown occurs.

The processes that are primarily responsible for the breakdown of a gas are ionization by collision, photo-ionization, and the secondary ionization processes. In insulating gases (also called electron-attaching gases) the process of attachment also plays an important role.

2.3.1 Ionization by Collision

The process of liberating an electron from a gas molecule with the simultaneous production of a positive ion is called ionization. In the process of ionization by collision, a free electron collides with a neutral gas molecule and gives rise to a new electron and a positive ion. If we consider a low-pressure gas column in which an electric field \mathcal{E} is applied across two plane parallel electrodes, as shown in Fig. 2.1 then, any electron starting at the cathode will be accelerated more and more between collisions with other gas molecules during its travel towards the anode. If the energy (ε) gained during this travel between collisions exceeds the ionization potential, V_i , which is the energy required to dislodge an electron from its atomic shell, then ionization takes place. This process can be represented as

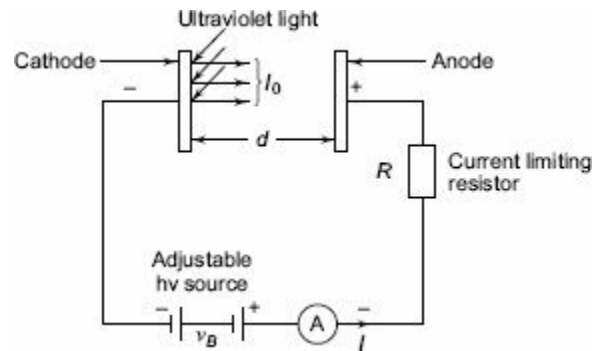
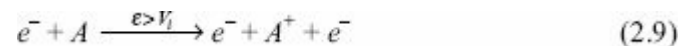


Fig. 2.1 Arrangement for study of a Townsend discharge



where A is the atom, A^{+} is the positive ion and e^{-} is the electron.

A few of the electrons produced at the cathode by some external means, say by ultra-violet light falling on the cathode, ionize neutral gas particles producing positive ions and additional electrons. The additional electrons, then, themselves make ‘ionizing collisions’ and thus the process repeats itself. This represents an increase in the electron current, since the number of electrons reaching the anode per unit time is greater than those liberated at the cathode. In addition, the positive ions also reach the cathode and on bombardment on the cathode give rise to secondary electrons.

2.3.2 Photo-ionization

The phenomena associated with ionization by radiation, or photo-ionization, involves the interaction of radiation with matter. Photo-ionization occurs when the amount of radiation energy absorbed by an atom or molecule exceeds its ionization potential.

There are several processes by which radiation can be absorbed by atoms or molecules. They are

- (a) excitation of the atom to a higher energy state, and
- (b) continuous absorption by direct excitation of the atom or dissociation of diatomic molecule or direct ionization, etc.

Just as an excited atom emits radiation when the electron returns to the lower state or to the ground state, the reverse process takes place when an atom absorbs radiation. This reversible process can be expressed as



Ionization occurs when

$$\lambda \leq c \cdot \frac{h}{V_i} \quad (2.11)$$

where, h is the Planck's constant, c is the velocity of light, λ is the wavelength of the incident radiation and V_i is the ionization energy of the atom. Substituting for h and c , we get

$$\lambda \leq \left(\frac{1.27}{V_i} \right) \times 10^{-6} \text{ cm}$$

where V_i is in electron volts (eV). The higher the ionization energy, the shorter will be the wavelength of the radiation capable of causing ionization. It was observed experimentally that a radiation having a wavelength of 1250 Å is capable of causing photo-ionization of almost all gases.

2.3.3 Secondary Ionization Processes

Secondary ionization processes by which secondary electrons are produced are the one which sustain a discharge after it is established due to ionization by collision and photo-ionization.

They are briefly described below.

(a) *Electron Emission due to Positive Ion Impact* Positive ions are formed due to ionization by collision or by photo-ionization, and being positively charged, they travel towards the cathode.

A positive ion approaching a metallic cathode can cause emission of electrons from the cathode by giving up its kinetic energy on impact. If the total energy of the positive ion, namely, the sum of its kinetic energy and the ionization energy, is greater than twice the work function of the metal then one electron will be ejected and a second electron will neutralise the ion. The probability of this process is measured as γ_i which is called the Townsend's secondary ionization coefficient due to positive ions and is defined as the net yield of electrons per incident positive ion. γ_i increases with ion velocity and depends on the kind of gas and electrode material used.

(b) *Electron Emission due to Photons* To cause an electron to escape from a metal, it should be given enough energy to overcome the surface potential barrier. The energy can also be supplied in the form of a photon of ultraviolet light of suitable frequency. Electron emission from a metal surface occurs at the critical condition (see [Eq. \(2.11\)](#))

$$h \cdot \nu \leq \phi$$

where ϕ is the work function of the metallic electrode. The frequency (ν) is given by the relationship

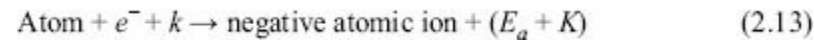
$$\nu = \frac{\phi}{h} \quad (2.12)$$

is known as the threshold frequency. For a clean nickel surface with $\phi = 4.5$ eV, the threshold frequency will be that corresponding to a wavelength $\lambda = 2755$ Å. If the incident radiation has a greater frequency than the threshold frequency, then the excess energy goes partly as the kinetic energy of the emitted electron and partly to heat the surface of the electrode. Since ϕ is typically a few electrons volts, the threshold frequency lies in the far ultraviolet region of the electromagnetic radiation spectrum.

(c) *Electron Emission due to Metastable and Neutral Atoms* A meta-stable atom or molecule is an excited particle whose lifetime is very large (10^{-3} s) compared to the lifetime of an ordinary particle (10^{-8} s). Electrons can be ejected from the metal surface by the impact of excited (metastable) atoms, provided that their total energy is sufficient to overcome the work function. This process is most easily observed with metastable atoms, because the lifetime of other excited states is too short for them to reach the cathode and cause electron emission, unless they originate very near to the cathode surface. Therefore, the yields can also be large nearly 100%, for the interactions of excited He atom with a clean surface of molybdenum, nickel or magnesium. Neutral atoms in the ground state also give rise to secondary electron emission if their kinetic energy is high (≈ 1000 eV). At low energies the yield is considerably less.

2.3.4 Electron Attachment Process

The types of collisions in which electrons may become attached to atoms or molecules to form negative ions are called attachment collisions. Electron attachment process depends on the energy of the electron and the nature of the gas and is a very important process from the engineering point of view. All electrically insulating gases, such as O_2 , CO_2 , Cl_2 , F_2 , C_2F_6 , C_3F_8 , C_4F_{10} , CCl_2F_2 , and SF_6 exhibit this property. An electron-attachment process can be represented as



The energy liberated as a result of this process is the kinetic energy K plus the electron affinity E_a . In the attaching or insulating gases, the atoms or molecules have vacancies in their outermost shells and, therefore, have an affinity for electrons. The attachment process plays a very important role in the removal of free electrons from an ionized gas when arc interruption occurs in gas-insulated switchgear. The effect of attachment on breakdown in gases is discussed in [Sec. 2.8](#) of this chapter.

2.4 TOWNSEND'S CURRENT GROWTH EQUATION

Referring to [Fig. 2.1](#), let us assume that n_0 electrons are emitted from the cathode. When one electron collides with a neutral particle, a positive ion and an electron are formed. This is called an ionizing collision. Let α be the average number of ionizing collisions made by an electron per centimetre travel in the direction of the field (α depends on gas pressure p and E/p , and is called the *Townsend's first ionization coefficient*). At any distance x from the cathode, let the number of electrons be n_x . When these n_x electrons travel a further distance of dx they give rise to ($\alpha n_x dx$) electrons.

$$\text{At } x = 0, n_x = n_0 \quad (2.14)$$

$$\text{Also, } \frac{dn_x}{dx} = \alpha n_x; \text{ or } n_x = n_0 \exp(\alpha x) \quad (2.15)$$

Then, the number of electrons reaching the anode ($x = d$) will be

$$n_d = n_0 \exp(\alpha d) \quad (2.16)$$

The number of new electrons created, on the average, by each electron is

$$\exp(\alpha d) - 1 = \frac{n_d - n_0}{n_0} \quad (2.17)$$

Therefore, the average current in the gap, which is equal to the number of electrons travelling per second will be

$$I = I_0 \exp(\alpha d) \quad (2.18)$$

where I_0 is the initial current at the cathode.

2.5 CURRENT GROWTH IN THE PRESENCE OF SECONDARY PROCESSES

The single avalanche process described in the previous section becomes complete when the initial set of electrons reaches the anode. However, since the amplification of electrons $[\exp(\alpha d)]$ is occurring in the field, the probability of additional new electrons being liberated in the gap by other mechanisms increases, and these new electrons create further avalanches. The other mechanisms are the following:

- (i) The positive ions liberated may have sufficient energy to cause liberation of electrons from the cathode when they impinge on it.
- (ii) The excited atoms or molecules in avalanches may emit photons, and this will lead to the emission of electrons due to photo-emission.
- (iii) The metastable particles may diffuse back causing electron emission.

The electrons produced by these processes are called secondary electrons. The secondary ionization coefficient γ is defined in the same way as α , as the net number of secondary electrons produced per incident positive ion, photon, excited particle, or metastable particle, and the total value of γ is the sum of the individual coefficients due to the three different processes, i.e. $\gamma = \gamma_1 + \gamma_2 + \gamma_3$. γ is called the Townsend's secondary ionization coefficient and is a function of the gas pressure p and E/p .

Following Townsend's procedure for current growth, let us assume

n'_0 = number of secondary electrons produced due to secondary (γ) processes.

Let n''_0 = total number of electrons leaving the cathode.

Then $n''_0 = n_0 + n'_0$ (2.19)

The total number of electrons n reaching the anode becomes,

$$n = n''_0 \exp(\alpha d) = (n_0 + n'_0) \exp(\alpha d);$$

and

$$n'_0 = \gamma [n - (n_0 + n'_0)] \leftarrow \text{[...] is \# of ions born by the electrons traveling from cathode to anode. Thus this expression means ions born by electron collision to atoms during its passage to anode hit cathode and their \# multiplied by secondary coefficient gives \# of secondary electrons.}$$

Eliminating n'_0 ,

$$n = \frac{n_0 \exp(\alpha d)}{1 - \gamma [\exp(\alpha d) - 1]}$$

or

$$I = \frac{I_0 \exp(\alpha d)}{1 - \gamma [\exp(\alpha d) - 1]} \quad (2.20)$$

2.6 TOWNSEND'S CRITERION FOR BREAKDOWN

Equation (2.20) gives the total average current in a gap before the occurrence of breakdown. As the distance between the electrodes d is increased, the denominator of the equation tends to zero, and at some critical distance $d = d_s$.

$$1 - \gamma[\exp(\alpha d) - 1] = 0 \quad (2.21)$$

For values of $d < d_s$, I is approximately equal to $\frac{I_0}{1 - \gamma[\exp(\alpha d) - 1]}$, and if the external source for the supply of θ is removed, I becomes zero. If $d = d_s$, $I \rightarrow \infty$ and the current will be limited only by the resistance of the power supply and the external circuit. This condition is called Townsend's breakdown criterion and can be written as

$$\gamma[\exp(\alpha d) - 1] = 1$$

Normally, $\exp(\alpha d)$ is very large, and hence the above equation reduces to

$$\gamma \exp(\alpha d) = 1 \quad (2.22)$$

For a given gap spacing and at a given pressure the value of the voltage V which gives the values of α and γ satisfying the breakdown criterion is called the spark breakdown voltage V_s and the corresponding distance d_s is called the sparking distance.

The Townsend mechanism explains the phenomena of breakdown only at low pressure, corresponding to $p \times d$ (gas pressure \times gap distance) values of 1000 torr-cm and below.

2.7 EXPERIMENTAL DETERMINATION OF COEFFICIENTS α AND γ

The experimental arrangement is shown in Fig. 2.2. The electrode system consists of two uniform field electrodes. The high-voltage electrode is connected to a variable high-voltage dc source (of 2 to 10 kV rating). The low-voltage electrode consists of a central electrode and a guard electrode. The central electrode is connected to the ground through the high resistance of an electrometer amplifier having an input resistance of 10^9 to 10^{13} ohms. The guard electrode is directly earthed. The electrometer amplifier measures currents in the range 10^{-14} to 10^{-8} A.

The electrode system is placed in an ionization chamber which is either a metal chamber made of chromium-plated mild steel or stainless steel, or a glass chamber. The electrodes are usually made of brass or stainless steel. The chamber is evacuated to a very high vacuum of the order of 10^{-4} to 10^{-6} torr. Then it is filled with the desired gas and flushed several times till all the residual gases and air are removed. The pressure inside the chamber is adjusted to a few torr depending on the gap separation and left for about half an hour for the gas to fill the chamber uniformly.

The cathode is irradiated using an ultra-violet (UV) lamp kept outside the chamber. The UV radiation produces the initiatory electrons (n_0) by photo-electric emission.

When the dc voltage is applied and when the voltage is low, the current pulses start appearing due to electrons and positive ions as shown in Figs 2.3a and 2.3b. These records are obtained when the current is measured using a cathode ray oscilloscope.

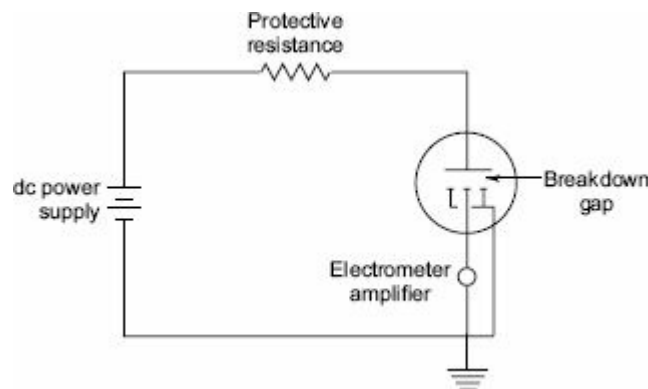
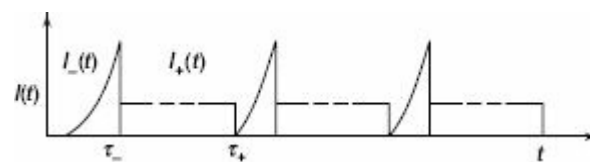
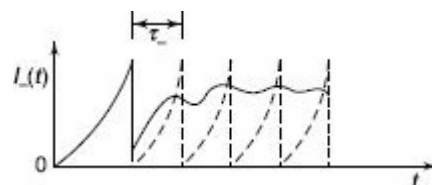


Fig. 2.2 Experimental arrangement to measure ionization coefficients α and γ



(a) When secondary electrons are produced at the cathode by positive ions Caption to figure 2.3



Caption to figure 2.3

(b) When secondary electrons are produced by photons at the cathode _____ ideal, _____ actual.
 $I(t)$ is the total current and I_- and I_+ are electron-ion currents. τ_- and τ_+ are the electron- and ion-

transit times.

Fig. 2.3 Current as a function of time

When the applied voltage is increased, the pulses disappear and an average dc current is obtained as shown in [Fig. 2.4](#). In the initial portion (T_0), the current increases slowly but unsteadily with the voltage applied. In the regions T_1 and T_2 , the current increases steadily due to the Townsend mechanism. Beyond T_2 the current rises very sharply, and a spark occurs.

For determining the α and γ coefficients, the voltage-current characteristics for different gap settings are obtained. From these results, a $\log I/I_0$ versus gap distance plot is obtained under constant field (E) conditions as shown in

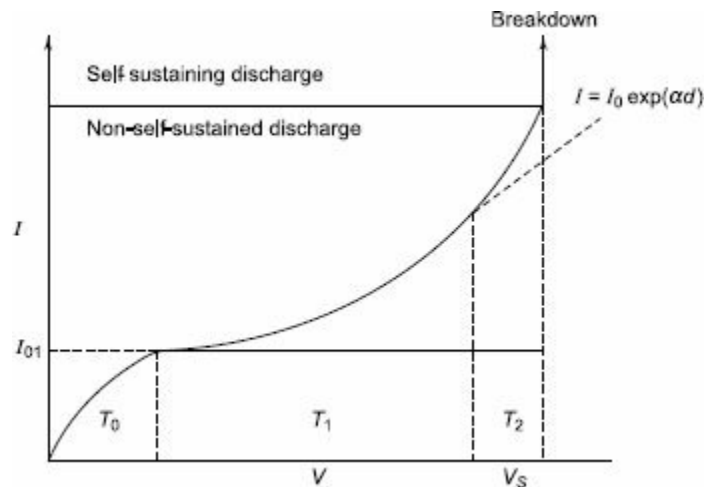


Fig. 2.4 Typical current growth curve in a Townsend discharge

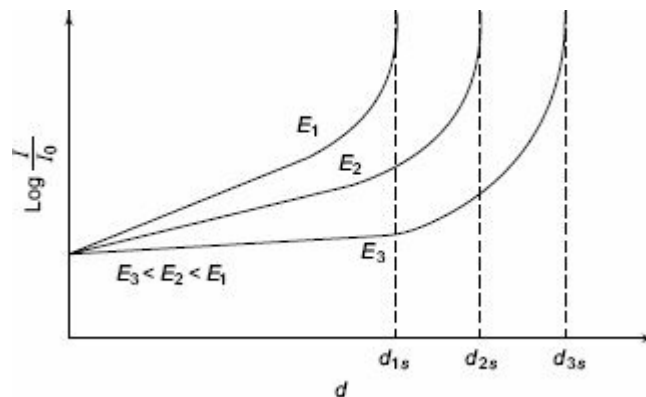


Fig. 2.5 Townsend type $\log (I/I_0)$ vs. d plot

[Fig. 2.5](#). The slope of the initial portion of the curves gives the value of α . Knowing α , γ can be found from [Eq. \(2.20\)](#) using points on the later upturn portion of the graphs. The experiment can be repeated for different pressures.

It can be easily seen that α/p and γ are functions of E/p . The spark-over voltage for any gap length d_s is $V_s = Ed_s$ where d_s is the critical gap length for that field strength as obtained from the graph. It may be noted that if I_0 , the initial current, is more, the average anode current I will also be more, but the relation $\log I/I_0$ versus d plot remains the same. Typical variation of α is shown in [Fig. 2.6](#).

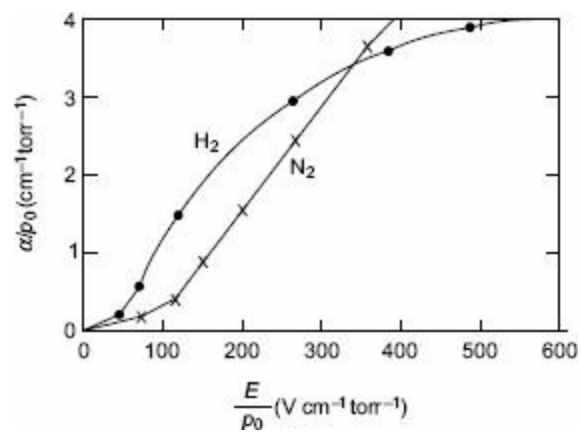


Fig. 2.6 The variation of α/p with E/p in hydrogen and nitrogen, p_0 in both x and y axes refers to values of pressure reduced to 0°C

2.8 BREAKDOWN IN ELECTRONEGATIVE GASES

It has been recognised that one process that gives high breakdown strength to a gas is the electron attachment in which free electrons get attached to neutral atoms or molecules to form negative ions. Since negative ions like positive ions are too massive to produce ionization due to collisions, attachment presents an effective way of removing electrons which otherwise would have led to current growth and breakdown at low-voltage. The gases in which attachment plays an active role are called electronegative gases.

The most common attachment processes encountered in gases are (a) the direct attachment in which an electron directly attaches to form a negative ion, and (b) the dissociative attachment in which the gas molecules split into their constituent atoms and the electronegative atom forms a negative ion. These processes may be symbolically represented as

(a) Direct attachment



(b) Dissociative attachment



A simple gas of this type is oxygen. Other gases are sulphur hexafluoride, freon, carbon dioxide, and fluorocarbons. In these gases, 'A' is usually sulphur or carbon atom, and 'B' is oxygen atom or one of the halogen atoms or molecules.

With such gases, the Townsend current growth equation is modified to include ionization and attachment. An attachment coefficient (η) is defined, similar to α , as the number of attaching collisions made by one electron drifting one centimetre in the direction of the field. Under these conditions, the current reaching the anode, can be written as

$$I = I_0 \frac{[\{\alpha/(\alpha - \eta)\} \exp(\alpha - \eta)d] - [\eta/(\alpha - \eta)]}{1 - \left\{ \gamma \frac{\alpha}{(\alpha - \eta)} [\{\exp(\alpha - \eta)d\} - 1] \right\}} \quad (2.25)$$

The Townsend breakdown criterion for attaching gases can also be deduced by equating the denominator in [Eq. \(2.17\)](#) to zero, i.e.,

[Eq. \(2.25\)](#)

$$\gamma \frac{\alpha}{(\alpha - \eta)} [\exp(\alpha - \eta)d - 1] = 1 \quad (2.26)$$

This shows that for $\alpha > \eta$, breakdown is always possible irrespective of the values of α , η , and γ . If on the other hand, $\eta > \alpha$ [Eq. \(2.26\)](#) approaches an asymptotic form with increasing value of d , and

$$\gamma \frac{\alpha}{(\alpha - \eta)} = 1; \text{ or } \alpha = \frac{\eta}{(1 - \gamma)} \quad (2.27)$$

Normally, γ is very small ($\leq 10^{-4}$) and the above equation can be written as $\alpha = \eta$. This condition puts a limit for E/p below which no breakdown is possible irrespective of the value of d , and the limit value is called the critical E/p . Critical E/p for SF_6 is $117 \text{ V cm}^{-1} \text{ torr}^{-1}$, and for CCl_2F_2 it is $121 \text{ V cm}^{-1} \text{ torr}^{-1}$ (both at 20°C). η values are also experimentally determined as described in [Sec.](#)

2.7. Typical values of η in SF_6 are shown in Fig. 2.7.

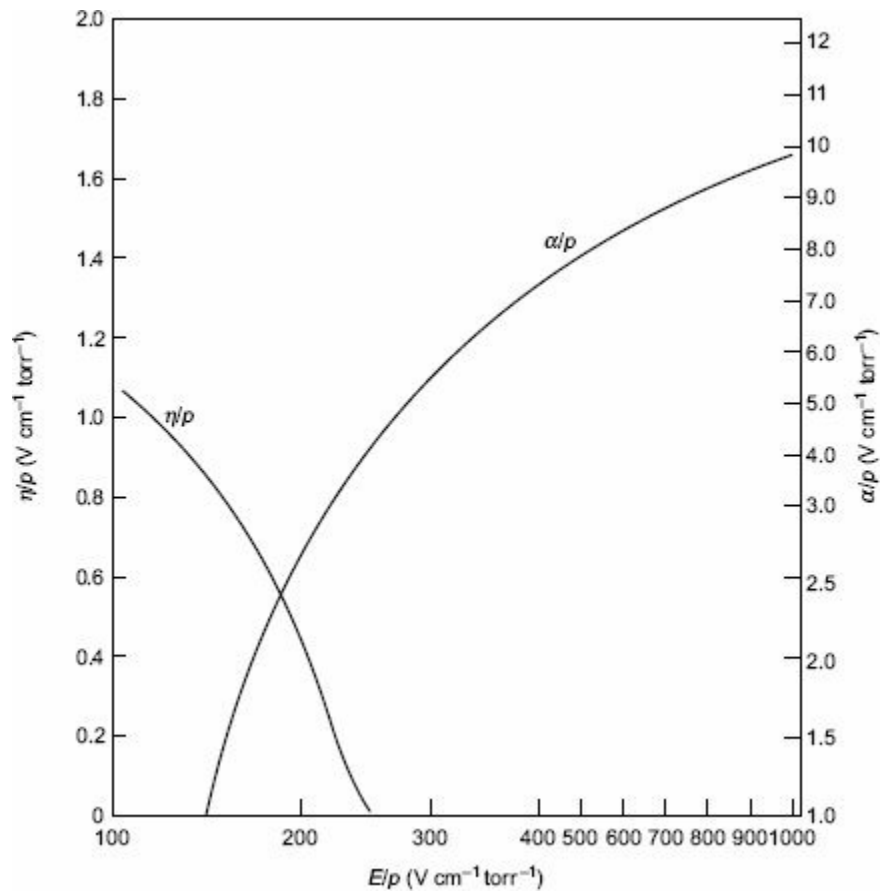


Fig. 2.7 Values of α/p and η/p as a function of E/p in SF_6 at $20^\circ C$

2.9 TIME LAGS FOR BREAKDOWN

In the previous section, the mechanism of spark breakdown is considered as a function of ionization processes under uniform field conditions. But in practical engineering designs, the breakdown due to rapidly changing voltages or impulse voltages is of great importance. Actually, there is a time difference between the application of a voltage sufficient to cause breakdown and the occurrence of breakdown itself. This time difference is called the time lag.

The 'Townsend criterion' for breakdown is satisfied, only if at least one electron is present in the gap between the electrodes. In the case of applied dc or slowly varying (50 Hz ac) voltages, there is no difficulty in satisfying this condition. However, with rapidly varying voltages of short duration ($\approx 10^{-6}$ s), the initiatory electron may not be present in the gap, and in the absence of such an electron breakdown cannot occur. The time t which lapses between the application of the voltage sufficient to cause breakdown and the appearance of the initiating electron is called a statistical time lag (t_s) of the gap. The appearance of electrons is usually statistically distributed. After the appearance of the electron, a time t_f is required for the ionization processes to develop fully to cause the breakdown of the gap, and this time is called the formative time lag (t_f). The total time $t_s + t_f = t$ is called the total time lag as shown in [Fig. 2.8](#).

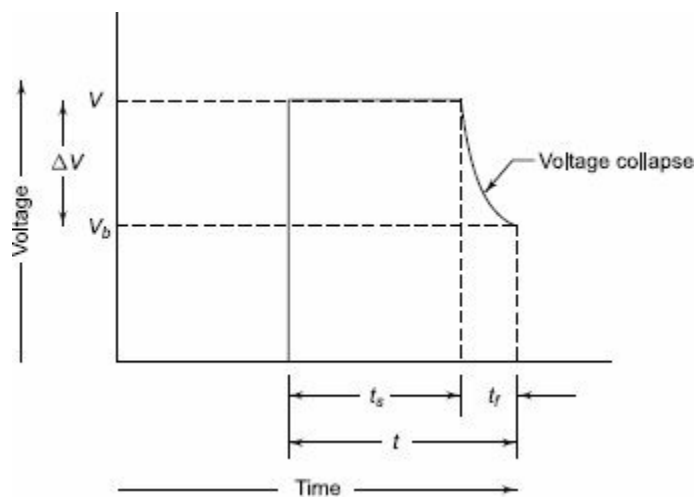


Fig. 2.8 Breakdown with a step function voltage pulse. t_s = statistical time; t_f = formative time; t = total time

The statistical time lag depends upon the amount of pre-ionization present in the gap. This in turn depends on the size of the gap and the quantity of radiation that produces the primary electrons. The appearance of such electrons is usually statistically distributed. The techniques generally used for irradiating the gaps include ultraviolet radiation, radio active materials and light sources.

The formative time lags depend mostly on the mechanism of the avalanche growth in the gap. In cases where the secondary electrons are produced only due to the bombardment of the cathode by the positive ions, the transit time of the positive ion from the anode to the cathode will predominantly contribute for the formative time lag.

The formative time lag is usually much shorter than the statistical time lag and therefore the statistical time lag can be determined by measuring the total time lag.

2.9.1 Voltage-time Characteristics

When an impulse voltage of a value V or higher is applied to a gap, breakdown will occur on each voltage application. The time lag will then depend on the rate of rise of the applied voltage and field uniformity. Therefore, for each gap configuration it is possible to construct a volt-time characteristic by applying a number of impulses of increasing magnitude and recording the time lag using an oscilloscope. A representative plot of such a characteristic is shown in [Fig. 2.10](#). In uniform and fairly non-uniform field gaps, the characteristic is sharply defined and rises steeply with increasing rate of rise of the applied voltage. In non-uniform field gaps there will be a large scatter in the results, and the time to breakdown will be less sensitive to the rate of rise of applied voltage. Hence, fairly uniform field gaps such as sphere gaps are often used as protective devices against over-voltages in electric power systems. The voltage-time characteristic is an important property of any insulating structure or equipment. It provides a basis for establishing the impulse strength of the insulation as well as for the design of the protective levels against over-voltages in power systems. For more details, see [Chapter 8](#).

Time lags are of considerable practical importance. For breakdown to occur, the applied voltage V should be greater than the static breakdown voltage V_s as shown in [Fig. 2.9](#). The difference in voltage $\Delta V = V - V_s$ is called the overvoltage, and the ratio V/V_s is called the impulse ratio. The variation of t_f with overvoltage (ΔV) is shown in [Fig. 2.9](#). The volt-time characteristics of different electrical apparatus are very important in insulation co-ordination.

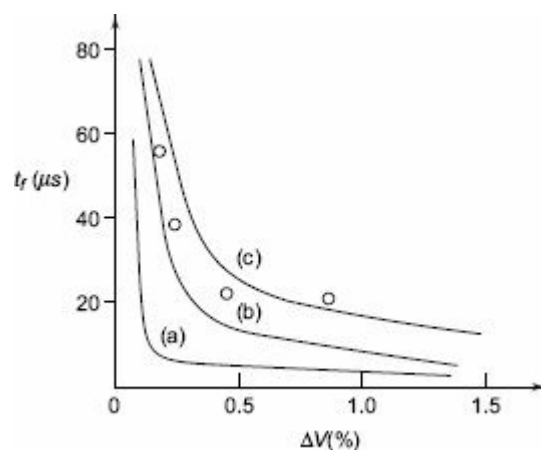


Fig. 2.9 Formative time lag (t_f) as a function of ΔV a, b, c are for different gap spacings, $^{\circ}$ experimental point—calculated

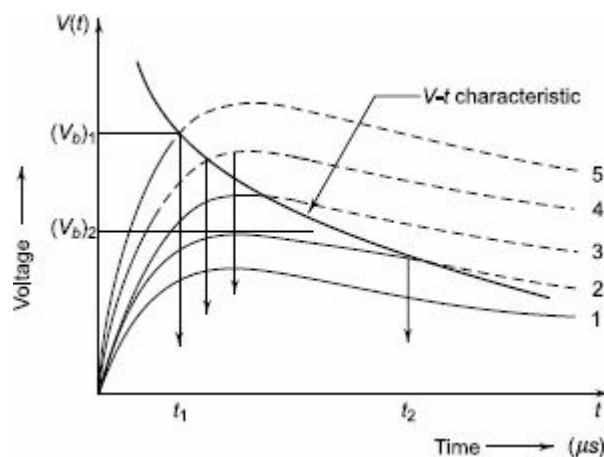


Fig. 2.10 Voltage-time characteristics

2.10 STREAMER THEORY OF BREAKDOWN IN GASES

Townsend mechanism when applied to breakdown at atmospheric pressure was found to have certain drawbacks. Firstly, according to the Townsend theory, current growth occurs as a result of ionization processes only. But in practice, breakdown voltages were found to depend on the gas pressure and the geometry of the gap. Secondly, the mechanism predicts time lags of the order of 10^{-5} s, while in actual practice breakdown was observed to occur at very short times of the order of 10^{-8} s. Also, while the Townsend mechanism predicts a very diffused form of discharge, in actual practice, discharges were found to be filamentary and irregular. The Townsend mechanism failed to explain all these observed phenomena and as a result, around 1940, Raether and, Meek and Loeb independently proposed the Streamer theory.

2.10.1 Streamer Theory

The growth of charge carriers in an avalanche in a uniform field is described by $e^{\alpha d}$. This is valid only as long as the influence of the space charge due to ions is very small compared to the applied field. In his studies on the effect of space charge on avalanche growth, Raether observed that when charge concentration was between 10^6 and 10^8 , the growth of the avalanche became weak. On the other hand, when the charge concentration was higher than 10^8 , the avalanche current was followed by a steep rise in the current between the electrodes leading to the breakdown of the gap. Both the slow growth at low charge concentrations and fast growth at high charge concentrations have been attributed to the modification of the originally applied uniform field (E) by the space charge P . [Figure 2.11](#) shows the electric field around the avalanche as it progresses along the gap and the resulting modification to the applied field. For simplicity, the space charge at the head of the avalanche is assumed to have a spherical volume containing negative charge at its top because of the higher electron mobility. Under these conditions, the field gets enhanced at the top of the avalanche with field lines from the anodes terminating on its head. Further, at the bottom of the avalanche, the field between electrons and ions reduces the applied field (E). Still further down, the field between cathode and the positive ions gets enhanced. Thus, the field distortion occurs and it becomes noticeable with a charge carrier number $n > 10^6$. For example, in nitrogen at $p = 760$ torr and with a gap distance of 2 cm, the filled field distortion will be about 1%. This 1% field distortion over the entire gap will lead to a doubling of the avalanche size, but as the distortion is significant only in the vicinity of the top of the avalanche its effect is still negligible. However, if a charge density in the avalanche approaches $n = 10^8$ the space charge filled field and the applied field will have the same magnitude and this leads to the initiation of a streamer. Thus, the space charge fields play an important role in the growth of avalanches in corona and spark discharges in non-uniform field gaps. It has been shown that transformation from an avalanche to a streamer generally occurs when the charge within the avalanche head reaches a critical value of $n_0 \exp(\alpha x_c) = 10^8$ or αx_c lies between 18 and 20, where x_c is the length of the avalanche in which the secondary electrons are produced by photo-ionization of gas molecules in the inter-electrode gap.

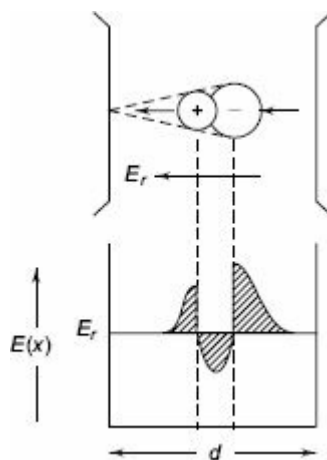


Fig. 2.11 Field distortion in a gap due to space charge

Further, cloud-chamber photographs of the avalanche development have shown that, under certain conditions, the space charge developed in an avalanche can transform the avalanche into streamers which lead to very rapid development of breakdown.

In the theories proposed by Raether and Meek, it has been shown that when the avalanche in the

gap reaches a critical size, the combined applied field and the space charge field cause intense ionization and excitation of the gas particles in front of the avalanche. Instantaneous recombination between positive ions and electrons releases photons which in turn produce secondary electrons by photo-ionization. These secondary electrons under the influence of the field in the gap develop into secondary avalanches as shown in Fig. 2.12. Since photons travel with the velocity of light, the photo-ionization process gives rise to rapid development of conduction channels across the gap.

On the basis of experimental observations Raether proposed an empirical expression for the streamer spark criterion of the form

$$\alpha x_c = 17.7 + \ln x_c + \ln (E_r/E) \quad (2.28)$$

where E_r is the space charged field directed radially at the head of the avalanche and E is the applied field.

The conditions for the transition from the avalanche to streamer assumes that the space charged field, E , approaches the externally applied field ($E = E_r$) and hence the breakdown criterion (Eq. (2.28)) becomes

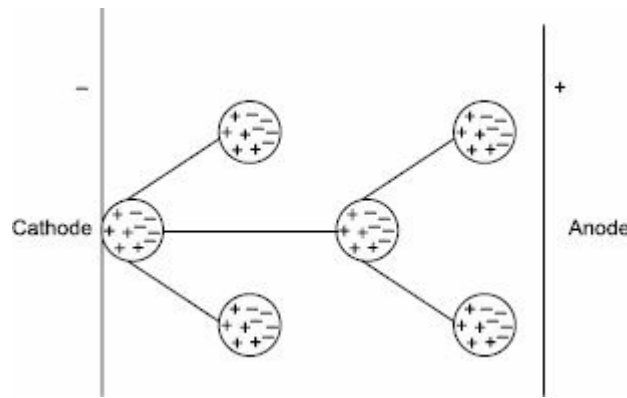


Fig. 2.12 Formation of secondary avalanches due to photo-ionization

$$\alpha x_c = 17.7 + \ln x_c \quad (2.29)$$

The minimum breakdown value for a uniform field gap by streamer mechanism is then obtained on the assumption that the transition from an avalanche to a streamer occurs when the avalanche has just crossed a gap, d . Thus, a minimum breakdown voltage by streamer mechanism occurs only when a critical length $x_c = d$.

Meek proposed a simple quantitative criterion to estimate the electric field that transforms an avalanche into a streamer. The field E_r produced by the space charge, at the radius r , is given by

$$E_r = 5.27 \times 10^{-7} \frac{\alpha \exp(\alpha x)}{(x/p)^{1/2}} \text{ V/cm} \quad (2.30)$$

where α is Townsend's first ionization coefficient, p is the gas pressure in torr, and x is the distance to which the streamer has extended in the gap. According to Meek, the minimum breakdown voltage is obtained when $E_r = E$ and $x = d$ in the above equation.

$$\alpha d + \ln \left(\frac{\alpha}{p} \right) = 14.5 + \ln \left(\frac{E}{p} \right) + \frac{1}{2} \ln \left(\frac{d}{p} \right) \quad (2.31)$$

This equation is solved between α/p and E/p at which a given p and d satisfy the equation. The breakdown voltage is given by the corresponding product of E and d .

The above simple criterion enabled an agreement between the calculated and the measured breakdown voltages. This theory also neatly fits in with the observed filamentary, crooked channels and the branching of the spark channels, and cleared up many ambiguities of the Townsend mechanism when applied to breakdown in a high-pressure gas across a long gap.

It is still controversial as to which mechanism operates in uniform field conditions over a given range of pd values. It is generally assumed that for pd values below 1000 torr-cm and gas pressures varying from 0.01 to 300 torr, the Townsend mechanism operates, while at higher pressures and pd values the Streamer mechanism plays the dominant role in explaining the breakdown phenomena.

2.11 PASCHEN'S LAW

It has been shown earlier (refer [Sec. 2.6](#)) that the breakdown criterion in gases is given as

$$\gamma[\exp(\alpha d) - 1] = 1 \quad (2.32)$$

where the coefficients α and γ are functions of E/p , i.e.,

$$\left(\frac{\alpha}{p}\right) = f_1\left(\frac{E}{p}\right)$$

and $\gamma = f_2\left(\frac{E}{p}\right)$

Also $E = \frac{V}{d}$

Substituting for E in the expressions for α and γ and rewriting [Eq. \(2.26\)](#) we have

$$f_2\left(\frac{V}{pd}\right)\left[\exp\left\{pd f_1\left(\frac{V}{pd}\right)\right\} - 1\right] = 1 \quad (2.33)$$

This equation shows a relationship between V and pd , and implies that the breakdown voltage varies as the product pd varies. Knowing the nature of functions f_1 and f_2 we can rewrite [Eq. \(2.32\)](#) as,

$$V = f(pd) \quad (2.34)$$

This equation is known as Paschen's law.

The Paschen's curve, the relationship between V and pd is shown in [Fig. 2.13](#). It is seen that the relationship between V and pd is not linear and has a minimum value for any gas.

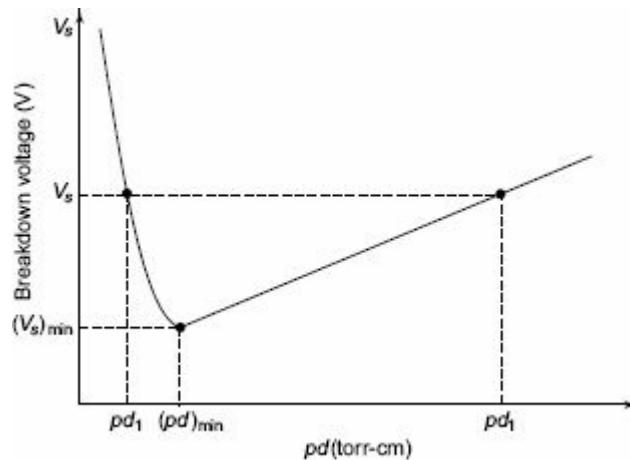


Fig. 2.13 Breakdown voltage- pd curve (Paschen's law)

This means that a breakdown voltage of a uniform field gap is a unique function of the product of p , the gas pressure and d , the electrode gap, for a particular gas and for a given electrode material.

From Paschen's law, the breakdown voltage of a spark gap can be obtained in terms of α and γ by rewriting the breakdown condition given in [Eq. \(2.32\)](#) and substituting for α and γ in terms of ' pd ' product. This gives rise to ' d ', the gap distance as

$$d = \frac{1}{\alpha} \left[\ln \left(1 + \frac{1}{\gamma} \right) \right]$$

$$= \frac{1}{pf_1 \left(\frac{v}{pd} \right)} \ln \left[1 + \frac{1}{f_2 \left(\frac{V}{pd} \right)} \right] \text{ where}$$

$\frac{\alpha}{p} = f_1 \left(\frac{E}{p} \right)$ and $\gamma = f_2 \left(\frac{E}{p} \right)$ f_1 and f_2 being some functions and $E = V/d$ 'α' may be assumed to follow an exponential function and may be written as

$$\alpha = Ap e^{-BpE} = Ap e^{-Bpdv}$$

substituting for 'α' and retaining γ

$$d = \frac{1}{Ap} e^{Bpdv} \ln \left[1 + \frac{1}{r} \right]$$

or

$$V = \frac{Bpd}{\ln \frac{Apd}{\ln \left(1 + \frac{1}{r} \right)}} \quad (2.34a)$$

The minimum value for V can be obtained by making $\frac{dV}{d(pd)} = 0$ which gives rise to

$$\left. \begin{aligned} pd_{\min} &= \frac{e}{A} \ln \left[1 + \frac{1}{r} \right] \quad \text{where } e = 2.178 \\ V_{\min} &= \frac{eB}{A} \ln \left[1 + \frac{1}{r} \right] \end{aligned} \right\} \quad (2.34b)$$

Paschen's Law is found to be valid over a wide range of pd values as shown in [Fig. 2.14](#). As can be seen from the figure, at higher pd values, the breakdown voltage in some gases is found to be slightly higher than the values at smaller gaps for the same values of pd . This departure from Paschen's law is probably due to the transition from the Townsend breakdown mechanism to the Streamer mechanism. On the other hand, at very low pressures, deviations from the Paschen's law are observed when the breakdown mechanism is not influenced by the properties of the gas but depends on the purity and property of the electrodes.

In order to account for the effect of temperature, Paschen's law is generally stated as $V = f(Nd)$, where N is the density of the gas molecules. This is necessary, because the pressure of the gas changes with temperature according to the gas law $pv = NRT$, where v is the volume of the gas, T is the temperature, and R is a constant.

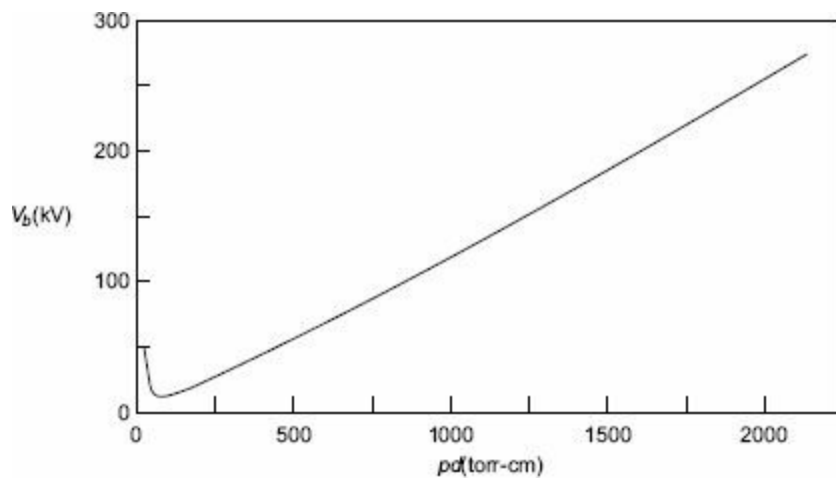


Fig. 2.14 Breakdown voltage (V_b) as a function of pd in SF_6 . (*Electrical Breakdown of Gases*, edited by J.M. Meek and J.D.Craggs, John Wiley, New York, 1978)

Based on the experimental results, the breakdown potential of air is expressed as a power function in pd as

$$V = 24.22 \left[\frac{293pd}{760T} \right] + 6.08 \left[\frac{293pd}{760T} \right]^{1/2} \quad (2.35)$$

It may be noted from the above formula that the breakdown voltage at constant pressure and temperature is not constant.

At 760 torr and 293 K.

$$E = V/d = 24.22 + \left[\frac{6.08}{\sqrt{d}} \right] \text{ kV/cm} \quad (2.36)$$

This equation yields a limiting value for E of 24 kV/cm for long gaps and a value $\left(\frac{293pd}{760T} \right) = 1$, which means a pressure of 760 torr at 20°C with 1 cm gap. This is the usually quoted breakdown strength of air at room temperature and at atmospheric pressure.

2.12 BREAKDOWN IN NON-UNIFORM FIELDS AND CORONA DISCHARGES

2.12.1 Corona Discharges

If the electric field is uniform, a gradual increase in voltage across a gap produces a breakdown of the gap in the form of a spark without any preliminary discharges. On the other hand, if the field is non-uniform, an increase in voltage will first cause a discharge in the gas to appear at points with highest electric field intensity, namely at sharp points or where the electrodes are curved or on transmission lines. This form of discharge is called a corona discharge and can be observed as a bluish luminescence. This phenomenon is always accompanied by a hissing noise, and the air surrounding the corona region becomes converted into ozone. Corona is responsible for considerable loss of power from high-voltage transmission lines, and it leads to the deterioration of insulation due to the combined action of the bombardment of ions and of the chemical compounds formed during discharges. Corona also gives rise to radio interference.

The voltage gradient required to produce visual ac corona in air at a conductor surface, called the corona inception field, can be approximately given for the case of parallel wires of radius r as

$$E_w = 30 md \left[1 + \frac{0.301}{\sqrt{dr}} \right] \quad (2.37)$$

For the case of coaxial cylinders, whose inner cylinder has a radius r the equation becomes

$$E_c = 31 md \left[1 + \frac{0.308}{\sqrt{dr}} \right] \quad (2.38)$$

where m is the surface irregularity factor which becomes equal to unity for highly polished smooth wires; d is the relative air density correction factor given by,

$$d = \frac{0.392b}{(273 + T)} \quad (2.39)$$

where b is the atmospheric pressure in torr, and T is the temperature in °C, $d = 1$ at 760 torr and 25°C. The expressions were found to hold good from atmospheric pressure down to a pressure of several torr.

On the high voltage conductors at high pressures there is a distinct difference in the visual appearance of the corona under positive and negative polarities of the applied voltage. When the voltage is positive, corona appears as a uniform bluish white sheath over the entire surface of the conductor. On the other hand, when the voltage is negative, the corona will appear like reddish glowing spots distributed along the length of the wire. Investigations with point-plane gaps in air showed that when point is negative, corona appears as current pulses called Trichel pulses, and the repetition frequency of these pulses increases as the applied voltage is increased and decreases with decrease in pressure. On the other hand, observations when the point is positive in air showed that the corona current increases steadily with voltage. At sufficiently high voltage, current amplification increases rapidly with voltage, up to a current of about 10^{-7} A, after which the current becomes pulsed with repetition frequency of about 1 kHz composed of small bursts. This form of corona is called burst corona. The average current then increases steadily with applied voltage leading to

breakdown.

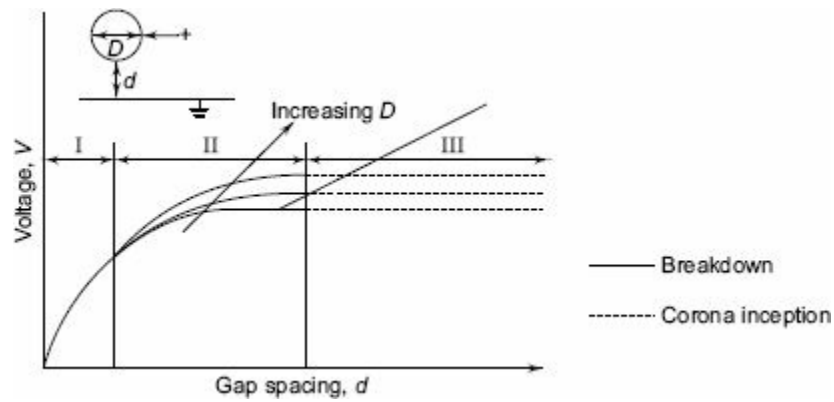


Fig. 2.15 Breakdown and corona inception characteristics for spheres of different diameters in sphere-plane gap geometry

The corona inception and breakdown voltages of the sphere-plane arrangement are shown in [Fig. 2.15](#). From this figure it can be seen that

- at small spacings (region I), the field is uniform, and the breakdown voltage mainly depends on the spacing;
- at fairly large spacings (region II), the field is non-uniform, and the breakdown voltage depends both on the sphere diameter and the spacing; and
- at large spacings (region III), the field is non-uniform, and the breakdown is preceded by corona and is controlled only by the spacing. The corona inception voltage mainly depends on the sphere diameter.

It may be summarized that the study of corona and non-uniform field breakdown is very complicated and investigations are still under progress.

2.12.2 Breakdown in Non-uniform Fields

In non-uniform fields, such as coaxial cylinders, point-plane and sphere-plane gaps, the applied field varies across the gap. Similarly, Townsend's first ionization coefficient (α) also varies with the gap. Hence, αd in Townsend's criterion [refer [Eq.\(2.22\)](#)] is rewritten by replacing αd by $\int_0^d \alpha dx$.

Townsend's criterion for breakdown now becomes

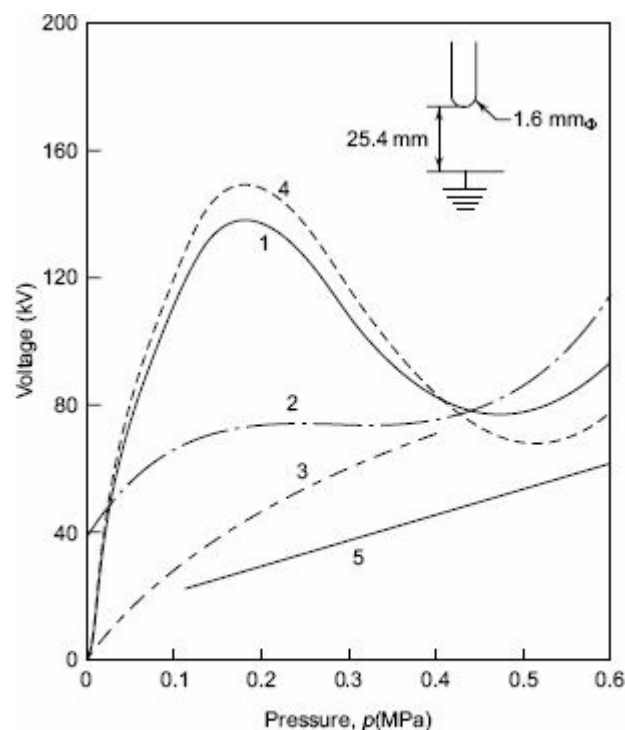
$$\gamma \left\{ \exp \left[\int_0^d \alpha dx \right] - 1 \right\} = 1 \quad (2.40)$$

Meek and Raether also discussed the non-uniform field breakdown process as applied to their Streamer theory, and Meek's equation [[Eq. \(2.27\)](#)] for the radial field at the head of an avalanche when it has crossed a distance x is modified as

$$E_r = \frac{5.27 \times 10^{-7} \alpha_x \exp \left(\int_0^x \alpha dx \right)}{(x/p)^{1/2}} \text{ V/cm} \quad (2.41)$$

where α_x is the value of α at the head of the avalanche, and p is the gas pressure. The criterion for the formation of the streamer is reached when the space charge field E_r approaches a value equal to the applied field at the head of the avalanche.

This equation has been successfully used for determining the corona onset voltages of many non-uniform geometries. However, the condition for the advancement of streamers has not been arrived at so far. [Figures 2.16 to 2.18](#) show the breakdown characteristics for SF_6 and SF_6/N_2 mixtures.



1. SF_6 positive dc breakdown
2. SF_6 positive impulse breakdown
3. SF_6 positive dc corona
4. SF_6 50 Hz ac breakdown
5. SF_6 50 Hz ac corona

Fig. 2.16 Breakdown characteristics of SF_6 and N_2 as a function of pressure

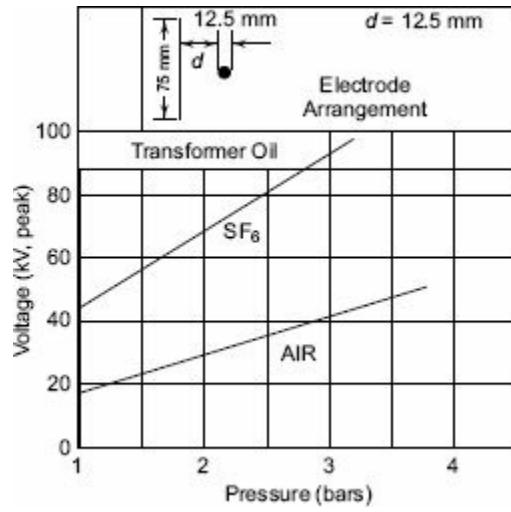


Fig. 2.17 Breakdown voltages as a function of pressure in SF_6

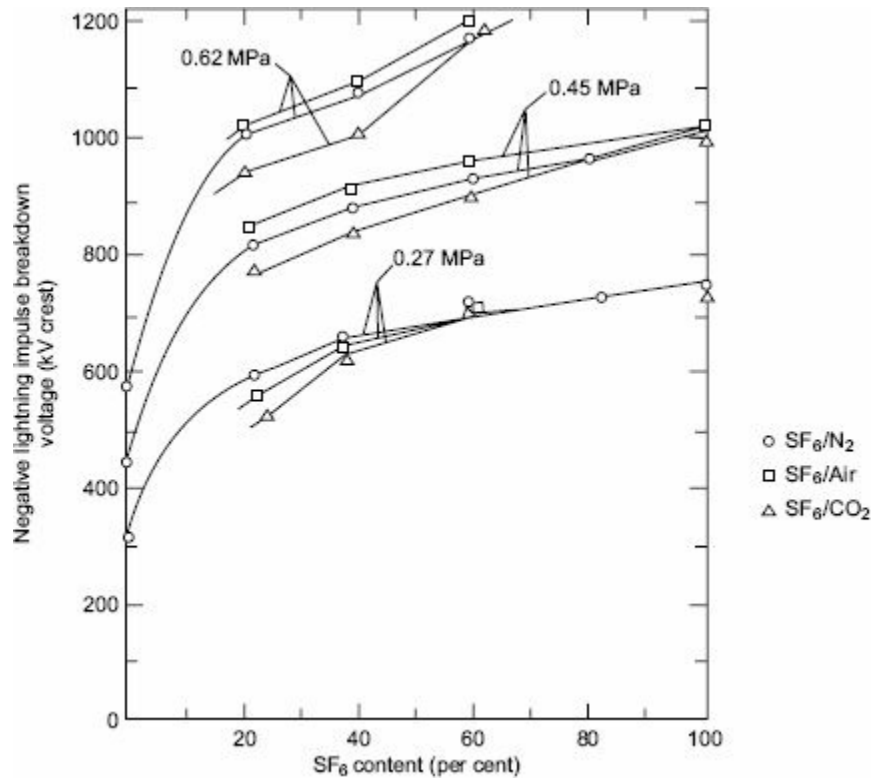


Fig. 2.18 Negative lightning impulse ($1.2/40 \mu s$) breakdown voltage in mixtures of SF_6 with N_2 , Air and CO_2 for coaxial electrode system

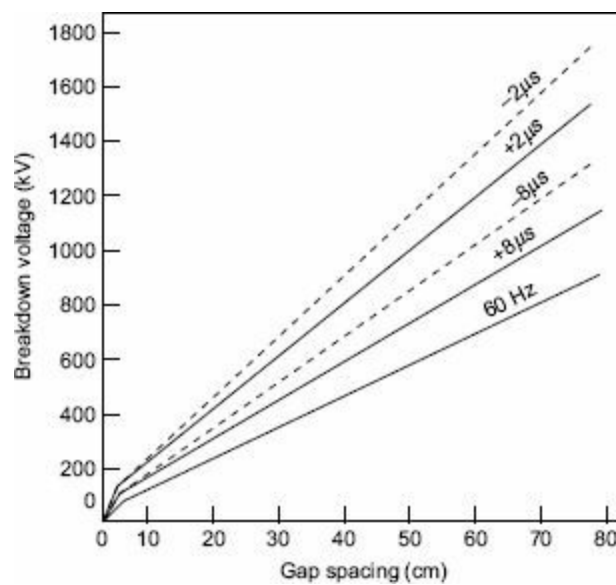


Fig. 2.19 Power frequency (60 Hz) and impulse breakdown voltage curves for a rod-rod gap in air at n.t.p. One rod is earthed. Absolute humidity is 6.5g/ft^3 . Impulse breakdown curves are for various times of breakdown on the wave tail. (Ref: B.S.S. 171:1959, power transformers)

From the practical engineering point of view, rod-rod gap and sphere-sphere gap are of great importance, as they are used for the measurement of high voltages and for the protection of electrical apparatus such as transformers. The breakdown characteristics of rod-rod gaps are shown in [Fig. 2.19](#). From this figure it can be seen that the breakdown voltages are higher for negative polarity. The breakdown voltages were also observed to depend on humidity in air. In the case of rod gaps the field is non-uniform, while in the case of sphere gaps field is uniform, if the gap is small compared with the diameter. In the case of sphere gaps, the breakdown voltages do not depend on humidity and are also independent of the voltage waveform. The formative time lag is quite small ($\sim 0.5 \mu\text{s}$) even with 5% over-voltage. Hence sphere gaps are used for breakdown voltage (peak value) measurements. These are further discussed in [Chapter 7 \(Sec. 7.2.6\)](#).

2.13 POST-BREAKDOWN PHENOMENA AND APPLICATIONS

This is the phenomenon which occurs after the actual breakdown has taken place and is of technical importance. Glow and arc discharges are the post-breakdown phenomena, and there are many devices that operate over these regions. In a Townsend discharge (see [Fig. 2.20](#)) the current increases gradually as a function of the applied voltage. Further, to this point (B) only the current increases, and the discharge changes from the Townsend type to Glow type (BC). Further increase in current results in a very small reduction in voltage across the gap (CD) corresponding to the normal glow region. The gap voltage again increases (DE), when the current is increased more, but eventually leads to a considerable drop in the applied voltage. This is the region of the arc discharge (EG). The phenomena that occur in the region CG are the post-breakdown phenomena consisting of glow discharge (CE) and the arc discharge (EG).

2.13.1 Glow Discharge

A glow discharge is characterized by a diffused luminous glow. The colour of the glow discharge depends on the cathode material and the gas used. The glow discharge covers the cathode partly and the space between the cathode, and the anode will have intermediate dark and bright regions. This is called normal glow. If the current in the *normal glow* is increased such that the discharge covers the entire cathode surface, then it becomes abnormal glow. In a glow discharge, the voltage drop between the electrodes is substantially constant, ranging from 75 to 300 V over a current range of 1 mA to 100 mA depending on the type of the gas. The properties of the glow discharge are used in many practical applications, such as cold-cathode gaseous voltage stabilized tubes (voltage regulation tubes or VR tubes), for rectification, as a relaxation oscillator, and as an amplifier.

2.13.2 Arc Discharge

If the current in the gap is increased to about 1 A or more, the voltage across the gap suddenly reduces to a few volts (20–50 V). The discharge becomes very luminous and noisy (region EG in Fig. 2.20). This phase is called the arc discharge and the current density over the cathode region increases to very high values of 10^3 to 10^7 A/cm². Arcing is associated with high temperatures, ranging from 1000°C to several thousand degrees celsius. The discharge will contain a very high density of electrons and positive ions, called the arc plasma. The study of arcs is important in circuit breakers and other switch contacts. It is a convenient high-temperature, high-intensity light source. It is used for welding and cutting of metals. It is the light source in lamps such as carbon arc lamp. High temperature plasmas are used for generation of electricity through magneto-hydro dynamic (MHD) or nuclear-fusion processes.

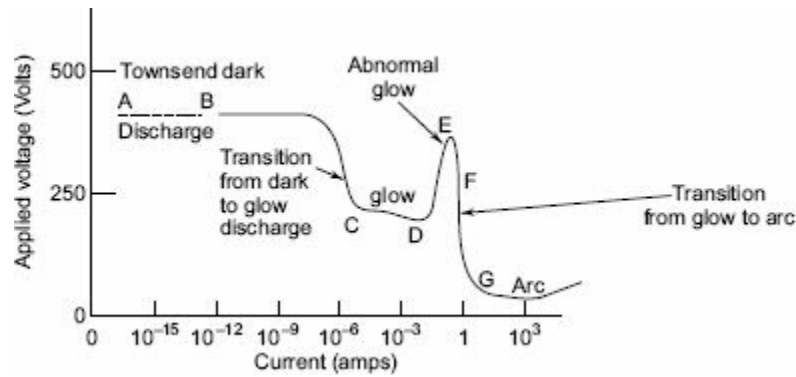


Fig. 2.20 *dc voltage-current characteristic of an electrical discharge with electrodes having no sharp points or edges*

2.14 PRACTICAL CONSIDERATIONS IN USING GASES AND GAS MIXTURES FOR INSULATION PURPOSES

Over the years, considerable amount of work has been done to adopt a specific gas for practical use. Before adopting a particular gas or gas mixture for a practical purpose, it is useful to gain a knowledge of what the gas does, what its composition is, and what the factors are that influence its performance. The greater the versatility of the operating performance demanded from an insulating gas or gas mixture, the more rigorous would be the requirements which it should meet. These requirements needed by a good dielectric do not exist in a majority of the gases. Generally, the preferred properties of a gaseous dielectric for high-voltage applications are

- high dielectric strength,
- thermal stability and chemical inactivity towards materials of construction,
- non-flammability and physiological inertness, and environmentally non-hazardous,
- low temperature of condensation,
- good heat transfer, and
- ready availability at moderate cost.

Sulphur hexafluoride (SF_6) which has received much study over the years has been found to possess most of the above requirements.

Of the above properties, dielectric strength is the most important property of a gaseous dielectric for practical use. The dielectric strength of gases is comparable with those of solid and liquid dielectrics (see [Fig. 2.21](#)).

It is clear that SF_6 has high dielectric strength and low liquefaction temperature, and it can be used over a wide range of operating conditions. SF_6 was also found to have excellent arc-quenching properties. Therefore, it is widely used as an insulating as well as arc-quenching medium in high-voltage apparatus such as high-voltage cables, current and voltage transformers, circuit-breakers and metal enclosed substations.

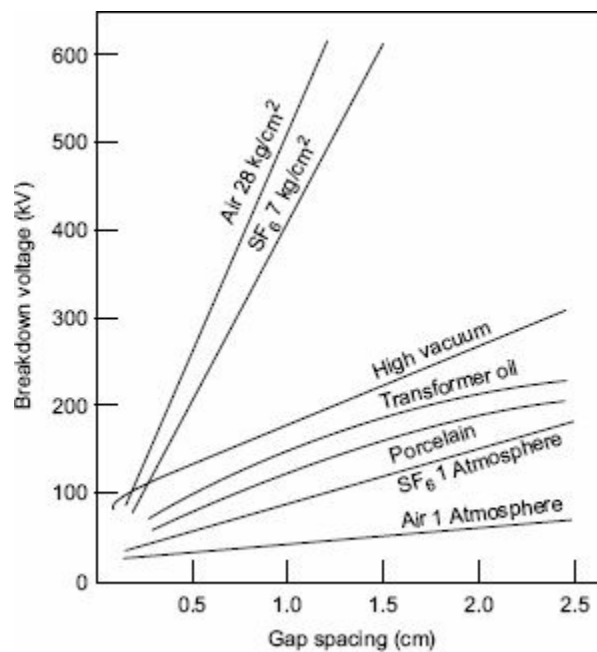


Fig. 2.21 *dc breakdown strength of typical solid, liquid, gas and vacuum insulations in uniform fields*

2.14.1 SF₆ and Other Gas Mixtures

SF₆ is widely used for applications in power system due to its high dielectric strength and good arc interruption properties. However, SF₆ gas has been found to be a greenhouse gas that causes environmental problems. The production and use of SF₆ gas has increased steadily and today it is about 10,000 metric tons due to leakages into the atmosphere from the electrical equipment. The concentration of SF₆ in the environment has been steadily increasing. The release of SF₆ into the atmosphere leads to concentration of large volumes of SF₆ gas in the upper atmosphere. SF₆ molecules absorb energy from the sun and radiate it into the atmosphere for long duration of time.

There has been a large concern for these environmental effects and therefore the electrical industry has been looking for an alternate gas or gas mixture to be used in electrical equipment which presently use SF₆ gas, as an insulating and arc interruption medium. The large amount of experimental data that is presently available suggest that 40% SF₆/60% N₂ mixtures have all the dielectric characteristics that make it suitable for use as insulation in high-voltage equipment. Ideally the gas mixture should be suitable for use in the existing equipment as well as in the equipment that will be designed and manufactured in future.

Extensive research work done in SF₆ and its mixtures with N₂, air and CO₂ has given breakdown values which are 80–90% of the pure SF₆ values as shown in [Table 2.1](#).

Table 2.1 Lightning impulse breakdown strength of SF₆/other gas mixtures

Mixture Ratio	Breakdown Strength (kV/cm)
100% SF ₆ gas	89.0
1% SF ₆ /99% Nitrogen	80.0
10% SF ₆ /90% Nitrogen	78.0
20% SF ₆ /80% Nitrogen	76.5
40% SF ₆ /60% Nitrogen	75.6
10% SF ₆ /90% CO ₂	76.5
20% SF ₆ /80% CO ₂	76.5
40% SF ₆ /60% CO ₂	75.5
10% SF ₆ /90% Air	77.0
20% SF ₆ /80% Air	76.5
40% SF ₆ /60% Air	75.6

The industry is looking for a gas mixture that can replace the pure SF₆ gas in the existing SF₆ insulated apparatus, requiring no change in hardware, test procedures or ratings. SF₆/N₂ mixture is the one that has been found to be a good replacement for SF₆. SF₆/N₂ mixtures have been used in Gas Insulated Transmission System and were found to perform well. Also, the work done so far has shown that the ability of SF₆/N₂ mixtures to quench high-current arcs is promising. The cost of such mixtures is low and are less sensitive to field non-uniformities present inside the equipment. In view of the above, the industry is trying to find out the optimum mixture ratio and the total pressure of the SF₆/N₂ mixture that would be required for a variety of applications. For many applications, such as Gas Insulated Transmission Systems, cables, capacitors, current transformers and voltage

transformers, mixtures with different SF₆ concentrations varying from 5% to 40%.

SF₆/N₂ mixtures show promise as a medium in circuit breakers. It has been found that a mixture containing 69% SF₆/31% N₂ gave higher recovery rate than pure SF₆ at the same partial pressure. It has also been shown that it is possible to further improve the arc interruption properties of SF₆ by using SF₆/N₂ or SF₆/He mixtures.

In summary, it may be said that there is an urgent need to significantly reduce the use of SF₆ gas and its leakage from power apparatus. Use of gas mixtures appears to be feasible, but it has to be ensured that there is no loss in the performance of the equipment. Therefore, further research has to be carried out to identify a suitable gas mixture, its pressure and its arc interruption capability to be used in the existing apparatus and the apparatus that will be designed and manufactured in future.

2.15 VACUUM INSULATION

2.15.1 Introduction

The idea of using vacuum for insulation purposes is very old. According to the Townsend theory, the growth of current in a gap depends on the drift of the charged particles. In the absence of any such particles, as in the case of perfect vacuum, there should be no conduction and the vacuum should be a perfect insulating medium. However, in practice, the presence of metallic electrodes and insulating surfaces within the vacuum complicate the issue and, therefore, even in vacuum, a sufficiently high-voltage will cause a breakdown.

In recent years, a considerable amount of work has been done to determine the electrical properties of high vacuum. This is mainly aimed at adopting such a medium for a wide range of applications in devices such as vacuum contactors and interrupters, high frequency capacitors and relays, electrostatic generators, microwave tubes, etc. The contactors and circuit breakers using vacuum as insulation are finding increasing applications in power systems.

2.15.2 What is Vacuum?

A vacuum system which is used to create vacuum is a system in which the pressure is maintained at a value much below the atmospheric pressure. In vacuum systems the pressure is always measured in terms of millimetres of mercury, where one standard atmosphere is equal to 760 millimetres of mercury at a temperature of 0°C. The term 'millimetres of mercury' has been standardized as 'Torr' by the International Vacuum Society, where one millimetre of mercury is taken as equal to one Torr. Vacuum may be classified as

High vacuum : 1×10^{-3} to 1×10^{-6} Torr

Very high vacuum : 1×10^{-6} to 1×10^{-8} Torr

Ultra high vacuum : 1×10^{-9} torr and below.

For electrical insulation purposes, the range of vacuum generally used is the 'high vacuum', in the pressure range of 10^{-3} Torr to 10^{-6} Torr.

2.15.3 Electron Emission in Vacuum

When the voltage across a small vacuum gap (< 2 mm) is increased, a relatively small current, mainly due to electrons, flows. For higher gaps (< 10 mm) small pulses of current, called microdischarges flow either independently or superposed over the steady current. For both the types of gaps, subsequent increase of applied voltage causes the breakdown of the gap.

Several mechanisms have been proposed to explain electron emission from metallic surfaces. The most widely accepted mechanism is the cold-emission model originally proposed by Fowler and Nordheim. Accordingly to this, the current density J due to field emission from sharp points on the electrode is given as:

$$J = AE^2 \exp[(-B\phi^{1.5} v(y))/E] A/m^2 \quad (2.42)$$

where $A = (1.54 \times 10^{-2})/[\phi t^2 (y)]$, $B = -6.831 \times 10^9$ and $\phi =$ work function of the metal.

The expression $t(y)$ and $v(y)$ are slow varying functions which are regarded as constants. The above equation therefore can be expressed as

$$\log [J/E^2] = -\log [1/A] (-B\phi^{1.5} v(y) (1/E))/2.3026 \quad (2.43)$$

Since A , ϕ and essentially $v(y)$ are constants, a plot of $\log J/E^2$ against the reciprocal of E produces a straight line having a negative slope. This straight line is often used to assess the applicability of Fowler-Nordheim relation of the experimental data. However, in the case of electrodes with large area, the protrusions and uneven surfaces become unknown geometry. Therefore, to take account of these factors, Alpert modified the above equation as follows:

$$\log [J/V^2] = -\log [1/(A'\beta^2)] (-B\phi^{1.5} v(y) [d/V])/2.3026\beta \quad (2.44)$$

where A' is the electrode area and d is the gap length, J has been replaced by $(1/A')$, and the modified field is written as a product of local field enhancement factor β and the average field $E (= V/d)$. The actual emitting area is replaced as $A'\beta^2$. [Equations \(2.42 to 2.44\)](#) have been experimentally confirmed by many investigators. If β is high and critical macroscopic field exceeds the field in the gap, the emitting site will explode releasing metal vapour.

In vacuum, electrode surfaces in long gaps produce low-power pulses called microdischarges. These discharges have durations of 0.1 to 100 ms, frequency of 0.1 to 100 Hz and amplitudes of ≤ 10 mA. They may be caused by small particles of electrode material that are pulled out from one electrode and strike the other, or the beam of electrons from a cathode that can vapourize a small quantity of electrode material. At a given pressure, the frequency of occurrence of microdischarges increase with increase in applied voltage, eventually leading to breakdown.

2.15.4 Vacuum Breakdown

In the Townsend type of discharge in a gas described earlier, electrons get multiplied due to various ionization processes and an electron avalanche is formed. In a high vacuum, even if the electrodes are separated by, say, a few centimetres, an electron crosses the gap without encountering any collisions. Therefore, the current growth prior to breakdown cannot be due to the formation of electron avalanches. However, if a gas is liberated in the vacuum gap, then, breakdown can occur in the manner described by the Townsend process. Thus, the various breakdown mechanisms in high vacuum aim at establishing the way in which the liberation of gas can be brought about in a vacuum gap.

During the last 70 years or so, many different mechanisms for breakdown in vacuum have been proposed. These can be broadly divided into three categories:

- (a) Particle exchange mechanism
- (b) Field emission mechanism
- (c) Clump theory

(a) Particle Exchange Mechanism

In this mechanism, it is assumed that a charged particle would be emitted from one electrode under the action of the high electric field, and when it impinges on the other electrode, it liberates oppositely charged particles due to ionization of adsorbed gases. These particles are accelerated by the applied voltage back to the first electrode where they release more of the original type of particles. When this process becomes cumulative, a chain reaction occurs which leads to the breakdown of the gap.

The particle-exchange mechanism involves electrons, positive ions, photons and the absorbed gases at the electrode surfaces. Qualitatively, an electron present in the vacuum gap is accelerated towards the anode, and on impact releases A positive ions and C photons. These positive ions are accelerated towards the cathode, and on impact each positive ion liberates B electrons and each photon liberates D electrons. This is shown schematically in Fig. 2.22. The breakdown will occur if the coefficients of production of secondary electrons exceeds unity. Mathematically, the condition for breakdown can be written as

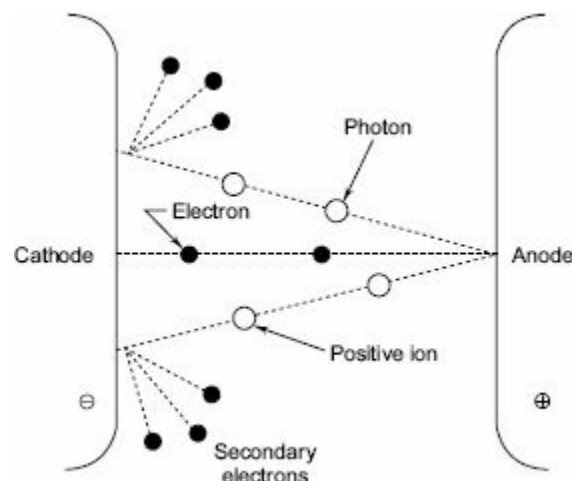


Fig. 2.22 Particle exchange mechanism of vacuum breakdown

$$(AB + CD) > 1$$

(2.45)

Later, Trump and Van de Graaff measured these coefficients and showed that they were too small for this process to take place. Accordingly, this theory was modified to allow for the presence of negative ions and the criterion for breakdown then becomes

$$(AB + EF) > 1 \tag{2.46}$$

where A and B are the same as before and E and F represent the coefficients for negative and positive ion liberation by positive and negative ions. It was experimentally found that the values of the product EF were close enough to unity for copper, aluminium and stainless steel electrodes to make this mechanism applicable at voltage above 250 kV

(b) Field Emission Theory

(i) *Anode Heating Mechanism* This theory postulates that electrons produced at small micro-projections on the cathode due to field emission bombard the anode causing a local rise in temperature and release gases and vapours into the vacuum gap. These electrons ionize the atoms of the gas and produce positive ions. These positive ions arrive at the cathode, increase the primary electron emission due to space charge formation and produce secondary electrons by bombarding the surface. The process continues until a sufficient number of electrons are produced to give rise to breakdown, as in the case of a low-pressure Townsend type gas discharge. This is shown schematically in [Fig. 2.23](#).

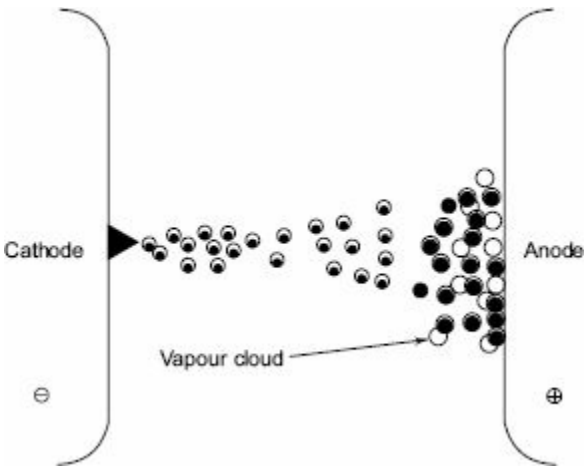


Fig. 2.23 Electron beam anode heating mechanism of vacuum breakdown

(ii) *Cathode Heating Mechanism* This mechanism postulates that near the breakdown voltages of the gap, sharp points on the cathode surface are responsible for the existence of the pre-breakdown current, which is generated according to the field emission process described below.

This current causes resistive heating at the tip of a point and when a critical current density is reached, the tip melts and explodes, thus initiating vacuum discharge. This mechanism is called field emission as shown schematically in [Fig. 2.24](#). Thus, the initiation of breakdown depends on the conditions and the properties of the cathode surface. Experimental evidence shows that breakdown takes place by this process when the effective cathode electric field is of the order of 10^6 to 10^7 V/cm.

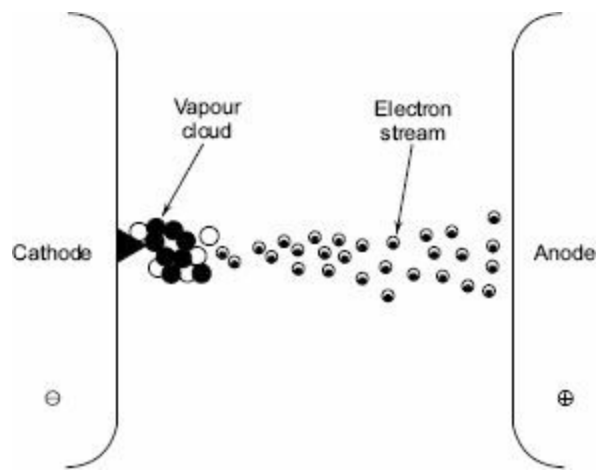
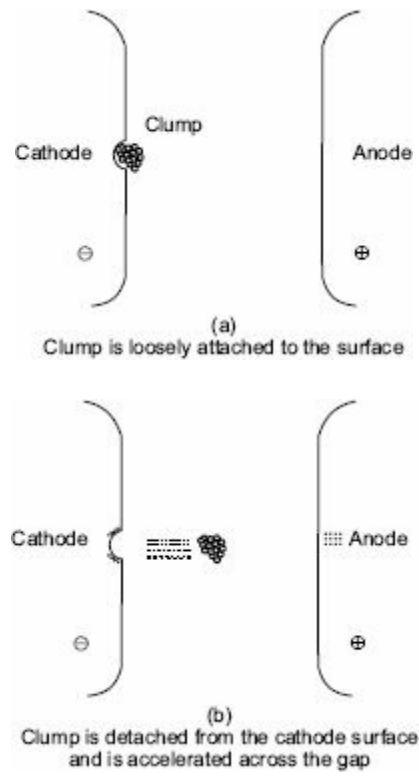


Fig. 2.24 Breakdown in vacuum caused by the heating of a microprojection on the cathode

(c) Clump Mechanism

Basically, this theory has been developed on the following assumptions ([Fig. 2.25](#)):

- (i) A loosely bound particle (clump) exists on one of the electrode surfaces.
- (ii) On the application of a high-voltage, this particle gets charged, subsequently gets detached from the mother electrode, and is accelerated across the gap.
- (iii) The breakdown occurs due to a discharge in the vapour or gas released by the impact of the particle at the target electrode.



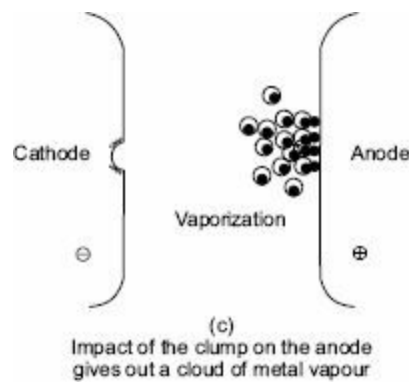


Fig. 2.25 (a, b, c) Clump mechanism of vacuum breakdown

Cranberg was the first to propose this theory. He initially assumed that breakdown will occur when the energy per unit area, W , delivered to the target electrode by a clump exceeds a value C' , a constant, characteristic of a given pair of electrodes. The quantity W is the product of gap voltage (V) and the charge density on the clump. The latter is proportional to the electric field E at the electrode of origin. The criterion for breakdown, therefore, is

$$VE = C' \quad (2.47)$$

In case of parallel plane electrodes the field $E = V/d$, where d is the distance between the electrodes. So the generalized criterion for breakdown becomes

$$V = (Cd)^{1/2} \quad (2.48)$$

where C is another constant involving C' and the electrode surface conditions.

Cranberg presented a summary of the experimental results which satisfied this breakdown criterion with reasonable accuracy. He stated that the origin of the clump was the cathode and obtained a value for the constant C as $60 \times 10^{10} \text{ V}^2/\text{cm}$ (for iron particles). However, the equation was later modified as $V = Cd^\alpha$, where α varies between 0.2 and 1.2 depending on the gap length and the electrode material, with a maximum at 0.6. The dependence of V on the electrode material, comes from the observations of markings on the electrode surfaces. Craters were observed on the anode and melted regions on the cathode or vice-versa after a single breakdown.

(d) Summary

Dielectric strength of vacuum is defined in different ways. In the case of vacuum insulated switchgear, it is the value of the voltage to cause the first breakdown that is important. However, when the gap breaks down repeatedly, the breakdown voltage increases with the number of breakdowns until it reaches a steady or conditioned value. This value is often taken as the breakdown strength of the vacuum gap.

Although there has been a large amount of work done on vacuum breakdown phenomena, so far, no single theory has been able to explain all the available experimental measurements and observations. Since experimental evidence exists for all the postulated mechanisms, it appears that each mechanism would depend, to a great extent, on the conditions under which the experiments were performed. The most significant experimental factors which influence the breakdown mechanism are: gap length, geometry and material of the electrodes, surface uniformity and treatment of the surface, presence of extraneous particles and residual gas pressure in the vacuum gap. It was observed that the correct

choice of electrode material, and the use of thin insulating coatings on electrodes in long gaps can increase the breakdown voltage of a vacuum gap. On the other hand, an increase of electrode area or the presence of particles in the vacuum gap will reduce the breakdown voltage.

K
TERMS
Y

- Conduction and breakdown in gases
- Collision Processes
- Mobility Diffusion Coefficient
- Electron Energy Distribution
- Collision Cross Section
- Mean Free Path
- Ionization Processes
- Primary and Secondary Processes
- Electron Emission and Attachment
- Current Growth and Townsend Mechanism
- Ionization Coefficients
- Breakdown in Gases
- Time Lags
- Streamer Mechanism
- Paschen's Law
- Corona Discharges
- Breakdown in Non-uniform Fields
- Post Breakdown Phenomenon
- Vacuum Breakdown

WORKED EXAMPLES

Example 2.1 *What will the breakdown strength of air be for small gaps (1 mm) and large gaps (20 cm) under uniform field conditions and standard atmospheric conditions?*

Solution The breakdown strength of air under uniform field conditions and standard atmospheric conditions is approximately given by

$$E = \frac{V}{d} = \left(24.22 + \frac{6.08}{d^{1/2}} \right) \text{ kV/cm}$$

Substituting for 1 mm gap,

$$E = 24.22 + \frac{6.08}{(0.1)^{1/2}} = 43.45 \text{ kV/cm}$$

For 20 cm gap, $E = 24.22 + \frac{6.08}{(20.1)^{1/2}} = 25.58 \text{ kV/cm}$

Example 2.2 In an experiment in a certain gas it was found that the steady state current is $5.5 \times 10^{-8} \text{ A}$ at 8 kV at a distance of 0.4 cm between the plane electrodes. Keeping the field constant and reducing the distance to 0.1 cm results in a current of $5.5 \times 10^{-9} \text{ A}$. Calculate Townsend's primary ionization coefficient α .

Solution The current at the anode I is given by

$$I_0 = \exp(\alpha d)$$

where $I = I_0$ is the initial current and d is the gap distance. Given,

$$\begin{aligned} d_1 &= 0.4 \text{ cm} & d_2 &= 0.1 \text{ cm} \\ I_1 &= 5.5 \times 10^{-8} \text{ A} & I_2 &= 5.5 \times 10^{-9} \text{ A} \end{aligned}$$

$$\frac{I_1}{I_2} = \exp(\alpha(d_1 - d_2))$$

i.e., $10 = \exp(\alpha \times 0.3)$
 i.e., $0.3\alpha = \ln(10) \quad \therefore \alpha = 7.676/\text{cm torr}$

Example 2.3 In [Example 2.2](#), if the breakdown occurred when the gap distance was increased to 0.9 cm, what is the value of γ ?

Solution

Breakdown occurs when $\gamma e^{\alpha d} = 1$

Here $\alpha = 7.676$ and $d = 0.9 \text{ cm}$

Hence, $\gamma e^{0.9 \times 7.676} \approx 1001$

$\therefore \gamma = 9.993 \times 10^{-4}$

Example 2.4 What will be the breakdown voltage of a spark gap in a gas at $pr = 760 \text{ torr}$ at 25°C if $A = 15/\text{cm}$, $B = 360/\text{cm}$, $d = 1 \text{ mm}$ and $\gamma = 1.5 \times 10^{-4}$?

Solution

$$V = \frac{(Bpd)}{\ln \frac{Apd}{\ln \left(1 + \frac{1}{\gamma} \right)}}$$

Here, $pd = 760 \times 0.1 = 76 \text{ torr cm}$

Substituting $V = \frac{(360 \times 76)}{\ln \frac{15 \times 76}{\ln \left[1 + \frac{1}{1.5} \times 10^4 \right]}} = 4885 \text{ volts}$

Example 2.5 What is the minimum spark-over voltage of the above gap in [Example 2.4](#) if $\gamma = 10^{-4}$ with all other parameters remaining the same.

Solution

$$V_{b \min} = \frac{Be}{A} \ln \left[1 + \frac{1}{\gamma} \right] = \frac{360}{15} \times 2.178 \times \ln \left[1 + \frac{1}{1.5} \times 10^4 \right] = 574 \text{ V}$$

Example 2.6 What is the critical threshold distance for sustained discharge if $\alpha = 2.43/\text{cm}$ and $\gamma = 6.823 \times 10^{-4}$.

Solution For critical discharge (d) breakdown

$$\gamma e^{\alpha d} \approx 1 \quad \text{or} \quad d = \frac{1}{\alpha} \ln \left(\frac{1}{\gamma} \right)$$

substituting for α and γ

$$d = \frac{1}{2.43} \ln \left(\frac{10^4}{6.823} \right) = 3.00 \text{ cm}$$

MULTIPLE-CHOICE QUESTIONS

- Electrical conduction in gases was first studied in 1905 by
 - Loeb
 - Maxwell
 - Townsend
 - Hertz
- According to Townsend current growth process the current (I) in a uniform electric field gap is
 - $I_0 e^{-\alpha d}$
 - $I_0 e^{\alpha d}$
 - $I_0 e^{\gamma d}$
 - $I_0 e^{-\gamma d}$
- The breakdown criterion in a uniform field electrode gap is
 - $\alpha^{-\gamma d} = 1$
 - $\alpha = \frac{\eta}{(1-\gamma)}$
 - $\gamma e^{\alpha d} = 1$
 - $\gamma e^{-\alpha d} = 1$
- An electronegative gas is one in which
 - positive ions are formed along with electrons
 - the gas has inherent negative charge
 - gas is ionized due to electron bombardment

(d) the gases in which electron gets attached to form negative ion

5. SF₆ is a

- (a) neutral gas
- (b) electronegative gas
- (c) ionizes easily to form ions
- (d) non-attaching gas

6. Ionization coefficients α , γ are functions of

- (a) applied voltage
- (b) pressure and temperature
- (c) electric field
- (d) ratio of electric field to pressure

7. Time lag for breakdown is

- (a) time difference between instant of applied voltage and occurrence of breakdown
- (b) time taken for the voltage to rise before breakdown occurs
- (c) time required for gas to breakdown under pulse application
- (d) none of the above.

8. Streamer mechanism of breakdown explains the phenomena of electrical breakdown of

- (a) very short spark gaps
- (b) when pd is less than 1000 torr-cm
- (c) very long gaps where field is non-uniform
- (d) spark gaps subjected to impulse voltages.

9. Paschen's law states that

- (a) breakdown voltage is a function of electric field
- (b) breakdown voltage is a function of pd
- (c) α and γ depends on E/p
- (d) electronegative gases have high breakdown voltage.

10. Minimum sparking potential of air is about

- (a) 100 V
- (b) 4.4kV
- (c) 40 V
- (d) 325 V

11. At standard temperature and pressure the electric field at which breakdown occur in air with a small gap d (cm) is given by

- (a) $30 + 6.08/d$
- (b) $24.2 + 6.08/d$
- (c) $24.2 + 6.08/\sqrt{d}$
- (d) $30d \left[1 + \frac{0.301}{\sqrt{d}} \right]$

12. For a 1 cm gap in air at 760 mm pressure and 20°C temperature, the breakdown voltage is

- (a) 24kV
- (b) 30.3kV
- (c) 22.92 kV
- (d) 40kV

13. Corona occurs before the breakdown in a sphere to ground air gap when ratio of gap distance to the radius of sphere is

- (a) >1.0
 (b) >3.0
 (c) >10
 (d) <1.0
4. The requirement of gases for insulation purpose is
 (a) high dielectric strength and thermal stability
 (b) high dielectric strength only
 (c) high thermal stability
 (d) high thermal stability and low temperature condensation.
5. The mechanism of breakdown in vacuum is due to
 (a) particle exchange
 (b) field emission
 (c) clump formation
 (d) all of the above.
6. SF_6 has the following property which is not favourable for use in electrical apparatus:
 (a) High dielectric strength
 (b) High arc quenching ability
 (c) It is not environmental friendly and causes global warming
 (d) None of the above
7. The breakdown voltage of gas or air with increase in pressure under uniform field has _____ relation with pressure
 (a) almost linear
 (b) square
 (c) non-linear
 (d) reciprocal
8. The breakdown voltage of a spark gap for impulse voltage _____ is compared to the breakdown voltage of power frequency ac
 (a) same
 (b) larger
 (c) smaller
 (d) cannot be predicted
9. Among the common gases that are used for electrical insulation, which gas has the highest breakdown strength at atmospheric pressure?
 (a) Air
 (b) Nitrogen
 (c) SF_6
 (d) Oxygen
10. Which of the following gas is a electronegative gas?
 (a) Air
 (b) O_2
 (c) SF_6
 (d) Both O_2 and SF_6

- | | | | | | |
|---------|---------|---------|---------|---------|---------|
| 1. (c) | 2. (b) | 3. (c) | 4. (d) | 5. (b) | 6. (d) |
| 7. (a) | 8. (c) | 9. (b) | 10. (d) | 11. (b) | 12. (b) |
| 13. (b) | 14. (a) | 15. (d) | 16. (d) | 17. (a) | 18. (b) |
| 19. (c) | 20. (d) | | | | |

REVIEW QUESTIONS

1. Explain the difference between photo-ionization and photo-electric emission.
2. Explain the term 'electron attachment'. Why are electron attaching gases useful for practical use as insulants when compared to non-attaching gases?
3. Describe the current growth phenomenon in a gas subjected to uniform electric fields.
4. Explain the experimental set-up for the measurement of pre-breakdown currents in a gas.
5. Define Townsend's first and second ionization coefficients. How is the condition for breakdown obtained in a Townsend discharge?
6. What are electronegative gases? Why is the breakdown strength higher in these gases compared to that in other gases?
7. Derive the criterion for breakdown in electronegative gases.
8. Explain the Streamer theory of breakdown in air at atmospheric pressure.
9. What are the anode and the cathode streamers? Explain the mechanism of their formation and development leading to breakdown.
10. What is Paschen's law? How do you account for the minimum voltage for breakdown under a given ' $p \times d$ ' condition?
11. Describe the various factors that influence breakdown in a gas.
12. What is vacuum? How is it categorized? What is the usual range of vacuum used in high voltage apparatus?
13. Describe how vacuum breakdown is different from normal breakdown of a gas.
14. Discuss the various mechanisms of vacuum breakdown.

PROBLEMS

1. Obtain the value of γ at breakdown for a parallel-plate electrode configuration under uniform electric field using Paschen's law if the gap distance is 1 cm, pressure is 760 torr, temperature is 30°C when breakdown voltage is 31, 500 volts.
(take $A = 15/\text{cm}$ and $B = 360/\text{cm}$)
2. For a certain gap with uniform field electrodes, α was 7.5/cm with a gap distance of 6 mm before breakdown. What will be the secondary ionization coefficient γ ?
3. In a certain experiment relating to study of breakdown in gases, the ratio of current obtained to initial current was 1.20, 1.80 and 2.25 for gap distances of 1.0, 3.0 and 4.0 cm respectively if E/p was constant at 160 V/cm-torr and pressure 0.1 torr, calculate the value of α and γ .
4. Obtain the value of ' α ' assuming that it follows exponential function with constants $A = 15$ and $B = 360$ with $E/p = 150$ V/cm-torr. If the secondary ionization coefficient $\gamma = 10^{-4}$, Calculate the minimum ' pd ' value and minimum breakdown voltage for the above values A , B and γ .
5. What can be the breakdown voltage of an air gap of 1 cm at a pressure of 70 torr and a temperature of 35°C?

(Hint: Use [Eq. 2.35](#))

6. Calculate the electric field that causes breakdown between two cylindrical conductors of radius 0.5 cm with gap spacing of 50 cm when pressure = 750 torr, temperature = 35°C.
(Hint: Use [Eqs 2.37](#) and [2.39](#))
7. If the breakdown voltage of two parallel plates with gap separation of 0.1 cm is 4.5 kV at atmospheric pressure of 760 torr and temperature 25°C, find the value of γ
(take $A = 15/\text{cm}$, $B = 360/\text{cm}$).

REFERENCES

1. Meek, J.M. and Craggs, J.D., *Electrical Breakdown of Gases*, John Wiley, New York (1978).
2. Raether, H., *Electron Avalanches and Breakdown in Gases*, Butterworth, London (1964).
3. Naidu, M.S. and Maller, V.N., *Advances in High Voltage Breakdown and Arc Interruption in SF₆ and Vacuum*, Pergamon Press, Oxford (1981).
4. Nasser, E., *Fundamentals of Gaseous Ionization and Plasma Electronics*, John Wiley, New York (1974).
5. Alston, L.L., *High Voltage Technology*, Oxford University Press, Oxford (1968).
6. Kuffel, E. E., Zaengl, W.S. and Kuffel, J., *High Voltage Engineering Fundamentals* (2nd edition), Butterworth-Heinemann (2000).
7. Christophorou, L.G., *Gaseous Dielectrics*, GD-2, Pergamon Press, New York (1980) .
8. Christophorou, L.G. and Dale, S.J., *Encyclopedia of Physical Science and Technology*, Edited by R.A. Mayords, **4**, pp. 246–292, Academic Press, New York (1987).
9. Wurtz, M., Adam, H. and Walcher, W., *Theory and Practice of Vacuum Technology*, FriedViewveg and Sohn, Braunschweig, Germany (1989).
10. Christophorou, L.G., Olthoff, J.K. and Green, D.S., *Gases for Electrical Insulation and Interruption: Possible, Present and Future Alternatives to Pure SF₆*, National Institute of Standards and Technology (USA), Technical Note 1425 (1997).
11. Alpert, D., *Journal of Vacuum Science and Technology*, **1**, pp. 35–50 (1964).
12. Latnam, R.V., *High Voltage Vacuum Insulation*, Academic Press, London (1981).
13. Meayats, G.A. and Proskurovasky, D.L., *Pulsed Electrical Discharges in Vacuum*, Springer Verlag, Berlin, Germany (1989).
14. Dielectric phenomenon in H.V. Engineering Peak F.W. and Hemphrey, H.K. McGraw-Hill publishing Co. U.S.A. 2002.

CHAPTER

3

Conduction and Breakdown in Liquid Dielectrics

3.1 LIQUIDS AS INSULATORS

Liquid dielectrics, because of their inherent properties, appear as though they would be more useful as insulating materials than either solids or gases. This is because both liquids and solids are usually 10^3 times denser than gases and hence, from Paschen's law it should follow that they possess much higher dielectric strength of the order of 10^7 V/cm. Also, liquids, like gases, fill the complete volume to be insulated and simultaneously will dissipate heat by convection. Oil is about 10 times more efficient than air or nitrogen in its heat transfer capability when used in transformers. Although liquids are expected to give very high dielectric strength of the order of 10 MV/cm, in actual practice the strengths obtained are only of the order of 100 kV/cm.

Liquid dielectrics are used mainly as impregnants in high-voltage cables and capacitors, and for filling up of transformers, circuit breakers, etc. Liquid dielectrics also act as heat transfer agents in transformers, and as arc-quenching media in circuit breakers. Petroleum oils (Transformer oil) are the most commonly used liquid dielectrics. Synthetic hydrocarbons and halogenated hydrocarbons are also used for certain applications. For very high-temperature applications, silicone oils and fluorinated hydrocarbons are employed. However, it may be mentioned that some of the isomers of poly-chlorinated diphenyls (generally called askerels) have been found to be very toxic and poisonous, and hence, their use has been almost stopped.

Liquid dielectrics normally are mixtures of hydrocarbons and are weakly polarised. When used for electrical insulation purposes, they should be free from moisture, products of oxidation and other contaminants. The most important factor that affects the electrical strength of an insulating oil is the presence of water in the form of fine droplets suspended in the oil. The presence of even 0.01% water in transformer oil reduces its electrical strength to 20% of the dry oil value. The dielectric strength of oil reduces more sharply, if it contains fibrous impurities in addition to water. [Table 3.1](#) shows the properties of some dielectrics commonly used in electrical equipment.

Of the insulating liquids shown in [Table 3.1](#), transformer oils are the cheapest and the most commonly used. The electrical properties of transformer oil are given in the above table. Oils used in the capacitors are similar to transformer oil but they are subjected to a very high degree of purification. Various kinds of oils are used in cables as impregnants for paper insulation and to improve their heat transfer capability. [Table 3.1](#) gives the dielectric properties of various liquid dielectrics used in cables, capacitors and in other special applications.

In practice, the choice of a liquid dielectric for a given application is made mainly on the basis of its chemical stability. Other factors such as saving of space, cost, previous usage, and susceptibility to the environmental influences are also considered.

Table 3.1 Dielectric properties of some liquid dielectrics

<i>Property</i>	<i>Transformer oil</i>	<i>Cable oil</i>	<i>Capacitor oil</i>	<i>PETEP oil</i>	<i>Silicone oils</i>
Breakdown strength at 20°C on 2.5 mm standard sphere gap	15 kV/mm	30 kV/mm	20 kV/mm	> 15 kV/mm	30–40 kV/mm
Relative permittivity (50 Hz)	2.2–2.3	2.3–2.6	2.1	2.7	2–73
Tan δ (50 Hz) (1 kHz)	0.001 0.0005	0.002 0.0001	0.25×10^{-3} 0.10×10^{-3}	0.1×10^{-3} 0.5×10^{-3}	10^{-3} 10^{-4}
Resistivity (ohm-cm)	10^{12} – 10^{13}	10^{12} – 10^{13}	10^{13} – 10^{14}	$> 10^{14}$	3×10^{14}
Specific gravity at 20°C	0.89	0.93	0.88–0.89	0.96–0.97	1.0–1.1
Viscosity at 20°C (CS)	30	30	30	80	10–1000
Acid value (mg/gm of KOH)	Nil	Nil	Nil	< 0.03	Nil
Refractive index	1.4820	1.4700	1.4740	1.4555	1.5000–1.6000
Saponification (mg of KOH/gm of oil)	0.01	0.01	0.01		< 0.01
Thermal expansion (20–100°C)	$7 \times 10^{-4}/^{\circ}\text{C}$	$7 \times 10^{-4}/^{\circ}\text{C}$	$7 \times 10^{-4}/^{\circ}\text{C}$	0.00075	$5 \times 10^{-4}/^{\circ}\text{C}$
Max. permissible water content (in ppm)	50	50	50	200	< 30 (negligible)

3.1.1 Classification of Liquid Dielectrics

In recent years, a substitute to mineral oils, other polyester oils have been developed which are extensively used in transformers in Europe and other countries. One such oil is the halogen-free Penta-Ethythrite-Tetra Fatty Acid Polyester oil (PETFP oil) which has very good electrical, physical and thermal properties (see [Table 3.1](#)). It is also biodegradable, i.e. when decomposed has almost negligible toxicity and does not contribute to pollution.

(a) Transformer Oil (Mineral Oil) As already mentioned, transformer oil is the most commonly used liquid dielectric in power apparatus. It is an almost colourless liquid consisting of a mixture of hydrocarbons which include paraffins, isoparaffins, naphthalenes and aromatics. When in service, the liquid in a transformer is subjected to prolonged heating at high temperatures of about 95°C, and consequently it undergoes a gradual ageing process. With time, the oil becomes darker due to the formation of acids and resins, or sludge in the liquid. Some of the acids are corrosive to the solid insulating materials and metal parts in the transformer. Deposits of sludge on the transformer core, on the coils and inside the oil ducts reduce circulation of oil and thus its heat-transfer capability gets considerably reduced. Complete specifications for the testing of transformer oils are given in IS 1866 (1983), IEC 296 (1969) and IEC 474 (1974).

(b) Synthetic Hydrocarbons Among synthetic liquid dielectrics, polyolefins are the dielectrics of choice for applications in power cables. Over 55% of synthetic hydrocarbons produced worldwide today are polyolefins. The most commonly used olefins are poly-butylene and alkylaromatic hydrocarbons (e.g., alkyl-benzene). Their general characteristics are very similar to those of mineral oils.

(c) Chlorinated Hydrocarbons Two aromatic hydrocarbons, benzene and diphenyl, are chlorinated to produce chlorinated aromatic compounds called askarels or simply polychlorinated biphenyl (PCB). They possess high fire point and excellent electrical properties. In recent years their use has been banned throughout the world, because they pose serious health hazards.

(d) Silicone Oils Silicone oils represent an alternative to PCBs but they are expensive. Even at a temperature of 150°C, they exhibit high long-term thermal stability. Silicone oils are resistant to most chemicals, and are oxidation resistant, even at higher temperatures. They can be used at higher temperatures than mineral oils. Silicone oils are an acceptable substitute for PCBs in transformers despite their slightly inferior nonflammable properties.

(e) Esters Natural esters such as castor oil has been used as a capacitor impregnant for many years, but currently two types of synthetic esters are being used, viz., organic esters and phosphate esters.

Organic esters have high boiling points in relation to their viscosity and, therefore, have high fire points. They have a good viscosity-temperature relationship and are used extensively in capacitors.

The phosphate esters have high boiling point and low flammability and therefore are used in transformers that are to be installed in hazardous areas.

(f) Latest Developments Some new oils have been introduced in recent years. These are being marketed under different commercial names, such as high-temperature hydrocarbon oil,

tetrachloroethylene and perfluoropolyether.

High Temperature Hydrocarbon (HTH) oils have good electrical insulating and adequate heat transfer properties. They are chemically similar to regular mineral transformer oils, but possess higher boiling points and higher fire points. However, they have higher viscosity which reduces heat transfer capability.

Table 3.2 Properties of High-Temperature Hydrocarbon (HTH) oils and Tetrachloroethylene (C_2Cl_4)

Property	HTH	C_2Cl_4
Dielectric strength, kV	43	43
Impulse breakdown, kV		
Negative polarity	118	—
Positive polarity	85	—
Dielectric constant, ϵ_r	2.38	2.365
Dissipation factor (%)		
100°C	0.4	—
50°C	0.4	0.05
250°C	$< 10^{-3}$	—
Flach point, °C	285	none
Fire point, °C	312	none
Pour point, °C	-30	-22
Viscosity, cSt		
100°C	16	0.36
50°C	85	0.42
250°C	350	0.55
Specific gravity, g/cm^3	0.877	1.620

Tetrachloroethylene (C_2Cl_4) is a nonflammable insulating fluid, and is used in mixtures with mineral oil. It has very low viscosity and therefore gives excellent heat transfer properties. Some typical properties of HTH oil and C_2Cl_4 are given below in [Table 3.2](#). Perfluoropolyether has been recently introduced in the European market with the trade name Galden HT40. It is a nonflammable oil and its boiling point exceeds 400°C. It possesses low-vapour pressure, so can be used as a good heat-transfer medium.

3.1.2 Characteristics of Liquid Dielectrics

Essentially, a liquid dielectric should possess good dielectric properties, excellent heat transfer characteristics and must be chemically stable under the range of conditions under which the equipment operates. These are briefly discussed below.

(a) Electrical Properties The electrical properties that are essential in determining the dielectric performance of a liquid dielectric are its

- (i) capacitance per unit volume or its relative permittivity
- (ii) resistivity
- (iii) loss tangent ($\tan \delta$) or its power factor which is an indication of the power loss under ac voltage application
- (iv) its ability to withstand high electric stresses.

Permittivities of most of the petroleum oils vary from 2.0 to 2.6 while those of silicone oils from 2.0 to 73 (see [Table 3.1](#)). In case of the non-polar liquids, the permittivity is independent of frequency but in the case of polar liquids, such as water, it changes with frequency. For example, the permittivity of water is 78 at 50 Hz and reduces to about 5.0 at 1 MHz.

Resistivities of insulating liquids used for high-voltage applications should be more than 10^{16} ohm-metre and most of the liquids in their pure state exhibit this property.

Power Factor of a liquid dielectric under ac voltage will determine its performance under load conditions. Power factor is a measure of the power loss and is an important parameter in cable and capacitor systems. However, in the case of transformers, the dielectric loss in the oil is negligible when compared to copper and iron losses. Pure and dry transformer oil will have a very low power factor varying between 10^{-4} at 20°C and 10^{-3} at 90°C at a frequency of 50 Hz.

Dielectric Strength is the most important parameter in the choice of a given liquid dielectric for a given application. The dielectric strength depends on the atomic and molecular properties of the liquid itself. However, under practical conditions the dielectric strength depends on the material of the electrodes, temperature, type of applied voltage, gas content in the liquid, etc., which change the dielectric strength by changing the molecular properties of the liquid. The above factors which control the breakdown strength and leads to electrical breakdown of the liquid dielectrics.

(b) Heat Transfer Characteristics In equipments filled with a liquid dielectric (transformer, cable, circuit breaker, etc.), heat is transferred mainly by convection. Under natural atmospheric cooling conditions convection (N) is given by

$$N = f[K^3 AC/\nu]^n \quad (3.1)$$

where K = thermal conductivity, A = coefficient of expansion, C = specific heat per unit volume, ν = kinematic viscosity, and $n = 0.25 \sim 0.33$. The main factors that control the heat transfer are thermal conductivity (K) and viscosity (ν). From [Eq. \(3.1\)](#) it can be seen that a higher value for K is preferable for apparatus likely to operate continuously at a high temperature. On the other hand, a low value of K and high viscosity can lead to localized overheating or even electrical 'burn out'.

Silicone oils do not exhibit these properties and therefore can pose severe overheating problems in equipment that use these oils.

(c) Chemical Stability In service, insulating liquids are subjected to thermal and electrical stresses in the presence of materials like O₂, water, fibres and decomposition products of solid insulation. These, either singly or in combination, cause degradation of the liquid with the result that soluble solid and gaseous products are found, which can result in corrosion, impairment of heat transfer, deterioration of electrical properties, increased dielectric losses, discharges and arcing. In the absence of any remedial action, this cycle continues and produces an ever-worsening liquid purity and equipment condition.

3.2 PURE LIQUIDS AND COMMERCIAL LIQUIDS

Pure liquids are those which are chemically pure and do not contain any other impurity even in traces of 1 in 10^9 , and are structurally simple. Examples of such simple pure liquids are *n*-hexane (C_6H_{14}), *n*-heptane (C_7H_{16}) and other paraffin hydrocarbons. By using simple and pure liquids, it is easier to separate out the various factors that influence conduction and breakdown in them. On the other hand, the commercial liquid oils which are not chemically pure, normally consist of mixtures of complex organic molecules which cannot be easily specified or reproduced in a series of experiments.

3.2.1 Purification

The main impurities in liquid dielectrics are dust, moisture, dissolved gases and ionic impurities. Various methods employed for purification are filtration (through mechanical filters, spray filters, and electrostatic filters), centrifuging, degassing and distillation, and chemical treatment (adding ion exchange materials such as alumina, fuller's earth, etc. and filtering). Dust particles when present become charged and reduce the breakdown strength of the liquid dielectrics, and they can be removed by careful filtration. Liquid will normally contain moisture and dissolve gases in small quantities. Gases like oxygen and carbon dioxide significantly affect the breakdown strength of the liquids, and hence it is necessary to control the amount of gas present. This is done by distillation and degassing. Ionic impurity in liquids, like water vapour which easily dissociates, leads to very high conductivity and heating of the liquid depending on the applied electric field. Water is removed using drying agents or by vacuum drying. Sometimes, liquids are shaken with concentrated sulphuric acid to remove wax and residue and washed with caustic soda and distilled water. A commonly used closed-cycle liquid purification system to prepare liquids as per the above requirements is shown in [Fig. 3.1](#). This system provides for cycling the liquid. The liquid from the reservoir flows through the distillation column where ionic impurities are removed. Water is removed by drying agents or frozen out in the low-temperature bath. The gases dissolved in the liquid are removed by passing them through the cooling tower and/or pumped out by the vacuum pumps. The liquid then passes through the filter where dust particles are removed. The liquid thus purified is then used in the test cell. The used liquid then flows back into the reservoir. The vacuum system thus helps to remove the moisture and other gaseous impurities.

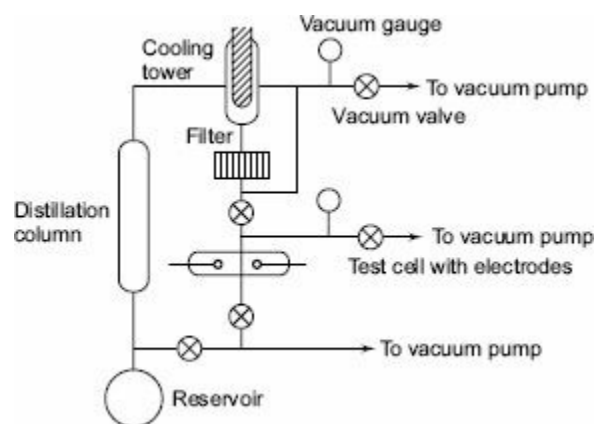


Fig. 3.1 *Liquid purification system with test cell*

3.2.2 Breakdown Tests

Breakdown tests are normally conducted using test cells. For testing pure liquids, the test cells used are small so that less quantity of liquid is used during testing. Also, test cells are usually an integral part of the purification system as shown in [Fig. 3.1](#). The electrodes used for breakdown voltage measurements are usually spheres of 0.5 to 1 cm in diameter with gap spacings of about 100–200 nm (i.e. 0.1 mm). The gap is accurately controlled by using a micrometer. Sometimes parallel plane uniform-field electrode systems are also used. Electrode separation is very critical in measurements with liquids, and also the electrode surface smoothness and the presence of oxide films have a marked influence on the breakdown strength. The test voltages required for these tests are usually low, of the order of 50–100 kV, because of small electrode spacings. The breakdown strengths and dc conductivities obtained in pure liquids are very high, of the order of 1 MV/cm and $10^{-18} - 10^{-20}$ mho/cm respectively, the conductivity being measured at electric fields of the order of 1 kV/cm. However, the corresponding values in commercial liquids are relatively low, as can be seen from [Table 3.1](#).

3.3 CONDUCTION AND BREAKDOWN IN PURE LIQUIDS

When low electric fields less than 1 kV/cm are applied, conductivities of 10^{-18} – 10^{-20} mho/cm are obtained. These are probably due to the impurities remaining after purification. However, when the fields are high (> 100 kV/cm) the currents not only increase rapidly, but also undergo violent fluctuations which will die down after some time. A typical mean value of the conduction current in hexane is shown in [Fig. 3.2](#).

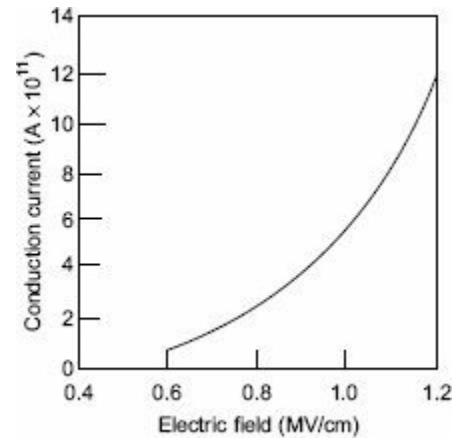


Fig. 3.2 Conduction current-electric field characteristic in hexane at high fields

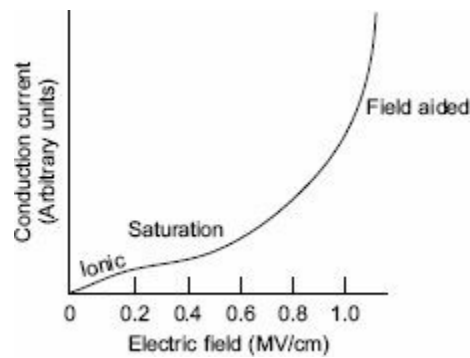


Fig. 3.3 Conduction current-electric field characteristic in a hydrocarbon liquid

This is the condition nearer to breakdown. However, if this figure is redrawn starting from very small currents, a current-electric field characteristic as shown in [Fig. 3.3](#), can be obtained. This curve will have three distinct regions as shown. At very low fields, the current is due to the dissociation of ions. With intermediate fields, the current reaches a saturation value, and at high fields the current generated because of the field-aided electron emission from the cathode gets multiplied in the liquid medium by a Townsend type of mechanism (see [Chapter 2](#)). The current multiplication also occurs from the electrons generated at the interfaces of liquid and impurities. The increase in current by these processes continues till breakdown occurs.

The exact mechanism of current growth is not known; however, it appears that the electrons are generated from the cathode by field emission of electrons. The electrons so liberated get multiplied by a process similar to Townsend's primary and secondary ionization in gases (see [Chapter 2, Sec. 2.2 to 2.5](#)). As the breakdown field is approached, the current increases rapidly due to a process similar to the primary ionization process and also the positive ions reaching the cathode generate secondary electrons, leading to breakdown. The breakdown voltage depends on the field, gap separation, cathode work-function, and the temperature of the cathode. In addition, the liquid viscosity, the liquid temperature, the density, and the molecular structure of the liquid also influence

the breakdown strength of the liquid. Typical maximum breakdown strengths of some highly purified liquids and liquefied gases are given in [Table 3.3](#).

Table 3.3 Maximum breakdown strengths of some liquids

Liquid	Maximum breakdown strength (MV/cm)
Hexane	1.1–1.3
Benzene	1.1
Transformer oil	1.0
Silicone	1.0–1.2
Liquid Oxygen	2.4
Liquid Nitrogen	1.6–1.9
Liquid Hydrogen	1.0
Liquid Helium	0.7
Liquid Argon	1.10–1.42

It has been observed that the increase in breakdown strength is more, if the dissolved gases are electronegative in character (like oxygen).

Similarly, the increase in the liquid hydrostatic pressure increases the breakdown strength. These properties are shown in [Figs 3.4](#) and [3.5](#).

To sum up, this type of breakdown process in pure liquids, called the electronic breakdown, involves emission of electrons at fields greater than 100 kV/cm. This emission occurs either at the electrode surface irregularities or at the interfaces of impurities and the liquid. These electrons get further multiplied by Townsend's type of primary and secondary ionization processes, leading to breakdown.

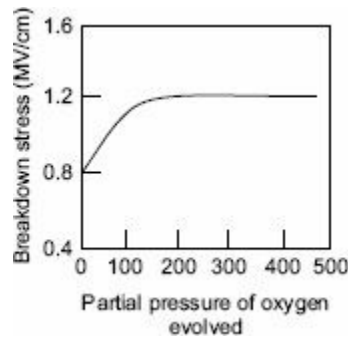


Fig. 3.4 Effect of oxygen gas evolved on the breakdown stress in *n*-hexane

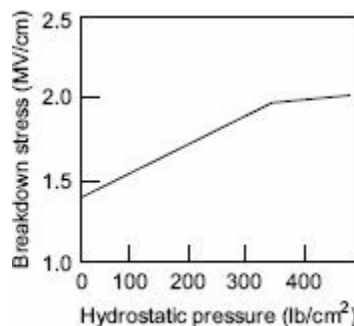


Fig. 3.5 Effect of hydrostatic pressure on breakdown stress in *n*-hexane

3.4 CONDUCTION AND BREAKDOWN IN COMMERCIAL LIQUIDS

As already mentioned, commercial insulating liquids are not chemically pure and have impurities like gas bubbles, suspended particles, etc. These impurities reduce the breakdown strength of these liquids considerably. The breakdown mechanisms are also considerably influenced by the presence of these impurities. In addition, when breakdown occurs in these liquids, additional gases and gas bubbles are evolved and solid decomposition products are formed. The electrode surfaces become rough, and at times explosive sounds are heard due to the generation of impulsive pressure through the liquid.

The breakdown mechanism in commercial liquids is dependent, as seen above, on several factors, such as the nature and condition of the electrodes, the physical properties of the liquid, and the impurities and gases present in the liquid. Several theories have been proposed to explain the breakdown in liquids, and they are classified as follows:

- (a) Suspended Particle Mechanism
- (b) Cavitation and Bubble Mechanism
- (c) Stressed Oil Volume Mechanism

These are explained briefly below.

3.4.1 Suspended Particle Theory

In commercial liquids, the presence of solid impurities cannot be avoided. These impurities will be present as fibres or as dispersed solid particles. The permittivity of these particles (ϵ_2) will be different from the permittivity of the liquid (ϵ_1). If we consider these impurities to be spherical particles of radius r , and if the applied field is E , then the particles experience a force F , where

$$F = \frac{1}{2} r^3 \frac{(\epsilon_2 - \epsilon_1)}{2\epsilon_1 + \epsilon_2} \text{grad } E^2 \quad (3.2)$$

This force is directed towards areas of maximum stress, if $\epsilon_2 > \epsilon_1$, for example, in the case of the presence of solid particles like paper in the liquid. On the other hand, if only gas bubbles are present in the liquid, i.e. $\epsilon_2 < \epsilon_1$, the force will be in the direction of areas of lower stress. If the voltage is continuously applied (dc) or the duration of the voltage is long (ac), then this force drives the particles towards the areas of maximum stress. If the number of particles present are large, they become aligned due to these forces, and thus form a stable chain bridging the electrode gap causing a breakdown between the electrodes.

If there is only a single conducting particle between the electrodes, it will give rise to local field enhancement depending on its shape. If this field exceeds the breakdown strength of the liquid, local breakdown will occur near the particle, and this will result in the formation of gas bubbles which may lead to the breakdown of the liquid.

The values of the breakdown strength of liquids containing solid impurities was found to be much less than the values for pure liquids. The impurity particles reduce the breakdown strength, and it was also observed that the larger the size of the particles, the lower were the breakdown strengths.

3.4.2 Cultivation and the Bubble Theory

It was experimentally observed that in many liquids, the breakdown strength depends strongly on the applied hydrostatic pressure, suggesting that a change of phase of the medium is involved in the breakdown process, which in other words, means that a kind of vapour bubble formed is responsible for breakdown. The following processes have been suggested to be responsible for the formation of the vapour bubbles:

- (a) gas pockets at the surfaces of the electrodes;
- (b) electrostatic repulsive forces between space charges which may be sufficient to overcome the surface tension;
- (c) gaseous products due to the dissociation of liquid molecules by electron collisions; and
- (d) vapourization of the liquid by corona type discharge from sharp points and irregularities on the electrode surfaces.

Once a bubble is formed, it will elongate in the direction of the electric field under the influence of electrostatic forces. The volume of the bubble remains constant during elongation. Breakdown occurs when the voltage drop along the length of the bubble becomes equal to the minimum value on the Paschen's curve (see [Chapter 2, Sec. 2.10](#)) for the gas in the bubble. The breakdown field is given as

$$E_0 = \frac{1}{(\epsilon_1 - \epsilon_2)} \left[\frac{2\pi\sigma(2\epsilon_1 + \epsilon_2)}{r} \left\{ \frac{\pi}{4} \sqrt{\left(\frac{V_b}{2rE_0} \right)^2 - 1} \right\} \right]^{1/2} \quad (3.3)$$

where σ is the surface tension of the liquid, ϵ_1 is the permittivity of the liquid, ϵ_2 is the permittivity of the gas bubble, r is the initial radius of the bubble assumed as a sphere and V_b is the voltage drop in the bubble (corresponding to minimum on the Paschen's curve). From this equation, it can be seen that the breakdown strength depends on the initial size of the bubble which in turn is influenced by the hydrostatic pressure and temperature of the liquid.

This theory does not take into account the production of the initial bubble and hence, the results given by this theory do not agree well with the experimental results. This [Fig. 3.6](#) is shown in [Fig. 3.6](#).

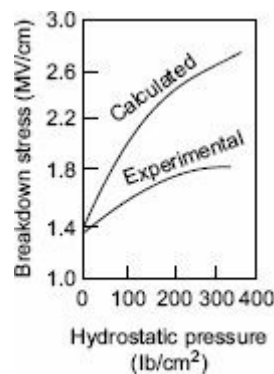


Fig. 3.6 Theoretical and experimental breakdown stresses in *n*-hexane

3.4.3 Thermal Mechanism of Breakdown

Another mechanism proposed to explain breakdown under pulse conditions is thermal breakdown. This mechanism is based on the experimental observations of extremely large currents just before breakdown. These high-current pulses are believed to originate from the tips of the microscopic projections on the cathode surface with densities of the order of 1 A/cm^3 . These high density current pulses give rise to localized heating of the oil which may lead to the formation of vapour bubbles. The vapour bubbles are formed when the energy exceeds 10^7 J/cm^2 . When a bubble is formed, breakdown follows, either because of its elongation to a critical size or when it completely bridges the gap between the electrodes. In either case, it will result in the formation of a spark. According to this mechanism, the breakdown strength depends on the pressure and the molecular structure of the liquid. For example, in *n*-alkanes the breakdown strength was observed to depend on the chain length of the molecule. This theory is only applicable at very small lengths ($\leq 100 \mu\text{m}$) and does not explain the reduction in breakdown strength with increased gap lengths.

3.4.4 Effect of Moisture Content on Breakdown Strength of Liquid Dielectrics

Usually, in commercial liquids like transformer oil, certain amount of moisture (water vapour) and a very little amount of water will be present. The maximum amount of water present in the oil of a good quality will be less than 50 ppm at an atmospheric temperature of about 30°C or less. Water present in the oil lowers the dielectric strength. At lower temperatures, the moisture is distributed as minute water globules, whereas at higher temperatures ($\geq 80^\circ\text{C}$), water begins to boil creating more number of vapour bubbles inside the liquid. Water globules or vapour bubbles are the reason for the reduction of the dielectric strength. The variation (lowering of) the breakdown strength for a 6 mm uniform field electrode gap is shown [Fig. 3.7](#).

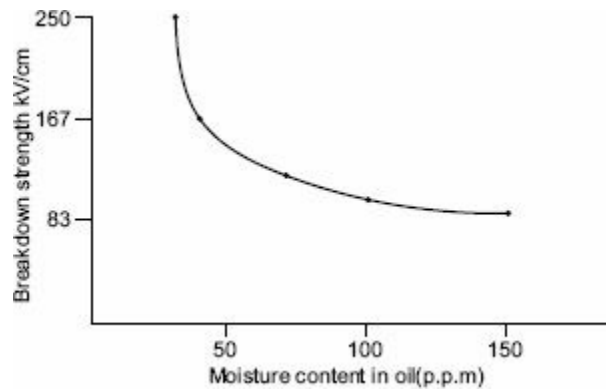


Fig. 3.7 Breakdown strength of oil as function of water content

3.4.5 Stressed Oil Volume Theory

In commercial liquids where minute traces of impurities are present, the breakdown strength is determined by the 'largest possible impurity' or 'weak link'. On a statistical basis, it was proposed that the electrical breakdown strength of the oil is defined by the weakest region in the oil, namely, the region which is stressed to the maximum and by the volume of oil included in that region. In non-uniform fields, the stressed oil volume is taken as the volume which is contained between the maximum stress (E_{\max}) contour and $0.9 E_{\max}$ contour. According to this theory, the breakdown strength is inversely proportional to the stressed oil volume.

The breakdown voltage is highly influenced by the gas content in the oil, the viscosity of the oil, and the presence of other impurities. These being uniformly distributed, increase in the stressed oil volume consequently results in a reduction in the breakdown voltage. The variation of the breakdown voltage stress with the stressed oil volume is shown in [Fig. 3.8](#).

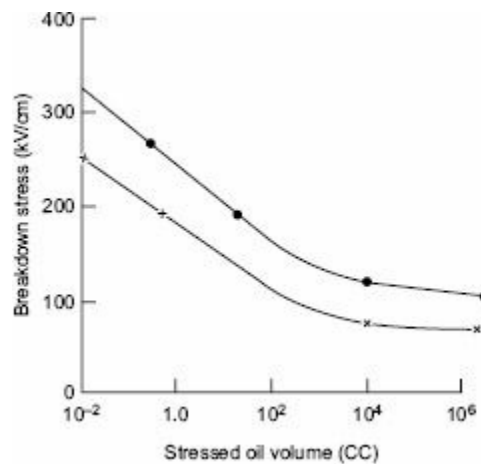


Fig. 3.8 Power frequency (50 Hz) ac breakdown stress as a function of the stressed oil volume ● With steady voltage rise × One minute withstand voltage

3.5 TESTING OF INSULATING OILS (FLUIDS): TRANSFORMER FLUIDS

Since the fluids (oils) used in electrical power equipment (Viz) Transformers etc are subjected to deterioration and contamination, their properties and quality is effectively reduced. Hence many tests have been developed to determine the condition of transformer and their insulating fluid in it. The following tests are the minimum to determine the quality and the suitability of the oils for future and continued use.

- *Dielectric Breakdown Test:* This is done using standard oil testing kit. The test cell has a standard spark gap setting (usually 2.5 mm). The one minute with stand voltage and spark over voltage with a voltage rise of 3 kV/Sec is done. The with stand should not be less than about 40 kV on the above gap and spark over voltage 50 kV For high voltage transformers the value should not be less than 1 kV for each primary kV and not less than 22 kV/mm.
- *Acid and Neutralization Tests:* This is a measure for acids formed due to oxidation. Also sludges and sediments are formed in oil due to oxidation and contact with moisture. The acidity is measured as a neutralization number with standard alkalis (KOH). For new and good hydrocarbon oils it should be less than 0.1 and for few PCB oils less then 0.2. However it should not go beyond 0. 3 for oils in use.
- *Moisture Content Test:* Moisture or water content in oils must be as minimum as possible and higher moisture content will reduce the dielectric strength very much. Hence periodic testing for moisture is done. The acceptable value for Hydrocarbon oils and PCB oils is less than 30 ppm.
- *Colour and Visual Particulate Testing:* This indicates the contaminants like dust particles, sludge etc. Colour is measured by comparing the light transmitted through it with standard colour scale. Max acceptable colour number is 3.

3.6 CONCLUSIONS

From the study of the above theories which attempt to explain the breakdown phenomenon in liquids, it is clear that no single theory can explain all the experimental observations satisfactorily. Therefore, recently developed fast optical techniques have been widely used to study the processes of liquid dielectric breakdown. After a thorough analysis and review of the data with the use of optical techniques, it is now clear that the understanding of the mechanism of liquid breakdown has advanced tremendously.

All the theories discussed above do not consider the dependence of breakdown strength on the gap length. They all try to account for the maximum obtainable breakdown strength only. However, the experimental evidence showed that the breakdown strength of a liquid depends on the gap length, given by the following expression,

$$V_b = Ad^n \tag{3.4}$$

where, d = gap length,

A = constant, and

n = constant, always less than 1.

The breakdown voltage also depends on the nature of the voltage, the mode in which the voltage is applied, and the time of application. The above relationship is of practical importance, and the electrical stress of a given oil used in design is obtained from this. During the last few years, research work is directed on the measurements of discharge inception levels in oil and the breakdown strengths of large volumes of oil under different conditions.

It may be summarized that the actual mechanism of breakdown in oil is not a simple phenomenon and the breakdown voltages are determined by experimental investigations only. Electrical stresses obtained for small volumes should not be used in the case of large volumes. As a general guideline, the properties of good dielectric oils for electrical purpose are tabulated (see [Table 3.1](#)), and the designer should satisfy himself on all the properties before acceptance.

[Table 3.4](#) gives the typical breakdown strengths for highly purified liquids and the design stresses actually used. A factor of safety of about 10 is used as can be seen from the data in the table. The reasons for such an approach can be understood from the various factors considered in the breakdown theories discussed.

Table 3.4 Power frequency design field strengths and breakdown field strengths for highly purified dielectric liquids—a comparison

Dielectric liquid	Used in (equipment)	Design field strength (MV/m)	Breakdown strength (MV/m)
Transformer oil	Transformers	2–5	100
<i>n</i> -hexane	Cables	13–20	132
Polybutane (Synthetic hydrocarbon)	Capacitors	10–25	109

In the next 20 years, transformer oils, which are derivatives of petroleum crude, may be in short supply. Therefore, various synthetic insulating oils have been examined as potential insulants in high-voltage apparatus. Among the synthetic oils, polybutane liquids have been used for some years in cables and paper capacitors. They are superior to transformer oils in various electrical properties including dielectric strength. Fluorocarbon and silicone liquids are also used in special apparatus. In

recent years, new liquids, such as high temperature hydrocarbon oils, tetrachloroethylene and tetrafluoropolyether have been successfully used as liquid dielectrics in high-voltage apparatus. However, their widespread use will require further evaluation of their properties.

K
T E R M S
Y

- Liquid Dielectrics
- Classification
- Characteristics and Properties
- Conduction and Breakdown in Pure Liquids
- Commercial Liquids
- Breakdown Mechanisms

WORKED EXAMPLES

Example 3.1 *In an experiment for determining the breakdown strength of transformer oil, the following observations were made. Determine the power law dependence between the gap spacing and the applied voltage of the oil.*

Gap spacing (mm)	:	4	6	10	12
Voltage at breakdown (kV)	:	90	140	210	255

Solution The relationship between the breakdown voltage and gap is normally given as

$$V = Kd^n$$

or, $\log V = \log K + n \log d$
 i.e., $\log V - \log K = n \log d$

or, $n = \frac{\log V - \log K}{\log d}$
 = slope of the straight line as shown in Fig. E.3.1
 = 0.947

From Fig. E.3.1, $K = 24.5$

∴ relationship between the breakdown voltage and the gap spacing for the transformer oil studied is

$$V = 24.5 d^{0.947}$$

where V is in kV and d is in mm.

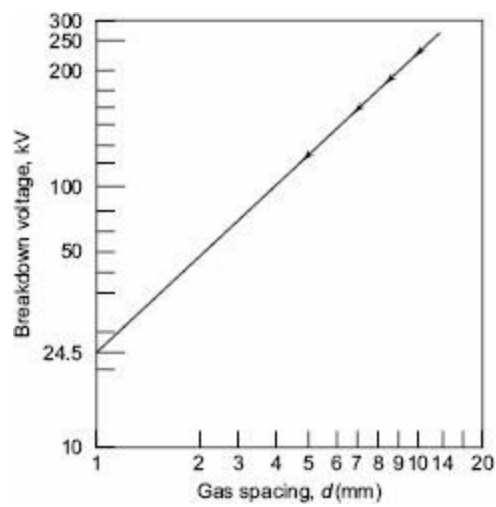


Fig. E.3.1 Breakdown voltage as a function of gap spacing

MULTIPLE-CHOICE QUESTIONS

- Transformer oil is
 - askeral
 - silicone oil
 - polyester
 - mineral oil
- The breakdown strength of mineral oil is about
 - 20 kV/mm
 - 50 kV/mm
 - 3 to 5 kV/mm
 - 30 to 40 kV/mm
- $\tan \delta$ for liquid insulants at 50 Hz should be less than
 - 0.1
 - 0.01
 - 0.001
 - 10^{-6}
- Dielectric constant of mineral oils is about
 - 1.5 to 2.0
 - 2.2 to 2.4
 - 3.0 to 3.5
 - 1.008
- DC conductivity of liquid dielectrics at low electric fields is about in Siemens
 - 10^{-6}
 - 10^{-12}
 - 10^{-18}
 - 10^{-30}
- Maximum dielectric strength obtained with pure liquids is about
 - 100 kV/mm
 - 10 kV/mm
 - 1 MV/mm

(d) 50 kV/mm

7. Conduction and breakdown in commercial liquids is affected by

- (a) solid particles
- (b) vapour or air bubbles
- (c) electrode material
- (d) all the above three factors a, b and c

8. The relation between breakdown strength and gap distance in liquid dielectrics is V_b

- (a) K/d
- (b) Kd^n
- (c) Kd^{-n}
- (d) $(K_1d + K_2)$

9. Stressed oil volume theory is applicable when

- (a) small volume of liquid is involved
- (b) large volume of liquid is involved
- (c) large gap distance is involved
- (d) pure liquids are involved

10. The parameters that affect the breakdown strength of liquids is

- (a) hydrostatic pressure and temperature
- (b) dissolved impurities
- (c) dielectric constant
- (d) pressure, temperature, dissolved impurities and suspended particles

11. Which of the following liquids has highest breakdown strength?

- (a) Mineral oils
- (b) Silicone oils
- (c) Chlorinated hydrocarbon oils
- (d) Polyolefins or esters

12. Which of the following property is important for a liquid to be used both for electrical insulation and cooling purposes?

- (a) Thermal conductivity
- (b) Viscosity
- (c) Viscosity temperature characteristic
- (d) Breakdown strength

13. For good insulating oil, the power factor or $\tan \delta$ at the given frequency of application should be

- (a) 0.1
- (b) less than 10^{-3}
- (c) 10^{-2} to 10^{-3}
- (d) 10^{-1} to 10^{-2}

14. The maximum breakdown strength that can be obtained with pure liquids like hexane is about

- (a) 1 MV/cm
- (b) 100 kV/cm
- (c) 250 to 300 kV/cm
- (d) 10 MV/cm

15. In a pure liquid dielectric, with the increase in hydrostatic pressure, the breakdown stress

- (a) increases linearly up to some extent and does not change afterwards

- (b) increases exponentially
- (c) decreases
- (d) none of the above

Answers to Multiple-Choice Questions

- | | | | | | |
|---------|---------|---------|---------|---------|---------|
| 1. (d) | 2. (a) | 3. (c) | 4. (b) | 5. (b) | 6. (a) |
| 7. (d) | 8. (b) | 9. (b) | 10. (d) | 11. (b) | 12. (c) |
| 13. (b) | 14. (a) | 15. (a) | | | |

REVIEW QUESTIONS

1. Explain the phenomena of electrical conduction in liquids. How does it differ from that in gases?
2. What are commercial liquid dielectrics, and how are they different from pure liquid dielectrics?
3. What are the factors that influence conduction in pure liquid dielectrics and in commercial liquid dielectrics?
4. Explain the various theories that explain breakdown in commercial liquid dielectrics.
5. What is “stressed oil volume theory”, how does it explain breakdown in large volumes of commercial liquid dielectrics?
6. What are the common liquid insulants used in an electrical apparatus? Briefly give their physical properties.
7. Why are both electrical and thermal properties important for liquids for use in an apparatus like a transformer?
8. What are the different methods and means for purification of liquid dielectrics?
9. Discuss the effect of the following parameters on the breakdown strength of liquids:
 - (a) Hydrastatic pressure
 - (b) Solid impurities
 - (c) Moisture content in the oil
10. In a experiment for determining the breakdown strength of transformer oil with standard electrodes, the following observations were obtained with two different types of oils. Determine the power law for breakdown and hence estimate the breakdown strength for a 1 cm gap (kV/cm).

(i) 'A' oil

Gap spacing (mm)	3	6	9	10
Bd. voltage (kV)	86	148	169	219

(ii) 'B' oil

Gap spacing (mm)	3	6	9	12
Bd. voltage (kV)	84	143	192	214

Answer

- (i) $V_b \approx 32.6 d^{0.84}$; $bds \approx 210$ kV/cm
 (ii) $V_b \approx 31.4 d^{0.82}$; $bds \approx 204$ kV/cm

REFERENCES

1. Adam Czewski, I., *Ionization, Conduction and Breakdown in Dielectric Liquids*, Taylor and Francis, London (1969).
2. Gallager, T.J., *Simple Dielectric Liquids*, Clarendon Press, Oxford (1975).
3. Hawley, R. and Zaky, A.A., *Conduction and Breakdown in Mineral Oil*, Peter Peregrinus,

London (1973).

4. Lewis, T.J., *Progress in Dielectrics*, Vol. 1, Heywood, London (1959), pp. 97–140.
5. Code of practice for maintenance and supervision of insulating oil in equipment, *IS:1866–1983*; also *IS: 6262–1971* (for $\tan \delta$ measurement) and *IS: 6792–1972* (for measurement of electrical strength).
6. “Specifications for new insulating oils for transformers and switchgear”, *IEC No. 269*, 1969.
7. “Oxidation tests for inhibited oils”, *IEC No. 474*, 1974.
8. Wilson, A.C.M., *Insulating liquids: Their uses, manufacture and properties*, Peter Peregrinus and IEE, London (1980).
9. Bartnikas, B. (ed), “Engineering Dielectrics, Vol II: Electrical Insulating Liquids”, *ASTM*, Philadelphia (1994).
10. Shugg, W.T., “Handbook of Electrical and Electronic Insulating Materials”, *IEEE Press*, New York (1995).
11. Bradwell, A., *Electrical Insulation*, Peter Peregrinus Ltd., London (1983).
12. McGrawth, P.B. and Nelson, J.K., “Optical studies of pre-breakdown events in liquid dielectrics,” *Proceedings IEE, Part A*, **124**, pp. 183–187 (1977).
13. Tanaka, T. and Greenwood, A., *Advanced Power Cable Technology*, CRC Press, Boca Roton, Florida (1983).
14. Watson, P.K., Quershi, M.I. and Chadband, W.B., “The growth of prebreakdown cavities in silicone fluids and the frequency of accompanying discharge pulses”, *IEEE Transactions on Electrical Insulation*, **EI-5**, No. 3, pp. 344-349 (June 1998).
15. Malik, N.H., Al-Arainy, A.A. and Quershi, M.I., *Electrical Insulation in Power Systems*, Marcel Dekker Inc., New York (1998).
16. Kuffel, E., Zaengl, W.S. and Kuffel, J., *High Voltage Engineering Fundamentals*, (2nd edition). Butterworth Heinemann, New York, (2000).
17. Arghi, S.M., Qureshi, M.I. and Chadband, W.G., *IEEE Transactions on Electrical Insulation*, **EI-26**, No. 4, pp. 663–672 (1994).
18. *Electrical Insulation in power systems* N.H. Malik etc. Taylor and Fransis, London 1998.

CHAPTER

4

Breakdown in Solid Dielectrics

4.1 INTRODUCTION

Solid dielectric materials are used in all kinds of electrical apparatus and devices to insulate one current-carrying part from another when they operate at different voltages. A good dielectric should have low dielectric loss, high mechanical strength, should be free from gaseous inclusions, and moisture, and be resistant to thermal and chemical deterioration. Solid dielectrics have higher breakdown strength compared to liquids and gases.

Solid insulating materials, which are generally used in practice, are of two types, namely, the organic materials, such as paper, wood and rubber, and the inorganic materials, such as mica, glass and procelain, and synthetic polymers, such as perspex, PVC, epoxy resins, etc. Some important properties of these materials which are used for insulation purposes in high-voltage apparatus are described later in this chapter.

Studies of the breakdown of solid dielectrics are of extreme importance in insulation studies. When breakdown occurs, solids get permanently damaged while gases fully and liquids partly recover their dielectric strength after the applied electric field is removed.

The mechanism of breakdown is a complex phenomenon in the case of solids, and varies depending on the time of application of voltage as shown in [Fig. 4.1](#). The various breakdown mechanisms can be classified as follows:

- (a) intrinsic or ionic breakdown,
- (b) electromechanical breakdown,
- (c) failure due to treeing and tracking,
- (d) thermal breakdown,
- (e) electrochemical breakdown, and
- (f) breakdown due to internal discharges.

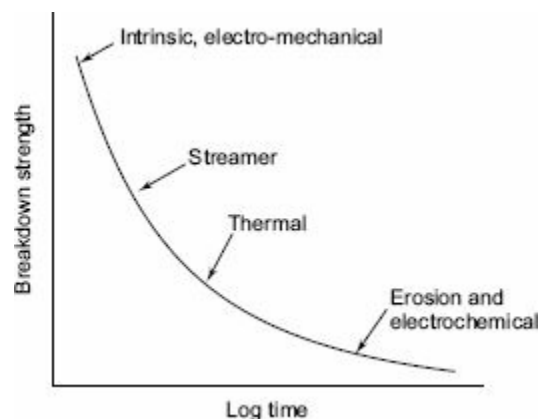


Fig. 4.1 Variation of breakdown strength with time after application of voltage

4.2 INTRINSIC BREAKDOWN

When voltages are applied only for short durations of the order of 10^{-8} s, the dielectric strength of a solid dielectric increases very rapidly to an upper limit called the *intrinsic electric strength*. Experimentally, this highest dielectric strength can be obtained only under the best experimental conditions when all extraneous influences have been isolated and the value depends only on the structure of the material and the temperature. The maximum electrical strength recorded is 15 MV/cm for polyvinyl-alcohol at -196°C . The maximum strength usually obtainable ranges from 5 MV/cm to 10 MV/cm.

Intrinsic breakdown depends upon the presence of free electrons which are capable of migration through the lattice of the dielectric. Usually, a small number of conduction electrons are present in solid dielectrics, along with some structural imperfections and small amounts of impurities. The impurity atoms, or molecules, or both, act as traps for the conduction electrons up to certain ranges of electric fields and temperatures. When these ranges are exceeded, additional electrons in addition to trapped electrons are released, and these electrons participate in the conduction process. Based on this principle, two types of intrinsic breakdown mechanisms have been proposed.

4.2.1 Electronic Breakdown

As mentioned earlier, intrinsic breakdown occurs in time of the order of 10^{-8} s and therefore is assumed to be electronic in nature. The initial density of conduction (free) electrons is also assumed to be large, and electron-electron collisions occur. When an electric field is applied, electrons gain energy from the electric field and cross the forbidden energy gap from the valence to the conduction band. When this process is repeated, more and more electrons become available in the conduction band, eventually leading to breakdown.

4.2.2 Avalanche or Streamer Breakdown

This is similar to breakdown in gases due to cumulative ionization. Conduction electrons gain sufficient energy above a certain critical electric field and cause liberation of electrons from the lattice atoms by collisions. Under uniform field conditions, if the electrodes are embedded in the specimen, breakdown will occur when an electron avalanche bridges the electrode gap.

An electron within the dielectric, starting from the cathode will drift towards the anode and during this motion gains energy from the field and loses it during collisions. When the energy gained by an electron exceeds the lattice ionization potential, an additional electron will be liberated due to collision of the first electron. This process repeats itself resulting in the formation of an electron avalanche. Breakdown will occur, when the avalanche exceeds a certain critical size.

In practice, breakdown does not occur by the formation of a single avalanche itself, but occurs as a result of many avalanches formed within the dielectric and extending step by step through the entire thickness of the material as shown in [Fig. 4.2](#). This can be readily demonstrated in a laboratory by applying an impulse voltage between point-plane electrodes with the point embedded in a transparent solid dielectric such as perspex.

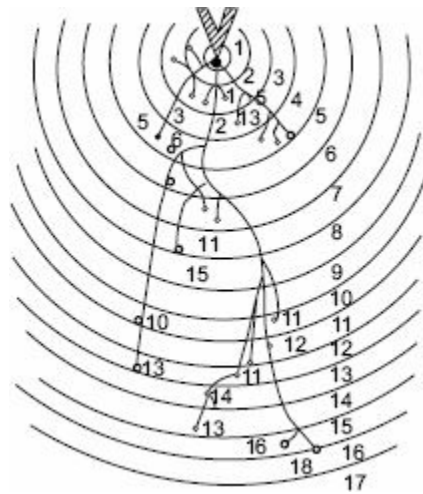


Fig. 4.2 Breakdown channels in perspex between point-plane electrodes. Radius of point 0.01 in, thickness 0.19 in. Total number of impulses 190. Number of channels produced 16; (n) point indicates end of nth channel. Radii of increases in units of 10^{-2} in.

Source: R. Cooper, *International Journal of Elec. Engg. Education*, vol. 1, 241 (1963)

4.3 ELECTROMECHANICAL BREAKDOWN

When solid dielectrics are subjected to high electric fields, failure occurs due to electrostatic compressive forces which can exceed the mechanical compressive strength. If the thickness of the specimen is d_0 and is compressed to a thickness d under an applied voltage V , then the electrically developed compressive stress is in equilibrium if

$$\epsilon_0 \epsilon_r \frac{V^2}{2d^2} = Y \ln \left[\frac{d_0}{d} \right] \quad (4.1)$$

where Y is the Young's modulus.

From Eq. (4.1),

$$V^2 = d^2 \left[\frac{2Y}{\epsilon_0 \epsilon_r} \right] \ln \left[\frac{d_0}{d} \right] \quad (4.2)$$

Usually, mechanical instability occurs when

$$d/d_0 = 0.6 \text{ or } d_0/d = 1.67$$

Substituting this in [Eq. \(4.2\)](#), the highest apparent electric stress before breakdown,

$$E_{\max} = \frac{V}{d_0} = 0.6 \left[\frac{Y}{\epsilon_0 \epsilon_r} \right]^{1/2} \quad (4.3)$$

The above equation is only approximate as Y depends on the mechanical stress. Also, when the material is subjected to high stresses the theory of elasticity does not hold good, and plastic deformation has to be considered.

Recently, this theory has been modified based on the concept of fracture mechanics. In the new mechanism, filamentary shaped cracks propagate through the dielectric material releasing both the electrostatic energy and the electromechanical strain energy stored in the material due to the applied electric field. This is analogous to the conventional mechanical crack propagation in brittle materials, whereby the cracks propagate spontaneously, if the strain energy released is greater than that required to overcome the toughness of the material (see Reference 13).

4.4 THERMAL BREAKDOWN

In general, the breakdown voltage of a solid dielectric should increase with its thickness. But this is true only up to a certain thickness above which the heat generated in the dielectric due to the flow of current determines the conduction.

When an electric field is applied to a dielectric, conduction current, however small it may be, flows through the material. The current heats up the specimen and the temperature rises. The heat generated is transferred to the surrounding medium by conduction through the solid dielectric and by radiation from its outer surfaces. Equilibrium is reached when the heat used to raise the temperature of the dielectric, plus the heat radiated out, equals the heat generated. The heat generated under dc stress E is given as

$$W_{dc} = E^2 \sigma \text{ W/cm}^3 \quad (4.4)$$

where, σ is the dc conductivity of the specimen.

Under ac fields, the heat generated

$$W_{ac} = \frac{E^2 f \epsilon_r \tan \delta}{1.8 \times 10^{12}} \text{ W/cm}^3 \quad (4.5)$$

where, f = frequency in Hz,

δ = loss angle of the dielectric material, and

E = rms value.

The heat dissipated (W_T) is given by

$$W_T = C_v \frac{dT}{dt} + \text{div} (K \text{ grad } T) \quad (4.6)$$

where C_v = specific heat of the specimen,

T = temperature of the specimen,

K = thermal conductivity of the specimen, and

t = time over which the heat is dissipated.

Equilibrium is reached when the heat generated (W_{dc} or W_{ac}) becomes equal to the heat dissipated (W_T). In actual practice, there is always some heat that is radiated out.

Breakdown occurs when W_{dc} or W_{ac} exceeds W_T . The thermal instability condition is shown in [Fig. 4.3](#). Here, the heat lost is shown by a straight line, while the heat generated at fields E_1 and E_2 are shown by separate curves. At field E_2 breakdown occurs both at temperatures T_A and T_B . In the temperature region of T_A and T_B heat generated is less than the heat lost for the field E_2 , and hence the breakdown will not occur.

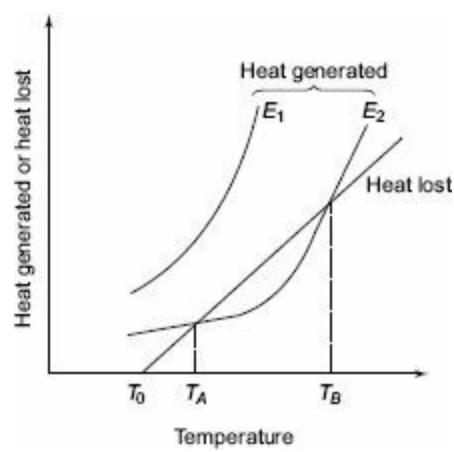


Fig. 4.3 Thermal instability in solid dielectrics

Table 4.1 Thermal breakdown stresses in dielectrics

Material	Maximum thermal breakdown stress in MV/cm	
	dc	ac
Muscovite mica	24	7.18
Rock salt	38	1.4
High grade porcelain	—	2.8
HV Steatite	—	9.8
Quartz—perpendicular to axis	1200	—
—parallel to axis	66	—
Capacitor paper	—	3.4–4.4
Polythene	—	3.5
Polystyrene	—	5.0

This is of great importance to practicing engineers, as most of the insulation failures in high-voltage power apparatus occur due to thermal breakdown. Thermal breakdown sets up an upper limit for increasing the breakdown voltage when the thickness of the insulation is increased. For a given loss angle and applied stress, the heat generated is proportional to the frequency and hence thermal breakdown is more serious at high frequencies. [Table 4.1](#) gives the thermal breakdown voltages of various materials under dc and ac fields.

It can be seen from this table that since the power loss under ac fields is higher, the heat generation is also high, and hence the thermal breakdown stresses are lower under ac conditions than under dc conditions.

4.5 BREAKDOWN OF SOLID DIELECTRICS IN PRACTICE

There are certain types of breakdown which do not come under either intrinsic breakdown or thermal breakdown, but actually occur after prolonged operation. These are, for example, breakdown due to tracking in which dry conducting tracks are formed on the surface of the insulation. These tracks act as conducting paths on the insulator surfaces leading to gradual breakdown along the surface of the insulator. Another type of breakdown in this category is the electrochemical breakdown caused by chemical transformations such as electrolysis, formation of ozone, etc. In addition, failure also occurs due to partial discharges which are brought about in the air pockets inside the insulation. This type of breakdown is very important in the impregnated paper insulation used in high-voltage cables and capacitors.

4.5.1 Chemical and Electrochemical Deterioration and Breakdown

In the presence of air and other gases some dielectric materials undergo chemical changes when subjected to continuous electrical stresses. Some of the important chemical reactions that occur are the following:

(a) Oxidation In the presence of air or oxygen, materials such as rubber and polyethylene undergo oxidation giving rise to surface cracks.

(b) Hydrolysis When moisture or water vapour is present on the surface of a solid dielectric, hydrolysis occurs and the materials lose their electrical and mechanical properties. Electrical properties of materials such as paper, cotton tape, and other cellulose materials deteriorate very rapidly due to hydrolysis. Plastics like polyethylene undergo changes, and their service life considerably reduces.

(c) Chemical Action Even in the absence of electric fields, progressive chemical degradation of insulating materials can occur due to a variety of processes such as chemical instability at high temperatures, oxidation and cracking in the presence of air and ozone, and hydrolysis due to moisture and heat. Since different insulating materials come into contact with each other in many practical apparatus, chemical reactions occur between these various materials leading to reduction in electrical and mechanical strength resulting in failure.

The effects of electrochemical and chemical deterioration could be minimized by carefully studying and examining the materials. High soda-content glass insulation should be avoided in moist and damp conditions, because sodium, being very mobile, leaches to the surface giving rise to the formation of a strong alkali which will cause deterioration. It was observed that this type of material will lose its mechanical strength within 24 hours, when it is exposed to atmospheres having 100% relative humidity at 70°C. In paper insulation, even if partial discharges are prevented completely, breakdown can occur due to chemical degradation. The chemical and electrochemical deterioration increases very rapidly with temperature, and hence high temperatures should be avoided.

4.5.2 Breakdown due to Treeing and Tracking

Polymeric insulation is widely used for many engineering applications as they are tough, light in weight and possess excellent dielectric properties. Also, they can be easily fabricated in any complicated shape as required in practical use. However, their life when used in high-voltage systems gets severely reduced by the degradation processes.

When a solid dielectric subjected to electrical stresses for a long time fails, normally two kinds of visible markings are observed on the dielectric materials. They are

- (a) the presence of a conducting path across the surface of the insulation; and
- (b) a mechanism whereby leakage current passes through the conducting path finally leading to the formation of a spark. Insulation deterioration occurs as a result of these sparks.

The spreading of spark channels during **tracking**, in the form of the branches of a tree is called **treeing**. **Tracking** is the formation of a continuous conducting paths across the surface of the insulation mainly due to surface erosion under voltage application. While in use, the insulator progressively gets coated with moisture that causes increased conduction leading to the formation of surface tracks.

Consider a system of a solid dielectric having a conducting film and two electrodes on its surface. In practice, the conducting film very often is formed due to moisture. On application of voltage, the film starts conducting, resulting in generation of heat, and the surface starts becoming dry. The conducting film becomes separate due to drying, and so sparks are drawn damaging the dielectric surface. With organic insulating materials such as paper and Bakelite, the dielectric carbonizes at the region of sparking, and the carbonized regions act as permanent conducting channels resulting in increased stress over the rest of the region. This is a cumulative process, and insulation failure occurs when carbonized tracks bridge the distance between the electrodes. This phenomenon, called **tracking**, is common between layers of bakelite, paper and similar dielectrics built of laminates.

On the other hand, **treeing** occurs due to the erosion of material at the tips of the spark. Erosion results in the roughening of the surfaces, and hence becomes a source of dirt and contamination. This causes increased conductivity resulting either in the formation of a conducting path bridging the electrodes or in a mechanical failure of the dielectric.

When a dielectric material lies between two electrodes as shown in [Fig. 4.4](#), there is a possibility for two different dielectric media, the air and the dielectric, to come in series. The voltages across the two media are as shown (V_1 across the air gap, and V_2 across the dielectric). The voltage V_1 across the air gap is given as,

$$V_1 = \frac{V d_1}{d_1 + \left(\frac{\epsilon_0}{\epsilon_1}\right) d_2} \quad (4.7)$$

where V is the applied voltage.

Since $\epsilon_2 > \epsilon_1$, most of the voltage appears across d_1 , the air gap. Sparking will occur in the air gap and, charge accumulation takes place on the surface of the insulation. Sometimes the spark erodes the surface of the insulation. As time passes, breakdown channels spread through the insulation in an irregular '**tree**' like fashion leading to the formation of conducting channels. This kind of channeling is called **treeing**.

Under ac voltage conditions treeing can occur in a few minutes or several hours. Hence, care must

be taken to see that no series air gaps or other weaker insulation gaps are formed.

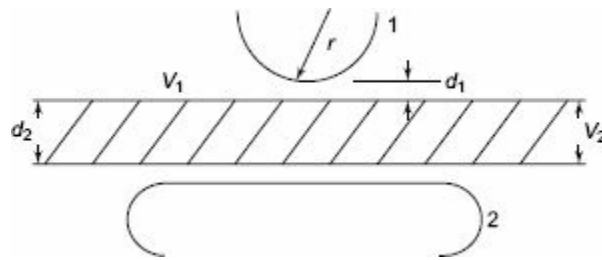


Fig. 4.4 Arrangement for study of treeing phenomenon 1 and 2 are electrodes

Usually, tracking occurs even at very low voltages of the order of about 100 V, whereas treeing requires high voltage. For testing of tracking, a number of international standard testing methods have been used. At present, the method that is generally preferred is the liquid contaminant inclined plane tracking method as described in the standards IEC 587 (1984) and ASTM-D-2303 (1984). IEC method is preferred as it can differentiate between two materials having the same initial tracking voltage but different times to track. Another method, which is also widely used, is described in the standard ASTM-D-495 (1973). In this method, no contaminant is used. The numerical value of the voltage that initiates tracking is called the 'tracking index' and is used to qualify the surface condition of the material under test.

Treeing can be prevented by having clean, dry, and undamaged surfaces and a clean environment. The materials chosen should be resistant to tracking. Sometimes moisture-repellant greases are used. But this needs frequent cleaning and regreasing. Increasing creepage distances should prevent tracking, but in practice the presence of moisture films defeat the purpose.

Usually, treeing phenomenon is observed in capacitors and cables, and extensive work is being done to investigate the real and natural causes of this phenomenon.

4.5.3 Breakdown due to Internal Discharges

Solid insulating materials, and to a lesser extent liquid dielectrics contain voids or cavities within the medium or at the boundaries between the dielectric and the electrodes. These voids are generally filled with a medium of lower dielectric strength, and the dielectric constant of the medium in the voids is lower than that of the insulation. Hence, the electric field strength in the voids is higher than that across the dielectric. Therefore, even under normal working voltages the field in the voids may exceed their breakdown value, and breakdown may occur.

Let us consider a dielectric between two conductors as shown in Fig. 4.5a. If we divide the insulation into three parts, an electrical network of C_1 , C_2 , and C_3 can be formed as shown in Fig. 4.5b. In this, C_1 represents the capacitance of the void or cavity, C_2 is the capacitance of the dielectric which is in series with the void, and C_3 is the capacitance of the rest of the dielectric. When the applied voltage is V , the voltage across the void, V_1 is given by the same Eq. (4.7a).

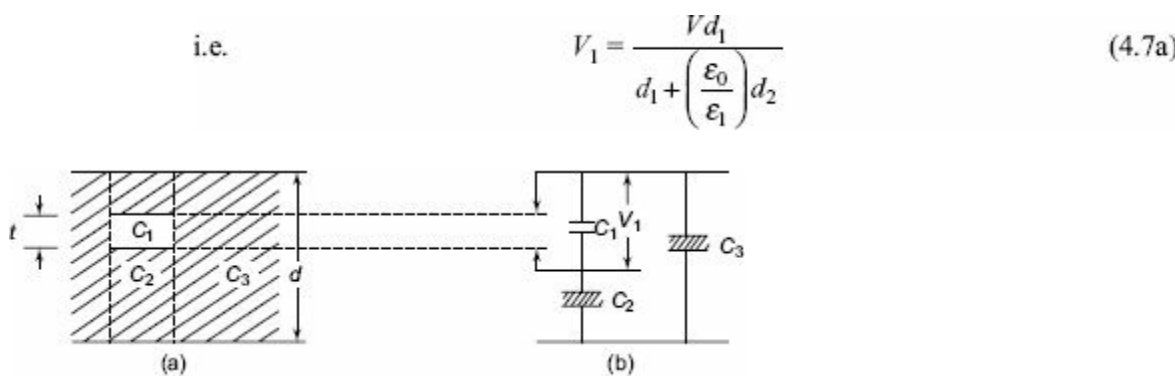


Fig. 4.5 Electrical discharge in a cavity and its equivalent circuit

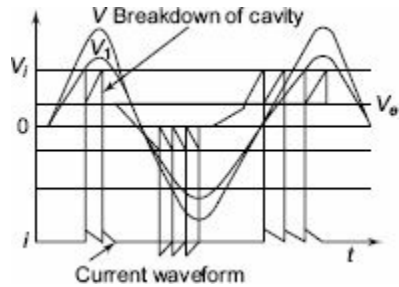


Fig. 4.6 Sequence of cavity breakdown under alternating voltages

where d_1 and d_2 are the thickness of the void and the dielectric, respectively, having permittivities ϵ_0 and ϵ_1 . Usually $d_1 \ll d_2$, and if we assume that the cavity is filled with a gas, then

$$V_1 = V \epsilon_r \left(\frac{d_1}{d_2}\right) \tag{4.8}$$

where ϵ_r is the relative permittivity of the dielectric.

When a voltage V is applied, V_1 reaches the breakdown strength of the medium in the cavity (V_i) and breakdown occurs. V_i is called the ‘discharge inception voltage’. When the applied voltage is ac, breakdown occurs on both the half cycles and the number of discharges will depend on the applied voltage. The voltage and the discharge current waveforms are shown in Fig. 4.6. When the first breakdown across the cavity occurs the voltage across it becomes zero. When once the voltage V_1

becomes zero, the spark gets extinguished and again the voltage rises till breakdown occurs again. This process repeats again and again, and current pulses as shown, will be obtained both in the positive and negative half cycles.

These internal discharges (also called partial discharges) will have the same effect as 'treeing' on the insulation. When the breakdown occurs in the voids, electrons and positive ions are formed. They will have sufficient energy and when they reach the void surfaces they may break the chemical bonds. Also, in each discharge there will be some heat dissipated in the cavities, and this will carbonize the surface of the voids and will cause erosion of the material. Channels and pits formed on the cavity surfaces increase the conduction. Chemical degradation may also occur as a result of the active discharge products formed during breakdown.

All these effects will result in a gradual erosion of the material and consequent reduction in the thickness of insulation leading to breakdown. The life of the insulation with internal discharges depends upon the applied voltage and the number of discharges. Breakdown by this process may occur in a few days or may take a few years.

4.6 BREAKDOWN IN COMPOSITE DIELECTRICS

4.6.1 Introduction

It is difficult to imagine a complete insulation system in an electrical equipment which does not consist of more than one type of insulation. If an insulation system as a whole is considered, it will be found that more than one insulating material is used. These different materials can be in parallel with each other, such as air or SF₆ gas in parallel with solid insulation or in series with one another. Such insulation systems are called *composite dielectrics*.

Composite insulating materials are generally composed of different chemical substances or they come into contact with materials of different compositions. Therefore, chemical reactions occur when a voltage is applied to them, and there will be a substantial increase in the rate of these reactions, if the applied voltage is continuous and high temperatures are present. Under these conditions, the composites undergo chemical deterioration leading to reduction in both the electrical and mechanical strengths.

The composite nature of an insulation system arises from the mechanical requirements involved in separating electrical conductors which are at different potentials. Also, parts of a single system that are normally composed of a single material, are in fact composite in nature. In actual practice, these single materials will normally have small volumes of another material present in their bulk. For example, a solid will contain gas pockets or voids, while a liquid or gas will contain metallic or dust particles, gas bubbles, etc. A commonly encountered composite dielectric is the solid/liquid combination or liquid impregnated flexible solid like thin sheets of paper or plastic. This type of composite dielectric is widely used in a variety of low and high voltage apparatus such as cables, capacitors, transformers, oil-filled switchgear, bushings, etc. In recent years, solid/SF₆ gas technology has become more acceptable.

All the desirable properties of composite dielectrics cannot be realised to the fullest extent owing to the presence of impurities in them. For example, in a solid/liquid system, the presence of gas bubbles in the liquid phase and cavities in the solid phase will give rise to a number of processes, both physical and chemical, which will reduce the dielectric strength of the system.

In the practical system, in order to reduce the undesirable effects mentioned above, composite insulation is used by combining different dielectrics either in series or in parallel such that it is possible to obtain superior dielectric properties than that possible for a single material of the same thickness.

4.6.2 Properties of Composite Dielectrics

A composite dielectric generally consists of a large number of layers arranged one over the other. This is called 'the layered construction' and is widely used in cables, capacitors and transformers. Three properties of composite dielectrics which are important to their performance are given below.

(a) Effect of Multiple Layers The simplest composite dielectric consists of two layers of the same material. Here, advantage is taken of the fact that two thin sheets have a higher dielectric strength than a single sheet of the same total thickness. The advantage is particularly significant in the case of materials having a wide variation in dielectric strength values measured at different points on its surface.

(b) Effect of Layer Thickness Increase in layer thickness normally gives increased breakdown voltage. In a layered construction, breakdown channels occur at the interfaces only and not directly through another layer. Also, a discharge having penetrated one layer cannot enter the next layer until a part of the interface also attains the potential which can produce an electric field stress comparable to that of the discharge channel.

The use of layered construction is very important in the case of insulating paper since the paper thickness itself varies from point to point and consequently the dielectric strength across its surface is not homogeneous. The differences in the thickness impart a rough surface to the paper which can produce an electric field stress comparable to that of the discharge channel. The rough surface of the paper also helps in better impregnation when tightly wound. On the other hand, the existence of areas with lower thickness in the paper can cause breakdown at these points at considerably lower voltages.

Various investigations on composite dielectrics have shown that

- (i) the discharge inception voltage depends on the thickness of the solid dielectric, as well as on the dielectric constant of both the liquid and solid dielectric, and
- (ii) the difference in the dielectric constants between the liquid and solid dielectrics does not significantly affect the rate of change of electric field at the electrode edge with the change in the dielectric thickness.

(c) Effect of Interfaces The interface between two dielectric surfaces in a composite dielectric system plays an important role in determining its pre-breakdown and breakdown strengths. Discharges usually occur at the interfaces and the magnitude of the discharge depends on the associated surface resistance and capacitance. When the surface conductivity increases, the discharge magnitude also increases, resulting in damage to the dielectric.

In a composite dielectric, it is essential to maintain low dielectric losses because they normally operate at high electric stresses. However, even in an initially pure dielectric liquid, when used under industrial conditions for impregnating solid dielectrics, impurities arise, resulting in increased dielectric losses. The effect of various impurities in causing the breakdown of composite dielectrics is discussed in the next section.

4.6.3 Mechanisms of Breakdown in Composite Dielectrics

As mentioned in the earlier section, if dielectric losses are low the cumulative heat produced will be low and thermal breakdown will not occur. However, several other factors can cause short and long time breakdown.

(a) Short-term Breakdown

If the electric field stresses are very high, failure may occur in seconds or even faster without any substantial damage to the insulating surface prior to breakdown. It has been observed that breakdown results from one or more discharges when the applied voltage is close to the observed breakdown value. There exists a critical stress in the volume of the dielectric at which discharges of a given magnitude can enter the insulation from the surface and propagate rapidly into its volume to cause breakdown. Experiments with single discharges on an insulating material have shown that breakdown occurs more rapidly when the electric field in the insulation is such that it assists the charged particles in the discharge to penetrate into the insulation, than when the field opposes their entry. Breakdown was observed to occur more readily when the bombarding particles are electrons, rather than positive ions. In addition, there are local field intensifications due to the presence of impurities and variations in the thickness of solid insulation and these local field intensifications play a very important role in causing breakdown under high field conditions; the actual effect being dependent on the field in the insulation before the discharge impinges on it. A more detailed description is given in the book by Bradley (Reference 4).

(b) Long-term Breakdown

Long-term breakdown is also called the ageing of insulation. The principal effects responsible for the ageing of the insulation which eventually leads to breakdown arise from the thermal processes and partial discharges. Partial discharges normally occur within the volume of the composite insulation systems. In addition, the charge accumulation and conduction on the surface of the insulation also contributes significantly towards the ageing and failure of insulation.

(i) Ageing and Breakdown due to Partial Discharges During the manufacture of composite insulation, gas-filled cavities will be present within the dielectric or adjacent to the interface between the conductor and the dielectric. When a voltage is applied to such a system, discharges occur within the gas-filled cavities. These discharges are called the 'partial discharges' and involve the transfer of electric charge between the two points in sufficient quantity to cause the discharge of the local capacitance. At a given voltage, the impact of this charge on the dielectric surface produces a deterioration of the insulating properties, in many ways, depending on the geometry of the cavity and the nature of the dielectric. The study of breakdown by partial discharges is very important in industrial systems.

The degree of ageing depends on the discharge inception voltage, V_i and the discharge magnitude. It has been shown that V_i is strongly dependent on the permittivity of the dielectric ϵ_r and the thickness of the cavity g . V_i can be estimated approximately by

$$V_i = \left(\frac{E_g}{\epsilon_r} \right) (t + \epsilon_r g) \quad (4.9)$$

where E_g is the breakdown stress of the cavity air gap of thickness g and t is the thickness of the dielectric in series with the cavity. For any given arrangement $(g + t)$ will be constant. Let us call this constant as C . Then, the above equation can be written as

$$V_i = \left(\frac{E_g}{\epsilon_r} \right) [(\epsilon_r - 1)g + C] \quad (4.10)$$

Differentiating, we get

$$\frac{dV_i}{dg} = \frac{\epsilon_r - 1}{\epsilon_r} \left[E_g + \left\{ g + \frac{C}{\epsilon_r - 1} \right\} \frac{dE}{dg} \right] \quad (4.11)$$

Here, E_g is always positive and dE/dg is always negative or zero.

In obtaining the above expressions, two assumptions have been made. One is that in the cavity the stress $E_g = \epsilon_r \cdot E$, where E is the electric field across the dielectric. The other is that within the cavity $E_{g(max)}/E_g = 1$. When these assumptions are valid, the Paschen's law can be used to explain the breakdown of the gas gap (cavity). However, the validity of the above assumptions depends upon the shape and dimensions of the cavity.

For the breakdown of the gas in the cavity to occur, the discharge has to start at one end and progress to the other end. As the discharge progresses, the voltage across the cavity drops due to charge accumulation on the cavity surface towards which it is progressing, and often the discharge gets extinguished. The discharge extinction voltage depends on the conditions inside the cavity. The discharge causes a rise in the temperature and pressure of the gas in the cavity and gaseous deterioration products are also formed. At high frequencies, when the discharges occur very rapidly, these may cause the extinction voltage levels to reach lower values in spite of the erosion of the cavity walls.

From the above analysis the following conclusions can be arrived at

- (i) for very small cavities, V_i decreases as the cavity depth increases, following the Paschen curve of gas breakdown.
- (ii) in spite of the erosion in the cavity walls, breakdown will not occur and the life of the insulation is very long if the applied voltage is less than $2V_i$.
- (iii) for applied voltages greater than $2V_i$, erosion is faster and therefore ageing of the insulation is quicker.
- (iv) the total capacitance of the cavity is not discharged as a single event but as a result of many discharges, each discharge involving only a small area of the cavity wall determined by the conductivity of the cavity surface in the region of the discharge.

Further details on ageing and breakdown due to partial discharges can be had from the book edited by A. Bradley (1984).

(ii) Ageing and Breakdown due to Accumulation of Charges on Insulator Surfaces

During discharges at the solid or liquid or solid-gas or solid-vacuum interfaces, certain quantity of charge (electrons or positive ions) gets deposited on the solid insulator surface. The charge thus deposited can stay there for very long durations, lasting for days or even weeks. The presence of this charge increases the surface conductivity, thereby increasing the discharge magnitude in subsequent

discharges. Increased discharge magnitude in subsequent discharges causes damage to the dielectric surface. Experiments using electro-photography and other methods have shown that transverse discharges occur on the faces of the dielectric, and these discharges cause a large area to be discharged instantaneously. Charges that exist in surface conductivity are due to the discharges themselves such that changes in discharge magnitude will occur spontaneously during the life of a dielectric.

It has been generally observed that the discharge characteristics change with the life of the insulation. This can be explained as follows: for clean surfaces, at the discharge inception voltage V_i , the discharge characteristic depends on the nature of the dielectric, its size and shape. The discharge normally consists of a large number of comparatively small discharges originating from sites on the insulator surface where the necessary discharge condition exists. After some time, erosion at these sites causes the discharges to decrease in number as well as in magnitude, and consequently total extinction may occur. With the passage of time, the phenomena involved become complex because the charges from the surface-induced conductivity add to the charge accumulation in the bulk due to partial discharges.

4.7 SOLID DIELECTRICS USED IN PRACTICE

The majority of the insulating systems used in practice are solids. They can be broadly classified into three groups: organic materials, inorganic materials and synthetic polymers. Some of these materials are listed in [Table 4.2](#) below.

Organic materials are those which are produced from vegetable or animal matter and all of them have similar characteristics. They are good insulators and can be easily adopted for practical applications. However, their mechanical and electrical properties always deteriorate rapidly when the temperature exceeds 100°C. Therefore, they are generally used after treating with a varnish or impregnation with an oil. Examples are paper and pressboard used in cables, capacitors and transformers.

Inorganic materials, unlike organic materials, do not show any appreciable reduction (< 10%) in their electrical and mechanical properties almost up to 250°C. Important inorganic materials used for electric applications are glasses and ceramics. They are widely used for the manufacturer of insulators, bushings, etc., because of their resistance to atmospheric pollutants and their excellent performance under varying conditions of temperature and pressure.

Table 4.2 Classification of solid insulation materials

Organic materials	Inorganic materials	Synthetic polymers	
		Thermoplastic	Thermosetting
Amber	Asbestos	Polyethylene	Bakelite
Cotton	Ceramics	Perspex	Epoxy resins
Paper	Glass	Polypropylene	Crosslinked
Pressboard	Mica	Polystyrene	Polyethelene
Rubber		Polyvinyl chloride	Phenolics
Wax			Elastomers
Wood		Polycarbonate	Melamine

Synthetic polymers are the polymeric materials which possess excellent insulating properties and can be easily fabricated and applied to the apparatus. These are generally divided into two groups, the thermoplastic and the thermosetting plastic types. Although they have low melting temperatures in the range 100–120°C, they are very flexible and can be moulded and extruded at temperatures below their melting points. They are widely used in bushings, insulators, etc. Their electrical use depends on their ability to prevent the absorption of moisture.

Some of the important dielectric properties of some of the above materials are discussed as follows.

Another way of classification of solid in insulating materials is based on the thermal endurance. The insulation is primarily meant to resist electrical stresses. In addition, it should also be able to withstand certain other stresses which the insulation encounters during manufacture, storage, and operation. The performance of the insulation depends on its operating temperature. The higher the temperature, the higher will be the rate of its chemical deterioration, and hence the lower will be its useful life. If a reasonably long life of an insulation is expected, its operating temperature must be maintained low. Therefore, it is necessary to determine the limits of temperature for the insulation, which will ensure safe operation over its expected life. Thus, the insulating materials are grouped into different classes O, A, B, and C with temperature limits of 90°C, 105°C, and 130°C for the first three classes and no specific limit fixed for class C. Classes O and A cover the various organic materials without and with impregnation respectively, while classes B and C cover inorganic

materials, respectively with and without a binder. With the advent of newer insulating materials, namely, the plastics and silicones, during the middle of this century, a need was felt to reorganize the classification of the insulating materials. This led IEC (International Electrotechnical Commission) to come up with the new categories:

Class Y (formerly O) 90°C Paper, cotton, silk, natural rubber, polyvinyl chloride, etc., without impregnation.

Class A 105°C Same as class Y but impregnated, and nylon.

Class E 120°C Polyethylene terephthalate (terylene fibre, melinex film), cellulose triacetate, polyurethanes, polyvinyl acetate enamel.

Class B 130°C Mica, fibreglass (alkali free alumino borosilicate), bitumenized asbestos, Bakelite, polyester enamel.

Class F 155°C As class B but with alkyd and epoxy-based resins.

Class H 180°C As class B with silicone resin binder, silicone rubber, aromatic polyamide (nomex paper and fibre), polyimide film (enamel, varnish and film), and estermide enamel.

Class C Above 180°C As class B, but with suitable non-organic binders; teflon (polytetrafluoroethylene), and other high-temperature polymers. Sub-groups in class C are 200°C, 220°C and 250°C and above.

The temperatures mentioned above cannot be regarded as the limiting operating temperatures but only as an index to compare the various insulating materials. All the international standards permit the equipment to work up to these temperatures, but in practice, certain differentials are allowed because of the overloads, other manufacturing advantages and economics.

4.7.1 Paper and Boards

The kind of paper normally employed for insulation purposes is a special variety known as tissue paper or Kraft paper. Paper and paper boards used for dielectric purposes are produced from cotton, organic fibres, mica, glass and ceramics. Generally, if the thickness of paper is 0.8 mm or higher it is called *paper board*. Boards of higher thickness are made by laminating many layers of paper with an adhesive to get the desired thickness. These are called pressboards and are used in transformers and bushings as supporting materials and insulating barriers. The thickness and density of paper vary depending on the application. Low-density paper (0.8 gms/cm^3) is preferred in high frequency capacitors and cables, while medium density paper is used in power capacitors. High-density papers are preferable in dc and energy storage capacitors and for the insulation of dc machines.

Paper is hygroscopic. Therefore, it has to be dried and impregnated with impregnants, such as mineral oil, chlorinated diphenyl and vegetable oils. The relative dielectric constant of impregnated paper depends upon the permittivity of cellulose of which the paper is made, and permittivity of the impregnant and the density of the paper. [Table 4.3](#) gives the dielectric constants for different densities of paper impregnated with different impregnants.

When very thin (thickness $8\text{--}20 \mu\text{m}$) paper is used, it is very essential to see that the number of conducting particles on the surface of the paper is minimum. The conventional method of detecting conducting particles is by means of using a roller and plate, the conduction being indicated by means of headphones.

Table 4.3 Classification of solid insulating materials

Impregnant	Density of paper (g/cm^3)		
	0.8	1.0	1.2
Trichlorodiphenyl at 20°C ($\epsilon_r = 6.1$)	6.28	6.30	6.40
Trichlorodiphenyl at 50°C ($\epsilon_r = 5.6$)	6.0	6.14	6.24
Pentachlorodiphenyl at 20°C ($\epsilon_r = 5.7$)	5.71	5.88	6.06
Transformer oil ($\epsilon_r = 2.2$)	3.26	3.72	4.30

4.7.2 Fibres

Fibres when used for electrical purposes will have the ability to combine strength and durability with extreme fineness and flexibility. The fibres used are both natural and human-made. They include cotton, jute, flax, wool, silk (natural fibres), rayon, nylon, terylene, Teflon, and fibreglass.

The properties of fibrous materials depends on the temperature and humidity. [Figures 4.7](#) and [4.8](#) show the variation of ϵ_r and $\tan \delta$ of various fibrous materials. It can be observed from these figures that ϵ_r decreases with temperature, while $\tan \delta$ is higher at lower frequencies. Most of the perfectly dried fibres have a dielectric constant between 3 and 8. The presence of ionic impurities (e.g., salt) considerably reduces the electrical resistance of the fibre. Artificial fibres, such as terylene and fibreglass absorb very little water and hence have very high resistance. [Table 4.4](#) gives the density, ϵ_r and $\tan \delta$ of various fibres.

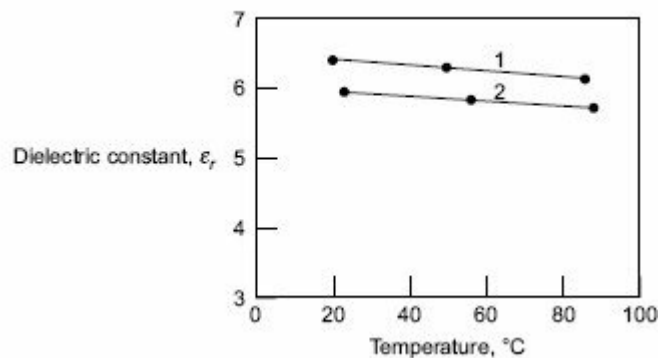
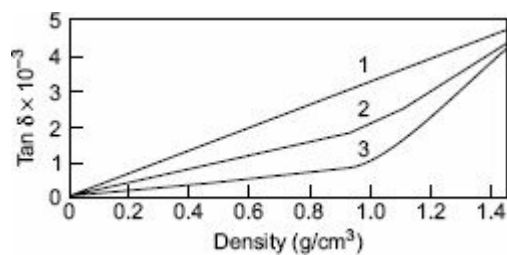


Fig. 4.7 Variation of dielectric constant, ϵ_r , with temperature for paper

1. Trichlorodiphenyl impregnated paper
2. Pentachlorodiphenyl impregnated paper



1. Trichlorodiphenyl impregnated paper;
2. Mineral oil impregnated paper; 3. Dry paper

Fig. 4.8 Variation of $\tan \delta$ with the density of paper

Table 4.4 Electrical properties of fibrous dielectrics

<i>Fibres</i>	<i>Density</i>	ϵ_r	$\tan \delta$
<i>Vegetable Fibre—Natural</i>			
Cotton	1.53	4.4–7.3	0.120
Flax	1.53	4.4–7.3	0.120
Jute	1.53	4.4–7.3	0.120
<i>Animal Fibre—Natural</i>			
Wool	1.31	1.52	0.016
Silk	1.30	3.4	0.016
<i>Man-made Fibres</i>			
Rayon	1.52	2.03	0.031
Acetate (cellulose acetate)	1.33	2.2	0.015
Nylon	1.14	2.51	0.053
(Polyamide)		(3.5–4.2)*	
Terylene (Decrom)	1.38	1.97	0.030
Teflon (P.T.F.E.)	2.30	1.9–2.2	0.001–0.003
Fibreglass	2.54	5–7	0.001–0.0025

* Dielectric constant when the material contains no air voids.

4.7.3 Mica and Its Products

Mica is the generic name of a class of crystalline mineral silicates of alumina and potash. It can be classified into four main groups: (i) muscovite, (ii) phlogopite, (iii) fibiolite, and (iv) lipidolite. The last two groups are hard and brittle and hence are unsuitable for electrical insulation purposes. Mica can be split into very thin flat laminae. It has got a unique combination of electrical properties, such as high dielectric strength, low dielectric losses, resistance to high temperatures and good mechanical strength. These have made it possible for it to be used in many electrical apparatus. Very pure mica is used for high-frequency applications. Spotted mica is used for low voltage insulation, such as for commutator segment separators, armature windings, switchgear and in electrical heating and cooling equipments. [Table 4.5](#) shows the electrical properties of mica.

Mica is built into sheet form by bounding together with a suitable resin or varnish. Depending on the type of application, mica can be mixed with the required type of resin to meet the operating temperature requirements. Micanite is another form of mica which is extensively used for insulation purposes. Mica splittings and mica powder are used as fillers in insulating materials, such as glass and phenolic resins. The use of mica as a filler results in improved dielectrics strength, reduced dielectric loss and improved heat resistance and hardness of the material. The grading of muscovite mica which is widely used for insulation purposes is described in the standard ASTM D 351 (1990).

Table 4.5 *Electrical properties of Muscovite and Phlogopite mica*

<i>Property</i>	<i>Muscovite</i>	<i>Phlogopite</i>
Chemical formula	$K_2O.3Al_2O_3.6SiO_2.2H_2O$	$K_2O.6MgO.Al_2O_3.6SiO_2.2H_2O$
Hardness(shore)	76–106	77–101
Tensile strength (0.02–0.05 mm thick)	17–36 kgf/mm ²	16–26 kgf/mm ²
Compressive strength (20 × 20 mm sample, 10–20 mm thick)	2000–5800 kgf/cm ²	1500–4600 kgf/cm ²
Dielectric strength (upto 30°C)	1000 kV/mm	700 kV/mm
Dielectric constant (1 kHz–3000MHz)	6–7.5	6–7.5
Loss tangent	0.03 (50 Hz) 0.001 (1 MHz)	0.03 (50 Hz) 0.001 (1 MHz)
Surface resistivity (60% humidity)	10^{11} – 10^{12} ohm-cm	10^{10} – 10^{11} ohm-cm
Volume resistivity (constant up to 200°C)	10^{14} – 10^{15} ohm-cm	10^{13} – 10^{14} ohm-cm

4.7.4 Glass

Glass is a thermoplastic inorganic material comprising complex systems of oxides (SiO_2). The dielectric constant of glass varies from 3.7 to 10 and the density varies from 2.2 to 6 g/cm^3 . At room temperature, the volume resistivity of glass varies from 10^{12} to 10^{20} ohm-cm. The dielectric loss of glass varies from 0.004 to 0.020 depending on the frequency. The losses are highest at lowest frequencies. The dielectric strength of glass varies from 3000 to 5000 kV/cm and decreases with increase in temperature, reaching half the value at 100°C . Glass is used as a cover and for internal supports in electric bulbs, electronic valves, mercury arc switches, X-ray equipment, capacitors and as insulators in telephones.

4.7.5 Ceramics

Ceramics are inorganic materials produced by consolidating minerals into monolithic bodies by high temperature heat treatment. Ceramics can be divided into two groups depending on the dielectric constant. Low-permittivity ceramics ($\epsilon_r < 12$) are used as insulators, while the high permittivity ceramics ($\epsilon_r > 12$) are used in capacitors and transducers.

[Tables 4.6](#) and [4.7](#) give the various dielectric properties of some ceramics commonly used for electrical insulation purposes.

Porcelain and steatite are dense and chemically inert to all alkalies and most of the acids. Therefore, they are corrosion-proof and resistant to contamination. Steatite possesses higher mechanical strength and low ϵ_r hence is used for making electronic components. Also, alumina (Al_2O_3) has replaced quartz because of its superior mechanical strength, better insulating properties and good thermal conductivity. It is used in the fabrication of high-current vacuum interrupters and a variety of electrical and ceramic components. Its powder is used for making sheets and various forms of composite insulators. At present, alumina based porcelains, because of their higher mechanical strength, are being widely used for suspension-type insulators and station type post insulators.

Table 4.6 Properties of low-permittivity ceramics

Property	HT porcelain	LT porcelain	Low loss steatite	Alumina	Forsterite
Chemical composition	50% Clay, 25% Feldspar, 25% Flint	50% Clay, 25% Feldspar, 25% Flint	3 MgO, 4 SiO ₂ , H ₂ O	95%	2MgO, SiO
Water absorption (p.p.m.)	0	0.5–2	0	0	0
Safe temperature (°C)	1000	900	1050	1600	1050
Dielectric strength (kV/mm)	25	3	8–25	16	8–12
ϵ_r	5–7	5–7	6	9	6
$\tan \delta \times 10^4$	50–100	100–200	10	5	3–4

Table 4.7 Properties of high-permittivity ceramics

Ceramics	Chemical composition	ϵ_r	$\tan \delta \times 10^4$
Magnesium metatitanate	MgTiO ₃	16	2
Strantium zirconate	SrZrO ₃	38	3
Titanium oxide	TiO ₂	90	5
Calcium titanate	CaTiO ₃	150	3
Strantium titanate	SrTiO ₃	200	5
Barium titanate	BaTiO ₃	1500	150

4.7.6 Rubber

Rubber is a natural or synthetic vulcanizable high polymer having high elastic properties. Electrical properties of rubber depend on the degree of compounding and vulcanizing. General impurities, chemical changes due to ageing, moisture content and variations in temperature and frequency have substantial effects on the electrical properties of rubber. Some important electrical properties and applications of different types of rubber are given in [Table 4.8](#).

Also, there are polymeric materials which exhibit elastic properties similar to those of rubber. The most commonly used polymeric materials are called elastomers. The most commonly used elastomers for high voltage applications are silicone rubber, Ethylene Propylene Rubber (EPR) and Ethylene Propylene Dien Monomer (EPDM).

Table 4.8 *Properties and applications of rubber*

Type of rubber	Water absorption (per cent)	ϵ_r (50 Hz)	$\tan \delta$ (50 Hz)	ac breakdown voltage kV/cm	Application and limitations
Natural rubber	0–4.8	2.9–6.6	0.02–0.1	100–390	Inexpensive, flexible, good electrical properties, resistant to corona, maximum operating temperature 60°C.
Polysar kryflex rubber and Styrene butadine rubber	0–4.5	3.8–6.2	0.02–0.09	80–380	Used for low voltage (< 11 kV) cables. Not good under weathering, water, oils, etc.
Butyl rubber and Polysar butyl rubber	0–2	2.2–3.2	0.003–0.03	80–200	Used in aerial, submarine and underground cables. Good electrical properties at low temperatures. Excellent resistance to tear, abrasion, acids, alkalies and chemicals.
Silicone rubber	0–3	2.6–3.4	0.006–0.02	90–390	Used in shipping and aircraft cables, transformers, lightning equipment, etc. High service temperature (150°C). Easily attacked by acids, alkalies and chlorinated compounds.

Silicone rubber insulation can be safely used in the temperature range of -55°C to 200°C . Silicone rubber exhibits good resistance to ozone, corona and changing weather conditions. It also has good resistance to alcohol, dilute acids, alkylies and almost all types of oils and waxes. However, silicone rubber shows signs of erosion in the presence of halogenated hydrocarbons, aromatic solvents, concentrated acids and steam.

Silicone rubber is widely used for cable insulation. High-temperature Vulcanized (HTV) silicone rubber is being used in the manufacture of outdoor high voltage insulators and also in the form of extended sheds on ceramic insulators to improve their performance under severely polluted conditions. For applications in outdoor high voltage insulators, another type of silicone rubber called the Room Temperature Vulcanized (RTV) rubber is also used.

Table 4.9 *Comparative properties of silicone rubber and EPDM*

<i>Property</i>	<i>HTV Silicone rubber</i>	<i>EPDM</i>
Dielectric strength (kV/mm)	20.01	19.7–31.5
Dielectric constant (1 MHz)	3.0–3.6	2.5–3.5
Dissipation factor (1 MHz)	0.005	0.007
Volume resistivity (Ω -m)	10^{13}	10^{14}
Specific gravity	1.15–1.55	0.85
Elongation, % (ASTM-D412)	200	200
Comparative abrasion resistance	Fair	Good
Water resistance	Good	Excellent
Maximum operating temp.	200°C	177°C
Flame resistance	Poor	Poor
Resistance to ozone	—	Excellent

Silicone rubber is immune to ultraviolet radiation. As on today, all the electrical utilities are attempting to use silicone rubber for the sheds of all types of overhead line insulators.

Ethylene-propylene rubber (EPR) is primary an extruded dielectric and is used in medium and high voltage power cables. Its electrical properties, such as electrical stability under wet conditions, flexibility and resistance to corona and water tree formation are very useful in these applications.

Three types of EPRs are in use for overhead line insulation purposes. They are ethylene-propylene monomer (EPM), EPDM and a copolymer of ethylene-propylene and silicone (ESP). All these types of EPRs are filled with alumina and other types of fillers. [Table 4.9](#) shows a comparison of the properties of silicone rubber and EPDM.

From the table it can be seen that EPDM has excellent resistance to ozone and water. EPRs are being employed successfully for distribution and transmission class insulators of up to 765 kV ratings. However, their long-term performance under pollution has been unsatisfactory. This type of insulators are still relatively new and will require a few more years in operation to discover the reasons for their pollution performance and to suggest improvements.

4.7.7 Plastics

Plastics (polymeric materials) used for electrical insulation purposes consist of long chain macromolecules with repeating monomer units. A polymer is named by putting the prefix *poly* in front of the monomer. For example, propylene monomer becomes polypropylene. Some of the polymers used in current insulation practice are: polyethylene, PTFE, PVC, polypropylene, polystyrene, polyisobutane (butyl rubber), polyester, polybutadiene, polymethyl meta-crylate (PMMA), etc.

Simple polymer chains form branches from the main chain. This is commonly found in polyethylene. This branching reduces the potential for regular molecular packing and reduces the density. As a result, in the case of polyethylene, low-density polyethylene is formed. Besides branching, polymers also have ‘cross links’ in which polymer chains are joined by short, long or even polymeric molecules resulting in one gigantic cross-linked polymer. Cross-linked polymers are generally obtained by using the curing technique. Polymers which are not cross-linked can be remoulded into other shapes and are called *thermoplastics*. Polyethylene, polycarbonate and acetal copolymers are examples of thermo-plastics used for insulation purposes. [Table 4.10](#) summarizes important dielectric properties of the thermoplastic materials used in practice.

Table 4.10 Properties of thermoplastics used for electrical insulation

Thermoplastics	Dielectric strength (kV/mm)	ϵ_r at		Tan at		Maximum service temperature °C
		60 Hz	10^6 Hz	60 Hz	10^6 Hz	
Polyphenylene sulphide	15.0	3.1	3.2	0.0003	0.0007	205
Polyether sulphone	15.7	3.5	3.5	0.001	0.004	180
Poly carbonate	15.0	3.2	3.0	0.009	0.01	130
Acetal homopolymer	15.0	3.7	3.7	—	0.0048	90
Acetal copolymer	15.0	3.7	3.7	0.001	0.006	105
Acrylic (PMMA)	19.7	3.7	2.2	0.05	0.3	95

Plastics are very widely used as insulating materials because of their excellent dielectric properties. Many new developments in electrical engineering and electronics would not have been possible without the development of plastics. Plastics are made by combining large numbers of small molecules into a few big ones. When small molecules link to form the bigger molecules of the plastics, many different types of structures result. Most thermoplastic resins approximate to a structure in which several thousand atoms are tied together in one direction. The thermosetting resins on the other hand, form a three-dimensional network. In view of the large number of plastics available, it will not be possible to deal with all of them, and only materials which are commonly used for insulation purposes are described.

(a) Polyethylene Polyethylene is a thermoplastic material which combines unusual electrical properties, high resistance to moisture and chemicals, easy processability, and low cost. It has got high resistivity and good dielectric properties at high frequencies, and therefore, is widely used for power and coaxial cables, telephone cables, multi-conductor control cables, TV lead-in wires, etc.

By varying the methods of manufacture different types of polyethylene are made with specific properties for different applications. They may have low density, medium density, high density or may be irradiated types. The dielectric properties of these are summarized in [Table 4.11](#).

Table 4.11 Electrical properties of polyethylene

Property	Low density polyethylene	Medium density polyethylene	High density polyethylene	Irradiated polyethylene
Volume resistivity (ohm-cm)	$> 10^{16}$	$> 10^{16}$	$> 10^{16}$	$> 10^{16}$
Dielectric strength (kV/cm)	170–280	200–280	180–240	720–1000
Dielectric constant (50 Hz– 10^6 Hz)	2.3	2.3	2.35	2.3
$\tan \delta$ (50 Hz– 10^6 Hz)	0.0002	0.0002	0.0002	0.0005
Arc resistance	melts	melts	melts	melts

(b) Fluorocarbon Plastics Polytetrafluoroethylene (PTFE), polychlorotri-fluoroethylene (PCTFE) and polyvinylidene (PVF₂) plastics come under this category. PTFE is the most thermally stable and chemically resistant of all the three. It is considered as one of the best plastics used for insulation because of its excellent electrical and mechanical properties. It can be used without decomposition up to temperatures of 327°C. It is widely used in almost all applications. PCTFE has higher dielectric constant and loss factor than PTFE, but melts at 1900C. PVF₂ can be worked in the temperature range –30°C to 150°C. It is used as thin wall insulation, as jacketing for computer wires and special control wires, and for tubing and sleeving for capacitors, resistors, terminal junctions, and solder sleeves. The electrical properties of fluorocarbons are tabulated in [Table 4.12](#).

Table 4.12 Properties of fluorocarbon plastics

Property	PTFE	PCTFE	PVF ₂
Volume resistivity (ohm-cm)	$> 10^{18}$	1.2×10^{18}	2×10^{14}
Dielectric strength (kV/cm)	200	210	104–512
Dielectric constant (50 Hz– 10^6 Hz)	2.0	2.3–2.8	8.4–6.49
$\tan \delta$ (50 Hz– 10^6 Hz)	< 0.0002	0.0012–0.0036	0.0491–0.15

(c) Nylon Nylon is a thermoplastic which possesses high impact, tensile, and flexural strengths over a wide range of temperature (0 to 3000°C). It also has high dielectric strength and good surface and volume resistivities even after lengthy exposure to high humidity. It is also resistant to chemical action, and can be easily moulded, extruded and machined. It is generally recommended for high frequency low loss applications. In electrical engineering, nylon mouldings are used to make coil forms, fasteners, connectors, washers, cable clamps, switch housings, etc.

Table 4.13 Dielectric properties of nylon

Property	Nylon 6/6	Nylon 6	Nylon 6/10
Volume resistivity (ohm-cm)	4.5×10^{13}	10×10^{13}	4×10^{14}
Dielectric strength (kV/cm)	154	176–204	190
Dielectric constant			
50 Hz	4.1	5.0–14.0	4.6
10^3 Hz	4.0	4.9–10.1	4.5
10^6 Hz	3.4	4.0–4.7	3.5
tan δ			
50 Hz	0.014	0.06–0.10	0.04
10^3 Hz	0.02	0.06–0.10	0.04
10^6 Hz	0.04	0.04–0.13	0.03

There are three different types of nylon commonly used. They are nylon 6/6, nylon 6 and nylon 6/10. The dielectric properties of these three types are given in [Table 4.13](#).

(d) Polyvinyl Chloride Polyvinyl chloride or PVC is used commercially in various forms. It is available as an unplasticized, tough, and rigid sheet material and can be easily shaped to any required form. It is chemically resistant to strong acids and alkalis and is insoluble in water, alcohol and organic solvents like benzene. The upper temperature limit of operation is about 60°C. The dielectric strength, volume resistivity and surface resistivity are relatively high. The dielectric constant and loss tangent are 3.0–3.3 and 0.015–0.02 respectively, at all frequencies up to 1 MHz.

PVC is also available as a highly plasticized flexible material, which is used extensively for wire covering, insulated sleeving, and cable sheathing in preference to natural rubber because of its resistance to the action of sunlight, water and oxygen.

(e) Polyesters Polyesters have excellent dielectric properties and superior surface hardness, and are highly resistant to most chemicals. They represent a whole family of thermosetting plastics produced by the condensation of dicarboxylic acids and dihydric alcohols, and are classified as either saturated or unsaturated types. Unsaturated polyesters are used in glass laminates and glass fibre reinforced mouldings, both of which are widely used for making small electrical components to very large structures. Saturated polyesters are used in producing fibres and film. Polyester fibre is used to make paper, mat and cloth for electrical applications. The film is used for insulating wires and cables in motors, capacitors and transformers. The dielectric properties of polyester compounds are given in [Table 4.14](#).

Table 4.14 Dielectric properties of polyesters

Property	Glass reinforced type		Cast resins	
	Premixed	Preformed	Rigid	Flexible
Volume resistivity (ohm-cm)	10^{12} – 10^{15}	10^{14}	10^{12} – 10^{14}	—
Dielectric constant				
50 Hz	5.3–7.3	3.8–6.0	3.3–4.3	4.4–8.1
10^3 Hz	4.68	4.0–6.0	3.2–4.3	4.5–7.1
10^6 Hz	5.6–6.4	3.5–5.5	3.2–4.3	4.1–5.7
tan δ				
50 Hz	0.01–0.04	0.01–0.04	0.006–0.05	0.026–0.031
10^3 Hz	—	0.01–0.05	0.006–0.04	0.016–0.050
10^6 Hz	0.008–0.022	0.01–0.03	0.017–0.019	0.020–0.060

Mylor polyester film is being largely used in preference to paper insulation. At power frequencies,

its dissipation factor is very low, and it decreases as the temperature increases. It has got a dielectric strength of 2000 kV/cm, and its volume resistivity is better than 10^{15} ohm-cm at 100°C. Its high softening point enables it to be used at temperatures above the operating limit of paper insulation. It has got high resistance to weathering and can be buried under the soil also. Therefore, this can be used for motor and transformer insulation at power frequencies and also for high frequency applications which are subjected to varying weather conditions.

(f) Polystyrenes

Polystyrenes are obtained when styrene is polymerized with itself or with other polymers or monomers producing a variety of thermoplastic materials with varying properties in different colours. Electrical grade polystyrenes have a dielectric strength comparable to that of mica, and have low dielectric losses which are independent of the frequency. Their volume resistivity is about 10^{19} ohm-cm and the dielectric strength is 200–350 kV/cm. The dielectric constant at 20°C is 2.55, and the loss tangent is 0.0002 at all frequencies up to 10,000 MHz.

Polystyrene films are extensively used in the manufacture of low loss capacitors, which will have a very stable capacitance and extremely high insulation resistance. Films and drawn threads of polystyrene are also used for high frequency and cable insulations.

4.7.8 Epoxy Resins

Epoxy resins are thermosetting types of insulating materials. They possess excellent dielectric and mechanical properties. They can be easily cast into desired shapes even at room temperature. They are very versatile, and their basic properties can be modified either by the selection of a curing agent or by the use of modifiers or fillers. They are highly elastic; samples tested under very high pressure, up to about 180,000 psi (12,000 atm) returned to their original shape after the load was removed, and the sample showed no permanent damage. Resistance to weathering and chemicals is also very good. The tensile strength of araldite *CT 200* and hardner *HV 901* is in the range 5.5–8.5 kg/mm², and the compressive strength is 11–13 kg/mm². The dielectric constant varies between 2.5 and 3.8. The dielectric loss factor is very small under power frequency conditions lying in the range 0.003–0.03. The dielectric strength is 75 kV/mm, when the specimen thickness is 0.025 mm or 1 mil. The volume resistivity of the material is of the order of 10¹³ ohm-cm.

Epoxy resin can be formed into an insulator of any desired shape for almost any type of high voltage application. Insulators, bushings, apparatus, etc., can be made out of epoxy resin. It can also be used for encapsulation of electronic components, generator windings and transformers. It is used for bonding of very diverse materials such as porcelain, wood, metals, plastics, etc. It is a very important adhesive used for sealing of high-vacuum joints. In any laboratory or industry in which electrical or electronic components or equipments are handled or manufactured, numerous occasions arise wherein epoxy resins can be used with an advantage saving time, labour and money.

To improve the electrical and mechanical properties of the end product of the epoxy resins (in which two components are mixed), they are loaded with fibre glass, fused silica and other particulate fillers. These fillers may form more than 50% of the weight of the epoxy. The relative permittivity of the epoxy resins can be higher in the range of 3.5 to 5. These epoxy resins are extensively used in high voltage switchgear and as insulation in rotating machines. They are also finding applications in transformer winding encapsulation and as insulating spacers in SF₆ Gas Insulated Transmission System (GITS), SF₆ circuit breakers and in SF₆ Gas Insulated Sub-stations (GIS). Glass-fiber reinforced epoxy rods and hydrated aluminium filled epoxys are widely used for overhead transmission line insulators, bushings and bus bar insulators.

4.7.9 High-Temperature High-Performance Polymers

High-performance polymer films are thermoplastic and are generally transparent. They are needed for use in applications where temperatures vary from very low (-269°C) to very high ($+400^{\circ}\text{C}$) values. Such applications include space shuttle solar arrays, high speed locomotive and other motor armature slot liners, capacitors, transformers, miniaturized electronic components, microprocessor chip carriers, cryogenic cables and other applications at cryogenic temperatures. Successful application of these polymers is due to the unique combination of their electrical, physical and mechanical properties and their ability to retain these properties over a wide temperature range, where other insulating materials may fail.

(a) Perfluoro Carbon Films

High temperature materials used in practice include Fluorocarbon films such as Teflon (PTFE) and Perfluoroalkoxyl (PFA), Polyimide films such as Kapton and its grades (made by DuPont), Polycarbonate (PC), Polyethylene (PE) and composites such as Polybenzomidole (PBI), Nomex and Kavalor. Important properties of these materials and their applications in electrical and electronic equipments/devices are described below.

Perfluoro carbon film is a transparent thermoplastic that can be heat sealed, metallized, laminated and used as an excellent adhesive. Teflon (PTFE), perfluoroalkoxy (PFA) and polyvinylidene fluoride (PVDF) are the perfluoro carbon films used for electrical insulation purposes. These films are chemically inert and will not dissolve in virtually any chemical except in molten alkyl-metal fluorine gas and chlorine trifluoride at higher temperatures and pressures. Teflon is the most inert of all the plastics. Perfluoro carbon films have high dielectric strength 26.5 kV/mm for 25 micrometers thick film and are non-wettable and non-charring. They have very low dielectric constant of 2.0 and low dielectric loss of 0.0002 at a frequency of 100 Hz which increases to 0.0007 at 100 MHz.

Some important characteristics of these films are given in [Table 4.15](#).

Table 4.15 Summary of characteristics of fluoropolymer films

Fluoropolymer	Advantages	Limitations
Polytetrafluoroethylene (PTFE)	Widest useful thermal range of all plastics (-267° to 260°C) unaffected by virtually all chemicals. Dielectric constant is relatively unchanged (about 2.1) with time, frequency or temperature.	Poor resistance to corona and radiation.
Perfluoroalkoxyl (PFA)	Dielectric, mechanical, thermal and chemical properties equal to PTFE. Better mechanical properties than PTFE above 150°C . Can be processed by conventional extrusion techniques.	Lower abrasion resistance and higher in price than PTFE.
Polyvinylidene fluoride (PVDF)	Can be solvated by organic esters and ketones as well as processed by conventional extrusion techniques. High abrasion resistance and resistance to UV and nuclear radiation.	Highest dielectric constant and dissipation factor of all fluoropolymers. Chemical resistance lowest. Useful thermal range -62° to 150°C

Perfluoro carbon films are mainly used under severe conditions of temperature and environment. Applications include wrapped insulation on high temperature wires and cables, motor coil, phase and ground insulation, as capacitor dielectric and as substrate for flexible printed circuits and flexible cables.

(b) Imidepolymers: Polyimide Film

(i) *General Properties* Polyimide film has the best thermal properties of all organic films. The film made by DuPont under the trade name *Kapton* in USA and by ICI with the trade name *Upilex*. Polyimide films possess unique properties of combinations that permit them to be used at extremely high and low temperatures.

Kapton film has no melting point and can be successfully used over the temperature range of -269°C to $+350^{\circ}\text{C}$. It can function continuously at 240°C without losing any of its properties. It retains its dielectric strength even at high temperatures. Physical properties include high tensile strength and high resistance to creep and abrasion. The dielectric properties other than the dielectric strength show reduction with increase in temperature. Resistance to radiation and ultraviolet light are very good. However, the film is vulnerable to attacks by alkalies and strong inorganic acids. The moisture absorption rate is the highest for all dielectric films.

(ii) *Dielectric Properties* The dielectric properties of Kapton HN film are given in [Table 4.16](#) below.

Table 4.16 Electrical properties of Kapton HN film

Property	Property Value at Film Thickness (μm)						Method
	7.6	12.7	25.4	50.8	76.2	127	
Dielectric Strength (kV/mm)	11.8	11.8	23.6	19.7	17.7	11.8	ASTM D-149-94 (Average of ten specimens). AC voltage at 500 V/sec rate of rise to the break-down voltage.
Volume Resistivity, ohm-cm at 200°C	10^{12}	10^{12}	10^{12}	10^{12}	10^{12}	10^{12}	ASTM D-257-93
Dielectric constant at 1 kHz	4.0	4.0	3.9	3.9	3.9	3.9	ASTM D-150-94. Using conducting silver paint electrodes, two-terminal system of measurement at standard conditions.
Dissipation factor at 1 kHz	0.0070	0.0050	0.0036	0.0036	0.0036	0.0036	Same as above

(iii) *Corona resistance of polyimide films* Like all organic materials, Kapton film is subject to damage by a corona discharge. At moderate rate of corona, equipments insulated with this material have not shown any damage due to corona up to 3000 hours. This means that brief exposure to corona discharges will not significantly affect the working life of the film. The experimental investigations on $25\ \mu\text{m}$ thick HN film showed that corona inception level does not depend on duration of applied voltage and pre-stressing of the insulating HN films. Therefore this film can be used to make insulated magnet wire, wrappers and slot insulation without fear of damage due to corona.

(iv) *Types of Kapton Film* There are three main types of Kapton films which are commercially

available.

- HN, an all-purpose that can be laminated, metallized or adhesive coated. It has been successfully used in a variety of applications at temperature as low as -269°C and as high as $+400^{\circ}\text{C}$.
- Type VN similar to type HN but with better dimensional stability.
- Type FN, a type HN film coated on both the sides with Teflon PTFE fluorocarbon resin to give it heat sealing, provide resistance to moisture entry and to enhance resistance to chemicals.

(v) *Applications in Electrical/Electronic Equipment/Devices* Kapton polyimide film can be used in a variety of electronic and electrical insulation applications, such as motor slot insulation, transformer and capacitor insulation, formed coil insulation, magnet wire insulation and for flexible printed circuits. Because of its relatively high cost, this film is mainly used where its unique properties make it the only suitable and also where its use permits economy in the design. It is used in motors where it replaces thicker dielectrics, thus making the motor more powerful without increasing its size. It is also used in aerospace electrical equipment where it is subjected to temporary overvoltages and in the construction of wire and cable where the film provides considerable savings in space with weight.

Further, the Kapton film is compatible with many high temperature impregnating varnishes including polyimides, epoxies, silicones and esterimides which are used in the manufacture of electrical equipment.

(c) Polycarbonate (PC) and Imide Polymers

One of the most recently developed resins is polycarbonate which is used for a variety of electrical and electronic applications. This polymer is manufactured by General Electric of USA. Polycarbonate film has good heat resistance, flexibility and dielectric characteristics. It is resistant to attack by oils, fats and dilute acids but is affected by alkalies and esters and aromatic hydrocarbon. Water vapour and gas transmission rates are relatively high. Because of its greater cost efficiency and heat resistance it is widely used in electrical industry for capacitors, conductor insulation, coil insulation and slot insulation. This is called lexan polymer.

Noryl, is a modified Polypropylene Oxide (PPC), is an amorphous material which has excellent electrical, mechanical and thermal properties and is used widely in electrical industry. On account of its flexibility, it is primarily used for wire and coil insulation. It can be operated continuously up to temperatures of 190°C .

Table 4.17 Electrical properties of polycarbonate and other polymers*

Polymer	Breakdown strength (kV/mm)	Thickness = 1.6 mm				Maximum operating temperature ($^{\circ}\text{C}$)
		ϵ_r at		$\tan \delta$ at		
		50 Hz	1 MHz	50 Hz	1 MHz	
<i>Lexan</i> (303 R)	20	3.0	2.9	0.0014	0.0067	150
<i>Noryl</i> (N 180)	23	3.32	2.55	0.0054	0.056	190
<i>Valox</i> (753)	24	4.65	3.4	0.0028	0.031	200
<i>Ultem</i> (2400)	24	3.76	3.07	0.0033	0.031	225

*Ref: GE Plastics, Catalogue No. elec 75, Engineering Materials in Electrical Industry.

Valox is a thermoplastic polyester and can be used up to 200°C with no loss in electrical

properties. It can also be filled with mineral and glass and these grades give higher temperature resistance and increased flexibility. These properties make it an ideal choice for use in circuit breakers, switches and plugs.

Among the Imide polymers, polyetherimide (PEI) film produced by General Electric with a trade name *Ultem*, was introduced into the market in 1993. It competes with polyimide film for applications in transformers and motors. The film has dielectric strength comparable to that of polyimide film but with higher thermal conductivity and lower moisture absorption at significantly less cost. Minimum film thickness is $25\ \mu\text{m}$. It retains its dielectric strength up to 250°C and is an ideal material for the fabrication of components designed in a hostile environment. [Table 4.17](#) gives the electrical properties of polycarbonate and other polymers.

In the previous sections details are given of a variety of insulating materials, commonly used for electrical insulation purposes. A good insulating material should have good dielectric strength, high mechanical strength, high thermal conductivity, very low loss factor, and high insulation resistance. The specific application of these materials in various power apparatus, electronic equipments, capacitors and cables are discussed in [Chapter 5](#).

In [Table 4.18](#), a comparison of electrical properties of commonly used high-temperature insulation is given

Table 4.18 *Electrical properties of high-temperature materials*

Material	Max. temperature of operation $^\circ\text{C}$	ϵ_r at 1 MHz	$\tan \delta$ at 1 MHz	Vol. resistivity ohm-m	Dielectric strength KV/cm
PTFE	260	2.1	0.003	$>10^{16}$	~ 20
PFA(Teflon)	260	2.1	0.003	$>10^{16}$	~ 22
FEP (Fluorinated ethylene Propylene)	205	2.1	0.003	$>10^{16}$	~ 20
PCTFE	200	2.5	0.006	$>10^6$	~ 20
Silicone rubber	200	3 to 3.6	—	$\approx 10^{15}$	—

K
T E R M S
Y

- Solid Dielectrics
- Breakdown Processes
- Intrinsic Breakdown
- Avalanche Breakdown
- Thermal Breakdown
- Treeing and Tracking
- Internal Discharges
- Composite Dielectrics
- Ageing Processes and Longterm Breakdon.
- Solid Dielectrics Materials, their Properties

WORKED EXAMPLES

Example 4.1 *A solid specimen of dielectric has a dielectric constant of 4.2, and $\tan \delta = 0.001$ at*

a frequency of 50 Hz. If it is subjected to an alternating field of 50 kV/cm, calculate the heat generated in the specimen due to the dielectric loss.

Solution Dielectric heat loss at any electric stress E [Eq. (4.5)]

$$= \frac{E^2 f \epsilon_r \tan \delta}{1.8 \times 10^{12}} \text{ W/cm}^3$$

For the specimen under study, the heat loss will be

$$= \frac{50 \times 50 \times 10^6 \times 50 \times 4.2 \times .001}{1.8 \times 10^{12}}$$

$$= 0.291 \text{ mW/cm}^3$$

Example 4.2 A solid specimen of dielectric dielectric constant of 4.0, shown in the figure has an internal void of thickness 1mm. The specimen is 1cm thick and is subjected to a voltage of 80 kV(rms). If the void is filled with air and if the breakdown strength of air can be taken as 30 kV(peak)/cm, find the voltage at which an internal discharge can occur.



Solution Referring to Fig. 4.5(a) and Eqs (4.7) and (4.8), the voltage that appears across the void is given as

$$V_1 = \frac{V d_1}{\left(d_1 + \frac{\epsilon_0}{\epsilon_1} d_2 \right)}$$

where, $d_1 = 1 \text{ mm}$

$$d_2 = 9 \text{ mm}$$

$$\epsilon_0 = 8.89 \times 10^{-12} \text{ F/m}$$

$$\epsilon_1 = \epsilon_r \epsilon_0 = 4.0 \epsilon_0$$

$$V_1 = \frac{V \times 1}{\left(1 + \frac{9}{4} \right)} = \left(\frac{4V}{13} \right)$$

The voltage at which the air void of 1 mm thickness breaks down is $3 \text{ kV/mm} \times 1 \text{ mm} = 3 \text{ kV}$

$$V_1 = \frac{13V}{4} = \frac{13 \times 3}{4} = \frac{39}{4}$$

$$= 9.75 \text{ kV (peak)}$$

The internal discharges appear in the sinusoidal voltage $80\sqrt{2} \sin \omega t \text{ kV}$ when the voltage reaches a value of 9.75 kV (see Fig. 4.6 for the discharge pattern).

Example 4.3 A coaxial cylindrical capacitor is to be designed with an effective length of 20 cm. The capacitor is expected to have a capacitance of 1000 pF and to operate at 15 kV, 500 kHz. Select a suitable insulating material and give the dimensions of the electrodes.

Solution The capacitance of the coaxial cylindrical capacitor is

$$\frac{2\pi\epsilon_0\epsilon_r l}{\ln \frac{d_2}{d_1}} \quad (1)$$

where l = length in metres, d_1 and d_2 are the diameters of the inner and outer electrodes, and ϵ_r = dielectric constant. The dielectric material that can be selected is either polyethylene or PTFE.

Choosing high-density polyethylene, its dielectric constant $\epsilon_r = 2.3$, and its breakdown stress is taken as 500 V/mil or 200 kV/cm. Allowing a factor of safety of 4, the maximum stress $E_{\max} = 50$ kV/cm. E_{\max} occurs near the inner electrode and is given by

$$E_{\max} = \frac{V}{r_1 \ln \frac{r_2}{r_1}} \quad (2)$$

From Eq. (1),

$$\ln \frac{d_2}{d_1} = \ln \frac{r_2}{r_1} = \frac{2\pi\epsilon_0\epsilon_r l}{\text{capacitance}}$$

$$= \frac{2\pi \frac{10^{-9}}{36\pi} \times 2.3 \times 0.2}{100 \times 10^{-12}} = 0.02556$$

\therefore

$$\frac{r_2}{r_1} = 1.026$$

From Eq. (2),

$$r_1 = \frac{V}{E_{\max} \ln \frac{r_2}{r_1}}$$

$$= \frac{15}{50 \times 0.02556} = 11.74 \text{ cm}$$

\therefore

$$r_2 = 1.026 \times 11.74 = 12.05 \text{ cm}$$

The thickness of the insulation is 3.1 mm (refer to [Tables 4.11](#) and [4.15](#) for the properties of the material).

MULTIPLE-CHOICE QUESTIONS

- The intrinsic breakdown strength of solid dielectrics is about
 - 50 to 100 kV/mm
 - 500 to 1000 kV/mm
 - 5 to 10 kV/mm
 - 1 to 5 kV/mm
- The usual mechanism of breakdown in solid dielectrics is
 - intrinsic breakdown
 - electromechanical breakdown
 - thermal breakdown

(d) chemical breakdown

3. Long-term deterioration and breakdown occurs in solid dielectrics due to

(a) thermal phenomenon

(b) surface discharges

(c) internal discharges

(d) treeing phenomenon

4. Paper insulation is mainly used in

(a) cables and capacitors

(b) transformers

(c) rotating machines

(d) circuit breakers

5. Thermal classification of insulating materials is done for

(a) gases

(b) liquids

(c) solids

(d) composite insulation

6. Breakdown is permanent in

(a) gases

(b) liquids

(c) solids

(d) in all the three

7. The material used for insulation that is exposed to atmosphere is

(a) ceramics and glass

(b) polyesters

(c) inorganic insulation

(d) rubber and plastics

8. For high frequency applications the following plastic is preferred

(a) polyethylene

(b) polyvinyl chloride (PVC)

(c) polyester

(d) polystyrene

9. The operating temperatures of polyethylene insulation is

(a) -30° to 50°

(b) -60° to 150°

(c) -50° to 80°

(d) 0° to 100°

10. Epoxy resins are used as insulation when

(a) composite insulation is required

(b) when cast in insulation mould is required

(c) for very high temperature applications are needed

(d) filler materials are required

11. Electromechanical breakdown occurs when the thickness due to electrical stress is compressed or reduced to about

(a) 0.9

(b) 0.8

(c) 0.7

(d) 0.6

2. Thermal breakdown occurs when the heat generated inside the insulating material is
 - (a) equal to or greater than the heat dissipated
 - (b) less than that the heat generated from the surface
 - (c) only under ac voltage application
 - (d) none of the above
3. Breakdown due to internal discharges develops
 - (a) in milliseconds
 - (b) in few seconds
 - (c) over a long duration of several days
 - (d) all the above
4. Electrochemical breakdown and deterioration of insulating material is due to
 - (a) temperature rise
 - (b) oxidation, hydrolysis or some other chemical action
 - (c) only due to hydrolysis and moisture effects
 - (d) none of the above
5. Aging in electrical insulating materials under an electrical field means
 - (a) gradual reduction in dielectric strength which may lead to breakdown
 - (b) decrease in insulation resistance of the materials
 - (c) progressive building up of disruptive discharges inside the material
 - (d) all the above
 - (e) none of the above

Answers to Multiple-Choice Questions

- | | | | | | |
|---------|---------|---------|---------|---------|---------|
| 1. (b) | 2. (c) | 3. (c) | 4. (a) | 5. (c) | 6. (c) |
| 7. (a) | 8. (d) | 9. (c) | 10. (b) | 11. (d) | 12. (a) |
| 13. (c) | 14. (b) | 15. (d) | | | |

REVIEW QUESTIONS

1. What do you understand by 'intrinsic strength' of a solid dielectric? How does breakdown occur due to electrons in a solid dielectric?
2. What is 'thermal breakdown' in solid dielectrics, and how is it practically more significant than other mechanisms?
3. Explain the different mechanisms by which breakdown occurs in solid dielectrics in practice.
4. How does the 'internal discharge' phenomena lead to breakdown in solid dielectrics?
5. What is a composite dielectric and what are its properties?
6. Describe the mechanism of short-term breakdown of composite insulation.
7. How do the temperature and moisture affect the breakdown strength of solid dielectrics?
8. What are the advantages of using plastic film insulation over the paper insulation?
9. What are the properties that make plastics more suitable as insulating materials?
10. What are the special features of epoxy resin insulation?
11. Explain the phenomenon 'treeing and tracking' in solid insulating materials under electrical stress. How does it lead to breakdown?
12. What is composite insulation? How does short-term breakdown differ from long-term

breakdown?

REFERENCES

1. O'Dwyer, J.J., *Theory of Dielectric Breakdown in Solids*, Clarendon Press, Oxford (1964).
2. Von Hippel, A., *Dielectric Materials and Applications*, John Wiley, New York (1964).
3. Clark, F.M., *Insulating Materials for Design and Engineering Practice*, John Wiley, New York (1962).
4. Bradley, A., *Electrical Insulation*, Peter Peregrinus, London (1984).
5. Gallagher, T.J. and Pearmain, A.F., *High Voltage Measurements, Testing and Design*, John Wiley and Sons, New York (1983).
6. Arora, R. and Mosch, W., *High Voltage Insulation Engineering*, Wiley Eastern Ltd., New Delhi, India (1995).
7. Khalifa, M.M. (Ed), *High Voltage Engineering: Theory and Practice*, Marcel Dekker, New York (1990).
8. Shugg, W.T., *Handbook of Electrical and Electronic Insulating Materials*, (2nd Edition), IEEE Press, New York (1995).
9. Sillars, R.W., *Electrical Insulating Materials and Their Applications*, Peter Peregrinus, London (1973).
10. Tanaka, T. and Greenwood, A., *Advanced Power Cable Technology*, CRC Press, Boca Raton, Florida, USA (1983).
11. Bartnikas, R. and Eichhorn, R.M. (Eds), *Engineering Dielectrics, Vol. I, "Corona Measurements and Interpretation"*, ASTM Publications, Philadelphia, USA (1983).
12. Bartnikas, R. and Eichhorn, R.M. (Eds), *Engineering Dielectrics, Vol. IIA, "Electrical Properties of Solid Insulating Materials: Molecular Structure and Electrical Behaviour"*, ASTM Publications, Philadelphia, USA (1983).
13. Dissado, L.D. and Fothergill, J.C., *Electrical Degradation and Breakdown in Polymers*, Peter Peregrinus, London (1992).
14. DuPont Catalogue No. H-3892-3 (Polyimide Films), (2000).
15. DuPont Catalogue No. H-04321-3 (Fluorocarbon Films), (1996).
16. Cherny, E.A., *IEEE Electrical Insulation Magazine*, Vol. 12, No. 3, pp. 7-15 (1996).
17. Hogate, R.C. and Swift, D.A., *IEEE Transactions on Power Delivery*, Vol. 15, No. 4, pp. 1944-1955 (1990).
18. *ASTM Standard*, "Natural Muscovite Block Mica and Thins Based on Visual Quality", D-351 (1990).
19. *IEC Publication*, "Standard Method for Evaluating Resistance to Tracking and Erosion of Electrical Insulating Materials under Severe Ambient Conditions", 587 (1984).
20. *ASTM Standard*, "Dielectric Breakdown Voltage and Dielectric Strength of Electrical Insulating Materials at Power Frequency", D-149 (1983).
21. *ASTM Standard*, "A.C. Loss Characteristics and Dielectric Constant of Electrical Insulating Materials", D-150 (1990).
22. *ASTM Standard*, "Standard Test Method for High Voltage, Low Current Dry Arc Resistance of Solid Electrical Insulation", D-495 (1973).

CHAPTER

5

Applications of Insulating Materials

5.1 INTRODUCTION

There is no piece of electrical equipment that does not depend on electrical insulation in one form or other to maintain the flow of electric current in desired paths or circuits. If due to some reasons the current deviates from the desired path, the potential will drop. An example of this is a short circuit and this should always be avoided. This is done by proper choice and application of insulation wherever there is a potential difference between neighbouring conducting bodies that carry current. There are four principal areas where insulation must be applied. They are between

- (a) coils and earth (phase-to-earth),
- (b) coils of different phases (phase-to-phase),
- (c) turns in a coil (inter-turn), and
- (d) the coils of the same phase (inter-coil).

In this chapter, we deal with the insulation systems in electrical equipments. First we deal with insulation in power apparatus under which insulation in rotating electrical machines, transformers and switchgear is discussed followed by the insulation in capacitors and cables.

5.2 APPLICATIONS IN POWER TRANSFORMERS

Transformers are the first to encounter lightning and other high-voltage surges. The transformer insulation has to withstand very high impulse voltages many times the power frequency operating voltages. The transformer insulation is broadly divided into

- (a) conductor or turn-to-turn insulation,
- (b) coil-to-coil insulation,
- (c) low-voltage coil-to-earth insulation,
- (d) high-voltage coil-to-low voltage coil insulation, and
- (e) high-voltage coil-to-ground insulation.

The low-voltage coil-to-ground and the high-voltage coil-to-low voltage coil insulations normally consist of solid tubes combined with liquid or gas filled spaces. The liquid or gas in the spaces help to remove the heat from the core and coil structure and also help to improve the insulation strengths. The inter-turn insulation is directly applied on the conductor as organic enamel in smaller rating transformers. In the large transformers paper or glass tape is wrapped on the rectangular conductors. In the case of layer to layer, coil-to-coil and coil-to-ground insulations, Kraft paper is used in smaller transformers, whereas thick radial spacers made of pressboard, glass fabric, or porcelain are used in the case of higher rating transformers.

Much of the insulation system used in oil-filled transformers consists of an oil-impregnated pressboard placed around the low and high-voltage windings and supported by the iron core. The thin oil layers within the multilayer pressboard structure result in high dielectric strength, which increases with pressboard density. In addition, the oil passing between the individual pressboard components of insulation structures allows the required heat dissipation in order to achieve necessary electrical and thermal performance.

Conductor insulation is usually paper. Paper by itself is not mechanically strong and dealing with copper conductors which are heavy, a much higher quantity of insulation in the form of pressboard will be required. Over the years, major developments have taken place to improve the quality of insulating materials. The most commonly used insulating board is made of wood or a mixture of wood and cotton. By using the relatively long cotton fibres, the oil impregnation of the wood materials becomes easier to accomplish. Other insulation systems at lower voltage ratings use cast resin as the insulation and air as the coolant. Higher temperature systems, on the other hand, employ synthetic fluids which include silicones and these are usually used in association with high-temperature solid-insulating materials, such as Nomex with resin or polyester glasses. These materials are much more expensive than paper or pressboard.

Gas-insulated power transformers use sheet-aluminium conductors for windings, a polymer film (Mylar) for turn-to-turn insulation, self-contained annular cooling ducts containing circulating cooling gas to cool the windings, and compressed SF₆ gas which insulates all the major gaps.

Transformer oil provides the required dielectric strength and insulation and also cools the transformer by circulating itself through the core and the coil structure. The transformer oil, therefore, should be in the liquid state over the complete operating range of temperatures between -40°C and $+50^{\circ}\text{C}$. The oil gets oxidized when exposed to oxygen at high temperatures, and the oxidation results in the formation of peroxides, water, organic acids and sludge. These products cause chemical deterioration of the paper insulation and the metal parts of the transformer. Sludge being heavy, reduces the heat transfer capabilities of the oil, and also forms as a heat insulating layer on the coil

structure, the core and the tank walls. In present-day transformers, the effects of oxidation are minimized by designing them such that access to oxygen itself is limited. This is done by the use of (a) sealed transformers, (b) by filling the air space with nitrogen gas, and (c) providing oxygen absorbers like activated clay or alumina.

When an arc discharge occurs inside a transformer, the oil decomposition occurs. The decomposition products consist of hydrogen and gaseous hydrocarbons which may lead to explosion. And hence, oil insulated transformers are seldom used inside buildings or other hazardous locations like mines. Under such conditions dry type or sulphur hexafluoride (SF_6) gas filled transformers are used.

5.2.1 Dry-Type Transformers

Apart from oil-filled distribution transformers, dry-type transformers have become important during the last few years. This type of transformers are mainly used in areas where use of oil-filled transformers is risky, such as in apartment complexes, cinema halls, water protection areas and some industrial enterprises.

Insulation of this type of transformers is nowadays done using prepregs. The advantages of these materials are good dielectric strength of the coil, easier production methods and elimination of expensive vacuum impregnation of the low voltage coils. Prepregs are mainly manufactured using the following baking materials: glass fibres, Nomex, aramide papers and multi-layers made of non-woven polyester and polyester films. Esterimide resins and epoxy resins are used as resin systems. It is important that the prepregs are free from any cracks. Prepregs have excellent adhesive capability, good ageing as well as good storage properties.

However, change from vacuum impregnation technology for low-voltage coils to prepreg technology is yet to become popular because of its high cost.

5.3 APPLICATIONS IN ROTATING MACHINES

Rotating machines are normally divided into two categories: those with voltage ratings less than 6,600 V are called low-voltage machines, and the others are high-voltage machines. Because of the difficulty of insulating at high voltages, machines above 22 kV rating are not built except under special conditions. Classes Y and C insulation find no application in rotating machines. Class E which was widely used in low-voltage machines for over 20 years is now being replaced by class F which is meant for high-voltage machines. Also, class F is being increasingly used in place of class B. Thus, class F appears to be the insulation of the future. Considerable progress has been made in recent years, in reducing the size of the machines for a given rating by use of class H materials, particularly, for small machines. However, the cost of class H materials (silicones, teflon) is very high, and hence they are used only under special conditions like severe overloads in traction motors and mill motors. The various materials used in modern rotating machines are tabulated in [Table 5.1](#). This is only a typical listing and may vary depending on the choice of the design engineer.

Mica has been used in the electrical industry since its inception. Normally, mica is available in the form of very thin splittings. Hence, it is bound to a supporting sheet of electrical grade paper or glass cloth with a suitable binding agent. The resulting mica sheets are known as micanite. Since mica splittings of fairly large surface area were not available, methods were evolved to make mica paper using mica of any size. The mica paper so obtained is not sufficiently strong or self-supporting. Hence, it has to be given a backing of glass cloth or other binding material such as epoxy resin. Epoxy-resin-bounded mica paper is extensively used in both low and high-voltage machines.

Table 5.1 Typical insulating material for rotating machines

Component	Low voltage machines			High voltage machines		
	Class E	Class B	Class F	Class B	Class F	
Turn-to-turn insulation	Polyvinyl acetal for both wire and strip conductors	Polyester enamel (wire) or phenolic bonded fibreglass (strip)	Estermide enamel (wire) or alkyd bonded fibreglass (strip)	Phenolic bonded fibreglass (strip)	Alkyd bonded fibreglass (strip)	
Coil-to-coil and phase-to-phase insulation	Inside the slots	Bakelized fabric strips	Bakelized fabric strips	Epoxy fibreglass strips	Shellac or bitumen bonded mica foil or tape on straight portions of the coils	Epoxy impregnated mica paper foil or tape on straight portions of the coil.
	On overhangs	Melinex film bonded to press paper	Alkyd bonded mica glass sheet	Nomex sheet	Alkyd varnished glass tape on coil ends and alkyd bonded mica sheet between layers	Epoxy varnished mica glass sheet between layers
Phase (or coil) to earth insulation	Melinex film bonded to press paper	Mica alkyd bonded to glass cloth	Nomex sheet	No extra insulation because the phase-to-phase insulation itself is sufficient.		
Slot closure (wedge)	Bakelized fabric strip	Bakelized fabric strip	Epoxy fibreglass strip	Bakelized fabric strip	Epoxy fibreglass strip	
Insulation for leads	Alkyd varnished terylene or glass tape or sleeving			Alkyd varnished glass tape		
Varnish for impregnation treatment	Alkyd phenolic	Alkyd phenolic	Estermide or epoxy	Alkyd-phenolic	Epoxy	

In modern insulation practice, there are various requirements of the insulating material for use in electric generators and motors. The selection of the right material depends on the power rating of the motor and the conditions under which it operates. Today, multilayer insulation is made of pressboard and polyester film or Nomex and polyester film, or non-woven polyester and polyester film, with or without impregnation. These are being used for slot insulation. Multi-layers made of Nomex or Kapton polyimide film are used for very high-temperature applications.

In the case of generators, a particularly important parameter is the insulation of rotors and stators

and its reliability. Individual manufacturers have developed their own insulation systems and changes, if any, in the insulation systems are done very carefully. For many decades rotors have been insulated with single layer glass or hard fabrics or with glass fabrics and/or Nomex. These are also used as winding insulation as well as slot insulation. The main insulation of the stators have always been mica based. In addition, conducting non-woven polyesters are used for corona protection both inside and at the edges. Particularly important parameter of an insulating system is the support between the winding bars, slots and the core laminations. Glass fiber reinforced epoxy wedge profiles which allows long service life are used for this purpose.

The maintenance of good mechanical properties is also equally important for the reliable operation of machines. The insulation should withstand the expansion and contraction during temperature cycles in large machines. These effects become very severe at the high temperatures observed in power generators of a very large size. Maintenance of good mechanical properties and thermal endurance are very essential in low voltage machines also.

5.4 APPLICATIONS IN CIRCUIT BREAKERS

A circuit breaker is a switch which automatically interrupts the circuit when a critical current or voltage rating is exceeded. Ac currents are considerably easier to interrupt than dc currents. Ac current interruption generally requires first to substitute an arc for part of the metallic circuit and then its deionization when the current goes through zero, so that the arc will not re-establish again.

Circuit breakers are also divided into two categories, namely, the low-voltage and high-voltage types. Low voltage breakers use synthetic resin mouldings to carry the metallic parts. For higher temperatures ceramic parts are used. When the arc is likely to come into contact with moulded parts, melanine or some special kind of alkyd resins are used because of their greater arc resistance.

Nowadays most of the circuit breakers that are in operation, use SF₆ gas or vacuum as insulating medium. While vacuum circuit breakers are available up to voltage ratings of 33 kV, SF₆ circuit breakers are manufactured up to the higher transmission voltage of 800 kV. Most of the present-day SF₆ circuit breaker designs are virtually maintenance free. This means that the arcing contacts and nozzles on the interrupters should have a long service life. Most arcing contacts are fitted with copper–tungsten alloy chips. This alloy is used to control both the erosion rate of the tips and the emission of copper vapour from the contacts.

The nozzle is the most important component of a buffer-type interrupter. The performance of the interrupter is governed by the nozzle geometry, shape, size and nozzle material. The materials normally chosen are either very pure PTFE or filled PTFE. Pure PTFE can produce carbon molecules absorbing the radiated arc energy. Filled PTFE gives better performance than pure PTFE. There are three types of filling materials used to make filled PTFE. They are, boron nitride, molybdenum and aluminium oxide. Although filled PTFE is slightly more expensive than pure PTFE, its consistent performance and extra long life justifies the use in high current interrupters. Further, epoxy and polyurethane and other polymeric materials are being widely used for potting, encapsulation and mouldings to replace other traditional materials in circuit breakers and transformers.

5.4.1 Arc Interruption in Gas Mixtures

Pure SF₆ gas is very efficiently used in the present-day circuit breakers for interrupting currents up to 63 kA and 80 kA. However, it is an expensive gas and at the normal operating pressure of 6 bar (g), it condenses at temperatures lower than -20°C. Therefore several gas mixtures have been studied with the objective of effectively using them in switchgear. One such mixture is SF₆/N₂ whose dielectric strength, is 80% of that of pure SF₆, but its interrupting performance does not compare favourably with that of pure SF₆ gas. The short circuit rating of SF₆/N₂ circuit breaker is normally lower, i.e., its value reduces to 40 kA from 50 kA for an SF₆ insulated circuit breaker.

With circuit breakers for voltage of 550 kV the number of interrupters per phase has reduced from 6 to 1 in recent years. Therefore, the dielectric performance has become very important. In circuit breakers, due to the very high temperatures produced during interruption, SF₆ gas decomposes into its various constituents, some of which are toxic. Long-term resistance of the insulating material to SF₆ decomposition products is essential and therefore most manufacturers use alumina-filled cast-resin insulators.

The different types of insulating materials used in the construction of high-voltage switchgear are classified in [Table 5.2](#). This includes some of the modern insulating materials for future applications. Of these, a few are widely used as major insulants. They are porcelain, synthetic resin bonded paper laminates, epoxy resins, SF₆ gas and vacuum.

Table 5.2 *Insulation in high-voltage switchgear*

<i>Materials</i>	<i>Applications</i>
Epoxy resins	Low-pressure castings for bushings, switchgear orifices, bus-bars, instrument transformers
Epoxy-resin-bonded glassfibre	For components such as arc control devices, circuit breaker operating rod
Polyester resins	Insulating lever for circuit breaker and phase barrier plate in switch board
Porcelain	Insulators and bushings of power transformers, circuit breakers and instrument transformers
Vulcanized fibre	Arc-chamber segments
Synthetic-resin-bonded paper	Bushings, arc chambers, etc.
Nylon	Injection mouldings for arc control devices in circuit breakers
Silicone rubber	Filling for moulded joint boxes in SF ₆ insulated circuit breakers

5.5 APPLICATIONS IN CABLES

In the recent years, natural rubber has been completely replaced by synthetic rubbers and plastics as cable insulation. The physical properties required for wire and cable insulation depend on the type of application. It should have good elongation and tensile strength and toughness, so that it will withstand handling during installation and service. It should also have low dielectric constant and power factor but high dielectric strength and insulation resistance. Also, during operation, because of overloading, the insulation may be exposed to high temperatures for long periods of time. This necessitates the insulation to have excellent resistance to ageing at high temperatures. The insulation should also be able to withstand long exposure to sunlight and various chemicals. Cables are also laid in rivers and under the sea. For these applications it should have very low water absorption. When cables have to operate at low temperature, the insulation should not become stiff and brittle. The partial discharges in the cable insulation should also be kept as low as possible.

The main types of insulants used in the cable industries are paper, rubber, plastics and compressed gas. Paper-insulated lead-sheathed cables are still used because of their reliability, high dielectric strength, low dielectric loss, and long life. The most commonly used insulating materials for low and medium-voltage (up to 3.3 kV) cables is polyvinylchloride (PVC). Polyethylene and cross-linked polyethylene are also used. PVC is not suitable for high voltage applications because of its high dielectric constant and high loss. It cannot be operated continuously at higher voltages, although it can be used up to 85°C continuous at low voltages. On the other hand, polyethylene has low dielectric constant and low loss with high dielectric strength. The best material for high-voltage and high-temperature operation is teflon (PTFE) which can be used up to 250°C. Silicone rubber has a high degree of heat resistance for continuous operation up to 150°C. It gives rise to very little carbon formation when destroyed by fire, and as such, it continues to function even after the fire. Hence it is used for aircraft cables where contamination with aircraft fuel can occur at very high temperatures.

Table 5.3 Cable insulations

Insulation	Maximum cable operating voltage ac (kV)	Range of operating temperature (°C)
(a) <i>Impregnated Paper</i>		
Solid type	95.0	-10 to 85
Oil-filled	400.0	-20 to 70
Gas-filled	400.0	-20 to 70
Varnished cloth	28.0	-10 to 80
(b) <i>Rubber</i>		
Synthetic-neoprene	0.6	-30 to 90
Synthetic-silicone	5.0	-40 to 150
Synthetic-butyl	28.0	-40 to 80
(c) <i>Plastics</i>		
PVC	0.6	-30 to 105
Polyethylene	15.0	-60 to 80
Teflon	5.0	-54 to 250
Fluorothenes	5.0	-54 to 150

In paper insulated cables the paper is impregnated with oil by the process of mass impregnation using free-flowing liquid. [Table 5.3](#) gives the various insulating materials used in cables and the maximum cable operating voltages and temperatures.

5.5.1 High-Voltage Cable Technology

High-voltage cables and the insulation technology used for their manufacture are given in [Table 5.4](#). The insulation is mainly paper based and is divided into three broad categories described as follows.

Table 5.4 *Insulation and technology of HV cables*

<i>Medium-Voltage (Up to 33 kV)</i>	<i>High-Voltage 33 to 400 kV and above</i>
Lapped paper, dried and impregnated with viscous or non-draining compound as per BS 6480, ESI 09-12, IEC 55	Lapped paper, dried and impregnated with low viscosity oil, as per C47, NGTS 3 : 5 : 1, IEC 141-1
Extruded PVC	Extruded vulcanised (EP) rubbers
Extruded Vulcanized (EP) rubbers as per BS 6622, IEC 502	Extruded cross-linked polyethylene (XLPE) TPS 2/12
Extruded cross-linked polyethylene (XLPE) as per BS 6622, IEC 502	

(a) Paper-Based Laminated Construction The construction of the above insulation of the high voltage cable is done by building up its thickness with a large number of layers of a thin sheet material like paper. Paper provides manufacturing flexibility and it is available in high electrical quality (cellulose paper). A multiple-layer construction has the advantage that a defective layer only marginally weakens the whole system both electrically and mechanically. For the purpose of design, an AC field strength of upto 15 kV/mm or (100 kV lightning impulse) is typical for low viscosity oil impregnated paper. Typical value of dielectric constant is 3.5 and that of dielectric loss factor ($\tan \delta$) is 0.0025.

(b) Polymeric Insulation Extrusion of a polymer to form the insulating wall of the cable offers the possibility of high production speed along with the advantages of polymeric materials. Polymers can be selected to have dielectric losses less than 10% of the cellulose paper and the intrinsic dielectric strength as high as 4 times that of oil impregnated paper and thermal conductance 30% higher. The disadvantage of this type of insulation is that a single defect can have a disastrous effect on the dielectric integrity of the whole cable. At voltages of 120 kV and below compounds of ethylene-propylene (EP) rubber are being used. The benefit of this material is that it is water resistant. An alternative to EP rubbers in XLPE.

5.6 APPLICATIONS IN POWER CAPACITORS

In most of the industrial applications, the power requirements are reactive in nature and a lagging current is drawn from the power lines. This requires additional generating capacity. This can be compensated by using capacitors which take a leading current in ac circuits. Hence, the greatest use of power capacitors is with the power frequency systems. Capacitors are made in simple units with voltage ratings for 220 to 13800 V with kVAR ratings varying from 0.5 to 25 kVAR. Power capacitors are normally made using impregnated paper dielectric. Power capacitors are also used for high-frequency applications, such as power-factor correction in high-frequency heaters and induction furnaces. At high frequencies, the dielectric losses increase very rapidly, and the capacitors have to be cooled externally using water cooling. Capacitors are also used in dc applications such as impulse voltage generators, energy storage, welding and high intensity flash X-ray and light photography.

Generally, power capacitors are made of several layers of insulation paper of adequate thickness and aluminium foil of 6-micron thickness as electrodes interleaved and wound. Single units are connected in parallel depending on the rating of the capacitor unit to be manufactured. These are placed in containers hermetically sealed, thoroughly dried, and then impregnated with insulating oil. The impregnating oils used are either mineral oil or chlorinated diphenyl oil. Capacitors made with mineral oil are quite expensive, and hence capacitors made with chlorinated diphenyl are preferred for power-factor correction applications because of their low cost and non-inflammability.

Properties required for the insulation paper for capacitor applications are high dielectric strength, low dielectric loss, high dielectric constant, uniform thickness, and minimum conducting particles. The recently discovered polypropylene film has low dielectric loss and higher operating voltage. However, paper is still widely used partly, mainly due to the reason that paper after impregnation offers many desirable properties required for use at high voltages in addition to economy.

The impregnants for power capacitors should have high dielectric strength, high dielectric constant, good chemical and thermal stability and adequate viscosity for efficient conduction of heat. Mineral oils with high aromatic content have traditionally been used. However, they have been replaced by a variety of synthetic oils such as di-isopropylnaphthalene (DIPN), mono-isopropylbiphenyl (MIPP) and phenylxylenhane (PXE) because of their high gas-absorbing abilities, high dielectric strength and dielectric constant. Properties of some of these impregnants used in capacitors are summarized in [Table 5.6](#). The dielectric properties of the tissue paper and the capacitor impregnants are given in [Table 5.5](#) and [5.6](#).

Table 5.5 Characteristics of tissue paper

(a) <i>Fibre Composition</i>	
Unbalanced sulphate	100%ASTM
Ash	less than 0.3%
Moisture	4 to 8%
(b) <i>Water Extract</i>	
Conductivity	less than 4 μ Siemens/cm
pH value	6.0–7.5
Chloride content	less than 5 mg/kg
Standard thickness	10, 12, 13, 14, 15, and 18 micron
Conducting particles	nil
Density	1 or 1.2 g/cm ³

Table 5.6 Properties of impregnating of high-voltage capacitors

Property	Impregnating oil				
	MO	DIPN	PXE	MIPB	PMS
Specific gravity	0.88	0.96	0.99	0.99	0.97
Viscosity 30° (cSt)	11.0	8.5	8.0	8.3	35
ϵ_r (50 Hz, 80°C)	2.18	2.48	2.51	2.55	2.65
Tan δ (50 Hz, 80°C)	0.01	0.005	0.005	0.005	0.08
Breakdown voltage (kV/mm)	28	32	32	32	14.5
Fire point (°C)	135	144	148	140	317
Pour point (°C)	-32	-47.5	-47.5	-50	-77

MO: Mineral Oil DIPN: Di-Isopropyl Naphthalene PXE: Phenylxyl ethane
MIPB: Mono Isopropyl Biphenyl PMS: Phenylmethyl Dimethyl Siloxane

The electrode material extensively used in aluminium foil of 6 microns thickness because of its high tensile strength, low specific resistance, high melting point, low specific gravity, low cost, and easy availability.

As already mentioned, the latest trend in capacitor manufacture is to replace paper by polypropylene plastic films. This results in a drastic reduction in size. Its use results in cheaper capacitors for high-voltage ratings because of its high working stress. As regards impregnants, askarels are harmful to the environment and hence are being banned. The latest trend is to develop other types of material. With this in view, research is being directed towards the use of vegetable oils like castor oil.

5.7 APPLICATIONS IN HIGH-VOLTAGE BUSHINGS

5.7.1 Condenser Bushings

At rated voltages higher than 52 kV, the condenser or capacitance graded bushing principle is generally used. The insulating material for such a bushing is paper which is treated. There are three types of such paper, viz., resin-bonded paper (RBP), oil-impregnated paper (OIP) and resin impregnated paper (RIP). The paper is generally wound onto a central tube and conducting layers are then inserted to form a series of concentric capacitors between the tube and the mounting flange. The diameter and length of each layer is designed such that the partial capacitances give a uniform axial stress distribution and control the radial stress within the limits of the insulating material.

In *resin bonded paper (RBP) bushings*, the paper is first coated with phenolic or epoxy resin and wound into a cylindrical form under heat and pressure, after inserting conducting layers at appropriate intervals. They are designed to operate at a maximum radial stress of 20 kV/cm. On the other hand, *oil impregnated paper bushings (OIP)* are made by winding untreated paper after inserting conducting layers at the appropriate positions and then impregnating with oil after vacuum drying. The paper used is generally an unleached kraft paper and the oil used is a mineral oil. Prior to impregnation, processing is carried out to ensure that the moisture and gas contents are low. These bushings are designed to operate at a typical radial stress of 40 kV/cm. *Resin impregnated paper bushings (RIP)* are being used up to voltages of 520 kV. In its manufacturing process, creped paper tape or sheet is wound onto a conductor and dried in an autoclave under strictly controlled heat and vacuum conditions. Epoxy resin is then added to fill the winding. These bushings are designed to operate at a radial stress of about 30 kV/cm.

5.8 APPLICATIONS IN FRACTIONAL HORSEPOWER MOTORS

(a) Small Generators and Starters These are mass-produced items and are used in the automobile industry. Therefore the insulation system must guarantee reliability, combined with good processing capability, mechanical strength and tolerance to severe short-thermal stress while in operation. For this kind of application, the following materials have been found to have excellent insulation properties, viz., presspaper reels, NMN multilayers (made of Nomex and polyester film) as well as saturated DMD (made from non-woven polyester and polyester film). These materials are cured with high-quality resin impregnation on both the sides.

(b) Small-size Motors These motors are made in large numbers and are used in automobile industry and in household appliances. They should give reliable service in operation which involve vibrations. Manufacturers of this type of motors use pressboard as the main insulation. In contrast to polyester film, pressboard has no melting point. This board has been widely used in small size motors over many decades. Further, in the case of electric power tools, the main insulation is the multilayer material made of pressboard and polyester film. The greatest advantages of this material is that it can withstand short-term thermal stresses.

In recent years, many new high-temperature polymers have been developed and are being widely used as insulating materials in small-size electric motors and generators and for a variety of electronic applications, including manufacture of PCB, electronic components, etc. Details of these materials involving their characteristics, operating temperature ranges and applications have already been described in the previous chapter ([Sec. 4.7](#), [Chapter 4](#)).

K
TERMS
Y

- Temperature Classification for Insulating Materials
- Application of Insulating Materials in Electrical Apparatus
- Transformers
- Rotating Machines
- Switchgear
- Cables, Capacitors and other Apparatus

MULTIPLE-CHOICE QUESTIONS

1. The most commonly used liquid for transformer insulation is
 - (a) mineral oil
 - (b) askerals
 - (c) silicone oil
 - (d) polyester oils
2. For generator coil insulation the class of insulation used is
 - (a) class A
 - (b) class B

(c) class C

(d) class F

3. The insulation used in high voltage circuit breakers of large power rating is

(a) air

(b) vacuum

(c) SF₆

(d) mineral oil

4. For HV cable insulation, the materials used are

(a) glass and ceramic

(b) silicone rubber

(c) XLPE

(d) paper-oil insulation

5. Askerals are not used as transformer or capacitor insulation in recent years because

(a) it has less dielectric strength

(b) its density and dielectric constant are high

(c) it decomposes easily giving out toxic gases

(d) it is highly flammable

6. Gas insulation is nowadays used in

(a) generators

(b) motors

(c) transformers

(d) circuit breakers and substations

7. Synthetic liquid dielectrics are mainly used in

(a) capacitors and cable insulation as impregnants

(b) In transformer insulation

(c) In circuit breakers

(d) all the three above a, b, and c

8. Resins and varnishes are mainly used for

(a) transformer coil impregnation

(b) Generator and motor coil impregnation

(c) In cable and capacitor insulation

(d) overhead line insulation

9. For high temperature applications such as few motor or generator coils with class F or H insulation the materials used are

(a) Polymer films (Mylar, etc.)

(b) Polyester films

(c) Glass fibre reinforced epoxy or polyester films

(d) PTFE or PXE films

10. In high-voltage switch gear, the insulation used inside the breaker (arc chambers) is

(a) Epoxy resin

(b) Porcelain

(c) Vulcanized

(d) Fibre and resin bonded glass fibre

- | | | | | | |
|--------|--------|--------|---------|--------|--------|
| 1. (a) | 2. (d) | 3. (c) | 4. (d) | 5. (c) | 6. (d) |
| 7. (a) | 8. (b) | 9. (c) | 10. (c) | | |

REVIEW QUESTIONS

1. Give the temperature classification for solid insulating materials. Why is this classification not done for liquids and gases?
2. How is transformer insulation divided? Briefly indicate the insulation arrangement indicating the insulating materials chosen.
3. How is the insulation arrangement done for different parts in switchgear?
4. Give the application of gases and gas mixtures as insulating medium in (a) High-Voltage Switchgear, and (b) High-Voltage Power Cables.
5. Indicate the solid insulation applications in
 - (a) Power Cables
 - (b) HV Bushings
 - (c) Small-size rotating machines (motors and generators)
6. Discuss the different insulating materials used for Motor and generator coils rated for voltages more than 6,600 V with class F or H insulation?
7. What are insulation requirements for high-voltage Air or SF₆ circuit breakers?
8. What are the different materials used in capacitor insulation? Discuss the insulation requirements for
 - (i) HVDC capacitors,
 - (ii) High rating power frequency capacitors, and
 - (iii) High frequency and impulse voltage capacitors.

REFERENCES

1. Clark, F.M. *Insulating Materials for Design and Engineering Practice*, John Wiley, New York (1962).
2. Black, R.M. and Reynolds, E.H., *Proc. I.E.E.* **112**(6), 1226 (1965).
3. Birks, J.B., *Modern Insulating Materials*, Haywood, London (1960).
4. Koritsky, Y.U., *Electrical Engineering Materials*, Mir Publishers, Moscow (1970).
5. Insulation Encyclopedia, *Journal of Insulation*, June-July (1970).
6. Insulation Directory, p. 163–207 (1969).
7. Palmer, S. and Sharpley, W.A., *Proc. I.E.E.*, **116**, 2029 (1969).
8. Micafil News, MNV 45/3e, August (1968).
9. Sillars, R.W., *Electrical Insulating Materials and Their Applications*, Peter Peregrinus, London (1973).
10. Schewarz, K.K., *Proc. I.E.E.*, **116**(10), 1735 (1969).
11. Guide for the Determination of Thermal Endurance Properties of Electrical Insulating Materials, I.E.C. Publication, 216–1, 1974.
12. Indian Standard Specifications *IS: 6380–1971*, *IS: 692–1973*, *IS: 6474–1971*, *IS: 1554–1964*, and *IS: 7098–1973*.
13. Von Hippel, A., *Dielectric Materials and Applications*, M.I.T. Press, Boston, Mass. (1962).
14. Johns, A.J. and Platts, J.R., *High Voltage Engineering and Testing*, Peter Peregrinus, London (1994).

15. Farneti, F. et al., "Reliability of underground and submarine high voltage cables", *CIGRE Montreal Symposium*, Paper S38–91 (1991).
16. Allan, D.J., "Power transformers the second century", *IEE Power Engineering Journal*, 5(1) (1991).
17. IEC 76 (BS 171) Power Transformers.
18. IEEEMA, *Symposium on electrical insulation (INSULEC)*, Bangalore (1997).
19. Shugg, W.T., *Handbook of electrical and electronic insulating materials* (2nd edition), IEEE Press, New York, (1995).
20. Tanaka, T. and Greenwood, A., *Advanced Power Cable Technology*, CRC Press, Boca Raton, Florida, USA (1983).
21. IEC 60085 and B.S. 2757–1994 on classes of insulation.

CHAPTER

6

Generation of High Voltages and Currents

In the fields of electrical engineering and applied physics, high voltages (dc, ac, and impulse) are required for several applications. For example, electron microscopes and X-ray units require high dc voltages of the order of 100 kV or more. Electrostatic precipitators, particle accelerators in nuclear physics, etc. require high voltages (dc) of several kilovolts and even megavolts. High ac voltages of one million volts or even more are required for testing power apparatus rated for extra high transmission voltages (400 kV system and above). High impulse voltages are required for testing purposes to simulate over voltages that occur in power systems due to lightning or switching action. For electrical engineers, the main concern of high voltages is for the insulation testing of various components in power systems for different types of voltages, namely, power frequency ac, high frequency, ac switching or lightning impulses. Hence, generation of high voltages in laboratories for testing purposes is essential and is discussed in this chapter.

Different forms of high voltages mentioned above are classified as

- (i) high dc voltages,
- (ii) high ac voltages of power frequency,
- (iii) high ac voltages of high frequency,
- (iv) high transient or impulse voltages of very short duration such as lightning over voltages, and
- (v) transient voltages of longer duration such as switching surges.

Normally, in high-voltage testing, the current under conditions of failure is limited to a small value (less than an ampere in the case of dc or ac voltages and few amperes in the case of impulse or transient voltages). But in certain cases, like the testing of surge diverters or the short-circuit testing of switchgear, high-current testing with several hundreds of amperes is of importance. Tests on surge diverters require high-surge currents of the order of several kiloamperes. Therefore, test facilities require high-voltage and high-current generators. High impulse current generation is also required along with voltage generation for testing purposes.

6.1 GENERATION OF HIGH DIRECT-CURRENT VOLTAGES

Generation of high dc voltages is mainly required in research work in the areas of pure and applied physics. Sometimes, high direct voltages are needed in insulation tests on cables and capacitors. Impulse generator charging units also require high dc voltages of about 100 to 200 kV. Normally, for the generation of dc voltages of up to 100 kV, electronic valve rectifiers are used and the output currents are about 100 mA. The rectifier valves require special construction for cathode and filaments since a high electrostatic field of several kV/cm exists between the anode and the cathode in the non-conduction period. The ac supply to the rectifier tubes may be of power frequency or may be of audio frequency from an oscillator. The latter is used when a ripple of very small magnitude is required without the use of costly filters to smoothen the ripple.

6.1.1 Half- and Full-Wave Rectifier Circuits

Rectifier circuits for producing high dc voltages from ac sources may be (a) half wave, (b) full wave, or (c) voltage doubler-type rectifiers. The rectifier may be an electron tube or a solid-state device. Nowadays single electron tubes are available for peak inverse voltages up to 250 kV, and semiconductor or solid state diodes up to 20 kV. For higher voltages, several units are to be used in series. When a number of units are used in series, transient voltage distribution along each unit becomes non-uniform and special care should be taken to make the distribution uniform.

Commonly used half-wave and full-wave rectifiers are shown in Fig. 6.1. In the half wave rectifier (Fig. 6.1a) the capacitor is charged to V_{\max} , the maximum ac voltage of the secondary of the high-voltage transformer in the conducting half cycle. In the other half cycle, the capacitor is discharged into the load. The value of the capacitor C is chosen such that the time constant CR_L is at least 10 times that of the period of the ac supply. The rectifier valve must have a peak inverse rating of at least $2V_{\max}$. To limit the charging current, an additional resistance R is provided in series with the secondary of the transformer (not shown in the figure).

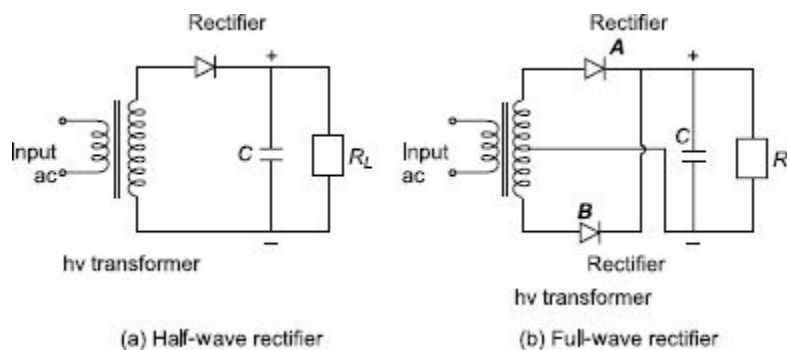


Fig. 6.1 Full- and half-wave rectifier

A full-wave rectifier circuit is shown in Fig. 6.1b. In the positive half-cycle, the rectifier A conducts and charges the capacitor C , while in the negative half-cycle, the rectifier B conducts and charges the capacitor. The source transformer requires a centre-tapped secondary with a rating of $2V$.

For applications at high voltages of 50 kV and above, the rectifier valves used are of special construction. Apart from the filament, the cathode and the anode, they contain a protective shield or grid around the filament and the cathode. The anode will usually be a circular plate. Since the electrostatic field gradients are quite large, the heater and the cathode experience large electrostatic forces during the non-conduction periods. To protect the various elements from these forces, the anode is firmly fixed to the valve cover on one side. On the other side, where the cathode and filament are located, a steel mesh structure or a protective grid kept at the cathode potential surrounds them so that the mechanical forces between the anode and the cathode are reflected on the grid structure only.

In modern high-voltage laboratories and testing installations, semiconductor rectifier stacks are commonly used for producing dc voltages. Semiconductor diodes are not true valves since they have finite but very small conduction in the backward direction. The more commonly preferred diodes for high-voltage rectifiers are silicon diodes with *Peak Inverse Voltage (PIV)* of 1 kV to 2 kV. However, for laboratory applications, the current requirement is small (a few milliamperes, and less than one ampere) and as such, a selenium element stack with PIV of up to 500 kV may be employed without the use of any voltage grading capacitors.

Both full wave and half-wave rectifiers produce dc voltages less than the ac maximum voltage.

Also, ripple or the voltage fluctuation will be present, and this has to be kept within a reasonable limit by means of filters.

Ripple Voltage with Half-Wave and Full-Wave Rectifiers When a full-wave or a half-wave rectifier is used along with the smoothing capacitor C , the voltage on no load will be the maximum ac voltage. But when on load, the capacitor gets charged from the supply voltage and discharges into load resistance R_L whenever the supply voltage waveform varies from peak value to zero value. These waveforms are shown in [Fig. 6.2](#). When loaded, a fluctuation in the output dc voltage δV appears, and is called a ripple. The ripple voltage δV is larger for a half-wave rectifier than that for a full-wave rectifier, since the discharge period in the case of half-wave rectifier is larger as shown in [Fig. 6.2](#). The ripple δV depends on (a) the supply voltage frequency f , (b) the time constant CR_L , and (c) the reactance of the supply transformer X_L . For half-wave rectifiers, the ripple frequency is equal to the supply frequency and for full-wave rectifiers, it is twice that value. The ripple voltage is to be kept as low as possible with the proper choice of the filter capacitor and the transformer reactance for a given load R_L .

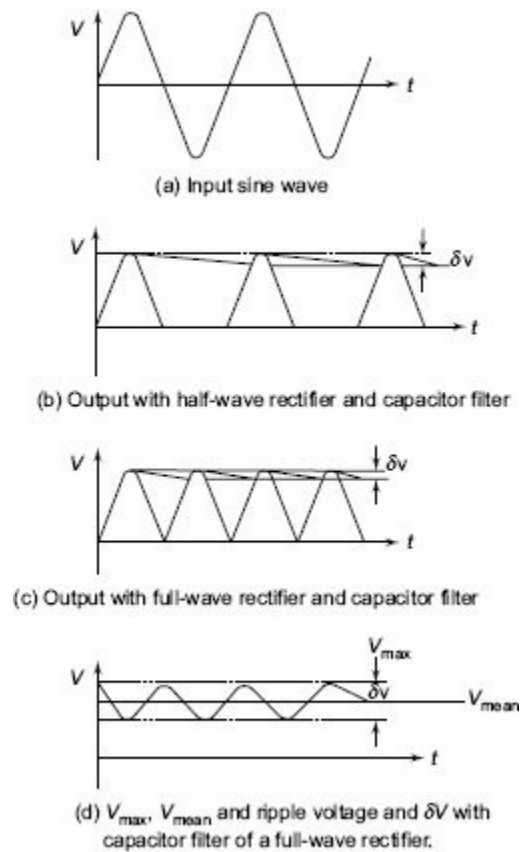


Fig. 6.2 Input and output waveforms of half- and full-wave rectifiers

6.1.2 Voltage Doubler Circuits

Both full-wave and half-wave rectifier circuits produce a dc voltage less than the ac maximum voltage. When higher dc voltages are needed, a voltage doubler or cascaded rectifier doubler circuits are used. The schematic diagram of voltage doublers are given in [Figs 6.3a](#) and [b](#).

In the voltage doubler circuit shown in [Fig. 6.3a](#), the capacitor C_1 is charged through rectifier R_1 to a voltage of $+V_{\max}$ with polarity as shown in the figure during the negative half cycle. As the voltage of the transformer rises to positive $+V_{\max}$ during the next half cycle, the potential of the other terminal of C_1 rises to a voltage of $+2V_{\max}$.

Thus, the capacitor C_2 in turn is charged through R_2 to $2V_{\max}$. Normally, the dc output voltage on load will be less than $2V_{\max}$, depending on the time constant C_2R_L and the forward charging time constants. The ripple voltage of these circuits will be about 2% for $R_L/r \leq 10$ and $X/r \leq 0.25$, where X and r are the reactance and resistance of the input transformer. The rectifiers are rated to a peak inverse voltage of $2V_{\max}$, and the capacitors C_1 and C_2 must also have the same rating. If the load current is large, the ripple also is more.

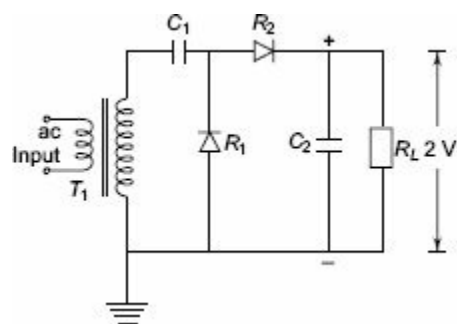


Fig. 6.3a Simple voltage doubler

Cascaded voltage doublers are used when larger output voltages are needed without changing the input transformer voltage level. A typical voltage doubler is shown in [Fig. 6.3b](#) and its input and output waveforms are shown in [Fig. 6.3c](#). The rectifiers R_1 and R_2 with transformer T_1 and capacitors C_1 and C_2 produce an output voltage of 2 V in the same way as described above. This circuit is duplicated and connected in series or cascade to obtain a further voltage doubling to 4 V. T is an isolating transformer to give an insulation for $2V_{\max}$ since the transformer T_2 is at a potential of $2V_{\max}$ above the ground. The voltage distribution along the rectifier string R_1 , R_2 , R_3 , and R_4 is made uniform by having capacitors C_1 , C_2 , C_3 , and C_4 of equal values. The arrangement may be extended to give 6 V, 8 V, and so on, by repeating further stages with suitable isolating transformers. In all the voltage doubler circuits, if valves are used, the filament transformers have to be suitably designed and insulated, as all the cathodes will not be at the same potential from ground. The arrangement becomes cumbersome if more than 4 V is needed with cascaded steps.

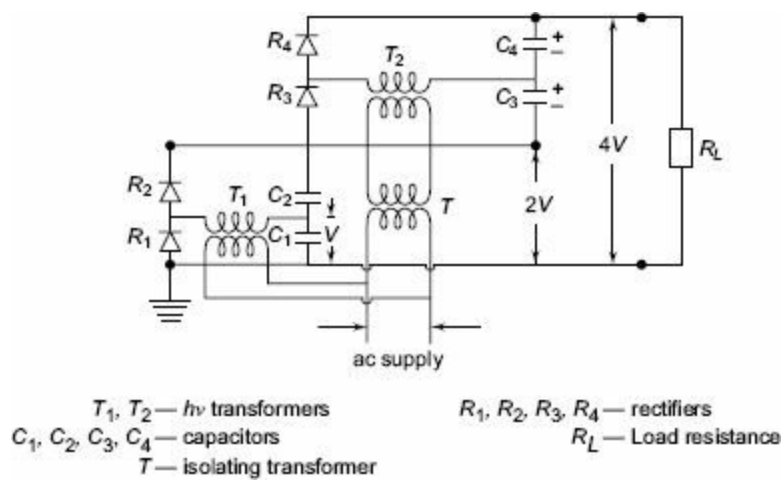
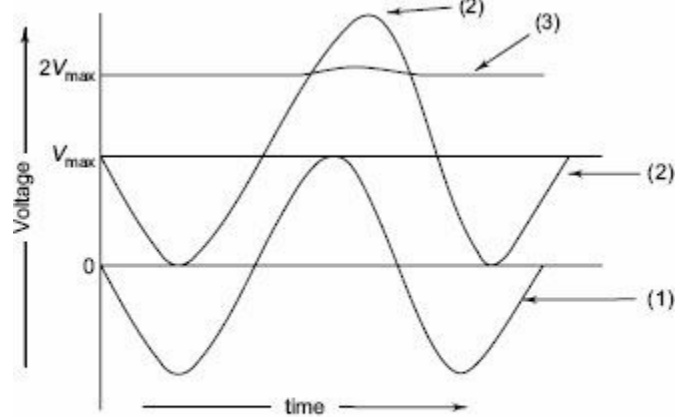


Fig. 6.3b Cascaded voltage doubler



- (1) ac input voltage waveform
- (2) ac output voltage waveform with capacitor filter
- (3) dc output voltage waveform with capacitor filter.

Fig. 6.3c Waveforms of ac voltage and the dc output voltage on no-load of the voltage doubler shown in Fig. 6.3b

Fig. 6.3 Voltage doubler circuits

6.1.3 Voltage Multiplier Circuits

Cascaded voltage multiplier circuits for higher voltages are cumbersome and require too many supply and isolating transformers. It is possible to generate very high dc voltages from single supply transformers by extending the voltage doubler circuits. This is simple and compact when the load current requirement is less than one milliampere, such as for cathode ray tubes, etc. Valve-type pulse generators may be used instead of conventional ac supply and the circuit becomes compact. A typical circuit of this form is shown in Fig. 6.4a.

The pulses generated in the anode circuit of the valve P are rectified and the voltage is cascaded to give an output of $n V_{max}$ across the load R_L . A trigger voltage pulse of triangular waveform (ramp) is given to make the valve switched on and off. Thus a voltage across the coil L is produced and is equal to $V_{max} = I\sqrt{L/C_P}$, where C_P is the stray capacitance across the coil of inductance L . A dc power supply of about 500 V applied to the pulse generator, is sufficient to generate a high voltage dc of 50 to 100 kV with suitable number of stages. The pulse frequency is high (about 500 to 1000 Hz) and the ripple is quite low ($< 1\%$). The voltage drop on the load is about 5% for load currents of about 150 μA . The voltage drops rapidly at high load currents.

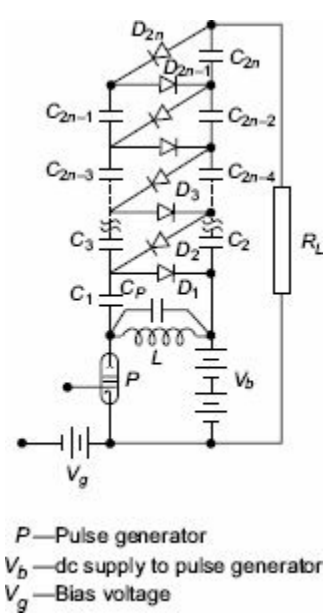


Fig. 6.4a Cascaded rectifier unit with pulse generator

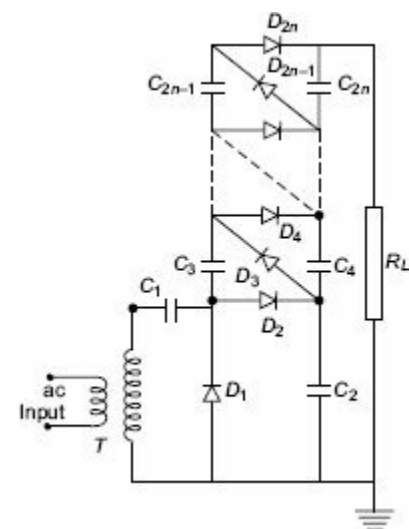


Fig. 6.4b Cockcroft-Walton voltage multiplier circuit

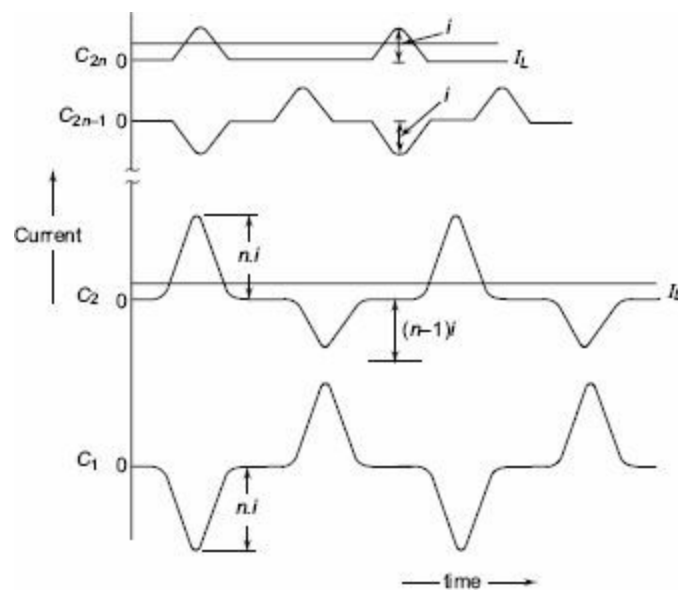


Fig. 6.4c Schematic current waveforms across the first and the last capacitors of the cascaded voltage multiplier circuit shown in [Fig. 6.4b](#)

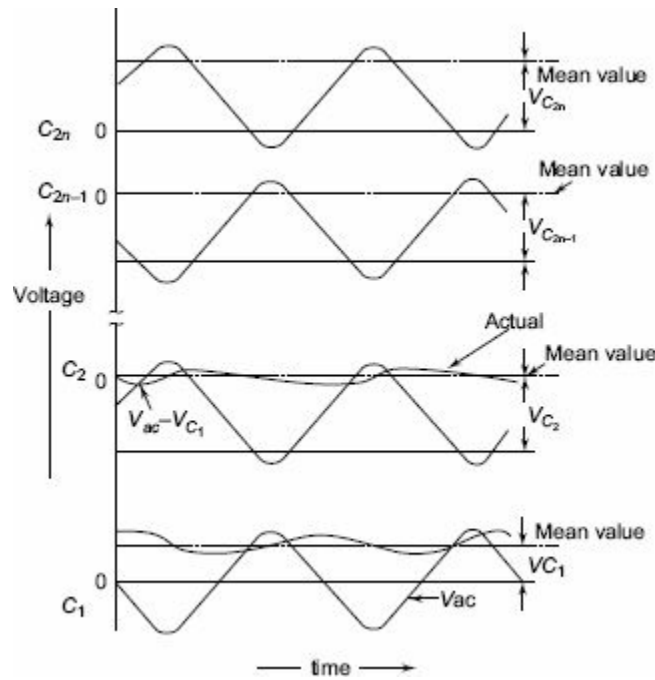


Fig. 6.4d Voltage waveforms across the first and the last capacitors of the cascaded voltage multiplier circuit shown in [Fig. 6.4b](#)

Voltage multiplier circuit using the Cockcroft-Walton principle is shown in [Fig. 6.4b](#). The first stage, i.e., D_1, D_2, C_1, C_2 , and the transformer T are identical as in the voltage doubler shown in [Fig. 6.3](#). For higher output voltage of $4, 6, \dots, 2n$ of the input voltage V , the circuit is repeated with cascade or series connection. Thus, the capacitor C_4 is charged to $4V_{\max}$ and C_{2n} to $2nV_{\max}$ above the earth potential. But the voltage across any individual capacitor or rectifier is only $2V_{\max}$.

The rectifiers $D_1, D_3, \dots, D_{2n-1}$ shown in [Fig. 6.4b](#) operate and conduct during the positive half cycles while the rectifiers D_2, D_4, \dots, D_{2n} conduct during the negative half cycles. Typical current and voltage waveforms of such a circuit are shown in [Figs 6.4c](#) and [6.4d](#) respectively. The voltage on C_2 is the sum of the input ac voltage, V_{ac} and the voltage across condenser C_1, V_{C1} as shown in [Fig. 6.4](#). The mean voltage on C_2 is less than the positive peak charging voltage ($V_{ac} + V_{C1}$). The voltage

across other capacitors C_2 to C_{2n} can be derived in the same manner (i.e.) from the difference between voltage across the previous capacitor and the charging voltage. Finally, the voltage after $2n$ stages will be $V_{ac} (n_1 + n_2 + \dots)$, where n_1, n_2, \dots are factors when ripple and regulation are considered in the next rectifier. The ripple voltage δV and the voltage drop ΔV in a cascaded voltage multiplier unit are shown in [Fig. 6.4e](#).

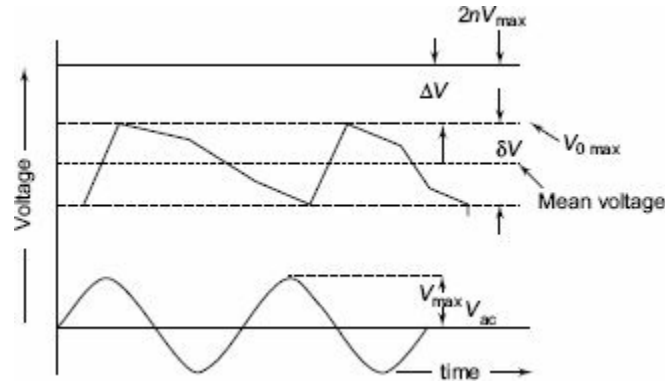


Fig. 6.4e Ripple voltage δV and the voltage drop ΔV in a cascaded voltage multiplier circuit shown in [Fig. 6.4b](#)

(a) Ripple in Cascaded Voltage Multiplier Circuits With load, the output voltage of the cascaded rectifiers is less than $2nV_{max}$, where n is the number of stages. The ripple and the voltage regulation of the rectifier circuit may be estimated as follows.

Let f = supply frequency,
 q = charge transferred in each cycle,
 I_1 = load current from the rectifier,
 t_1 = conduction period of the rectifiers,
 t_2 = non-conduction period of rectifiers, and
 δV = ripple voltage (peak to peak)

Referring to [Fig. 6.3a](#), when load current I_1 is supplied from capacitor C_2 to load R_L during the non-conducting period, the charge transferred per cycle from the capacitor C_2 to the load during the non-conduction period t_2 is q , and is related as follows.

$$I_1 = \frac{dq}{dt} \approx \frac{q}{t_2}$$

Since $t_1 \ll t_2$ and $t_1 + t_2 = \frac{1}{f}$ (i.e., the period of the ac supply voltage),

$$t_2 = \frac{1}{f}$$

Also, $q = C_2 \delta V$

Hence, $\delta V = \text{the ripple} = \frac{I_1}{f C_2}$

At the same time a charge q is transferred from C_1 to C_2 during each cycle equal to $I_1/f C_2$. Thus the total voltage drop that occurs will be $I_1 I f C_1 + 2 I_1 I f C_1$.

Hence, regulation = mean voltage drop from $2V_{max}$

$$= \frac{I_1}{f} \left[\frac{1}{C_1} + \frac{2}{C_2} \right] \quad (6.1)$$

Therefore, the mean output voltage $= 2V_{max} - \frac{I_1}{f} \left(\frac{1}{C_1} + \frac{2}{C_2} \right)$.

For the cascade circuit, on no load, the voltages between stages are raised by $2V_{max}$ giving an output voltage of $2nV_{max}$ for n stages.

Referring to [Fig. 6.4b](#), to find an expression for the total ripple voltage, let it be assumed that all capacitances C_1, C_2, \dots, C_{2n} be equal to C . Let q be the charge transferred from C_{2n} to the load per cycle.

Then the ripple at the capacitor C_{2n} will be $\frac{I_1}{fC}$.

Simultaneously, C_{2n-2} transfers as charge q to the load and to C_{2n-1} .

Hence, the ripple at the capacitor C_{2n-2} is $\frac{2I_1}{fC}$.

Similarly, C_{2n-4} transfers a charge q to the load, to C_{2n-3} , and to C_{2n-2} .

Therefore, the ripple at capacitor C_{2n-4} is $\frac{3I_1}{fC}$.

Proceeding in the same way, the ripple at C_2 will be $\frac{nI_1}{fC}$.

Hence, for n stages the total ripple (peak to peak) will be

$$\delta V_{total} = \frac{I_1}{fC} [1 + 2 + 3 \dots + n] = \frac{I_1}{fC} \frac{(n)(n+1)}{2} \quad (6.2)$$

$$\text{and the average ripple} = \frac{\delta V_{total}}{2} = \frac{I_1}{4fC} (n)(n+1) \quad (6.2a)$$

The major contribution to the ripple is from the lowest or ground end capacitors, C_1, C_2, C_3, C_4 , etc. Ripple can be reduced if the capacitance of these capacitors is increased proportionately, i.e., C_1, C_2 are made nC , C_3, C_4 are made $(n-1)C$ and so on so that the total ripple will be equal to

$$\frac{nI_1}{fC}$$

Note: ‘ n ’ capacitors here mean $n/2$ stages only since two capacitors from each stage or a doubler unit.

(b) Voltage Drop on Load and Regulation The change of average voltage across the load from the no load theoretical value expressed as a percentage of no load voltage is called the regulation. The change in voltage (i.e.) the voltage drop ‘ ΔV ’ is caused due to the ripple δV , and the capacitors not getting charged to the full voltage V_m when they are supplying the load current I_1 .

The voltage drop under load condition ΔV is found by assuming that all the capacitors are of equal value ‘ C ’. It is seen from the analysis of ripple that all the capacitors are not charged to $2V_{max}$. The capacitor C_{2n} is charged to $(2V_{max} - n I_1/fC)$ only instead of $2V_{max}$ because the charge given through C_{2n-1} in one cycle is equal to a voltage drop of $n I_1/fC$. This is because, in each stage the loss of charge equal to a voltage drop of I_1/fC to the load. In a similar manner the capacitor C_{2n-2} is charged to only $[2V_{max} - n I_1/fC - n I_1/fC - (n-1) I_1/fC]$ since the reduction in voltage at this stage is further equal to $n I_1/fC$ at the capacitor C_{2n-1} and $(n-1) I_1/fC$ at capacitor C_{2n-2} . Thus, if the voltage drops

at each of the capacitor C_{2n} , C_{2n-2} , etc., to C_2 are designated as ΔV_{2n} , ΔV_{2n-2} , ... ΔV_2 , the total voltage drop will be

$$\begin{aligned}\Delta V_{2n} &= \frac{nI_1}{fC} = \frac{I_1}{fC} [2n - n] \\ \Delta V_{2n-2} &= \frac{nI_1}{fC} + \frac{nI_1}{fC} + \frac{(n-1)I_1}{fC} = \frac{I_1}{fC} [2n + n - 1] \\ &= \frac{I_1}{fC} [2n + 2(n-1) - (n-1)] \\ &\quad \dots \\ &\quad \dots \\ &\quad \dots \\ &\quad \dots \\ \Delta V_4 &= \frac{I_1}{fC} [2n + 2(n-1) + \dots + 2] \\ &= \frac{I_1}{fC} [2n + 2(n-1) + \dots + 2.2 - 2] \\ \Delta V_2 &= \frac{I_1}{fC} [2n + 2(n-1) + \dots + 2.1 - 1]\end{aligned}$$

Summing up all the voltage drops,

$$\begin{aligned}\Delta V &= \frac{I_1}{fC} \sum_{n=1}^n \Delta V_{2n} = \frac{I_1}{fC} \left\{ \sum_{n=1}^n n \cdot 2n - \sum_{n=1}^n n \right\} \\ &= \frac{I_1}{fC} \left[\sum_1^n 2n^2 - \sum_1^n n \right] \\ &= \frac{I_1}{fC} \left[2 \cdot \frac{(n)(n+1)(2n+1)}{6} - \frac{n(n+1)}{2} \right] \\ &= \frac{I_1}{fC} \left[n(n+1) \left(\frac{2n+1}{3} - \frac{1}{2} \right) \right] \\ &= \frac{I_1}{fC} \left[\frac{n(n+1)(4n-1)}{6} \right] \\ &= \frac{I_1}{fC} \left[\frac{2n^3}{3} + \frac{n^2}{2} - \frac{n}{6} \right] \tag{6.3}\end{aligned}$$

It is seen from [Eq. \(6.3\)](#) that most of the voltage drop is at the lowest stage capacitors C_1 , C_2 , C_3 , C_4 , etc. Hence it is advantageous to increase their values to be proportional to the stage number counted from the top. In other words C_1 C_2 may be chosen as nC , C_3 C_4 as $(n-1)C$, etc.

For large values of n (≥ 5), $\frac{n^2}{2}$ and $\frac{n}{6}$ terms in [Eq. \(6.3\)](#) will become small compared to $\frac{2}{3}n^3$ and may be neglected; then the optimum number of stages for the minimum voltage drop may be expressed as

$$n_{\text{optimum}} = \sqrt{\frac{V_{\text{max}} f C}{I}} \quad (6.4)$$

where I is the load current.

Thus, for a multiplier or a cascaded circuit with $f = 50$ Hz, $C = 0.1 \mu\text{F}$, $V_{\text{max}} = 100$ kV and $I = 5$ mA, the number of stages $n = 10$.

The regulation can be improved by increasing f but an upper limit is set by the high voltage appearing across the inductances and high capacitor currents which are considerable. At present, the Cockcroft-Walton type voltage multipliers are available using selenium rectifiers and a.c. supply frequencies of 500 to 1000 Hz for output voltages of more than one million volts and load currents of 30 mA.

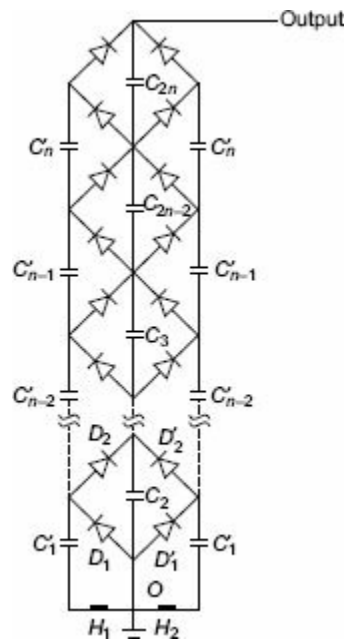


Fig. 6.5a One-phase, two-pulse,

The voltage multiplier described in [Sec. 6.1.3](#) is a single pulse voltage multiplier since it has only one rectified wave or pulse per cycle. Hence its ripple content is high. In order to reduce the ripple as well as regulation and to improve the efficiency and power output, two or more pulse units per cycle are preferred. Single or three phase bridge is used as the basic rectifier or stage and the multiplier circuit is built in the same manner as that of the Cockcroft-Walton multiplier.

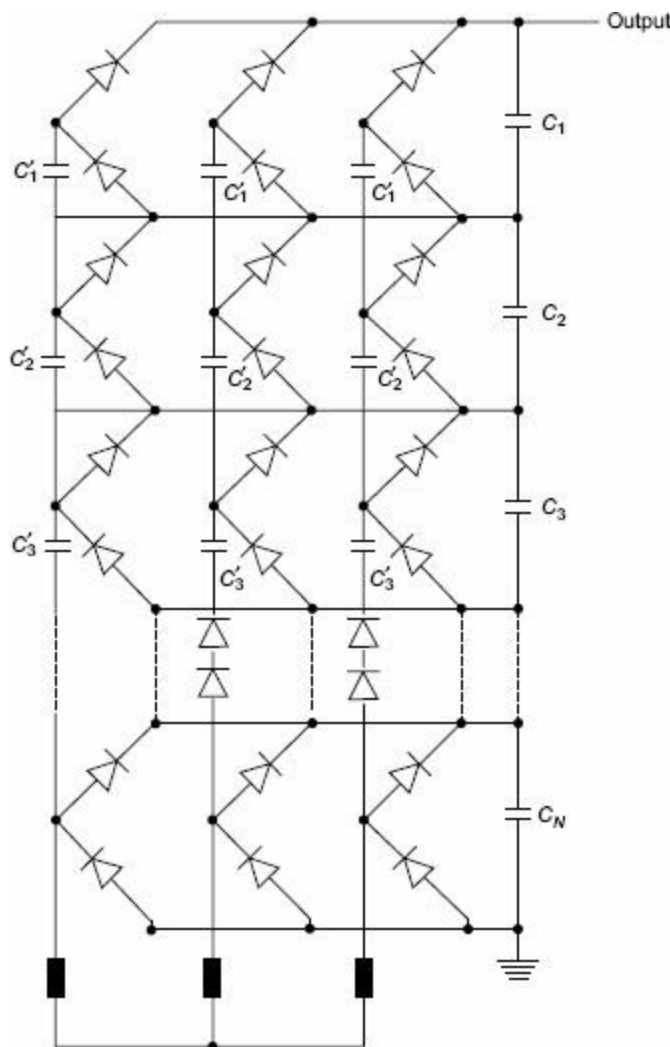


Fig. 6.5b Three-phase, six-pulse, voltage multiplier circuit

The arrangement for single phase two pulse and three phase six pulse circuits are shown in [Figs 6.5\(a\)](#) and [6.5\(b\)](#) respectively.

(c) Single-phase Two-pulse Cascade Multiplier The basic voltage doubler unit consisting of D_1, D_2, C_1, C_2 is replaced by the bridge circuit D_1, D_2, D'_1, D'_2 , with an extra capacitor C'_1 . The centre tap of the supply transformer is connected to the junction of rectifiers D_1, D_2 . The arrangement is simply an addition of another voltage doubler circuit D'_1, D'_2, C'_1, C'_2 along with the transformer H_1H_2 for the negative cycle rectification.

The multiplier circuit is built for both positive and negative cycle rectification and the arrangement is called *Symmetrical Cascade Unit*. The ripple for this arrangement is $nI/2fC$ as against $n(n + 1)I/2fC$ with all capacitors of value equal to C and the regulation is $\frac{nI}{3fC} \left(\frac{n^2}{2} + 1 \right)$.

(d) Three-phase Six-pulse Arrangement The three-phase six-pulse arrangement is a 3-phase bridge or Gratz circuit cascaded into a multiplier unit as shown in [Fig. 6.5b](#). Two more multiplier units for the other two phases of the three phase supply are connected in parallel to build this circuit. The ripple in this case is reduced to $\frac{nI}{6fC}$ and regulation to $\frac{nI}{3fC} \left(\frac{n^2}{6} - \frac{n}{4} + \frac{1}{3} \right)$

The two-pulse circuit requires double the number of diodes and one and a half times the capacitors required for single-pulse circuits. The six-pulse circuit requires twice the number of diodes and

capacitors used in a single-pulse circuit and as such, the cost increases. But the regulation and ripple are very much reduced and requirements needed in the specifications of dc test sources are easily met with much smaller ratings for the capacitors. Further, large currents required for pollution testing can be obtained only with three-phase six-pulse arrangement.

6.1.4 Electrostatic Machines: Basic Principle

In electromagnetic machines, current-carrying conductors are moved in a magnetic field, so that the mechanical energy is converted into electrical energy. In electrostatic machines, charged bodies are moved in an electric field against the electrostatic field in order that mechanical energy is converted into electrical energy. Thus, if an insulated belt with a charge density δ moves in an electric field ' $E(x)$ ' between two electrodes with separation ' s ' then

- (i) the charge on the strip of belt at a distance dx is $dq = \delta b \cdot dx$ where b is the width of the belt, and
- (ii) the force on the belt, F is

$$F = \int_0^s E(x) \cdot dq = \int_0^s \delta \cdot b \cdot E(x) dx$$

If the belt moves with a velocity, v , then the mechanical power P , required to move the belt is

$$P = F \cdot v = \delta \cdot b \cdot v \int_0^s E(x) dx$$

The current, I , in the system is given as

$$I = dq/dt = \delta b \cdot dx/dt = \delta \cdot b \cdot v$$

and the potential difference, V , between the electrodes is

$$V = \int_0^s E(x) dx$$

Thus, in an electrostatic machine, the mechanical power required to move the belt at a velocity v , i.e., $P = F \cdot v$ is converted into the electrical power, $P = VI$, assuming that there are no losses in the system. The Van de Graaff generator is one such electrostatic machine which generates very high voltages, with small output current ([Plate 1](#)).

(a) Van de Graaff Generators The schematic diagram of a Van de Graaff generator is shown in [Fig. 6.6](#). The generator is usually enclosed in an earthed metallic cylindrical vessel and is operated under pressure or in vacuum. Charge is sprayed onto an insulating moving belt from corona points at a potential of 10 to 100 kV above earth and is removed and collected from the belt connected to the inside of an insulated metal electrode through which the belt moves. The belt is driven by an electric motor at a speed of 1000 to 2000 metres per minute. The potential of the high voltage electrode above the earth at any instant is $V = Q/C$, where Q is the charge stored and C is the capacitance of the high-voltage electrode to earth. The potential of the high-voltage electrode rises at a rate

$$\frac{dV}{dt} = \frac{1}{C} \frac{dQ}{dt} = \frac{I}{C} \quad \text{where } I \text{ is the net charging current.}$$

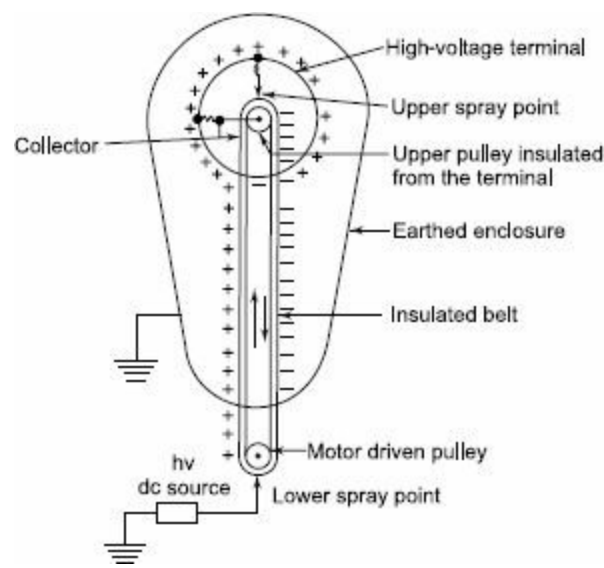


Fig. 6.6 Van de Graff generator

A steady potential will be attained by the high-voltage electrode when the leakage currents and the load current are equal to the charging current. The shape of the high-voltage electrode is so made with re-entrant edges as to avoid high surface field gradients, corona and other local discharges. The shape of the electrode is nearly spherical.

The charging of the belt is done by the lower spray points which are sharp needles and connected to a dc source of about 10 to 100 kV, so that the corona is maintained between the moving belt and the needles. The charge from the corona points is collected by the collecting needles from the belt and is transferred on to the high-voltage electrode as the belt enters into the high-voltage electrode. The belt returns with the charge dropped, and fresh charge is sprayed onto it as it passes through the lower corona point. Usually, in order to make the charging more effective and to utilize the return path of the belt for charging purposes, a self-inducing arrangement or a second corona-point system excited by a rectifier inside the high-voltage terminal is employed. To obtain a self-charging system, the upper pulley is connected to the collector needle and is therefore maintained at a potential higher than that of the high-voltage terminal. Thus, a second row of corona points connected to the inside of the high-voltage terminal and directed towards the pulley above its point of entry into the terminal gives a corona discharge to the belt. This neutralizes any charge on the belt and leaves an excess of opposite polarity to the terminal to travel down with the belt to the bottom charging point. Thus, for a given belt speed the rate of charging is doubled.

The charging current for unit surface area of the belt is given by $I = bv\delta$, where b is the breadth of the belt in metres, v is the velocity of the belt in m/sec, and δ is the surface charge density in coulombs/m². It is found that δ is $\leq 1.4 \times 10^{-5}$ C/m² to have a safe electric field intensity normal to the surface. With $b = 3$ m and $v = 3$ m/s, the charging current will be approximately 125 μ A. The generator is normally worked in a high-pressure gaseous medium, the pressure ranging from 5 to 15 atm. The gas may be nitrogen, air, air-freon (CCl₂F₂) mixture, or sulphur hexafluoride (SF₆).

Van de Graaff generators are useful for very high-voltage and low-current applications. The output voltage is easily controlled by controlling the corona source voltage and the rate of charging. The voltage can be stabilized to 0.01%. These are extremely flexible and precise machines for voltage control.

(b) Electrostatic Generators Van de Graaff generators are essentially high-voltage but low-

power devices, and their power rating seldom exceeds few tens of kilowatts. As such, electrostatic machines which effectively convert mechanical energy into electrical energy using variable capacitor principle were developed. These are essentially duals of electromagnetic machines and are constant voltage variable capacitance machines. An electrostatic generator consists of a stator with interleaved rotor vanes forming a variable capacitor and operates in vacuum.

The current through a variable capacitor is given by $I = \frac{dV}{dt} + V \frac{dC}{dt}$ where C is a capacitor charged to a potential V .

The power input into the circuit at any instant is

$$P = VI = CV \frac{dV}{dt} + V^2 \frac{dC}{dt} \quad (6.5)$$

If $\frac{dC}{dt}$ is negative, mechanical energy is converted into electrical energy.

With the capacitor charged with a dc voltage V , $C \frac{dV}{dt} = 0$ and the power output will be $P = V^2 \frac{dC}{dt}$.

A schematic diagram of a synchronous electrostatic generator with interleaved stator and rotor plates is shown in Fig. 6.7. The rotor is insulated from the ground, and is maintained at a potential of V . The rotor to stator capacitance varies from C_m to C_0 and the stator is connected to a common point between two rectifiers across the dc output which is $-E$ volts. When the capacitance of the rotor is maximum (C_m), the rectifier **B** does not conduct and the stator is at ground potential. The potential E is applied across the rectifier α and V is applied across C_m . As the rotor rotates, the capacitance C decrease and the voltage across C increases.

Thus, the stator becomes more negative with respect to ground. When the stator reaches the line potential $-E$ the rectifier **A** conducts, and further movement of the rotor causes the current to flow from the generator. Rectifier **B** will now have E across it and the charge left in the generator will be $Q_0 = C_0 (V + E) + E (C_s + C_r)$, where C_s is the stator capacitance to earth, C_r is the capacitance of rectifier **B** to earth, and C_0 is the minimum capacitance value of C (stator to rotor capacitance).

A generator of this type with an output voltage of one MV and a field gradient of 1 MV/cm in high vacuum and having 16 rotor poles, 50 rotor plates of 4 feet maximum and 2 feet minimum diameter, and at a speed of 4000 rpm would develop 7 MW of power.

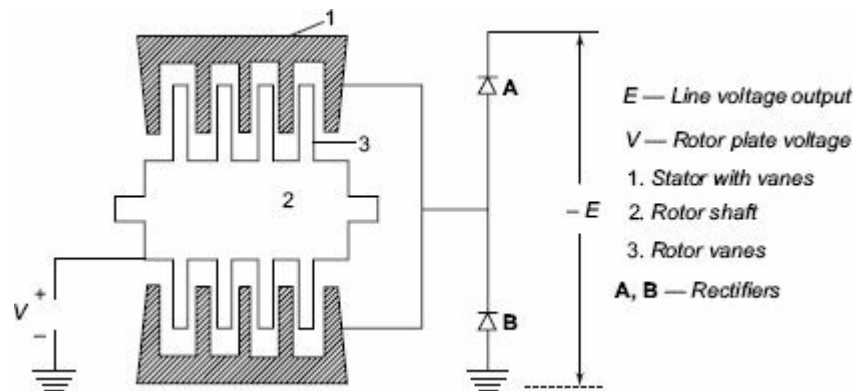


Fig. 6.7 Electrostatic generator

6.1.5 Regulation of dc Voltages

The output voltage of a dc source, whether it is a rectifier or any other machine, changes with the load current as well as with the input voltage variations. In order to maintain a constant voltage at the load terminals, it is essential to have a regulator circuit which corrects the variation in voltage. It is essential to keep the change in voltage between $\pm 0.1\%$ to $\pm 0.001\%$ depending on the applications.

A dc voltage regulator consists of detecting elements which sense the change in voltage from the desired value and controlling elements actuated by the detector in such a manner as to correct the changes. The regulators are generally of two types (a) series type, and (b) shunt or parallel type. Schematic diagrams of these regulators are given in [Fig. 6.8](#).

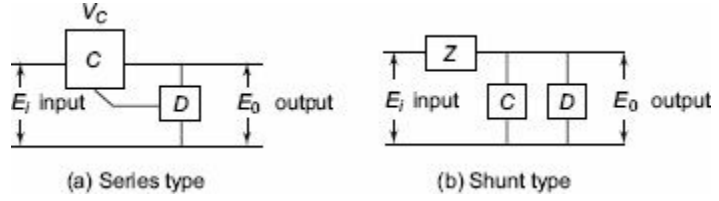


Fig. 6.8 Schematic diagram of voltage stabilizers

If ΔE_0 is the change in E_0 as a result of a change of ΔE_i in E_i , then the stabilization ratio S is defined as

$$S = \frac{[\Delta E_i / E_i]}{[\Delta E_0 / E_0]} = \frac{\Delta E_i}{\Delta E_0} \frac{E_0}{E_i} \tag{6.6}$$

A second parameter R_0 is introduced to define completely the functional performance of a regulator. R_0 is the effective internal resistance of the regulator as seen from the output terminals.

$$R_0 = \frac{\Delta E_0}{\Delta I_0}$$

where ΔE_0 is the change in the output voltage caused due to a change in load current of ΔI_0 , with the input voltage remaining constant.

The regulation R is defined as,

$$R = \frac{[\Delta E_0 / E_0]}{[\Delta I_0 / I_0]} = \frac{R_0}{R_L} \tag{6.7}$$

where R_L is the load resistance.

Typical series type regulator and degenerative feedback system of voltage regulation are shown in [Figs 6.9a](#) and [b](#) respectively.

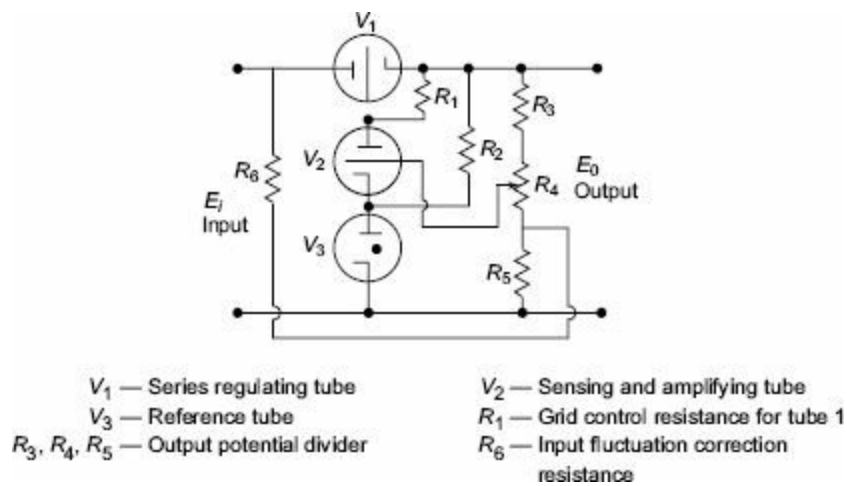


Fig. 6.9a Series dc voltage regulator

[Figure 6.9a](#) shows the simplified diagram of a series type of voltage regulator. Here the gas tube V_3 provides the reference voltage which keeps the potential of the cathode of the tube V_2 constant. When the output voltage E_0 changes, the current through the divider R_2 , R_4 and R_5 changes, and hence the bias voltage of the tube V_2 with respect to its cathode changes in the opposite manner (reduces when the output voltage increases and vice versa). Thus, the grid potential of V_1 is altered in such a manner as to oppose the variation in output voltage E_0 ; that is, the voltage drop across the tube V_1 reduces, if the output voltage decreases and vice versa. Resistance R_6 together with R_5 provides a voltage input to the dc amplifier (the detector) in proportion to fluctuations in the input voltage in such a way as to reduce the effect of these variations in the output voltage.

A convenient method of regulating high dc voltages is the degenerative feedback system, shown in [Fig. 6.9b](#). The fluctuations in the output voltage are measured by a detecting device, amplified by a dc amplifier and fed back into the high-voltage set so as to correct for the original fluctuations. The detecting device in the above circuit is the potential divider of ratio $\beta = R_1/(R_1 + R_2)$. The amplifier is directly coupled and the difference in potential between the tapping on the divider and the amplifier grid voltage is made up by the battery voltage V .

The output voltage E_0 is given as follows:

$$E_0 = NE_i - I_i R_i - Ae \tag{6.7a}$$

where N = ratio between the output voltage of the hv set and the main supply voltage, E_i ,

I_i = load current,

R_i = internal resistance of the hv set,

A = gain of the feedback amplifier,

e = amplifier input voltage.

Since $e = \beta E_0 - V$, the output voltage becomes

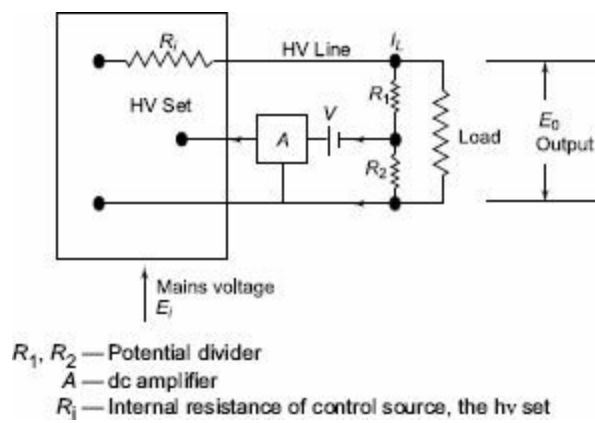


Fig. 6.9b Degenerative feedback system of voltage regulation

$$E_0 = NE_i - I_l R_i - (\beta E_0 - V) A = NE_i - I_l R_i - A\beta E_0 + AV$$

or, $E_0(1 + A\beta) = NE_i + AV - I_l R_i$

or,
$$E_0 = \frac{NE_i}{(1 + A\beta)} + \frac{AV}{(1 + A\beta)} - \frac{I_l R_i}{(1 + A\beta)}$$

For large values of A

$$E_0 = \frac{AV}{(1 + A\beta)} \approx \frac{V}{\beta}$$

The stabilization ratio = $[\Delta E_i/E_i]/[\Delta E_0/E_0] = 1 + A\beta$.

In practice, values of $A\beta$ of the order of 1000 are common. It can be seen that for given value of A , stabilization ratio can be increased by making β as large as possible.

Stabilities to about 2 parts in 10^4 in high voltage are easily obtained by this method if load changes are kept small.

6.2 GENERATION OF HIGH ALTERNATING VOLTAGES

When test voltage requirements are less than about 300 kV, a single transformer can be used for test purposes. The impedance of the transformer should be generally less than 5% and must be capable of giving the short-circuit current for one minute or more depending on the design. In addition to the normal windings, namely, the low- and high-voltage windings, a third winding known as meter winding is provided to measure the output voltage. For higher voltage requirements, a single-unit construction becomes difficult and costly due to insulation problems. Moreover, transportation and erection of large transformers become difficult. These drawbacks are overcome by series connection or cascading of the several identical units of transformers, wherein the high voltage windings of all the units effectively come in series.

Schematic diagrams of the cascade transformer units are shown in [Figs 6.10](#) and [6.11](#).

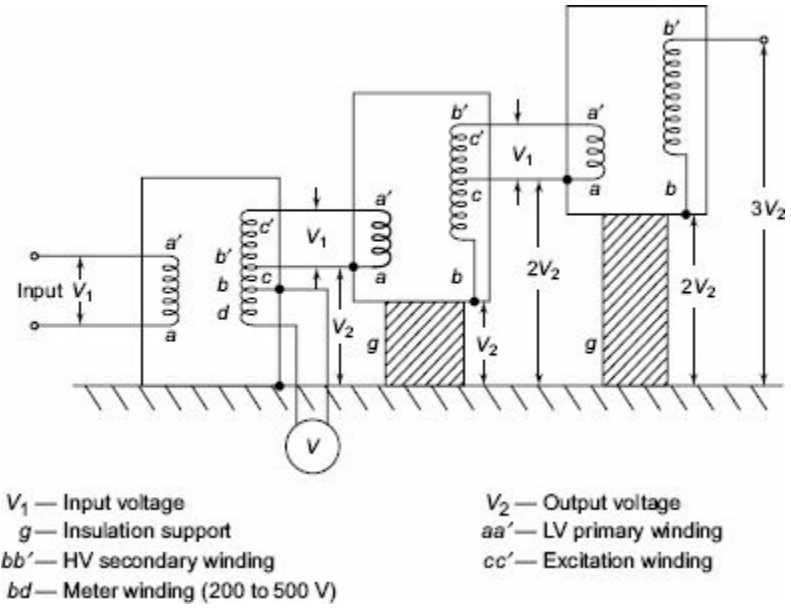


Fig. 6.10 Cascade transformer connection (schematic)

Fig. 6.11 Cascade transformer unit with isolating transformers for excitation

Testing of an hv apparatus or insulation always involves supplying of capacitive loads with very low power dissipation. Thus if C is the capacitance of the test object, V is the rms value of the nominal output voltage of the transformer at an angular frequency ω then the nominal rating of the transformer in kVA will be $P = K \cdot v^2 \omega C$, where $K (> 1.0)$ is a factor to account for any extra capacitance in the test circuit like that of the measuring capacitance divider, etc. K may have values of the order of 2 or more for very high voltages (> 1 MV). Typical capacitance values for high capacitance test objects like power transformers, cables, etc. are as follows:

Power transformers (rating < 1 MVA)	1000 pF
Power transformers (rating > 1 MVA)	1000–10,000 pF
High-voltage power cables (with solid insulation)	250–300 pF/m
High-voltage power cables (with gas insulation)	50–80 pF/m
Metal-clad sub-station with gas insulation (GIS)	100–10,000 pF

The charging currents for the test apparatus may range from 10 mA at 100 kV to a few milliamperes in the megavolt range. As such the transformers should have only a short time rating (10 to 15 min) for high power ratings, as compared to those with nominal power ratings.

Large testing transformers rated for more than 1 MVA at 1 MV are nowadays designed for outdoor use only. The design is of the type mentioned in the second scheme and ensures that the units are enclosed by large-size metal rings to prevent corona, and are terminated with near spherical polycone electrodes. Modern test transformers are built to withstand transients during the flashover of the test object. However, particular care need to be taken to see that steady state voltage distribution within the cascade units is uniform. Sometimes reactor compensation may have to be provided for excessive load currents of capacitive nature. Cascade transformers are very expensive apparatus and are difficult to repair. Therefore it is necessary to limit the high short-circuit currents by using limiting reactors in the input stage.

Power Supply for ac Test Circuits Large cascade transformers units are supplied power through a separate motor-generator set or by means of voltage regulators. Supply through a voltage regulator will be cheaper, and will be more flexible in the sense that the units in the cascade set can be operated in cascade, or in parallel, or as three-phase units. It is also necessary that the impedance of the voltage regulating transformer is low in all voltage positions, from the minimum to the rated value.

6.2.2 Resonant Transformers

The equivalent circuit of a high-voltage testing transformer consists of the leakage reactance of the windings, the winding resistances, the magnetizing reactance, and the shunt capacitance across the output terminal due to the bushing of the high-voltage terminal and also that of the test object. This is shown in Fig. 6.12a with its equivalent circuit in Fig. 6.12b. It may be seen that it is possible to have series resonance at power frequency ω , if $(L_1 + L_2) = 1/\omega C$. With this condition, the current in the test object is very large and is limited only by the resistance of the circuit. The waveform of the voltage across the test object will be purely sinusoidal. The magnitude of the voltage across the capacitance C of the test object will be

$$V_C = \left| \frac{-jVX_C}{R + j(X_L - X_C)} \right| = \frac{V}{R} X_C = \frac{V}{\omega CR} \tag{6.8}$$

where R is the total series resistance of the circuit.

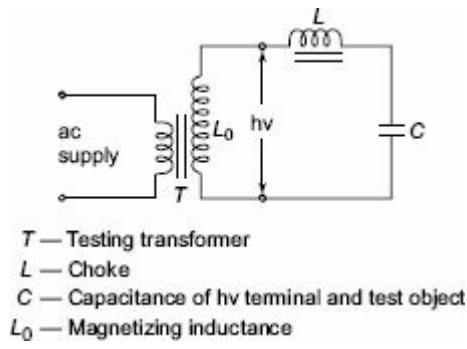


Fig. 6.12a Transformer

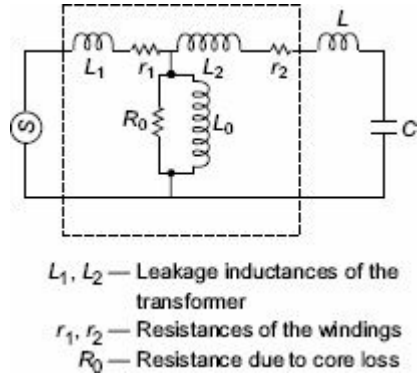


Fig. 6.12b Equivalent circuit

The factor $X_C/R = 1/\omega CR$ is the Q factor of the circuit and gives the magnitude of the voltage multiplication across the test object under resonance conditions. Therefore, the input voltage required for excitation is reduced by a factor $1/Q$, and the output kVA required is also reduced by a factor $1/Q$. The secondary power factor of the circuit is unity.

This principle is utilized in testing at very high voltages and on occasions requiring large current outputs such as cable testing, dielectric loss measurements, partial discharge measurements, etc. A transformer with 50 to 100 kV voltage rating and a relatively large current rating is connected together with an additional choke, if necessary. The test condition is set such that $(\omega(L_e + L) = 1/\omega C$ where L_e is the total equivalent leakage inductance of the transformer including its regulating transformer. The chief advantages of this principle are

- (a) it gives an output of pure sine wave,
- (b) power requirements are less (5 to 10% of total kVA required),
- (c) no high-power arcing and heavy current surges occur if the test object fails, as resonance ceases at the failure of the test object,
- (d) cascading is also possible for very high voltages,
- (e) simple and compact test arrangement, and
- (f) no repeated flashovers occur in case of partial failures of the test object and insulation recovery. It can be shown that the supply source takes Q number of cycles at least to charge the test specimen to the full voltage.

The disadvantages are the requirements of additional variable chokes capable of withstanding the full test voltage and the full current rating.

A simplified diagram of the series resonance test system is given in Fig. 6.12c and that of the parallel resonant test system in 6.12d. A voltage regulator of either the auto-transformer type or the induction regulator type is connected to the supply mains and the secondary winding of the exciter transformer is connected across the hv reactor, L , and the capacitive load C . The inductance of the reactor L is varied by varying its air gap and operating range is set in the ratio 10 : 1.

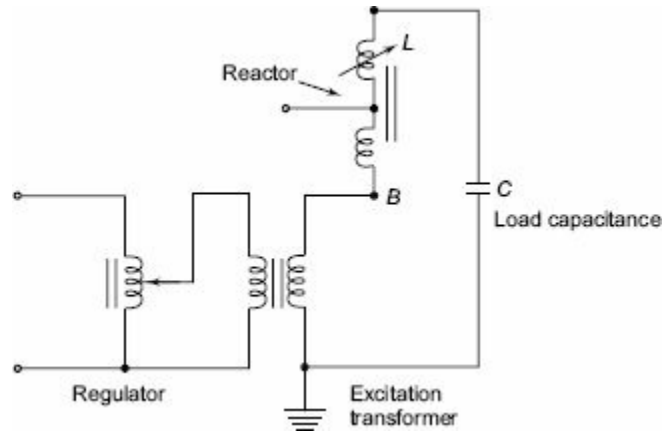


Fig. 6.12c Series resonant ac test system

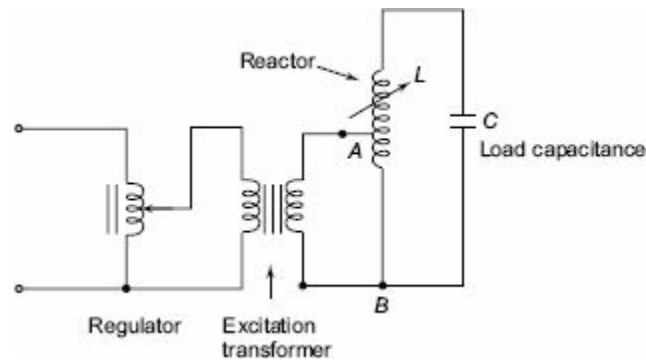


Fig. 6.12d Parallel resonant ac test system

Ratings: Regulator: 10 - 100 kVA
 Excitation transformer: 10 - 100 kVA with an output voltage of about 10 kV
 Reactor voltage — each unit up to 300 kV

Fig. 6.12 Resonant transformer and equivalent circuit

Capacitance C comprises of the capacitance of the test object, capacitance of the measuring voltage

divider, capacitance of the high-voltage bushing, etc. The Q -factor obtained in these circuits will be typically of the order of 50. In the parallel resonant mode the high voltage reactor is connected as an auto-transformer and the circuit is connected as a parallel resonant circuit. The advantage of the parallel resonant circuit is that more stable output voltage can be obtained along with a high rate of rise of test voltage, independent of the degree of tuning and the Q -factor. Single unit resonant test systems are built for output voltages up to 500 kV, while cascaded units for outputs up to 3000 kV, 50/60 Hz are available.

6.2.3 Generation of High-Frequency ac High Voltages

High-frequency high voltages are required for rectifier dc power supplies as discussed in Sec. 6.1. Also, for testing electrical apparatus for switching surges, high frequency high voltage damped oscillations are needed which need high-voltage high-frequency transformers. The advantages of these high-frequency transformers are:

- (i) the absence of iron core in transformers and hence saving in cost and size,
- (ii) pure sine-wave output,
- (iii) slow build-up of voltage over a few cycles and hence no damage due to switching surges, and
- (iv) uniform distribution of voltage across the winding coils due to subdivision of coil stack into a number of units.

The commonly used high-frequency resonant transformer is the Tesla coil, which is a doubly tuned resonant circuit shown schematically in Fig. 6.13a. The primary voltage rating is 10 kV and the secondary may be rated to as high as 500 to 1000 kV. The primary is fed from a dc or ac supply through the capacitor C_1 . A spark gap G connected across the primary is triggered at the desired voltage V_1 which induces a high self-excitation in the secondary. The primary and the secondary windings (L_1 and L_2) are wound on an insulated former with no core (air-cored) and are immersed in oil. The windings are tuned to a frequency of 10 to 100 kHz by means of the capacitors C_1 and C_2 .

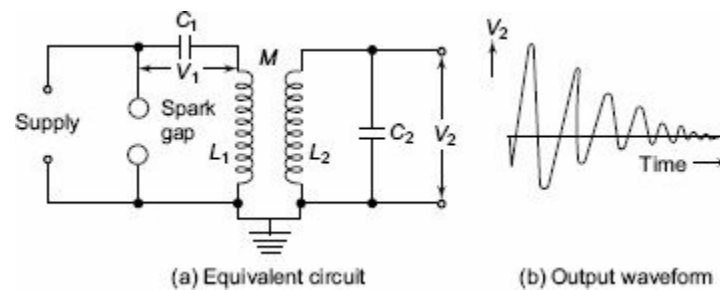


Fig. 6.13 Tesla coil equivalent circuit and its output waveform

The primary coil is wound on an insulator fibre tube of about 1 m length to represent a cylindrical or helical winding and consists of a few tens of turns (usually copper strip or tubings). The secondary winding is spaced quite away from the primary winding on another concentric fibre or pyrex tube with a few thousand turns. The whole assembly will be immersed in an oil tank under pressure. With separate bushings taken out for the primary and the secondary windings, the primary winding is supplied through a high-voltage capacitor rectifier unit rated for 10 kV to 50 kV or more and the power rating of the transformer may be 10 kVA or more.

The output voltage V_2 is a function of the parameters L_1, L_2, C_1, C_2 , and the mutual inductance M . Usually, the winding resistances will be small and contribute only for damping of the oscillations.

The analysis of the output waveform can be done in a simple manner neglecting the winding resistances. Let the capacitor C_1 be charged to a voltage V_1 when the spark gap is triggered. Let a current i_1 flow through the primary winding L_1 and produce a current i_2 through L_2 and C_2 .

$$\text{Then, } V_1 = \frac{1}{C_1} \int_0^t i_1 dt + L_1 \frac{di_1}{dt} + M \frac{di_2}{dt} \quad (6.9)$$

$$\text{and, } 0 = \frac{1}{C_2} \int_0^t i_2 dt + L_2 \frac{di_2}{dt} + M \frac{di_1}{dt}$$

The Laplace transformed equations for the above are

$$\frac{V_1}{s} = \left[L_1 s + \frac{1}{C_1 s} \right] I_1 + M s I_2 \quad (6.10)$$

and,

$$0 = [M s] I_1 + \left[L_2 s + \frac{1}{C_2 s} \right] I_2$$

where I_1 and I_2 are the Laplace transformed values of i_1 and i_2 .

The output voltage V_2 across the capacitor C_2 is

$$V_2 = \frac{1}{C_2} \int_0^t i_2 dt; \text{ or its transformed equation is}$$

$$V_2(s) = \frac{I_2}{C_2 s} \quad (6.11)$$

where $V_2(s)$ is the Laplace transform of V_2 .

The solution for V_2 from the above equations will be

$$V_2 = \frac{-M V_1}{\sigma L_1 L_2 C_2} \frac{1}{\gamma_2^2 - \gamma_1^2} [\cos \gamma_1 t - \cos \gamma_2 t] \quad (6.12)$$

where,

$$\sigma^2 = 1 - \frac{M^2}{L_1 L_2} = 1 - K^2$$

K = coefficient of coupling between the windings L_1 and L_2

$$\gamma_1^2 = \frac{\omega_1^2 + \omega_2^2}{2} + \sqrt{\left(\frac{\omega_1^2 + \omega_2^2}{2} \right)^2 - \sigma^2 \omega_1^2 \omega_2^2}$$

$$\gamma_2^2 = \frac{\omega_1^2 + \omega_2^2}{2} - \left[\left(\frac{\omega_1^2 + \omega_2^2}{2} \right)^2 - \sigma^2 \omega_1^2 \omega_2^2 \right]^{1/2}$$

$$\omega_1 = \frac{1}{\sqrt{L_1 C_1}} \text{ and } \omega_2 = \frac{1}{\sqrt{L_2 C_2}}$$

The output waveform is shown in [Fig. 6.13b](#).

The peak amplitude of the secondary voltage V_2 can be expressed as,

$$V_{2\max} = V_1 e \sqrt{\frac{L_2}{L_1}} \quad (6.13)$$

where,

$$e = \frac{2\sqrt{1 - \sigma^2}}{\sqrt{(1 + a)^2 - 4\sigma a}}$$

$$a = \frac{L_2 C_2}{L_1 C_1} = \frac{\omega_1^2}{\omega_2^2}$$

A more simplified analysis for the Tesla coil may be presented by considering that the energy stored in the primary circuit in the capacitance C_1 is transferred to C_2 via the magnetic coupling. If W_1 is the energy stored in C_1 and W_2 is the energy transferred to C_2 and if the efficiency of the transformer is η , then

$$W = \frac{1}{2} \eta C_1 V_1^2 = \left(\frac{1}{2} C_2 V_2^2 \right) \quad (6.14)$$

from which

$$V_2 = V_1 \sqrt{\eta \frac{C_1}{C_2}} \quad (6.14a)$$

It can be shown that if the coefficient of coupling K is large the oscillation frequency is less, and for large values of the winding resistances and K , the waveform may become a unidirectional impulse. This is shown in the next sections while dealing with the generation of switching surges.

6.3 GENERATION OF IMPULSE VOLTAGES

6.3.1 Standard Impulse Waveshapes

Transient overvoltages due to lighting and switching surges cause steep build-up of voltage on transmission lines and other electrical apparatus. Experimental investigations showed that these waves have a rise time of 0.5 to 10 μs and decay time to 50% of the peak value of the order of 30 to 200 μs . The waveshapes are arbitrary, but mostly unidirectional. It is shown that lightning overvoltage wave can be represented as double exponential waves defined by the equation

$$V = V_0 [\exp(-\alpha t) - \exp(-\beta t)] \quad (6.15)$$

where α and β are constants of microsecond values.

The above equation represents a unidirectional wave which usually has a rapid rise to the peak value and slowly falls to zero value. The general waveshapes is given in Fig. 6.14. Impulse waves are specified by defining their rise or front time, fall or tail time to 50% peak value, and the value of the peak voltage. Thus 1.2/50 μs , > 1000 kV wave represents an impulse voltage wave with a front time of 1.2 μs , fall time to 50% peak value of 50 μs , and a peak value of 1000 kV. When impulse waveshapes are recorded, the initial portion of the wave may not be clearly defined or sometimes may be missing. Moreover, due to disturbances it may contain superimposed oscillations in the rising portion. Hence, the front and tail times have to be redefined.

Referring to the waveshape in Fig. 6.14, the peak value α is fixed and referred to as 100% value. The points corresponding to 10% and 90% of the peak values are located in the front portion (points C and D). The line joining these points is extended to cut the time axis at O_1 . O_1 is taken as the virtual origin. 1.25 times the interval between times t_1 and t_2 corresponding to points C and D (projections on the time axis) is defined as the front time, i.e., 1.25 ($O_1 t_2 - O_1 t_1$). The point E is located on the wave tail corresponding to 50% of the peak value, and its projection on the time axis is t_4 . $O_1 t_4$ is defined as the fall or tail time. In case the point C is not clear or missing from the waveshape record, the point corresponding to 30% peak value F is taken and its projection t'_1 is located on time axis. The wave front time in that case will be defined as 1.67 ($O_1 t_3 - O_1 t'_1$). The tolerances that can be allowed in the front and tail times are respectively $\pm 30\%$ and $\pm 20\%$. Indian standard specifications define 1.2/50 μs wave to be the standard lightning impulse. The tolerance allowed in the peak value is $\pm 3\%$.

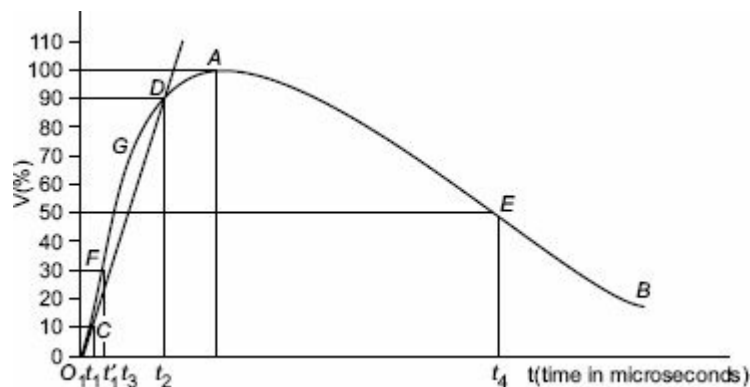


Fig. 6.14 Impulse wave and its definitions

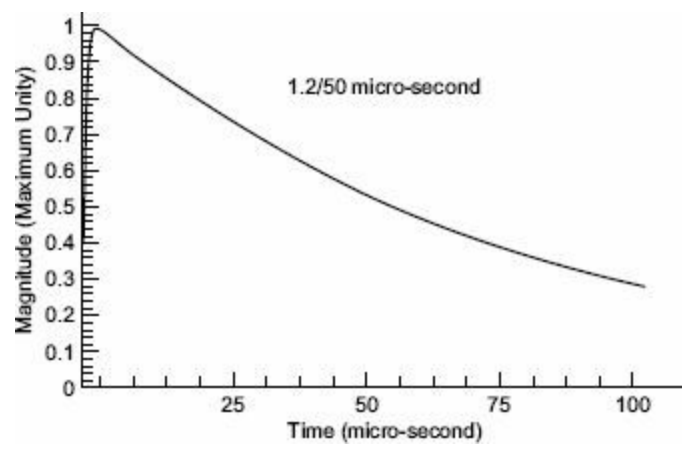


Fig. 6.14a *Typical 1.2/50 μ s waveform*

6.3.2 Theoretical Representation of Impulse Waves

The impulse waves are generally represented by [Eq. \(6.15\)](#) given earlier. V_0 in the equation represents a factor that depends on the peak value. For impulse wave of $1.2/50 \mu s$, $\alpha = -0.0146$, $\beta = -2.467$, and $V_0 = 1.04$ when time t is expressed in microseconds, α and β control the front and tail times of the wave respectively. Values of α and β for different waveforms are given in [Table 6.1](#).

Table 6.1 Values of α and μ for different waveforms (Double exponential type) (t in m seconds)

Wave form	α	β	V_0
0.5/5	0.1793	3.714	1.225
1/5	0.2650	1.294	1.892
1/50	0.01477	1.933	1.039
1.2/50	0.01460	2.467	1.046
1.5/40	0.01907	1.482	1.072
4/10	0.1866	0.3978	3.677
8/20	0.0535	0.113	2.010

6.3.3 Circuits for Producing Impulse Waves

A double exponential waveform of the type mentioned in Eq. (6.15) may be produced in the laboratory with a combination of a series $R-L-C$ circuit under over damped conditions or by the combination of two $R-C$ circuits. Different equivalent circuits that produce impulse waves are given in Figs 6.15a to d. Out of these circuits, those shown in Figs 6.15a to 6.15d are commonly used. Circuit shown in Fig. 6.15a is limited to model generators only, and commercial generators employ circuits shown in Figs 6.15b to 6.15d.

A capacitor (C_1 or C) previously charged to a particular dc voltage is suddenly discharged into the waveshaping network ($L - R$ or $R_1 R_2 C_2$ or other combination) by closing the switch S . The discharge voltage $V_0(t)$ shown in Fig. 6.15 gives the desired double exponential waveshape.

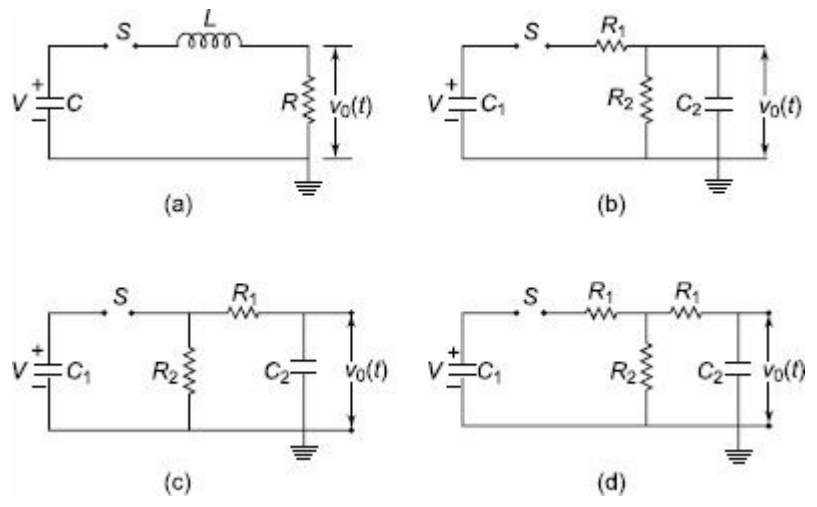


Fig. 6.15 Circuits for producing impulse waves

(a) **Analysis of Impulse Generator Circuit of Series R-L-C Type** Referring to Fig. 6.15a the current through the load resistance R is given by

$$V = \frac{1}{C} \int_0^t i dt + Ri + L \frac{di}{dt} \tag{6.16}$$

with initial condition at $t = 0$ being $i(0) = 0$ and the net charge in the circuit $q = 0$. Writing the above equation as a Laplace transform equation,

$$V/s = \left(\frac{1}{Cs} + R + Ls \right) I(s)$$

or,

$$I(s) = \frac{V}{L} \left[\frac{1}{s^2 + \frac{Rs}{L} + \frac{1}{LC}} \right]$$

The voltage across the resistor R (which is the output voltage) is, $v_0(s) = I(s) R$; hence,

$$v_0(s) = V \frac{R}{L} \frac{1}{s^2 + \frac{Rs}{L} + \frac{1}{LC}}$$

For an overdamped condition, $R/2L \geq 1/\sqrt{LC}$

Hence, the roots of the equation $s^2 + \frac{Rs}{L} + \frac{1}{LC}$ are

$$\alpha = s_1 = \frac{-R}{2L} + \sqrt{\left(\frac{R}{2L}\right)^2 - \frac{1}{LC}}$$

$$\beta = s_2 = \frac{-R}{2L} - \sqrt{\left(\frac{R}{2L}\right)^2 - \frac{1}{LC}}$$

The solution of the equation for $v_0(t)$ is

$$v_0(t) = \frac{V\left(\frac{R}{2L}\right)}{\left[\frac{R^2}{4L^2} - \frac{1}{LC}\right]^{1/2}} [\exp(-\alpha t) - \exp(-\beta t)] \quad (6.17)$$

$$= V_0 [\exp(-\alpha t) - \exp(-\beta t)] \quad (6.17a)$$

where,

$$V_0 = \frac{V\left(\frac{R}{2L}\right)}{\left[\frac{R^2}{4L^2} - \frac{1}{LC}\right]^{1/2}} = \frac{V}{\left[1 - \frac{4L}{CR^2}\right]^{1/2}} \quad (6.17b)$$

The sum of the roots $(\alpha + \beta) = -\frac{R}{2L}$

and, the product of the roots $\alpha\beta = \frac{1}{LC}$ (6.17c)

The wave-front and the wave-tail times are controlled by changing the values of R and L simultaneously with a given generator capacitance C ; choosing a suitable value for L , β or the wave-front time is determined and α or the wave-tail time is controlled by the value of R in the circuit. The advantage of this circuit is its simplicity. But the waveshape control is not flexible and independent. Another disadvantage is that the basic circuit is altered when a test object which will be mainly capacitive in nature, is connected across the output. Hence, the waveshape gets changed with the change of test object.

(b) Analysis of the Other Impulse Generator Circuits The most commonly used configurations for impulse generators are the circuits shown in [Figs 6.15b](#) and [c](#). The advantages of these circuits are that the wave front and wave tail times are independently controlled by changing either R_1 or R_2 separately. Secondly, the test objects which are mainly capacitive in nature from part of C_2 .

For the configuration shown in [Fig. 6.15b](#), the output voltage across C_2 is given by $v_0(t) = \frac{1}{C_2} \int_0^t i_2 dt$.

Performing Laplace transformation, $\frac{1}{C_2 s} I_2(s) = v_0(s)$

where i_2 is the current through C_2 .

Taking the current through C_1 as i_1 and its transformed value as $I_1(s)$,

$$I_2(s) = \left[\frac{R_2}{R_2 + \frac{1}{C_2 s}} \right] I_1(s)$$

$$I_1(s) = \frac{V}{s} \frac{1}{\frac{1}{C_1 s} + R_1 + \frac{R_2 \cdot \frac{1}{C_2 s}}{R_2 + \frac{1}{C_2 s}}}$$

where, $\frac{R_2 \cdot \frac{1}{C_2 s}}{R_2 + \frac{1}{C_2 s}}$ represents the impedance of the parallel combination of R_2 and C_2

Substitution of $I_1(s)$ gives

$$v_0(s) = \left[\frac{1}{C_2 s} \frac{R_2}{R_2 + \frac{1}{C_2 s}} \right] \left[\frac{V}{s} \frac{1}{\frac{1}{C_1 s} + R_1 + \frac{R_2(1/C_2 s)}{R_2 + (1/C_2 s)}} \right]$$

After simplification and rearrangement,

$$v_0(s) = \frac{V}{R_1 C_2} \left[\frac{1}{s^2 + \left(\frac{1}{C_1 R_1} + \frac{1}{C_2 R_2} + \frac{1}{C_2 R_1} \right) s + \frac{1}{C_1 C_2 R_1 R_2}} \right] \quad (6.18)$$

Here, the roots of the equation (α and β)

$$s^2 + \left[\frac{1}{C_1 R_1} + \frac{1}{C_2 R_2} + \frac{1}{C_2 R_1} \right] s + \frac{1}{C_1 C_2 R_1 R_2}$$

are found from the relations,

$$\alpha + \beta = - \left[\frac{1}{C_1 R_1} + \frac{1}{C_2 R_2} + \frac{1}{C_2 R_1} \right] \quad (6.19)$$

$$\alpha \beta = \frac{1}{C_1 C_2 R_1 R_2}$$

Taking inverse transform of $v_0(s)$ gives

$$v_0(t) = \frac{V}{R_1 C_2 (\alpha - \beta)} [\exp(-\alpha t) - \exp(-\beta t)] \quad (6.20)$$

Usually, $\frac{1}{C_1 R_1}$ and $\frac{1}{C_2 R_2}$ will be much smaller compared to $\frac{1}{R_1 C_2}$.

Hence, the roots may be approximated as

$$\alpha \approx \frac{1}{R_1 C_2} \text{ and } \beta = \frac{1}{R_2 C_1} \quad (6.21)$$

Following a similar analysis, it may be shown that the output waveform for the circuit configuration

of 6.15c will be

$$v_0(t) = \frac{VC_1R_2\alpha\beta}{(\beta - \alpha)} [\exp(-\alpha t) - \exp(-\beta t)]$$

where α and β are the roots of the Eq. (6.19). The approximate values of α and β given by Eq. (6.21) are valid for this circuit also.

The equivalent circuit given in Fig. 6.15d is a combination of the configurations of Fig. 6.15b and Fig. 6.15c. The resistance R_1 is made into two parts and kept on either side of R_2 to give greater flexibility for the circuits. For series R - L - C circuit, LC and RC products for different wave forms are given in Table 6.2.

Table 6.2 'LC' and 'RC' products for producing different waveforms with R - L - C Ckt

Waveform	LC	RC	Voltage efficiency
0.5/5	0.788	6.43	95.4
1/5	1.80	5.60	88.1
1/10	3.16	12.9	95.4
1.5/40	15.6	55.4	97.8
1/50	11.6	70.6	98.8
8/20	65	6.955	50.0

(R in Ohms, C in μF and L in μH)

(c) Restrictions on the Ratio of the Generator and Load Capacitances, C_1/C_2 on the Circuit Performance For a given waveshape, the choice of R_1 and R_2 to control the wave-front and wave-tail times is not entirely independent but depends on the ratio of C_1/C_2 . It can be shown mathematically that

$$R_2 = P(y)/C_1 \text{ and } R_1 = Q(y)/C_1$$

where $y = C_1/C_2$ and P and Q are functions of y . In order to get real values for R_1 and R_2 for a given waveshape, a maximum and minimum value of y exists in practice. This is true whether the configuration of Fig. 6.15b or 6.15c is used. For example, with the circuit of Fig. 6.15b, the ratio of C_1/C_2 cannot exceed 3.35 for a $1/5 \mu s$ waveshape. Similarly, for a $1/50 \mu s$ waveshape the ratio C_1/C_2 lies between 6 and 106.5. If the configuration chosen is 6.15c, the minimum value of C_1/C_2 for $1/5 \mu s$ waveshape is about 0.3 and that for the $1/50 \mu s$ waveshape is about 0.01. The reader is referred to High-Voltage Laboratory Techniques by Craggs and Meek for further discussion on the restrictions imposed on the ratio C_1/C_2 .

(d) Effect of Circuit Inductances and Series Resistance on the Impulse Generator Circuits

The equivalent circuits shown in Figs 6.15a to d, in practice comprise of several stray series inductances. Further, the circuits occupy considerable space and will be spread over several metres in a testing laboratory. Each component has some residual inductance and the circuit loop itself contributes for further inductance. The actual value of the inductance may vary from $10 \mu H$ to several hundreds of microhenries. The effect of the inductance is to cause oscillations in the wave-front and in the wave-tail portions. Inductances of several components and the loop inductance are

shown in Fig. 6.16a. Figure 6.16b gives a simplified circuit for considering the effect of inductance. The effect of the variation of inductance on the waveshape is shown in Fig. 6.16c. If the series resistance R_1 is increased, the wave front oscillations are damped, but the peak value of the voltage is also reduced. Sometimes, in order to control the front time a small inductance is added.

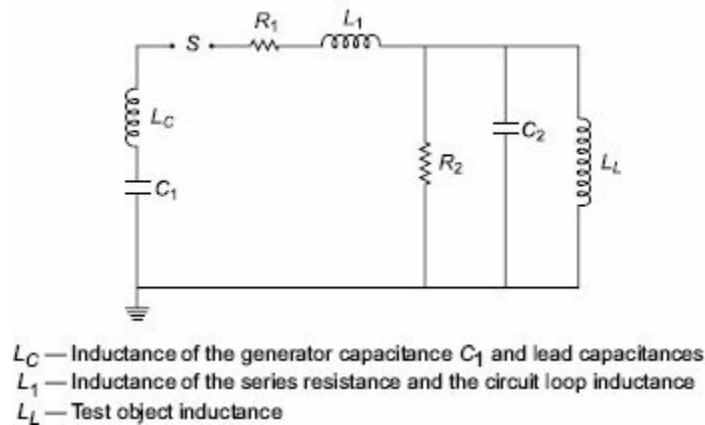


Fig. 6.16a Series inductances in impulse generator circuit

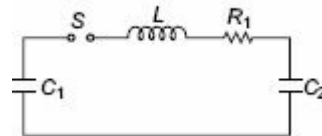


Fig. 6.16b Simplified circuit for calculation of wave-front time $L = L_C + L_1 + \text{any other added inductance}$

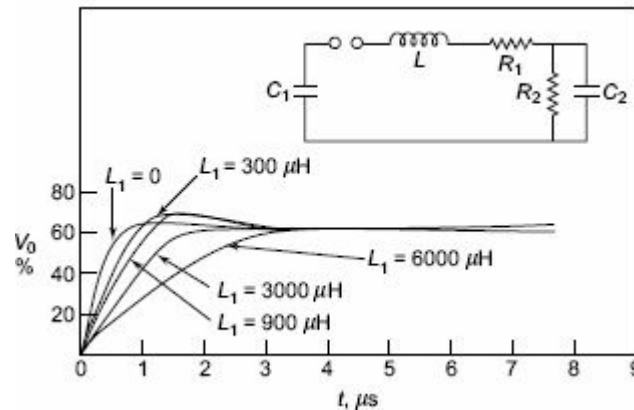


Fig. 6.16c Effect of series inductance on wave-front time. V_0 is the percentage of charging voltage V , to which C_1 is charged

(e) Impulse Generators for Testing Objects having Large Capacitance When test objects with large capacitances are to be tested ($C > 5 \text{ nF}$), it is difficult to generate standard impulses with front time within the specified tolerance of $\pm 30\%$ and the specified less than 5% tolerance in the overshoot. This is mainly because of the effect of the inductance of the impulse generator and the front resistors. Normally the inductance of the impulse generator will be about 3 to 5 μH per stage and that of the leads about 1 $\mu\text{H}/\text{m}$. Also the front resistor which is usually of bifilar type, has inductance of about 2 $\mu\text{H}/\text{unit}$. An overshoot in the voltage wave of more than 5% will occur $R/(\sqrt{L/C}) \leq 1.38$, where R is the front resistance, L is the generator inductance and C is the equivalent capacitance of the generator given by $C = C_1 \cdot C_2 / (C_1 + C_2)$.

(f) Impulse Generators for Test Objects with Inductance Often impulse generators are required to test equipment with large inductance, such as power transformers and reactors. Usually, generating the impulse voltage wave of proper time-to-front and obtaining a good voltage efficiency are easy, but obtaining the required time-to-tail as per the standards will be very difficult. The equivalent circuit for medium and low inductive loads will be as shown in Fig. 6.16d. For the calculation of time-to-tail the circuit can still be approximated as a series C - R - L circuit. As the value $R/(\sqrt{L/C})$ decreases, the overshoot and the swing of the wave to the opposite polarity increases thereby deviating from the standard wave shape. Therefore, it is necessary to keep the value of the effective resistance R in the circuit large. One method of doing this is to connect a large resistance, R_2 in parallel with the test object or to connect the untested winding of the transformer (load) with a suitable resistance. Another method that can be used is to increase the generator capacitance with which the time-to-tail also increases, but without altering the time-to-front and the overshoot. Figure 6.16d gives the circuit arrangement for inductive loads and 6.16e gives the requirement of energy and capacitance of the impulse voltage generator. Figure B of 6.16e gives the generator capacitance required to give the time-to-tail values in the range of 40 to 60 μ s at different inductive loads.

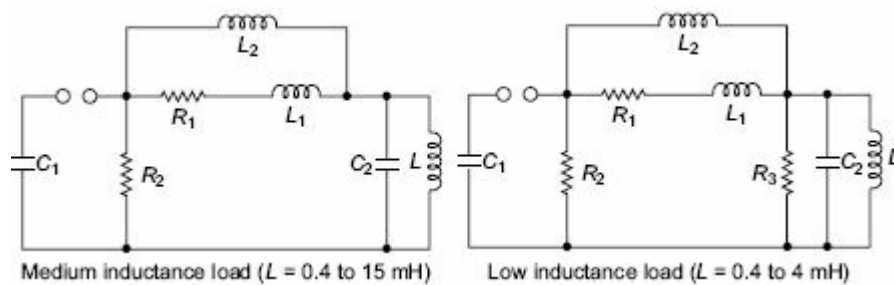


Fig. 6.16d Effect of inductive loads on impulse voltage generator circuits

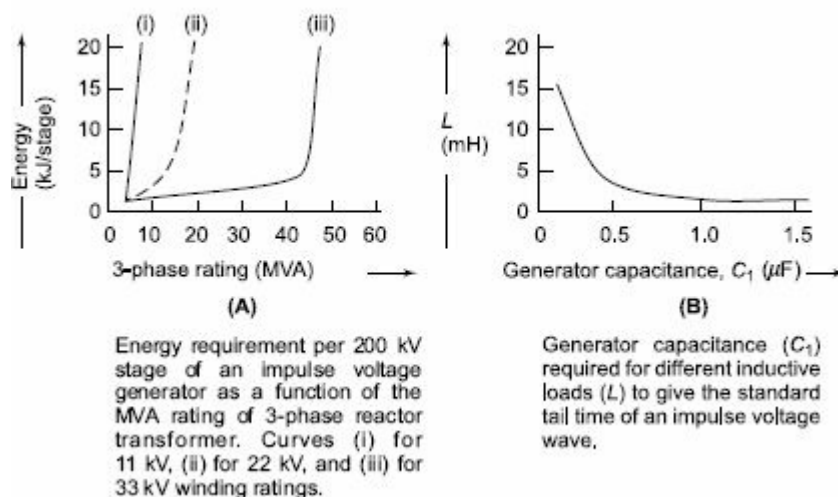


Fig. 6.16e Requirements of an impulse voltage generator energy and capacitance for the testing of the transformer (reactor) winding using standard impulse voltages

Fig. 6.16 Series inductance in impulse generator circuits and its effect on waveshape

(g) Waveshape Control Generally, for a given impulse generator of Fig. 6.15b or c the generator capacitance C_1 and load capacitance C_2 will be fixed depending on the design of the generator and the test object. Hence, the desired waveshape is obtained by controlling R_1 and R_2 . The following

approximate analysis is used to calculate the wave-front and wave-tail times.

The resistance R_2 will be large. Hence, the simplified circuit shown in [Fig. 6.16b](#) is used for wave front time calculation. Taking the circuit inductance to be negligible during charging, C_1 charges the load capacitance C_2 through R_1 . Then the time taken for charging is approximately three times the time constant of the circuit and is given by

$$t_1 = 3.0 R_1 \frac{C_1 C_2}{C_1 + C_2} = 3 R_1 C_e \quad (6.22)$$

where $C_e = \frac{C_1 C_2}{C_1 + C_2}$. If R_1 is given in ohms and C_e in microfarads, t_1 is obtained in microseconds.

For discharging or tail time, the capacitances C_1 and C_2 may be considered to be in parallel and discharging occurs through R_1 and R_2 . Hence, the time for 50% discharge is approximately given by

$$t_2 = 0.7 (R_1 + R_2) (C_1 + C_2) \quad (6.23)$$

These formulae for t_1 and t_2 hold good for the equivalent circuits shown in [Figs 6.15b](#) and [6.15c](#). For the circuit given in [Fig. 6.15d](#), R is to be taken as $2R_1$. With the approximate formulae, the wave front and wave tail times can be estimated to within $\pm 20\%$ for the standard impulse waves.

6.3.4 Multistage Impulse Generators—Marx Circuit

In the above discussion, the generator capacitance C_1 is to be first charged and then discharged into the wave-shaping circuits. A single capacitor C_1 may be used for voltages up to 200 kV. Beyond this voltage, a single capacitor and its charging unit may be too costly, and the size becomes very large. The cost and size of the impulse generator increases at a rate of the square or cube of the voltage rating. Hence, for producing very high voltages, a bank of capacitors are charged in parallel and then discharged in series. The arrangement for charging the capacitors in parallel and then connecting them in series for discharging was originally proposed by Marx. Nowadays, modified Marx circuits are used for the multistage impulse generators.

The schematic diagram of Marx circuit and its modification are shown in [Figs 6.17a](#) and [6.17b](#), respectively. Usually the charging resistance R_s is chosen to limit the charging current to about 50 to 100 mA, and the generator capacitance C is chosen such that the product CR_s is about 10 s to 1 min. The gap spacing is chosen such that the breakdown voltage of the gap G is greater than the charging voltage V . Thus, all the capacitances are charged to the voltage V in about 1 minute. When the impulse generator is to be discharged, the gaps G are made to spark over simultaneously by some external means. Thus, all the capacitors C get connected in series and discharge into the load capacitance or the test object. The discharge time constant CR_1/n (for n stages) will be very very small (microseconds), compared to the charging time constant CR_s which will be few seconds. Hence, no discharge takes place through the charging resistors R_s . In the Marx circuit is of [Fig. 6.17a](#) the impulse wave-shaping circuit is connected externally to the capacitor unit. In [Fig. 6.17b](#), the modified Marx circuit is shown, wherein the resistances R_1 and R_2 are incorporated inside the unit. R_1 is divided into n parts equal to R_1/n and put in series with the gap G . R_2 is also divided into n parts and arranged across each capacitor unit after the gap G . This arrangement saves space, and also the cost is reduced. But, in case the waveshape is to be varied widely, the variation becomes difficult. The additional advantages gained by distributing R_1 and R_2 inside the unit are that the control resistors are smaller in size and the efficiency (V_0/ZnV) is high.

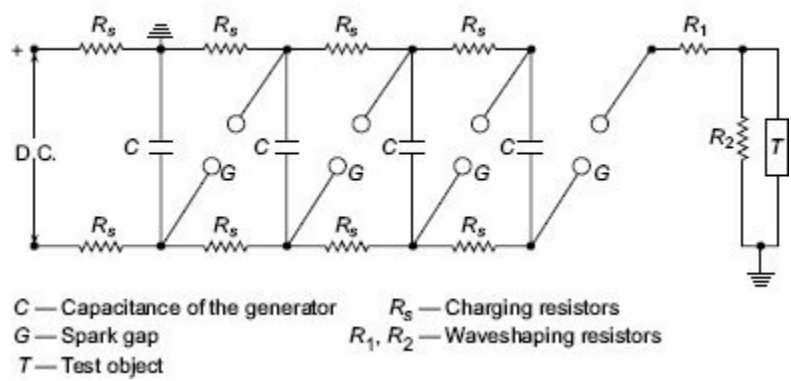


Fig. 6.17a Schematic diagram of Marx circuit arrangement for multistage impulse generator

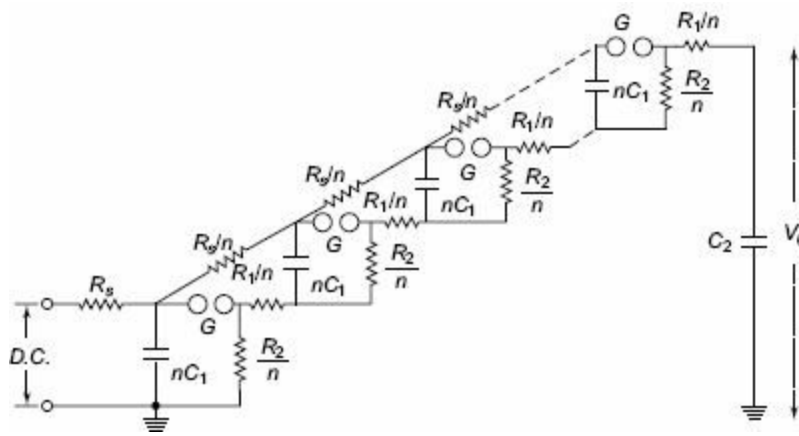


Fig. 6.17b Multistage impulse generator incorporating the series and wave tail resistances with in the generator

Impulse generators are nominally rated by the total voltage (nominal), the number of stages, and the gross energy stored. The nominal output voltage is the number of stages multiplied by the charging voltage. The nominal energy stored is given by $\frac{1}{2} C_1 V^2$ where $C_1 = C/n$ (the discharge capacitance) and V is the nominal maximum voltage (n times charging voltage). A 16-stage impulse generator having a stage capacitance of $0.280\mu\text{F}$ and a maximum charging voltage of 300 kV will have an energy rating of 192 kW. The height of the generator will be about 15 m and will occupy a floor area of about 3.25×3.00 m. The waveform of either polarity can be obtained by suitably changing the charging unit polarity ([Plate 3](#)).

6.3.5 Components of a Multistage Impulse Generator

A multistage impulse generator requires several components parts for flexibility and for the production of the required waveshape. These may be grouped as follows:

(i) *dc Charging Set* The charging unit should be capable of giving a variable dc voltage of either polarity to charge the generator capacitors to the required value.

(ii) *Charging Resistors* These will be non-inductive high value resistors of about 10 to 100 kilo-ohms. Each resistor will be designed to have a maximum voltage between 50 and 100 kV.

(iii) *Generator Capacitors and Spark Gaps* These are arranged vertically one over the other with all the spark gaps aligned. The capacitors are designed for several charging and discharging operations. On dead short circuit, the capacitors will be capable of giving 10 kA of current. The spark gaps will be usually spheres or hemispheres of 10 to 25 cm diameter. Sometimes spherical ended cylinders with a central support may also be used.

(iv) *Wave-shaping Resistors and Capacitors* Resistors will be non-inductive wound type and should be capable of discharging impulse currents of 1000 A or more. Each resistor will be designed for a maximum voltage of 50 to 100 kV. The resistances are bifilar wound on non-inductive thin flat insulating sheets. In some cases, they are wound on thin cylindrical formers and are completely enclosed. The load capacitor may be of compressed gas or oil filled with a capacitance of 1 to 10 nF.

Modern impulse generators have their wave-shaping resistors included internally with a flexibility to add additional resistors outside, when the generator capacitance is changed (with series parallel connection to get the desired energy rating at a given test voltage). Such generators optimize the set of resistors. A commercial impulse voltage generator uses six sets of resistors ranging from 1.0 ohm to about 160 ohms with different combinations (with a maximum of two resistors at a time) such that a resistance value varying from 0.7 ohm to 235 ohms per stage is obtained, covering a very large range of energy and test voltages. The resistors used are usually resin cast with voltage and energy ratings of 200 to 250 kV and 2.0 to 5.0 kW. The entire range of lightning and switching impulse voltages can be covered using these resistors either in series or in parallel combination.

(v) *Triggering System* This consists of trigger spark gaps to cause spark breakdown of the gaps (see [Sec. 6.5](#)).

(vi) *Voltage Dividers* Voltage dividers of either damped capacitor or resistor type and an oscilloscope with recording arrangement are provided for measurement of the voltages across the test object. Sometimes a sphere gap is also provided for calibration purposes (see [Chapter 7](#) for details).

(vii) *Gas Insulated Impulse Generators* Impulse generators rated for 4 MV or above will be very tall and require large space. As such they are usually located in open space and are housed in an insulated enclosure. The height of a 4.8 MV unit may be around 30 m. To make the unit compact, a compressed gas, such as N₂ or SF₆ may be used as the insulation.

Impulse generators are needed to generate very fast transients having time duration of 0.5/5 or 0.1/1.0 μ s waves for testing Gas Insulated Systems (GIS) that are coming up nowadays. The energy

needed for testing of this type of equipment is small (less than 30 kJ) and the load capacitance is usually less than 500 pF.

Generation of Very Fast Transients

IEC specifies that the standard wave form of the fast transients can be either 0.2/2 or 0.3/3.0 μ second wave with front-time tolerance of about 60% and tail-time tolerance of 30%. When testing motor or generator coils, the test specimen is a 'R-L' load where as with GIS the load is capacitive. Hence, generation of exact wave form without oscillations or distortions is extremely difficult.

The impulse generator used to generate such wave forms consists of a capacitor of 0.01 to 0.1 μ F discharging into a load capacitor in parallel with the test object (either 'R-L' like motor coils or capacitive like GIS) through a few sections of 'L-C' unit pulse-shaping network ([Fig. 6.21](#)).

6.3.6 Generation of Switching Surges

Nowadays, in extra-high-voltage transmission lines and power systems, switching surge is an important factor that affects the design of insulation. All transmission lines rated for 220 kV and above, incorporate switching surge spark overvoltage for their insulation levels. A switching surge is a short duration transient voltage produced in the system due to a sudden opening or closing of a switch or circuit breaker or due to an arcing at a fault in the system. The waveform is not unique. The transient voltage may be an oscillatory wave or a damped oscillatory wave of frequency ranging from few hundred hertz to few kilohertz. It may also be considered as a slow rising impulse having a wave front time of 0.1 to 10 μs , and a tail time of one to several μs . Thus, switching surges contain larger energy than the lightning impulse voltages.

Several circuits have been adopted for producing switching surges. They are grouped as (i) impulse generator circuit modified to give longer duration waveshapes, (ii) power transformers or testing transformers excited by dc voltages giving oscillatory waves and these include Tesla coils.

Standard switching impulse voltage is defined, both by the Indian Standards and the IEC, as 250/2500 μs wave, with the same tolerances for time-to-front and time-to-tail as those for the lightning impulse voltage wave, i.e., time-to-front of $(250 \pm 50) \mu\text{s}$ and time-to-half value of $(2500 \pm 500) \mu\text{s}$. Other switching impulse voltage waves commonly used for testing the lightning arresters are 250/1500 μs with a tolerance of $\pm 500 \mu\text{s}$ in time-to-half value.

[Figure 6.18](#) shows the impulse generator circuits modified to give switching surges. The arrangement is the same as that of an impulse generator. The values of R_1 and R_2 for producing waveshapes of long duration, such as 100/1000 μs or 400/4000 μs , will range from 1 to 5 kilo-ohms and 5 to 20 kilo-ohms respectively. Thus, R_1 is about 20 to 30% of R_2 . The efficiency of the generator gets considerably reduced to about 50% or even less. Moreover, the values of the charging resistors R_1 are to be increased to very high values as these come in parallel with R_2 in the discharge circuit.

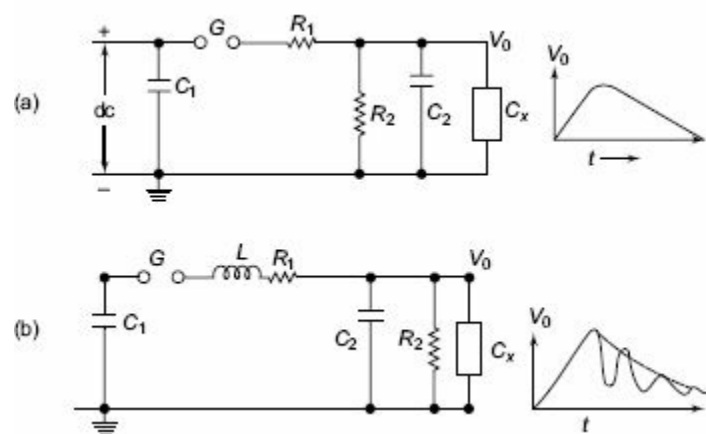


Fig. 6.18 Circuits for producing switching surge voltages. Also, shown are the output waveshapes across the load C_x .

The circuit given in [Fig. 6.18b](#) produces unidirectional damped oscillations. With the use of an inductor L , the value of R_1 is considerably reduced, and the efficiency of the generator increases. The damped oscillations may have a frequency of 1 to 10 kHz depending on the circuit parameters. Usually, the maximum value of the switching surge obtained is 250 to 300 kV with an impulse generator having a nominal rating of 1000 kV and 25 kW. Bellaschi et al. used only an inductor L of low resistance to produce switching impulse up to 500 kV. A sphere gap was included in parallel with the test object for voltage measurement and also for producing chopped waves.

Switching surges of very high peaks and long duration can be obtained by using the circuit shown in Fig. 6.19. An impulse generator condenser C_1 charged to a low voltage dc (20 to 25 kV) is discharged into the low-voltage winding of a power or testing transformer. The high-voltage winding is connected in parallel to a load capacitance C_2 , a potential divider R_2 , a sphere gap S , and test object. Through an autotransformer action, switching surge of proper waveshape can be generated across the test object. The efficiency obtained by this method is high but the transformer should be capable of withstanding very high voltages.

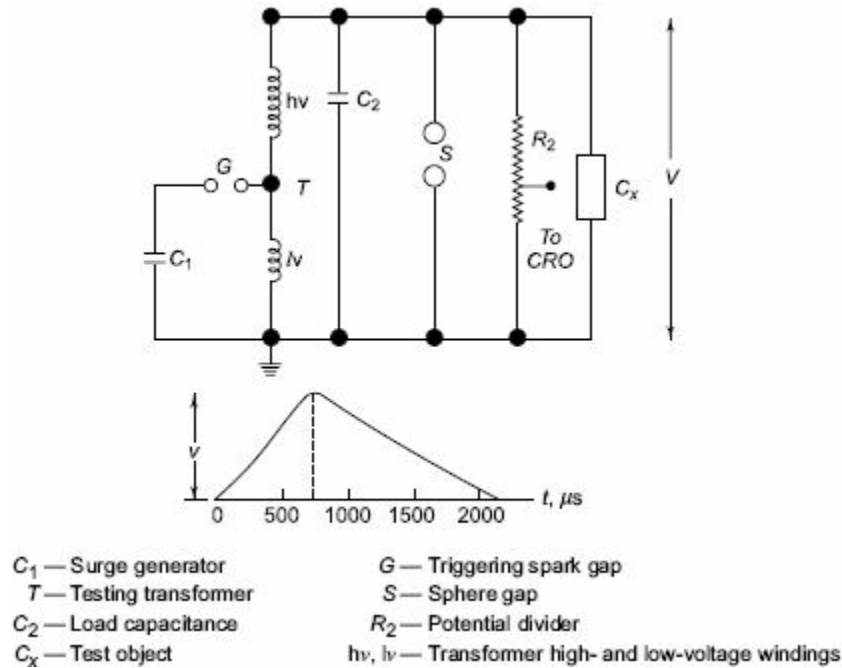


Fig. 6.19 Circuit for producing switching surges using a transformer

Multi-Test Sets for High-Voltage Testing

In many small laboratories like in the teaching institutions, small industries and utility organizations, the requirements of high voltages may be less than about 200 kV, 50 Hz, ac, 400 kV dc and 400 kV standard lightning and switching impulse voltages. The power requirements will be around 5 kVA or kVA and the energy requirement will be less than 1.5 kJ. For such applications, flexible and universally interchangeable modular systems of the above voltage and energy ratings are available under different trade names. These systems mainly consist of the following:

(i) *ac Testing Transformers* With continuous power ratings of 3 to 5 kVA with a short time rating about 150%. The unit can be one single transformer of up to 100 kV (rms), or 2 to 3 units connected in cascade with voltage ratings up to 300 kV (rms).

(ii) *dc Units* Ac transformer with the addition of a rectifier unit and a filter capacitor, with ripple factor at rated current less than 5% and a voltage drop or regulation less than 10%, for a single stage output of about 100 kV (half-wave rectifier) constitute a dc set. dc sets are available as multi-stage voltage doubler units with one pulse output, or as a quadruple unit of up to 400 kV rating with the same specifications. In either case, the power ratings will be about 3 to 5 kVA continuous. The rectifier stacks used are the selenium diode type.

(iii) Impulse Voltage Units Marx circuit of 2 to 4 stages can be assumed using the transformer and dc rectifier unit described earlier for an output voltage of about 400 kV (peak) using a one stage rectifier unit. The necessary wave front and wave tail resistors and load capacitances are normally provided. The units are assembled with modular components mounted on suitable insulating columns. The units normally have voltage efficiency of about 90%.

All the basic units are clearly and compactly arranged. By having increased number of units the system can be expanded to obtain higher and desired type of voltage. Control cubicles/boxes are provided for the control and measurement of voltages. The units can be mounted on wheels or located permanently in a test hall of size 4 m × 3 m × 3 m.

Multi-test sets are currently being manufactured and assembled in India by some leading manufacturers of high-voltage test equipments.

6.4 GENERATION OF IMPULSE CURRENTS

Lightning discharges involve both high voltage impulses and high current impulses on transmission lines. Protective gear like surge diverters have to discharge the lightning currents without damage. Therefore, generation of impulse current waveforms of high magnitude (= 100 kA peak) find application in test work as well as in basic research on non-linear resistors, electric arc studies, and studies relating to electric plasmas in high current discharges.

6.4.1 Definition of Impulse Current Waveforms

The waveshapes used in testing surge diverters are 4/10 and 8/20 μs , the figures respectively representing the nominal wave-front and wave-tail times (see [Fig. 6.14](#)). The tolerances allowed on these are $\pm 10\%$ only. Apart from the standard impulse current waves, rectangular waves of long duration are also used for testing. The waveshape should be nominally rectangular in shape. The rectangular waves generally have durations of the order of 0.5 to 5 μs , with rise and fall times of the waves being less than $\pm 10\%$ of their total duration. The tolerance allowed on the peak value is $+20\%$ and -0% (the peak value may be more than the specified value but not less). The duration of the wave is defined as the total time of the wave during which the current is at least 10% of its peak value.

6.4.2 Circuit for Producing Impulse Current Waves

For producing impulse currents of large value, a bank of capacitors connected in parallel are charged to a specified voltage and are discharged through a series R - L circuit as shown in Fig. 6.20. C represents a bank of capacitors connected in parallel which are charged from a dc source to a voltage up to 200 kV. R represents the dynamic resistance of the test object and the resistance of the circuit and the shunt. L is an air cored high current inductor, usually a spiral. If the capacitor is charged to a voltage V and discharged when the spark gap is triggered, the current i_m will be given by the equation

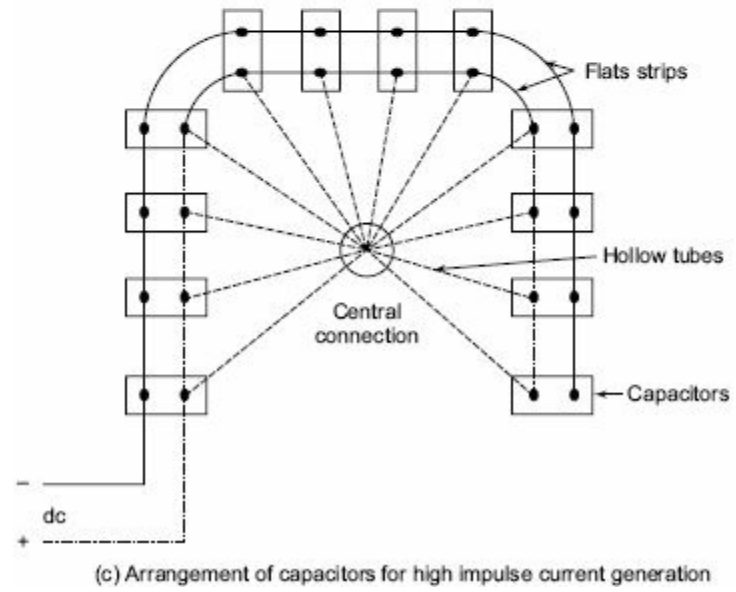
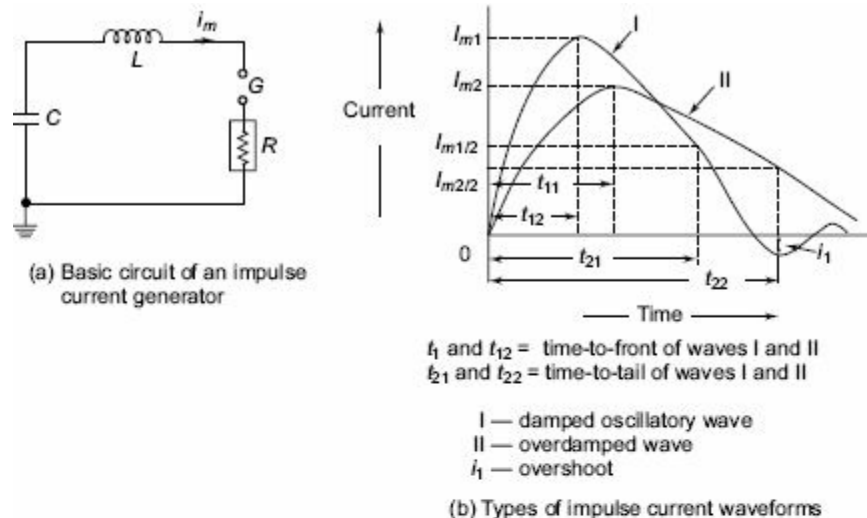


Fig. 6.20 Impulse current generator circuit and its waveform

$$V = Ri_m + L \frac{di_m}{dt} + \frac{1}{C} \int_0^t i_m dt \tag{6.24}$$

The circuit is usually underdamped, so that

$$\frac{R}{2} < \sqrt{L/C}$$

Hence, i_m is given by
$$i_m = \frac{V}{\omega L} [\exp(-\alpha t)] \sin(\omega t) \quad (6.25)$$

where
$$\alpha = \frac{R}{2L} \text{ and } \omega = \sqrt{\frac{1}{LC} - \frac{R^2}{4L^2}} \quad (6.25a)$$

The time taken for the current i_m to rise from zero to the first peak value is

$$t_1 = t_f = \frac{1}{\omega} \sin^{-1} \frac{\omega}{\sqrt{LC}} = \frac{1}{\omega} \tan^{-1} \frac{\omega}{\alpha} \quad (6.26)$$

The duration for one half cycle of the damped oscillatory wave t_2 is

$$t_2 = \frac{\pi}{\sqrt{\frac{1}{LC} - \frac{R^2}{4L^2}}} \quad (6.27)$$

It can be shown that the maximum value of i_m is normally independent of the value of V and C for a given energy $W = \frac{1}{2} CV^2$, and the effective inductance L . It is also clear from [Eq. \(6.25\)](#) that a low inductance is needed in order to get high current magnitudes for a given charging voltage V .

The present practice as per IEC standards is to adopt waveform II shown in [Fig. 6.20](#), and to define the waveform and wave tail times similar to the definition given for impulse voltage waves. Thus, the current i_m is expressed as follows.

$$I_m = e^{-\alpha t} \{e^{+\beta t} - e^{-\beta t}\} = I_0 \{e^{(-\alpha+\beta)t} - e^{-(\alpha+\beta)t}\}$$

where
$$\alpha = -R/2L \text{ and } \beta = \sqrt{\frac{R^2}{4L^2} - \frac{1}{LC}}$$

with this definition, time to front $t_1 = t_f \Rightarrow 1/\beta \tanh^{-1} \beta/\alpha$ and the time to tail t_2 is a complex function of both β and α .

For a 8/20 μS wave, the values of t_1 , t_2 and peak value of I_m are deduced as $\alpha = 0.0535 \times 10^6$, $\beta = 0.113 \times 10^6$ and $I_m = VC/14$ with $LC = 65$.

Values of R , L and C are expressed in ohms, Henries and Farads and V , I are expressed in kV and kA.

6.4.3 Generation of High Impulse Currents

For producing large values of impulse currents, a number of capacitors are charged in parallel and discharged in parallel into the circuit. The arrangement of capacitors is shown in [Fig. 6.20c](#). In order to minimize the effective inductance, the capacitors are subdivided into smaller units. If there are n_1 groups of capacitors, each consisting of n_2 units and if L_0 is the inductance of the common discharge path, L_1 is that of each group and L_2 is that of each unit, then the effective inductance L is given by

$$L = L_0 + \frac{L_1}{n_1} + \frac{L_2}{n_1 n_2}$$

Also, the arrangement of capacitors into a horse-shoe shaped layout minimizes the effective load inductance ([Plate 4](#)).

The essential parts of an impulse current generator are

- (i) a dc charging unit giving a variable voltage to the capacitor bank,
- (ii) capacitors of high value (0.5 to 5 μF) each with very low self-inductance, capable of giving high short circuit currents,
- (iii) an additional air cored inductor of high current value,
- (iv) proper shunts and oscillograph for measurement purposes, and
- (v) a triggering unit and spark gap for the initiation of the current generator.

6.4.4 Generation of Rectangular Current Pulses

Generation of rectangular current pulses of high magnitudes (few hundred amperes and duration up to 5 ms) can be done by discharging a pulse network or cable previously charged. The basic circuit for producing rectangular pulses is given in Fig. 6.21. The length of a cable or an equivalent pulse forming network is charged to a specified dc voltage. When the spark gap is short-circuited, the cable or pulse network discharges through the test object.

To produce a rectangular pulse, a coaxial cable of surge impedance $\sqrt{L_0/C_0}$ (where L_0 is the inductance and C_0 is the capacitance per unit length) is used. If the cable is charged to a voltage V and discharged through the test object of resistance R , the current pulse I is given by $I = V/(Z_0 + R)$. A pulse voltage $RV/(R + Z_0)$ is developed across the test object R , and the pulse current is sustained by a voltage wave $(V-IR)$. For $R = Z_0$, the reflected wave from the open end of the cable terminates the pulse current into the test object, and the pulse voltage becomes equal to $V/2$.

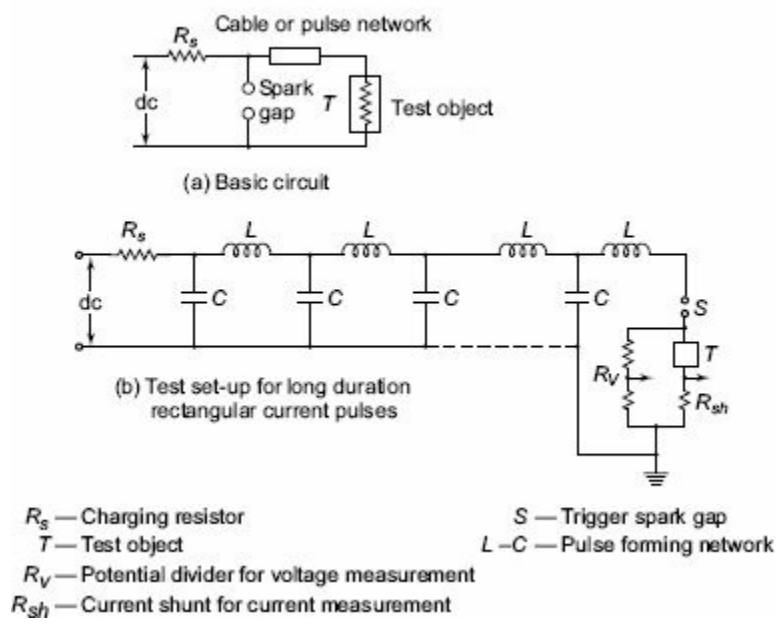


Fig. 6.21 Basic circuit and schematic set-up for producing rectangular current pulses

In practice, it is difficult to get a coaxial cable of sufficient capacitance and length. Often artificial transmission lines with lumped L and C as shown in Fig. 6.21b are used. Usually, 6 to 9 $L-C$ sections will be sufficient to give good rectangular waves. The duration of the pulse time in seconds (t) is given by $t = 2(n-1)\sqrt{LC}$, where n is the number of sections used, C is the capacitance per stage or section, and L is the inductance per stage or section.

The current waveforms produced by an artificial line or pulse network and a coaxial cable are shown in Figs 6.22a and b.

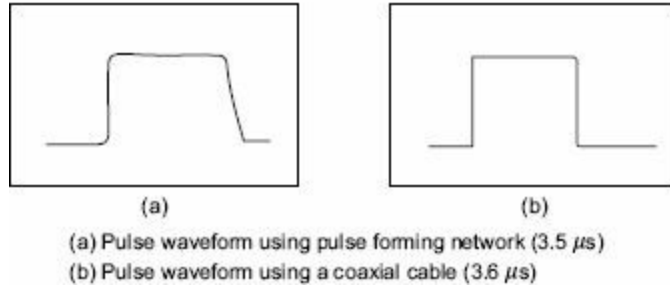


Fig. 6.22 *Current waveforms produced by rectangular current generators*

6.5 TRIPPING AND CONTROL OF IMPULSE GENERATORS

In large impulse generators, the spark gaps are generally sphere gaps or gaps formed by hemispherical electrodes. The gaps are arranged such that sparking of one gap results in automatic sparking of other gaps as overvoltage is impressed on the other. In order to have consistency in sparking, irradiation from an ultra-violet lamp is provided from the bottom to all the gaps.

To trip the generator at a predetermined time, the spark gaps may be mounted on a movable frame, and the gap distance is reduced by moving the movable electrodes closer. This method is difficult and does not assure consistent and controlled tripping.

A simple method of controlled tripping consists of making the first gap a three electrode gap and firing it from a controlled source. [Figure 6.23](#) gives the schematic arrangement of a three-electrode gap. The first stage of the impulse generator is fitted with a three-electrode gap, and the central electrode is maintained at a potential in between that of the top and the bottom electrodes with the resistors R_1 and R_1 . The tripping is initiated by applying a pulse to the thyatron G by closing the switch S . The capacitor C produces an exponentially decaying pulse of positive polarity. The pulse goes and initiates the oscilloscope time base. The thyatron conducts on receiving the pulse from the switch S and produces a negative pulse through the capacitance C_1 at the central electrode of the three electrode gap. Hence, the voltage between the central electrode and the top electrode of the three electrode gap goes above its sparking potential and thus the gap conducts. The time lag required for the thyatron firing and breakdown of the three electrode gap ensures that the sweep circuit of the oscilloscope begins before the start of the impulse generator voltage. The resistance R_2 ensures decoupling of voltage oscillations produced at the spark gap entering the oscilloscope through the common trip circuit.

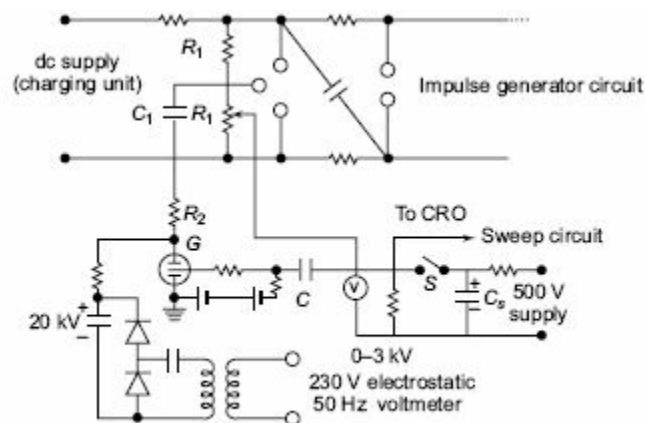


Fig. 6.23 *Tripping of an impulse generator with a three electrode gap*

The three-electrode gap requires larger space and an elaborate construction. Nowadays a trigatron gap shown in [Fig. 6.24](#) is used, and this requires much smaller voltage for operation compared to the three-electrode gap. A trigatron gap consists of a high-voltage spherical electrode of suitable size, an earthed main electrode of spherical shape, and a trigger electrode through the main electrode. The trigger electrode is a metal rod with an annular clearance of about 1 mm fitted into the main electrode through a bushing. The trigatron is connected to a pulse circuit as shown in [Fig. 6.24b](#). Tripping of the impulse generator is effected by a trip pulse which produces a spark between the trigger electrode and the earthed sphere. Due to space charge effects and distortion of the field in the main gap, sparkover of the main gap occurs. The trigatron gap is polarity sensitive and a proper polarity pulse

should be applied for correct operation.

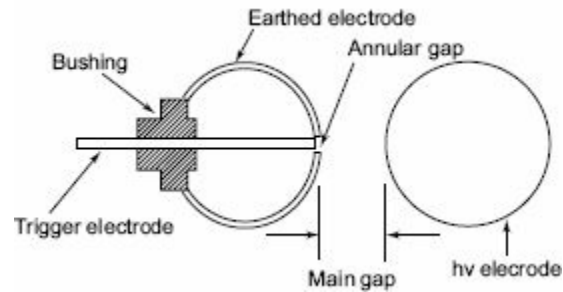
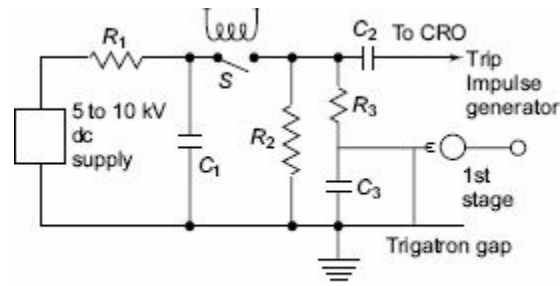


Fig. 6.24a Trigonon gap



(b) Tripping circuit using a trigatron

Fig. 6.24b Trigonon gap and tripping circuit

K
T E R M S
Y

- Generation of High Voltages
- dc Voltages
- Half and Full-wave Rectifiers
- Voltage Doublers and Multipliers
- Ripple and Regulation
- Electrostatic Machines
- Van de Graaff Generator
- Generation of High ac Voltages
- Testing Transformers
- Cascade Transformers
- Resonant Transformers
- Tesla Coil
- Impulse Voltages
- Wave Definition
- Standard Wave
- Circuits for Impulse Voltages
- Analysis of Impuse Circuits
- Multi-stage Impulse Generators
- Components
- Switching Surges
- Very Fast Transients G.I.S.
- Multi-test Sets
- Impulse Current Generators

- Rectangular Current Pulse Generation
- Tripping and Control of Impulse Generators

WORKED EXAMPLES

Example 6.1 A Cockcroft-Walton type voltage multiplier has eight stages with capacitances, all equal to $0.05 \mu\text{F}$. The supply transformer secondary voltage is 125 kV at a frequency of 150 Hz . If the load current to be supplied is 5 mA , find (a) the percentage ripple, (b) the regulation, and (c) the optimum number of stages for minimum regulation or voltage drop.

Solution (a) Calculation of Percentage Ripple

$$\text{The ripple voltage } \delta V = \frac{1}{fC} \frac{(n)(n+1)}{2}$$

$I = 5 \text{ mA}$, $f = > 150 \text{ Hz}$, $C = 0.05 \mu\text{F}$, number of stages = 8.

Hence $n = 16$ (number of capacitors)

$$\therefore \delta V = \frac{5 \times 10^{-3}}{150 \times 0.05 \times 10^{-6}} \times \frac{16 \times 17}{2} = 90.7 \text{ kV}$$

$$\% \text{ ripple} = \frac{\delta V \times 100}{16V_{\max}} = \frac{90.7 \times 100}{2 \times 125 \times 8} = 4.53\%$$

(b) Calculation of Regulation

$$\begin{aligned} \text{Voltage drop, } \Delta V &= \frac{1}{fC} \left(\frac{2}{3}n^3 + \frac{n^2}{2} - \frac{n}{6} \right) \\ &= \frac{5 \times 10^{-3}}{150 \times 0.05 \times 10^{-6}} \left[\left(\frac{2}{3} \times 8^3 \right) + \left(\frac{1}{2} \times 8^2 \right) - \frac{8}{6} \right] \\ &= 248 \text{ kV} \end{aligned}$$

$$\begin{aligned} \therefore \text{regulation} \left(\frac{V}{2nV_{\max}} \right) &= \frac{248}{2 \times 8 \times 125} = \frac{124}{1000} \\ &= 12.4\% \end{aligned}$$

(c) Calculation of Optimum Number of Stages (n_{optimum}) Since $n > 5$,

$$\begin{aligned}
 n_{\text{optimum}} &= \sqrt{V_{\text{max}} f C / I} \\
 &= \sqrt{\frac{125 \times 150 \times 0.05 \times 10^{-6} \times 10^{+3}}{5 \times 10^{-3}}} \\
 &= \sqrt{125 \times 1.5} \\
 &= 13.69 = 14 \text{ stages}
 \end{aligned}$$

Example 6.2 A 100 kVA, 400 V/250 kV testing transformer has 8% leakage reactance and 2% resistance on 100 kVA base. A cable has to be tested at 500 kV using the above transformer as a resonant transformer at 50 Hz. If the charging current of the cable at 500 kV is 0.4 A, find the series inductance required. Assume 2% resistance for the inductor to be used and the connecting leads. Neglect dielectric loss of the cable. What will be the input voltage to the transformer?

Solution The maximum current that can be supplied by the testing transformer is

$$\frac{100 \times 10^3}{250 \times 10^3} = 0.4 \text{ A}$$

X_C = Reactance of the cable is

$$\frac{V_C}{I} = \frac{500 \times 10^3}{0.4} = 1250 \text{ k}\Omega$$

X_L = Leakage reactance of the transformer is

$$\frac{\%X}{100} \times \frac{V}{I} = \frac{8}{100} \times \frac{250 \times 10^3}{0.4} = 50 \text{ k}\Omega$$

At resonance,

$$X_C = X_L$$

Hence, additional reactance needed

$$= 1250 - 50 = 1200 \text{ k}\Omega$$

Inductance of additional reactance (at 50 Hz frequency)

$$\frac{1200 \times 10^3}{2\pi \times 50} = 3820 \text{ H}$$

R = Total resistance in the circuit on 100 kVA base is 2% + 2% = 4%. Hence, the ohmic value of the resistance

$$= \frac{4}{100} \times \frac{250 \times 10^3}{0.4} = 25 \text{ k}\Omega$$

Therefore, the excitation voltage E_2 on the secondary of the transformer

$$\begin{aligned}
 &= I \times R \\
 &= 0.4 \times 25 \times 10^3 \\
 &= 10 \times 10^3 \text{ V or } 10 \text{ kV}
 \end{aligned}$$

The primary voltage or the supply voltage, E_1

$$= \frac{10 \times 10^3 \times 400}{250 \times 10^3}$$

$$= 16 \text{ V}$$

$$\text{Input kW} = \frac{16}{400} \times 100 = 4.0 \text{ kW}$$

(The magnetizing current and the core losses of the transformer are neglected.)

Example 6.3 An impulse generator has eight stages with each condenser rated for $0.16 \mu\text{F}$ and 125 kV . The load capacitor available is 1000 pF . Find the series resistance and the damping resistance needed to produce $1.2/50 \mu\text{s}$ impulse wave. What is the maximum output voltage of the generator, if the charging voltage is 120 kV ?

Solution Assume the equivalent circuit of the impulse generator to be as shown in [Fig. 6.15b](#).

$$C_1, \text{ the generator capacitance} = \frac{0.16}{8} \text{ } 0.02 \mu\text{F}$$

$$C_2, \text{ the load capacitance} = 0.001 \mu\text{F}$$

$$t_1, \text{ the time to front} = 1.2 \mu\text{s}$$

$$= 3.0 R_1 \frac{C_1 C_2}{C_1 + C_2}$$

$$\therefore R_1 = 1.2 \times 10^{-6} \frac{C_1 + C_2}{C_1 C_2} \times \frac{1}{3}$$

$$= 1.2 \times 10^{-6} \frac{0.021 \times 10^{-6}}{0.02 \times 0.001 \times 10^{-12}} \times \frac{1}{3} = 420 \Omega$$

$$t_2, \text{ time to tail} = 0.7 (R_1 + R_2) (C_1 + C_2)$$

$$= 50 \times 10^{-6}$$

or $0.7 (420 + R_2) (0.021 \times 10^{-6}) = 50 \times 10^{-6}$

or $R_2 = 2981 \Omega$

The dc charging voltage for eight stages is

$$V = 8 \times 120 = 960 \text{ kV}$$

The maximum output voltage is

$$\frac{V}{R_1 C_2 (\alpha - \beta)} (e^{-\alpha t_1} - e^{-\beta t_1})$$

where $\alpha = \frac{1}{R_1 C_2}$, $\beta = \frac{1}{R_2 C_1}$ and V is the dc charging voltage.

Substituting for R_1 , C_1 and R_2 , C_2 ,

$$\alpha = 0.7936 \times 10^6$$

$$\beta = 0.02335 \times 10^6$$

$$\therefore \text{maximum output voltage} = 932.6 \text{ kV.}$$

Example 6.4 An impulse current generator has a total capacitance of $8 \mu\text{F}$. The charging voltage is 25 kV . If the generator has to give an output current of 10 kA with $8/20 \mu\text{s}$ waveform, calculate (a) the circuit inductance, and (b) the dynamic resistance in the circuit. (Ref. [Sec. 6.4.2](#), Eq. 6.28)

Solution For an $8/20 \mu\text{s}$ impulse wave,

$$\alpha = R/2L = 0.0535 \times 10^{+6} \text{ (Ref. Tables 6.1 and 6.2)}$$

and, the product $LC = 65$. Given $C = 8 \mu\text{F}$. (L in μH , C in μF , and R in ohms)

Therefore, the circuit inductance is

$$\frac{65}{C} = 8.125 \mu\text{H}$$

$$\begin{aligned} \text{The dynamic resistance } 2L\alpha &= 2 \times \frac{65 \times 10^{-6}}{8} \times 0.0535 \times 10^{+6} \\ &= 0.8694 \text{ ohms} \end{aligned}$$

$$\text{Peak current is given by } \frac{VC}{14} = 10 \text{ kA}$$

(V in kV , C in μF , and I in kA),

\therefore charging voltage needed is

$$V = \frac{14 \times 10}{8} = 15.5 \text{ kV}$$

Example 6.5 (Alternative Solution for Example 6.4): Assuming the wave to have a time-to-front of $8 \mu\text{s}$, the time-to-first half cycle of the damped oscillatory wave will be $20 \mu\text{s}$. Then

Solution

$$t_1 = t_f = 1/\omega [\text{arc tan } (\omega/\alpha)] = 8 \mu\text{s}$$

$$\text{and } t_2 = \pi/\omega = 20 \mu\text{s}$$

$$\text{Therefore, } \omega = \pi/t_2 = \pi \times 10^6/20 = 0.1571 \times 10^6$$

$$\text{arc tan } (\omega/\alpha) = \omega/\alpha = 1.2566$$

$$\text{i.e. } \omega/\alpha = 0.8986 \text{ radians}$$

$$\text{and } \alpha = 0.1748 \times 10^6.$$

$$\text{Then, } \sqrt{1/(LC) - \alpha^2} = 0.1571 \times 10^6.$$

Substituting the value of α and simplifying,

$$LC = 32.47 \times 10^{12}, \text{ hence } L = 4.06 \mu\text{H}$$

$$\text{and } R = 2 \times L \times \alpha = 1.419 \text{ ohm}$$

$$i_m = V/\omega L \times \text{Exp } (-\alpha) = 10 \text{ kA}$$

$$V = \omega L \times 10 \times \text{Exp } (-\alpha) = 25.8 \text{ kV.}$$

Example 6.6 A 12-stage impulse generator has $0.126 \mu\text{F}$ capacitors. The wave-front and the wave-tail resistances connected are 800 ohms and 5000 ohms respectively. If the load capacitor is 1000 pF , find the front and tail times of the impulse wave produced.

$$\text{Solution The generator capacitance } C_1 = \frac{0.126}{12} = \mu\text{F}$$

$$\text{The load capacitance } C_2 = 0.001 \mu\text{F}$$

Resistances, $R_1 = 800$ ohms and $R_2 = 5000$ ohms

$$\begin{aligned} \therefore \text{time to front, } t_1 &= 3(R_1) \left(\frac{C_1 C_2}{C_1 + C_2} \right) \\ &= 3 \times 800 \times \frac{(0.0105 \times 10^{-6} \times 0.001 \times 10^{-6})}{(0.0105 + 0.001) \times 10^{-6}} \\ &= 2.19 \mu\text{s} \\ \text{time to tail, } t_2 &= 0.7(R_1 + R_2)(C_1 + C_2) \\ &= 0.7(800 + 5000) \times (0.0105 + 0.001) \times 10^{-6} \\ &= 46.7 \mu\text{s} \end{aligned}$$

Example 6.7 A Tesla coil has a primary winding rated for 10 kV. If L_p , L_2 and coefficient of coupling K are 10 mH, 200 mH, and 0.6 respectively find the peak value of the output voltage if the capacitance in the primary side is $2.0 \mu\text{F}$ and that on the secondary side is 1 nF. Neglect the winding resistance. Find also the highest resonant frequency produced with rated voltage applied.

Solution $M = K \sqrt{L_1 L_2} = 0.6 \sqrt{2000} = 26.82$ mH

$$\begin{aligned} \omega_1 &= \frac{1}{\sqrt{L_1 C_1}} = \frac{1}{\sqrt{10 \times 10^{-3} \times 2 \times 10^{-6}}} \\ &= 7.07 \times 10^3 \text{ radians/second} \\ \sigma &= \sqrt{1 - K^2} = 0.8 \\ \omega_2 &= \frac{1}{\sqrt{L_2 C_2}} = \frac{1}{\sqrt{200 \times 10^{-3} \times 1 \times 10^{-9}}} \\ &= 7.07 \times 10^4 \text{ radius/second} \\ \gamma_2^2 &= \frac{\omega_1^2 + \omega_2^2}{2} + \sqrt{\left(\frac{\omega_1^2 + \omega_2^2}{2} \right)^2 - \sigma^2 \omega_1^2 \omega_2^2} \end{aligned}$$

and

$$\gamma_1^2 = \frac{\omega_1^2 + \omega_2^2}{2} - \sqrt{\left(\frac{\omega_1^2 + \omega_2^2}{2} \right)^2 - \sigma^2 \omega_1^2 \omega_2^2}$$

Substituting for ω_1^2 , ω_2^2 and σ , we get

$$\begin{aligned} \gamma_2 &= 70.83 \times 10^3 \text{ rad/s} \\ \gamma_1 &= 5.645 \times 10^3 \text{ rad/s} \end{aligned}$$

Hence the highest frequency produced = $\frac{\gamma_2}{2\pi} = 11.27$ kHz

Peak value of output voltage

$$V_2 (\text{peak}) = \frac{VM}{\sigma L_1 L_2 C_2} \frac{1}{(\gamma_2^2 - \gamma_1^2)}$$

$$= \frac{10 \times 10^3 \times 26.32 \times 10^{-3}}{0.80 \times (10 \times 200 \times 10^{-6}) (1 \times 10^{-9})} \times \frac{1}{(70.83^2 - 5.645^2) \times 10^6}$$

$$= 33.61 \text{ kV}$$

Note: The turns ratio $\cong \sqrt{L_2/L_1} = \sqrt{200/10} = 4.47$. Hence, output peak cannot be more than 44.7 kV

Example 6.8 In Example 6.7, if the energy efficiency is 5%, calculate the output voltage.

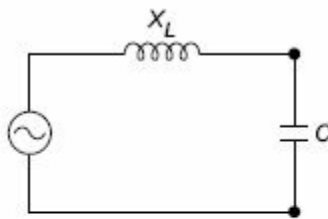
$$V_2 = V_1 \sqrt{n \frac{C_1}{C_2}}$$

$$= 10 \sqrt{\frac{0.05 \times 2 \times 10^{-6}}{1 \times 10^{-9}}} = 10\sqrt{10} = 31.6 \text{ kV}$$

Note: Normally Tesla coils have poor energy efficiency as most of the energy is consumed in the resistance of the windings as well as at the spark gaps.

Example 6.9 A 6.6 kV/350 kV, 350 kVA, 50 Hz testing transformer when tested had the following observations: (a) No load voltage rise on HV side was 1% more than the rated value when 6.6 kV was applied on primary side. (b) The rated short circuit current was obtained on HV side when shorted with 8% rated voltage on primary side. Calculate (i) self-capacitance of transformer along with its hv side bushing, and (ii) leakage reactance neglecting resistance.

Solution



Equivalent circuit of transformer

$$X_2 = \text{short-circuit or equivalent impedance of transformers}$$

$$= \frac{0.8V}{I}$$

Referring to secondary side

$$I = \frac{350 \text{ kVA}}{350 \text{ kV}} = 1 \text{ A}$$

$$\therefore V = 350 \text{ kV} \quad \therefore X_L = \frac{0.08 \times 350}{1} = 28 \text{ k}\Omega$$

Rise in voltage = $0.01 \text{ V} = I_0 X_L$ (I_0 is current drawn by line self-capacitance C)

$$\therefore I_0 = \frac{0.01 \text{ V}}{X_L} = \frac{0.01 \times 350 \text{ kV}}{28 \text{ k}\Omega} = \frac{1}{8} = 0.125 \text{ A}$$

Voltage across the terminals = voltage across the self-capacitance 'C'

$$\therefore I_0 X_C = 1.01 \text{ V} = 1.01 \times 350 \text{ kV}$$

$$\therefore X_C = \frac{1}{\omega C} = \frac{1}{100\pi C} = \frac{1.01 \times 350 \text{ kV}}{0.125}$$

$$\text{Self-capacitance } C = 1.125 \times 10^{-9} \quad \therefore \text{ or } 1.125 \text{ nF}$$

Example 6.10 A model impulse generator has a capacitance of $1 \mu\text{F}$ rated to 10 kV and uses series R - L - C circuit to produce $1/50 \mu$ second voltage wave. (a) Determine the resistance and inductance needed to produce the same and the output voltage across the resistance 'R'. (b) If the same circuit is to be used to produce $8/20 \mu$ second impulse voltage wave, what are the other parameters?

Solution Referring to Fig. 6.15 a for $1/50 \mu$ second wave form, for a series R - L - C circuit

$$CR = 70.6 \text{ and } LC = 11.6 \text{ from Table 6.2}$$

$$\text{since } C = 1 \mu\text{F}$$

$$R = \frac{70.6}{1} = 70.6 \Omega \text{ and } L = \frac{11.6}{1} = 11.6 \mu\text{H}$$

The voltage efficiency of the circuit is 98.8% and hence the output voltage in $988 \times 10 = 9.88 \text{ kV}$

(b) Referring to Fig. 8.20a and Table 6.2,

for $8/20 \mu$ second double exponential wave $LC = 65$

$$\therefore L = \frac{65}{1} = 65 \mu\text{H} \text{ Also, } \alpha = \frac{R}{2L} = 0.0535$$

(L in μH and C in μF)

$$\therefore R = 2L\alpha = 6.955 \Omega$$

$$I_{\text{peak}} = VC/14 = \frac{10 \times 1}{14} = 0.714 \text{ kA and } 714 \text{ A}$$

MULTIPLE-CHOICE QUESTIONS

1. Peak to peak ripple is defined as

- the difference between average dc voltage and peak value
- the difference between maximum and minimum dc voltage
- the difference between maximum ac and average dc voltages
- the difference between ac (rms) and average dc voltages

2. In a voltage doubler circuit peak to peak ripple is if C : capacitance, I : load current, and f = frequency)

(a) $= (3If/C)$

(b) $= 2If/fC$

(c) $= 3I/fC$

(d) $= I/fC$

3. Optimum number of stages for Cockcroft Walton voltage multiplier circuit are (if V_{\max} = supply voltage, f = frequency, I = load current, C = stage capacitance)

(a) $\sqrt{V/IfC}$

(b) $\sqrt{IfC/V}$

(c) $\sqrt{Vf/IC}$

(d) $\sqrt{VfC/I}$

4. A Van de Graaff generator has a belt speed of 2.5 m/s, charge density of $10 \mu\text{c}/\text{m}^2$ and a belt width 2 m. The maximum charging current is

(a) $50 \mu\text{A}$

(b) $5 \mu\text{A}$

(c) $2 \mu\text{A}$

(d) $12.5 \mu\text{A}$

5. The nominal rating of a testing transformer in kVA is given by (if ω = supply frequency, C = capacitance loading and V = output voltage)

(a) $0.5 V^2 \omega C$

(b) $V^2 \omega C$

(c) $1.5 V^2 \omega C$

(d) $10 V^2 \omega C$

6. In testing with a resonant transformer, the output voltage is

(a) rectangular wave

(b) triangular wave

(c) trapezoidal wave

(d) pure sine wave

7. Parallel resonant transformer test system is used when

(a) large test voltages are needed

(b) stable output voltage with high rate of rise of voltage is needed

(c) large current is needed

(d) when high frequency test voltage is needed

8. Tesla coil is used for

(a) generation of sinusoidal output voltages

(b) generation of very high voltages

(c) generation of rectangular voltages

(d) generation of high frequency ac voltages

9. Time to front of a impulse voltage wave-form is defined as

(a) 1.25 times the interval between 0.1 to 0.9 of peak value

(b) time interval between 0.1 to 0.9 of peak value

(c) 1.67 times the interval between 0.1 to 0.9 of peak value

(d) 1.25 times the interval between 0.3 to 0.9 of peak value.

10. The approximate value of time to front in an impulse voltage generator is

(a) $3 R_1 C_1$

(b) $2.3 R_1 C_1$

(c) $3.0 R_1 \frac{(C_1 C_2)}{C_1 + C_2}$

(d) $(0.7)(R_1 + R_2)(C_1 + C_2)$

1. An impulse voltage generator has a generator capacitance of $0.01 \mu\text{F}$, load capacitance of 1 nF , front resistance of $R_1 = 110 \Omega$ and tail resistance of $R_2 = 400 \Omega$. The tail time is
 - (a) $40 \mu\text{s}$
 - (b) $55 \mu\text{s}$
 - (c) $50 \mu\text{s}$
 - (d) $10 \mu\text{s}$
2. The value of charging voltage used in a medium-size impulse generator is
 - (a) 10 to 50 kV
 - (b) 50 to 100 kV
 - (c) 500 kV
 - (d) any value
3. The voltage efficiency of a normal impulse generator for generation of switching impulses is
 - (a) less than 30%
 - (b) 80 to 90%
 - (c) 40 to 60%
 - (d) 10 to 90%
4. A 16-stage impulse voltage generator has stage capacitance of $0.125 \mu\text{F}$ and a charging voltage of 200 kV. The energy rating in kJ is
 - (a) 40
 - (b) 50
 - (c) 80
 - (d) 640
5. In an impulse current generator the capacitors are connected in
 - (a) series
 - (b) parallel
 - (c) connected in parallel while charging and in series while discharging
 - (d) connected in series while charging and parallel while discharging
6. Multi test kits used in high-voltage laboratories consist of
 - (a) ac, dc and impulse voltage test units
 - (b) ac and dc test units
 - (c) dc and impulse test units
 - (d) ac, dc impulse voltage and current test units
7. Impulse current generator output wave-form is
 - (a) damped oscillatory wave
 - (b) overdamped wave
 - (c) critically damped wave
 - (d) can be damped waved or damped oscillatory wave
8. To minimise the inductance in impulse current generator circuits
 - (a) capacitor are connected in parallel

- (b) capacitors are subdivided into smaller units
(c) air core inductors are used in series
(d) discharge path is made into a rectangular path
9. A trigetron gap is used with
(a) cascade transformer units
(b) impulse current generator
(c) impulse voltage generator
(d) dc voltage double units
10. A oscillatory impulse waveform is represented by
(a) $e^{-at} \cos bt$
(b) $e^{+at} \cos bt$
(c) $e^{-at} - e^{-bt}$
(d) $e^{at} - e^{bt}$
11. With in the limits of regulation and ripple, the maximum voltage and current rating to which a 'dc' voltage multiplier can be built in
(a) 1 MV, 10 ma
(b) 2 MV, 20 ma
(c) 1 MV, 100 ma
(d) no limitation
12. The energy rating of different resistors in impulse generators of medium and large size is
(a) less than 1 kJ
(b) 10 to 20 kJ
(c) 1 to 2 kJ
(d) 2 to 5 kJ
13. Impulse generators needed to test gas-insulated systems are required to produce impulse voltages waves of
(a) 0.1/1 or 0.3/3 μ second
(b) $\frac{1}{10}$ and $\frac{1}{50}$ μ second
(c) 1.2/50 and 25/250 μ second
(d) 4/20 and 8/20 μ second
14. Voltage stabilizers used for regulating high dc voltages are
(a) series type
(b) shunt type
(c) both series and shunt type
(d) shunt or series or degenerative
15. Typical capacitive loading on a testing transformers rated for 100 kVA, 250 kV will be about
(a) less than 1 nF
(b) 3 to 5 nF
(c) 10 to 50 nF
(d) 50 to 100 nF

- | | | | | | |
|---------|---------|---------|---------|---------|---------|
| 1. (b) | 2. (c) | 3. (d) | 4. (a) | 5. (c) | 6. (d) |
| 7. (b) | 8. (d) | 9. (a) | 10. (c) | 11. (a) | 12. (b) |
| 13. (c) | 14. (a) | 15. (b) | 16. (a) | 17. (d) | 18. (b) |
| 19. (c) | 20. (a) | 21. (b) | 22. (d) | 23. (a) | 24. (c) |
| 25. (b) | | | | | |

REVIEW QUESTIONS

1. Explain with diagrams, different types of rectifier circuits for producing high dc voltages.
2. What are the special features of high-voltage rectifier valves? How is proper voltage division between the valves ensured, if a number of tubes are used in series?
3. Why is a Cockcroft-Walton circuit preferred for voltage multiplier circuits? Explain its working with a schematic diagram.
4. Give the expression for ripple and regulation in voltage multiplier circuits. How are the ripple and regulation minimized?
5. Describe, with a neat sketch, the working of a Van de Graaff generator. What are the factors that limit the maximum voltage obtained?
6. Explain the different schemes for cascade connection of transformers for producing very high ac voltages.
7. Why is it preferable to use isolating transformers for excitation with cascade transformer units, if the power requirement is large?
8. What is the principle of operation of a resonant transformer? How is it advantageous over the cascade connected transformers?
9. What is a Tesla coil? How are damped high-frequency oscillations obtained from a Tesla coil?
10. Define the front and tail times of an impulse wave. What are the tolerances allowed as per the specifications?
11. Give different circuits that produce impulse waves explaining clearly their relative merits and demerits.
12. Give the Marx circuit arrangement for multistage impulse generators. How is the basic arrangement modified to accommodate the wave time control resistances?
13. How are the wave-front and wave-tail times controlled in impulse generator circuits?
14. Explain the different methods of producing switching impulses in test laboratories.
15. Explain the effect of series inductance on switching impulse waveshapes produced.
16. Describe the circuit arrangement for producing lightning current waveforms in laboratories.
17. How is the circuit inductance controlled and minimized in impulse current generators?
18. How are rectangular current pulses generated for testing purposes? How is their time duration controlled?
19. Explain one method of controlled tripping of impulse generators. Why is controlled tripping necessary?
20. What is a trigatron gap? Explain its functions and operation.

PROBLEMS

1. An impulse generator has 12 capacitors of $0.12 \mu\text{F}$, and 200 kV rating. The wave-front and wave-tail resistances are $1.25 \text{ k}\Omega$ and $4 \text{ k}\Omega$ respectively. If the load capacitance including that of the test object is 1000 pF , find the wave-front and wave-tail times and the peak voltage of

impulse wave produced.

2. An 8-stage impulse generator has $1.2 \mu\text{F}$ capacitors rated for 167 kV. What is its maximum discharge energy? If it has to produce a $1/50 \mu\text{s}$ waveform across a load capacitor of $15,000 \text{ pF}$, find the values of the wave front and wave tail resistances.
3. Calculate the peak current and waveshape of the output current of the following generator. Total capacitance of the generator is $53 \mu\text{F}$. The charging voltage is 200 kV. The circuit inductance is 1.47 mH , and the dynamic resistance of the test object is 0.051 ohms .
4. A single-phase testing transformer rated for 2 kV/350 kV, 3500 kVA, 50 Hz on testing yields the following data: (i) No-load voltage on HV side = 2% higher than the rated value when the input voltage is 2 kV on the LV side (ii) Short circuit test with HV side shorted, rated current was obtained with 10% rated voltage on the input side. Calculate the self-capacitance on the HV side and the leakage reactance referred to the HV side. Neglect resistance.
5. Determine the ripple voltage and regulation of a 10 stage Cockcroft-Walton type dc voltage multiplier circuit having a stage capacitance = $0.01 \mu\text{F}$, supply voltage = 100 kV at a frequency of 400 Hz and a load current = 10 mA.
6. A voltage doubler circuit has $C_1 = C_2 = 0.01 \mu\text{F}$ and is supplied from a voltage source of $V = 100 \sin 3141 \text{ kV}$. If the dc output current is to be 4 mA, calculate the output voltage and the ripple.
7. The primary and secondary winding inductances of a Tesla coil are 0.093 H and 0.011 H respectively with a mutual inductance between the windings equal to 0.026 H . The capacitance included in the primary and secondary circuits are respectively $1.5 \mu\text{F}$ and 18 nF . If the Tesla coil is charged through a 10 kV DC supply, determine the output voltage and its waveform. Neglect the winding resistances.
8. An impulse current generator is rated for 60 kW seconds. The parameters of the circuit are $C = 53 \mu\text{F}$, $L = 1.47 \mu\text{H}$ and the dynamic resistance = 0.0156 ohm . Determine the peak value of the current and the time-to-front and the time-to-tail of the current waveform.
9. A high voltage testing laboratory is required to test apparatus with a capacitance of the order of 2000 p.F. used in a 230kV system. If the test voltage requirement is 2.2 times the system rated voltage, determine the rating of the test transformer at 50 Hz operation.
10. A cable test unit is required to test cables of 5000 pf at 200 kV. The testing transformer available is 230 V/50 kV, 15 kVA with 2.5% resistance and 6% reactances. Determine the inductance required for resonant testing and input voltage to the testing transformer. Assume the resistance of inductor and leads to be 2.5%.
11. Three 350 kV, 350 kVA testing transformers are connected in cascade and have a short circuit impedance of 5%. Determine (i) the full load current, (ii) the short circuit current, (iii) maximum capacitive load that can be tested without exceeding the power rating.
12. In Question 6.31 determine (a) the maximum capacitive load that can be tested at 350 kV, if all the transformers are connected in parallel, and (b) the maximum line charging current that can be given by the unit if all the transformers are connected in star to supply a 3 phase line.

Answers to Problems

1. $t_1 = 3.41 \mu\text{s}$, $t_2 = 40.4 \mu\text{s}$, peak output voltage = 1655 kV
2. Energy = 133 kJ, $R_1 = 24.4 \text{ ohms}$, $R_2 = 409.6 \text{ ohms}$
3. $I_m = 97.6 \text{ kA}$, $I(t) = 121.6 e^{-\omega t} \sin \omega t$

$$a \Rightarrow 1.7347 \times 10^4, \omega = 11.19 \times 10^4$$

$$t_1 = 12.67 \mu s, t_2 = 28.07 \mu s$$

4. 17.8nF, 3.5kohms
5. Ripple = 137.5 kV, 6.88%, regulation = 715kV, 35.75%
6. Output = 186 kV, ripple = 24 kV
7. output wave $9.22 (\cos \gamma_1 t - \cos \gamma_2 t)$ kV
 $\gamma_1 = 1.606 \times 10^3, \gamma_2 = 71.13 \times 10^3$
8. $I_m = 266.2$ kA, $I(t) = 286 e^{-\infty} \sin \omega t$
 $\alpha = 5.306 \times 10^3, \omega = 113.2 \times 10^3$
 $t_1 = 13.46 \mu s, t_2 = 22.75 \mu s$
9. $V = 500$ kV, 150 kVA
10. Inductance 1708 H, $V_L = 11.5$ V
11. $I_{full\ load} = 0.33$ A, $I_{short\ ckt} = 6.67$ A, $C_1 = 3.03$ nF at 1050 kV, 50 Hz
(Total ratings is 350 kVA only)
12. (a) $C_L = 9.09$ nF at 50 Hz, 350 kV
(b) 0.33 A at 600 kV

REFERENCES

1. Craggs, J.D. and Meek, J.M., *High Voltage Laboratory Technique*, Butterworths, London (1954).
2. Heller, H. and Veverka, A., *Surge Phenomenon in Electrical Machines*, Illifce and Company, London (1969).
3. Dieter Kind, *An Introduction to High Voltage Experimental Technique*, Wiley Eastern, New Delhi (1979).
4. Gallanher, T.J. and Pearman, A.J., *High Voltage Measurement, Testing and Design*, John Wiley and Sons, New York (1982).
5. Kuffel, E., Zaengl, W. and Kuffel, J., *High Voltage Engineering*, Butterworth Heinemann (2000).
6. Begamudre, R.D., *E.H.V a.c. Transmission Engineering*, Wiley Eastern, New Delhi (1986).
7. Niels Hilton Cavillius, *High Voltage Laboratory Planning*, Emil Haefely and Company, Basel, Switzerland (1988).
8. "High Voltage Technology for Industry and Utilities", *Technical Literature of Hippotronics Inc.*, Brewster, New York, USA.
9. "High-Voltage Testing Techniques", Part-2, *Test Procedures*. IEC Publication Number 60-2-1973.
10. "Standard Techniques for High-Voltage Testing", *IEEE Standard no. 4-1978*.
11. Mazen Abdul Salam, *High-Voltage Engineering* Marcel Dekker Inc. New York 2001.
12. Rihond Reid, "High-Voltage Resonant Testing", *Proceedings of IEEE PES Winter Conference*, Paperno. C74-038-6, 1974.
13. Kannan, S.R. and Narayana Rao, Y., "Prediction of Parameters for Impulse Generator for Transformer Testing", *Proceedings of IEE*, Vol. 12, No. 5, pp. 535-538, 1973.
14. Glaninger, P., "Impulse Testing of Low Inductance Electrical Equipment", *2nd International Symposium on High Voltage Technology*, Zurich, pp. 140-144, 1975.
15. Khalifa, M., (ed.), *High-Voltage Engineering: Theory and Practice*, Marcel Dekker Inc., New York (1990).

16. Rea, M. and Yan, K., *IEEE Trans. on Industry Application*, **31**, No. 3, pp. 507-512, (1995).
17. IEC 60-1, "High-Voltage Test Technique", IEC, Geneva, Switzerland (1989).
18. Mizuno, A. and Hori, Y., *IEEE Trans. on Industry Application*,. **24**, No. 3, pp. 387-394 (1988).
19. Kamase, Y., Shimiza, M., Nagahama, T. and Mizuno, A., *IEEE Trans. on IndustryApplication*, **29**, No. 4, pp. 793-797 (1993).
20. Ryan, H.M., High-Voltage Engineering and Testing I.E.T. England.

CHAPTER

7

Measurement of High Voltages and Currents

In industrial testing and research laboratories, it is essential to measure the voltages and currents accurately, ensuring perfect safety to the personnel and equipment. Hence a person handling the equipment as well as the metering devices must be protected against over voltages and also against any induced voltages due to stray coupling. Therefore, the location and layout of the devices are important. Secondly, linear extrapolation of the devices beyond their ranges are not valid for high-voltage meters and measuring instruments, and they have to be calibrated for the full range. Electromagnetic interference is a serious problem in impulse voltage and current measurements, and it has to be avoided or minimized. Therefore, even though the principles of measurements may be same, the devices and instruments for measurement of high voltages and currents differ vastly from the low-voltage and low-current devices. Different devices used for high-voltage measurements may be classified as in [Tables 7.1](#) and [7.2](#).

7.1 MEASUREMENT OF HIGH DIRECT-CURRENT VOLTAGES

Measurement of high dc voltages as in low-voltage measurements, is generally accomplished by extension of meter range with a large series resistance. The net current in the meter is usually limited to one to ten microamperes for full-scale deflection. For very high voltages (1000 kV or more) problems arise due to large power dissipation, leakage currents, and limitation of voltage stress per unit length, change in resistance due to temperature variations, etc. Hence, a resistance potential divider with an electrostatic voltmeter is sometimes better when high precision is needed. But potential dividers also suffer from the disadvantages stated above. Both series resistance meters and potential dividers cause current drain from the source. Generating voltmeters are high impedance devices and do not load the source. They provide complete isolation from the source voltage (high-voltage) as they are not directly connected to the high-voltage terminal and hence are safer. Spark gaps such as sphere gaps are gas discharge devices and give an accurate measure of the peak voltage. These are quite simple and do not require any specialized construction. But the measurement is affected by the atmospheric conditions like temperature, humidity, etc. and by the vicinity of earthed objects, as the electric field in the gap is affected by the presence of earthed objects. But sphere gap measurement of voltages is independent of the waveform and frequency.

Table 7.1 High-voltage measurement techniques

Type of voltage	Method or technique
(a) dc voltages	(i) Series resistance microammeter
	(ii) Resistance potential divider
	(iii) Generating voltmeters
	(iv) Sphere and other spark gaps
(b) ac voltages (power frequency)	(i) Series impedance ammeters
	(ii) Potential dividers (resistance or capacitance type)
	(iii) Potential transformers (electromagnetic or CVT)
	(iv) Electrostatic voltmeters
	(v) Sphere gaps
(c) ac high frequency voltages, impulse voltages, and other rapidly changing voltages	(i) Potential dividers with a cathode ray oscillograph (resistive or capacitive dividers)
	(ii) Peak voltmeters
	(iii) sphere gaps

Table 7.2 High-current measurement techniques

Type of current	Device or technique
(a) Direct currents	(i) Resistive shunts with milliammeter
	(ii) Hall effect generators
	(iii) Magnetic links
(b) Alternating currents (Power frequency)	(i) Resistive shunts
	(ii) Electromagnetic current transformers
(c) High frequency ac, impulse and rapidly	(i) Resistive shunts
	(ii) Magnetic potentiometers or Rogowski coils

changing currents (iii) Magnetic links

Hall effect generators

7.1.1 High Ohmic Series Resistance with Microammeter

High dc voltages are usually measured by connecting a very high resistance (few hundreds of megaohms) in series with a microammeter as shown in Fig. 7.1. Only the current flowing through the large calibrated resistance R is measured by the moving coil microammeter. The voltage of the source is given by

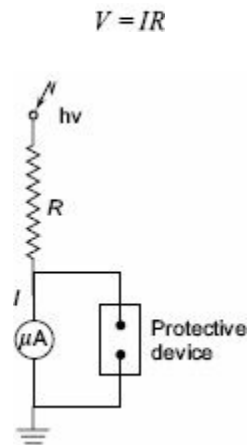


Fig. 7.1 Series resistance micrometer

The voltage drop in the meter is negligible, as the impedance of the meter is only few ohms compared to few hundred megaohms of the series resistance R . A protective device like a paper gap, a neon glow tube, or a zener diode with a suitable series resistance is connected across the meter as a protection against high voltages in case the series resistance R fails or flashes over. The ohmic value of the series resistance R is chosen such that a current of one to ten microamperes is allowed for full-scale deflection. The resistance is constructed from a large number of wire wound resistors in series. The voltage drop in each resistor element is chosen to avoid surface flashovers and discharges. A value of less than 5 kV/cm in air or less than 20 kV/cm in good oil is permissible. The resistor chain is provided with corona-free terminations. The material for resistive elements is usually a carbon-alloy with temperature coefficient less than $10^{-4}/^{\circ}\text{C}$. Carbon and other metallic film resistors are also used. A resistance chain built with $\pm 1\%$ carbon resistor located in an airtight transformer oil-filled PVC tube, for 100 kV operation had very good temperature stability. The limitations in the series resistance design are

- (i) power dissipation and source loading,
- (ii) temperature effects and long time stability,
- (iii) voltage dependence of resistive elements, and
- (iv) sensitivity to mechanical stresses.

Series resistance meters are built for 500 kV dc with an accuracy better than 0.2%.

7.1.2 Resistance Potential Dividers for dc Voltages

A resistance potential divider with an electrostatic or high impedance voltmeter is shown in [Fig. 7.2](#). The influence of temperature and voltage on the elements is eliminated in the voltage divider arrangement. The high-voltage magnitude is given by $[(R_1 + R_2)/R_2] v_2$, where v_2 is the dc voltage across the low-voltage arm R_2 . With sudden changes in voltage, such as switching operations, flashover of the test objects, or source short circuits, flashover or damage may occur to the divider elements due to the stray capacitance across the elements and due to ground capacitances. To avoid these transient voltages, voltage controlling capacitors are connected across the elements. A corona-free termination is also necessary to avoid unnecessary discharges at high voltage ends. A series resistor with a parallel capacitor connection for linearization of transient potential distribution is shown in [Fig. 7.3](#). Potential dividers are made with 0.05% accuracy up to 100 kV, with 0.1% accuracy up to 300 kV, and with better than 0.5% accuracy for 500 kV.

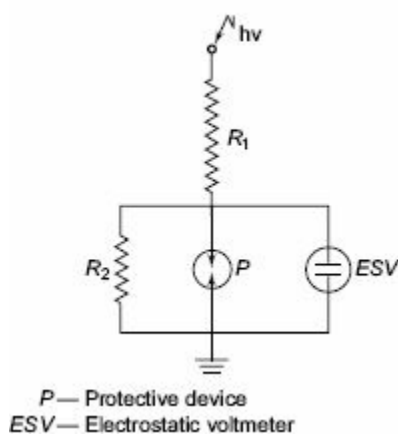


Fig. 7.2 Resistance potential divider with an electrostatic voltmeter

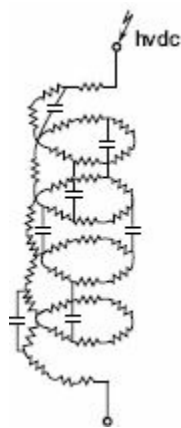


Fig. 7.3 Series resistor with parallel capacitors for potential linearization for transient voltages

HVDC Divider for HVDC Transmission System

In case of dc voltage measurements in HVDC transmission system, the voltage divider used should measure (a) steady dc voltage, (b) ripple voltage, and (c) any transient voltages. Hence, the divider requires to have a wide bandwidth from dc to several kHz with a fast response to voltage changes. Hence, a compensated resistive voltage divider (*RC* divider) is preferred ([Fig. 7.25a](#) and [b](#)). The resistance component of the divider is made of high-precision low-inductance component resistors connected in series as needed for the primary voltage and a defined current (usually 1 mA or 0.5 mA). Grading capacitors are connected in parallel to the resistors to facilitate ripple measurement and also protect against high transient voltages. The dividers are commercially available for voltages up to ± 800 kV dc with frequency accuracy $\pm 0.4\%$ or better. The other features are

- Temperature coefficient ≤ 15 ppm/ $^{\circ}\text{C}$
- Time stability of divider accuracy $\leq 0.002\%$ /year
- Step response time $< 33 \mu\text{s}$
- Frequency response > 10 kHz

7.1.3 Generating Voltmeters

High-voltage measuring devices employ generating principle when source loading is prohibited (as with Van de Graaff generators, etc.) or when direct connection to the high-voltage source is to be avoided. A generating voltmeter is a variable capacitor electrostatic voltage generator which generates current proportional to the applied external voltage. The device is driven by an external synchronous or constant speed motor and does not absorb power or energy from the voltage measuring source.

(a) Principle of Operation The charge stored in a capacitor of capacitance C is given by $q = CV$. If the capacitance of the capacitor varies with time when connected to the source of voltage V , the current through the capacitor

$$i = \frac{dq}{dt} = V \frac{dC}{dt} + C \frac{dV}{dt} \quad (7.1)$$

For dc voltages $dV/dt = 0$. Hence,

$$i = \frac{dq}{dt} = V \frac{dC}{dt} \quad (7.2)$$

If the capacitance C varies between the limits C_0 and $(C_0 + C_m)$ sinusoidally as

$$C = C_0 + C_m \sin \omega t$$

the current i is

$$i = i_m \cos \omega t$$

where

$$i_m = VC_m \omega$$

(i_m is the peak value of the current). The rms value of the current is given by

$$i_{\text{rms}} = \frac{VC_m \omega}{\sqrt{2}} \quad (7.3)$$

For a constant angular frequency ω , the current is proportional to the applied voltage V . More often, the generated current is rectified and measured by a moving coil meter. Generating voltmeter can be used for ac voltage measurements also provided the angular frequency ω is the same or equal to half that of the supply frequency.

A generating voltmeter with a rotating cylinder consists of two exciting field electrodes and a rotating two pole armature driven by a synchronous motor at a constant speed n . The ac current flowing between the two halves of the armature is rectified by a commutator whose arithmetic mean may be calculated from:

$$i = \frac{n}{30} \Delta CV, \quad \text{where } \Delta C = C_{\text{max}} - C_{\text{min}}$$

For a symmetric voltage $C_{\min} = 0$. When the voltage is not symmetrical, one of the electrodes is grounded and C_{\min} has a finite value. The factor of proportionality, ΔC is determined by calibration.

This device can be used for measuring ac voltages provided the speed of the drive-motor is half the frequency of the voltage to be measured. Thus a four-pole synchronous motor with 1500 rpm is suitable for 50 Hz. For peak value measurements, the phase angle of the motor must also be so adjusted that C_{\max} and the crest value occur at the same instant.

Generating voltmeters employ rotating sectors or vanes for variation of capacitance. [Figure 7.4](#) gives a schematic diagram of a generating voltmeter. The high voltage source is connected to a disc electrode S_3 which is kept at a fixed distance on the axis of the other low voltage electrodes S_0 , S_1 and S_2 . The rotor S_0 is driven at a constant speed by a synchronous motor at a suitable speed (1500, 1800, 3000, or 3600 rpm). The rotor vanes of S_0 cause periodic change in capacitance between the insulated disc S_2 and the hv electrode S_3 . The shape and number of the vanes of S_0 and S_1 are so designed that they produce sinusoidal variation in the capacitance. The generated ac current through the resistance R is rectified and read by a moving coil instrument. An amplifier is needed, if the shunt capacitance is large or longer leads are used for connection to rectifier and meter. The instrument is calibrated using a potential divider or sphere gap. The meter scale is linear and its range can be extended by extrapolation. Typical calibration curves of a generating voltmeter are given in [Figs 7.5a](#) and [b](#).

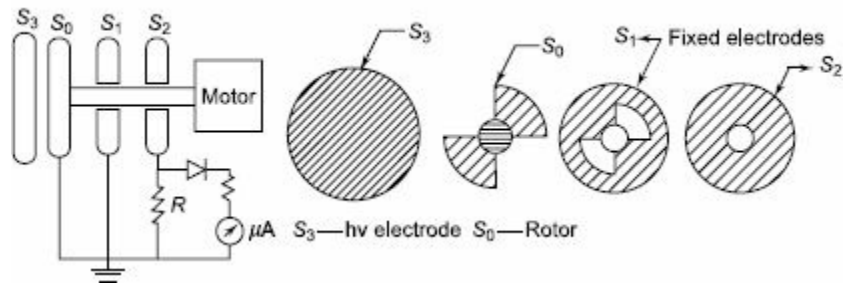


Fig. 7.4 Schematic diagram of a generating voltmeter (rotating vane type)

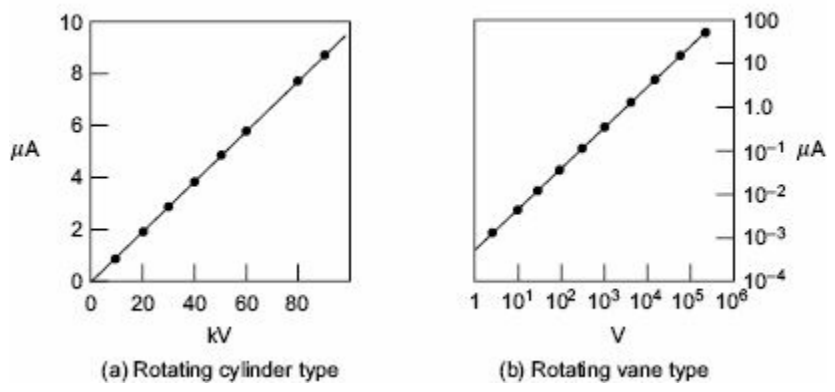


Fig. 7.5 Calibration curves for a generating voltmeter

(b) Advantages of Generating Voltmeters

- (i) No source loading by the meter,
- (ii) No direct connection to high voltage electrode,
- (iii) Scale is linear and extension of range is easy, and

- (iv) A very convenient instrument for electrostatic devices such as Van de Graaff generator and particle accelerators.

(c) Limitations of Generating Voltmeters

- (i) They require calibration,
- (ii) Careful construction is needed and is a cumbersome instrument requiring an auxiliary drive, and
- (iii) Disturbance in position and mounting of the electrodes make the calibration invalid.

7.1.4 Measurement of dc and ac Electric Fields

Electric fields exist in the near vicinity of very high voltage power lines, EHV substations and other power apparatus. At present EHV and UHV transmission systems with ratings of 750 kV ac and higher and ± 500 kV and higher have become common. People throughout the world are more concerned about the electric fields on account of their biological, and ecological effects and possible shock hazards. Hence development of electric field meters and measurement of electric fields have become essential.

(a) dc Electric Field Strength (E) Meters

The electric field strength E can be measured by using (i) variable capacitor probe or generating voltmeter, or (ii) a vibrating plate capacitor. These devices determine the electrical field intensity E by measuring either the induced charges or currents sensed by the electrodes.

(i) *Variable Capacitor Field Meter* If a metallic electrode is kept in an electric field E , the total charge induced on its surface A is given by

$$Q = \epsilon A E = \epsilon \int E dA \quad (7.4)$$

If the area of the sensing electrode varies and the variation of the area of the sensing electrode is periodic, then the current flowing through the measuring electrode to the ground is

$$I = \frac{dq}{dt} = \frac{1}{T} \int \frac{dq}{dt} \cdot dt = \frac{(q_{\max} - q_{\min})}{T} \quad (7.4a)$$

and hence the average value of electric field is

$$E = \frac{(q_{\max} - q_{\min})}{\epsilon_0 A T} = \frac{q_{\max}}{\epsilon_0 A T} = \frac{i}{\epsilon_0 A} \text{ if } q_{\min} = 0 \quad (7.4b)$$

Hence the electric field is proportional to the current, I

The arrangement of electrodes is shown in [Fig. 7.6a](#). The sensing electrode which is in the form of a circular disc is divided into sectors and shielded by a rotating shutter which rotates at an angular velocity ω . The shutter is driven at a constant speed by a motor. Two opposite sectors of the sensing electrodes are grounded and the other two are connected to ground through a measuring resistance R . The voltage across the resistance is measured and from this the electric field intensity E is determined. The induced current signal (voltage) is rectified by a phase sensitive detector operating with suitable phase angle relative to the movement of the shutter and is calibrated in terms of electric field E .

(ii) *Vibrating Plate Field Meter* This meter consists of a fixed face plate with an aperture. A vibrating plate or electrode is located below the face plate and is made to oscillate at a fixed rate by a driver motor [[Fig. 7.6b](#)]. Due to the vibrating motion of the driver plate a variable voltage K between the two plates, i.e., the face plate and the vibrating plate is generated. This is essentially a variable capacitor and the electric field E is proportional to the voltage generated V . The instrument is calibrated by placing it in a known electric field.

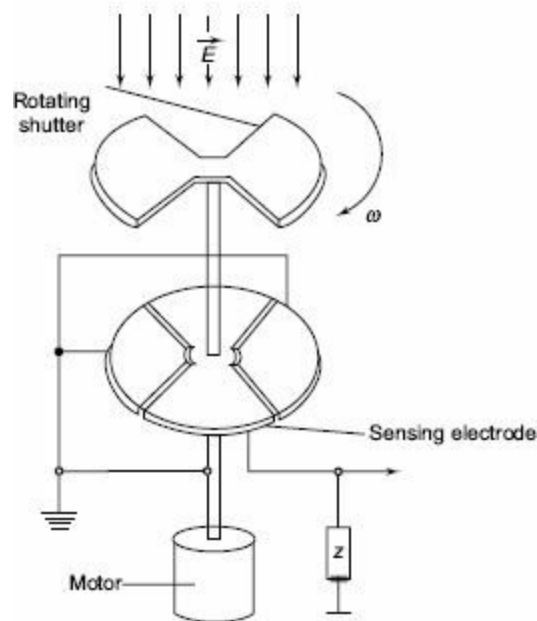


Fig 7.6a variable capacity, dc field meter

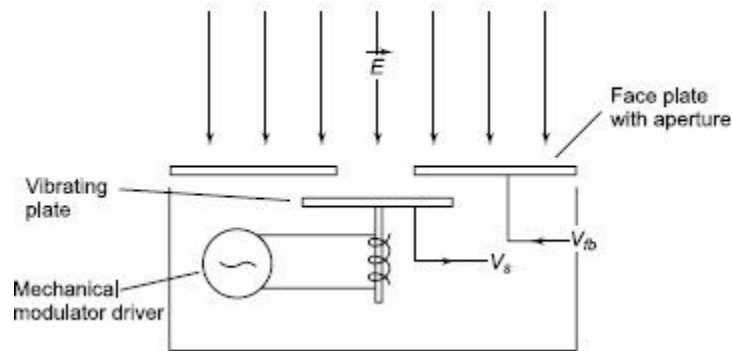


Fig 7.6b vibrating plate field meter

(b) ac Field Strength Meter: The Capacitor Probe

AC electric field is usually measured by introducing a small fixed capacitance probe into the field area and measuring the induced charge on it. Since the electric field between the plates of the capacitor is proportional to the charge induced on the plates of the capacitor and varies because of the variation of the ac electric field, the capacitive current is a measure for the field. Usually the electrodes of the field (capacitive) probe are spherical or parallel plates as shown in [Fig. 7.6c](#).

The charge Q induced on the surface of a conductor in an electric field E for a spherical electrode is given by $Q = 3 \pi a^2 \epsilon_0 E = K \epsilon_0 E$

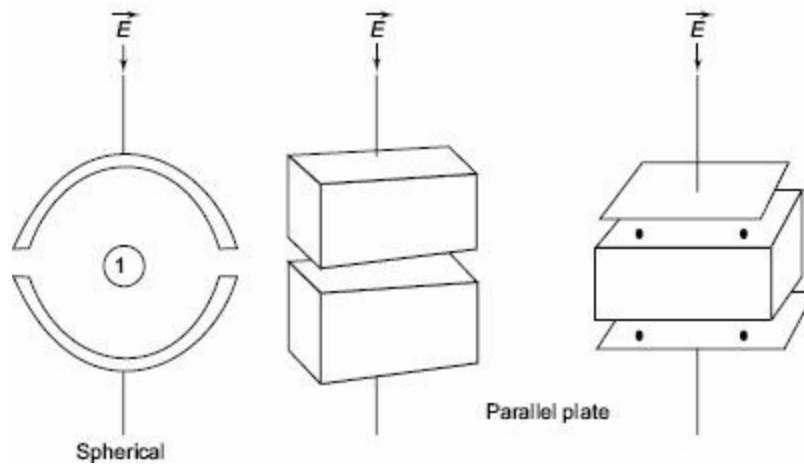


Fig 7.6c Types of electrodes for field probe

(The surface charge density over a hemisphere is given by $3 \pi a^2 \epsilon_0 E \cos \theta$ and integrating over the surface area gives the above value)

If the electric field is ac and given by $E \sin \omega t$, the current through the probe is given by

$$I = dq/dt = K \omega \epsilon_0 E \cos \omega t$$

The rms value of the current is proportional to E . Depending on the type of probe electrode used the value of K is determined and is included. The current is usually measured through a rectifier meter. This meter can be used over a wide range of frequencies but must be recalibrated for that frequency. The accuracy of the meter is about 0.5% and depends on the harmonic content, atmospheric conditions like temperature, humidity, etc., and the position or location of the meter in the electric field.

7.1.5 Measurement of Ripple Voltage in dc Systems

It has been discussed in the previous chapter that dc rectifier circuits contain ripple, which should be kept low ($\ll 3\%$). Ripple voltages are ac voltages of non-sinusoidal nature, and as such oscillographic measurement of these voltages is desirable. However, if a resistance potential divider is used along with an oscilloscope, the measurement of small values of the ripple δV will be inaccurate.

A simple method of measuring the ripple voltage is to use a capacitance-resistance (C - R) circuit and measure the varying component of the ac voltage by blocking the dc component. If V_1 is the dc source voltage with ripple (Fig. 7.7a) and V_2 is the voltage across the measuring resistance R , with C acting as the blocking capacitor, then

$$V_2(t) = V_1(t) - V_{dc} = \text{ripple voltage}$$

The condition to be satisfied here is $\omega CR \gg 1$.

Measurement of Ripple with CRO

The detailed circuit arrangement used of this purpose is shown in Fig. 7.7b. Here, the capacitance ' C ' is rated for the peak voltage. It is important that the switch ' S ' be closed when the CRO is connected to the source so that the CRO input terminal does not receive any high-voltage signal while ' C ' is being charged. Further, C should be larger than the capacitance of the cable and the input capacitance of the CRO , taken together.

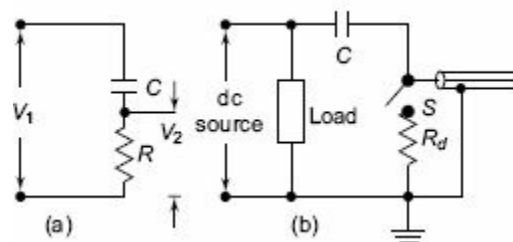


Fig. 7.7 Circuit arrangement for the measurement of ripple voltage

7.2 MEASUREMENT OF HIGH AC AND IMPULSE VOLTAGES

Measurement of high ac voltages employ conventional methods like series impedance voltmeters, potential dividers, potential transformers, or electrostatic voltmeters. But their designs are different from those of low-voltage meters, as the insulation design and source loading are the important criteria. When only peak value measurement is needed, peak voltmeters and sphere gaps can be used. Often, sphere gaps are used for calibration purposes. Impulse and high frequency ac measurements invariably use potential dividers with a cathode ray oscillograph for recording voltage waveforms. Sphere gaps are used when peak values of the voltage are only needed and also for calibration purposes.

7.2.1 Series Impedance Voltmeters

For power frequency ac measurements the series impedance may be a pure resistance or a reactance. Since resistances involve power losses, often a capacitor is preferred as a series reactance. Moreover, for high resistances, the variation of resistance with temperature is a problem, and the residual inductance of the resistance gives rise to an impedance different from its ohmic resistance. High resistance units for high voltages have stray capacitances and hence a unit resistance will have an equivalent circuit as shown in [Fig. 7.8](#). At any frequency ω of the ac voltage, the impedance of the resistance R is

$$i = \frac{dq}{dt} = V \frac{dC}{dt} + C \frac{dV}{dt} \quad (7.1)$$

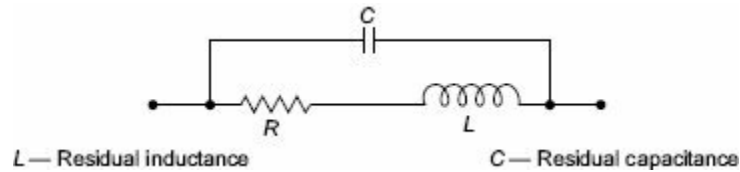


Fig. 7.8 Simplified lumped parameter equivalent circuit of a high ohmic resistance R

If ωL and ωC are small compared to R

$$i = \frac{dq}{dt} = V \frac{dC}{dt} + C \frac{dV}{dt} \quad (7.1)$$

and the total phase angle is

$$i = \frac{dq}{dt} = V \frac{dC}{dt} + C \frac{dV}{dt} \quad (7.1)$$

This can be made zero and independent of frequency, if

$$i = \frac{dq}{dt} = V \frac{dC}{dt} + C \frac{dV}{dt} \quad (7.1)$$

For extended and large dimensioned resistors, this equivalent circuit is not valid and each elemental resistor has to be approximated with this equivalent circuit.

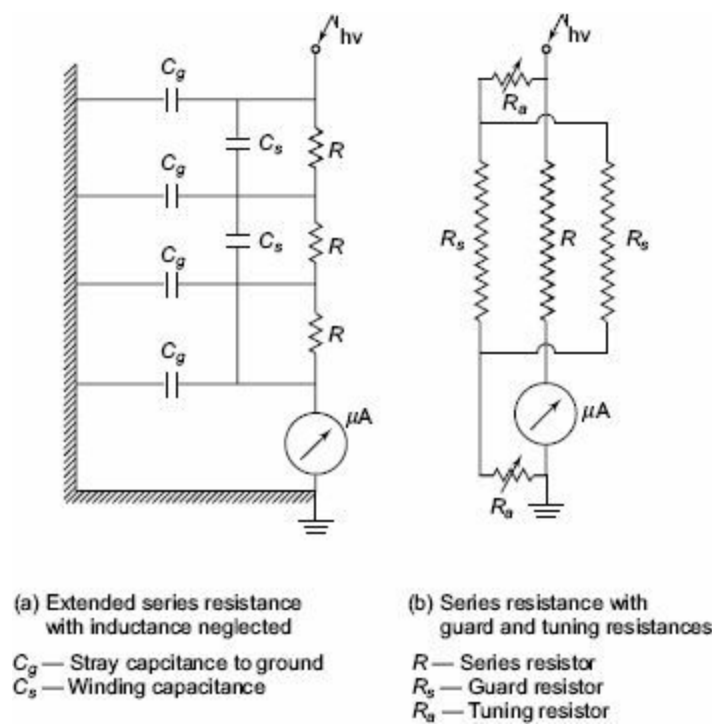


Fig. 7.9 Extended series resistance for high ac voltage measurements

The entire resistor unit then has to be taken as a transmission line equivalent, for calculating the effective resistance. Also, the ground or stray capacitance of each element influences the current flowing in the unit, and the indication of the meter results in an error. The equivalent circuit of a high voltage resistor neglecting inductance and the circuit of compensated series resistor using guard and tuning resistors is shown in [Figs 7.9a](#) and [b](#) respectively. Stray ground capacitance effects (refer [Fig. 7.9b](#)) can be removed by shielding the resistor R by a second surrounding spiral R_s , which shunts the actual resistor but does not contribute to the current through the instrument. By tuning the resistors R_a , the shielding resistor and potentials may be adjusted with respect to the actual measuring resistor so that the resulting compensation currents between the shield and the measuring resistors provide a minimum phase angle.

Series Capacitance Voltmeter

To avoid the drawbacks pointed out earlier, a series capacitor is used instead of a resistor for ac high voltage measurements. The schematic diagram is shown in [Fig. 7.10](#). The current I_c through the meter is

$$I_c = j \omega CV \quad (7.9)$$

where, C = capacitance of the series capacitor,
 ω = angular frequency, and
 V = applied ac voltage.

If the ac voltage contains harmonics, error due to changes in series impedance occurs. The rms value of the voltage V with harmonics is given by

$$V = \sqrt{V_1^2 + V_2^2 + \dots + V_n^2} \quad (7.10)$$

where V_1, V_2, \dots, V_n represent the rms value of the fundamental, second ... and nth harmonics.

The currents due to these harmonics are

$$\begin{aligned} I_1 &= \omega C V_1 \\ I_2 &= 2 \omega C V_2, \dots, \end{aligned} \quad (7.11)$$

and $I_n = n \omega C V_n$

Hence, the resultant rms currents is:

$$I = \omega C (V_1^2 + 4V_2^2 + \dots + n^2 V_n^2)^{1/2} \quad (7.12)$$

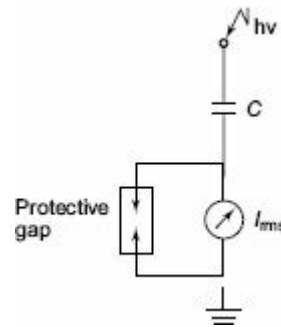


Fig. 7.10 Series capacitance with a milliammeter for measurement of high ac voltages

With a 10% fifth harmonic only, the current is 11.2% higher, and hence the error is 11.2% in the voltage measurement.

This method is not recommended when ac voltages are not pure sinusoidal waves but contain considerable harmonics.

Series capacitance voltmeters were used with cascade transformers for measuring rms values up to 1000 kV. The series capacitance was formed as a parallel plate capacitor between the high voltage terminal of the transformer and a ground plate suspended above it. A rectifier ammeter was used as an indicating instrument and was directly calibrated in high voltage rms value. The meter was usually a 0-100 $\mu\alpha$ moving coil meter and the overall error was about 2%.

7.2.2 Capacitance Potential Dividers and Capacitance Voltage Transformers

The errors due to harmonic voltages can be eliminated by the use of capacitive voltage dividers with an electrostatic voltmeter or a high impedance meter such as a TVM. If the meter is connected through a long cable, its capacitance has to be taken into account in calibration. Usually, a standard compressed air or gas capacitor is used as C_1 (Fig. 7.11), and C_2 may be any large capacitor (mica, paper, or any low loss capacitor). C_1 is a three terminal capacitor and is connected to C_2 through a shielded cable, and C_2 is completely shielded in a box to avoid stray capacitances. The applied voltage V_1 is given by

$$V_1 = V_2 \left(\frac{C_1 + C_2 + C_m}{C_1} \right) \quad (7.13)$$

where C_m is the capacitance of the meter and the connecting cable and the leads and V_2 is the meter reading.

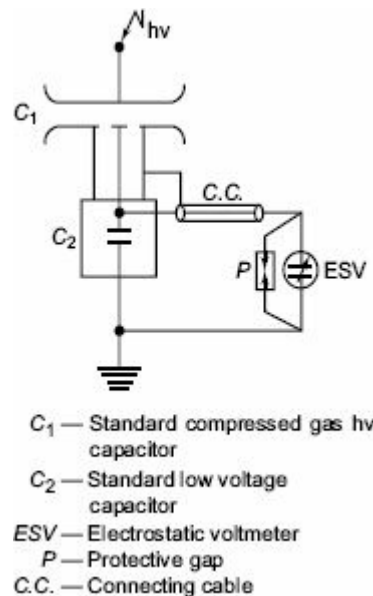


Fig. 7.11 Capacitance potential divider

(a) Capacitance Voltage Transformer=CVT Capacitance divider with a suitable matching or isolating potential transformer tuned for resonance condition is often used in power systems for voltage measurements. This is often referred to as CVT. In contrast to simple capacitance divider which requires a high impedance meter like a TVM or an electrostatic voltmeter, a CVT can be connected to a low impedance device like a wattmeter pressure coil or a relay coil. CVT can supply a load of a few VA. The schematic diagram of a CVT with its equivalent circuit is given in Fig. 7.12. C_1 is made of a few units of high-voltage capacitors, and the total capacitance will be around a few thousand picofarads as against a gas filled standard capacitor of about 100 pF. A matching transformer is connected between the load or meter M and C_2 . The transformer ratio is chosen on economic grounds, and the hv winding rating may be 10 to 30 kV with the l.v. winding rated from 100 to 500 V. The value of the tuning choke L is chosen to make the equivalent circuit of the CVT purely resistive or to bring resonance condition. This condition is satisfied when

$$\omega(L + L_T) = \frac{1}{\omega(C_1 + C_2)} \quad (7.14)$$

where, L = inductance of the choke, and

L_T = equivalent inductance of the transformer referred to hv side.

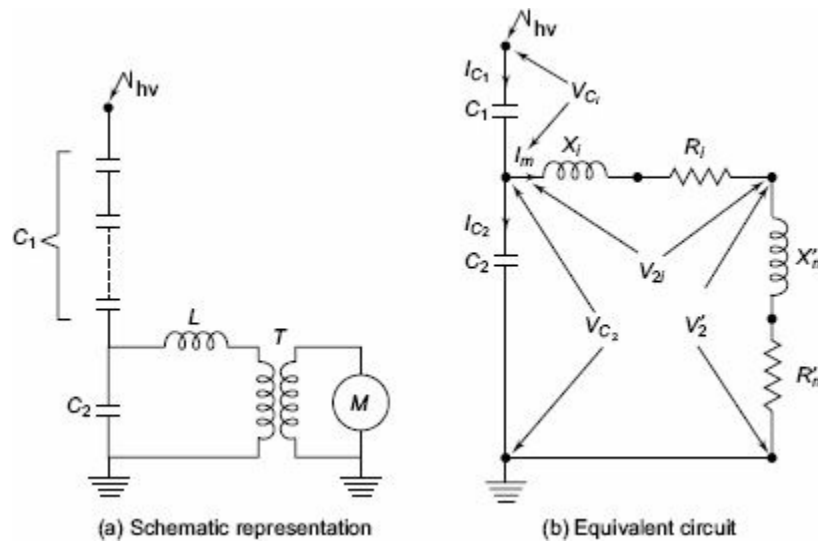


Fig. 7.12 Capacitive voltage transformer (CVT)

The phasor diagram of the CVT under resonant conditions is shown in Fig. 7.13. The meter reactance, X_m is neglected and is taken as a resistance load R_m when the load is connected to the voltage divider side. The voltage across the potential transformer $V_2 = I_m R_m$ and the voltage across the capacitor $= V_2 + I_m (R_e + jX_e)$. The phasor diagram is written taking V_1 as the reference phasor. $V_1 = V_{C1} + V_{C2}$ and total current $= I_m + I_C$. It can be seen that with proper tuning V_2 will be in phase with V_1 . The potential transformer resistance and reactance are not shown separately and are included in R_i and X_i , the resistance and reactance of tuning inductor L.

The voltage ratio,
$$a = \frac{V_1}{V_2} = \frac{V_{C1} + V_{Ri} + V_2}{V_2} \quad (7.15)$$

Neglecting the reactance drop $I_m X_e$, V_{Ri} is the voltage drop across the tuning inductor and the transformer resistance. The voltage V_2 (meter voltage) will be in phase with the input voltage V_1 .

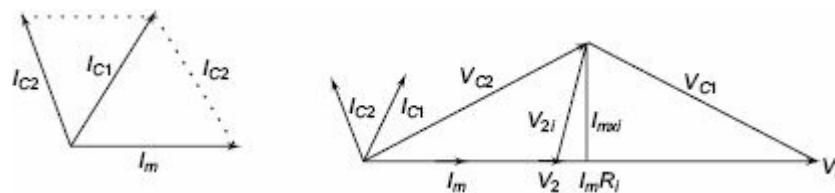


Fig. 7.13 Phasor diagram of a CVT under resonance conditions

The advantages of a CVT are

- (i) simple design and easy installation,
- (ii) can be used both as a voltage measuring device for meter and relaying purposes and also as a coupling condenser for power line carrier communication and relaying.
- (iii) frequency independent voltage distribution along elements as against conventional magnetic potential transformers which require additional insulation design against surges, and
- (iv) provides isolation between the high-voltage terminal and low-voltage metering.

The disadvantages of a CVT are the

- (i) voltage ratio is susceptible to temperature variations, and
- (ii) problem of inducing ferro-resonance in power systems.

(b) *Resistance Potential Dividers* Resistance potential dividers suffer from the same disadvantages as series resistance voltmeters for ac applications. Moreover, stray capacitances and inductances ([Figs 7.7](#) and [7.8](#)) associated with the resistances make them inaccurate, and compensation has to be provided. Hence, they are not generally used.

7.2.3 Potential Transformers (Magnetic Type)

Magnetic potential transformers are the oldest devices for ac measurements. They are simple in construction and can be designed for any voltage. For very high voltages, cascading of the transformers is possible. The voltage ratio is:

$$\frac{V_1}{V_2} = a = \frac{N_1}{N_2} \quad (7.16)$$

where V_1 and V_2 are the primary and secondary voltages, and N_1 and N_2 are the respective turns in the windings.

These devices suffer from the ratio and phase angle errors caused by the magnetizing and leakage impedance of the transformer windings. The errors are compensated by adjusting the turns ratio with the tappings on the high-voltage side under load conditions. Potential transformers (PT) do not permit fast rising transient or high frequency voltages along with the normal supply frequency, but harmonic voltages are usually measured with sufficient accuracy. With high-voltage testing transformers, no separate potential transformer is used, but a PT winding is incorporated with the high voltage windings of the testing transformer.

With test objects like insulators, cables, etc. which are capacitive in nature, a voltage rise occurs on load with the testing transformer, and the potential transformer winding gives voltage values less than the actual voltages applied to the test object. If the percentage impedance of the testing transformer is known, the following correction can be applied to the voltage measured by the PT winding of the transformer.

$$V_2 = V_{20} (1 + 0.01 v_x C / C_N) \quad (7.17)$$

where, V_{20} = open circuit voltage of the PT winding,

C_N = load capacitance used for testing,

C = test object capacitance ($C \ll C_N$), and

v_x = % reactance drop in the transformer.

7.2.4 Electrostatic Voltmeters

(a) Principle In electrostatic fields, the attractive force between the electrodes of a parallel plate capacitor is given by

$$F = \left| \frac{-\delta W_s}{\delta s} \right| = \left| \frac{\delta}{\delta s} \left(\frac{1}{2} CV^2 \right) \right| = \left| \frac{1}{2} V^2 \frac{\delta C}{\delta s} \right|$$
$$= \frac{1}{2} \epsilon_0 V^2 \frac{A}{s^2} = \frac{1}{2} \epsilon_0 A \left(\frac{V}{s} \right)^2 = \frac{d^2}{2825} \left(\frac{V}{s} \right)^2 \text{ gm.wt} \quad (7.18)$$

where, V = applied voltage between plates,

C = capacitance between the plates,

A = area of cross-section of the plates,

d = diameter of plates,

s = separation between the plates,

ϵ_0 = permittivity of the medium (air or free space), and

W_s = work done in displacing a plate

When one of the electrodes is free to move, the force on the plate can be measured by controlling it by a spring or balancing it with a counter weight. For high-voltage measurements, a small displacement of one of the electrodes by a fraction of a millimetre to a few millimetres is usually sufficient for voltage measurements. As the force is proportional to the square of the applied voltage, the measurement can be made for ac or dc voltages.

(b) Construction Electrostatic voltmeters are made with parallel plate configuration using guard rings to avoid corona and field fringing at the edges. An absolute voltmeter is made by balancing the plate with a counter weight and is calibrated in terms of a small weight. Usually the electrostatic voltmeters have a small capacitance (5 to 50 pF) and high insulation resistance ($R > 10^{13} \Omega$). Hence, they are considered devices with high input impedance. The upper frequency limit for ac applications is determined from the following considerations:

- (i) natural frequency of the moving system,
- (ii) resonant frequency of the lead and stray inductances with meter capacitance, and
- (iii) the R - C behaviour of the retaining or control spring (due to the frictional resistance and elastance).

An upper frequency limit of about one MHz is achieved in careful designs. The accuracy for ac voltage measurements is better than $\pm 0.25\%$, and for dc voltage measurements it may be $\pm 0.1\%$ or less.

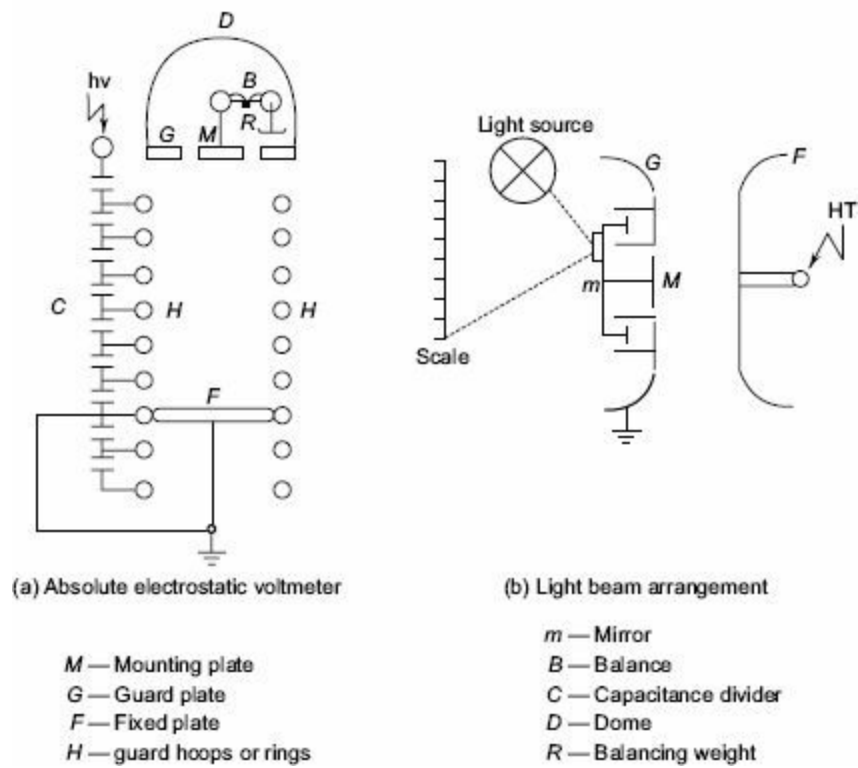


Fig. 7.14 Electrostatic voltmeter

The schematic diagram of an absolute electrostatic voltmeter is given in Fig. 7.14. It consists of parallel-plane disc-type electrodes separated by a small distance. The moving electrode is surrounded by a fixed guard ring to make the field uniform in the central region. In order to measure the given voltage with precision, the disc diameter is to be increased, and the gap distance is to be made less. The limitation on the gap distance is the safe working stress (V/s) allowed in air which is normally 5 kV 1cm or less. The main difference between several forms of voltmeters lies in the manner in which the restoring force is obtained. For conventional versions of meters, a simple spring control is used, which actuates a pointer to move on the scale of the instruments. In more versatile instruments, only small movements of the moving electrodes is allowed, and the movement is amplified through optical means (lamp and scale arrangement as used with moving coil galvanometers). Two air vane dampers are used to reduce vibrational tendencies in the moving system, and the elongation of the spring is kept minimum to avoid field disturbances. The range of the instrument is easily changed by changing the gap separation so that V/s or electric stress is the same for the maximum value in any range. Multi-range instruments are constructed for 600 kV rms and above.

The constructional details of an absolute electrostatic voltmeter is given in Fig. 7.14a. The control torque is provided by a balancing weight. The moving disc *M* forms the central core of the guard ring *G* which is of the same diameter as the fixed plate *F*. The cap *D* encloses a sensitive balance *B*, one arm of which carries the suspension of the moving disc. The balance beam carries a mirror which reflects a beam of light. The movement of the disc is thereby magnified. As the spacing between the two electrodes is large, the uniformity of the electric field is maintained by the guard rings *H* which surround the space between the discs *F* and *M*. The guard rings *H* are maintained at a constant potential in space by a capacitance divider ensuring a uniform special potential distribution.

Some instruments are constructed in an enclosed structure containing compressed air, carbon dioxide, or nitrogen. The gas pressure may be of the order of 15 atm. Working stresses as high as 100 kV/cm may be used in an electrostatic meter in vacuum. With compressed gas or vacuum as medium,

the meter is compact and much smaller in size.

7.2.5 Peak Reading ac Voltmeters

In some occasions, the peak value of an ac waveform is more important. This is necessary to obtain the maximum dielectric strength of insulating solids, etc. When the waveform is not sinusoidal, rms value of the voltage multiplied by $\sqrt{2}$ is not correct. Hence a separate peak value instrument is desirable in high voltage applications.

(a) *Series Capacitor Peak Voltmeter* When a capacitor is connected to a sinusoidal voltage source, the charging current $i_0 = \int_0^t v dt = j \omega CV$ where V is the rms value of the voltage and Ω is the angular frequency. If a half-wave rectifier is used, the arithmetic mean of the rectifier current is proportional to the peak value of the ac voltage. The schematic diagram of the circuit arrangement is shown in [Fig. 7.15](#). The dc meter reading is proportional to the peak value of the value V_m or

$$V_m = \frac{I}{2\pi f C}$$

where I is the dc current read by the meter and C is the capacitance of the capacitor. This method is known as the Chubb-Frotschue method for peak voltage measurement.

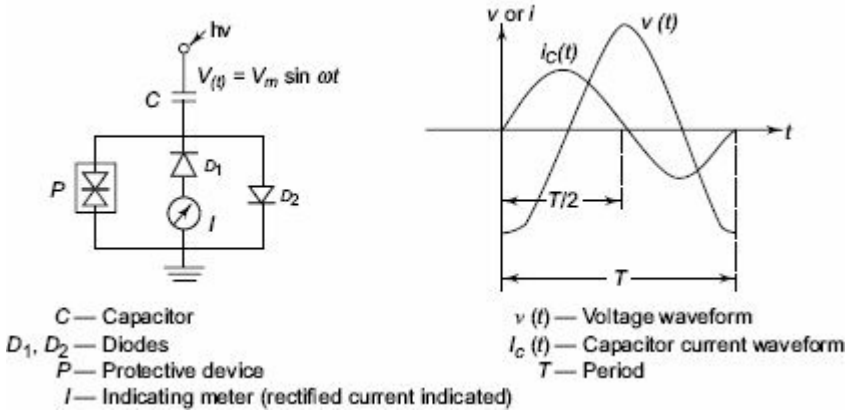


Fig. 7.15 Peak voltmeter with a series capacitor

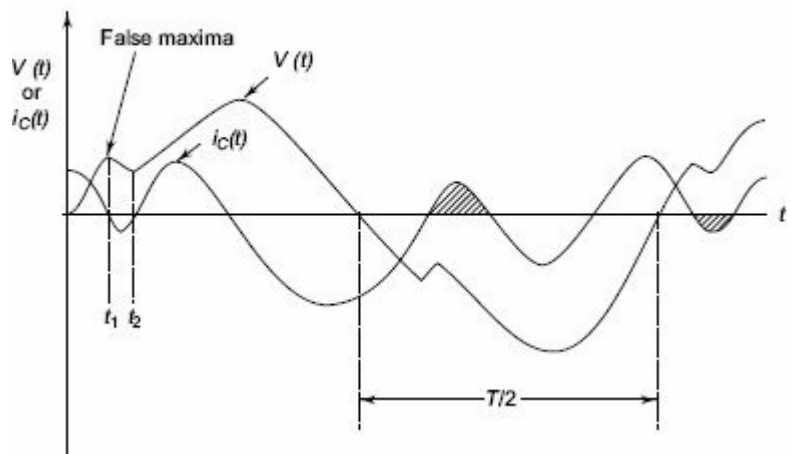


Fig. 7.16 Voltage waveform with harmonic content showing false maxima

The diode D_1 is used to rectify the ac current in one half cycle while D_2 by-passes in the other half cycle. This arrangement is suitable only of positive or negative half cycles and hence is valid only

when both half cycles are symmetrical and equal. This method is not suitable when the voltage waveform is not sinusoidal but contains more than one peak or maximum as shown in [Fig. 7.16](#). The charging current through the capacitor changes its polarity within one half cycle itself. The shaded areas in [Fig. 7.16](#) give the reverse current in any one of the half cycles and the current within that period subtracts from the net current. Hence the reading of the meter will be less and is not proportional to V_m as the current flowing during the intervals $(t_1 - t_2)$ etc. will not be included in the mean value. The 'second' or the false maxima is easily spotted out by observing the waveform of the charging current on an oscilloscope. Under normal conditions with ac testing, such waveforms do not occur and as such do not give rise to errors. But pre-discharge currents within the test circuits cause very short duration voltage drops which may introduce errors. This problem can also be overcome by using a resistance R in series with capacitor C such that $CR \ll 1/\omega$ for 50 Hz application.

The error due to the resistance

$$\frac{\Delta V}{V} = \frac{V - V_m}{V} = \left(1 - \frac{1}{1 + \omega^2 C^2 R^2}\right) \quad (7.19)$$

where, V = actual value, and
 V_m = measured value

In determining the error, the actual value of the angular frequency Ω has to be determined.

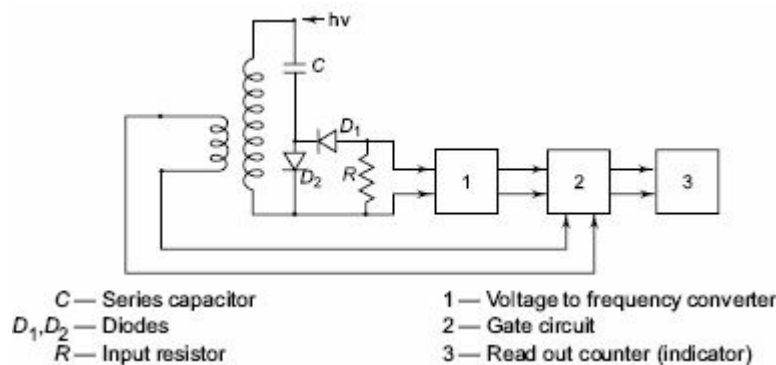


Fig. 7.17 Digital peak voltmeter

The different sources that contribute to the error are

- (i) the effective value of the capacitance being different from the measured value of C .
- (ii) imperfect rectifiers which allows small reverse currents.
- (iii) non-sinusoidal voltage waveforms with more than one peak or maxima per half cycle.
- (iv) deviation of the frequency from that of the value used for calibration.

As such, this method in its basic form is not suitable for waveforms with more than one peak in each half cycle.

A digital peak reading meter for voltage measurements is shown in [Fig. 7.17](#).

Instead of directly measuring the rectified charging current, a proportional analog voltage signal is derived which is then converted into a proportional mean frequency, f_m . The frequency ratio f/f_m is measured with a gate circuit controlled by the ac power frequency (f) and a counter that opens for an adjustable number of periods $\Delta t = p/f$. During this interval, the number of impulses counted, n , is

$$n = f_m \cdot \Delta t = p \cdot \frac{f_m}{f} = 2pCV_mAR \quad (7.20)$$

where p is a constant of the instrument and A represents the conversion factor of the ac to dc converter. $A = f_m / (R i_m)$; i_m is the rectified current through resistance R . An immediate reading of the voltage in kV can be obtained by suitable choice of the parameter R and the number of periods p . The total estimated error in this instrument was less than 0.35%. Conventional instruments of this type are available with less than 2% error.

(b) Peak Voltmeters with Potential Dividers Peak voltmeters using capacitance dividers, designed by Boulder *et al.*, are shown in Fig. 7.18a. The voltage across C_s is made use of in charging the storage capacitor C_s . R_d is a discharge resistor employed to permit variation of V_m whenever V_2 is reduced. C_s is charged to a voltage proportional to the peak value to be measured. The indicating meter is either an electrostatic voltmeter or a high impedance VTVM. This discharge time constant $C_s R_d$ is designed to be about 1 to 10 s. This gives rise to a discharge error which depends on the frequency of the supply voltage. To compensate for the charging and discharging errors due to the resistances, the circuit is modified as shown in Fig. 7.18b. Measurement of the average peak is done by a microammeter. Rabus' modification to compensate the charging errors is given in Fig. 7.18c.

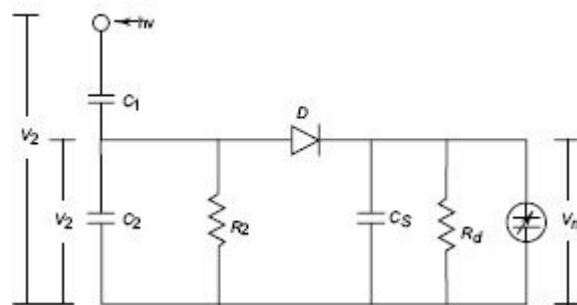


Fig. 7.18a Peak voltmeter with a capacitor potential divider and electrostatic voltmeter

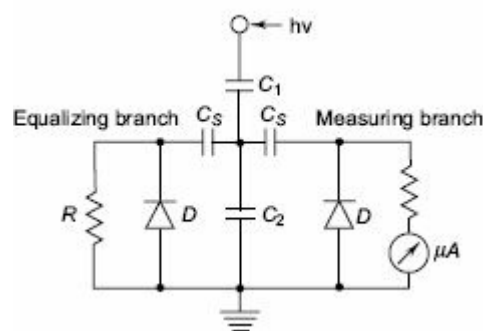
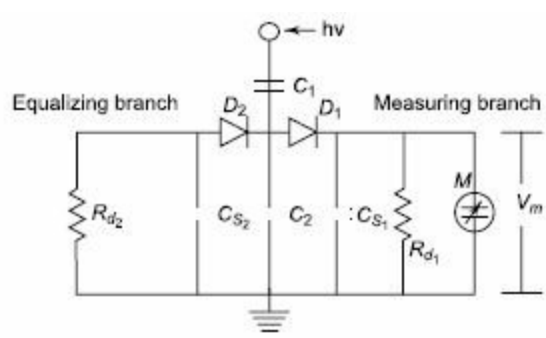


Fig. 7.18b Peak voltmeter as modified by Haefely (Ref. 8)



M — Electrostatic voltmeter
or T.V.M. of high impedance

$C_{S2} = C_{S1} + C \text{ meter}$
 $Rd_2 = Rd_1$

Fig. 7.18c Peak voltmeter with equalizing branch as designed by Rabus (Ref. 9)

Gap spacing (cm)	Sphere diameter (cm)																
	5		10		15		25		50		100		150		200		
	A	B	A	B	A	B	A	B	A	B	A	B	A	B	A	B	
0.5	17.4	17.4	16.9	16.8	16.9	16.9											
1.0	32.0	32.0	31.7	31.7	31.7	31.4	31.2	31.4									
1.5	44.7	45.5	44.7	45.1	44.7	45.1	44.7	44.7									
2.0	57.5	58.0	58.0	58.0	58.0	58.0	58.0	58.0									
2.5			71.5	71.5	71.5	71.5	71.5	71.5	71.5	71.5							
3.0			85.0	85.0	85.0	85.0	85.0	85.0	85.0	85.0							
3.5			95.5	96.0	97.0	97.0	97.0	97.0	97.0	97.0							
4.0			106.0	108.0	108.0	110.0	110.0	110.0	110.0	110.0							
5.0			(123.0)	(127.0)	127.0	132.0	135.0	136.0	136.0	136.0							
7.5					(181.0)	(187.0)	195.0	196.0	199.0	199.0							
10.0							257	268	259	259	262	262	262	262	262	262	262
12.5							277	294	315	317							
15.0							(309)	(331)	367	374	383	384	384	384	384	384	384
17.5							(336)	(362)	413	425							
20.0									452	472	500	500	500	500	500	500	500
25.0									520	545	605	610					
30.0									(575)	(610)	700	715	730	735	735	740	740
35.0									(725)	(755)	785	800					
40.0											862	885	940	950	960	965	965
45.0											925	965					
50.0											1000	1020	1110	1130	1160	1170	1170
75.0											(1210)	(1260)	1420	1460	1510	1590	1590
100.0															1870	1900	1900

Table 7.4 Sphere gap sparkover voltages in kV (peak) in air for ac, dc, and impulse voltage of either polarity for symmetrical sphere gaps at temperature: 20°C and pressure: 760 torr

Gap spacing (cm)	Sphere diameter (cm)								Remarks
	5	10	15	25	50	100	150	200	
0.5	17.5	16.9	16.5						For spacings less than 0.5 D, the accuracy is ±3% and for spacing ≥ 0.5 D, the accuracy is ±5%.
1.0	32.2	31.6	31.3	31.0					
1.5	46.1	45.8	45.5	45.0					
2.0	58.3	59.3	59.2	59.0					
2.5	69.4	72.4	72.9	73.0					
3.0	(79.3)	84.9	85.8	86.0					
4.0		107.0	111.0	113.0	112.0				
5.0		128.0	134.0	138.0	138.0	137.0	137.0	137.0	
8.0		(177)	194.0	207.0	214.0				
10.0				248.0	263.0	266.0	267.0	267.0	
12.0				286.0	309.0				
14.0				320.0	353.0				
16.0				352.0	394.0				
18.0					452.0				
20.0					495.0	504.0	511.0	511.0	
25.0					558.0	613.0	628.0	632.0	
30.0						744.0	741.0	746.0	
35.0						812.0	848.0	860.0	
40.0						902.0	950.0	972.0	
50.0						1070.0	1140.0	1180.0	
60.0						(1210)	1320.0	1380.0	
70.0							1490.0	1560.0	
80.0							(1640)	1730.0	
90.0								1900.0	
100.0								2050.0	

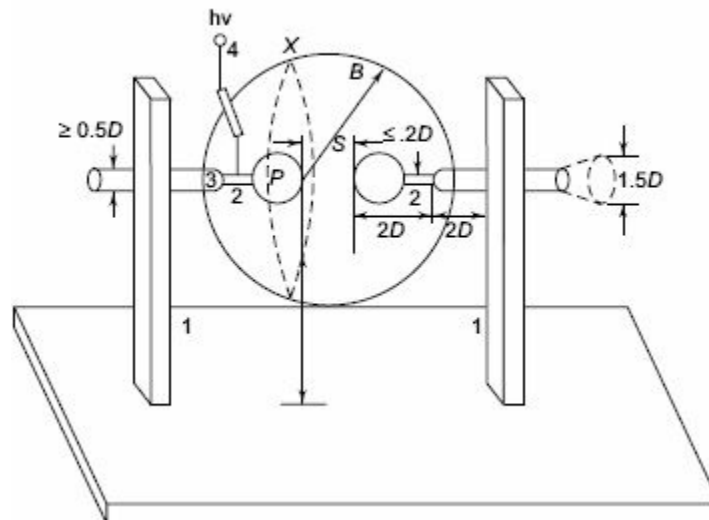


Fig. 7.19b Horizontal arrangement of sphere gap (Legend as in Fig. 7.19a)

In the ease of ac peak value and dc voltage measurements, the applied voltage is uniformly

increased until sparkover occurs in the gap. Generally, a mean of about five breakdown values is taken when they agree to within $\pm 3\%$.

In the case of impulse voltages, to obtain 50% flashover voltage, two voltage limits, differing by not more than 2% are set such that on application of lower limit value either 2 or 4 flashovers take place and on application of upper limit value 8 or 6 flashovers take place respectively. The mean of these two limits is taken as 50% flashover voltage. In any case, a preliminary sparkover voltage measurement is to be made before actual measurements are made.

The flashover voltage for various gap distances and standard diameters of the spheres used are given in [Tables 7.3](#) and [7.4](#) respectively. The values of sparkover voltages are specified in BS : 358, IEC Publication 52 of 1960 and IS: 1876 of 1962. The clearances necessary are shown in [Figs 7.19a](#) and [7.19b](#) for measurements to be within $\pm 3\%$. The value of A and B indicated in the above figures are given in [Table 7.5](#).

(b) Sphere Gap Construction and Assembly

Sphere gaps are made with two metal spheres of identical diameters D with their shanks, operating gear, and insulator supports ([Fig. 7.19a](#) or [b](#)). Spheres are generally made of copper, brass, or aluminium; the latter is used due to low cost. The standard diameters for the spheres are 2, 5, 6.25, 10, 12.5, 15, 25, 50, 75, 100, 150, and 200 cm. The spacing is so designed and chosen such that flashover occurs near the sparking point P. The spheres are carefully designed and fabricated so that their surfaces are smooth and the curvature is uniform. The radius of curvature measured with a spherometer at various points over an area enclosed by a circle of $0.3 D$ around the sparking point should not differ by more than $\pm 2\%$ or the nominal value. The surface of the sphere should be free from dust, grease, or any other coating. The surface should be maintained clean but need not be polished. If excessive pitting occurs due to repeated sparkovers, they should be smoothed. The dimensions of the shanks used, the grading ring used (if necessary) with spheres, the ground clearances, etc. should follow the values indicated in [Figs 7.19a](#) and [7.19b](#) and [Table 7.5](#). The high voltage conductor should be arranged such that it does not affect the field configuration. Series resistance connected should be outside the shanks at a distance $2D$ away from the high voltage sphere or the sparking point P.

Table 7.5 Clearances for sphere gaps

D (cm)	Value of A		Value of B (min)
	Min	Max	
up to 6.25	$7 D$	$9 D$	$14 S$
10 to 15	$6 D$	$8 D$	$12 S$
25	$5 D$	$7 D$	$10 S$
50	$4 D$	$6 D$	$8 S$
100	$3.5 D$	$5 D$	$7 S$
150	$3 D$	$4 D$	$6 S$
200	$3 D$	$4 D$	$6 S$

A and B are clearances as shown in [Figs 7.19a](#) and [7.19b](#).

D = diameter of the sphere; S = spacing of the gap; and $S/D \leq 0.5$.

Irradiation of sphere gap is needed when measurements of voltages less than 50 kV are made with sphere gaps of 10 cm diameter or less. The irradiation may be obtained from a quartz tube mercury

vapour lamp of 40 W rating. The lamp should be at a distance B or more as indicated in [Table 7.5](#).

(c) Factors Influencing the Sparkover Voltage of Sphere Gaps

Various factors that affect the sparkover voltage of a sphere gap are

- (i) near by earthed objects,
- (ii) atmospheric conditions and humidity,
- (iii) irradiation, and
- (iv) polarity and rise time of voltage waveforms.

Detailed investigations of the above factors have been made and analysed by Craggs and Meek , Kuffel and Abdullah , Kuffel, Davis and Bowlder, and several other investigators. Only a few important factors are presented here.

(i) effect of near by Earthed Objects The effect of nearby earthed object was investigated by Kuffel by enclosing the earthed sphere inside an earthed an earthed cylinder. It was observed that the sparkover voltage is reduced. The reduction was observed to be

$$\Delta V = m \log (B/D) + C \quad (7.21)$$

Where, ΔV = percentage reduction,
 B = diameter of earthed enclosing cylinder,
 D = diameter of the spheres,
 S = spacing, and m and C are constants.

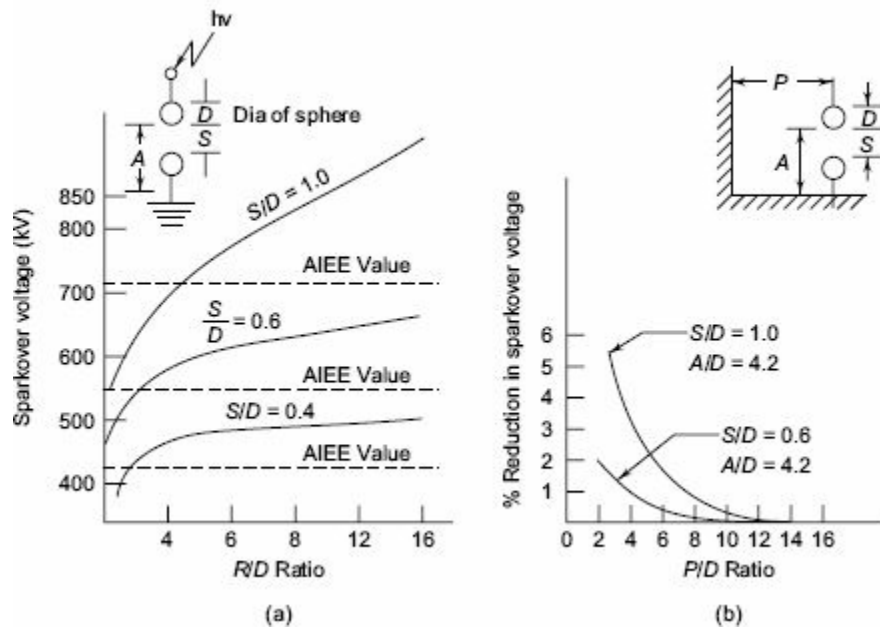


Fig. 7.20 Influence of ground planes on sparkover voltage

The reduction was less than 2% for $S/D \leq 0.5$ and $B/D \geq 0.8$. Even for $S/D = 1.0$ and $B/D \geq 1.0$ the reduction was only 3%. Hence, if the specifications regarding the clearances are closely observed the error is within the tolerances and accuracy specified. The variation of breakdown voltage with A/D ratio is given in Figs 7.20a and b for a 50 cm sphere gap. The reduction in voltage is within the accuracy limits, if S/D is kept less than 0.6 A in the above ratio, A is the distance from sparking point

to horizontal ground plane (also shown in [Fig. 7.20](#)).

(ii) Effect of Atmospheric Conditions The sparkover voltages of a spark gap depends on the air density which varies with the changes in both temperature and pressure. If the sparkover voltage is V under test conditions of temperature T and pressure p torr and if the sparkover voltage is V_0 under standard conditions of temperature $T = 20^\circ\text{C}$ and pressure $p = 760$ torr, then

$$V = kV_0$$

where k is a function of the air density factor d , given by

$$d = \frac{p}{760} \left(\frac{293}{273 + T} \right) \quad (7.22)$$

The relationship between d and k is given in [Table 7.6](#).

Table 7.6 Relation between correction factor k and air density factor d

d	0.70	0.75	0.80	0.85	0.90	0.95	1.0	1.05	1.10	1.15
k	0.72	0.77	0.82	0.86	0.91	0.95	1.0	1.05	1.09	1.12

The sparkover voltage increases with humidity. The increase is about 2 to 3% over normal humidity range of 8 g/m^3 to 15 g/m^3 . The influence of humidity on sparkover voltage of a 25 cm sphere gap for 1 cm spacing is presented in [Fig. 7.21](#). It can be seen that the increase in sparkover voltage is less than 3% and the variation between ac and dc breakdown voltages is negligible ($< 0.5\%$).

Hence, it may be concluded that (i) the humidity effect increases with the size of spheres and is maximum for uniform field gaps, and (ii) the sparkover voltage increases with the partial pressure of water vapour in air, and for a given humidity condition, the change in sparkover voltage increases with the gap length. As the change in sparkover voltage with humidity is within 3%, no correction is normally given for humidity.

(iii) Effect of Irradiation Illumination of sphere gaps with ultra-violet or X-rays aids easy ionization in gaps. The effect of irradiation is pronounced for small gap spacings. A reduction of about 20% in sparkover voltage was observed for spacings of $0.1 D$ to $0.3 D$ for a 1.3 cm sphere gap with dc voltages. The reduction in sparkover voltage is less than 5% for gap spacings more than 1 cm, and for gap spacings of 2 cm or more it is about 1.5%. Hence, irradiation is necessary for smaller sphere gaps of gap spacing less than 1 cm for obtaining consistent values.

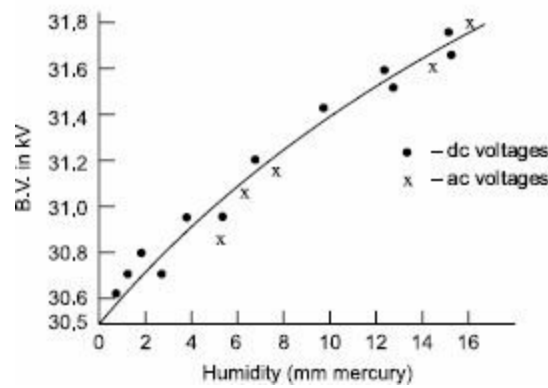


Fig. 7.21 Influence of humidity on dc and ac breakdown voltages (25 cm dia sphere gap, 1 cm spacing)

(iv) Effect of Polarity and Waveform

It has been observed that the sparkover voltages for positive and negative polarity impulses are different. Experimental investigation showed that for sphere gaps of 6.25 to 25 cm diameter, the difference between positive and negative dc voltages is not more than 1%. For smaller sphere gaps (2 cm diameter and less) the difference was about 8% between negative and positive impulses of 1/50 μs waveform. Similarly, the wave-front and wave-tail durations also influence the breakdown voltage. For wave fronts of less than 0.5 μs and wave tails less than 5 μs the breakdown voltages are not consistent and hence the use of sphere gap is not recommended for voltage measurement in such cases.

(d) Uniform Field Electrode Gaps

Sphere gaps, although widely used for voltage measurements, have only limited range with uniform electric field. Hence, it is not possible to ensure that the sparking always takes place along the uniform field region. Rogowski [see Craggs and Meek⁽¹⁾] presented a design for uniform field electrodes for sparkover voltages up to 600 kV. The sparkover voltage in a uniform field gap is given by

$$V = AS + B\sqrt{S}$$

where A and B are constant, S is the gap spacing in cm, and V is the sparkover voltage.

Typical uniform field electrodes are shown in Fig. 7.22. The constants A and B were found to be 24.4 and 7.50 respectively at a temperature $T = 25^\circ C$ and pressure = 760 torr. Since the sparking potential is a function of air density, the sparkover voltage for any given air density factor d (see Eq. 7.22) is modified as

$$V = 24.4 dS + 7.50 \sqrt{dS} \tag{7.23}$$

Bruce [see Craggs *et al.*⁽¹⁾ and Kuffel *et al.*⁽²⁾]. made uniform field electrodes with a sine curve in the end region. According to Bruce, the electrodes with diameters of 4.5, 9.0, and 15.0 in can be used for maximum voltages of 140, 280, and 420 kV respectively. For the Bruce profile, the constants A and B are respectively 24.22 and 6.08. Later, it was found that with humidity the sparkover voltage increases, and the relationship for sparkover voltage was modified as

$$V = 6.66 \sqrt{dS} + [24.55 + 0.41 (0.1e - 1.0)]dS \tag{7.24}$$

where, $V = \text{sparkover voltage, kV}_{dc}$ (in kV_{dc}),

$e = \text{vapour pressure of water in air (mmHg)}$.

The constants A and B differ for ac, dc, and impulse voltages. A comparison between the sparkover voltages (in air at a temperature of 20°C and a pressure of 760 torr) of a uniform field electrode gap and a sphere gap is given in [Table 7.7](#). From this table it may be concluded that within the specified limitations and error limits, there is no significant difference among the sparkover voltages of sphere gaps and uniform field gaps.

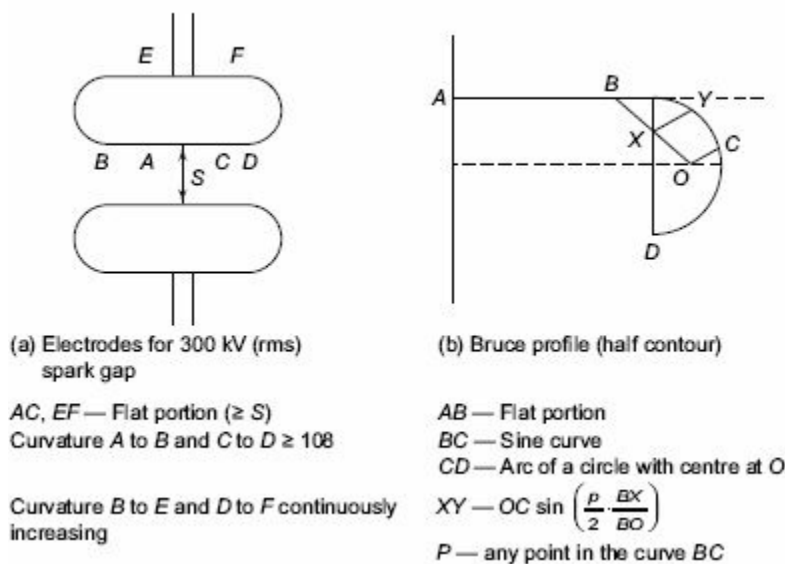


Fig. 7.22 Uniform field electrode spark gap

Table 7.7 Sparkover voltage of uniform field gaps and sphere gaps at $T = 20^\circ\text{C}$ and $pr = 760$ torr

Gap spacing (cm)	Sparkover voltage with uniform field electrodes as measured by			Sphere gap sparkover voltage (kV)
	Ritz (kV)	Bruce (kV)	Schumann (kV)	
0.1	4.54	—	4.50	4.6
0.2	7.90	7.56	8.00	8.0
0.5	17.00	16.41	17.40	17.0
1.0	31.35	30.30	31.70	31.0
2.0	58.70	57.04	59.60	58.0
4.0	112.00	109.00	114.00	112.0
6.0	163.80	160.20	166.20	164.0
8.0	215.00	211.00	216.80	215.0
10.0	265.00	261.1	266.00	265.0
12.0	315.00	311.6	—	312.0

The sparkover voltage of uniform field electrode gaps can also be found from calculations. However, no such calculation is available for sphere gaps. In spite of the superior performance and accuracy, the uniform field spark gap is not usually used for measurement purposes, as very accurate finish of the electrode surfaces and careful alignment are difficult to obtain in practice.

(e) Rod Gaps

A rod gap is also sometimes used for approximate measurement of peak values of power frequency voltages and impulse voltages. IEEE recognise that this method gives an accuracy within $\pm 8\%$. The rods will be either square edged or circular in cross-section. The length of the rods may be 15 to 75

cm and the spacing varies from 2 to 200 cm. The sparkover voltage, as in other gaps, is affected by humidity and air density. The power frequency breakdown voltage for 1.27 cm square rods in air at 27°C and at a pressure of 760 torr with the vapour pressure of water of 15.5 torr is given in [Table 7.8](#). The humidity correction is given in [Table 7.9](#). The air density correction factor can be taken from [Table 7.6](#).

Table 7.8 Sparkover voltage for rod gaps

Gap spacing (cm)	Sparkover voltage (kV)	Gap spacing (cm)	Sparkover voltage (kV)
2	26	30	172
4	47	40	225
6	62	50	278
8	72	60	332
10	81	70	382
15	102	80	435
20	124	90	488
25	147	100	537

The rods are 1.27 cm square edged at $t = 27^\circ\text{C}$, $p = 760$ torr, and vapour pressure of water = 15.5 torr.

Table 7.9 Humidity correction for rod gap sparkover voltages

Vapour pressure of water (torr)	2.54	5	10	15	20	25	30
Correction factor %	-16.5	-13.1	-6.5	-0.5	4.4	7.9	10.1

In case of impulse voltage measurements, the IEC and IEEE recommend horizontal mounting of rod gaps on insulators at a height of 1.5 to 2.0 times the gap spacing above the ground. One of the rods is usually earthed. For 50% flashover voltages, the procedure followed is the same as that for sphere gaps. Corrections for humidity for $1/5 \mu\text{s}$ impulse and $1/5 \mu\text{s}$ impulse waves of either polarity are given in [Fig. 7.23](#). The sparkover voltages for impulse waves are given in [Table 7.10](#).

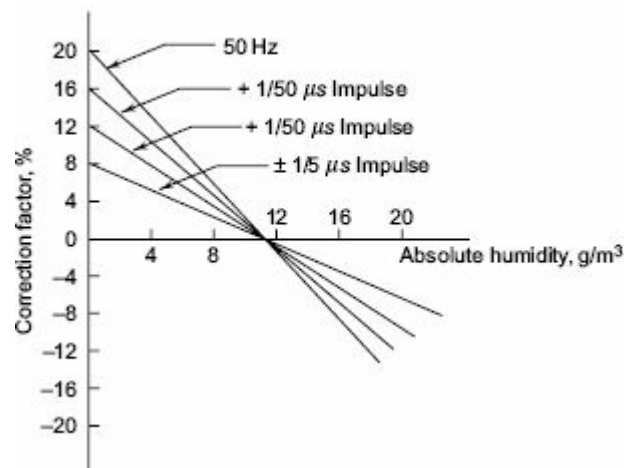


Fig. 7.23 Correction factor for rod gaps

Table 7.10 Sparkover voltages of rod gaps for impulse voltages at temperature = 20°C, pressure = 760 torr and humidity = 11 g/m³

<i>Gap length (cm)</i>	<i>1/5 μ s wave (kV)</i>		<i>1/50 μ s wave (kV)</i>	
	<i>Positive</i>	<i>Negative</i>	<i>Positive</i>	<i>Negative</i>
5	60	66	56	61
10	101	111	90	97
20	179	208	160	178
30	256	301	226	262
40	348	392	279	339
50	431	475	334	407
60	513	557	397	470
80	657	701	511	585
100	820	855	629	703

7.2.7 Potential Dividers for Impulse Voltage Measurements

Potential or voltage dividers for high-voltage impulse measurements, high frequency ac measurements, or for fast rising transient voltage measurements are usually either resistive or capacitive or mixed element type. The low-voltage arm of the divider is usually connected to a fast recording oscillograph or a peak reading instrument through a delay cable. A schematic diagram of a potential divider with its terminating equipment is given in [Fig. 7.24](#). Z_1 is usually a resistor or a series of resistors in case of a resistance potential divider, or a single or a number of capacitors in case of a capacitance divider. It can also be a combination of both resistors and capacitors. Z_2 will be a resistor or a capacitor or an $R-C$ impedance depending upon the type of the divider. Each element in the divider, in case of high-voltage dividers, has a self-resistance or capacitance. In addition, the resistive elements have residual inductances, a terminal stray capacitance to ground, and terminal to terminal capacitances.

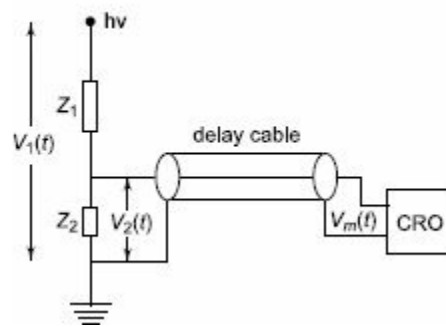


Fig. 7.24 Schematic diagram of a potential divider with a delay cable and oscilloscope

The lumped-circuit equivalent of a resistive element is already shown in [Fig. 7.8](#) the equivalent circuit of the divider with inductance neglected is of the form shown in [Fig. 7.9a](#). A capacitance potential divider also has the same equivalent circuit as in [Fig. 7.8a](#), where C_s will be the capacitance of each elemental capacitor, C_g will be the terminal capacitance to ground, and R will be the equivalent leakage resistance and resistance due to dielectric loss in the element. When a step or fast rising voltage is applied at the high voltage terminal, the voltage developed across the element Z_2 will not have the true waveform as that of the applied voltage. The cable can also introduce distortion in the waveshape. The following elements mainly constitute the different errors in the measurements:

- (i) residual inductance in the elements;
- (ii) stray capacitance occurring
 - (a) between the elements,
 - (b) from sections and terminals of the elements to ground, and
 - (c) from the high voltage lead to the elements or sections;
- (iii) The impedance errors due to
 - (a) connecting leads between the divider and the test objects, and
 - (b) ground return leads and extraneous current in ground leads; and
- (iv) parasitic oscillations due to lead and cable inductances and capacitance of high-voltage terminal to ground.

The effect to residual and lead inductances becomes pronounced when fast rising impulses of less than one microsecond are to be measured. The residual inductances damp and slow down the fast

rising pulses. Secondly, the layout of the test objects, the impulse generator, and the ground leads also require special attention to minimize recording errors. These are discussed in Sec. 7.4.

(a) Resistance Potential Divider for Very Low Impulse Voltages and Fast Rising Pulses A simple resistance potential divider consists of two resistances R_1 and R_2 in series ($R_1 \gg R_2$) (see [Fig. 7.25](#)). The attenuation factor of the divider or the voltage ratio is given by

$$a = \frac{V_1(t)}{V_2(t)} = 1 + \frac{R_1}{R_2} \quad (7.25)$$

The divider element R_2 , in practice, is connected through the coaxial cable to the oscilloscope. The cable will generally have a surge impedance Z_0 and this will come in parallel with the oscilloscope input impedance (R_m, C_m). R_m will generally be greater than one megaohm and C_m may be 10 to 50 picofarads. For high frequency and impulse voltages (since they also contain high frequency fundamental and harmonics), the ratio in the frequency domain will be given by

$$a = \frac{V_1}{V_2} = 1 + \frac{R_1}{(R_2/1 + j\omega R_2 C_m)} \quad (7.26)$$

Hence, the ratio is a function of the frequency. To avoid the frequency dependence of the voltage ratio a , the divider is compensated by adding an additional capacitance C_1 across R_1 . The value of C_1 , to make the divider independent of the frequency, may be obtained from the relation, meaning that the time constant of both the arms should be the same. This compensation is used for the construction of high-voltage dividers and probes used with oscilloscopes. Usually, probes are made with adjustable values of C_m so that the value of C_m can include any stray capacitance including that of a cable, etc. A typical high-voltage probe with a four nanosecond rise time rated for 40 kV (peak) has an input impedance of 100 M Ω in parallel with 2.7 pF. The output waveforms of a compensated divider are shown in [Fig. 7.25c](#) with over and under compensation for a square wave input. In [Fig. 7.25c](#) (i) is shown the waveform of an R - C divider when C_1 is too large or overcompensated, while in [Fig. 7.25c](#) (iii) is shown the waveform when C_1 is small or undercompensated. For the exponential slope or for the rising portion of the wave, the time constant $\tau = [R_1 R_2 / (R_1 + R_2)] (C_1 + C_m)$. This will be too large when the value of C_1 is greater than that required for correct compensation, i.e., $R_1 C_1 = R_2 C_m$ and hence an overshoot with an exponential decay occurs as shown in [Fig. 7.25c](#) (i). For under compensation, the charging time is too high and as such an exponential rise occurs as shown in [Fig. 7.25c](#) (iii). The schematic circuit of a compensated oscilloscope probe is shown in [Fig. 7.26](#).

$$\frac{R_1}{R_2} = \frac{C_m}{C_1} \quad (7.27)$$

or,

$$R_1 C_1 = R_2 C_m$$

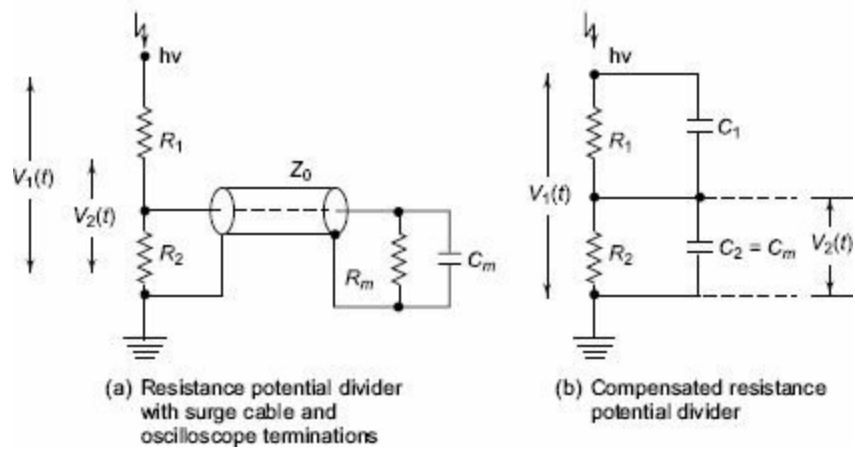


Fig. 7.25a and b Resistance potential dividers

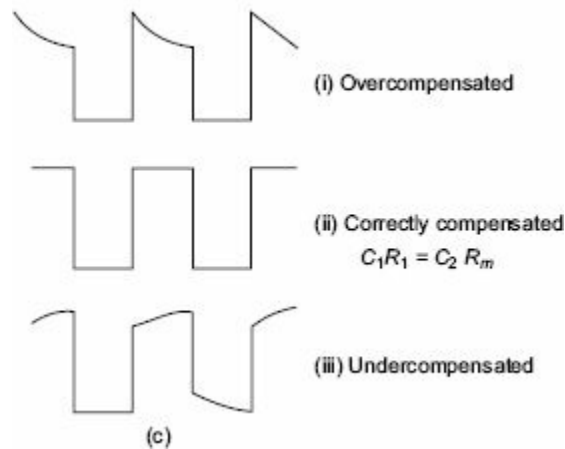


Fig. 7.25c Output of compensated resistance voltage divider for different degrees of compensation

(b) Potential Dividers Used for High-Voltage Impulse Measurements In a resistance potential divider, R_1 and R_2 are considered as resistors of small dimensions in the previous section. For voltages above 100 kV, R_1 is no longer small in dimension and is usually made of a number of sections. Hence the divider is no longer a small resistor of lumped parameters, but has to be considered as an equivalent distributed network with its terminal to ground capacitances and intersectional series capacitances as shown in Fig. 7.27. The total series resistance R'_1 is made of n resistors of value R'_1 and $R = nR'_1$. C_g is the terminal to ground capacitance of each of the resistor elements R'_1 , and C_s is the capacitance between the terminals of each section. The inductance of each element (L'_1) is not shown in the figure as it is usually small compared to the other elements (i.e., R'_1 , C_s and C_g). This type of divider produces a non-linear voltage distribution along its length and also acts like an R - C filter for applied voltages. The output of such divider for various values of C_g/C_s ratio is shown in Fig. 7.28 for a step input. By arranging guard rings at various elemental points, the equivalent circuit can be modified as shown Fig. 7.29, where C_h represents the stray capacitance introduced between the high voltage lead and the guard elements. This reduces the distortion introduced by the original divider (Plate 5).

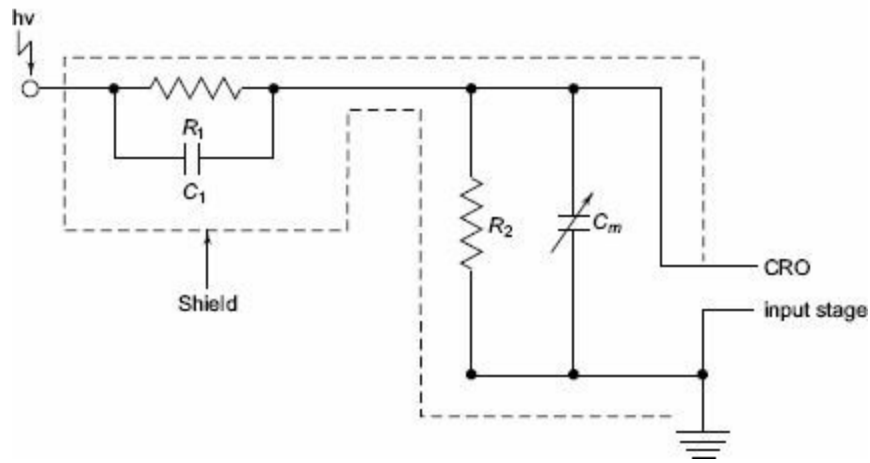


Fig. 7.26 Schematic circuit arrangement of a cathode ray oscilloscope voltage

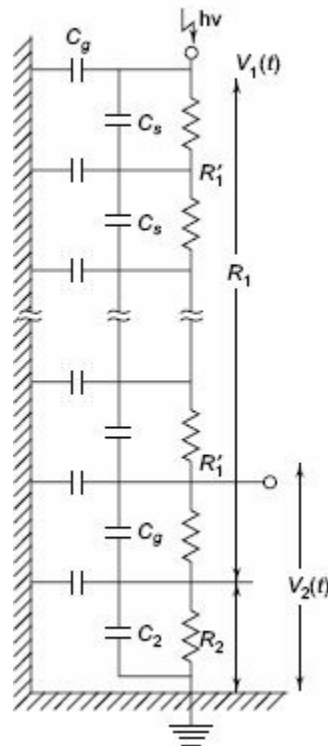


Fig. 7.27 Resistance potential divider ground capacitances

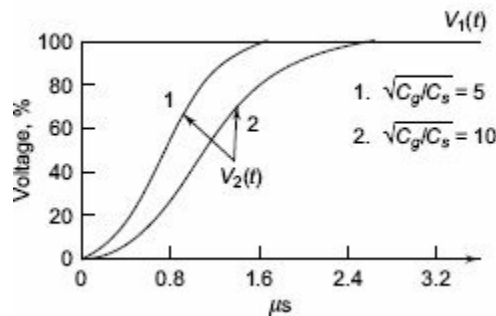


Fig. 7.28 Output of the divider with inter-sectional and shown in Fig. 7.27 for a step input

(c) **Capacitance Voltage Dividers** Capacitance voltage dividers are ideal for measurement of fast rising voltages and pulses. The capacitance ratio is independent of the frequency, if their leakage resistance is high enough to be neglected. But usually the dividers are connected to the source voltage

through long leads which introduce lead inductances and residual resistances. Also, the capacitance used for very high-voltage work is not small in dimension and hence cannot be considered as a lumped element. Therefore, the output of the divider for high frequencies and impulses is distorted as in the case of resistance dividers.

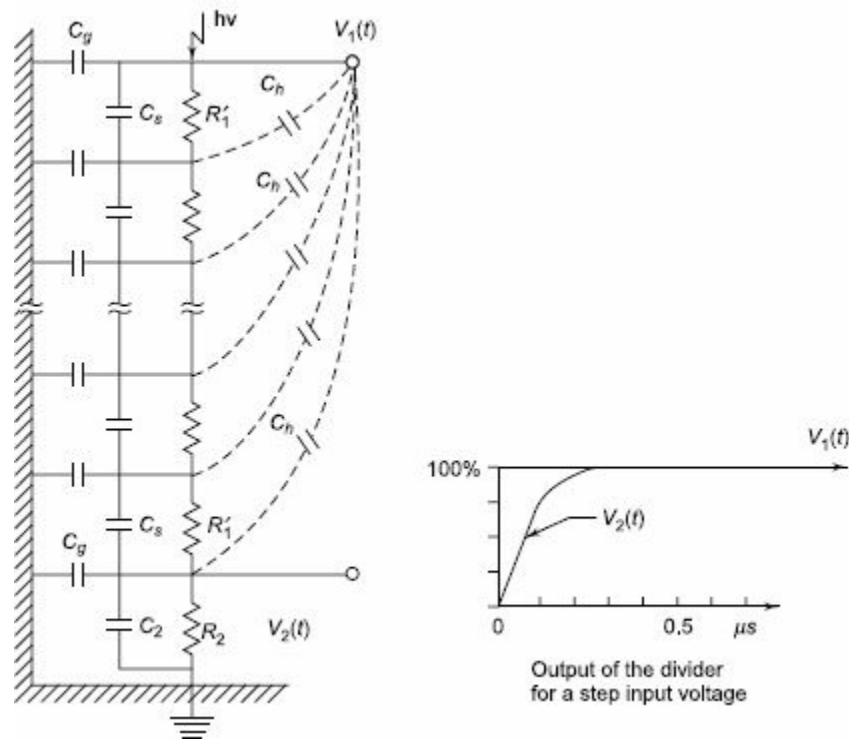


Fig. 7.29 Equivalent circuit of a resistance potential divider with shield and guard rings

(d) Pure Capacitance Dividers A pure capacitance divider for high voltage measurements and its electrical equivalent network without stray elements is shown in Fig. 7.30. The ratio of the divider

$$a = \frac{V_1(t)}{V_2(t)} = 1 + \frac{C_2}{C_1} \quad (7.28)$$

Capacitance C_1 is formed between the hv terminal of the source (impulse generator) and that of the test object or any other point of measurement. The CRO is located within the shielded screen surrounding capacitance C_2 , C_2 includes the capacitance used, the lead capacitance, input capacitance of the CRO, and other ground capacitances. The advantage of this connection is that the loading on the source is negligible; but a small disturbance in the location of C_2 or hv electrode or the presence of any stray object nearby changes the capacitance C_1 , and hence the divider ratio is affected.

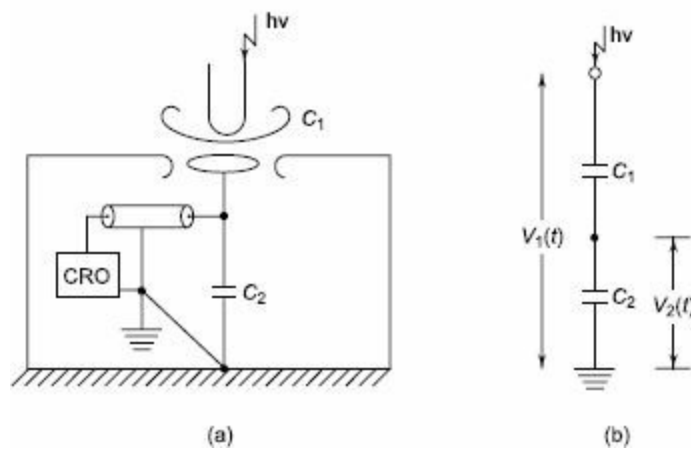


Fig. 7.30 Capacitance voltage divider for very high voltages and electrical equivalent circuit

In many cases, a standard air or compressed gas capacitor is used which has coaxial cylindrical construction. Accurate ratios that could be calculated up to 1000 : 1 have been achieved for a maximum impulse voltage of 350 kV, and the upper frequency limit is about 10 MHz. For smaller or moderately high voltages (up to 100 kV) capacitance dividers are built with an upper frequency limit of 200 MHz.

Another type of design frequently used is to make C_1 to consist of a number of capacitors C'_1 in series for the given voltage V_1 . In such cases the equivalent circuit is similar to that of a string insulator unit used in transmission lines (Fig. 7.31). The voltage distribution along the capacitor chain is non-linear and hence causes distribution of the output wave. But the ratio error is constant and is independent of frequency as compared to resistance dividers. A simplified equivalent circuit is shown in Fig. 7.31b, which can be used if $C_1 \ll C_2$ and $C_g \ll C_1$.

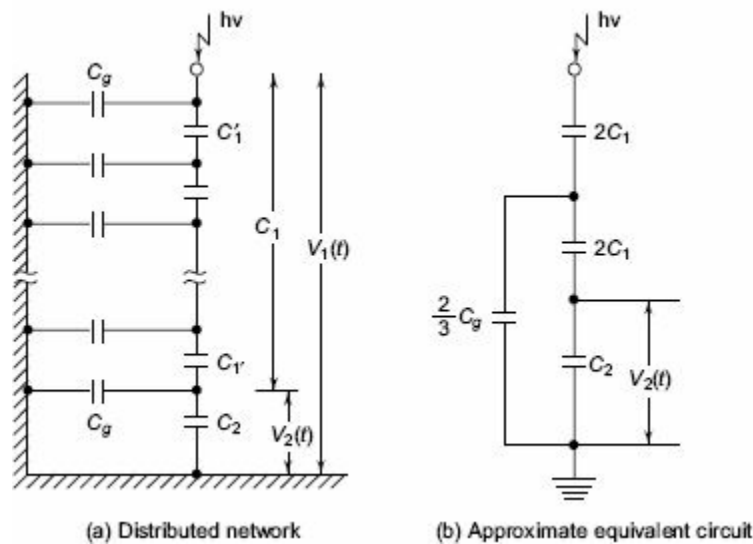


Fig. 7.31 Capacitance voltage divider with distributed network and its equivalent circuit

The voltage ratio is

$$a = \frac{V_1(t)}{V_2(t)} \approx \left[1 + \frac{C_2}{C_1} \right] \left[1 + \frac{C_g}{6C_1} \right] \quad (7.29)$$

This ratio is constant and gives an error of less than 5% when $C_1 = 3C_g$. This equivalent circuit is quite satisfactory up to 1 MHz.

(e) Field Controlled Voltage Dividers The electrostatic or capacitive field distribution of a shield or guard ring placed over a resistive divider to enforce a uniform field in the neighbourhood and along the divider may be adopted for high voltage measurements. The schematic diagram is shown in [Fig. 7.32](#) and its equivalent circuit is same as that given in [Fig. 7.29](#). The shield is of the form of a cone. R_1 is a non-linear resistance in the sense the resistance per unit length is not the same but is variable. The main advantage is that the capacitance per unit length is small and hence loading effect is reduced. Sometimes the parallel resistance R_2 together with the lead inductance and shunt capacitances cause oscillations as shown in [Fig. 7.33a](#). The oscillations can be reduced by adding a damping resistance R_d as shown in [Fig. 7.32](#).

Such dividers are constructed for very high voltages (up to 2 MV) with response times less than 30 ns. The resistance column, R_1 is made of woven resistance of 20 kilo-ohms. The step response of such a divider is shown in [Fig. 7.33](#), with and without a damping resistor. With a proper damping resistor (R_d) the response time is much less and the overshoot is reduced.

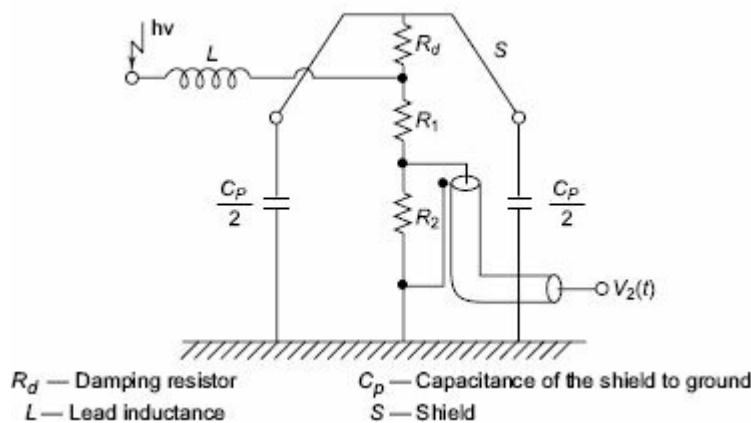


Fig. 7.32 Field-controlled resistance divider with a damping resistor

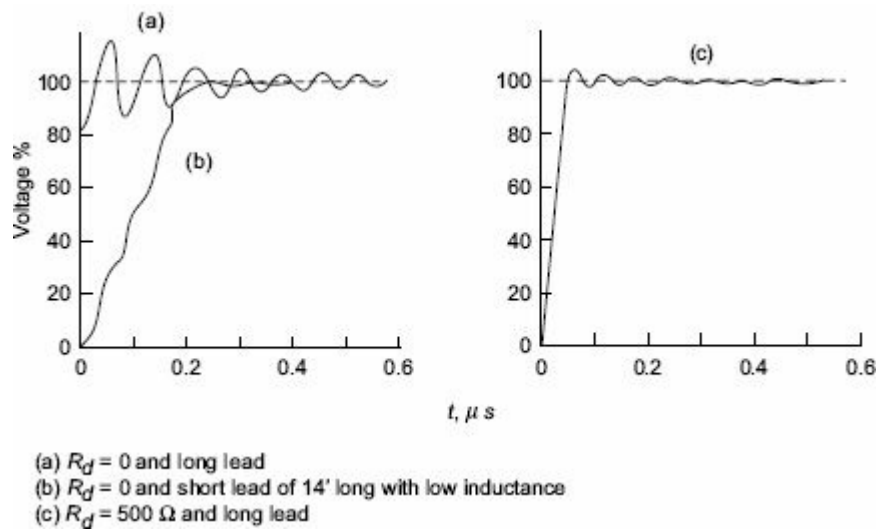


Fig. 7.33 Step response of field controlled voltage divider of [Fig. 7.32](#)

(f) Mixed R-C Potential Dividers Mixed potential dividers use R-C elements in series or in parallel. One method is to connect capacitance in parallel with each R'_1 element. This is successfully employed for voltage dividers of rating 2 MV and above. A better construction is to make an R-C series element connection. The equivalent circuit of such a construction is shown in [Fig. 7.34](#). Such

dividers are made up to 5 MV with response times less than 30 ns. The low voltage arm R_2 is given “ L peaking” by connecting a variable inductance L in series with R_2 . The step response of the divider and the schematic connection of low voltage arm are shown in Fig. 7.35. However, for a correctly designed voltage divider L peaking will not be necessary.

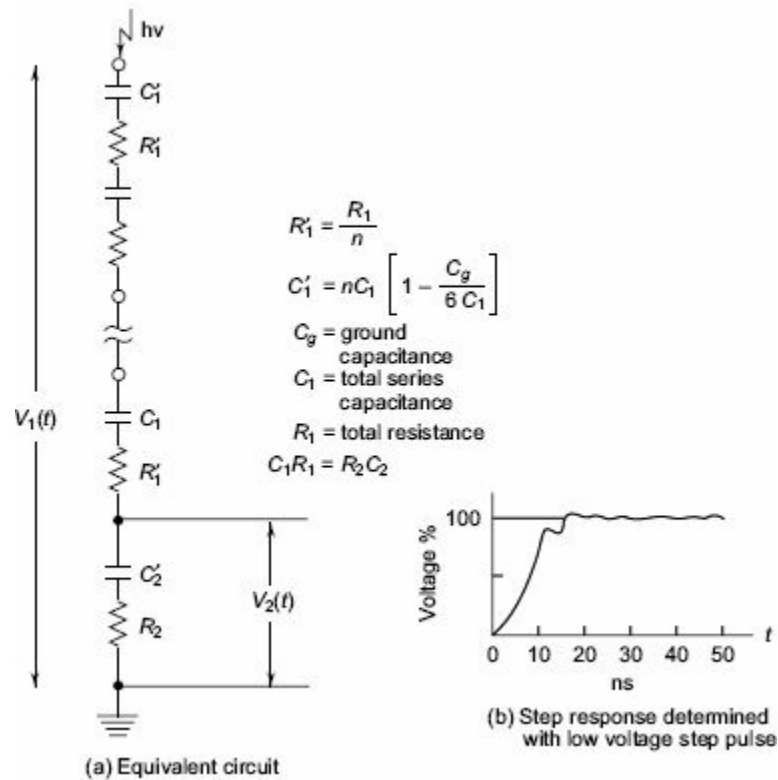


Fig. 7.34 Equivalent circuit of a series R - C voltage divider and its step response

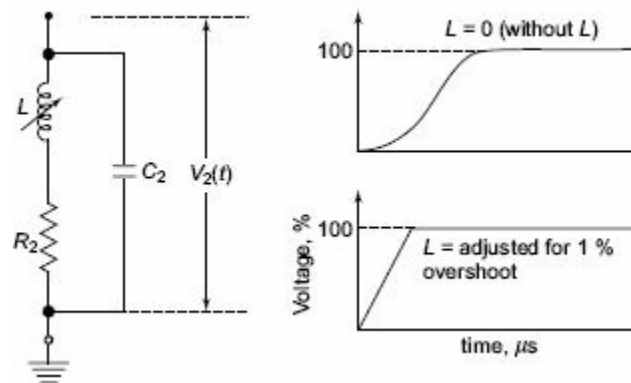
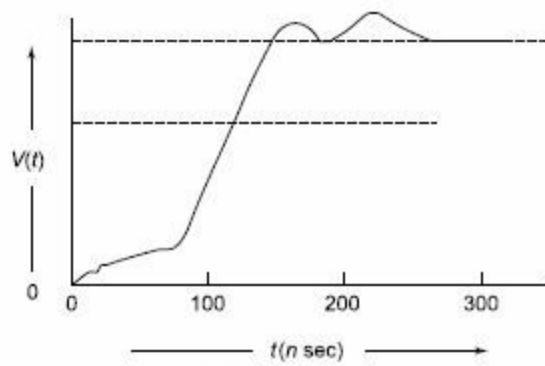


Fig. 7.35 L peaking in low-voltage arm and step response of the divider with L peaking

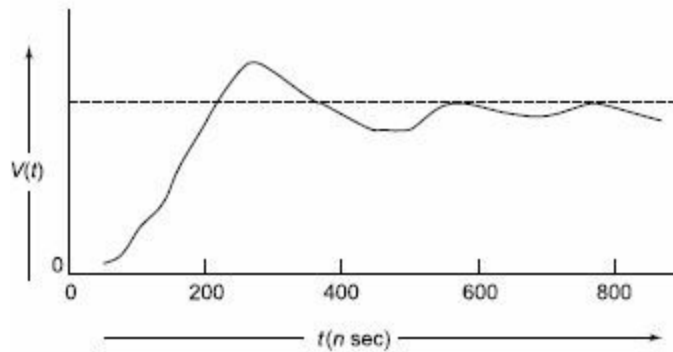
(g) R - C Potential Dividers for 2 MV Rating and above

Voltage dividers used for measuring more than one million volts attenuate the measuring signal to a value in the range of 100 V to few hundreds of volts.



(i) Optimally damped

Response time : 50 n sec
 Front time : 50 n sec
 Overshoot : $\approx 3\%$
 Parameters : $R_1 = 1000 \Omega$
 $C_1 = 360 \text{ pF}$
 Damping resistance : 500 Ω
 $(R_d + R_1) C_1 = R_2 C_2$



(ii) Underdamped

Response time : 4 n sec
 Front time : 110 n sec
 Overshoot : $\approx 30\%$
 Parameters : $R_1 = 256 \Omega$
 $C_1 = 400 \text{ pF}$
 Damping resistance : 0 Ω
 $R_1 C_1 = R_2 C_2$

Fig. 7.36 Step response of a 4 MV R-C divider

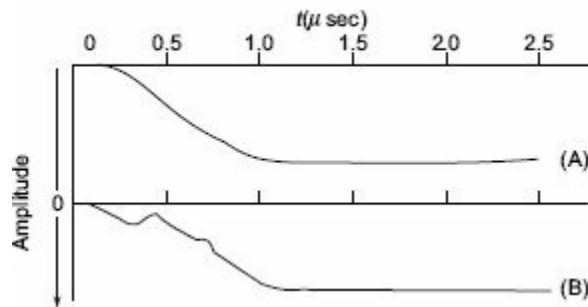


Fig. 7.37 Record of the front portion of a lightning impulse wave with underdamped (curve A) and optimally damped (curve B) dividers for a negative polarity wave when both dividers are connected in parallel

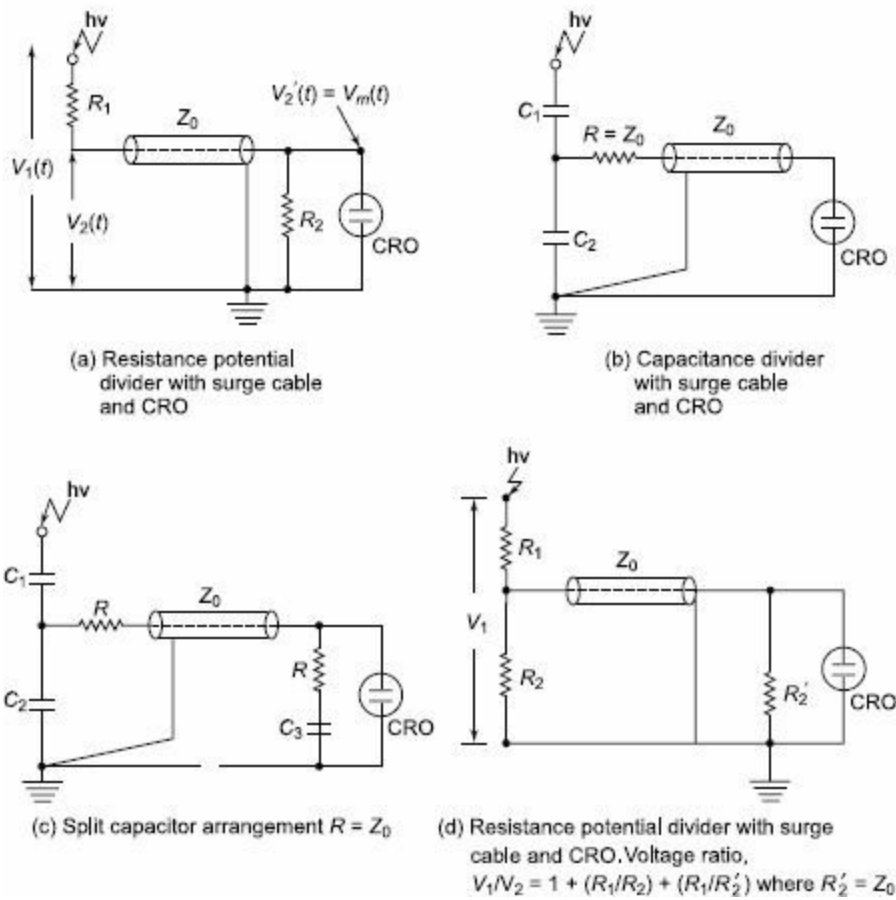


Fig. 7.38 Potential divider arrangements

The criteria required to assess the dividers are (i) the shape of the voltage in the test arrangement should be transferred without any distortion to the LV side, (ii) simple determination of transfer behaviour should be ensured, and (iii) they should be suitable for multipurpose use, i.e., for use with ac power frequency voltages, switching impulse voltages as well as with lightning impulse voltages. This condition necessitates that the dividers should have broad bandwidths. The above requirements are generally met by (a) optimally damped R-C dividers, (b) underdamped or low-damped R-C dividers. The high-voltage arm of such dividers consists of series R-C units while the secondary arm is usually an R-C series or parallel circuit. In case of optimally damped dividers, $R_1 = 4\sqrt{L_1/C_g}$ where L_1 is the inductance of the high-voltage lead and the HV portion of the divider, and C_g is the equivalent capacitance to ground. Usually this resistance will be 400 to 1000 ohms. On the other hand, for low or underdamped dividers, R_1 will be equal to 0.25 to 1.5 times $\sqrt{L/C_1}$ where L is the inductance for the complete measuring loop and C_1 is the capacitance of the HV part of the divider. In this case the normal value of R_1 lies between 50 and 300 ohms. The step response of the two types of dividers mentioned above is shown in [Fig. 7.36](#). In actual practice, because of the large time constant $(R_d + R_1) C_1$, the optimal damped divider affects the voltage shape at the test object. Standard lightning impulses sometimes cannot be generated to the correct standard specifications. As such, R-C potential dividers are not suitable for measurements with test objects of very low capacitance. The low or underdamped R-C divider acts as a load capacitance and is suitable for applications over a broad bandwidth, i.e., ac, switching impulses, lightning impulses, chopped waves, etc. Underdamped R-C dividers are also suitable for measurement of steep fronted impulse waves. A typical record of lightning impulse wave (1.2/50 μs wave) obtained using both the above types of dividers is shown in [Fig. 7.37](#). It may be noted that even though the step response is poor in the case of underdamped

dividers, they can be used to measure the standard impulse wave to a better accuracy.

(h) Different Connections Employed with Potential Dividers Different arrangements and connections of voltage or potential dividers with a cathode ray oscilloscope are shown in Figs 7.38 and 7.39.

A simple arrangement of a resistance divider is shown in Fig. 7.38a. The possible errors are (i) $R_2 \parallel Z_0$ (surge impedance of the cable), (ii) capacitance of the cable and CRO shunting R_2 and hence introducing distortion, (iii) attenuation or voltage drop in surge cable Z_0 , and (iv) ground capacitance effect. These errors are already discussed in Sec. 7.2.7. To avoid reflections at the junction of the cable and R_2 , R_2 is varied and adjusted to give the best possible step response. When a unit step voltage is applied to the circuit shown in Fig. 7.38b, the effect of the cable is to take a fraction of the voltage $[C_1 / (C_1 + C_2)]$ into it and cause reflections at the input end. In the beginning the cable acts like a resistance of value $= Z_0$ the surge impedance, but later behaves like a capacitor of value equal to the total capacitance of the cable. This behaviour introduced distortion and is compensated by using a split capacitor connection as shown in Fig. 7.38c with $(C_1 + C_2) = (C_3 + C_k)$ [C_k capacitance of the cable]. On the other hand if $C_i / (C_1 + C_2 + C_k) = 0.1$, the error will be less than 1.5%.

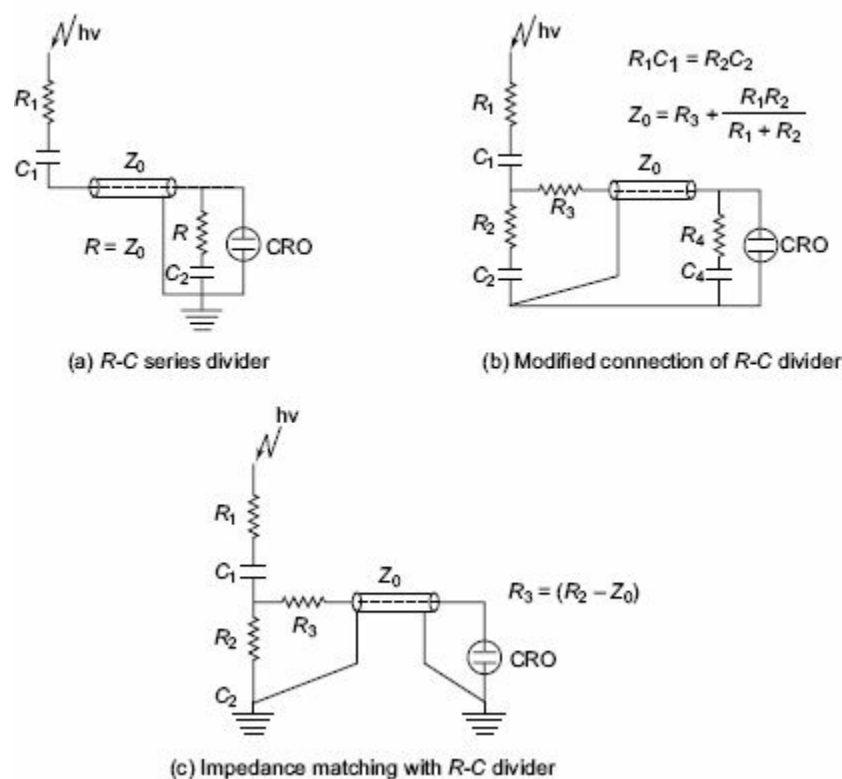


Fig. 7.39 Mixed potential divider arrangements

The arrangements for mixed potential dividers are shown in Fig. 7.39. The arrangement shown in Fig. 7.39a is modified and improved in the arrangement of Fig. 7.39b.

$$R_1 C_1 = \frac{C_2 Z_0 (C_1 + C_2 + C_k)}{(C_1 + C_2)} \quad (7.30)$$

$$Z_0 = R_3 + \left(\frac{R_1 R_2}{R_1 + R_2} \right), \text{ and } R_1 C_1 = R_2 C_3 \quad (7.31)$$

The response is greatly improved. The arrangement shown in [Fig. 7.38c](#) is simple and gives the desired impedance matching.

(i) Low-Voltage Arms of the Measuring System Connected to Voltage Dividers The mode of connection and the layout arrangement of the secondary arm of the divider is very critical for the distortion less measurement of fast transients. The LV arm of the divider itself introduces large distortions if not properly connected. Different corrections employed for connecting the LV arm to the measuring instrument via the signal cables are shown in [Figs 7.38](#) and [7.39](#). The signal cable Z_0 may be assumed to be loss-free so that the surge impedance, $z_0 = \sqrt{L/C}$ is independent of the frequency and the travel time for the signal, $\tau_0 = \sqrt{L/C}$ (refer to [Chapter 8](#) for details). In the case of resistance dividers, the cable matching is achieved by having a pure resistance, $R_2 = Z_0$ at the end of the cable. The surge cable Z_0 and the resistance R_2 form an integral part of the cable system. Typically, Z_0 has values of 50 or 75 ohms. In actual practice, signal cables do have losses due to skin effect at high frequencies and hence Z_0 becomes a complex quantity. Thus, the matching of R_2 with Z_0 should be done at high frequencies or with a step input as indicated earlier. In the case of long cables, the cable resistance including that of the shield wire should be taken as a part of the matching resistance. The divider ratio in the case of the connection shown in [Fig. 7.38](#) is

$$a = V_1/V_2 = 1 + R_1/R_2 + R_1/R'_2 \text{ and}$$

$$R'_2 = Z_0 \tag{7.32}$$

For the capacitance dividers, the signal cable cannot be completely matched. A low ohmic resistance connected in parallel with C_2 would load the LV arm and hence, the output gets decreased. Connection of a resistance $R = Z_0$ at the input end (see [Figs 7.38](#) and [7.39](#)) will make the voltage across the CRO the same as that across C_2 . The transient voltage ratio, at $t = 0$ is given as

$$a = V_1/V_2 = 1 + C_2/C_1 \text{ and}$$

$$\text{effective} = 1 + (C_2 + C_k)/C_1 \text{ for } t \gg 2 T_0 \tag{7.33}$$

where C_k is the cable capacitance.

Thus, an initial overshoot of $\Delta V = C_k/(C_1 + C_2)$ will appear. This will be either small or negligible for medium and low cable lengths, and for high values of capacitance C_2 . This error can be avoided and the response improved in the case of $R-C$ dividers by using the arrangements shown in [Fig. 7.39c](#).

Usually, the LV arms are made co-axial and are enclosed in metal boxes that are solidly grounded. The series resistors used in $R-C$ divider forms an integral part of the divider's LV arm. Further, all the LV arm capacitors and resistors should have a very low inductance. A typical LV arm arrangement is shown in [Fig. 7.40](#).

7.2.8 Peak-Reading Voltmeters for Impulse Voltages

Sometimes it is enough if the peak of an impulse voltage wave is measured; its waveshape might already be known or fixed by the source itself. This is highly useful in routine impulse testing work. The methods are similar to those employed for ac voltage crest value measurements. The instrument

is normally connected to the low voltage arms of the potential dividers described in [Sec. 7.2.7](#). The basic circuit along with its equivalent circuit and the response characteristic is shown in [Fig. 7.41](#). The circuit consists of only rectifiers.

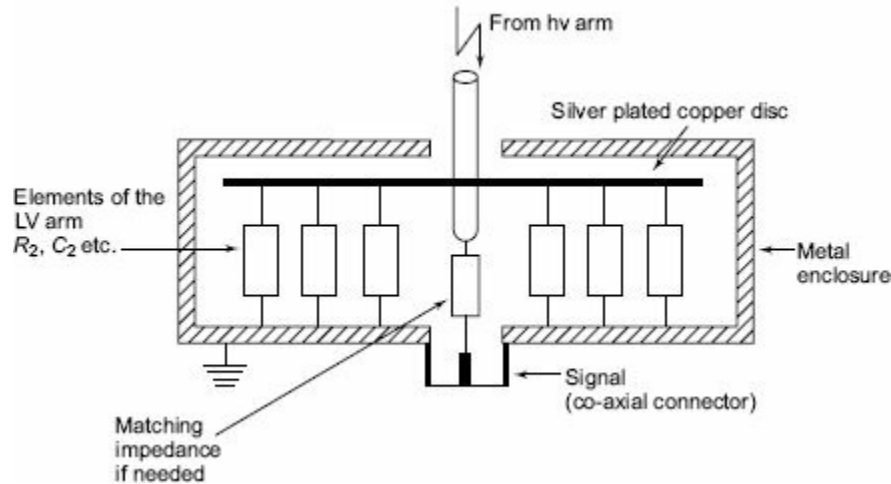


Fig. 7.40 LV arm layout for voltage dividers

Diode D conducts for positive voltages only. For negative pulses, the diode has to be connected in reverse. When a voltage impulse $v(t)$ appears across the low voltage arm of the potential divider, the capacitor C_m is charged to the peak value of the pulse. When the amplitude of the signal starts decreasing the diode becomes reverse biased and prevents the discharging of the capacitor C_m . The voltage developed across C_m is measured by a high impedance voltmeter (an electrostatic voltmeter or an electrometer). As the diode D has finite forward resistance, the voltage to which C_m is charged will be less than the actual peak of the signal, and is modified by the R - C network of the diode resistance and the measuring capacitance C_m . The error is shown in [Fig. 7.41c](#). The error can be estimated if the waveform is known. The actual forward resistance of the diode D (dynamic value) is difficult to estimate, and hence the meter is calibrated using an oscilloscope. Peak voltmeters for either polarity employing resistance dividers and capacitance dividers are shown in [Fig. 7.42](#). In this arrangement, the voltage of either polarity is transferred into a proportional positive measuring signal by a resistive or capacitive voltage divider and a diode circuit. An active network with feedback circuit is employed in commercial instruments, so that the fast rising pulses can also be measured. Instruments employing capacitor dividers require discharge resistance across the low-voltage arm to prevent the build-up of dc charge.

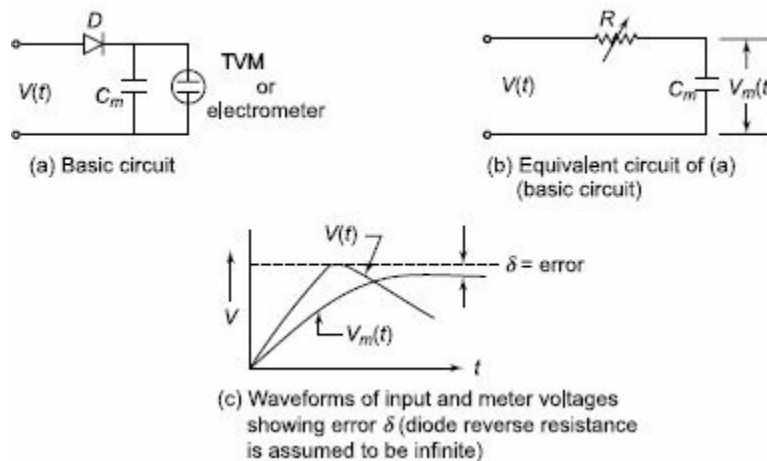


Fig. 7.41 A peak reading voltmeter and its equivalent circuit (*R-C approximation*)

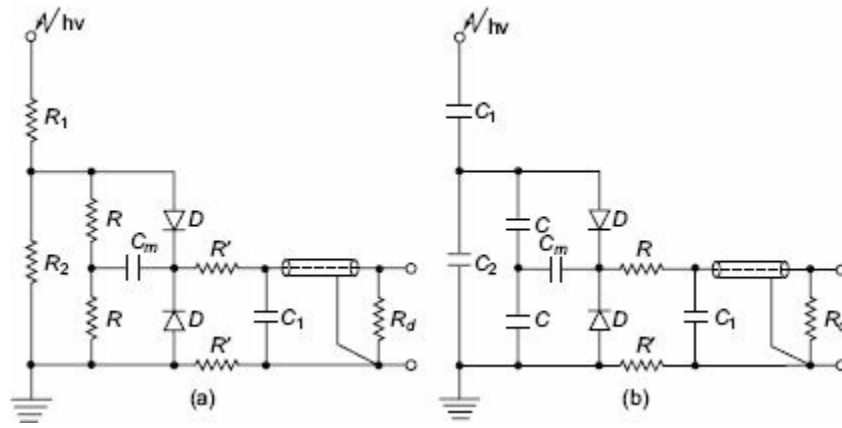


Fig. 7.42 Peak reading voltmeter for either polarity with (a) resistance divider, and (b) capacitance divider

7.3 MEASUREMENT OF HIGH CURRENTS=DIRECT, ALTERNATING, AND IMPULSE

In power systems, it is often necessary to measure high currents, arising due to short circuits. For conducting temperature rise and heat run tests on power equipments like conductors, cables, circuit breakers, etc., measurement of high currents is required. During lightning discharges and switching transients also, large magnitudes of impulse and switching surge currents occur, which require special measuring techniques at high potential levels.

7.3.1 Measurement of High Direct Currents

High magnitude direct currents are measured using a resistive shunt of low ohmic value. The voltage drop across the resistance is measured with a millivoltmeter. The value of the resistance varies usually between $10 \mu\Omega$ and $10 \mu\Omega$. This depends on the heating effect and the loading permitted in the circuit. High current resistors are usually oil immersed and are made as three or four terminal resistances (see Fig. 7.43). The voltage drop across the shunt is limited to a few millivolts (< 1 Volt) in power circuits.

Typical shunt used for measurement of current in HVDC transmission system is shown in Fig. 7.43c. The voltage drop across the shunt, which is an analog signal, is converted into a digital/optical signal and is sent via a fibre-optic cable to the ground-level instrument.

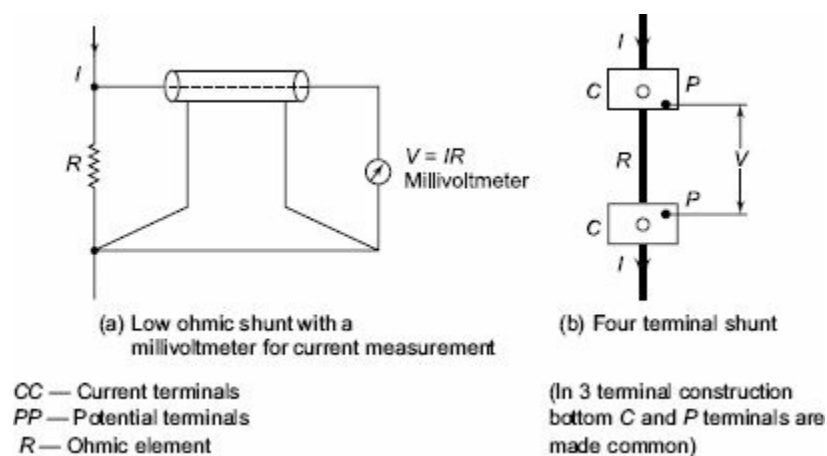


Fig. 7.43 Calibrated ohmic shunt for dc current measurements

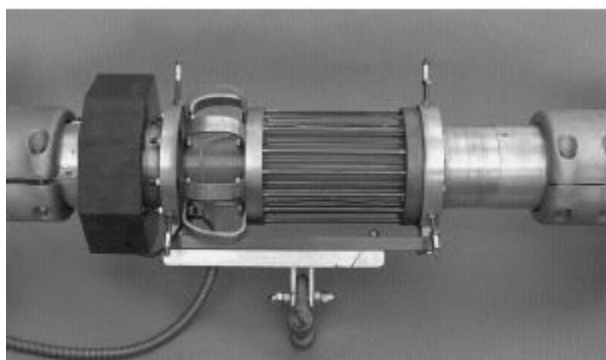


Fig 7.43c HVDC shunt assembly

(a) dc Current Transformer

Principle Transformer operates on the principle of ampere turn balance, i.e. the primary ampere turns ($N_1 I_1$) are balanced by the secondary ampere turns ($N_2 I_2$) where N_1 and N_2 are the turns in the primary and secondary windings and I_1 and I_2 are the respective currents in these windings. With dc current in the primary winding, core saturation occurs due to the non-linearity of the $B-H$ curve of the core.

When a high-frequency excitation is given to the third or excitation winding located on the same core, the current through the secondary winding will have a distorted waveform containing a large-amplitude second harmonic. A fourth winding is added and a second harmonic current is injected in the opposite direction to make the harmonic current zero. The injected current will be proportional to

the primary dc current and hence will give the measurement of dc current. Schematic diagram of a dc current transformer is shown in [Fig. 7.44](#)

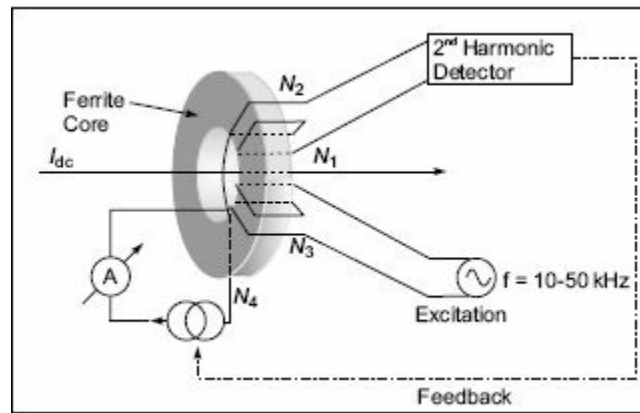


Fig. 7.44 DC CT schematic diagram

- The advantages of dc CT are the following:
- It gives isolation to high voltages.
- Power loss is much less compared to dc shunt, and the conductor through which the dc current flows need not be broken for connecting to the mains.

(b) Hall Generators for dc Measurements

The principle of the ‘Hall effect’ is made use of in measuring very high direct currents. If an electric current flows through a metal plate located in a magnetic field perpendicular to it, Lorentz forces will deflect the electrons in the metal structure in a direction normal to the direction of both the current and the magnetic field. The charge displacement generates an emf in the normal direction, called the “Hall voltage”. The Hall voltage is proportional to the current i , the magnetic flux density B , and the reciprocal of the plate thickness d ; the proportionality constant R is called the *Hall coefficient*

$$V_H = R \frac{B_i}{d} \quad (7.34)$$

For metals, the Hall coefficient is very small, and hence semi-conductor materials are used for which the Hall coefficient is high.

In large current measurements, the current carrying conductor is surrounded by an iron cored magnetic circuit, so that the magnetic field intensity $H = (1/\delta)$ is produced in a small air gap in the core. The Hall element is placed in the air gap (of thickness d), and a small constant dc current is passed through the element. The schematic arrangement is shown in [Fig. 7.44a](#). The voltage developed across the Hall element in the normal direction is proportional to the dc current I . It may be noted that the Hall coefficient R depends on the temperature and the high magnetic field strengths, and suitable compensation has to be provided when used for measurement of very high currents.

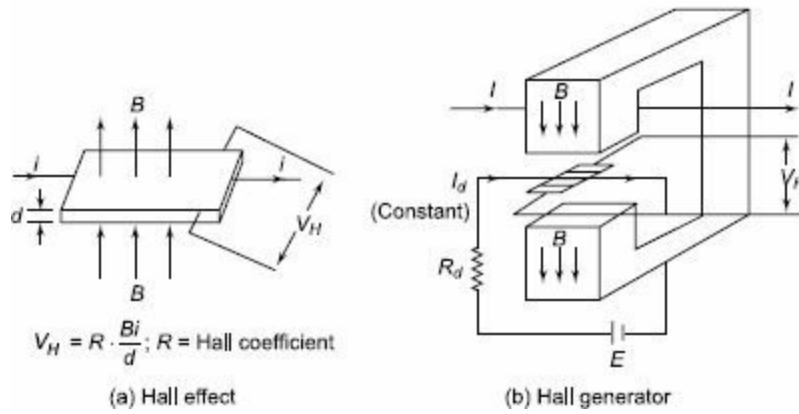


Fig. 7.44a Hall generator for measuring high dc currents

Hall generators can be used for measurement of unidirectional ac and impulse currents also. With proper design of Hall-element dimensions and addition of compensating circuits, the bandwidth of the Hall generator can be increased to about 50 MHz. As such, these generators can be used for the measurement of post arc currents and unidirectional impulse currents.

7.3.2 Measurement of High-Power Frequency Alternating Currents

Measurement of power frequency currents are normally done using current transformers only, as use of current shunts involves unnecessary power loss. Also the current transformers provide electrical isolation from high voltage circuits in power systems. Current transformers used for extra high voltage (EHV) systems are quite different from the conventional designs as they have to be kept at very high voltages from the ground. A new scheme of current transformer measurements introducing electro-optical technique is described in [Fig. 7.45](#). A voltage signal proportional to the measuring current is generated and is transmitted to the ground through an electro-optical device. Light pulses proportional to the voltage signal are transmitted by a glass-optical fibre bundle to a photo detector and converted back into an analog voltage signal. Accuracies better than $\pm 0.5\%$ have been obtained at rated current as well as for high short circuit currents. The required power for the signal converter and optical device are obtained from suitable current and voltage transformers as shown in [Fig. 7.45](#).

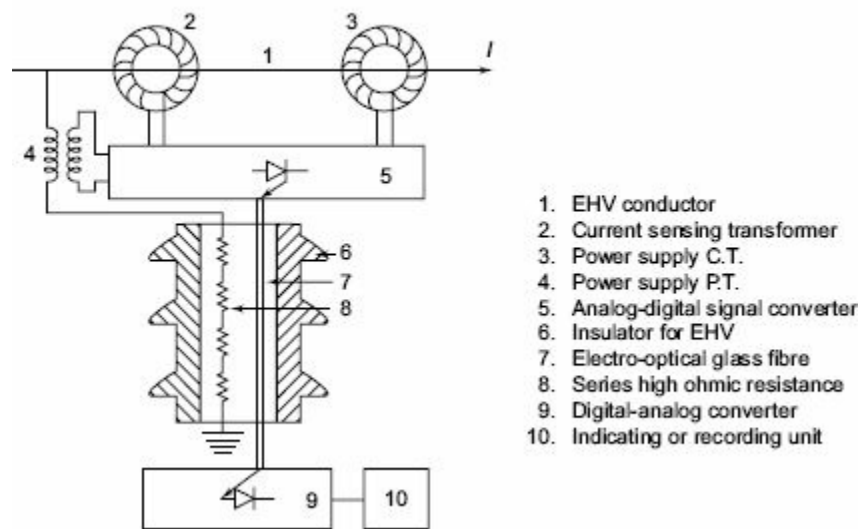


Fig. 7.45 Current transformer with electro-optical signal converter for EHV systems

7.3.3 Measurement of High Frequency and Impulse Currents

In power system applications as well as in other scientific and technical fields, it is often necessary to determine the amplitude and waveforms of rapidly varying high currents. High impulse currents occur in lightning discharges, electrical arcs and post-arc phenomenon studies with circuit breakers, and with electric discharge studies in plasma physics. The current amplitudes may range from a few amperes to few hundred kiloamperes. The rate of rise for such currents can be as high as 10^6 to 10^{12} A/s, and rise times can vary from few microseconds to few nano seconds. In all such cases the sensing device should be capable of measuring the signal over a wide frequency band. The methods that are frequently employed are (i) resistive shunts, (ii) magnetic potentiometers or probes, and (iii) the Faraday and Hall effect devices.

The accuracy of measurement varies from 1 to 10%. In applications where only peak value measurement is required, peak reading voltmeters described in Sec. 7.2.8 may be employed with a suitable shunt.

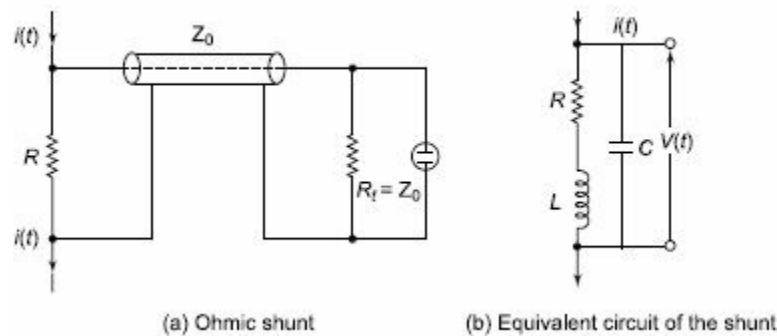


Fig. 7.46 Calibrated low ohmic shunt and its equivalent circuit for impulse current measurements

Resistive Shunts

The most common method employed for high impulse current measurements is a low ohmic pure resistive shunt shown in Fig. 7.46. The equivalent circuit is shown in Fig. 7.46b. The current through the resistive element R produces a voltage drop $v(t) = i(t)R$. The voltage signal generated is transmitted to a CRO through a coaxial cable of surge impedance Z_0 . The cable at the oscilloscope end is terminated by a resistance $R_t = Z_0$ to avoid reflections. The resistance element, because of its large dimensions will have a residual inductance L and a terminal capacitance C . The inductance L may be neglected at low frequencies (ω), but becomes appreciable at higher frequencies (ω) when ωL is of the order of R . Similarly, the value of C has to be considered when the reactance $1/\omega C$ is of comparable values. Normally L and C become significant above a frequency of 1 MHz. The resistance value usually ranges from $10 \mu\Omega$ to few milliohms, and the voltage drop is usually about a few volts. The value of the resistance is determined by the thermal capacity and heat dissipation of the shunt.

The voltage drop across the shunt in the complex frequency domain may be written as

$$V(s) = \frac{(R + Ls)}{(1 + RCs + LCs^2)} I(s) \quad (7.35)$$

where s is the complex frequency or Laplace transform operator and $V(s)$ and $I(s)$ are the transformed quantities of the signals $v(t)$ and $i(t)$. With the value of C neglected it may be approximated as

It may be noted here that the stray inductance and capacitance should be made as small as possible for better frequency response of the shunt. The resistance shunt is usually designed in the following manner to reduce the stray effects.

- (i) Bifilar flat strip design,
- (ii) Coaxial tube or Park's shunt design, and
- (iii) Coaxial squirrel cage design.

(i) Bifilar Strip Shunt The bifilar design (Fig. 7.47) consists of resistor elements wound in opposite directions and folded back, with both ends insulated by a teflon or other high quality insulation. The voltage signal is picked up through a ultra high frequency (UHF) coaxial connector. The shunt suffers from stray inductance associated with the resistance element, and its potential leads are linked to a small part of the magnetic flux generated by the current that is measured. To overcome these problems, coaxial shunts are chosen.

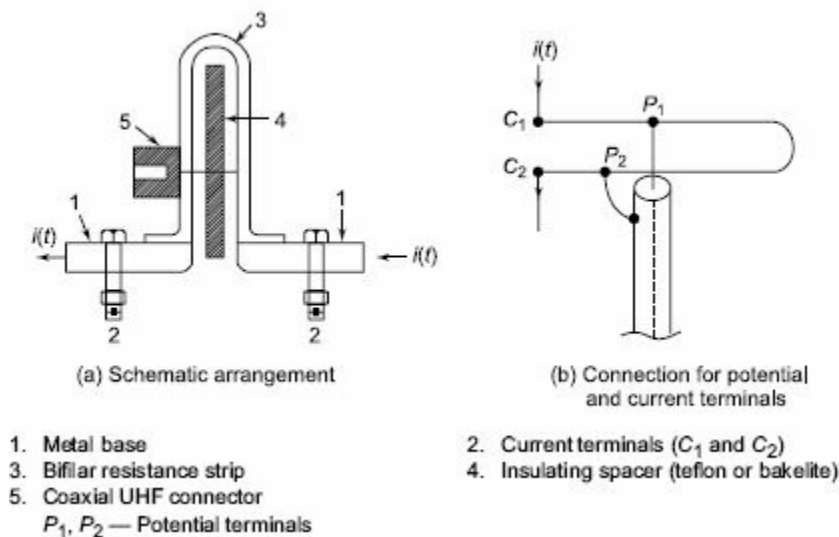


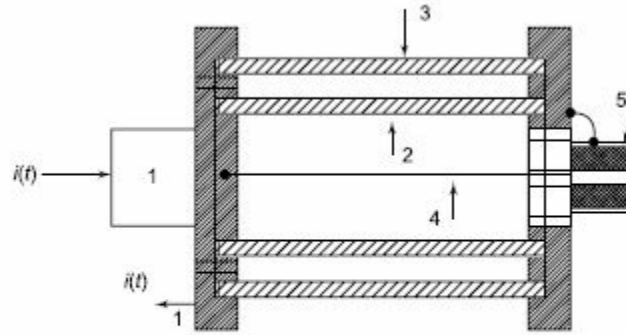
Fig. 7.47 Bifilar flat strip resistive shunt

(ii) Coaxial Tubular or Park's Shunt In the coaxial design (Fig. 7.48), the current is made to enter through an inner cylinder or resistive element and is made to return through an outer conducting cylinder of copper or brass. The voltage drop across the resistive element is measured between the potential pick-up point and the outer case. The space between the inner and the outer cylinder is air and hence acts like a pure insulator. With this construction, the maximum frequency limit is about 1000 MHz and the response time is a few nanoseconds. The upper frequency limits is governed by the skin effect in the resistive element. The equivalent circuit of the shunt is given in Fig. 7.49. The step response and the frequency response are shown in Fig. 7.50. The inductance L_0 shown in Fig. 7.49 may be written as

$$L_0 = \frac{\mu dl}{2\pi r} \quad (7.37)$$

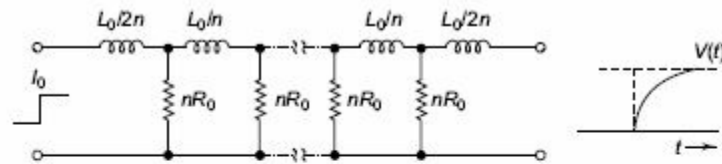
where, $\mu = \mu_0 \mu_r$; the magnetic permeability, $\mu_0 = 4\pi \times 10^{-7}$

d = thickness of the cylindrical tube,
 l = length of the cylindrical tube, and
 r = radius of the cylindrical tube

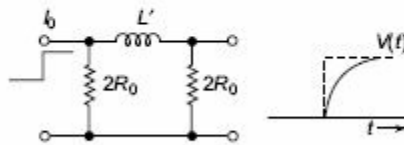


1. Current terminals
2. Coaxial cylindrical resistive element
3. Coaxial cylindrical return conductor (copper or brass tube)
4. Potential pick up lead
5. UHF coaxial connector

Fig. 7.48 Schematic arrangement of a coaxial ohmic shunt



(a) Exact equivalent circuit



(b) Simplified circuit

L_0 — Inductance
 R_0 — dc resistance
 n — Number of sections per unit length
 $L' = 0.43 L_0$

Fig. 7.49 Simplified and exact equivalent circuits of a coaxial tubular shunt

The effective resistance is given by

$$R = \frac{V(t)}{I_0} = R_0 \theta(\omega t) \tag{7.38}$$

where R_0 = the dc resistance; L_0 = inductance for dc currents and $\theta(\omega t)$ is the theta function of type 3 and is equal to

$$\left[1 + 2 \sum_{n=1}^{\infty} (-1)^n \exp(-n^2 \omega t) \right]$$

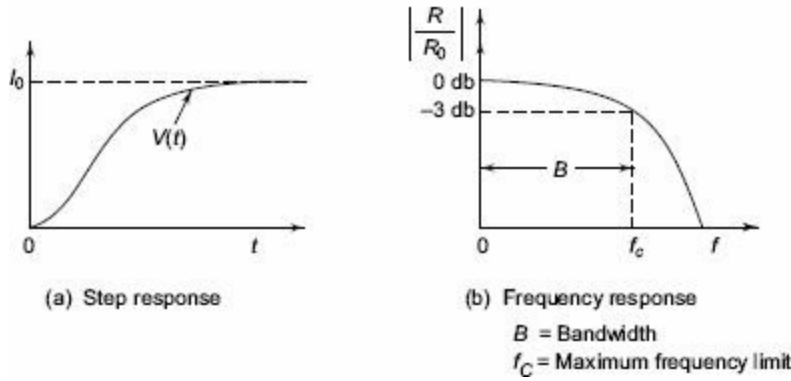


Fig. 7.50 Step and frequency responses of a coaxial tubular shunt

in which

$$\omega = \frac{(\pi^2 R_0)}{L_0}$$

$V(t)$ = signal developed; and I_0 is the step current.

The effective impedance of the shunt for any frequency/according to Silsbee is given by

$$Z = \frac{R_0(1+j)\delta}{\sinh[(1+j)\delta]} \tag{7.39}$$

where, R_0 = dc resistance Ω ,

$$\delta = 2 \pi d \sqrt{(f\mu)/\rho},$$

ρ = resistivity of the material, Ω -cm,

d = thickness of the tube, cm,

f = frequency, Hz, and

μ = permeability as defined earlier.

The simplified equivalent circuit shown in [Fig. 7.49](#) is convenient to calculate the rise time of the shunt. The rise time accordingly is given by,

$$T = 0.237 \frac{\mu d^2}{\rho}$$

and the bandwidth is given by

$$B = \frac{1.46R}{L_0} = \frac{1.46\rho}{\mu d^2} \tag{7.40}$$

The coaxial tubular shunts were constructed for current peaks up to 500 kA; shunts constructed for current peaks as high as 200 kA with di/dt of about 5×10^{10} A/s have induced voltages less than 50 V and the voltage drop across the shunt was about 100 V.

(iii) Squirrel-Cage Shunts In certain applications, such as post arc current measurements, high ohmic value shunts which can dissipate larger energy are required. In such cases tubular shunts are not suitable due to their limitations of heat dissipation, larger wall thickness, and the skin effect. To overcome these problems, the resistive cylinder is replaced by thick rods or strips, and the structure

resembles the rotor construction of double squirrel-cage induction motor. The equivalent circuit for squirrel-cage construction is different, and complex. The shunts show peaky response for step input, and a compensating network has to be designed to get optimum response. In Fig. 7.51, the step response (Fig. 7.51a) and frequency response (Fig. 7.51b) characteristics are given. Rise times of better than 8 ns with bandwidth more than 400 MHz were obtained for this type of shunts. A typical R-C compensating network used for these shunts is shown in Fig. 7.52.

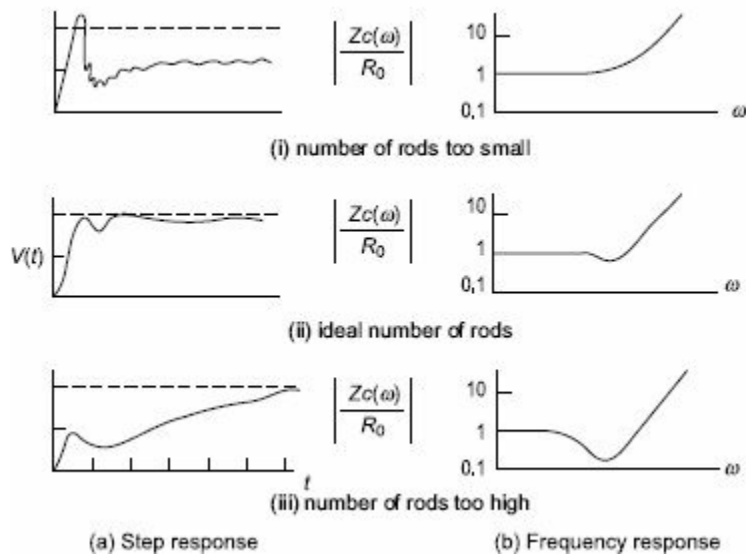


Fig. 7.51 Response of squirrel cage shunt for different number of rods

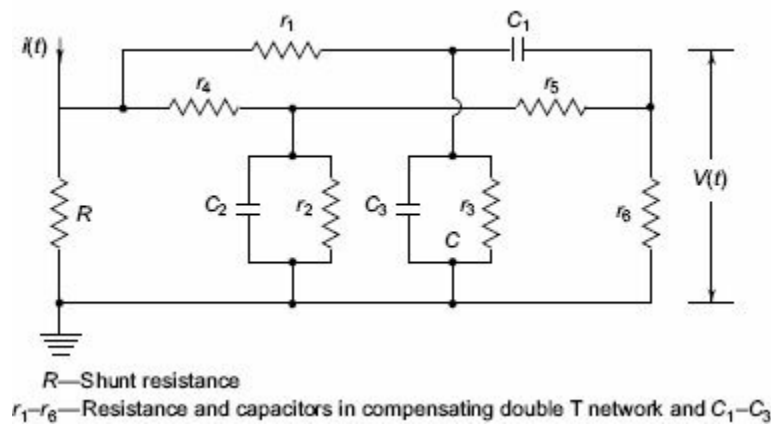


Fig. 7.52 Compensating network for squirrel cage shunts

(iv) Material and Technical Data for the Current Shunts The important factor for the materials of the shunts is the variation of the resistivity of the material with temperature. In Table 7.11 physical properties of some materials with low temperature coefficient, which can be used for shunt construction are given.

The importance of the skin effect has been pointed out in the coaxial shunt design. The skin depth d for a material of conductivity σ at any frequency f is given by

$$d = \frac{1}{\sqrt{\pi f \mu \sigma}} \quad (7.41)$$

Skin depth, d , is defined as the distance or depth from the surface at which the magnetic field intensity is reduced to '1/e' ($e = 2.718 \dots$) of the surface value for a given frequency f . Materials of

low conductivity ζ (high resistivity materials) have large skin depth and hence exhibit less skin effect.

It may be stated that low ohmic shunts of coaxial type or squirrel cage type construction permit measurements of high currents with response times less than 10 ns.

Table 7.11 Properties of resistive materials

Property	Material				
	Constantan	Manganin	Nichrome	German silver	Ferro-alloy
Resistivity ρ at 20°C ($\Omega\text{-m}$)	0.49×10^{-6}	0.43×10^{-6}	1.33×10^{-6}	0.23×10^{-6}	0.49×10^{-6}
Temperature coefficient per °C (10^{-6})	30	20	20	≈ 50	40
Density at 20°C kg/litre	8.9	8.4	8.1	≈ 7.5	8.8
Specific heat kilo calories/kg°C	0.098	0.097	0.11	≈ 0.1	≈ 0.1

7.3.4 Measurement of High Impulse Currents: Other Techniques (Rogowski Coils Current Transformers and Magnetic Links)

(a) Rogowski Coils If a coil is placed surrounding a current carrying conductor, the voltage signal induced in the coil is $v_i(t) = M dI(t)/dt$ where M is the mutual inductance between the conductor and the coil, and $I(t)$ is the current flowing in the conductor. Usually, the coil is wound on a nonmagnetic former of toroidal shape and is coaxially placed surrounding the current-carrying conductor. The number of turns on the coil is chosen to be large, to get enough signal induced. The coil is wound cross-wise to reduce the leakage inductance. Usually, an integrating circuit (see Fig. 7.53) is employed to get the output signal voltage proportional to the current to be measured. The output voltage is given by

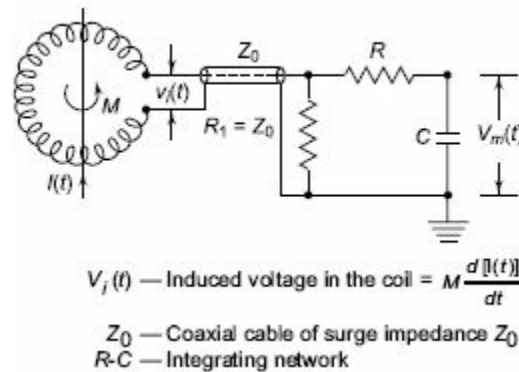


Fig. 7.53 Rogowski coil for high impulse current measurements

$$V_m(t) = \frac{1}{CR} \int_0^t v_i(t) dt = \frac{M}{CR} I(t) \quad (7.42)$$

Rogowski coils with electronic or active integrator circuits have large bandwidths (about 100 MHz). At frequencies greater than 100 MHz the response is affected by the skin effect, the capacitance distributed per unit length along the coil, and due to the electromagnetic interferences. However, miniature probes having nanosecond response time are made using very few turns of copper strips for UHF measurements.

(b) Magnetic Links Magnetic links are short high retentivity steel strips arranged on a circular wheel or drum. These strips have the property that the remanent magnetism for a current pulse of 0.5/5 ms is same as that caused by a dc current of the same value. Hence, these can be used for measurement of peak value of impulse currents. The strips will be kept at a known distance from the current carrying conductor and parallel to it. The remanent magnetism is then measured in the laboratory from which the peak value of the current can be estimated. These are useful for field measurements, mainly for estimating the lightning currents on the transmission lines and towers. By using a number of links, accurate measurement of the peak value, polarity, and the percentage oscillations in lightning currents can be made.

The rate of rise of impulse currents can be measured using the magnetic links by placing them within the magnetic field of inductors which carry the main current to be measured. The inductors are connected in series with different values of resistances giving different time constants. Hence the

magnetic links record the peak currents whose values are different. Knowing the time constants of the resistance – inductance combination, the mean rate of rise of current in the main circuit is estimated.

7.3.5 Other Techniques for Impulse Current Measurements

(i) **Hall Generators** Hall generators described earlier can be used for ac and impulse current measurements also. The bandwidth of such devices was found to be about 50 MHz with suitable compensating devices and feedback. The saturation effect in magnetic core can be minimized, and these devices are successfully used for post arc and plasma current measurements.

(ii) **Faraday Generator or Ammeter** When a linearly polarized light beam passes through a transparent crystal in the presence of a magnetic field, the plane of polarization of the light beam undergoes rotation.

The angle of rotation α is given by

$$\alpha = VBl \quad (7.43)$$

where, V = a constant of the crystal which depends on the wavelength of the light,
 B = magnetic flux density, and
 l = length of the crystal.

To measure the waveform of a large current in an EHV system an arrangement shown in Fig. 7.54 may be employed. A beam of light from a stabilized light source is passed through a polarizer P_1 to fall on a crystal F placed parallel to the magnetic field produced by the current I . The light beam undergoes rotation of its plane of polarization. After passing through the analyser, the beam is focused on a photomultiplier, the output of which is fed to a CRO. The output beam is filtered through a filter M , which allows only the monochromatic light. The relation between the oscillograph display and the current to be measured are complex but can be determined. The advantages of this method are that (i) there is no electric connection between the source and the device, (ii) no thermal problems even for large currents of several kiloamperes, and (iii) as the signal transmission is through an optical system, no insulation problems or difficulties arise for EHV systems. However, this device does not operate for dc currents.

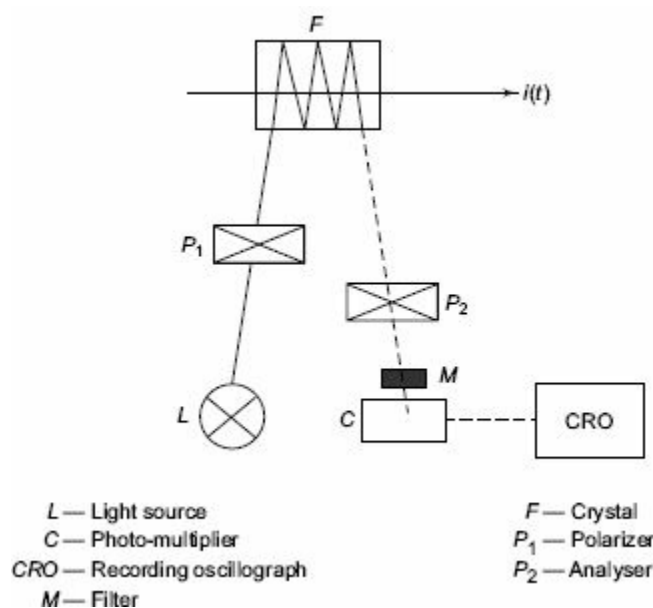


Fig. 7.54 Magneto-optical method of measuring impulse currents

(iii) Current Transformers Measurement of high frequency currents such as fault currents in power systems, switching current transients and impulse currents during impulse testing of transformers can be measured using current transformers with an air core or a ferrite core. The transformer will have a toroidal core with central bar primary or wound primary with single turn.

The secondary side of the current with N_1 primary and N_2 secondary turns is given by (with perfect ampere turn balance)

$$I_2(t) = \frac{N_1 I(t)}{N_2}$$

Usually, the secondary winding is terminated by a resistance R_2 and a CRO will be connected through a cable of surge impedance Z terminated by a resistance R equal to the surge impedance. The current I_3 through the cable and terminating resistance R is

$$I_3(t) = \frac{R_2}{R + R_2 + Z_0} I_2(t)$$

and the voltage across the resistance

$$R = V(t) = I_3(t) R = \left[\frac{R R_2}{R + R_2 + Z_0} \right] I_2(t)$$

$$I_2(t) = \frac{N_1}{N_2} \frac{R R_2}{R + R_2 + Z_0} I_1(t)$$

Usually, R_2 is also made equal to Z_0 to avoid reflections in case of impulse currents.

The unit is usually made into an epoxy resin cast unit with primary and secondary terminals brought out on either side of the unit.

The advantages of the current transformer are electrical isolation and wide measuring range with tapped turns on secondary side from 10 A to 10 kA or more. The main limitations are limited bandwidth of less than 1 MHz, and distortion in the waveform.

Current Transformers Current transformers with either air cores or ferrite cores are used for measurement of high-impulse currents. Usually, they have a toroidal core with a central hole through which the primary or conductor in which the current is to be measured will be inserted. The core can be of a split-type also. The secondary winding consists of a few turns (up to 500). The bandwidth of such transformers may be typically 40 Hz to 1 MHz for a peak current of 1000 A with an output voltage across the secondary between 0.5 to 5 V when terminated by 50 Ω . The typical insulation level provided between the primary and secondary windings is about 4 kV. Rf current transformers are typically designed for a peak current of 50 kA with a maximum rms current of 200 A. The rise time is about 0.1 ms and bandwidth 4 MHz with an output of 0.01 V/A with 50 Ω termination. The CTS have typical error of less than 2% with waveform distortion of less than 5% for standard impulse current waves. The VA rating can be from 0.5 VA to as high as 5 kVA. The bandwidth reduces as the VA ratings increase.

7.4 CATHODE-RAY OSCILLOGRAPHS FOR IMPULSE VOLTAGE AND CURRENT MEASUREMENTS

When waveforms of rapidly varying signals (voltages or currents) have to be measured or recorded, certain difficulties arise. The peak values of the signals in high voltage measurements are too large, may be several kilovolts or kiloamperes. Therefore, direct measurement is not possible. The magnitudes of these signals are scaled down by voltage dividers or shunts to smaller voltage signals. The reduced signal $V_m(t)$ is normally proportional to the measured quantity. The procedure of transmitting the signal and displaying or recording it is very important. The associated electromagnetic fields with rapidly changing signals induce disturbing voltages, which have to be avoided. The problems associated in the above procedure are discussed in this section.

7.4.1 Cathode-Ray Oscillographs for Impulse Measurements

Modern oscillographs are sealed tube, hot cathode oscilloscopes with photographic arrangement for recording the waveforms. The cathode ray oscilloscope for impulse work normally has input voltage range from 5 m V/cm to about 20 V/cm. In addition, there are probes and attenuators to handle signals up to 600 V (peak to peak). The bandwidth and rise time of the oscilloscope should be adequate. Rise times of 5 ns and bandwidth as high as 500 MHz may be necessary.

Sometimes high-voltage surges test oscilloscopes do not have vertical amplifier and directly require an input voltage of 10 V. They can take a maximum signal of about 100 V (peak to peak) but require suitable attenuators for large signals.

Oscilloscopes are fitted with good cameras for recording purposes. Tektronix model 7094 is fitted with a lens of 1 : 1.2 polaroid camera which uses 10,000 ASA film which possesses a writing speed of 9 cm/ns.

With rapidly changing signals, it is necessary to initiate or start the oscilloscope time base before the signal reaches the oscilloscope deflecting plates, otherwise a portion of the signal may be missed. Such measurements require an accurate initiation of the horizontal time base and is known as *triggering*. Oscilloscopes are normally provided with both internal and external triggering facility. When external triggering is used, as with recording of impulses, the signal is directly fed to actuate the time base and then applied to the vertical or *Y* deflecting plates through a delay line. The delay is usually 0.1 to 0.5 μ s. The delay is obtained by the following:

1. A long interconnecting coaxial cable 20 to 50 m long. The required triggering is obtained from an antenna whose induced voltage is applied to the external trigger terminal.
2. The measuring signal is transmitted to the CRO by a normal coaxial cable. The delay is obtained by an externally connected coaxial long cable to give the necessary delay. This arrangement is shown in [Fig. 7.55](#).
3. The impulse generator and the time base of the CRO are triggered from an electronic tripping device. A first pulse from the device starts the CRO time base and after a predetermined time a second pulse triggers the impulse generator.

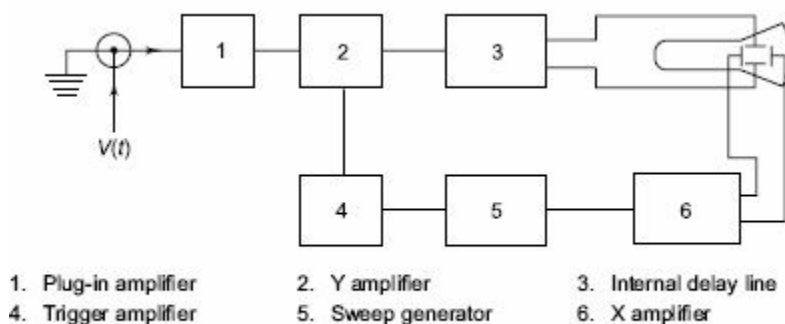


Fig. 7.55 Simplified block diagram of surge test oscilloscopes

7.4.2 Instrument Leads and Arrangement of Test Circuits

It is essential that leads, layout, and connections from the signal sources to the CRO are to be arranged such that the induced voltages and stray pick-ups due to electromagnetic interference are avoided. For slowly varying signals, the connecting cables behave as either capacitive or inductive depending on the load at the end of the cable. For fast-rising signals, however, the cables have to be accounted as transmission lines with distributed parameters. A travelling wave or signal entering such a cable encounters the surge impedance of the cable. To avoid unnecessary reflections at the cable ends, it has to be terminated properly by connecting a resistance equal to the surge impedance of the cable. In cables, the signal travels with a velocity less than that of light which is given by

$$v = \frac{C}{\sqrt{\epsilon_r \mu_r}}$$

where $C = 3 \times 10^8$ m/s and ϵ_r and μ_r are the relative permittivity and relative permeability respectively of the cable materials. Therefore, the cable introduces a finite propagation time

$$t = \frac{1}{v} \times \text{length of the cable}$$

Measuring devices such as oscilloscopes have finite input impedance, usually about 1 to 10 MW resistance in parallel with a 10 to 50 pF capacitance. This impedance at high frequencies ($f = 100$ MHz) is about 80Ω and thus acts as a load at the end of a surge cable. This load attenuates the signal at the CRO end.

Cables at high frequencies are not lossless transmission lines. Because of the ohmic resistance loss in the conductor and the dielectric loss in the cable material, they introduce attenuation and distortion to the signal. Cable distortion has to be eliminated as far as possible. Cable shields also generate noise, voltages due to ground loop currents and due to the electromagnetic coupling from other conductors. In [Fig. 7.56](#), the ground loop currents and their path is indicated. To eliminate these noise voltage multiple shielding arrangement as shown in [Fig. 7.57](#) may have to be used.

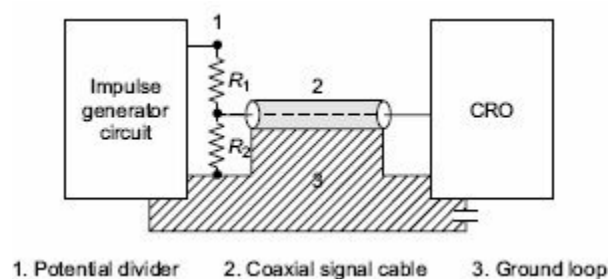


Fig. 7.56 Ground loops in impulse measuring systems

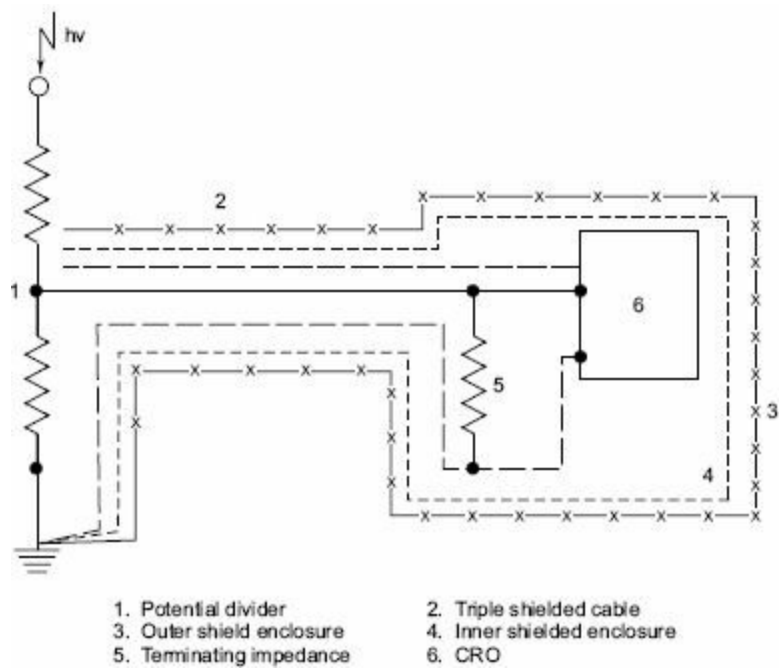


Fig. 7.57 Impulse measurements using multiple shield enclosures and signal cable

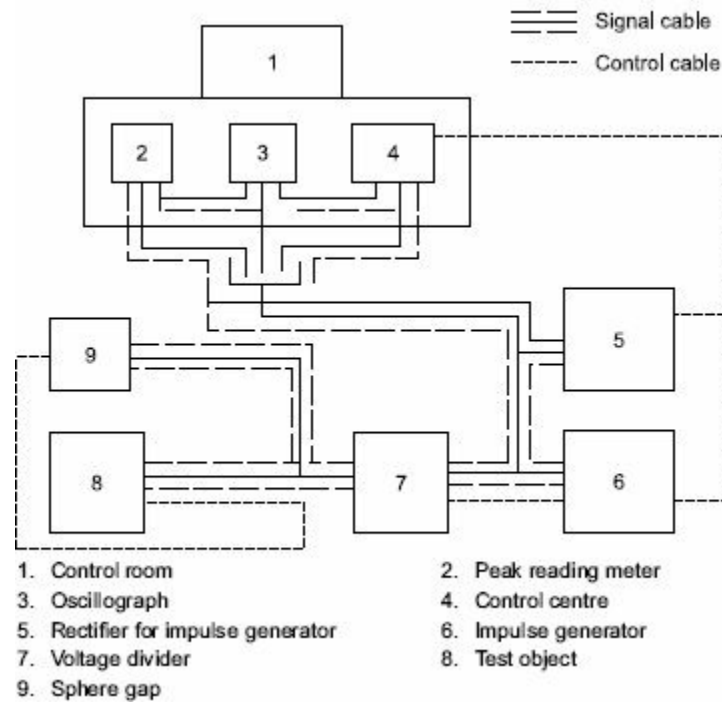


Fig. 7.58 Layout of an impulse testing laboratory with control and signal cables

Another important factor is the layout of power and signal cables in the impulse testing laboratories. Power and interconnecting cables should not be laid in a zig-zag manner and should not be cross-connected. All power cables and control cables have to be arranged through earthed and shielded conduits. A typical schematic layout is shown in [Fig. 7.58](#). The arrangement should provide for branched writing from the cable tree and should not form loops. Where environmental conditions are so severe that true signal cannot be obtained with all countermeasures, electro-optical techniques for transmitting signal pulses may have to be used.

7.4.3 The Impulse Test and Analysing System

It is extremely difficult to control and adjust the impulse wave shapes for different load conditions as in the case of large capacitive loads, very low inductors or coils, transformers with high inductance and capacitance. Further, whenever the tests require comparison of test records, the resolution and uncertainty in measurements will affect the test results and the recorders should be capable of detecting even small deviations or changes. Stringent conditions are imposed on the measuring systems, such as in the case of calibrations, diagnostic procedures, and transfer function analysis (e.g., as in transformer testing and fault diagnostics).

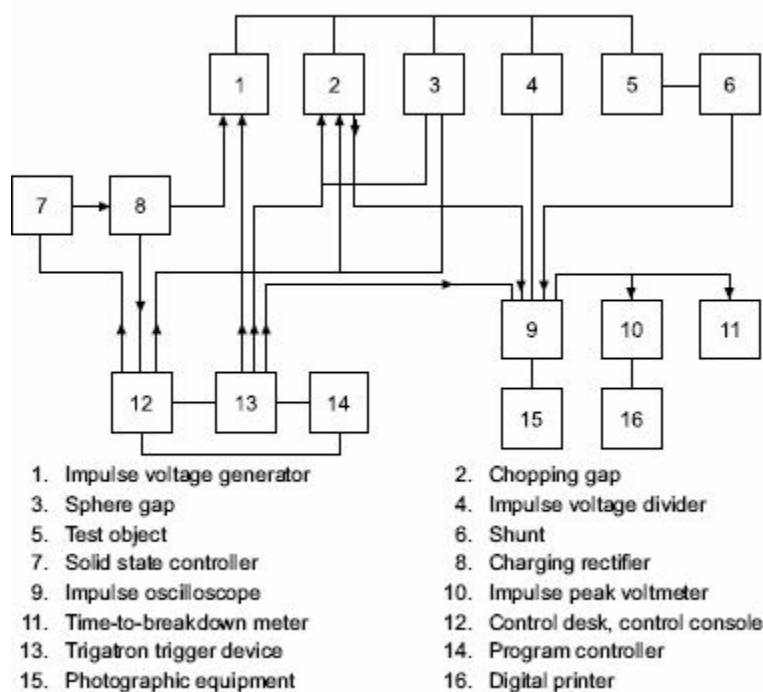


Fig. 7.59 Block diagram of impulse voltage test system

A modern impulse test measuring and analysing system consists of a multichannel digital control and recording systems with 32 bit microprocessor controller recorder and analyser ([Plate 6](#)). The inputs from the measuring voltage dividers, current shunts, etc. are fed through a cable transmission system and A-D converter. The control signals are fed to the charging unit, the trigger gaps of impulse generator, to chopping gaps, etc. Preset operations can be performed from the controller. Variable memory depths up to or more than 128 kilo data points are available. Common impulse shapes can be analysed automatically for such computations, such as (i) getting difference function of two waves, (ii) the Fourier analysis and FFT depicting the original wave in time domain and its Fourier transform in frequency domain, (iii) Transfer function, i.e. the ratio of neutral current to test voltage ratio in frequency domain, and (iv) the coherence function such as comparison of impulse wave at reduced test level and at full voltage level, etc. The software is normally available in common PC operating systems such as MS WINDOWS. Typical schematic diagram of a test and analysing system is shown in [Fig. 7.59](#).

This block diagram is provided for better comprehension of the system layout. All essential components are contained therein. Some components may be omitted, depending on the specific application. The connections indicated in the drawing are of a functional nature and do not necessarily correspond with system wiring.

- High-voltage and Current Measurements
- dc Voltage Measurements
- Potential Dividers
- Generating Voltmeters
- Electric Field Meters
- Measurement of Ripple Voltage
- ac Voltage Measurements
- Series Impedance Meters
- Potential Dividers
- CVTS
- Electrostatic Meters
- Peak Voltmeters
- Sphere Gap Measurements
- Impulse Voltage Measurements
- Potential Dividers
- Response Characteristics
- LV Arms
- Peak Voltmeters
- CRO
- Impulse Measuring Systems
- Impulse Current Measurements
- Shunts
- High Current Transformers

WORKED EXAMPLES

Example 7.1 *A generating voltmeter has to be designed so that it can have a range from 20 to 200 kV dc. If the indicating meter reads a minimum current of $2\mu\text{A}$ and maximum current of $25\mu\text{A}$, what should the capacitance of the generating voltmeter be?*

Solution Assume that the driving motor has a synchronous speed of 1500 rpm.

$$I_{\text{rms}} = \frac{VC_m}{\sqrt{2}} \omega$$

where, V = applied voltage,
 C_m = capacitance of the meter, and
 ω = angular speed of the drive

$$\text{Substituting, } 2 \times 10^{-6} = \frac{20 \times 10^3 \times C_m}{\sqrt{2}} \times \frac{1500}{60} \times 2\pi$$

$$\begin{aligned} \therefore C_m &= 0.9 \text{ p.F} \\ \text{At } 200 \text{ kV, } I_{\text{rms}} &= \frac{200 \times 10^3 \times 0.9 \times 10^{-12} \times 1500}{\sqrt{2} \times 60} 2\pi = 20.0 \text{ } \mu\text{A} \end{aligned}$$

The capacitance of the meter should be 0.9 pF. The meter will indicate 20 kV at a current 2 μ A and 200 kV at a current of 20 μ A.

Example 7.2 Design a peak reading voltmeter along with a suitable microammeter such that it will be able to read voltages, up to 100 kV (peak). The capacitance potential divider available is of the ratio 1000 : 1.

Solution Let the peak reading voltmeter be of the Haefely type shown in [Fig. 7.18b](#).

Let the micro-ammeter have the range 0–10 μ A.

The voltage available at the C_2 arm = $100 \times 10^3 \times = 100 \text{ V (peak)}$

The series resistance R in series with the micro-ammeter

$$= \frac{100}{10 \times 10^{-6}} = 10^7 \Omega$$

$$C_s R = 1 \text{ to } 10 \text{ s}$$

Taking the higher value of 10 s, $C_s = \frac{10}{10^7} = 1 \text{ } \mu\text{F}$

The values of C_s and R are 1 μ F and $10^7 \Omega$.

Example 7.3 Calculate the correction factors for atmospheric conditions, if the laboratory temperature is 37°C, the atmospheric pressure is 750 mmHg, and the wet bulb temperature is 27°C.

Solution

$$\text{Air density factor, } d = \frac{p}{760} \frac{293}{(273+t)}$$

$$\text{At } t = 37^\circ\text{C } d = \frac{750}{760} \frac{263}{310} = 0.9327$$

From [Table 7.6](#), air density correction factor $K = 0.9362$. From [Fig. 10.1](#), the absolute humidity (by extrapolation) corresponding to the given temperature is 18 g/m³. From [Fig. 10.2](#), the humidity correction factor for 50 Hz (curve *a*) is 0.925.

(Note: No humidity correction is needed for sphere gaps.)

Example 7.4 A resistance divider of 1400 kV (impulse) has a high-voltage arm of 16 kilo-ohms and a low-voltage arm consisting 16 members of 250 ohms, 2 watt resistors in parallel. The divider is connected to a CRO through a cable of surge impedance 75 ohms and is terminated at the other end through a 75 ohm resistor. Calculate the exact divider ratio.

Solution hv arm resistance, $R_1 = 16,000$ ohms

lv arm resistance, $R_2 = \frac{250}{16}$ ohms

Terminating resistance, $R'_2 = 75$ ohms

hence, the divider ratio, $a = 1 + R_1/R_2 + R_1/R'_2$
 $= 1 + 16,000 \times 16/250 + 16,000/75$
 $= 1 + 1024 + 213.3 = 1238.3$

Example 7.5 *The HV arm of an R-C, divider has 15 numbers of 120 ohms resistors with a 20pF capacitor to ground from each of the junction points. The LV arm resistance is 5 ohms. Determine the capacitance needed in the LV arm for correct compensation.*

Solution

Ground capacitance per unit = $C'_g = 20$ pF

Effective ground capacitance = $C_e = (2/3) C_g$

$= 2/3 (15 \times 20)$ (Refer Fig. 7.31)
 $= 200$ pF

This capacitance is assumed to be between the centre tap of the hv arms and the ground as shown in Figs 7.31 and 7.29.

Here, $R_1/2 = 15 \times 120/2 = 900$ ohms
 $R_2 = 5$ ohms

Then, the effective time constant of the divider,

$= (R_1/2 \cdot (2/3) C_g) = R_1 C_e/2$
 $= [(900 \times 200) \times 10^{-12}]/2 = 90$ ns

Making the LV arms time constant to be the same as that of the hv arms; the capacitance required for compensation is calculated as

$R_2 C_2 = 90$ ns
 $\therefore C_2 = 90/5$ nF = 18×10^{-9} F

Example 7.6 *A coaxial shunt is to be designed to measure an impulse current of 50 kA. if the bandwidth of the shunt is to be at least 10MHz and if the voltage drop across the shunt should not exceed 50 V, find the ohmic value of the shunt and its dimensions.*

Solution

Resistance of the shunt (max) $R = \frac{50}{50 \times 10^2} = 1$ mΩ

Taking the simplified equivalent circuit of the shunt as give in [Fig. 7.49b](#)

$$\text{Bandwidth } B = \frac{1.46R}{L_0} = 10 \text{ MHz}$$

d, the thickness of the cylindrical resistive tube is taken from the consideration of the bandwidth as

$$\begin{aligned} \text{or, } L_0 &= \frac{1.46R}{B} = \frac{1.46 \times 10^{-2}}{10 \times 10^6} \\ &= 1.46 \times 10^{-10} \text{ H or } 0.146 \text{ nH} \end{aligned}$$

where,

$$B = \frac{1.46\rho}{\mu d^2}$$

where, r = resistivity of the material,

$$\mu = \mu_0 = 4\pi \times 10^{-7} \text{ H/m, and}$$

d = thickness of the tube in metres

Let r = radius of the resistive tube,

l = length of the resistive tube,

d = thickness of the resistive tube, and

ρ = resistivity of the tube material.

$$\text{Then the bandwidth } B = \frac{1.46\rho}{\mu d^2}$$

Let the length l be taken as 10 cm or 10^{-1} m;

where, $\mu = \mu_0 \mu_r = \mu_0$

$$\text{Substituting } B = 10^7 \text{ Hz}$$

$$\rho = 30 \times 10^{-8} \Omega\text{m}$$

$$\mu_0 = 4\pi \times 10^{-7}$$

$$d = \frac{1.46\rho}{\mu B} = \sqrt{\frac{1.46 \times 30 \times 10^{-8}}{4\pi \times 10^{-7} \times 10^7}}$$

$$= 0.187 \times 10^{-3} \text{ m} = 0.187 \text{ mm}$$

For the return conductor the outer tube can be taken to have a length = 10 cm, radius = 30 mm, and thickness = 1 mm, and it can be made from copper or brass.

Example 7.7 A Rogowski coil is to be designed to measure impulse currents of 10 kA having a rate of change of current of 10 A/s. The current is read by a TVM as a potential drop across the integrating circuit connected to the secondary. Estimate the values of mutual inductance, resistance, and capacitance to be connected, if the meter reading is to be 10 V for full-scale deflection.

Solution

$$V_m(t) = \frac{M}{CR} I(t) \text{ for } \frac{1}{CR} \ll \omega \text{ (Eq. 7.42),}$$

taking the peak values

$$\frac{M}{CR} = \frac{V_m(t)}{I(t)} = \frac{10}{10^4} = 10^{-3}$$

The time interval of the change of current assuming sinusoidal variation is

$$\frac{10^4}{10^{11}} = 10^{-7} \text{ s} = \frac{1}{4} \text{ of a cycle}$$

∴ frequency = $\frac{10^7}{4}$ Hz

and, $\omega = 2\pi f = \frac{\pi}{2} \times 10^7$

Taking $\frac{1}{CR} = \frac{\omega}{10\pi} = \frac{10^6}{2}$

$$CR = \frac{2}{10^6}$$

$$M = 10^{-3} CR = 10^{-3} \frac{2}{10^6}$$

$$= 2 \times 10^{-9} \text{ H or } 2 \text{ nH.}$$

Taking $R = 2 \times 10^3 \Omega$,

$$C = \frac{CR}{R} = \frac{2 \times 10^{-9}}{2 \times 10^3} = 10^{-9} \text{ F or } 1000 \text{ pF}$$

(It should be noted that for a given frequency, $X_c \ll R$; otherwise the low frequency response will be poor. Here, X_c at $f = 10^7/4$ is 60Ω only.)

Example 7.8 *If the coil in Example 7.7 is to be used for measuring impulse current of $8/20 \mu\text{s}$ wave and of the same peak current, what should be the R-C integrating circuit.*

Solution In this case, the lowest frequency to be read should be at least $\frac{1}{3}$ to $\frac{1}{5}$ of the lowest frequency component present in the waveform.

The frequency corresponding to the tail time is

$$\frac{1}{20 \times 10^{-6}} = 50 \text{ kHz}$$

∴ lowest frequency to be read is

$$50 \times \frac{1}{5} = 10 \text{ kHz} \quad \therefore \omega = 2\pi \times 10^4 \text{ radians}$$

Taking $\frac{1}{CR} = \frac{\omega}{10\pi}$

$$= \frac{2\pi \times 10^4}{10\pi} = 2 \times 10^3$$

$$M = 10^{-3} \times \frac{1}{2 \times 10^3} = 0.5 \times 10^{-6} \text{ H, or } 0.5 \mu\text{H}$$

(X_c at a frequency of 10 kHz is about 60Ω which is very much less than R .)

MULTIPLE-CHOICE QUESTIONS

1. A generating voltmeter is used to measure
 - (a) impulse voltages
 - (b) ac voltages
 - (c) dc voltages
 - (d) high-frequency ac voltages
2. A series capacitance voltmeter can measure
 - (a) dc voltages
 - (b) ac voltage (rms value)
 - (c) ac voltage (peak value)
 - (d) impulse voltages
3. CVT when tuned does not have
 - (a) ratio error
 - (b) phase angle error
 - (c) both ratio and phase angle errors
 - (d) temperature error
4. Electrostatic voltmeters can measure
 - (a) only dc voltage
 - (b) both dc and ac voltages up to high frequency
 - (c) impulse voltages
 - (d) ac, dc and impulse voltages
5. Sphere gaps are used to measure
 - (a) dc voltages
 - (b) ac peak voltages
 - (c) dc, ac peak and impulse voltages
 - (d) only dc and ac peak voltages.
6. Sphere gap measurement is linear and valid for gap spacing less than or equal to
 - (a) radius of the sphere
 - (b) diameter of the sphere
 - (c) half the radius of sphere
 - (d) two times diameter of the sphere
7. The main factors that affect the sparkover voltage of sphere gap are
 - (a) humidity and waveform
 - (b) nearby earthed objects and atmospheric conditions
 - (c) diameter of the sphere
 - (d) gap spacing, diameter and waveform
8. For an RC divider to be compensated, the condition is
 - (a) $R_1C_1=R_2C_2$
 - (b) $R_1C_2=R_2C_1$
 - (c) $R_1C_1 = R_2 C_g$
 - (d) $(R_1+R_2)(C_1 + C_2)\mu s.$
9. Compensated capacitance divider for high voltages (1 MV) generally has a bandwidth of
 - (a) 10 MHz
 - (b) 1 MHz
 - (c) 100 MHz

(d) 1000 MHz.

10. In a pure capacitive divider, the ground capacitance C_g is represented by adding additional capacitance from central point of hv capacitor to the ground and is equal to
- (a) C_g
 - (b) $C_g/3$
 - (c) $2C_g/3$
 - (d) $C_g/2$.
11. For an optimally damped $R-C$ divider, the damping resistance R_1 connected in hv arm is equal to (L = high voltage lead inductance, and C_g = equivalent ground capacitance)
- (a) $4\sqrt{L/C_g}$
 - (b) $2\sqrt{L/C_g}$
 - (c) $\sqrt{L/C_g}$
 - (d) $\frac{1}{2}\sqrt{L/C_g}$
12. The surge impedance of a measuring cable with its resistance neglected, C_g is (if L and C are inductance and capacitance of cable per unit length)
- (a) $\sqrt{L/C}$
 - (b) $2\sqrt{L/C}$
 - (c) $2\sqrt{LC}$
 - (d) $\sqrt{C/L}$
13. Hall generators are normally used to measure
- (a) impulse voltages
 - (b) unidirectional impulse currents
 - (c) any type of impulse currents
 - (d) large ac currents
14. For measuring high impulse currents, the best type of shunt is
- (a) squirrel cage
 - (b) bifilar strip
 - (c) disc
 - (d) coaxial tubular (Park type)
15. The skin depth for resistance material used for impulse shunts is given by
- (a) $(\pi f \mu \sigma)^{1/2}$
 - (b) $(\pi f \mu \sigma)^{-1/2}$
 - (c) $2\sqrt{\pi f \mu \sigma}$
 - (d) $0.5 (\pi f \mu \sigma)^{-1/2}$
16. Rogowski coils and high frequency current transformers have bandwidth of about
- (a) 100 KHz
 - (b) 10 MHz
 - (c) 1.0 MHz
 - (d) 1100 Hz
17. An $R-C$ voltage divider has hv arm capacitance, $C_1 = 600$ pF, resistance = 400Ω and equivalent ground capacitance $C_g = 240$ pF. The effective time constant of the divider in nanoseconds is
- (a) 108
 - (b) 90
 - (c) 69
 - (d) 32.
18. Shunts used for measuring impulse currents, in the range 10 kA-50 kA will have a resistance of the order of

- (a) 10 to 25m Ω
 - (b) 0.1 to 1 m Ω
 - (c) 100 to 500 m Ω
 - (d) 0.1 to 1.0 Ω .
19. The type of measuring device preferred for measurement of impulse currents of short duration is
- (a) Park's tubular shunt
 - (b) current transformer
 - (c) Hall generator
 - (d) Faraday ammeter.
20. Secondary arm of a resistance impulse voltage divider consists of
- (a) a few resistors connected in series
 - (b) a few resistors connected in parallel
 - (c) a single wire wound resistor of very high power rating
 - (d) a linear resistor in parallel with a non-linear resistor of high power rating
21. The resistivity of the materials used as shunts for high currents will be in the range (Ω - cm)
- (a) 1 to 5×10^{-5}
 - (b) $\approx 10^{-3}$
 - (c) 0.5×10^{-6} to 0.5×10^{-7}
 - (d) 0.2×10^{-6} to 1.5×10^{-6}
22. In high frequency and RF current transformers, the secondary winding is terminated with a resistance of
- (a) 1 Ω
 - (b) 10 Ω
 - (c) 1kW
 - (d) 50 Ω or 75 Ω
23. To measure a high-voltage of peak value about 150 kV, the suitable sphere gap would be (diameter in cm)
- (a) 5 or 10
 - (b) 10 or 15
 - (c) 15 or 25
 - (d) 50 or 100
24. With a series capacitor voltmeter, a large error will result in when the
- (a) capacitance is larger
 - (b) meter used is an electromechanical meter
 - (c) voltage to be measured is non-sinusoidal and contains harmonics
 - (d) none above
25. Sphere-gap measurement of peak voltage has an error of
- (a) $< \pm 1\%$
 - (b) 5 to 10%
 - (c) 3 to 5%
 - (d) $< 3\%$

- | | | | | | |
|---------|---------|---------|---------|---------|---------|
| 1. (c) | 2. (c) | 3. (b) | 4. (b) | 5. (c) | 6. (a) |
| 7. (b) | 8. (a) | 9. (c) | 10. (c) | 11. (a) | 12. (a) |
| 13. (b) | 14. (d) | 15. (a) | 16. (b) | 17. (d) | 18. (a) |
| 19. (a) | 20. (b) | 21. (d) | 22. (d) | 23. (c) | 24. (c) |
| 25. (d) | | | | | |

REVIEW QUESTIONS

- Discuss the different methods of measuring high dc voltages. What are the limitations in each method?
- Describe the generating voltmeter used for measuring high dc voltages. How does it compare with a potential divider for measuring high dc voltages?
- Compare the relative advantages and disadvantages of using a series resistance microammeter and a potential divider with an electrostatic voltmeter for measuring high dc voltages?
- Why are capacitance voltage dividers preferred for high ac voltage measurements?
- What is capacitance voltage transformer? Explain with phasor diagram how a tuned capacitance voltage transformer can be used for voltage measurements in power systems.
- Explain the principle and construction of an electrostatic voltmeter for very high voltages. What are its merits and demerits for high-voltage ac measurements?
- Give the basic circuit for measuring the peak voltage of (a) ac voltage, and (b) impulse voltage. What is the difference in measurement technique in the above two cases?
- Explain how a sphere gap can be used to measure the peak value of voltages. What are the parameters and factors that influence such voltage measurement?
- Compare the use of uniform field electrode spark gap and sphere gap for measuring peak values of voltages.
- What are the conditions to be satisfied by a potential divider to be used for impulse work?
- Give the schematic arrangement of an impulse potential divider with an oscilloscope connected for measuring impulse voltages. Explain the arrangement used to minimize errors.
- What is a mixed potential divider? How is it used for impulse voltage measurements?
- Explain the different methods of high current measurements with their relative merits and demerits.
- What are the different types of resistive shunts used for impulse current measurements? Discuss their characteristics and limitations.
- What are the requirements of an oscillograph for impulse and high frequency measurements in high-voltage test circuits?
- Explain the necessity of earthing and shielding arrangements in impulse measurements and in high-voltage laboratories. Give a sketch of the multiple shielding arrangements used for impulse voltage and current measurements.
- Explain with schematic diagrams how dc current can be measured using dc current transformers.
- How is a compensated dc potential divider used to measure the dc voltage in HVDC systems?

PROBLEMS

- A generating voltmeter is to read 250 kV with an indicating meter having a range of (0-20) μA calibrated accordingly. Calculate the capacitance of the generating voltmeter when the driving motor rotates at a constant speed of 1500 r.p.m.

2. The effective diameter of the moving disc of an electrostatic voltmeter is 15 cm with an electrode separation of 1.5 cm. Find the weight in grams that is necessary to be added to balance the moving plate when measuring a voltage of 50 kV dc. Derive the formula used. What is the force of attraction between the two plates when they are balanced?
3. A compensated resistance divider has its high-voltage arm consisting of a series of resistance whose total value is 25 kilo-ohms shunted by a capacitance of 400 pF. The LV arm has a resistance of 75 ohms. Calculate the capacitance needed for the compensation of this divider.
4. What are the usual sources of errors in measuring high impulse voltages by resistance potential dividers? How are they eliminated? An impulse resistance divider has a high-voltage arm with a 5000 ohm resistance and the LV arm with a 5 ohm resistance. If the oscilloscope is connected to the secondary arm through a cable of surge impedance 75 ohms, determine, (i) the terminating resistance, and (ii) the effective voltage ratio.
5. A mixed R - C divider has its hv arm consisting of a capacitance of 400 pF in series with a resistance of 100 ohms. The LV arm has a resistance of 0.175 ohm in series with a capacitance C_2 . What should be the LV arm capacitance for correct compensation? The divider is connected to a CRO through a measuring cable of 75 ohms surge impedance. What should be the values of R_4 and C_4 (see [Fig. 7.38b](#)) in the matching impedance? Determine the voltage ratio of the divider.
6. A bifilar strip shunt has a resistance of 100 m Ω and inductance of 0.1 μ H with a parallel capacitance of 5 pF across its terminal. What will be its step response. Determine the rise time of the shunt.
7. Determine the dimensions of a co-axial tubular shunt with nominal resistance of 1 m Ω and rise time of 10 ns. Take the resistivity of the material as 50×10^{-6} Ω -cm and length of the shunt not to exceed 15 cm.
8. A Rogowski coil is to measure 20 kA peak current with a maximum di/dt of 10^4 A/ μ s. A 0–10 V electronic voltmeter is connected across the integrating circuit of the coil. Estimate the mutual inductance of the coil and resistance and capacitance of the integrating circuit to be used.
9. An electrostatic voltmeter has an effective plate diameter of 50 cm with a gap separation of 30 cm. Find the force between the plates when measuring a dc voltage of 100 kV. What is the maximum voltage that can be measured if the electric field E is to be not more than 5 kV/cm.
10. A co-axial shunt has the following dimensions length = 10 cm, radius of resistive tube 2.5 cm, thickness = 0.2 mm and ρ = resistivity = 50×10^{-6} Ω cm. Determine the resistance, inductance and band width of the shunt. What will be the voltage drop across the shunt if 10 kA peak current passes through it.

Answers to Problems

1. 0.72 pF
2. 88.57 g
3. 0.133 μ F
4. $R_3 = 70$ ohms, $R_4 = 75$ ohms, Ratio = 1067.7
5. $C_2 = 0.228$ μ F, $C_4 = 533.3$ pF, $R_4 = 75$ ohms
6. 0.02 ns
7. Radius of resistive tube = 2.54 cm
8. $M = 0.22$ μ H, $R = 10$ k Ω , $C = 4$ nF

9. 15.02 g wt, 150 kV
10. $R = 1.6 \text{ m}\Omega$ $L = 0.16 \text{ }\mu\Omega$, Band width = 14.5 MHz, $K=16V$

REFERENCES

1. Craggs, J.D. and Meek, J.M., *High Voltage Laboratory Techniques*, Butterworths Scientific Publications, London (1964).
2. Kuffel, E. and Abdullah, M., *High Voltage Engineering*, Pergamon Press, Oxford (1970).
3. Schwab, A.J., *High Voltage Measurement Technique*, M.I.T. Press, Cambridge, Massachusetts (1972).
4. Bowlder, G.W., *Measurement in High Voltage Test Circuits*, Pergamon Press, Oxford (1975).
5. Hylten Cavallius, N., *High Voltage Laboratory Planning*, Haefely and Co., Basel, Switzerland (1988).
6. Trump, G.J. and Van De Graaff *et al.*, "Generator voltmeter of high voltage sources", *Rev. Sci. Instr.*, 11, 54 (1940).
7. Hamwell and Van Voorhis, "An electrostatic generating voltmeter", *Rev. Sci. Instr.*, 4, 540 (1933).
8. Haefely and Co., "H.V meter for peak and rms value measurements", Druckschirf, BD., 6589 Basel (1967).
9. Rabus, W., "Measurements of surges by V.T.V.M. and electrostatic voltmeters", *ETZ(A)*, 75, 6761 (1953).
10. Blalock *et al.*, "A capacitive voltage divider for UHV outdoor testing", *Tr. IEEE PAS*, PAS-89, 1404 (1970).
11. Ziegler, "Highly stable 150 kV voltage divider", *Tr. IEEEIM*, IM-19, 395 (1970).
12. Koshrt, F., "Hall generators for high dc current measurements", *ETZ (A)*, 77, 487 (1956).
13. Thomas, R.F., "Fastlightpulse measuring schemes", *Tr. IEEE* IM-17, 12 (1968).
14. Mckibbin, F., "Use of delta modulation in pulse transmission system", *IEEE Trans.*, 6, 55 (1970).
15. Witt, R., "Response of low resistance shunts for impulse currents", *Eleteckric*, 47, 54 (1960).
16. Schwab, A., "Low ohmic resistors for impulse currents", *Transaction 12, of H.V. Laboratory*, University of Karlsruhe 1972.
17. Heumann, K., "Magnetic potentiometer of high precision", *Tr. IEEEIM*, IM-15, 242 (1966).
18. Thomas, R.T., *et al.*, "High impulse current and voltage measurements", *Tr. IEEEIM*, IM-19, 102 (1970).
19. Cassidy, E.C., *et al.*, "Electro-optical H.V. pulse measurement techniques", *Tr. IEEEIM*, IM-19, 395 (1970).
20. Zaengel, W., "Impulse voltage dividers and leads", *Bull, SEV*, 61, 1003 (1970).
21. Faser, K., "Transient behaviour of damped capacitive voltage dividers of millionvolts", *Tr. IEEEPAS*, 93.116 (1974).
22. Hylten Cavallius, N., *et al.*, "A new approach to minimise response errors in the measurement of high voltages", *Tr. IEEE PAS*, Vol. PAS – 102, 2077 (1983).
23. Hylten Cavallius, N., *et al.*, "Response errors of shunts", *Int. Symp, on High Voltage Engineering, Paper No. 61.05*, Athens, Greece (1983).
24. IEC 52, "Recommendation for Voltage Measurement by Means of Sphere Gaps (One Sphere Earthed)", Geneva, Switzerland (1960).
25. "Recovery Voltage Meter" Type 5461, *TETTEX Instruments*, Dietikon-Zurich, Switzerland.
26. IEC 60-1 (1989), "High voltage test techniques-Part 1: General specifications and test

requirements.”

27. IEC 60–2 (1984), “High voltage test techniques – Part 2: Measuring Systems.”
28. Wolf, J., and Voign, G., “A new solution for the extension of the load range of impulse generators”, *ISH Montreal* (1977) pp. 363–366.
29. IEC 1083–1 (1991), “Digital recorders for measurements in high-voltage impulse tests – Part 1: Requirements for digital recorders.”
30. IEC 790 (1984), “Oscilloscopes and peak voltmeters for impulse tests.”
31. ELECTRA 136, June (1991), “Measurements of standard switching impulse voltages by means of sphere gaps (one sphere earthed)”, *CIGRE WG 33–03*.
32. IEC 60183–1 (2001), Instruments and software used for measurements in high voltage impulse test – Part 1: Requirements for instruments.
33. HIAS – “High Resolution Impulse Analysing System”. *Bulletin E 147* (E. Haefely & Cie, Ltd.), Based 16, Switzerland.
34. IEC 1083–2 (1996), Digital recorders for measurements in high-voltage impulse tests – Part2: Evaluation of software used for the determination of the parameters of impulse wave-forms”.
35. Mazen Abdel Salam. High Voltage Engineering, Marcel Dekker U.S.A 2001.

CHAPTER

8

Overvoltage Phenomenon and Insulation Coordination in Electric Power Systems

It is essential for electrical power engineers to reduce the number of outages and preserve the continuity of service and electric supply. Therefore, it is necessary to direct special attention towards the protection of transmission lines and power apparatus from the chief causes of overvoltages in electric systems, namely lightning overvoltages and switching overvoltages. Lightning overvoltage is a natural phenomenon, while switching overvoltages originate in the system itself by the connection and disconnection of circuit breaker contacts or due to initiation or interruption of faults. Switching overvoltages are highly damped short duration overvoltages. They are ‘temporary overvoltages’ of power frequency or its harmonic frequency, either sustained or weakly damped, and originate in switching and fault-clearing processes in power systems. Although both switching and power frequency overvoltages have no common origin, they may occur together, and their combined effect is important in insulation design. The probability of lightning and switching overvoltages coinciding together is very small and hence can be neglected. The magnitude of lightning voltages appearing on transmission lines does not depend on line design and hence lightning performance tends to improve with increasing insulation level, that is, with system voltage. On the other hand, switching overvoltages are proportional to operating voltage. Hence, there is a system operating voltage at which the emphasis changes from lightning to switching surge design, this being important above 500 kV. In the range of 300 kV to 765 kV, both switching overvoltages and lightning overvoltages have to be considered, while for ultra high voltages (> 700 kV), perhaps switching surges may be the chief condition for design considerations.

For the study of overvoltages, a basic knowledge of the origin of overvoltages, surge phenomenon, and its propagation is desirable. The present chapter is therefore devoted to a summary of the above topics.

8.1 NATURAL CAUSES FOR OVERVOLTAGES—LIGHTNING PHENOMENON

Lightning phenomenon is a peak discharge in which charge accumulated in the clouds discharges into a neighbouring cloud or to the ground. The electrode separation, i.e., cloud-to-cloud or cloud-to-ground is very large, perhaps 10 km or more. The mechanism of charge formation in the clouds and their discharge is quite a complicated and uncertain process. Nevertheless, a lot of information has been collected since the last fifty years and several theories have been put forth for explaining the phenomenon. A summary of the various processes and theories is presented in this section.

8.1.1 Charge Formation in the Clouds

The factors that contribute to the formation or accumulation of charge in the clouds are too many and uncertain. But during thunderstorms, positive and negative charges become separated by the heavy air currents with ice crystals in the upper part and rain in the lower parts of the cloud. This charge separation depends on the height of the clouds, which range from 200 to 10,000 m, with their charge centres probably at a distance of about 300 to 2000 m. The volume of the clouds that participate in lightning flashover are uncertain, but the charge inside the cloud may be as high as 1 to 100 C. Clouds may have a potential as high as 10^7 to 10^8 V with field gradients ranging from 100 V/cm within the cloud to as high as 10 kV/cm at the initial discharge point. The energies associated with the cloud discharges can be as high as 250 kWh. It is believed that the upper regions of the cloud are usually positively charged, whereas the lower region and the base are predominantly negative except the local region, near the base and the head, which is positive. The maximum gradient reached at the ground level due to a charged cloud may be as high as 300 V/cm, while the fair weather gradients are about 1 V/cm. A probable charge distribution model is given in [Fig. 8.1](#) with the corresponding field gradient near the ground.

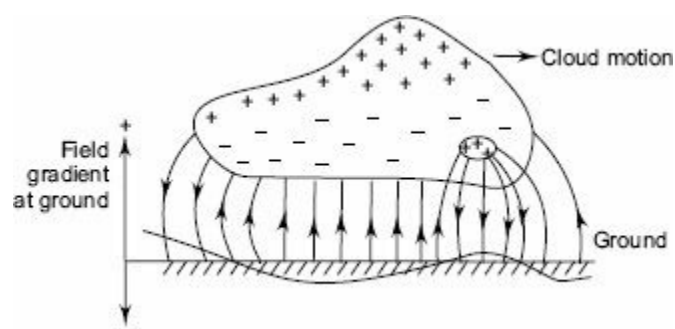


Fig. 8.1 Probable field gradient near the ground corresponding to the probable charge distribution in a cloud

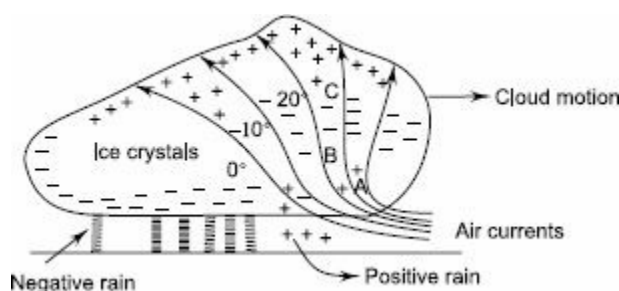


Fig. 8.2 Cloud model according to Simpson's theory

According to the Simpson's theory ([Fig. 8.2](#)) there are three essential regions in the cloud to be considered for charge formation. Below region *A*, air currents travel above 800 cm/s, and no raindrops fall through. In region *A*, air velocity is high enough to break the falling raindrops causing a positive charge spray in the cloud and negative charge in the air. The spray is blown upwards, but as the velocity of air decreases, the positively charged water drops recombine with the larger drops and fall again. Thus, region *A*, eventually becomes predominantly positively charged, while region *B* above it, becomes negatively charged by air currents. In the upper regions in the cloud, the temperature is low (below freezing point) and only ice crystals exist. The impact of air on these crystals makes them negatively charged, thus the distribution of the charge within the cloud becomes as shown in [Fig. 8.2](#).

However, the above theory is obsolete and the explanation presented is not satisfactory. Recently,

Reynolds and Mason proposed modification, according to which the thunder clouds are developed at heights 1 to 2 km above the ground level and may extend up to 12 to 14 km above the ground. For thunder clouds and charge formation air currents, moisture and specific temperature range are required.

The air currents controlled by the temperature gradient move upwards carrying moisture and water droplets. The temperature is 0°C at about 4 km from the ground and may reach -50°C at about 12 km height. But water droplets do not freeze as soon as the temperature is 0°C . They freeze below -40°C only as solid particles on which crystalline ice patterns develop and grow. The larger the number of solid sites or nuclei present, the higher is the temperature ($> -40^{\circ}\text{C}$) at which the ice crystals grow. Thus in clouds, the effective freezing temperature range is ground -33°C to -40°C . The water droplets in the thunder cloud are blown up by air currents and get super cooled over a range of heights and temperatures. When such freezing occurs, the crystals grow into large masses and due to their weight and gravitational force start moving downwards. Thus, a thunder cloud consists of supercooled water droplets moving upwards and large hail stones moving downwards.

When the upward moving supercooled water droplets act on cooler hail stone, it freezes partially, i.e., the outer layer of the water droplets freezes forming a shell with water inside. When the process of cooling extends to inside warmer water in the core, it expands, thereby splintering and spraying the frozen ice shell. The splinters being fine in size are moved up by the air currents and carry a net positive charge to the upper region of the cloud. The hail stones that travel downwards carry an equivalent negative charge to the lower regions of the cloud and thus negative charge builds up in the bottom side of the cloud.

According to Mason, the ice splinters should carry only positive charge upwards. Water being ionic in nature has concentration of H^+ and OH^- ions. The ion density depends on the temperature. Thus, in an ice slab with upper and lower surfaces at temperatures T_1 and T_2 , ($T_1 < T_2$), there will be a higher concentration of ions in the lower region. However, since H^+ ions are much lighter, they diffuse much faster all over the volume. Therefore, the lower portion which is warmer will have a net negative charge density, and hence the upper portion, i.e., cooler region will have a net positive charge density. Hence, it must be appreciated, that the outer shells of the frozen water droplets coming into contact with hail stones will be relatively cooler (than their inner core—warmer water) and therefore acquire a net positive charge. When the shell splinters, the charge carried by them in the upward direction is positive.

According to the Reynold's theory, which is based on experimental results, the hail packets get negatively charged when impinged upon by warmer ice crystals. When the temperature conditions are reversed, the charging polarity reverses. However, the extent of the charging and consequently the rate of charge generation was found to disagree with the practical observations relating to thunder clouds. This type of phenomenon also occurs in thunder clouds.

Rate of Charging of Thunder Clouds Mason considered thunder clouds to consist of a uniform mixture of positive and negative charges. Due to hailstones and air currents the charges separate vertically. If λ is a factor which depends on the conductivity of the medium, there will be a resistive leakage of charge from the electric field built up, and this should be taken into account for cloud charging.

Let E be the electric field intensity, v be the velocity of separation of charges, and ρ the charge density in the cloud. Then, the electric field intensity E is given by

$$\frac{dE}{dt} + \lambda = \rho v \quad (8.1)$$

Hence
$$E = \frac{\rho v}{\lambda} [1 - \exp(-\lambda t)] \quad (8.2)$$

This equation assumes initially $E = 0$ at $t = 0$, the start of charge separation, i.e. there is no separation initially.

Let Q_s be the separated charge and Q_g be the generated charge, then

$$\rho = \frac{Q_s}{Ah} \quad (8.3a)$$

and
$$E = \frac{Q_s}{A\epsilon_0} \quad (8.3b)$$

where ϵ_0 is the permittivity of the medium, A is the cloud area and h is the height of the charged region.

From [Eq. \(8.2\)](#), on substitution

$$Q_g = \frac{Q_s h}{v[1 - \exp(-\lambda t)]} = \frac{M}{v[1 - \exp(-\lambda t)]} \quad (8.4)$$

where $M = Q_s \cdot h =$ the electric moment of the thunderstorm.

The average values observed for thunder-clouds are

$$\text{time constant} = \frac{1}{\lambda} = 20 \text{ s}$$

electric moment $M = 110 \text{ C-km}$ and

time for first lightning flash to appear, $t = 20 \text{ s}$

The velocity of separation of charges, $v = 10$ to 20 m/s .

Substituting these values, we get

$$\begin{aligned} Q_g &= \frac{20,000}{v} \text{ C} \\ &= \frac{20,000}{20} \text{ C} = 1000 \text{ C for } v = 20 \text{ m/s} \end{aligned}$$

Calculations using Mason's theory show that a maximum charge transfer of $3 \times 10^{-3} T \text{ esu/cm}^2$ of contact surface for a contact period of 0.01 s , where T is the temperature difference.

The theory and observations of Reynolds *et al.*, gave values of $5 \times 10^{-9} \text{ esu}$ per crystal impact for a temperature difference of 5°C . Mason's theory seems to give much higher values, yet it explains the phenomenon satisfactorily.

8.1.2 Mechanism of Lightning Strokes

When the electric field intensity at some point in the charge concentrated cloud exceeds the breakdown value of the moist ionized air (≈ 10 kV/cm), an electric streamer with plasma starts towards the ground with a velocity of about 1/10 times that of the light, but may progress only about 50 m or so before it comes to a halt emitting a bright flash of light. The halt may be due to insufficient build-up of electric charge at its head and not sufficient to maintain the necessary field gradient for further progress of the streamer. But after a short interval of about $100 \mu\text{s}$, the streamer again starts out repeating its performance. The total time required for such a stepped leader to reach the ground may be 20 ms. The path may be quite lustrous, depending on the local conditions in air as well as the electric field gradients. Branches from the initial leader may also be formed. Since the progress of this leader stroke is by a series of jumps, it is referred as stepped leader. The picture of a typical leader stroke taken with a Boy's camera is shown in [Fig. 8.3](#).

The lightning stroke and the electrical discharges due to lightning are explained based on the 'streamer' or 'kanel' theory for spark discharges in long gaps with non-uniform electric fields. The lightning consists of a few separate discharges starting from a leader discharge and culminates in return strokes or main discharges.

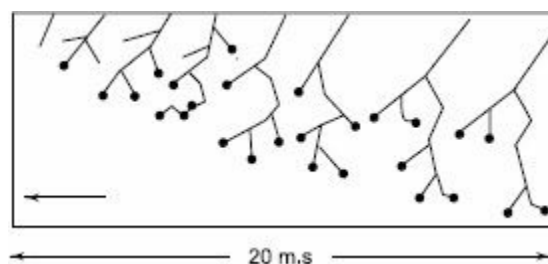


Fig. 8.3 Propagation of a stepped leader stroke from a cloud (* Bright tips recorded)

The velocity of the leader stroke of the first discharge may be 1.5×10^7 cm/s, of the succeeding leader strokes about 10^8 cm/s, and of their turn strokes may be 1.5×10^9 to 1.5×10^{10} cm/s (about 0.05 to 0.5 times the velocity of light).

After the leader touches the ground, the return stroke follows. As the leader moves towards the ground, positive charge is directly accumulated under the head of the stroke or canal. By the time the stroke reaches the ground or comes sufficiently near the ground, the electrical field intensity on the ground side is sufficiently large to build up the path. Hence, the positive charge returns to the cloud neutralizing the negative charge, and hence a heavy current flows through the path. The velocity of the return or main stroke ranges from 0.05 to 0.5 times the velocity of light, and currents will be of the order of 1000 to 250,000 A. The return strokes vanish before they reach the cloud, suggesting that the charge involved is that conferred to the stroke itself. The duration of the main or return stroke is about $100 \mu\text{s}$ or more. The diameters of the return strokes were estimated to be about 1 to 2 cm but the corona envelop may be approximately 50 cm. The return strokes also may develop branches but the charges in the branches are neutralized in succession so that their further progress is arrested. A Boy's camera picture of return stroke is shown in [Fig. 8.4](#).

After the completion of the return stroke, a much smaller current of 100 to 1000 A may continue to flow which persists approximately for 20 ms. Due to these currents, the initial breakdown points in the cloud are considerably reduced and discharges concentrate towards this point. Therefore, additional reservoirs of charge become available due to penetration of a cloud mass known as preferred paths and lead to repeated strokes. The leader strokes of the repeated strokes progress with

much less velocity ($\approx 1\%$ of that of light) and do not branch. This stroke is called continuous leader, and return stroke for this leader follows with much less current. The interval between the repeated strokes may be from 0.6 ms to 500 ms with an average of 30 ms. Multiple strokes may last for 1 s. The total duration of the lightning may be more than 1 s. The current from the ground by the main return stroke may have a peak value of 250,000 A, and rates of rise may be as high as 100 kA/ μ s or 10^{11} A/s. The time intervals between successive strokes, the number of successive strokes, the duration of lightning discharges the discharge current, the rate of rise of current, and wavefront and wave tail times and their probability distribution are given in [Figs 8.5](#) to [8.10](#).

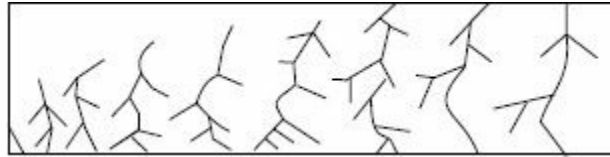


Fig. 8.4 *Development of the main or return stroke*

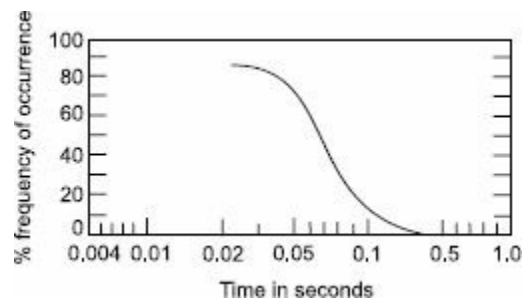


Fig. 8.5 *Time interval between successive strokes (ERA average curve)*

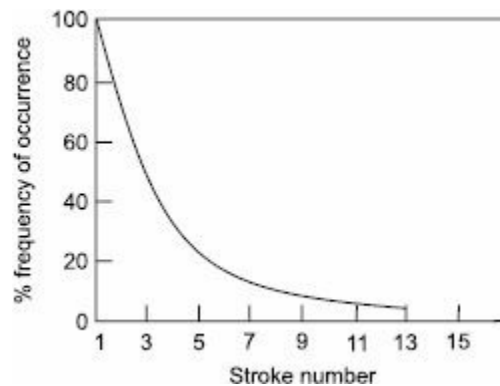
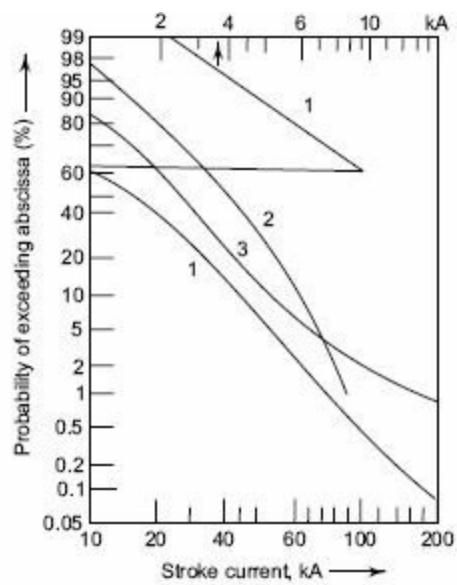
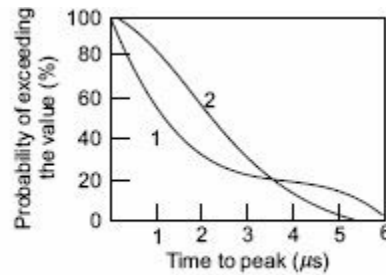


Fig. 8.6 *Number of strokes in lightning discharges (ERA average curve)*



1. AIEE committee (1950) 2. Anderson (1968) 3. CIGRE (1972)

Fig. 8.7 Cumulative distributions of lightning stroke currents (peak values)



1. McEachron (1941) 2. Anderson (1968)

Fig. 8.8 Time to peak of lightning stroke currents

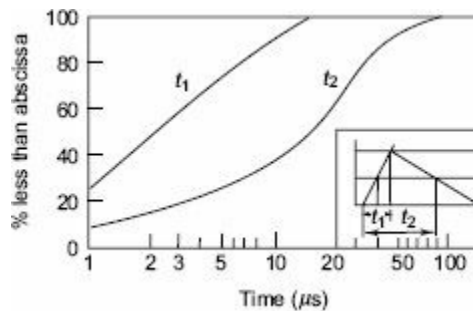


Fig. 8.9 Wavefront and wave tail times of lightning strokes (Ref: Muller Hiller Brand, 1965)

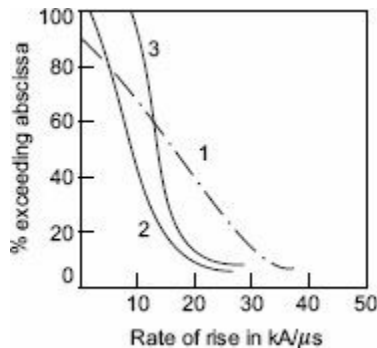


Fig. 8.10 Rate of rise of current of lightning strokes

(Ref: Westing house T and D reference book)

1. *Bergen—43 records on transmission tower*
2. *Norinder—magnetic field measurements*
3. *McEachron—strokes on Empire State Building by CRO measurements*

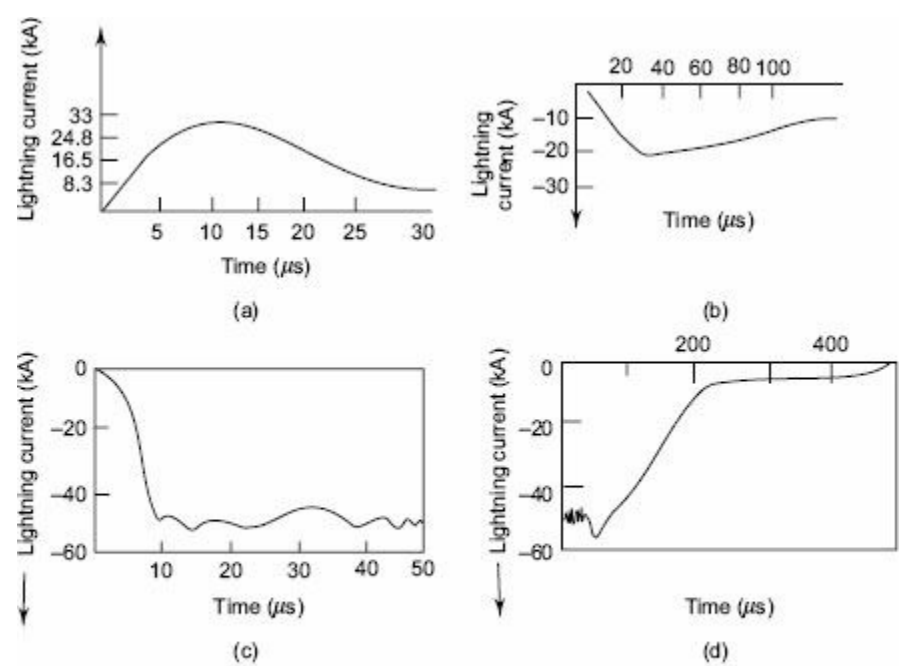
8.1.3 Parameters and Characteristics of the Lightning Strokes

The parameters and characteristics of lightning include the amplitude of the currents, the rate of rise, the probability distribution of the above, and the waveshapes of the lightning voltages and currents.

Typical oscillograms of the lightning current and voltage waveshapes on a transmission line are shown in Figs 8.11 and 8.12. The lightning current oscillograms indicate an initial high current portion which is characterized by short front times up to $10 \mu s$. The high current peak may last for some tens of microseconds followed by a long-duration low current portion lasting for several milliseconds. This last portion is normally responsible for damages (thermal damage). Lightning currents are usually measured either directly from high towers or buildings or from the transmission tower legs. The former gives high values and does not represent typical currents that occur on electrical transmission lines, and the latter gives inaccurate values due to non-uniform division of current in legs and the presence of ground wires and adjacent towers. Measurements made by several investigators and committees indicated the large strokes of currents ($> 100 \text{ kA}$) are possible (Fig. 8.7). It was shown earlier that tall objects attract a large portion of high current strokes, and this would explain the shift of the frequency distribution curves towards higher currents.

Other important characteristics are time to peak value and its rate of rise. From the field data, it was indicated that 50% of lightning stroke currents have a rate of rise greater than $7.5 \text{ kA}/\mu s$, and for 10% strokes it exceeded $25 \text{ kA}/\mu s$. The duration of the stroke currents above half the value is more than $30 \mu s$.

Measurements of surge voltages indicated that a maximum voltage, as high as 5,000 kV, is possible on transmission lines, but on the average, most of the lightning strokes give rise to voltage surges less than 1000 kV on lines. The time to front of these waves varies from 2 to $10 \mu s$ and tail times usually vary from 20 to $100 \mu s$. The rate of rise of voltage, during rising of the wave may be typically about $1 \text{ MV}/\mu s$.



(a) to a capacitive balloon (CIGRE)
 (b) on Empire State Building (McEachron)
 (c) and (d) on transmission line tower (Berger)

Fig. 8.11 Typical lightning current oscillograms (Ref: Westinghouse T and D reference book)

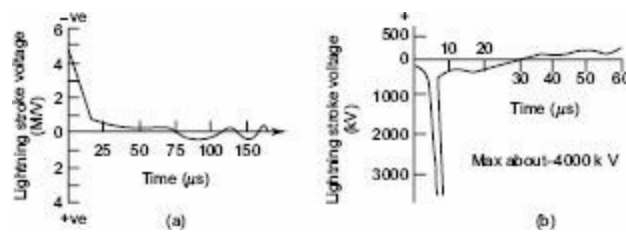


Fig. 8.12 Typical lightning stroke voltage on a transmission line without ground wire (Ref: Bell et al., 'Transactions AIEE, Vol. 50,1931)

Lightning strokes on transmission lines are classified into two groups—the direct strokes and the inducted strokes. When a thunder cloud directly discharges onto a transmission line tower or line wires it is called a direct stroke. This is the most severe form of the stroke. However, for bulk of the transmission systems the direct strokes are rare and only the induced strokes occur.

When the thunderstorm generates negative charge at its ground end, the earth objects develop induced positive charges. The earth objects of interest to electrical engineers are transmission lines and towers. Normally, it is expected that the lines are unaffected because they are insulated by string insulators. However, because of high field gradients involved, the positive charges leak from the tower along the insulator surfaces to the line conductors. This process may take quite a long time, of the order of some hundreds of seconds. When the cloud discharges to some earthed object other than the line, the transmission line is left with a huge concentration of charge (positive) which cannot leak suddenly. The transmission line and the ground will act as a huge capacitor charged with a positive charge and hence overvoltages occur due to these induced charges. This would result in a stroke and hence the name 'induced lightning stroke'.

Sometimes, when a direct lightning stroke occurs on a tower, the tower has to carry huge impulse currents. If the tower footing resistance is considerable, the potential of the tower rises to a large value, steeply with respect to the line and consequently a flashover may take place along the insulator strings. This is known as *back flashover*.

8.1.4 Mathematical Model for Lightning

During the charge formation process, the cloud may be considered to be a nonconductor. Hence, various potentials may be assumed at different parts of the cloud. If the charging process is continued, it is probable that the gradient at certain parts of the charged region exceeds the breakdown strength of the air or moist air in the cloud. Hence, local breakdown takes place within the cloud. This local discharge may finally lead to a situation where in a large reservoir of charges involving a considerable mass of cloud hangs over the ground, with the air between the cloud and the ground as a dielectric. When a streamer discharge occurs to ground by first a leader stroke, followed by main strokes with considerable currents flowing, the lightning stroke may be thought to be a current source of value I_0 with a source impedance Z_0 discharging to earth. If the stroke strikes an object of impedance Z , the voltage built across it may be taken as

$$V = IZ$$
$$= I_0 \frac{ZZ_0}{Z + Z_0} \quad (8.5)$$

$$= I_0 \frac{Z}{1 + \frac{Z}{Z_0}} \quad (8.6)$$

The source impedance of the lightning channels are not known exactly, but it is estimated to be about 1000 to 3000 Ω . The objects of interest to electrical engineers, namely, transmission line, etc. have surge impedances less than 500 Ω (overhead lines 300 to 500 Ω , ground wires 100 to 150 Ω , towers 10 to 50 Ω , etc.). Therefore, the value Z/Z_0 will usually be less than 0.1 and hence can be neglected. Hence, the voltage rise of lines, etc., may be taken to be approximately $V = I_0 Z$, where I_0 is the lightning stroke current and Z the line surge impedance.

If a lightning stroke current as low as 10,000 A strikes a line of 400 Ω surge impedance, it may cause an overvoltage of 4000 kV. This is a heavy overvoltage and causes immediate flashover of the line conductor through its insulator strings.

In case a direct stroke occurs over the top of an unshielded transmission line, the current wave tries to divide into two branches and travel on either side of the line. Hence, the effective surge impedance of the line as seen by the wave is $Z_0/2$ and taking the above example, the overvoltage caused may be only 10,000 x (400/2) = 2000 kV. If this line were to be a 132 kV line with an eleven 10 inch disc insulator string, the flashover of the insulator string will take place, as the impulse flashover voltage of the string is about 950 kV for a 2 μs front impulse wave.

The incidence of lightning strokes on transmission lines and sub-stations is related to the degree of thunderstorm activity. It is based on the level of *Thunderstorm Days (TD)* known as *Isokeraunic Level* defined as the number of days in a year when thunder is heard or recorded in a particular location. But this indication does not often distinguish between the ground strokes and the cloud-to-cloud strokes. If a measure of ground flashover density (N_g) is obtained, then the number of ground flashovers can be computed from the TD level. From the past records and the past experience, it is found that

$$N_g = (0.1 \text{ to } 0.2) \text{ TD/strokes/km}^2\text{-year.}$$

It is reported that TD is between 5 and 15 in Britain, Europe and Pacific west of North America,

and is in the range of 30 to 50 in Central and Eastern states of U.S.A. A much higher level is reported from South Africa and South America. No literature is available for the different regions in India, but a value of 30 to 50 may be taken for the coastal areas and for the central parts of India.

High incidence of lightning strokes causes direct and induced voltages in overhead lines. Further, high resistivity soils and regions like deserts, hills or mountain regions where effective earthing and low ground resistance is difficult, give rise to overvoltage problems due to lightning on power lines. Lightning accounts for most of the power interruptions.

The ground flashover density (N_g) is given by

$$N_g = K_1(TD)^b \text{ where}$$

$$K_1 = 0.04 \text{ and } b = 1.25 \text{ (Anderson) or}$$

$$K_1 = 0.054 \text{ and } b = 1.1 \text{ (Mac Gorman)}$$

From the experimental and field data collected, the number of lightning strokes or flashes on to an overhead line in open grounds with no nearby ground or tall objects can be estimated as

$$N = Ng(2.8 h^{0.6} + b/10)$$

h = height of the tower in metres, and
 b = width of the base of the tower.

The above empirical formula is of importance in estimating the number of lightning interruptions on power lines.

(a) Overvoltages due to Indirect Strokes A direct lightning stroke is one that hits either a

- (i) shielding wire (ground wire),
- (ii) tower, or
- (iii) phase conductor of a overhead powerline.

An indirect stroke is defined as one that strikes the ground, a nearby object around a power line or an earthed structure longer and higher than the power line and causes induced voltages.

The voltage induced on the power line by an indirect stroke can be due to the following reasons:

- (a) A charged cloud above the power line induces bound charges when the cloud discharges. Bound charges are released giving rise to travelling waves on power lines. (Please see [Sec. 8.1.5](#) for travelling waves)
- (b) Charges released by stepped leader strokes of a lightning stroke also give rise to the above effect.
- (c) Residual charge in the return stroke induces over voltages (electrostatic effect).
- (d) The rate of change of current in the return stroke induces overvoltage due to electromagnetic effects. The induced voltage computation is quite complex and is obtained by solving the equation.

$$V_i = \left[\nabla \phi + \frac{\delta A}{\delta t} \right] h$$

where V_i = induced voltage

- ϕ = electric potential caused by static charges (electrostatic)
- A = magnetic vector potential due to lightning currents (electromagnetic)
- h = height of conductor above the ground

Typical lightning parameters are given as

Total charge $\approx 80 \text{ C}$

Front duration $\approx 20 \mu\text{s}$

Max $dI/dt \approx 2.4 \text{ kA}/\mu\text{s}$

Stroke duration $\approx 230 \mu\text{s}$

(b) Model for Lightning Stroke Effect and Computation of Induced Voltages In lightning studies, the strokes to ground are of importance as they induce over-voltages on transmission lines and in nearby objects. Hence, a model based on lightning return stroke is presented here which assumes that the lightning channel is straight, vertical and normal to the ground plane. The return stroke current $I(z, t)$ is assumed as function of vertical co-ordinate z and time t and the initial current $I(0, t)$ is of importance in engineering applications. The electromagnetic fields associated with the lightning current and the lightning induced voltages are calculated based on the return stroke current equations taken as

$$i(z, t) = i(t - z/v) \quad z < vt$$

$$i(z, t) = 0 \quad z > vt$$

where, v is the return stroke velocity assuming that the current pulse propagates without attenuation and distortion in the upward channel. Since the current varies both in space and time, the electric field and magnetic field associated with it can be calculated using Maxwell's equations for time-varying fields.

Whenever a transmission line is nearer to the stroke channel there will be a coupling between the line and the stroke channel. The total voltage induced on the line is computed by solving the coupling equations involving the total induced voltage $u(x, t)$ and the induced current $i(x, t)$ assuming that the transmission line is in the direction x .

The factors that influence the lightning induced voltages on transmission lines are (i) the ground conductivity, (ii) the leader stroke current, and (iii) corona. The induced voltages based on the model are modified taking into account these parameters. With computer analysis, the prediction of overvoltage on the transmission lines and lightning performance of the line, i.e. flashover rate of the line insulation, is quite accurate.

8.1.5 Travelling Waves on Transmission Lines

Any disturbance on a transmission line or system such as sudden opening or closing of line, a short circuit or a fault results in the development of over voltages or over currents at that point. This disturbance propagates as a travelling wave to the ends of the line or to a termination, such as, a sub-station. Usually, these travelling waves are high-frequency disturbances and travel as waves. They may be reflected, transmitted, attenuated or distorted during propagation until the energy is absorbed. Long transmission lines are to be considered as electrical networks with distributed electrical elements. In Fig. 8.13, a typical two-wire transmission line is shown along with the distributed electrical elements, R , L , C and G .

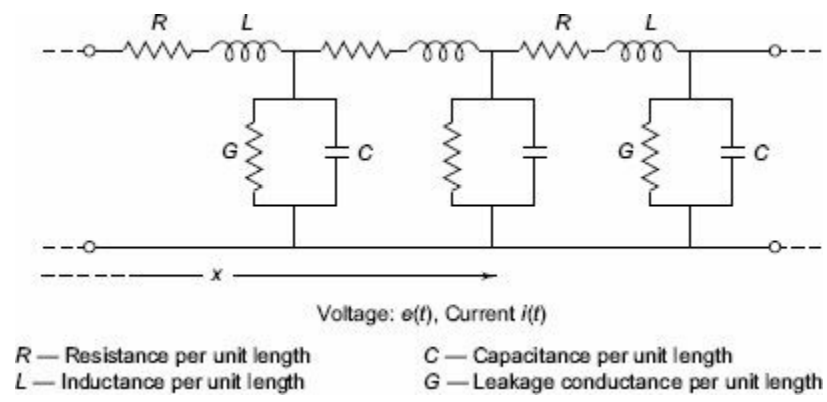


Fig. 8.13 Distributed characteristic of a long transmission line

The propagation of any travelling wave, say, a voltage wave can be analysed by considering an elemental length of the line dx . The voltage drop in the positive x -direction in the elemental length dx due to the inductance and resistance is

$$dV = \frac{\delta V}{\delta x} \cdot dx = iRdx + \frac{\delta \Psi}{\delta t} \tag{8.7}$$

Here, $\delta \Psi$ is the change of flux linkages and is equal to $i.L.dx$, where i the current through the line.

$$\begin{aligned} dV &= iR \cdot dx + \frac{\delta}{\delta t} (i \cdot dx) \\ &= \left(R + L \frac{\delta}{\delta t} \right) i \cdot dx \end{aligned} \tag{8.8}$$

The shunt current through the leakage conductance (G) and capacitance (C) is

$$di = \frac{\delta i}{\delta x} \cdot dx = VG \cdot dx + \frac{\delta}{\delta t} (V \cdot dx) \tag{8.9}$$

Here, $\nabla \Phi$ is the change in electrostatic field flux and is equal to $V C \cdot dx$, where V is the potential at the point x .

$$\begin{aligned} di &= VG \cdot dx + \frac{\delta}{\delta t} (VC \cdot dx) \\ &= \left(G + C \frac{\delta}{\delta t} \right) V \cdot dx \end{aligned}$$

Hence, the above equations can be written as

$$\frac{dV}{dx} = R + L \left(\frac{di}{dt} \right) \text{ and } \frac{di}{dx} = G + C \left(\frac{dV}{dt} \right)$$

Taking Laplace transform with respect to the time variable t , the equations can be put in the operation form as

$$\frac{\delta V}{\delta x} = (R + Ls) \cdot i = Z \cdot i,$$

and
$$\frac{\delta i}{\delta x} = (G + Cs) V = YV$$

where, $Z = (R + Ls)$ and $Y = (G + Cs)$

Eliminating i and V from above equations and differentiating w.r.t. x , we get

$$\begin{aligned} \frac{\delta^2 V}{\delta x^2} &= Z \frac{\delta i}{\delta x} \\ &= YZV = \gamma^2 V \end{aligned} \quad (8.10)$$

$$\begin{aligned} \frac{\delta^2 i}{\delta x^2} &= Y \frac{\delta V}{\delta x} \\ &= YZi = \gamma^2 i \end{aligned} \quad (8.10a)$$

where the product $YZ = \gamma^2 = RG + (RC + LG)s + LCs^2$.

The above two equations are called *wave equations* or *telegraphic equations*. The solutions for the above equations can be written in the form

$$V = e^{\gamma x} f_1(t) + e^{-\gamma x} f_2(t) \quad (8.11)$$

and
$$i = -\sqrt{Y/Z} [e^{\gamma x} f_1(t) - e^{-\gamma x} f_2(t)] \quad (8.11a)$$

where $f_1(t)$ and $f_2(t)$ are any arbitrary functions that satisfy the boundary conditions. The operator γ is simplified as

$$\begin{aligned} \gamma &= [(R + Ls)(G + Cs)]^{1/2} = \frac{1}{\sqrt{LC}} [(s + R/L)^{1/2} (s + G/C)]^{1/2} \\ &= 1/v [s + \alpha]^2 - \beta^2]^{1/2} \end{aligned} \quad (8.12)$$

where, $v = 1/\sqrt{LC}$ = propagation velocity (8.12a)

$$\alpha = 1/2 (R/L + G/C) = \text{attenuator constant} \quad (8.12b)$$

and
$$\beta = 1/2 (R/L - G/C) = \text{wavelength constant or phase constant} \quad (8.12c)$$

Also
$$\begin{aligned} \sqrt{Y/Z} &= [(G + Cs)/(R + Ls)] \\ &= \sqrt{C/L} [(s + \alpha - \beta)/(s + \alpha + \beta)]^{1/2} = Y(s) \end{aligned}$$

$Y(s)$ is called the surge admittance, the reciprocal of which

$$Z(s) = \sqrt{L/C} [(s + \alpha + \beta)/(s + \alpha - \beta)]^{-1/2} \quad (8.13)$$

$Z(s)$ is called the surge impedance of the transmission line.

(a) Classification of Transmission Lines

Transmission lines are usually classified as

- (i) lines with no loss or ideal lines,
- (ii) lines without distortion or distortionless lines,
- (iii) lines with small losses, and
- (iv) lines with infinite and finite length defined by all the four parameters.

(i) *Ideal Lines* A line is said to be an ideal line if $R = 0$ and $G = 0$. In this case the surge impedance of the line is $Z = \sqrt{L/C}$, and the surge admittance of the line is $Y = \sqrt{C/L}$. The solution for the voltage and current waves for this type of line is obtained as

$$V = f_1(t + x/v) + f_2(t - x/v) \quad (8.14)$$

$$i = Y [f_2(t - x/v) - f_1(t + x/v)] \quad (8.14a)$$

The function $f_2(t - x/v)$ represents the forward travelling wave and the function $f_1(t + x/v)$ represents the backward travelling wave. The propagation velocity for either wave is given as

$$v = 1/\sqrt{LC}$$

(ii) *Distortionless Lines* If, for any line $R/L = G/C = \alpha$ then, $\gamma = \sqrt{ZY} = \sqrt{LC}(s + \alpha)$ and the surge impedance is

$$Z(s) = \sqrt{L/C} \quad (8.15)$$

For these conditions, the solution for the wave Eqs (8.10) and (8.10a) will be modified as

$$V = \exp(\alpha x/v) f_1(t + x/v) + \exp(-\alpha x/v) f_2(t - x/v) \quad (8.16)$$

and
$$i = (1/Z) [\exp(-\alpha x/v) f_2(t - x/v) - \exp(\alpha x/v) f_1(t - x/v)] \quad (8.17)$$

The voltage and current waves for an ideal line represented by Eqs (8.14) and (8.14a) will be of the same shape. However, for a distortionless line, their magnitudes will decrease by the factor $\exp(\pm \alpha x/v)$, which is the reduction with respect to the distance x . The solutions can be rearranged by putting

$$\lambda_1 = t + x/v \text{ and } \lambda_2 = t - x/v$$

Under these conditions,

$$\begin{aligned} V &= \exp[\alpha(\lambda_1 - t)] f_1(\lambda_1) + \exp[\alpha(\lambda_2 - t)] f_2(\lambda_2) \\ &= \exp(-\alpha t) [\exp(\lambda_1) f_1(\lambda_1) + \exp(\lambda_2) f_2(\lambda_2)] \\ &= \exp(-\alpha t) [f_3(\lambda_1) + f_4(\lambda_2)] \\ &= \exp(-\alpha t) [f_3(t + x/v) + f_4(t - x/v)] \end{aligned} \quad (8.16a)$$

Similarly,
$$i = \frac{\exp(-\alpha t)}{Z} [f_4(t - x/v) - f_3(t + x/v)] \quad (8.17a)$$

Thus, the attenuation can be either with respect to the distance, x or the time, t . Equations (8.16) and (8.17) are more useful if the voltage distribution at $t = 0$ (initial condition) is specified.

(iii) *Line with Small Losses* In this type of lines, the time constants of the line are large, i.e., R/L and G/C are small. Then γ can be approximated to be equal to $(s + \alpha/v)$, and $Y(s)$ to be equal to

$\sqrt{C/L}(1-\beta/s)$. Under these conditions, the solutions for the voltage and the current waves become

$$V = \exp(\alpha x/v) \cdot f_1(t+x/v) + \exp(-\alpha x/v) \cdot f_2(t+x/v)$$

and

$$i = Y(s) \cdot V$$

$$= Y(s) [\exp(-\alpha x/v) \cdot f_2(t-x/v) + \exp(\alpha x/v) \cdot f_1(t+x/v)] + V\beta \left[\exp(\alpha x/v) \int_{-x/v}^t (t+x/v) dt - \exp(-\alpha x/v) \int_{x/v}^t f_2(t-x/v) \cdot dt \right] \quad (8.18)$$

$$= Y(s) [\exp(-\alpha x/v) \cdot f_2(t-x/v) + \exp(\alpha x/v) \cdot f_1(t+x/v)] + V\beta \left[\exp(\alpha x/v) \int_{-x/v}^t (t+x/v) dt - \exp(-\alpha x/v) \int_{x/v}^t f_2(t-x/v) \cdot dt \right] \quad (8.19)$$

The voltage Eq. (8.18) is similar to Eq. (8.14) and the current Eq. (8.19) is similar to Eq. (8.14a), along with the other expression containing the time integral of the functions f_1 and f_2 .

In a line with small losses, voltage solution shows that the voltage wave is the same as that in the case of distortionless line. However, the solution for the current wave differs by an amount equal to the energy loss in the resistance of the line. Thus, this solution is valid only for small intervals of time, i.e. for small values of $(t+x/v)$.

(iv) Exact Solution for Lines of Finite or Infinite Length Defined by all the Four Parameters The exact solution of the wave equation of this type of lines is quite complex and is normally of little practical importance. However, some of the inferences that can be drawn are

- the current and the voltage wave are dissimilar
- the attenuation and distortion due to normal line resistance and leakage conductance are of little consequence
- the surge impedance $Z(s) = e(s)/i(s)$ is a complex function and is not uniquely defined.

(b) Attenuation and Distortion of Travelling Waves

As a travelling wave moves along a line, it suffers both attenuation and distortion. The decrease in the magnitude of the wave as it propagates along the line is called attenuation. The elongation or change of wave shape that occurs is called distortion. Sometimes, the steepness of the wave is reduced by distortion. Also, the current and voltage wave shapes become dissimilar even though they may be the same initially. Attenuation is caused due to the energy loss in the line and distortion is caused due to the inductance and capacitance of the line. The energy loss may be in the conductor resistance as modified by the skin effect, changes in ground resistance, leakage resistance and non-uniform ground resistances, etc. The changes in the inductance are due to the skin effect, the proximity effect and non-uniform distribution effect of currents, and the nearness to steel structures such as transmission towers. The variation in capacitance is due to capacitance change in the insulation nearest to the ground structures, etc. If the wave shapes remain approximately the same, then the surge impedance can be taken to be constant, in which case the attenuation can be estimated. The other factor that contributes for the attenuation and distortion is the corona on the lines. For distortionless lines, the attenuation is approximated as a loss function $\phi(V)$, considering that the attenuation is due to the energy lost per unit length of the line in the resistance as the wave travels. It can be shown that

$$\phi(V) = -C \frac{dV^2}{dt} \quad (8.20)$$

For different line conditions, $\phi(V)$ and attenuation are as follows:

(i) *For Lines Having all the Parameters R, L, G and C*

$$\phi(V) = [(RC + LG)/LC]V^2 \quad (8.21)$$

$$\text{and } dV/dt = -\alpha V, \text{ where } \alpha = (1/2) [R/L] + (G/C) \quad (8.22)$$

From [Eq. \(8.20\)](#), α is called the attenuation factor.

$$\text{Hence } V = V_0 \exp(-\alpha t) \quad (8.23)$$

Hence $V = V_0 \exp(-\alpha t)$ (8.23)

where the initial voltage at $t = 0$ is taken as V_0 .

(ii) *The Skilling Formula* If $\phi(V)$ is assumed to be equal to $\beta(V - V_c)$, where V_c is critical corona voltage; then

$$dV/dt = -\beta/2c((V - V_c)/V)$$

and if the initial voltage at $t = 0$ is taken as V_0 , then

$$(V_0 - V) + V_c \ln [(V_0 - V_c)/(V - V_c)] = (\beta/2c)t \quad (8.24)$$

(iii) *The Quadratic Formula* If $\phi(V)$ is assumed to vary as

$$(V - V_c)^2, \text{ then, } dV/dt = (-\gamma/2c) [(V_0 - V_c)/(V - V_c)]^2$$

Integrating the above equation, we get

$$[(V_0 - V) \cdot V_c / (V_0 - V_c)(V - V_c)] + \ln [(V_0 - V_c)/(V - V_c)] = \gamma/2c \quad (8.25)$$

(iv) *The Foust and Manger formula* Here, $\phi(V)$ is assumed to be equal to λV^3 , so that

$$\frac{dV}{dt} = (-\lambda/2c)V^2$$

It follows from the above equation that

$$V = V_0/(1 + KV_0 t) \quad (8.26)$$

$$\text{where } K = \lambda/2c.$$

The Foust and Manger formula is simpler for the purpose of calculation and the exponential attenuation obtained in [Eq. \(8.23\)](#) can be used easily for all mathematical operations.

(v) *Attenuation due to Corona* The effect of corona is to reduce the crest of the voltage wave

under propagation, limiting the peak value to the critical corona voltage. Hence, the excess voltage above the critical voltage will cause power loss by ionising the surrounding air. This mechanism is explained as follows: the travelling wave is divided into a number of sections corresponding to different voltage levels, each voltage level corresponding to a different velocity of propagation since each lamination ionises a different diameter of the air layer surrounding the conductor and hence have different capacitances. Hence, a distortion is caused in the wave shape. This explanation ignores the power loss due to corona. The mechanism of corona power loss as explained by Skilling is as follows:

The charges liberated by the ionisation of air surrounding the conductor takes such positions on the conductor so as to make the critical field intensity (gradient) for air to reach values that cannot be exceeded. The supply of space charge to the above regions continue as long as the voltage is increasing and the energy is supplied. After the crest of wave is reached and the wave is trailing, the space charge remains constant in magnitude. The only energy loss caused during this period is due to the diffusion of ions, a process which is very slow. Based on this explanation Skilling gives the formula for corona power loss as $P = K(V - V_c)^2$, where V_c is the critical corona voltage and K is a constant.

(c) Reflection and Transmission of Waves at Transition Points

Whenever there is an abrupt change in the parameters of a transmission line, such as an open circuit or a termination, the travelling wave undergoes a transition, part of the wave is reflected or sent back and only a portion is transmitted forward. At the transition point, the voltage or current wave may attain a value which can vary from zero to two times its initial value. The incoming wave is called the incident wave and the other waves are called the reflected and transmitted waves at the transition point. Such waves are formed according to the Kirchhoff's laws and they satisfy the line differential equations. In [Fig. 8.14](#), shows a typical general transition point.

Let the transformed equations for line impedances be $Z_1(s)$, $Z_2(s)$... $Z_n(s)$, and the impedance to the ground $Z_g(s)$ be the total impedance as seen from the transition point $Z(s)$ and looking beyond the transition point, $Z_0(s)$. Taking the transition point T as reference, the distance along the line away from the transition point of the line is taken as negative, so that the incoming wave towards the transition point is counted as travelling in the positive direction. Taking the lines as lossless lines, the relations can be written as follows:

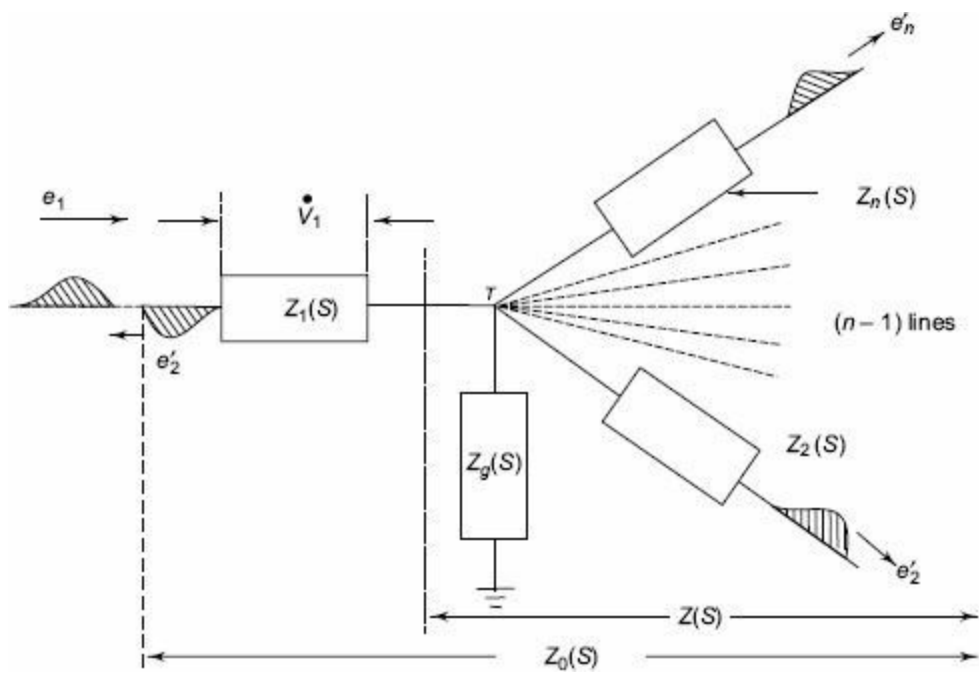


Fig. 8.14 Transition point (T) and the propagation of the wave at the transition point

$$\text{and} \quad \left. \begin{aligned} e_1/i_1 &= Z_1 \text{ (incident wave),} \\ e'_1/i'_1 &= -Z_1 \text{ (reflected wave)} \\ e''_k/i''_k &= Z_k \text{ (transmitted wave)} \end{aligned} \right\} \quad (8.27)$$

In the above equation, e , i , etc., are the unprimed quantities for the incident waves, single primed quantities e' , i' , etc. are for the reflected waves and the double primed quantities e'' , i'' , etc. are for the transmitted waves.

$$\text{At the junction point } T, \quad i_0 = i_1 + i'_1$$

$$\text{and} \quad e_0 = e_1 + e'_1 = Z_0(s) \cdot i_0 \quad (8.28)$$

From Eqs (8.27) and (8.28), the reflected voltage wave is

$$e'_1 = \left[\frac{Z_0(s) - Z_1}{Z_0(s) + Z_1} \right] \cdot e_1 \quad (8.29)$$

and the reflected current wave is

$$i'_1 = \left[\frac{Z_0(s) - Z_1}{Z_0(s) + Z_1} \right] \cdot i_1 \quad (8.30)$$

The junction voltage e_0 and the total current i_0 are given by

$$e_0 = \left[\frac{2Z_0(s)}{Z_0(s) + Z_1} \right] \cdot e_1 \quad \text{and} \quad i_0 = \left[\frac{2e_1}{Z_0(s) + Z_1} \right] \quad (8.31)$$

The coefficients multiplying the incident quantities are called the reflection coefficients.

The impedance of any line is given by $Z_k(s) + Z_k$.

Hence, the total impedance $Z_0(s) = Z_1(s) + Z(s)$

$$\text{i.e.} \quad Z_0(s) = Z_1(s) + 1 / \left[\frac{1}{Z_g(s)} + \left(\sum_{k=2}^n \frac{1}{Z_k(s) + Z_k} \right) \right] \quad (8.32)$$

Solving the above equations, the junction potential e_0 can be written as

$$e_0 = Z(s) \cdot i_0 = [2Z(s)/Z_0(s) + Z_1] \cdot e_1$$

and the ground current, $i_g = e_1/Z_g(s)$

$$= 2[\{Z(s)/Z_g(s)\} \cdot \{e_1/(Z_0(s) + Z_1)\}] \quad (8.33)$$

The transmitted voltage and current waves through any line K ($2 < K < n$) can be expressed as

$$e''_k = [\{2Z(s)/(Z_0(s) + Z_1)\} \cdot \{Z_K/(Z_K(s) + Z_K)\}] \cdot e_1 \quad (8.34)$$

and
$$i_k = [\{2Z(s)/(Z_0(s) + Z_1)\} \cdot \{e_1/(Z_K(s) + Z_K)\}]$$

The voltage drop V_K across any lumped $Z_K(s)$ is given by

$$V_K = [\{2Z(s)/(Z_0(s) + Z_1)\} \cdot \{Z_K(s)/(Z_K(s) + Z_K)\}] \cdot e_1 \quad (8.35)$$

All the above functions are in the transformed form as functions of 's' (the Laplace transform operator), and the inverse transform gives the desired time functions.

In simpler cases where the junction consists of two impedances only, the reflection and transmission coefficients become simpler and are given by reflection coefficient γ and

$$\gamma = (Z_2 - Z_1)/(Z_2 + Z_1)$$

the transmission coefficient is $(1 + \gamma)$ for voltage waves. The reflected and transmitted waves are then given by

$$e' = \gamma e, i' = -\gamma i, e'' = (1 + \gamma) \cdot e \text{ and } i'' = (1 + \gamma) \cdot i \quad (8.36)$$

It may be easily verified that

$$e/i = Z_1, e'/i' = -Z_1, \text{ and } e''/i'' = Z_2 \quad (8.37)$$

Solutions for lines terminated with lumped impedances can be easily worked out and the solutions for few cases are given in [Sec. 8.1.6](#). The above analysis of the travelling waves indicate how the waves are modified at transition points. There can be doubling effect at the junction point which contributes to the over voltages in power system networks. In many overvoltage calculations, travelling wave analysis will be useful for overvoltage and over current calculations.

Successive Reflections and Lattice Diagrams In many problems involving short cable lengths, or lines tapped at intervals, the travelling waves encounter successive reflections at the transition point. It is exceedingly difficult to calculate the multiplicity of these reflections and in his book, Bewley has given the lattice or time-space diagrams from which the motion of reflected and transmitted waves and their positions at every instant can be obtained. The principles observed in the lattice diagrams are as follows:

- (i) All waves travel downhill, i.e. into the positive time.
- (ii) The position of the wave at any instant is given by means of the time scale at the left of the lattice

diagram.

- (iii) The total potential at any instant of time is the superposition of all the waves which arrive at that point until that instant of time, displaced in position from each other by time intervals equal to the time differences of their arrival.
- (iv) Attenuation is included so that the amount by which a wave is reduced is taken care of.
- (v) The previous history of the wave, if desired can be easily traced. If the computation is to be carried out at a point where the operations cannot be directly placed on the lattice diagram, the arms can be numbered and the quantity can be tabulated and computed.

The above comprehensive description can be understood by considering the example shown in [Fig. 8.15](#).

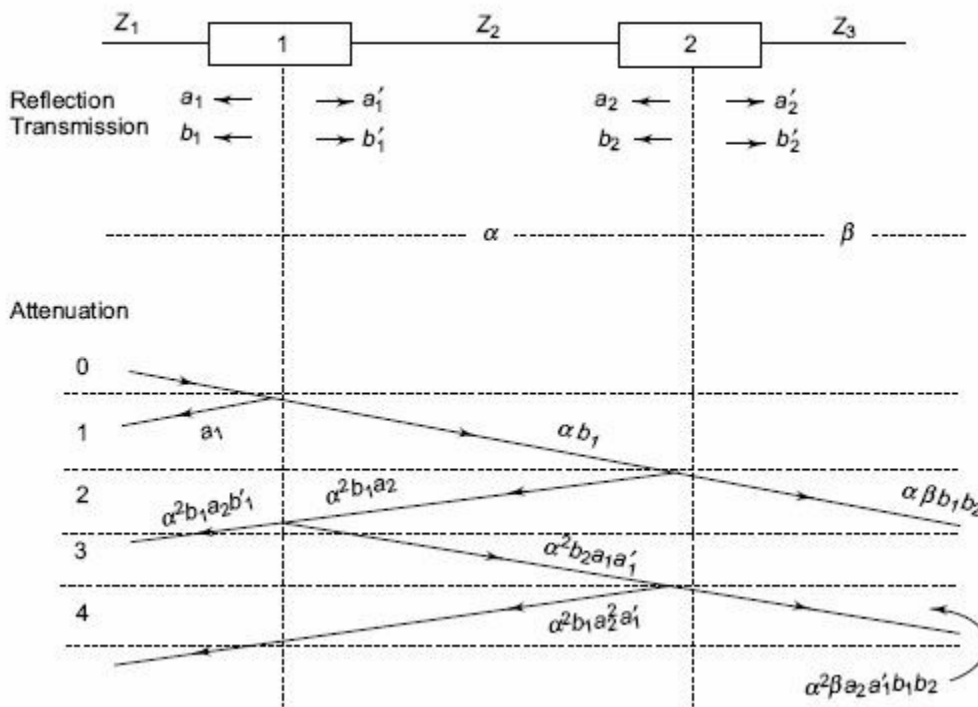


Fig. 8.15 Reflection lattice of a travelling wave

In the arrangement shown in the figure, there are two junctions 1 and 2. The travel times for the waves are different through Z_1 , Z_2 , and Z_3 . The lines with surge impedances Z_1 , Z_2 , and Z_3 are connected on either side of the junctions. Let α and β be the attenuation coefficients for the two sections Z_2 and Z_3 . Let a_1 and a'_1 be the reflection coefficients for the waves approaching from the left and the right at junction 1, and a_2 and a'_2 be the corresponding reflection coefficients at junction 2. Similarly, let b_1 and b'_1 be the transmission coefficients for the waves that approach from the left and the right at junction 1, and the corresponding coefficients be b_2 and b'_2 at junction 2. To construct the lattice diagram, the position O is taken when the wave coming from Z_1 reaches junction 1. Junction 2 is taken to scale at the time interval equal to the travel time through the line Z_2 between the junctions 1 and 2. The diagram is drawn by choosing a suitable time scale. The reflection and the transmission factors are marked as shown in the figure. The process of calculation is indicated on the slope of the lines in the diagram. The process can be continued for up to the required time interval. A numerical example illustrating the use of the above technique for the computation is given under worked examples (Example 8.6).

8.1.6 Behaviour of Rectangular Travelling Wave [Unit Step Function $U(t)$] at Transition Points—Typical Cases

Reflection and transmission of a travelling wave at junction points of unequal impedances in a transmission line are of great importance in transmission systems. Depending on the type of impedance at transition points, the travelling wave is modified, and sometimes a voltage rise or build-up of voltage can occur. The following cases are of practical importance and as such are discussed here. The solution is obtained using the Laplace Transforms rather than using operational calculus, as many of the readers may not be familiar with the Heaviside Operational Calculus.

Case (i) Open-ended Transmission Line of Surge Impedance Z

Let the voltage of travelling wave incident on the line be

$$e = EU(t)$$

then, $Z_1 = Z$ and $Z_2 = \infty$

$$\begin{aligned} \therefore \text{coefficient of reflection} \quad \Gamma &= \frac{(Z_2 - Z_1)}{(Z_2 + Z_1)} \\ &= \frac{(1 - Z_1/Z_2)}{(1 + Z_1/Z_2)} \end{aligned}$$

$$\begin{aligned} \text{Substituting} \quad \Gamma &= \frac{(1 - Z/\infty)}{(1 + Z/\infty)} \\ &= 1 \end{aligned}$$

\therefore voltage of the reflected wave, $e' = \Gamma e = e = E U(t)$ and the voltage of the transmitted wave, $e'' = (1 + \Gamma)e = 2e = 2EU(t)$

Hence the voltage at the open end rises to double its value.

Case (ii) Short-circuited Line

Voltage of the wave, $e = EU(t)$

Surge impedances $Z_1 = Z$ and $Z_2 = 0$

$$\therefore \text{coefficient of reflection,} \quad \Gamma = \frac{0 - Z}{0 + Z} = -1$$

\therefore voltage of the reflected wave, $e' = \Gamma \cdot e$
 $= -EU(t)$

The voltage of the transmitted wave, $e'' = (1 + \Gamma)e = 0$

Further i' , the magnitude of the reflected current wave

$$\begin{aligned} &= \left| -\frac{e'}{Z} \right| \\ &= \frac{EU(t)}{Z} \text{ (the magnitude of the incident current wave)} \end{aligned}$$

The total current at the junction point

$$i_0 = (i + i') = 2i$$

Thus, the current at the junction point rises to double the value of the incident current wave.

Case (iii) Line Terminated with a Resistance Equal to the Surge Impedance of the

Line

In this case, $Z_1 = Z$ and $Z_2 = R = Z$

\therefore coefficient of reflection,

$$\Gamma = \frac{(R - Z)}{(R + Z)} = 0$$

\therefore voltage of the reflected wave, e' is $\Gamma e = 0$

The voltage of the transmitted wave is $(1 + \Gamma)e = e$

Thus, there is no reflected wave. There is no discontinuity of the line, and the travelling wave proceeds without reflection and disappears. It is very important to note that there will be no reflections at the junction, if a transmission line or cable is terminated with a resistance equal to the surge impedance of the line or cable.

Case (iv) Line Terminated with a Capacitor

In this case, $e = E U(t)$, $Z_1 = Z$, and $Z_2 = \frac{1}{Cs}$

where s is the Laplace transform operator.

$$\begin{aligned} \text{The coefficient of reflection } \Gamma &= \frac{(Z_2 - Z_1)}{(Z_2 + Z_1)} \\ &= \frac{\left(\frac{1}{Cs} - Z\right)}{\left(\frac{1}{Cs} + Z\right)} \\ &= \frac{(1 - CZs)}{(1 + CZs)} \end{aligned}$$

The voltage of the reflected wave, $e' = \Gamma e$

$$\begin{aligned} \text{Taking the Laplace transform, } e'(s) &= \frac{(1 - CZs)}{(1 + CZs)} \frac{E}{s} \\ &= \left[1 - \frac{2CZs}{1 + CZs}\right] \frac{E}{s} \\ &= \left[\frac{1}{s} - \frac{2CZs}{1 + CZs}\right] E \end{aligned}$$

Taking the inverse transform

$$e' = [1 - 2 \exp(-t/CZ)] EU(t)$$

The voltage of the Laplace transformed transmitted wave,

$$\begin{aligned}
e''(s) &= (1 + \Gamma) e(s) \\
e''(S) &= (1 + \Gamma) \frac{E}{s} \\
&= \left[1 + \frac{(1 - CZs)}{(1 + CZs)} \right] \frac{E}{s} \\
&= \left[2 - \frac{(2CZs)}{(1 + CZs)} \right] \frac{E}{s} \\
&= \left[\frac{1}{s} - \frac{CZ}{(1 + CZs)} \right] \frac{2E}{s}
\end{aligned}$$

Taking the inverse transforms

$$e'' = 2 \left[1 - \exp\left(-\frac{t}{CZ}\right) \right] EU(t)$$

From the expression for e'' , it can be inferred that the steepness of the front is reduced and the wave rises slowly in an exponential manner. The capacitor initially acts as a short circuit and is charged through the line impedance Z . The voltage at the junction point finally rises to twice the magnitude of the incident wave.

Case (v) Line Terminated by an Inductance L

In this case, $e = EU(t)$

$$Z_1 = Z, \text{ and } Z_2 = Ls$$

$$\text{The coefficient of reflection } \Gamma = \frac{(Ls - Z)}{(Ls + Z)} = \frac{\left(s - \frac{Z}{L}\right)}{\left(s + \frac{Z}{L}\right)}$$

Voltage of the reflected wave, $e' = \Gamma e$

$$\begin{aligned}
\therefore e'(s) &= \frac{\left(s - \frac{Z}{L}\right)}{\left(s + \frac{Z}{L}\right)} \frac{E}{s} \\
&= \left[\frac{1}{s + \frac{Z}{L}} - \frac{Z/L}{s\left(s + \frac{Z}{L}\right)} \right] E
\end{aligned}$$

Taking inverse transforms,

$$e' = - \left[1 - 2 \exp\left(-\frac{Z}{L}t\right) \right] EU(t)$$

Voltage of the transformed transmitted wave, $e''(s) = (1 + \Gamma)e(s)$

$$\begin{aligned} \therefore e''(s) &= \left[1 + \frac{\left(s - \frac{Z}{L}\right)}{\left(s + \frac{Z}{L}\right)} \right] \frac{E}{s} \\ &= \frac{2E}{\left(s + \frac{Z}{L}\right)} \end{aligned}$$

$$\therefore e'' = 2E \exp\left(-\frac{Z}{L}t\right)$$

The voltage across the inductor initially rises to double the value of the incident wave and decays exponentially. This is of importance when long lines are terminated with inductors or transformers on open circuit.

Case (vi) Line having a Series Inductor

Let the surge impedance of the line be Z before and after the series inductor L . Considering the junction point after the inductor L , $e = E U(t)$, $Z_1 = (Z + Ls)$, and $Z_2 = Z$.

$$\text{The coefficient of reflection } \Gamma = \frac{(Z_2 - Z_1)}{(Z_2 + Z_1)}$$

Voltage of the transformed reflected wave, $e'(s) = \Gamma e(s)$

$$\begin{aligned} \therefore e'(s) &= -\frac{Ls}{2Z + Ls} \frac{E}{s} \\ &= -\frac{EL}{2Z + Ls} \\ &= -\frac{1}{\left(s + 2\frac{Z}{L}\right)} E \end{aligned}$$

Taking the inverse transform,

$$e' = -E \exp\left(-\frac{2Z}{L}t\right)$$

$$e''(s) = (1 + \Gamma)E = \left[\frac{E}{s} - \frac{E}{\left(s + 2\frac{Z}{L}\right)} \right]$$

$$\therefore e'' = \left[1 - \exp\left(-\frac{2Z}{L}t\right) \right] EU(t)$$

As seen from the expression for e'' , the steepness of the propagated wave through the inductor, i.e., the transmitted wave into the second portion of the line is reduced. The series inductor produced the same effect as that of a shunt capacitor on a transmission line.

Case (vii) Line Terminated with a Transformer (Taken as an L-C Parallel Combination)

$$e = EU(t)$$

$$Z_1 = Z$$

$$Z_2 = L \text{ and } C \text{ in parallel}$$

i.e.,

$$Z_2 = \frac{\left(LS \frac{1}{Cs} \right)}{\left(LS + \frac{1}{Cs} \right)}$$

$$= \frac{s}{C} \left(\frac{1}{s^2 + \frac{1}{LC}} \right)$$

∴ coefficient of reflection,

$$\Gamma = \frac{(Z_2 + Z_1)}{(Z_2 + Z_1)} = \frac{\left(\frac{s}{C(s^2 + 1/LC)} - Z \right)}{\left(\frac{s}{C(s^2 + 1/LC)} + Z \right)}$$

$$= - \frac{(s^2 - s/CZ + 1/LC)}{(s^2 + s/CZ + 1/LC)}$$

$$\therefore 1 + \Gamma = \frac{\left(2 \frac{s}{CZ} \right)}{\left(s^2 + \frac{s}{CZ} + \frac{1}{LC} \right)}$$

Let $\frac{1}{CZ} = \alpha$ and $\frac{1}{LC} = \omega_0^2$ so that Γ can be written as

$$\Gamma = - \frac{(s^2 - \alpha s + \omega_0^2)}{(s^2 + \alpha s + \omega_0^2)}$$

and

$$1 + \Gamma = \frac{2\alpha s}{(s^2 + \alpha s + \omega_0^2)}$$

$$e'(s) = \Gamma e(s) = \frac{(s^2 - \alpha s + \omega_0^2)}{(s^2 + \alpha s + \omega_0^2)} \left(\frac{E}{s} \right)$$

The reflected wave,

$$= - \left(\frac{1}{s} - \frac{2\alpha}{(s^2 + \alpha s + \omega_0^2)} \right) E$$

Taking the inverse transform.

$$e' = - \left\{ -1 - \frac{2\alpha}{n-m} [\exp(-mt) - \exp(-nt)] \right\} EU(t) \text{ if } \omega_0^2 < \left(\frac{\alpha}{2} \right)^2$$

where n and m are roots of $(s^2 + \alpha s + \omega_0^2)$.

$$e = - E U(t) \left[1 - \frac{2\alpha}{\sqrt{\omega_0^2 - (\alpha/2)^2}} \times \exp(-\alpha/2)t \right]$$

Or

$$\times \sin \sqrt{\omega_0^2 - \left(\frac{\alpha}{2} \right)^2} t \quad \text{if } \omega_0^2 > (\alpha/2)^2$$

The transmitted wave, $e''(s) = (1 + \Gamma) e(s) = \frac{2\alpha E}{S^2 + \alpha s + \omega_0^2} \frac{E}{s}$

$$= \frac{2\alpha E}{S^2 + \alpha s + \omega_0^2}$$

Taking the inverse transform

$$e'' = \frac{2\alpha}{n-m} [\exp(-mt) - \exp(-nt)] EU(t), \text{ if } \omega_0^2 < (\alpha/2)^2$$

and
$$e'' = \left[\frac{2\alpha}{\sqrt{\omega_0^2 - (\alpha/2)^2}} \exp(-\alpha/2t) \sin \sqrt{\omega_0^2 - (\alpha/2)^2} t \right] EU(t)$$
 if $\omega_0^2 > (\alpha/2)^2$

The transmitted wave reaching the transformer will be either a double exponential (standard impulse type) or a damped sinusoidal wave and the steepness of the wave front gets reduced.

The above analysis shows that travelling wave is modified at the transition points, and the steepness of the wave front is reduced in certain cases. There can be doubling effect at the junction points such as an open ended line or an inductance termination. These also contribute for further overvoltages at the transition points in a transmission system.

8.2 OVERVOLTAGE DUE TO SWITCHING SURGES, SYSTEM FAULTS AND OTHER ABNORMAL CONDITIONS

8.2.1 Introduction

Till the time when the transmission voltages were about 220 kV and below, overvoltages due to lightning were of very high order and overvoltages generated inside the system were not of much consequence. In later years, with increase in transmission voltages (400 kV and above), the overvoltages generated inside the system reached the same order of magnitude as those of lightning overvoltages, or higher. Secondly, the overvoltages thus generated last for longer durations and therefore are severe and more dangerous to the system. Unlike the lightning overvoltages, the switching and other types of overvoltages depend on the normal voltage of the system and hence increase with increased system voltage. In insulation co-ordination, where the protective level of any particular kind of surge diverter is proportional to the maximum voltage, the insulation level and the cost of the equipment depends on the magnitudes of these overvoltages. In the EHV range, it is the switching surge and other types of overvoltages that determine the insulation level of the lines and other equipment and consequently, they also determine their dimensions and costs.

8.2.2 Origin of Switching Surges

The making and breaking of electric circuits with switchgear may result in abnormal overvoltages in power systems having large inductances and capacitances. The overvoltages may go as high as six times the normal power frequency voltage. In circuit breaking operation, switching surges with a high rate of rise of voltage may cause repeated restriking of the arc between the contacts of a circuit breaker, thereby causing destruction of the circuit breaker contacts. The switching surges may include high natural frequencies of the system, a damped normal frequency voltage component, or the restriking and recovery voltage of the system with successive reflected waves from terminations.

8.2.3 Characteristics of Switching Surges

The waveshapes of switching surges are quite different and may have origin from any of the following sources.

- (i) De-energizing of transmission lines, cables, shunt capacitor, capacitor banks, banks, etc.
- (ii) Disconnection of unloaded transformers, reactors, etc.
- (iii) Energization or reclosing of lines and reactive loads
- (iv) Sudden switching off of loads
- (v) Short circuits and fault clearances
- (vi) Resonance phenomenon like ferro-resonance, arcing grounds, etc.

Typical waveshapes of the switching surges are given in [Figs 8.16a to e](#).

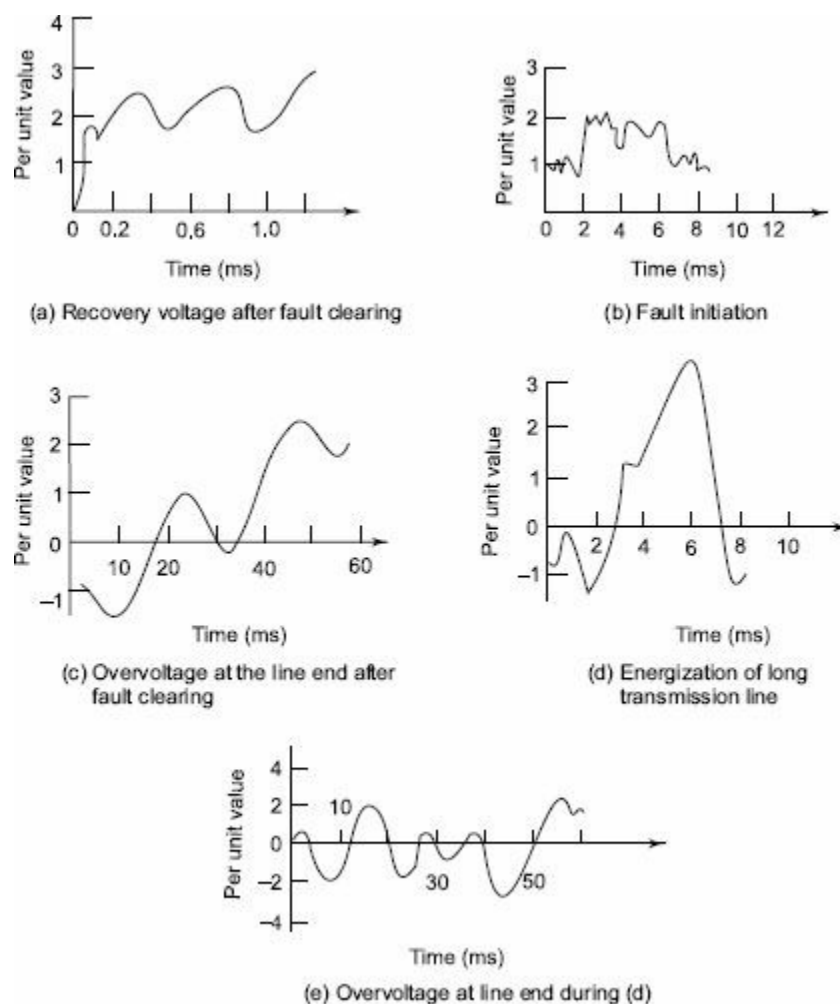


Fig. 8.16 Typical waveshapes of switching surge voltages

From the figures of the switching surges it is clear that the overvoltages are irregular (oscillatory or unipolar) and can be of high frequency or power frequency with its harmonics. The relative magnitudes of the overvoltages may be about 2.4 p.u. in the case of transformer energizing and 1.4 to 2.0 p.u. in switching transmission lines.

(a) Switching Overvoltages in EHV and UHV Systems

The insulation has the lowest strength for switching surges with regard to long air gaps. Further, switching overvoltages are of relatively higher magnitudes as compared to the lightning overvoltages for UHV systems. Overvoltages are generated in EHV systems when there is a sudden release of

internal energy stored either in the electrostatic form (in the capacitance) or in the electromagnetic form (in the inductance). The different situations under which this happens are summarized as

- (i) interruption of low inductive currents (current chopping) by high speed circuit breakers. This occurs when the transformers or reactors are switched off
- (ii) interruption of small capacitive currents, such as switching off of unloaded lines, etc.
- (iii) ferro-resonance condition

This may occur when poles of a circuit breaker do not close simultaneously

- (iv) energization of long EHV or UHV lines

Transient overvoltages in the above cases can be of the order of 2.0 to 3.3 p.u. and will have magnitudes of the order of 1200 kV to 2000 kV on 750 kV systems. The duration of these overvoltages varies from 1 to 10 ms depending on the circuit parameters. It is seen that these are of comparable magnitude or even higher than those that occur due to lightning. Sometimes the overvoltages may last for several cycles. The other situations of switching that give rise to switching overvoltages of short duration (0.5 to 5 ms) and lower magnitudes (2.0 to 2.5 p.u.) are

- (a) single pole closing of circuit breaker
- (b) interruption of fault current when the $L-G$ or $L-L$ fault is cleared
- (c) resistance switching used in circuit breakers
- (d) switching lines terminated by transformers
- (e) series capacitor compensated lines
- (f) sparking of the surge diverter located at the receiving end of the line to limit the lightning overvoltages

The overvoltages due to the above conditions are studied or calculated from

- (a) mathematical modelling of a system using digital computers
- (b) scale modelling using transient network analysers
- (c) by conducting field tests to determine the expected maximum amplitude of the overvoltages and their duration at different points on the line. The main factors that are investigated in the above studies are
 - (i) the effect of line parameters, series capacitors and shunt reactors on the magnitude and duration of the transients.
 - (ii) the damping factors needed to reduce the magnitude of over-voltages
 - (iii) the effect of single pole closing, restriking and switching with series resistors in circuit breakers on the overvoltages, and
 - (iv) the lightning arrester spark over characteristics.

It is necessary in EHV and UHV systems to control the switching surges to a safe value of less than 2.5 p.u. or preferably to 2.0 p.u. or even less. The measures taken to control or reduce the overvoltages are

- (i) one step or multi-step energization of lines by preinsertion of resistors,
- (ii) phase controlled closing of circuit breakers with proper sensors,
- (iii) drainage of trapped charges on long lines before the reclosing of the lines, and
- (iv) limiting the overvoltages by using surge diverters.

The first three methods, if used properly will limit the switching overvoltages between 1.5 to 2.0

p.u.

In [Table 8.1](#), a summary of the extent of overvoltages that can be developed under various conditions of switching is given.

Table 8.1 Overvoltages due to switching operations under different conditions Maximum value of the system line-to-ground voltage = 1.0 p.u.

Sl.no.	Type of operation	Overvoltage (p.u.)
1	Switching an open ended line with:	
	(a) infinite bus as source with trapped charges on line	4.1
	(b) infinite bus as source without trapped charges	2.6
	(c) de-energising an unfaulted line with a restrike in the circuit breaker	2.7
	(d) de-energising an unfaulted line with a line to ground fault (about 270 km in length)	1.3
2	(a) Switching a 500 kV line through an autotransformer, 220 kV/500 from the L.V. side	2.0
	(b) switching a transformer terminated line	2.2
	(c) series capacitor compensated line with 50% compensation	2.2
	(d) series capacitor compensated line with shunt reactor compensation	2.6
3	High speed reclosing of line after fault clearance	3.6

(b) Overvoltage due to Switching Operations in Gas-Insulated Sub-stations

Nowadays, gas-insulated sub-stations and systems in voltage ranges of 33 kV to 400 kV have come up due to land and space limitations in urban and highly populated areas. Very fast transient voltages are generated during switching operations such as

- (i) closing ground switch
- (ii) fault clearing
- (iii) opening or closing a disconnecter switch underload, etc.

A large number of pre-or re-strikes occur during a disconnecter switch or circuit breaker operations. The switching behaviour and pattern of voltages are shown in [Fig. 8.17](#)(a to c). During the opening operation, sparking occurs as soon as the voltage between the source and load side exceeds the dielectric strength of the gap between the contacts. After restrike high frequency current flows through the spark gap and will equalize the capacitive load voltage and source voltage. The frequency of pulse generated is given by

$$f = \frac{1}{4T} = \frac{75}{d} \text{ where}$$

where T is the transit time of the line in GIS (μs)

d duct length in meters and f = frequency in MHz

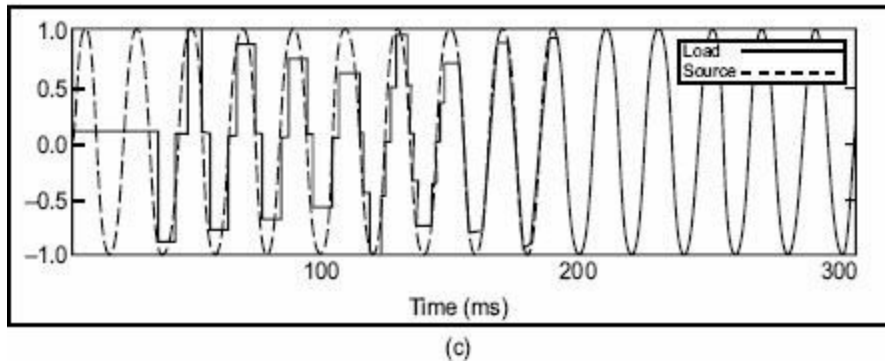
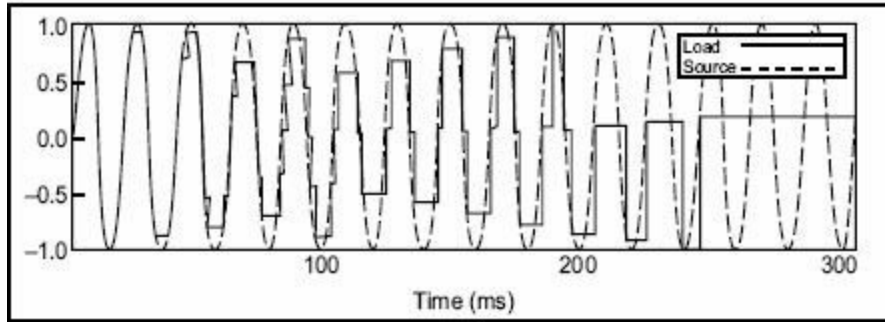
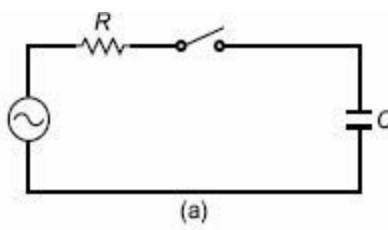


Fig. 8.17 Variation of load- and source-side voltages during disconnector switching: (a) scheme of the equivalent circuit, (b) opening operation, and (c) closing operation

f is found to be about 5 to 10 MHz which is equivalent to a fast transient of duration $0.1 \mu s$ (100 ns). A typical transient voltage wave form is shown in [Fig. 8.17 d and e](#).

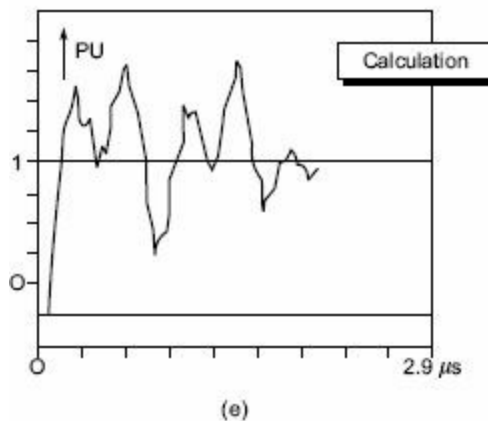
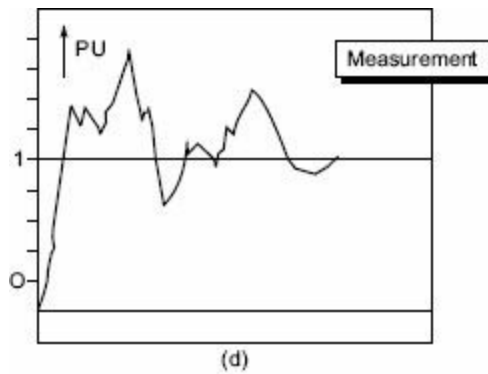


Fig. 8.17 *(d and e) Measurement and simulation of overvoltages in a GIS at closing a switch*

8.2.4 Power Frequency Overvoltages in Power Systems

The power frequency overvoltages occur in large power systems and they are of much concern in EHV systems, i.e., systems of 400 kV and above. The main causes for power frequency and its harmonic overvoltages are

- (a) sudden loss of loads,
- (b) disconnection of inductive loads or connection of capacitive loads,
- (c) Ferranti effect, unsymmetrical faults, and
- (d) saturation in transformers, etc.

Overvoltages of power frequency harmonics and voltages with frequencies nearer to the operating frequency are caused during tap changing operations, by magnetic or ferro-resonance phenomenon in large power transformers, and by resonating overvoltages due to series capacitors with shunt reactors or transformers.

The duration of these overvoltages may be from one to two cycles to a few seconds depending on the overvoltage protection employed.

(a) Sudden Load Rejection Sudden load rejection on large power systems causes the speeding up of generator prime movers. The speed governors and automatic voltage regulators will intervene to restore normal conditions. But initially both the frequency and voltage increase. The approximate voltage rise, neglecting losses, etc. may be taken as

$$v = \frac{f}{f_0} E' \left[\left(1 - \frac{f}{f_0} \right) \frac{x_s}{x_c} \right] \quad (8.38)$$

where x_s is the reactance of the generator (\approx the sum of the transient reactances of the generator and the transformer), x_c is the capacitive reactance of the line at open end at increased frequency, E' the voltage generated before the over-speeding and load rejection, f is the instantaneous increased frequency, and f_0 is the normal frequency.

This increase in voltage may go to as high as 2.0 per unit (p.u.) value with 400 kV lines. The voltage at the sending end is affected by the line length, short circuit MVA at sending end bus, and reactive power generation of the line (due to line capacitive reactance and any shunt or series capacitors). Shunt reactors may reduce the voltage to 1.2 to 1.4 p.u.

(b) Ferranti Effect Long uncompensated transmission lines exhibit voltage rise at the receiving end. The voltage rise at the receiving end V_2 is approximately given by

$$V_2 = \frac{V_1}{\cos \beta l} \quad (8.39)$$

where, V = sending end voltage,

l = length of the line,

β = phase constant of the line [Eq. \(8.12c\)](#)

$$\approx \left[\frac{(R + j\omega L)(G + j\omega C)}{LC} \right]^{1/2}$$

\approx about 6° per 100 km line at 50 Hz frequency. R , L , G , and C are as defined in [Sec. 8.1.5](#), and

ω = angular frequency for a line shown in [Fig. 8.18](#).

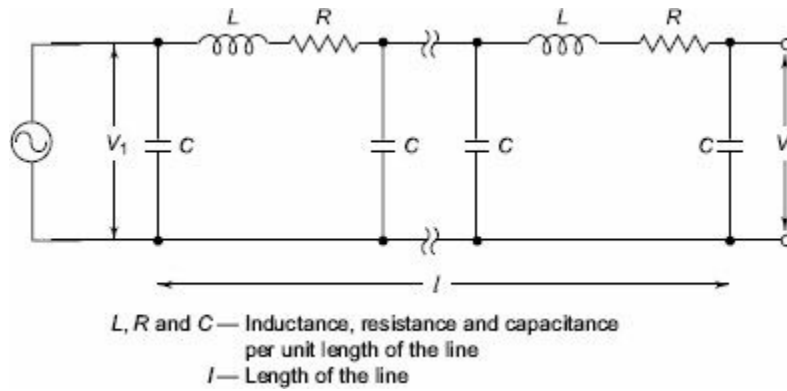


Fig. 8.18 Typical uncompensated long transmission line

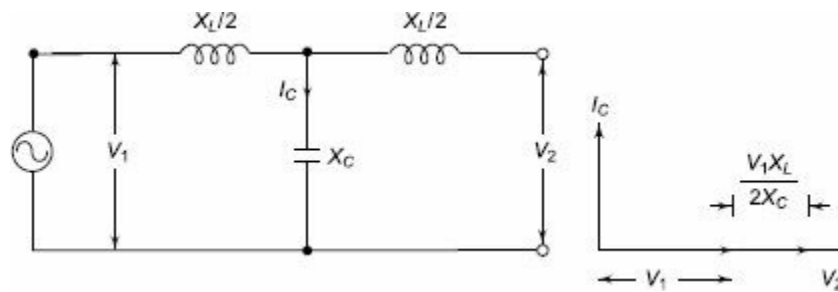


Fig. 8.19 Vector (phase) diagram of an open circuited uncompensated line showing Ferranti effect

Considering that the line capacitance is concentrated at the middle of the line, under open circuit conditions at the receiving end, the line charging current

$$I_C \approx j\omega CV_1 = \frac{V_1}{X_C} \quad (8.40)$$

$$\text{and the voltage } V_2 \approx V_1 \left[1 - \frac{X_L}{2X_C} \right] \quad (8.41)$$

where, X_L = line inductive reactance, and
 X_C = line capacitive reactance.

This approximation is shown in [Fig. 8.19](#).

Equation (8.39) gives a better approximation when the line distributed parameters R , L , G , and C per unit length are known.

Transmission line approximation for line in [Fig. 8.18](#).

(c) Ground Faults and Their Effects Single line to ground faults cause rise in voltages in other healthy phase. Usually, with solidly grounded systems, the increases in voltage (phase to ground value) will be less than the line-to-line voltage. With effectively ground systems, i.e. with

$$\frac{X_0}{X_1} \leq 3.0 \text{ and } \frac{R_0}{X_1} \leq 1.0$$

(where, R_0 and X_0 are zero sequence resistance and reactance and X_1 is the positive sequence reactance of the system), the rise in voltage of the healthy phases does not usually exceed 1.4 per unit.

(d) Saturation Effects When voltages above the rated value are applied to transformers, their magnetizing currents (no load currents also) increase rapidly and may be about the full rated current for 50% overvoltage. These magnetizing currents are not sinusoidal in nature but are of a peaky waveform. The third, fifth, and seventh harmonic contents may be 65%, 35%, and 25% of the exciting current of the fundamental frequency corresponding to an overvoltage of 1.2 p.u. For third and its multiple harmonics, zero sequence impedance values are effective, and delta connected windings suppress them. But the shunt connected capacitors and line capacitances can form resonant circuits and cause high third harmonic overvoltages. When such overvoltages are added, the voltage rise in the lines may be significant. For higher harmonics a series resonance between the transformer inductance and the line capacitance can occur which may produce even higher voltages.

8.2.5 Control of Overvoltages due to Switching

The overvoltages due to switching and power frequency may be controlled by

- (a) energization of transmission lines in one or more steps by inserting resistances and withdrawing them afterwards,
- (b) phase controlled closing of circuit breakers,
- (c) drainage of trapped charges before reclosing,
- (d) use of shunt reactors, and
- (e) limiting switching surges by suitable surge diverters.

(a) Insertion of Resistors It is normal and a common practice to insert resistances R in series with circuit breaker contacts when switching on but short circuiting them after a few cycles. This will reduce the transients occurring due to switching. The voltage step applied is first reduced to $Z_0/(R + Z_0)$ per unit where Z_0 is the surge impedance of the line. It is reflected from the far end unchanged and again reflected back from the near end with reflection factor $(R - Z_0)/(R + Z_0)$ per unit. If $R = Z_0$, there is no reflection from the far end. The applied step at the first instance is only 0.5 per unit.

When the resistor is short circuited, a voltage step equal to the instantaneous voltage drop enters the line. If the resistor is kept for a duration larger than 5 ms (for 50 Hz sine wave = 1/4 cycle duration), it can be shown from successive reflections and transmissions, that the overvoltage may reach as high as 1.2 p.u. for a line length of 500 km. But for conventional opening of the breaker, the resistors have too high an ohmic value to be effective for resistance closing. Therefore, pre-insertion of suitable value resistors in practice is done to limit the overvoltage to less than 2.0 to 2.5 p.u. Normal time of insertion is 6 to 10 ms.

(b) Phase-Controlled Switching Overvoltages can be avoided by controlling the exact instances of the closing of the three phases separately. But this necessitates the use of complicated controlling equipment and therefore is not adopted.

(c) Drainage of Trapped Charge When lines are suddenly switching off, 'electric charge' may be left on capacitors and line conductors. This charge will normally leak through the leakage path of the insulators, etc. Conventional potential transformers (magnetic) may also help the drainage of the charge. An effective way to reduce the trapped charges during the lead time before reclosing is by temporary insertion of resistors to ground or in series with shunt reactors and removing before the closure of the switches.

(d) Shunt Reactors Normally, all EHV lines will have shunt reactors to limit the voltage rise due to the Ferranti effect. They also help in reducing surges caused due to sudden energizing. However, shunt reactors cannot drain the trapped charge but will give rise to oscillations with the capacitance of the system. Since the compensation given by the reactors will be less than 100%, the frequency of oscillation will be less than the power frequency and overvoltages produced may be as high as 1.2 p.u. Resistors in series with these reactors will suppress the oscillations and limit the overvoltages.

Limiting the switching and power frequency overvoltages by using surge diverters is discussed in the next section.

8.2.6 Protection of Transmission Lines against Overvoltages

Protection of transmission lines against natural or lightning overvoltages and minimizing the lightning overvoltages are done by suitable line designs, providing guard and ground wires, and using surge diverters. Switching surges and power frequency overvoltages are accounted for by providing greater insulation levels and with proper insulation co-ordination. Hence, the above two protection schemes are dealt with separately in the next two sections.

Protection against Lightning Overvoltages and Switching Surges of Short Duration

Overvoltages due to lightning strokes can be avoided or minimized in practice by

- (a) shielding the overhead lines by using ground wires above the phase wires,
- (b) using ground rods and counter-poise wires, and
- (c) including protective devices like expulsion gaps, protector tubes on the lines, and surge diverters at the line terminations and substations.

(a) Lightning Protection Using Shielded Wires or Ground Wires Ground wire is a conductor run parallel to the main conductor of the transmission line supported on the same tower and earthed at every equally and regularly spaced towers. It is run above the main conductor of the line. The ground wire shields the transmission line conductor from induced charges, from clouds as well as from a lightning discharge. The arrangements of ground wires over the line conductor is shown in [Fig. 8.20](#).

The mechanism by which the line is protected may be explained as follows. If a positively charged cloud is assumed to be above the line, it induces a negative charge on the portion below it, of the transmission line. With the ground wire present, both the ground wire and the line conductor get the induced charge. But the ground wire is earthed at regular intervals, and, as such, the induced charge is drained to the earth; only the potential difference between the ground wire and the cloud and that between the ground wire and the transmission line wire will be in the inverse ratio of their respective capacitances [assuming the cloud to be a perfect conductor and the atmospheric medium (air) a dielectric]. As the ground wire is nearer to the line wire, the induced charge on it will be much less and hence the potential rise will be quite small. The effective protection or shielding given by the ground wire depends on the height of the ground wire above the ground (h) and the protection or shielding angle θ_s (usually 30°) as shown in [Fig. 8.20](#).

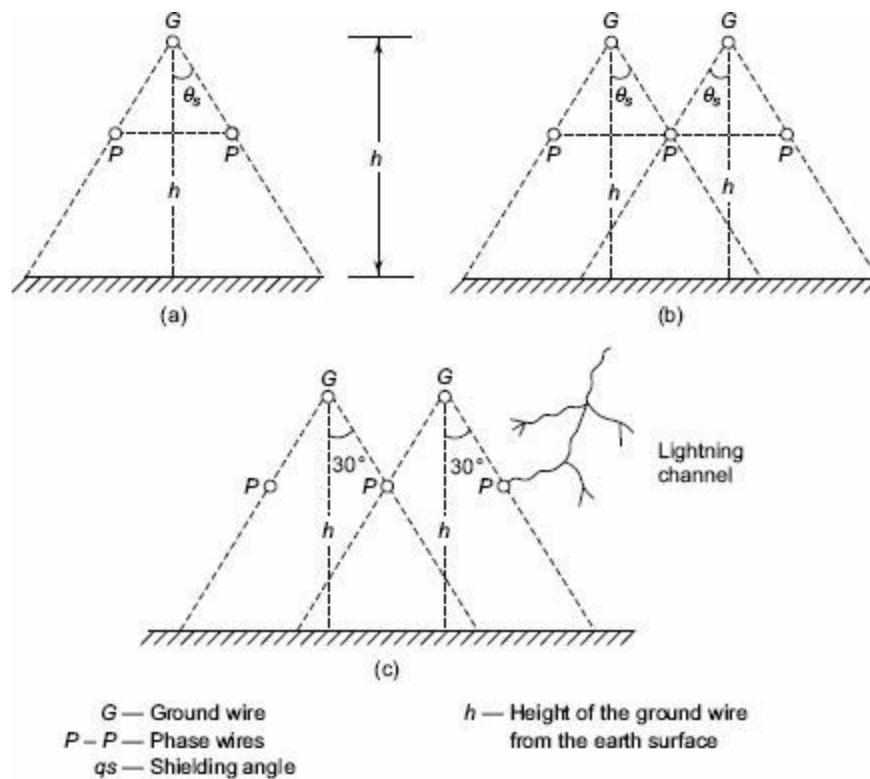


Fig. 8.20 Shielding arrangement of overhead lines by ground wires

The shielding angle $\theta_s \approx 30^\circ$ was considered adequate for tower heights of 30 m or less. The shielding wires may be one or more depending on the type of the towers used. But for EHV lines, the tower heights may be up to 50 m, and the lightning strokes sometimes occur directly to the line wires as shown in Fig. 8.20. The present trend in fixing the tower heights and shielding angles is by considering the ‘flashover rates’ and failure probabilities.

(b) Protection Using Ground Rods and Counter-Poise Wires When a line is shielded, the lightning strikes either the tower or the ground wire. The path for drainage of the charge and lightning current is (a) through the tower frame to ground, (b) through the ground line in opposite directions from the point of striking. Thus the ground wire reduces the instantaneous potential to which the tower top rises considerably, as the current path is in three directions. The instantaneous potential to which tower top can rise is

$$V_T = \frac{I_0 Z_T}{\left(1 + \frac{Z_T}{Z_S}\right)} \quad (8.42)$$

where, Z_r = surge impedance of the tower, and
 Z_s = surge impedance of the ground wire.

If the surge impedance of the tower, which is the effective tower footing resistance, is reduced, the surge voltage developed is also reduced considerably. This is accomplished by providing driven ground rods and counter-poise wires connected to tower legs at the tower foundation.

Ground rods are a number of rods about 15 mm diameter and 2.5 to 3 m long, driven into the ground. In hard soils the rods may be much longer and can be driven to a depth of, say, 50 m. They are usually made of galvanized iron or copper-bearing steel. The spacings of the rods, the number of rods, and the depth to which they are driven depend on the desired tower footing resistance. With 10

rods of 4 m long and spaced 5 m apart, connected to the legs of the tower, the dynamic or effective resistance may be reduced to 10 Ω .

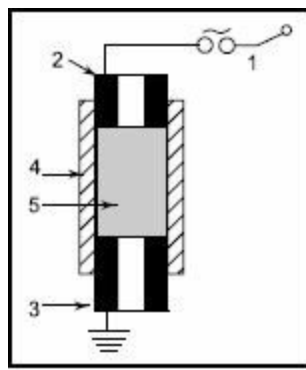
The above effect is alternatively achieved by using counter-poise wires. Counter-poise wires are wires buried in the ground at a depth of 0.5 to 1.0 m, running parallel to the transmission line conductors and connected to the tower legs. These wires may be 50 to 100 m long. These are found to be more effective than driven rods and the surge impedance of the tower may be reduced to as low as 25 Ω . The depth does not materially affect the resistance of the counter-poise, and it is only necessary to bury them to a depth enough to prevent theft. It is desirable to use a larger number of parallel wires than a single wire. But it is difficult to lay counterpoise wires compared to ground or driven rods.

(c) Protective Devices

In regions where lightning strokes are intense or heavy, the overhead lines within these zones are fitted with shunt protected devices. On the line itself two devices known as expulsion gaps and protector tubes are used. Line terminations, junctions of lines, and sub-stations are usually fitted with surge arresters.

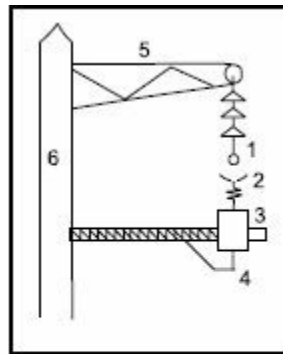
(i) Expulsion Gaps Expulsion gap is a device which consists of a spark gap together with an arc-quenching device which extinguishes the current arc when the gaps breakover due to overvoltages. A typical such arrangement is shown in [Fig. 8.21a](#). This essentially consists of a rod gap in air in series with a second gap enclosed within a fibre tube. In the event of an overvoltage, both the spark gaps breakdown simultaneously. The current due to the overvoltage is limited only by the tower footing resistance and the surge impedance of the ground wired. The internal arc in the fibre tube due to lightning current vapourizes a small portion of the fibre material. The gas thus produced, being a mixture of water vapour and the decomposed fibre product, drive away the arc products and ionized air. When the follow-on power frequency current passes through zero value, the arc is extinguished and the path becomes open circuited. Meanwhile the insulation recovers its dielectric strength, and the normal conditions are established. The lightning and follow-up power frequency currents together can last for 2 to 3 half cycles only. Therefore, generally no disturbance in the network is produced. For 132 or 220 kV lines, the maximum current rating may be about 7,500 A.

(ii) Protector Tubes A protector tube is similar to the expulsion gap, in construction and principle. It also consists of a rod or spark gap in air formed by the line conductor and its high-voltage terminal. It is mounted underneath the line conductor on a tower. The arrangement is shown in [Fig. 8.21b](#). The hollow gap in the expulsion tube is replaced by a nonlinear element which offers a very high impedance at low currents but has low impedance for high or lightning currents. When an overvoltage occurs and the spark gap breaks down, the current is limited both by its own resistance and the tower footing resistance. The overvoltage on the line is reduced to the voltage drop across the protector tube. After the surge current is diverted and discharged to the ground, the follow-on normal power frequency current will be limited by its high resistance. After the current zero of power frequency, the spark gap recovers the insulation strength quickly. Usually, the flashover voltage of the protector tube is less than that of the line insulation, and hence it can discharge the lightning overvoltage effectively.



1. External series gap
2. Upper electrode
3. Ground electrode
4. Fibre tube
5. Hollow space

Fig. 8.21a *Expulsion gap*



1. Line conductor on string insulator
2. Series gap
3. Protector tube
4. Ground connection
5. Cross arm
6. Tower body

Fig. 8.21b *Protector tube mounting*

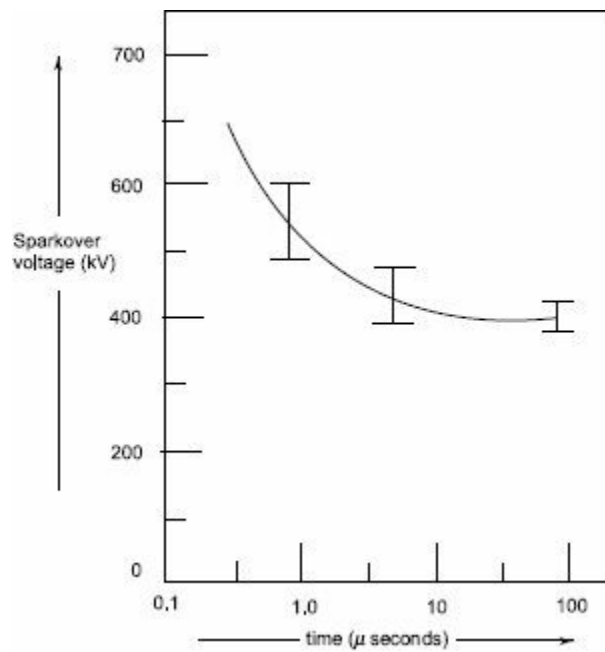


Fig. 8.22 *Volt-time characteristic of a standard rod-rod gap*

(iii) *Rod Gaps* A much simpler and effective protection device is a rod-gap (refer [Sec. 7.2.7](#)-rod-gaps, in [Chapter 7](#)). However, it does not meet the complete requirement. The sparkover voltage of a rod gap depends on the atmospheric conditions. A typical volt-time characteristic of a 67 cm-rod gap is shown in [Fig. 8.22](#), with its protective margin. There is no current limiting device provided so as to limit the current after sparkover, and hence a series resistance is often used. Without a series resistance, the sparking current may be very high and the applied impulse voltage suddenly collapses to zero thus creating a steep step voltage, which sometimes proves to be very dangerous to the apparatus to be protected, such as transformer or the machine windings. Nevertheless, rod gaps do provide efficient protection where thunderstorm activity is less and the lines are protected by ground wires.

(iv) *Surge Arresters or Lightning Arresters* Surge diverters or lightning arresters are devices used at sub-stations and at line terminations to discharge the lightning overvoltages and short duration switching surges. These are usually mounted at the line end at the nearest point to the sub-station. They have a flashover voltage lower than that of any other insulation or apparatus at the sub-station. These are capable of discharging 10 to 20 kA of long duration surges ($8/20 \mu\text{s}$) and 100 to 250 kA of the short duration surge currents ($1/5 \mu\text{s}$). The characteristics and detailed discussion of the surge arresters are presented in [Sec. 8.3.1](#).

8.3 PRINCIPLES OF INSULATION COORDINATION ON HIGH-VOLTAGE AND EXTRA HIGH-VOLTAGE POWER SYSTEMS

Electric power supply should ensure reliability and continuity to the utility concerns. Hence, the power lines and sub-stations are to be operated and protected against overvoltages such that the number of failures are as few as possible. At the same time, the cost involved in the design, installation, and operation of the protective devices should not be too high. Hence, a gradation of system insulation and protective device operation is to be followed, keeping in view the importance of the various equipment involved.

Generally, sub-stations contain transformers, switchgear, and other valuable equipment with non-self-restoring insulation, which have to be protected against failures and internal destruction. For other apparatus, which contain self-restoring insulation, like string insulators, they may be allowed to flashover in air. But the flashovers should be kept to a minimum so that the system disturbances are the least. Hence, lightning and switching surge protection requires establishment of protective voltage levels called shunt protection levels, by means of protective devices like lightning arresters.

The lightning impulse withstand level known as the *Basic Impulse Level (BIL)* is established for each system nominal voltage for different apparatus. Various equipment and their component parts should have their BIL above the system protective level, by a suitable margin. This margin is usually determined with respect to air insulation by statistical methods. For non-self-restoring insulation like the transformer insulation, the margin limit is fixed using conventional methods.

For system voltages below 400 kV, the switching surges are not of importance. If the BIL is chosen correctly, relative to the prevailing protective level, the equipment will have an adequate switching surge level. For higher system voltages, since the switching surges are of higher magnitude compared to the lightning overvoltages, switching surge magnitudes are of importance and the following criterion is to be adopted.

- (i) The flashover voltage of a protective device is chosen such that it will not operate for switching overvoltages and other power frequency and its harmonic overvoltages. But other long duration overvoltages, namely, sustained overvoltage due to faults and even the above-mentioned overvoltages may sometimes cause thermal overloading due to leakage currents. Therefore, the BIL has to be higher.
- (ii) For EHV systems, it may be economical to use a protective device for limiting the overvoltages due to lightning as well as switching surges to a particular level. At present, there are surge arresters which operate for both types of overvoltages mentioned above. In such cases, it is preferable to assign to each protected equipment a *Switching Impulse Level (SIL)*, so that there is a small margin above the controlled switching surge level, so that the surge diverters operate on switching surges, only when the controlling devices fail. Normally, only rod gaps and lightning arresters are used as protective devices for protection, and their characteristics are considered here.

The ideal requirements of a protective device connected in parallel or in shunt are the following:

- (a) It should not usually flashover for power frequency overvoltages.
- (b) The volt-time characteristics of the device must lie below the withstand voltage of the protected apparatus or insulation. The marginal difference between the above two should be adequate to

allow for the effects of distance, polarity, atmospheric conditions, changes in the characteristics of the devices due to ageing, etc.

(c) It should be capable of discharging high energies contained in surges and recover insulation strength quickly.

(d) It should not allow power frequency follow-on current to flow.

The behaviour of shunt connected protective devices like rod gaps and surge diverters along with transformer insulation is given in Fig. 8.23.

In Fig. 8.23a, the transformer insulation strength is given as a volt-time characteristic. Figure 8.23b gives the relative insulation strengths of the transformer (curve A), rod gaps (curves B and C), and that of a lightning arrester (curve D).

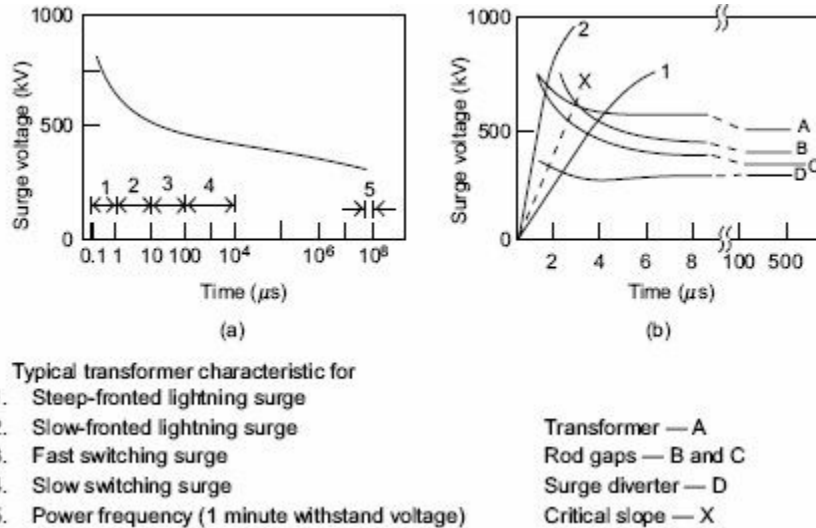


Fig. 8.23 Volt-time characteristics of transformer rod gaps and surge diverters

A lightning arrester protects the transformer insulation in the entire time region. The rod gap protects the transformer insulation, only if the rate of rise of surge is less than the critical slope (curve X). Thus, if the surge voltage rise is as shown by curve

1, rod gap flashes and protects the transformer, if the surge voltage rise follows curve 2, only the surge diverter can protect the transformer insulation.

Rod gaps are simple and cheap devices but do not meet all the requirements of a protective device. Moreover, their flashover characteristics depend on the atmospheric conditions, polarity of the wave, and wave shape. Also, it may give rise to very steep impulse waves on the transformer windings as chopped waves, because no current limiting resistance is used. Chopped impulse waves may lead to the destruction of the transformer turn-to-turn insulation. But still, rod gaps provide reasonable protection where lightning surge levels are low, and steep fronted surges are controlled by overhead ground wires.

8.3.1 Surge Arresters

These are non-linear resistors in series with spark gaps which act as fast switches. A typical surge arrester or lightning arrester is shown in [Fig. 8.24b](#) and its characteristics are given in [Fig. 8.25](#). A number of non-linear resistor elements made of silicon carbide are stacked one over the other into two or three sections. They are usually separated by spark gaps (see [Fig. 8.24b](#)). The entire assembly is housed in a porcelain water-tight housing. The volt-ampere characteristic of a resistance element is of the form

$$I = kV^a \quad (8.43)$$

where, I_d = discharge current,

V = applied voltage across the element, and k and a are constants depending on the material and dimensions of the element.

The dynamic characteristics are shown in [Fig. 8.25a](#).

When a surge voltage (V_i of [Fig. 8.25b](#)) is applied to the surge arrester, it breaks down giving the discharge current i_d and maintains a voltage V_d across it. Thus, it provides a protection to the apparatus to be protected above the protective level V_p (see [Fig. 8.25b](#)).

The lighter designs operate for smaller duration of currents, while the heavy duty surge arresters with assisted or active gaps are designed for high currents and long duration surges. The lighter design arresters can interrupt 100 to 300 A of power frequency follow-on current and about 5000 A of surge currents. If the current is to be more and has to be exceeded, the number of series elements has to be increased or some other method to limit the current has to be used. In heavy duty arresters, the gaps are so arranged that the arc burns in the magnetic field of the coils excited by power frequency follow-on currents. During lightning discharges, a high voltage is induced in the coil by the steep front of the surge, and sparking occurs in an auxiliary gap. For power frequency follow-on currents, the auxiliary gap is extinguished, as sufficient voltage will not be present across the auxiliary gap to maintain an arc. The main gap arcs occur in the magnetic field of the coils. The magnetic field, aided by the horn-shaped main gap electrodes, elongates the arc and quenches it rapidly. The follow-on current is limited by the voltage drop across the arc and the resistance element. During surge discharge the lightning protective level becomes low.

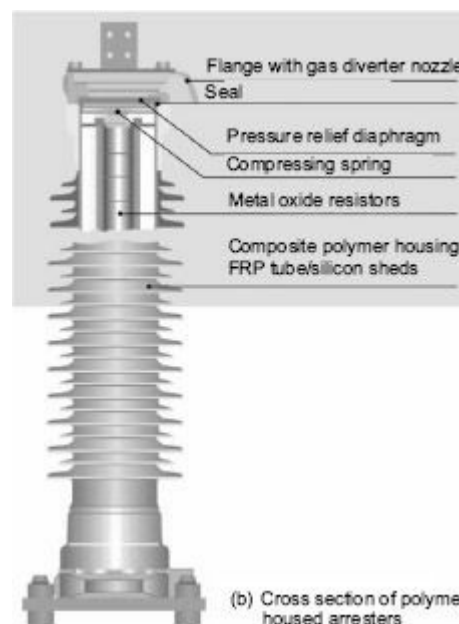


Fig. 8.24a Metal Oxide (ZnO) surge arrester in polymer housing

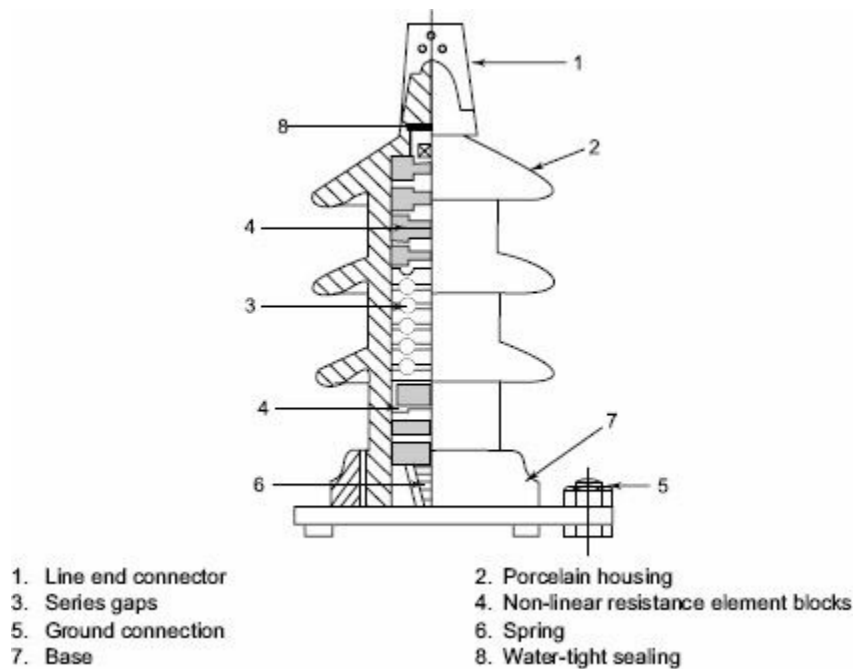


Fig. 8.24b Non-linear element surge arrester

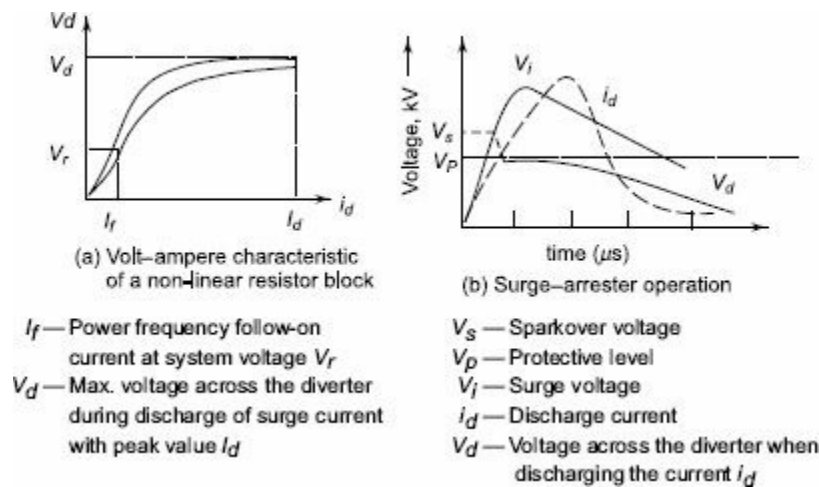


Fig. 8.25 Characteristics of a surge arrester

Sometimes, it is possible to limit the power frequency and other overvoltages after a certain number of cycles using surge arresters. The permissible voltage and duration depend on the thermal capacity of the arrester. The rated arrester voltage is normally chosen so that it is not less than the power frequency overvoltage expected (line to ground) at the point of installation, under any faulty or abnormal operating condition.

Typical characteristics of surge arresters in the voltage range 100 to 200 kV, 10 kA (heavy duty type) are given in [Table 8.2](#).

Table 8.2 Characteristics of 100-200 kV surge arresters 10 kA and heavy duty type (Ref. 14)

Characteristics		Per unit values (referred to the rated values of the diverter)
1.	Maximum 1.2/50 μ s surge 2.2 to 2.8 sparkover voltage	
2.	Maximum front of wave sparkover voltage	2.9 to 3.1
3.	Maximum switching impulse sparkover voltage	2.3 to 3.0
4.	Maximum discharge voltage (V_d) for 8/20 μ s current wave	

5 kA
10 kA
20 kA

2.0 to 2.7
2.2 to 3.0
2.5 to 3.3

(a) Surge Arresters for EHV Systems The selection of surge arrester voltage rating for EHV and UHV systems depends on

- (i) the rate of rise of voltage,
- (ii) the type of system to be handled, i.e., whether effectively grounded or grounded through an impedance etc., and
- (iii) operating characteristic of the arrester.

The usual type of surge arresters used for the above purposes are

- (i) silicon carbide arresters with spark gaps,
- (ii) silicon carbide arresters with current limiting gaps, and
- (iii) the gapless metal oxide (zinc oxide) arresters.

The first two types of arresters have a $V - I$ characteristic of the nature of $V = KI^n$, where n varies between 0.5 and 0.6 for the elements. The time to sparkover for the first type of arresters is around 1 to 2 μs and the voltage is limited to 2.0 p.u. of the power frequency voltage. The $V - I$ characteristics of arresters with no spark gaps are not enough to limit the power frequency follow-on current, while the arresters with the spark gap provided will have a high limiting voltage. Further, arresters with spark gaps are not very well suited to limit the switching overvoltages. However, recent developments in solid state technology have led to the development of metal oxide non-linear resistors. With the use of these materials, the new class of surge arresters that can handle very small to very large current, with almost constant voltage across them, have been developed. One such arrester is the zinc oxide (ZnO) arrester which uses a base material of ZnO) sintered into a different insulating medium such as BiO_3 . The $V - I$ characteristic of such a unit is of the form $V \propto I^n$ where $n = 0.02$ to 0.03. The $V - I$ characteristics of silicon carbide and zinc oxide arresters are shown in [Fig. 8.26a](#) for comparison.

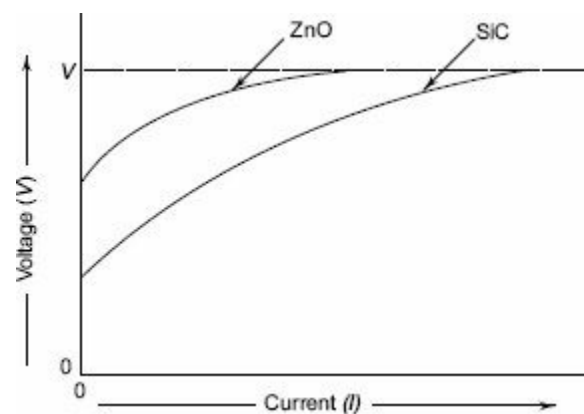


Fig. 8.26a Typical $V - I$ characteristics of silicon carbide (SiC) and zinc oxide (ZnO) surge diverters

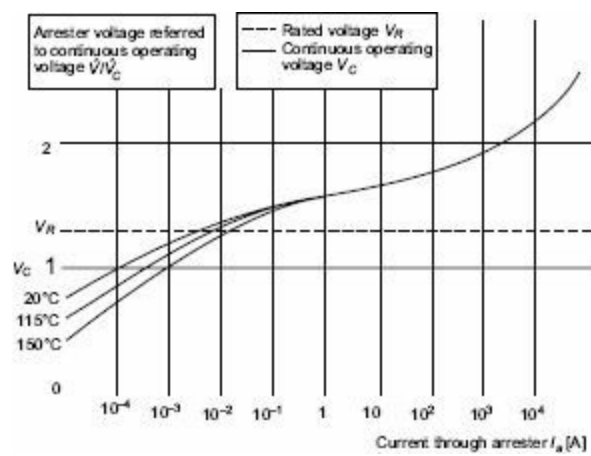


Fig. 8.26b Current/Voltage characteristic of non-linear metal oxide arrester

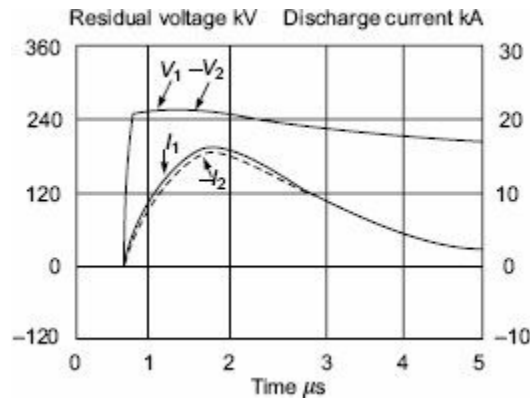


Fig. 8.26c Typical voltage and current oscillograms obtained for positive negative impulse surge test on an arrester

The advantages of zinc oxide arresters for EHV systems are

- (i) they are simple in construction,
- (ii) they have flat V - I characteristic over a wide current range, and
- (iii) the absence of a spark gap that produces steep voltage gradients when sparking occurs.

The main disadvantage of zinc oxide arresters is the continuous flow of power frequency current and the consequent power loss. Voltage grading system is not needed for each of the units of the zinc oxide arresters used in EHV systems. A typical 400 kV line arrester may be rated at 15 kA and may have a resistance of 100 ohms at the peak current rating.

Surge arresters for dc systems have severe requirements compared to ac systems and they

- Have to protect the equipment from overvoltages
- Should not have any effect on the power system during normal operation
- Should be capable of withstanding surges and dissipate energy without incurring any damage

The requirements are the following:

- Offer low resistance during surges so that overvoltage is limited to a low level
- Very high resistance during normal operation to avoid power loss and energy loss
- They must operate satisfactorily under earthquakes, polluted atmospheres, under high and low temperature conditions, etc.

[Figure 8.24a](#) shows a cross-sectional view of a typical ZnO arrester housed in a polymeric housing

for application in HVDC systems. The assembly consists of a number of ZnO discs piled one over the other and compressed by a suitable spring. A pressure relief valve is provided so that any gases or decomposed products released are sent out. The volt-ampere characteristic of a single disc of metal oxide element is shown in Fig. 8.26b and voltage-current oscillogram for positive and negative impulses of 20 kA arrester unit is shown in Fig. 8.26c. The volt-ampere characteristic is extremely flat and has power law $V = KI^n$, n between 0.05 to 0.2.

(b) Protection of Lines with Surge Arresters Since surge arresters are devices that provide low resistance paths for overvoltages through an alternate ground path, their operating characteristics and application is of importance. The spark gap inside the arrester acts as a fast acting switch while non-linear arrester elements provide the low impedance ground path. The arrester voltage at its terminal when connected to a line of surge impedance Z to ground, is given as

$$V = [2(R + r)/(R + r + Z)] u(t) \quad (8.44)$$

where, Z is the line surge impedance,

R is the resistance of the non-linear element,

r is the ground to earth resistance, and

$u(t)$ is the surge voltage.

The Thevenin equivalent circuit for the arrester is shown in Fig. 8.27.

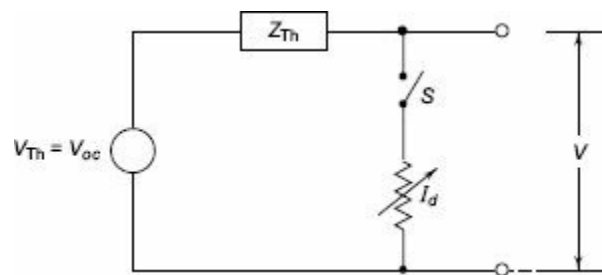


Fig. 8.27 Equivalent circuit of a surge arrester

The switch S is open for voltages less than the sparkover voltage of the surge arrester V_s , while it is closed for voltage magnitudes greater than V_s . The closing of the switch is represented by injecting a voltage cancellation wave having a negative amplitude equal to the potential difference between the voltage that appears when the switch is open V_{oc} , and the voltage developed across the impedance of the device after the switch is closed. Z_{Th} is the impedance of the system viewed from the terminals of the protective device.

8.3.2 Equipment Insulation Level and Insulation Coordination of Sub-stations

For steep fronted lightning waves at sub-stations and at different points on lines, the voltages at sub-stations may exceed the protective level depending on the distances involved and the arrester locations. Hence, it is necessary to decide the number of locations for arresters to optimize the overall cost. For high-voltage sub-stations, it is usual to instal surge arresters between a transformer and its circuit breaker, in order to protect the transformer from current chopping and the overvoltage due to it. Further, nearness of the arrester to the transformer offers better protection. The basic insulation level is often determined by giving a margin of 30% to the protective level of surge arrester and selecting the next nearest standard BIL. The standard values of BIL for system voltages from 145 to 765 kV are given in Tables 8.3 and 8.4. When a surge arrester is used to give switching surge protection also, the margin allowed is only 15%. The insulation level for lines and other equipment is to be chosen separately. The selection of this level for lines depends on the atmospheric conditions, the lightning activity, insulation pollution present and the acceptable outage or failure rate of the line.

Table 8.3 *Insulation levels (BIL) for various system voltages (Ref. 15)*

Highest voltage of the system equipment <i>kV (rms)</i>	Impulse withstand voltage for standard impulse waves		Power frequency withstand voltage with respect to earth	
	Full insulation <i>kV (peak)</i>	Reduced insulation <i>kV (peak)</i>	Full insulation <i>kV (rms)</i>	Reduced insulation <i>kV (rms)</i>
145	650	550	275	230
		450		185
245	1050	—	460	—
		900	—	395
		825	—	360
		750	—	325
362	—	1300	—	570
		1175	—	510
		1050	—	461
420	—	1675	—	740
		1550	—	680
		1425	—	630
		1300	—	570
525	—	1800	—	790
		1675	—	740
		1550	—	680
		1425	—	630
765	—	2400	—	1100
		2100	—	980
		1950	—	920
		1800	—	870

Table 8.4 *Standard insulation levels for equipment (> 300 kV) (Ref. 15)*

Highest voltage for equipment	Base for per unit voltage values	Rated switching impulse voltage		Ratio between lightning and switching withstand voltages	Rated lightning withstand voltage
U_m kV (rms)	$\left(U_m \frac{\sqrt{2}}{\sqrt{3}} \right)$	kV pu	kV (peak)		kV (peak)
300	245	3.06	750	1.13	850
		3.45	850	1.27	950
362	296	2.86	850	1.12	950
				1.24	1050
		3.20	950	1.12	1050
				1.24	1175
420	343	2.76	950	1.12	1050
				1.24	1175
		3.06	1050	1.12	1175
				1.24	1300
525	429	2.45	1050	1.36	1425
				1.12	1175
				1.24	1300
				1.36	1425
		2.74	1175	1.12	1300
				1.21	1425
765	625			1.32	1550
		2.08	1300	1.10	1425
				1.19	1550
				1.38	1800
		2.28	1425	1.09	1550
				1.28	1800
				1.47	2100
		2.48	1550	1.16	1800
		1.26	1950		
				1.55	2400

The protective level of the sub-station insulation depends on the station location, the protective level of the arrester, and the line shielding used. The line insulation in the end spans near the sub-station is normally reduced to limit the lightning overvoltages reaching the sub-station. In a sub-station, the busbar insulation level is the highest to ensure continuity of supply. The circuit breakers, isolators, instrument and relay transformers, etc., are given the next lower level. Since the power transformer is the costly and sensitive device, the insulation level for it is the lowest.

The illustrate the principles of insulation co-ordination, an example of a 132 kV sub-station is given below.

Nominal system voltage	: 132 kV
Highest system voltage	: 145 kV
Highest system voltage to ground	$145 \times \frac{\sqrt{2}}{\sqrt{3}} = 119$ kV (peak)
Expected switching surge overvoltage	
(Table 8.1) 3.0p.u.	: 3 X 119 = 357 kV (peak)
<i>(a) Surge arrester</i>	
Rating	: 123 kV
Front of wave sparkover voltage	: 510kV(peak)
V_d (discharge voltage at 10 kA, 8/20 μ s impulse current wave)	: 443 kV (peak)
<i>(b) Transformer</i>	
Impulse withstand voltage	: 550 kV (peak)
Induced voltage (withstand) level	: 230 kV (rms)

Impulse protective margin $\frac{.550 - 443}{443} \times 100 = 24\%$

(c) *Switchgear*

Impulse withstand voltage : 650 kV (peak)

Bus insulation impulse withstand voltage : 650 kV (peak)

In case a rod gap is used for the protection of a transformer, the rod gap with a negative sparkover voltage of 440 kV (59 cm gap) may be chosen to give the 25% margin. The protection is good for surges having a front time not shorter than $2 \mu s$. But the switching surge sparkover voltage which is about 380 kV is very near the maximum switching surge generated in the system and hence may cause many outages. If a rod gap of 66 cm is used, the protection becomes doubtful, as the impulse sparkover voltage for $2 \mu s$ front wave is 600 kV

8.3.3 Insulation Levels at Sub-stations with Protective Zones

(a) Magnitude and Shape of the Incoming Voltage Surges Direct strokes to phase conductors near the station point are very dangerous as they cause very high currents to flow through the surge arrester. The discharge voltages developed across the arrester elements are very high and the arresters may get destroyed. Therefore, the stations are completely shielded from direct strokes. The shielding is sometimes effected up to about 2 km on either side of the station. This protected zone gives the surges to originate only from outside regions. Usually, the voltage wave at the station entrance is estimated by assuming a voltage magnitude at the beginning of the protected zone as equal to 1.3 times the negative critical flashover voltage of the line insulation. It is also important that the sloping off of the point of the surge is helpful for the effective performance of the surge arrester. Back flashovers are also important. There is a risk of a more severe surge occurring in the case of back flashovers. The probability of the occurrence of this depends on the rate of the back flashover of the protected zone and its length.

(b) Equipment Insulation Level For steep-fronted travelling waves, the voltages at different points in the sub-station can exceed the protective level by amounts that depend on the distance from the arrester location, the steepness of the wave front and other electrical parameters. Hence, it is necessary to decide the number of locations at which surge arresters are to be located and their ratings. It necessary to keep this number to a minimum. Also, care must be taken regarding switching overvoltages generated due to current chopping which may destroy the transformer or the equipment near the circuit breakers. The Basic Impulse Level (BIL) is often determined as simply 1.25 to 1.30 times the protective level offered by the surge arrester. Usually, the next higher BIL value from the standard values is chosen. This is quite sufficient for smaller stations and station ratings up to 220 kV. For bigger stations and stations of importance, the 'distance effect' discussed in the next section is to be suitably allowed for, when surge arresters are to be used for SIL also; a margin of 15 to 20% is normally allowed over the protective level. Distance effect is negligible for long fronted switching surges.

(c) Distance Effect Usually the circuit breaker, the transformer and other equipment are placed at finite distances from the surge arrester and connected through a short distance over head line or cable. When a surge arises, it suffers multiple reflections between each of the equipment which may give rise to overvoltages of considerable magnitude (the travel time is usually less than a μs). It can be shown that when a surge arrester, a breaker and a transformer are in line, the voltage that can build up at a distance D from the surge arrester point is given as $V(D) = V_p + 2ST$, where V_p is the sparkover voltage/protective level, S is the steepness of the wave front, and T is the travel time $= D/v$. Here, v is the velocity of the wave travel, assuming that the line extends to a large distance such that no reflections come from the line end. The maximum value of $V(D)$ is attained when $2T = T_0$, the sparkover time of the arrester. The above simple expression shows that the transfer surge impedance is very high. The ratio of the transformer terminal voltage, V_T to that of the protective level V_p is a function of (T/T_0) . For steep fronted waves, sometimes V_T may exceed even $2V_p$. It has been shown that in a 330 kV sub-station, a 1.2/50 ms, 1500 kV incoming wave can give rise to a surge of peak value 1250 kV having rise time of 2 ms at the bus terminals (neglecting the transfer capacitance), whereas the protective level offered by the surge arrester at the transformer terminal is only 750 kV.

The transformer terminals may get a surge voltage of 930 kV peak. This has been verified by computer calculations for a $1/50 \mu\text{s}$ wave, on a line connected to a 330 kV station.

8.3.4 Insulation Co-ordination in EHV and UHV Systems

The insulation design of EHV and UHV stations is based on the following principles

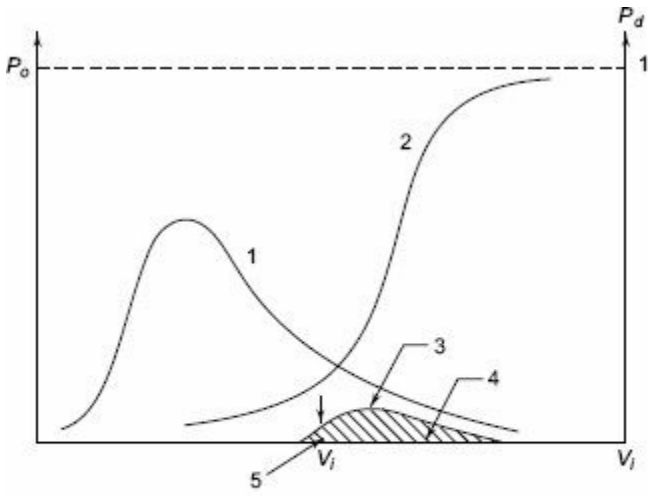
- (i) stations have transformers and other valuable equipment that have non-self restoring insulation, and
- (ii) the protective levels for lightning surges and switching surges are almost equal and even overlap. If the basic impulse level for the equipment or the system is chosen, then this level cannot give protection against the switching impulses. Hence, a separate switching impulse level (SIL) has to be chosen. It is, therefore, desirable to use protective devices for limiting both lightning and switching overvoltages. As such, the switching impulse insulation level above the controlled switching surge level has to be adopted so that the surge arresters operate only rarely on switching overvoltages when the controls of the control devices for switching voltages fail. A general guideline that can be adopted for different EHV and UHV system for maximum switching surge levels are given in [Table 8.5](#).

Table 8.5 Maximum switching surge level at different line voltages

Highest system voltage (kV)	420	525	765	1150
Maximum switching surge level (kV) = highest system voltage multiplied by	2.5	2.25	2.0	1.8 to 1.9

It is now necessary to allow a suitable margin in the insulation level above the maximum switching surge overvoltage and also permit a little risk for failure in the interest of economical adoption of insulation levels. Usually statistical methods are adopted based on a given risk of flashover which is calculated by combining the flashover voltage distribution function of the insulation structures with the overvoltage probability density function.

Let $P_0(V_i) dV_i$ be the probability of a surge voltage occurring as an overvoltage between V_i and $(V_i + dV_i)$. Let the probability for flashover of the insulation be $P_d(V_i)$. Then probability of both the above events occurring simultaneously in V_i and $(V_0 + V_i)$ will be given by $P_0(V_i) P_d(V_i)$. The risk of failure over the entire voltage range then becomes



1. $P_o(V_i)$
2. $P_d(V_i)$
3. $P_o(V_i) P_d(V_i)$
4. Risk of failure, $R = \int P_o(V_i) P_d(V_i) dV_i$
5. Probability density of failure at the value V_1

Fig. 8.28 Risk of failure as a function of the probability of the occurrence of a surge voltage [$P_o(V_i)$] and the probability of the insulation flashover [$P_d(V)$]

$$\text{Risk of failure, } R = \int_0^{V_i} P_o(V_i) \cdot P_d(V_i) \cdot dV_i \quad (8.45)$$

If a number of insulation structures such as string of insulators are subjected to a switching surge, then the failure is adjusted for appropriate probability, considering all the individual probabilities simultaneously.

The risk of failure is graphically represented in [Fig. 8.28](#).

A simplified procedure to evaluate the risk of failure is given by the IEC which defines the safety factor as a ratio of the statistical overvoltage to that of statistical withstand voltage (T). The former voltage is the voltage likely to exceed 2% of all the overvoltages, while the latter is the 90% probability voltage for failure which is given as $(CFO - 1.3 \sigma)$, where σ is the standard deviation of the overvoltage distribution function and CFO is the critical flashover voltage. A graph between the risk of failure and the statistical safety factor is given by the IEC and is shown in [Fig. 8.29](#). It is evident from this figure that increasing the statistical safety factor will reduce the risk of failure but will cause an increase in the cost of insulation to be provided. For non-self-restoring insulations like that of transformers, etc., the withstand voltage is expressed in terms of the breakdown voltage values.

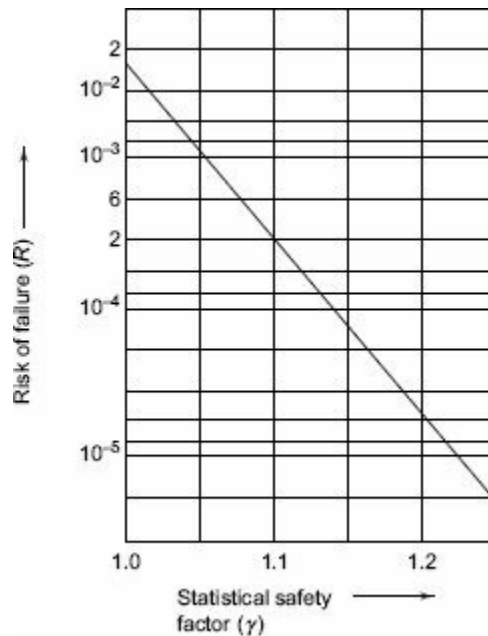


Fig. 8.29 Relation between the risk of failure (R) and the statistical safety factor (τ)

The protective level provided by the protective devices like the surge arresters is established in the same manner as that for other apparatus, the difference being that the surge arresters must absorb the surge. The safety margin is arrived at by considering the risk factor R for the device used for the protection and the insulation structure to be protected, giving a safe margin.

In normal practice, the insulation level and the protective safety margin are arrived at by

- (i) selecting the risk of failure R ,
- (ii) the statistical safety factor, γ , and
- (iii) then fixing the withstand voltage and designing the insulation level of any equipment or apparatus corresponding to 90% or 95% of the withstand voltage thus fixed.

This type of approach may be understood as follows:

Let $P_0(V_i)$ represent the probability of occurrence of an overvoltage of magnitude V_{os} and has only 2% chance to cause the failure of the insulation. This voltage is known as *statistical overvoltage*. Let V_{ds} be the voltage that causes only 10% or less breakdowns or failures, when applied to the insulation system. Also, let $P_d(V_i)$ represent the statistical withstand voltage corresponding to the voltage V_{ds} for the given insulation system. These probabilities are shown in Fig. 8.30. The statistical safety factor, τ defined earlier, is given as the ratio V_{ds}/V_{os} . This statistical parameter τ , if increased, reduces the risk of failure R . This is illustrated in Fig. 8.30, where if the curve of the insulation flashover voltage [$P_d(V_i)$] if shifted towards the right, will increase the safety factor and reduce the risk of failure. Hence, as has been stated earlier, proper selection of R and τ is to be done.

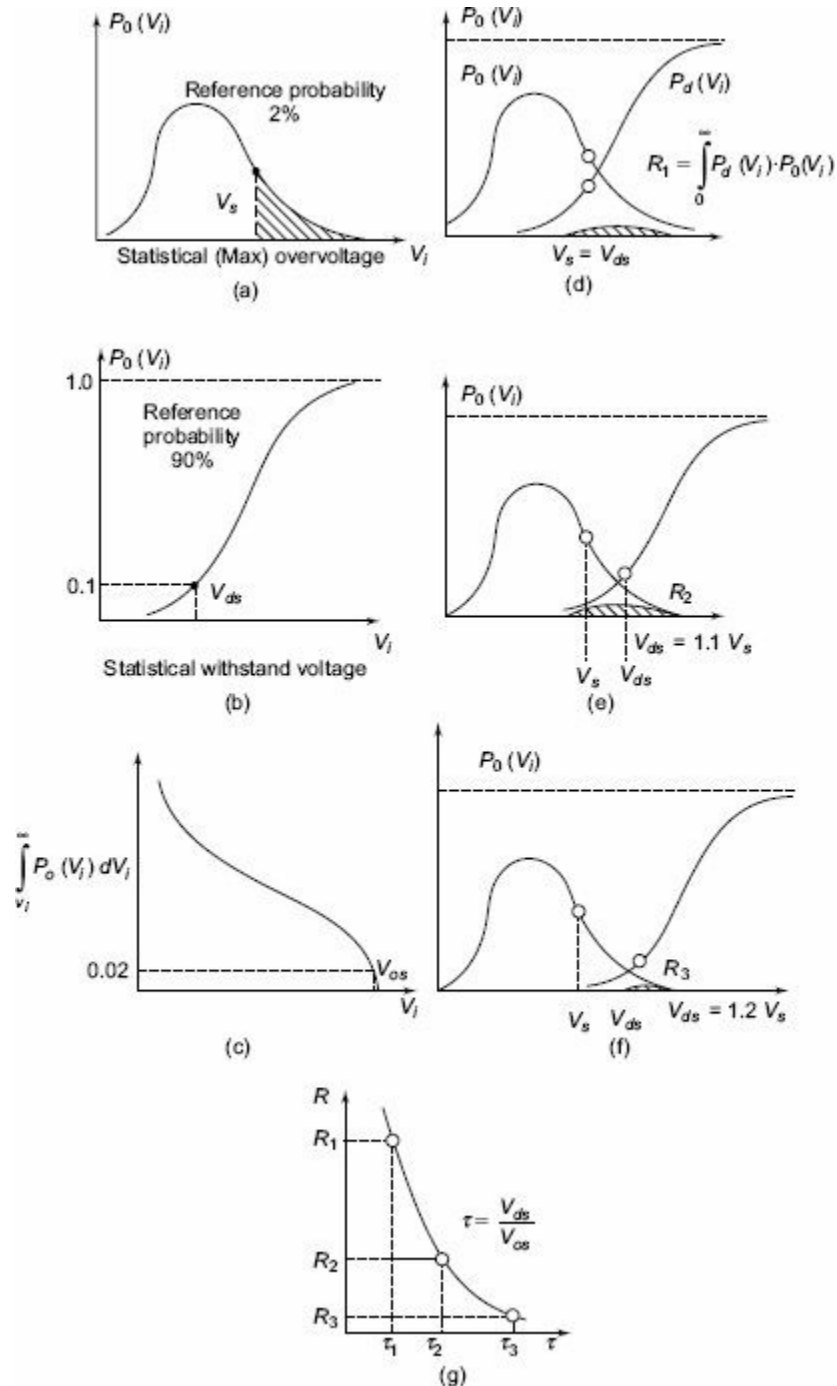


Fig. 8.30 The statistical safety factor (τ) and its relation to the risk of failure (R)

For proper insulation co-ordination, a certain margin of safety has to be provided by properly

choosing the “protective level” the protective devices, such as spark gaps and surge arresters, and proper insulation level for the equipment and the apparatus. The correlation between the two is illustrated in [Fig. 8.31](#).

In the figure, R_g gives the risk factor for the protective gap with $P_g(V_i)$ as its probability density function for failure and the overvoltage probability density function $P_o(V_i)$ occurring. The probability density function for insulation (to be protected) is given by $P_i(V_i)$ and R_i is its risk factor. The safety margin which is the difference between $P_g(V_i)$ and $P_i(V_i)$ is also shown. In reality, this computation is not simple and deviation in the occurrence of overvoltages greatly influences the risk factors and the safe margin usually gets reduced.

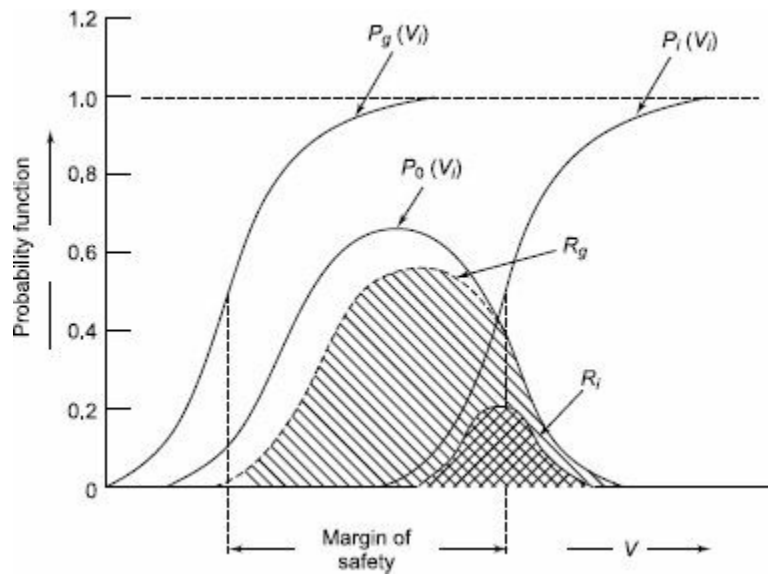


Fig. 8.31 Protective margin (margin of safety) and risk of failure provided by a protective device

The insulation co-ordination and safety margins fixed for a typical 750 kV station can be as follows:

surge-arrester voltage rating	: 590 kV
maximum sealed-off value of the power frequency harmonics	: 950 kV
lightning surge protective level	: 1450 kV
switching surge protective level	: 1200 kV
transformer or reactor BIL	: 1800 kV
transformer or reactor SIL	: 1500 kV
circuit breaker and other apparatus SIL	
when closed	: 1350 kV
when open	: 1500 kV
the maximum switching surge level taken as (2.0 p.u.)	: 1250 kV

If the 765 kV line uses a V type insulator string with 35 standard type disc insulators, then the CFO for lightning surges will be about 1350 kV. These values overlap with the SIL of the circuit breaker and other apparatus. Then, a suitable design for a conductor to tower clearance and for the conductor to ground clearance have to be given.

Surge diverter or lightning arrester is the main device that is used in power systems and sub-

stations to limit the overvoltages. Hence, proper selection and approach to determine the rating of arrester without damage to itself is of importance. In EHV and UHV systems the arresters used are gapless ZnO type. The arrester must have proper

- (i) **MCOV**: The maximum power frequency continuous operating voltage
- (ii) **TOV**: Temporary power frequency overvoltage that can appear on it
- (iii) **Energy**: The energy-dissipating capacity, i.e., energy to be absorbed by it when limiting the surge voltages.

Discharge currents usually considered for protection and voltage protective levels are

- (i) 10 kA, 8/20 *ms* lightning Impulse current, and
- (ii) 2 kA 36/90 *ms* switching Impulse current.

Suitable margin for energy capability and arrester protective level to take care of very fast transient (VFT) and distance effect (distance between arrester and equipment to be protected if it is greater than 20 m) is also taken into account.

The facts mentioned are illustrated with the following 500 kV system:

Minimum MCOV (taking 10% over nominal voltage is $\frac{500 \times 1.1}{\sqrt{3}} = 317.5$ kV

Hence choose an arrester of rating 332 kV, 5 minutes and 450 kV, 1 second rating.

Typical discharge voltage levels of the above arrester are

Nominal voltage reading = 400 kV

Discharge level of 10 kA, impulse current: 870 kV

Discharge level for 2 kA switching surge current = 760 kV

Referring to tables 8.3, 8.4 the BIL and SIL for a 500 kV (525 kV max) reduced insulation are 1425 kV and 1175 kV respectively with BIL to SIL level ratio 1.21

Hence, the protective margins are

- (i) Impulse protective margin $\frac{1425 - 870}{1425} \times 100 = 39\%$
- (ii) Switching impulse protective margin $\frac{500 \times 1.1}{\sqrt{3}} = 317.5$ kV

Thus, adequate margin (35 to 40%) is obtained by choosing surge diverter of 400 kV power frequency rating.

To conclude insulation coordination in power systems at sub-stations is to choose a protective device (surge arrester) such that its characteristics give sufficient but not very high protective margin.

- K**
T E R M S
Y
- Overvoltages
 - Lightning Phenomenon
 - Lightning Characteristics
 - Model for Lightning
 - Travelling Waves on Transmission Lines
 - Reflection and Transmission of Waves
 - Lattice Diagrams
 - Overvoltages due to Switching
 - Switching Surge Characteristics
 - Lightning Protection
 - Surge Arresters

WORKED EXAMPLES

Example 8.1 A 3-phase single circuit transmission line is 400 km long. If the line is rated for 220 kV and has the parameters, $R = 0.1$ ohms/km, $L = 1.26$ mH/km, $C = 0.009$ μ F/km, and $G = 0$, find (a) the surge impedance, and (b) the velocity of propagation neglecting the resistance of the line. If a surge of 150kV and infinitely long tail strikes at one end of the line, what is the time taken for the surge to travel to the other end of the line?

Solution

$$\begin{aligned} \text{Velocity of propagation} &= \frac{1}{\sqrt{LC}} = \frac{1}{\sqrt{1.26 \times 10^{-3} \times 0.009 \times 10^{-6}}} \\ &= 3 \times 10^5 \text{ km/s} \end{aligned}$$

$$\text{Surge impedance} = \sqrt{\frac{L}{C}} = \sqrt{\frac{1.26 \times 10^{-3}}{9 \times 10^{-9}}} = 374.2 \Omega$$

Time taken for the surge to travel to the other end is

$$= \frac{400}{3 \times 10^5} = 1.33 \text{ m s}$$

Example 8.2 A transmission line of 500- Ω surge impedance is connected to a cable of 60 Ω surge impedance at the other end. If a surge of 500 kV travels along the line to the junction point. Find the voltage build-up at the junction?

Solution

$$e = 500 U(t) \text{ kV}$$

$$Z_1 = 500 \Omega$$

$$Z_2 = 60 \Omega$$

Coefficient of reflection,

$$\Gamma = \frac{(Z_2 - Z_1)}{(Z_2 + Z_1)} = \frac{(500 - 60)}{(500 + 60)} = 0.786$$

Magnitude of the transmitted wave to the cable

$$\begin{aligned} &= (1 + \Gamma) e = (1.786) \times 500 \\ &= 893 \text{ kV} \\ &= \text{junction voltage} \end{aligned}$$

Example 8.3 An infinite rectangular wave on a line having a surge impedance of 500 Ω strikes a transmission line terminated with a capacitance of 0.004 μ F. Calculate the extent to which the wavefront is retarded?

Solution

$$e = E U(t), Z_1 = 500 \Omega, \text{ and } Z_2 = \frac{1}{Cs} = \frac{10^9}{4s}$$

$$\Gamma = \frac{Z_2 - Z_1}{Z_2 + Z_1} = \frac{\left(\frac{10^9}{4s} - 500\right)}{\left(\frac{10^9}{4s} + 500\right)} = \frac{(10^9 - 2000s)}{(10^9 + 2000s)}$$

Hence,

$$(1 + \Gamma) = \frac{2 \times 10^9}{(10^9 + 2000s)} = \frac{10^6}{\left(\frac{10^6}{2} + s\right)}$$

$$e''(s) \text{ voltage across capacitor} = (1 + \Gamma) e(s)$$

$$= \frac{10^6}{\left(\frac{10^6}{2} + s\right)} \frac{E}{s}$$

Taking inverse transforms

$$e'' = 2 E \left[1 - \exp\left(-\frac{t}{2 \times 10^{-6}}\right) \right]$$

Taking the rise time to be $3CZ$, the wave is retarded by

$$3 \times 2 \times 10^{-6} = 6 \times 10^{-6} \text{ s} \\ \text{or by } 6 \mu\text{s.}$$

Example 8.4 A 10 MVA, 132 kV transformer is connected to the end of a transmission line of surge impedance 400Ω . The transformer has an equivalent capacitance of $0.002 \mu\text{F}$ and leakage inductance of 16 H . If a rectangular wave of 1000 kV travels through the line and strikes the transformer, find the surge voltage on the transformer?

Solution

$e = 1000 U(t)$ kV; $Z_1 = 400 \Omega$, $Z_2 =$ combination of L and C given as,

$$\left[\frac{s}{C \left(s^2 + \frac{1}{LC} \right)} \right]$$

$$\alpha = \frac{1}{CZ} = \frac{1}{0.002 \times 400 \times 10^{-6}} = 1.25 \times 10^6$$

$$\omega_0 = \frac{1}{\sqrt{LC}} = \frac{1}{\sqrt{16 \times 0.002 \times 10^{-6}}}$$

or,
$$\omega_0^2 = \frac{10^6}{0.032} = 3.125 \times 10^7$$

$$(\alpha/2)^2 > \omega_0^2$$

Hence the voltage across the transformer = $e''(s)$

$$= (1 + \Gamma) e(s) = \frac{2\alpha E}{s^2 + \alpha s + \omega_0^2}$$

and the inverse transform is

$$e''(s) = \left[\left(\frac{2a}{n-m} \right) \exp(-mt) - \exp(-nt) \right] EU(t)$$

where n and m are the roots of the denominator $s^2 + \alpha s + \omega_0^2 = 0$

i.e. $n = 1.25 \times 10^6$, and $m = 30$

$$e = 1000 U(t) \text{ kV}$$

$$\therefore e'' = + \frac{2.5 \times 10^6}{1.2497 \times 10^6} [\exp(-30t) - \exp(-1.25 \times 10^6 t)]$$

$$= 2000 [\exp(-30t) - \exp(-1.25 \times 10^6 t)]$$

(The incident wave is modified to a double exponential wave when it reaches the transformer terminal.)

Example 8.5 An underground cable of inductance 0.189 mH/km and of capacitance 0.3 mF/km is connected to an overhead line having an inductance of 1.26 mH/km and capacitance of 0.009 mF/km. Calculate the transmitted and reflected voltage and current waves at the junction, if a surge of 200 kV travels to the junction, (i) along the cable, and (ii) along the overhead line.

Solution

Surge impedance of the cable $Z_1 = \sqrt{\frac{L_1}{C_1}} = \sqrt{\frac{0.189 \times 10^{-3}}{0.3 \times 10^{-6}}} = 25.1 \Omega$

Surge impedance of the line $Z_2 = \sqrt{\frac{L_2}{C_2}} = \sqrt{\frac{1.26 \times 10^{-3}}{0.009 \times 10^{-6}}} = 374.2 \Omega$

When the surge travels along the cable

$$\Gamma = \frac{(374.2 - 25.1)}{(374.2 + 25.1)} = 0.8742$$

The reflected wave, $e' = \Gamma e = 0.8742 \times 200 \text{ kV} = 174.84 \text{ kV}$

The transmitted wave, $e'' = (1 + \Gamma)e = 1.8742 \times 200 \text{ kV} = 374.84 \text{ kV}$

The reflected current wave, $I' = \frac{e'}{Z_1} = \frac{174.84 \times 10^3}{25.1} = 6.97 \text{ kA}$

The transmitted current wave,

$$I'' = \frac{e''}{Z_2} = \frac{374.84 \times 10^3}{374.20} = 1.002 \text{ kA}$$

When the wave travels along the line

$$\Gamma = \frac{(25.1 - 374.2)}{(25.1 + 374.2)} = -0.8742$$

\therefore reflected wave $= e' = \Gamma e = -174.84 \text{ kV}$

The transmitted wave $= e'' = (1 + \Gamma)e = (1 - 0.8742) \times 200 = 25.16 \text{ kV}$

The transmitted current wave $= I''$

$$= \frac{e''}{Z_2} = \frac{25.16}{25.1} = 1.006 \text{ kA}$$

The reflected current wave $= I'$

$$= \frac{e'}{Z_1} = \frac{-174.84}{374.2} \\ = 0.467 \text{ kA or } 467 \text{ A}$$

Example 8.6 *A long transmission line is energised by a unit-step voltage 1.0 V at the sending end and is open circuited at the receiving end. Construct the Bewley lattice diagram and obtain the value of the voltage at the receiving end after a long time. Take the attenuation factor $\alpha = 0.8$.*

Solution Let the time of travel of the wave = 1 unit

At the receiving end

Reflection coefficient $\gamma = (\infty - Z)/(\infty + Z) = 1.0$

Transmission coefficient $= 1 + \gamma = 2.0$

At the sending end

Reflection coefficient $\gamma = (0 - Z)/(0 + Z) = -1.0$

Transmission coefficient $= 1 + \gamma = 0$

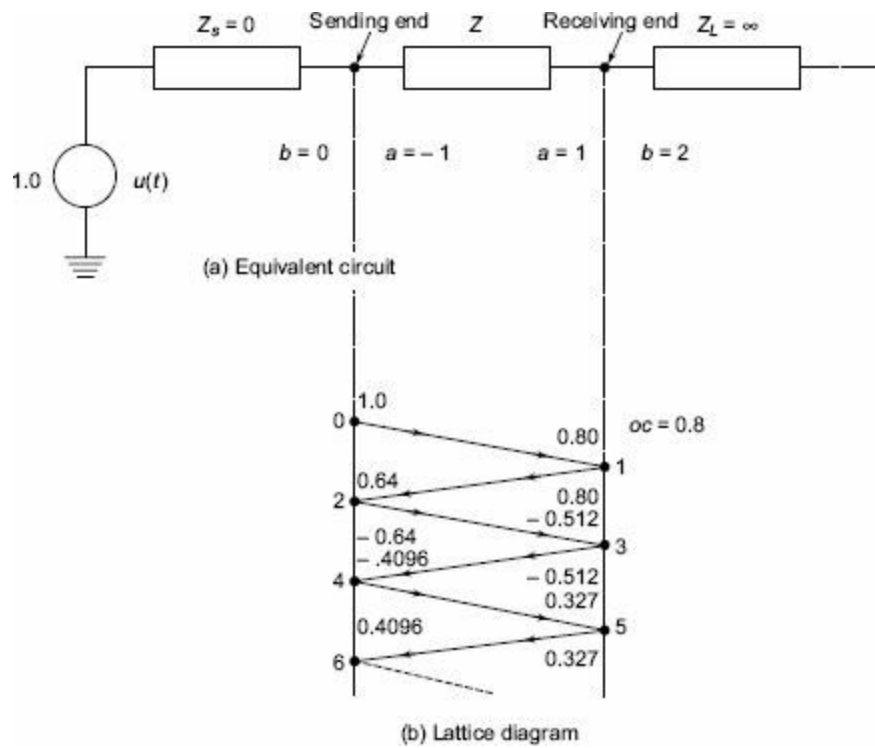


Fig. E.8.6 Equivalent circuit and lattice diagram of a transmission line

Since the source impedance $Z_s = 0$ and Z_2 , the open receiving end impedance is ∞ (infinity), as shown in the lattice diagram of Fig. E.8.6(b).

From the lattice diagram, the wave magnitudes are tabulated as shown below:

At the receiving end	At the sending end	Time unit
1	0	0
1	1	α
$1 + \alpha^2$	2	2α
1	3	$2\alpha - \alpha^3$
$1 - \alpha^4$	4	$2\alpha - \alpha^3$
1	5	$2\alpha - 2\alpha^3 + \alpha^5$
$1 + \alpha^6$	6	$2\alpha - 2\alpha^3 + 2\alpha^5$

The voltage at the receiving end after $4n$ units of time is

$$V = 2(\alpha - \alpha^3 + \alpha^5 - \dots) u(t) \\ = 2\alpha \left[\frac{1 - \alpha^{4(n+1)}}{1 + \alpha^2} \right] u(t)$$

Voltage at the receiving end after a long time (i.e. $t = \infty$) is

$$V_{\infty} u(t) = [2\alpha / (1 + \alpha^2)] u(t)$$

Substituting $\alpha = 0.8$, we get $V_{\infty} = 0.9756 u(t)$.

Example 8.7 Determine the sparkover voltage and the arrester current when a surge arrester is connected at the end of a transmission line having a surge impedance of 400Ω . Assume that a surge of 1000 kV (peak) strikes the arrester. The surge arrester characteristics for impulse currents may be taken as follows:

Surge current (kA)	1.5	3.0	5.0	10.0
Arrester voltage (kV)	264	308	336	360

Solution

(a) Calculation of spark over voltage with the line terminated

Assuming that the line is terminated, the equivalent voltage is twice the surge voltage = 2000 kV. Neglecting the ground and arrester resistances, the maximum arrester current

$$= 2 \times 2000/400 = 5 \text{ kA}$$

Referring to [Fig. E.8.7](#), the characteristics is cut by the line, $\tan^{-1} Z$ at $V_d = 330 \text{ kV}$. Hence the voltage drop across the arrester is 330 kV and the current through the arrester 3.9 kA. For steep fronted current waves, the voltage drop due to lead inductance is taken to be 5% more. Hence, the sparkover voltage, $V_d = 350 \text{ kV}$.

(b) Calculation of surge arrester sparkover voltage when the line is continuous If the line is continuous, the Thevenin equivalent voltage is

$$= \text{surge voltage} = 1000 \text{ kV}$$

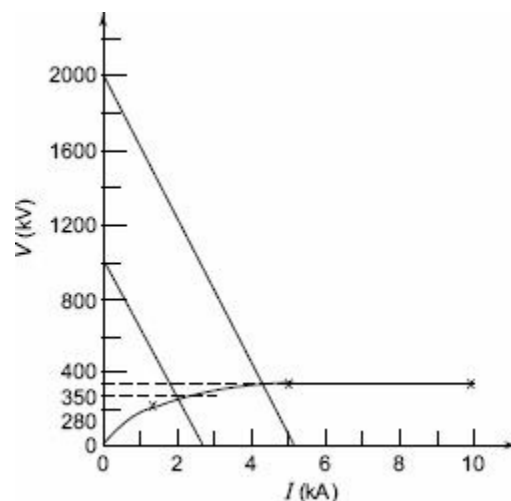


Fig. E.8.7 *V-I characteristic of a surge arrester*

Hence, the maximum arrester current = $1000/400 = 2.5 \text{ kA}$.

From [Fig. 8.7](#), the sparkover voltage = 280 kV and the arrester current = 1.8 kA. Adding 5% extra voltage for the steep-fronted current waves, the sparkover voltages, $V_d = 295 \text{ kV}$.

Example 8.8 *A transmission line has the following line constants $R = 0.1 \text{ ohm/km}$, $L = 1.26 \text{ mH/km}$, $C = 0.009 \mu\text{F/km}$, and $G = 0$. If the line is a 3-phase line and is charged from one end at a line voltage of 230 kV, find the rise in voltage at the other end, if the line length is 400 km.*

Solution

Method 1 Neglecting the resistance of the line,

$$V_2 = V_1 \left(1 - \frac{X_L}{2X_C} \right)$$

$$X_L = j\omega L = j(314) (1.26 \times 10^{-3} \times 400) = j 158.26 \Omega$$

$$X_C = -j/\omega C = -j (10^6/314 \times 0.009 \times 400) = -j 884.6 \Omega$$

$$\begin{aligned} \therefore V_2 &= V_1 \left[1 - \frac{j158.26}{2(-j884.6)} \right] \\ &= V_1 (1 + 0.0896) \end{aligned}$$

The given line voltage = 230 kV

$$\therefore \text{phase voltage} = \frac{230}{\sqrt{3}} = 132.8 \text{ kV}$$

Hence, the rise in voltage = $0.0896 \times 132.8 \text{ kV} = 11.9 \text{ kV}$

Method 2 Considering all the parameters,

$$V_2 = \frac{V_1}{\cos \beta l}$$

where β is the phase constant of the line and l is the length of the line.

$(\alpha + j\beta)$ = transmission line constant

$$\begin{aligned} &= \sqrt{(R + j\omega L)(G + j\omega C)} \\ &= [(0.1 + j314 \times 1.26 \times 10^{-3})(j \times 314 \times 0.009 \times 10^{-6})]^{1/2} \\ (\alpha + j\beta) &= 400 [(0.1 + j314 \times 1.26 \times 10^{-3})(j314 \times 0.009 \times 10^{-3})]^{1/2} \\ &= (0.1962 + j0.3822) \text{ rad} \end{aligned}$$

$$\therefore \cos \beta l = 0.9278$$

$$V_1 = \frac{230}{\sqrt{3}} = 132.8 \text{ kV}$$

$$\begin{aligned} \therefore V_2 &= \frac{V_1}{\cos \beta l} \\ &= V_1 \times 1.0778 \\ &= 143.13 \text{ kV} \end{aligned}$$

Hence, the rise in voltage is 10.33 kV.

Note: Even with resistance neglected, the rise in voltage is changed by 1.58 kV or -1.2% . Hence, in such calculations the effect of the line resistance is negligible.

Example 8.9 Work out the insulation coordination for a 220 kV sub-station with the following data. Take BIL as 1050 kV and BIL to SIL ratio as 1.24.

Solution

Highest system voltage for 220 kV = 245 kV

Highest system voltage to ground = $245 \times \frac{\sqrt{2}}{\sqrt{3}} \approx 295 \text{ kV}$. 200 kV

Expected switching surge voltage = 3.0 p.u = 600 kV

Choosing lightning arrester of 196 kV(200 kV)

Front of wave impulse spark overvoltage = 760 kV Discharge voltage for 5 kA = 690 kV

Discharge voltage for 2 kA switching surge current = 615 kV

SIL for 220 kV system $1050/1.24 = 850$ kV

Protective margin for lightning impulses

$$= \frac{1050 - 690}{1050} = \frac{360}{1050} = 34.3\%$$

Protective margin for switching surges

$$= \frac{850 - 615}{850} = 27.6\%$$

The margin when the lightning arrester just sparks over is $\frac{1050 - 760}{1050} = 27.5\%$ ¹⁰⁵⁰

The protective level is adequate (more than 25%)

(The lightning-arrester data is taken from the data published by a surge-arrester manufacturer)

MULTIPLE-CHOICE QUESTIONS

- The electrical field developed within clouds before a lightning stroke occurs can be of the order of
 - 0.1 kV/cm
 - 1.0 kV/cm
 - 100 kV/cm
 - 10 kV/cm
- The maximum voltage gradient at the ground level due to a charged cloud before lightning strikes, can be as high as
 - 1 V/cm
 - 30 V/cm
 - 30 V/m
 - 300 V/cm
- The velocity of wind currents required for charge separation inside the moving clouds is of the order
 - 1 to 5m/s
 - 5 to 10m/s
 - 10 to 20m/s
 - 50 to 200m/s
- Velocity of leader strokes in lightning discharges is about
 - 1.5×10^5 cm/s
 - 1.5×10^6 cm/s
 - 1.5×10^7 m/s
 - 1.5×10^8 m/s
- The velocity of return or main stroke may be of the order of (C = velocity of light)
 - 0.01 C
 - 0.001 C
 - 0.1 C
 - 0.8 C

6. The peak value of lightning stroke currents are of the order
- 100 A
 - 1000 A
 - 10 to 100 kA
 - 10^6 A
7. The cumulative probability of a 10 kA lightning stroke current (peak) is about
- 0.6
 - 0.2
 - 0.1
 - 0.98
8. The rate of rise of current (dI/dt) in lightning strokes is
- 1 kA/ μ s
 - 100 kA/ μ s
 - 100 A/ms
 - 1000 kA/ms
9. The ground flashover density (N_g) in any region due to lightning activity is about (TD = thunderstorm days)
- 0.1 to 0.2 TD/km²-year
 - 1 to 2 TD/km²-year
 - 30 to 50 TD/km²-year
 - 5 to 15 TD/km²-year
10. Surge impedance of loss less transmission line is (if L — inductance/m, C — capacitance/m)
- $\sqrt{C/L}$
 - $\sqrt{L/C}$
 - \sqrt{LC}
 - \sqrt{LC}
11. The attenuation constant of a transmission line in terms all the parameters R , L , G and C is
- $\frac{R}{L} + \frac{G}{C}$
 - $\left[\frac{R}{L} + \frac{G}{C} \right]^{1/2}$
 - $\frac{1}{2} \left[\frac{R}{L} + \frac{G}{C} \right]$
 - $\frac{R}{L} - \frac{G}{C}$
12. The reflection coefficient for a travelling voltage wave at a junction of two impedances Z_1 and Z_2 is
- $\frac{(Z_1 + Z_2)}{(Z_1 - Z_2)}$
 - $\frac{(Z_2 - Z_1)}{(Z_2 + Z_1)}$
 - $\frac{2Z_1}{(Z_1 + Z_2)}$
 - $\frac{2Z_2}{(Z_1 + Z_2)}$
13. A 400 Ω overhead line is connected to a cable having a surge impedance of 50 Ω , the transmission coefficient into the cable is
- 2/9
 - 1/4

- (c) $-16/9$
 (d) $1/9$
4. For surge-voltage computation, a transformer is represented by an equivalent circuit of
 (a) $R-L$ parallel network
 (b) $L-C$ parallel network
 (c) $R-L$ series network
 (d) $R-L-C$ series network
5. Switching overvoltage in power system networks are of the order of
 (a) 1.5pu
 (b) 2.5to3.5pu
 (c) 10pu or more
6. Overhead transmission lines are protected from lightning overvoltages by
 (a) counter poise wires
 (b) protector tubes
 (c) ground or shield wires above the main conductors
 (d) shunt reactors.
7. In order to limit the overvoltages developed on ground wires due to lightning strokes, the tower footing resistance should be less than
 (a) 1000 Ω
 (b) 100 Ω
 (c) 25 Ω
 (d) 1 Ω
8. For a typical heavy duty (10 kA rated) surge arrester, the discharge voltage at rated current will be of the order of
 (a) 1 pu
 (b) less than 2.0 pu
 (c) more than 3.5 pu
 (d) 2.2 to 3.0 pu
9. The material used in gap less surge arresters used in hv power system is
 (a) graphite
 (b) aluminium oxide
 (c) zinc oxide
 (d) silicon carbide
10. Material that is used in surge arresters for EHV and UHV power systems
 (a) silicon carbide
 (b) zinc oxide
 (c) aluminium oxide
 (d) metal oxides.
11. The volt ampere characteristic of a non-linear resistor used in surge arrester is given by
 (a) $V=KI^2$
 (b) $V=KI^n$
 (c) $V=KT^n$
 (d) $V=K_1I+K_2I^{-1}$.
12. The equivalent circuit of a surge arrester may be represented as:

- (a) capacitor
 - (b) an inductor
 - (c) non-linear resistor
 - (d) resistor
23. Basic impulse level (BIL) of a power system is defined as
- (a) the minimum Insulation Impulse withstand voltage of any power equipment or apparatus
 - (b) the maximum power frequency withstand voltage of any power equipment or apparatus
 - (c) the minimum power frequency withstand voltage of any apparatus or power equipment
 - (d) the peak value of highest system voltages.
24. The BIL of a power system is usually chosen as
- (a) 25% to 30% more than the protective level offered by the protective devices (surge arresters etc.)
 - (b) 50% more than the protective level offered by the protective devices (surge arresters etc.)
 - (c) 5 to 10% more than the protective level offered by the protective devices (surge arresters etc.)
 - (d) highest lightning surge voltage expected.
25. In EHV and UHV system the type of surge diverter used for overvoltage protection is
- (a) valve type Si C arrester
 - (b) gapless ZnO arrester
 - (c) gapless Si C arrester
 - (d) rod gap
26. The duration of switching surges in GIS is
- (a) ms
 - (b) microseconds
 - (c) few nanoseconds and less than a microsecond
 - (d) few tens of micro seconds
27. Indirect strokes near overhead transmission lines induce overvoltages due to
- (a) electrostatic induction
 - (b) both electrostatic and electromagnetic induction
 - (c) only electromagnetic induction
 - (d) conduction currents through line conductors
28. In EHV and UHV system, ratio of BIL to SIL will be usually
- (a) less than unity
 - (b) more than 1.5
 - (c) 1.5 to 2.0
 - (d) 1.2 to 1.5
29. The purpose of insulation coordination is to
- (a) limit the overvoltages
 - (b) to protect the electrical apparatus against overvoltages
 - (c) to grade the insulation of different power apparatus and overhead lines such that the least important and easily replaceable apparatus flashes or fails first and the most important one is protected to the highest level.
 - (d) None of the above a, b or c.
30. The maximum rate of rise of surge currents that occur in overhead lines is
- (a) 2 to 3 kA/ms
 - (b) less than 1 kA/ms

- (c) 5 to 10 kA/ms
- (d) greater than 10 kA/ms

Answers to Multiple-Choice Questions

- | | | | | | |
|---------|---------|---------|---------|---------|---------|
| 1. (d) | 2. (d) | 3. (c) | 4. (c) | 5. (c) | 6. (c) |
| 7. (a) | 8. (b) | 9. (a) | 10. (b) | 11. (c) | 12. (b) |
| 13. (a) | 14. (b) | 15. (b) | 16. (c) | 17. (c) | 18. (d) |
| 19. (d) | 20. (c) | 21. (b) | 22. (c) | 23. (a) | 24. (a) |
| 25. (b) | 26. (c) | 27. (b) | 28. (d) | 29. (c) | 30. (a) |

REVIEW QUESTIONS

1. Explain the different theories of charge formation in clouds.
2. What are the mechanisms by which lightning strokes develop and induce overvoltages on overhead power lines?
3. Give the mathematical models for lightning discharges and explain them.
4. What are the causes for switching and power frequency overvoltages? How are they controlled in power systems?
5. What are the different methods employed for lightning protection of overhead lines?
6. Explain with suitable figures the principles and functioning of (a) expulsion gaps, and (b) protector tubes.
7. What is a surge arrester? Explain its function as a shunt protective device.
8. What is meant by insulation co-ordination? How are the protective devices chosen for optimal insulation level in a power system?
9. With suitable illustrations, explain how insulation level is chosen for various equipment in a 230/132 kV sub-station.
10. Write short notes on
 - (a) Rod gaps used as protective devices
 - (b) Ground wires for protection of overhead lines
11. Derive the expressions for the voltage and current waves on long transmission lines and obtain the surge impedance of the line.
12. Define 'surge impedance' of a line. Obtain the expressions for voltage and current waves at a junction or transition point.
13. Explain the terms 'attenuation and distortion' of travelling waves propagating on overhead lines. What is the effect of corona on the transmission lines?
14. Explain the importance of switching overvoltages in EHV power systems. How is protection against overvoltages achieved?
15. Explain the different aspects of insulation design and insulation co-ordination adopted for EHV systems.

PROBLEMS

1. A transmission line of surge impedance, Z_A equal to 500Ω is connected through a cable of surge impedance 50Ω to another line of surge impedance Z_B equal to 600Ω . A travelling wave of $100 u(t)$ kV travels from the 500Ω line towards the 600Ω line through a cable. Calculate the voltage at the junction of the 500Ω line and the cable, after the first and second reflections.

- A 500 kV, 2 ms rectangular wave travels on a line having a surge impedance of 350Ω and approaches a termination with a capacitance C equal to 300 pF. Determine the magnitudes of the reflected and transmitted waves.
- A 220 kV, 3-phase line has a horizontal configuration of conductors 5 m apart. The ground clearance is 15 m. Find the position and the number of ground wires required.
- A long transmission line of 370 ohm surge impedance is connected to two cables each of surge impedance of 50 ohm and 75 ohm. If a surge of $100 e^{-0.1t}$ at $u(t)$ (t in ms) strikes the transmission line and cables, determine (i) the junction voltage, and (ii) the voltage wave transmitted through each of the cables.
- Estimate the overvoltage produced on the insulator string on a transmission line tower if a 10 kA lightning stroke directly hits the tower ground wire. Assume the surge impedance of line to be 400 ohms, surge impedance of ground wire of 350 ohms, tower footing resistance of 40 ohms and tower surge impedance — 135 ohms.
- A transmission line has the following line constants: $L = 1.26$ mH/km and $C = 0.009$ μ F/km. If the line is a 3-phase line and is charged from one end at a line voltage of 400 kV, 50 Hz, find the rise in voltage at the other end, if the line length is 250 km. The line resistance and leakage conductance may be neglected.
- An underground cable of 0.18 mH/km inductance and of 0.5 μ F/km capacitance is connected to an overhead line having an inductance of 1.26 mH/km and capacitance of 0.009 μ F/km. Calculate the transmitted and reflected voltage waves, and the junction voltage if the surge of 500 kV travels to the junction (i) along the cable, and (ii) along the overhead line.

Answers to Problems

- Junction voltage after 1st reflection = 18.2 kV Junction voltage after 2nd reflection = 27.9 kV
- Reflected wave: $500 (1 - 2 e^{-0.9524t}) [u(t) - u(t - 2)]$ kV, $t = \beta$ s Transmitted wave: $1000 [1 - e^{-0.9524t}] [u(t) - u(t - 2)]$ kV, $t = \beta$ s
- Two wires at a height of 4.33 m above conductor level, i.e. 19.33 m above ground level
- Junction voltage $185 e^{-0.1t} u(t)$ kV
Transmitted voltage through 50 Ω cable = $9 \times e^{-0.1t} u(t)$
Transmitted voltage through 75 Ω cable = $6 \times e^{-0.1t} u(t)$
- 87.5 kV assuming the ground wire is spread on either side of the tower.

REFERENCES

- Bewley, L.V., *Travelling Waves on Transmission Systems*, Dover Publications Inc., New York (1963).
- Lewis, W.W., *Protection of Transmission Lines and Systems against Lightning*, Dover Publications., Inc. New York (1965).
- Transmission and Distribution Reference Book*, Westinghouse Electric Corporation and Oxford University Press, New Delhi (1962).
- Marshall, J.L., *Lightning Protection*, John Wiley and Sons, New York (1973).
- Diesendorf, W., *Insulation Coordination in H.V. Electric Power Systems*, Butterworths, London (1974).
- Begamudre, R.D., E.H.V, *A.C. Transmission Engineering*, Wiley Eastern, New Delhi (1986).
- Golde, R.H., *Lightning*, Vol. 1 and 2, Academic Press, London (1977).

8. Black, R.M. and E.H. Reynolds, "Ionization and irradiation effects in high voltage dielectric materials", *Journal of Institute of Engineers*, London, **112**, 1226 (1965).
9. Bell, E., *et al.*, "Lightning investigations on 220 kV systems", *Tr. AIEE*, **150**, 1101 (1931).
10. Muller Hiller Brand, *et al.*, "Lightning counter measurements", *Proc. IEE*, **112**, 203 (1965).
11. Anderson, J.G., *EHV Transmission Reference Book*, Edison Electric Co, New York, 1968.
12. *CIGRE Report No. 22*, 139 (1972).
13. Newman, S.E., *et al.*, "Insulation coordination in H.V. stations", *English Electric Journal*, **13**, No. 3, 120 (1953).
14. "Insulation co-ordination", *IEC Technical Committee 28, Report No. 35* (1970).
15. *IEC Publication* on "Insulation coordination", No. 71, (5th edition), (1972).
16. Phelps., J.D., *et al.*, "765 kV station insulation co-ordination" *Tr. IEEE PAS, PAS-88*, 1377 (1965).
17. Kuffel, E. and Zaengl, W., "*High Voltage Engineering Fundamentals*", Pergamon Press, Oxford, England, 1984.
18. Andresson, R.B. and Erickson, A.J., "Lightning Parameters for Engineering Application", *Electra*, No. 69 (1980).
19. Chowdhuri, P., "Estimation of flashover rates of overhead power distribution lines by lightning strokes to nearby ground", *IEEE Trans. on Power Delivery*, Vol. 4, No. 3, July (1989).
20. Uman, M.A., *The lightning discharge*, Academic Press Inc., Orlando, Florida, (1987).
21. Nucci, C.A., Guerrieri, S., Correia de Barros, M.T. and Rachid, F., "Influence of corona on the voltages induced by nearby lightning on overhead distribution lines", *IEEE Trans. on Power Delivery*, 15, No. 4, pp. 1265-1273, October (2000).
22. Erikson, A.J., "The incidence of lightning strikes to power lines" *IEEE Power Delivery*, **PWRD-2**, No. 3, July (1987).
23. Brown, J.D., Fisher, F.A., Neugebauer, W. and Panek, J., *Insulation-design criteria, Transmission line reference book*, 2nd edition, EPRI, (1982).
24. "Electric System Issues at the turn of the 21st Century", *CIGRE Electra*, Special Issue (2000).
25. Dugan, R., McGranaghan, M.F. and Beaty, H.W., *Electrical Power Systems Quality*, McGraw-Hill (1996).
26. Tesche, F.M., Lanoz., M. and Karlsson, T., *EMC analysis methods and computational models*, John Wiley and Sons (1997).
27. Henriksen, T., "Calculation of lightning overvoltages using EMTP", *Proc. Int. Conf. on Power Systems Transients*, Lisbon, Sept. 3-7 (1995).
28. Agrawal, A.K., *et al.*, "Transient Response of a multiconductor transmission line excited by non uniform e.m. fields" *Tr IEEE on EMC Vol: EMC-2*, no 2, pp. 119-129, May 1980.
29. "Carlo Albero Nucci: Modelling of Lightning return strokes: Key note speech", 12 ISH, Page 20-26, Aug. 2001.
30. *The Electrical Power Engineering Hand Book*, Editor in Chief L.L. Grigsby CRC Press/IEEE New York 2001.

CHAPTER

9

Non-Destructive Testing of Materials and Electrical Apparatus

9.1 INTRODUCTION

Electrical insulating materials are used in various forms to provide insulation for the apparatus. The insulating materials may be solid, liquid, gas, or even a combination of these, such as paper impregnated with oil. These materials should possess good insulating properties over a wide range of operating parameters, such as a wide temperature range (0°C to 110°C) and a wide frequency range (dc to several MHz in the radio and high-frequency ranges). Since it is difficult to test the quality of an insulating material after it forms part of an equipment, suitable tests must be done to ensure their quality in the said ranges of operation. Also, these tests are devised to ensure that the material is not destroyed as in the case of high-voltage testing.

These tests are mainly done to assess the electrical properties, such as the resistivity (dc), the dielectric constant, and loss factor over a wide frequency range. In high-voltage apparatus, the quality of insulation is assessed by measuring the loss factor at high voltages and also by conducting partial discharge tests to detect any deterioration or faults in the internal insulation of the apparatus.

These tests may be conducted at a desired temperature or over a temperature range by keeping the test specimen in controlled temperature ovens. Knowledge of the variation of electrical properties over the operating range can be obtained from these tests and this will help the design engineer to take into account such variations in the design of electrical insulation for equipment.

9.2 MEASUREMENT OF DIRECT CURRENT RESISTIVITY

9.2.1 Specimens and Electrodes

The specimen shape and the electrode arrangement should be such that the resistivity can be easily calculated. For a solid specimen, the preferable shape is a flat plate with plane and parallel surfaces, usually circular. The specimens are normally in the form of discs of 5 to 10 cm diameter and 3 to 12 mm thickness.

If the electrodes are arranged to be in contact with the surfaces of the specimen, the measured resistance will be usually greater due to the surface conductivity effects. Often, a three-electrode arrangement shown in Fig. 9.1 is used. The electrode which completely covers the surface of the specimen is called the 'unguarded' electrode and is connected to the high-voltage terminal. The third electrode which surrounds the other measuring electrode is connected to a suitable terminal of the measuring circuit. The width of this 'guard' electrode must be at least twice the thickness of the specimen, and the unguarded electrode must extend to the outer edge of the guard electrode. The gap between the guarded and guard electrodes should be as small as possible. The effective diameter of the guarded electrode is greater than the actual diameter and is given as follows.

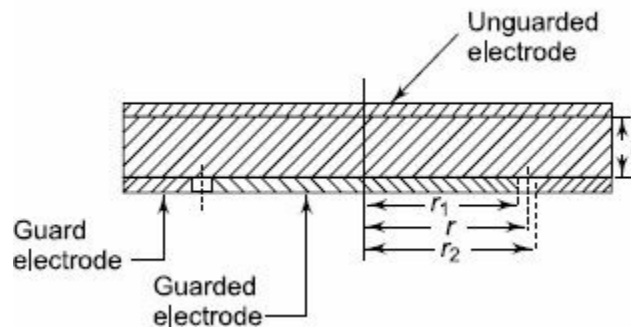


Fig. 9.1 The three-electrode system

Let r_1 , r_2 , and r be the radii of the guarded electrode, guard electrode including the gap, and the effective radius of the guarded electrode. Let the gap width = g and the specimen thickness = t . Then from references 5 to 6,

$$r = r_1 + \frac{g}{2} - \delta \quad (9.1)$$

where,
$$\frac{\delta}{t} = \frac{2}{\pi} \ln \cosh \left(\frac{\pi g}{4t} \right)$$

9.2.2 Electrode Materials

For accurate measurements, the electrodes should have very good contact with the surface of the insulator specimen. Hence, it is necessary to use some type of thin metallic foil (usually of lead or aluminium about 10 to 50 μm thickness), usually pressed on to the surface by a roller and made to stick by using a conducting adhesive like petroleum jelly or silicone grease. The electrodes are made simultaneously by cutting out a narrow strip by means of a compass provided with a narrow cutting edge. Sometimes conducting silver paint is also used for electrode deposition. Evaporated metal deposition on the specimen surface or use of mercury electrodes, applied by floating the specimen on a pool of mercury using confining rings with sharp edges for holding the metal, are also convenient.

9.2.3 Measuring Cells

The three-terminal electrode system and the measuring cell used are shown in [Fig. 9.2](#). The measuring cell is usually a shallow metal box provided with insulating terminals. The box itself is connected to the guard electrode and is grounded if the guard terminal is grounded. The connecting lead for the guarded electrode is taken through a shielded wire. In case the unguarded electrode is grounded, the entire box is to be placed on insulated supports and is to be placed in a grounded shield to eliminate induced voltages, and the lead from the guard electrode is doubly shielded.

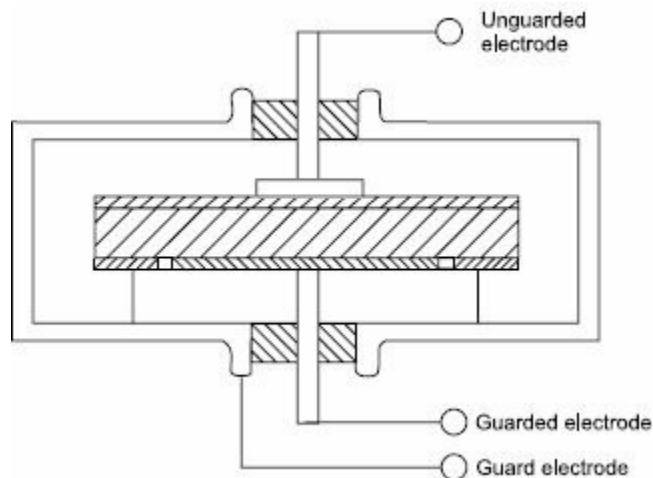


Fig. 9.2 *Three-terminal cell for study of solids*

In the simple two-terminal system, the measuring cell itself is the grounded support for the specimen and a small solid wire is connected to the high-voltage terminal of the measuring circuit, as can be seen from [Fig. 9.3](#). This is a simple and compact arrangement for quick measurements and requires less skill.

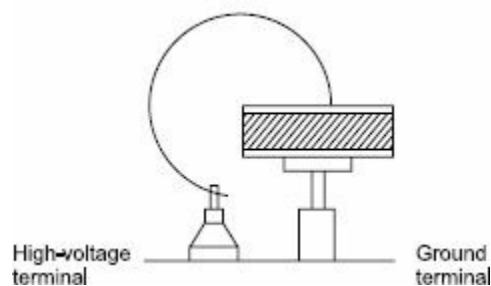


Fig. 9.3 *Stiff-wire connection for two-terminal measurement*

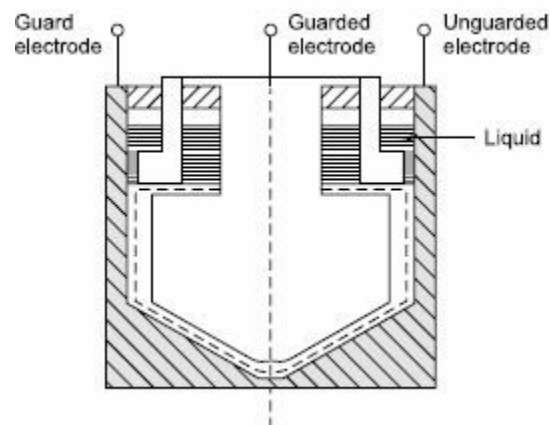


Fig. 9.4 *Three-terminal cell for study of liquids* Guard electrode

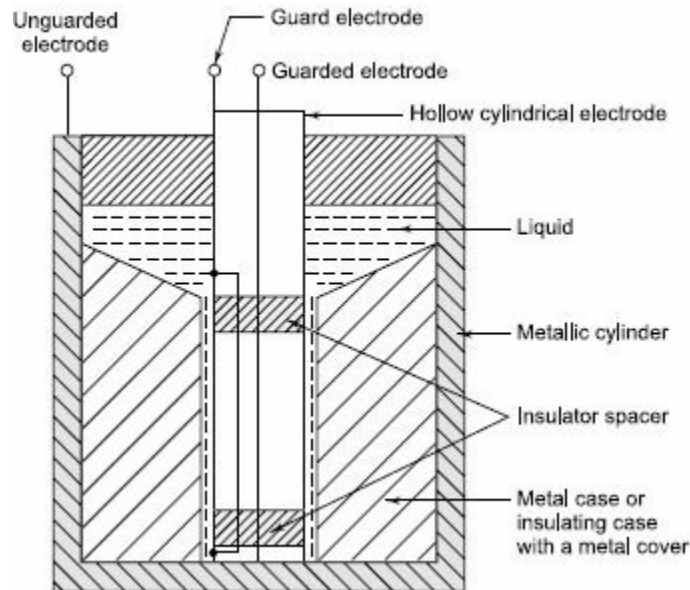


Fig. 9.5 *Three-terminal cell for study of liquids*

The arrangement used for the study of liquids is shown in [Fig. 9.4](#). This consists of an outer cylindrical case and an inner cylinder with a cylindrical guard electrode. The opposing surfaces of the measuring electrodes should be carefully finished to give a polished surface, and a uniform spacing of about 0.25 mm is maintained. The insulation should be able to maintain the alignment of the electrode even at the highest temperatures used and should still allow easy disassembling and cleaning. Another simple arrangement of the three-electrode system for the study of liquids is shown in [Fig. 9.5](#). This consists of a metallic cylindrical container with concentric hollow cylindrical electrodes as guard and guarded electrodes. The inner surface of the container electrode (unguarded) and the outer surfaces of the guard and unguarded electrodes should be carefully finished and a clearance of about 0.25 to 0.5 mm should be accurately maintained. The arrangement requires less liquid (usually only about 1 to 2 ml).

9.2.4 Measuring Circuits

A simple measuring circuit for the measurement of resistance is shown in Fig. 9.6. The galvanometer is first calibrated by using a standard resistance of 1 to 10 M Ω ($\pm 0.5\%$ or $\pm 1\%$). If necessary, a standard universal shunt is used with the galvanometer. The deflection in cm per microampere of current is noted. The specimen (R_p) is inserted in the circuit as shown in Fig. 9.6, and maintaining the same supply voltage, the galvanometer current is observed by adjusting the universal shunt, if necessary. The galvanometer gives a maximum sensitivity of 10^{-9} A/cm deflection and a dc amplifier has to be used along with the galvanometer for higher sensitivities (up to 10^{-12} to 10^{-13} A/cm).

The resistance of the specimen is given by

$$R_p = \frac{V}{(D \times G)} \quad (9.2)$$

where, D = deflection in cm (with specimen), and
 G = galvanometer sensitivity.

$$G = \left(\frac{V}{R_s} \right) \times \left(\frac{1}{n} \right) \times \left(\frac{1}{D_s} \right)$$

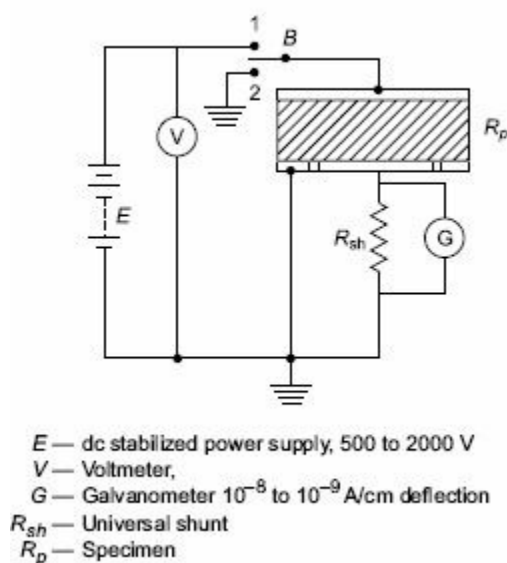


Fig. 9.6 dc galvanometer arrangement

in which, n = the universal shunt ratio,

D_s = deflection in cm with the standard resistance in position,

R_s = standard resistance used for calibration, and

V = the supply voltage.

It may be noted that the deflection with the specimen in the circuit, will change with time. The initial high deflections indicate the high charging current required by the dielectric specimen. For the purpose of calculations, the steady current obtained after a considerably long changing time should only be taken. Switch B is used to discharge the specimen after the measurements are complete and as well as for the initial discharging before the measurements are undertaken.

In Fig. 9.7, the dc galvanometer of Fig. 9.6 is replaced by a dc amplifier for resistivity

measurements. Here, the dc amplifier is used as a null detector. A separate potentiometer circuit is used for obtaining a signal e equal and opposite to the voltage drop across the standard resistance R_s . At balance, the voltage drop across R_s is effectively made zero. Any ac voltage appearing across the standard resistance R_s is amplified only by the net gain of the amplifier which is small. Using a recording meter after the dc amplifier in this arrangement, the volt-ampere-time curves for long durations, of the order of several hours (day also) can be obtained. This type of information is essential to determine the relaxation time at low frequencies or with dc.

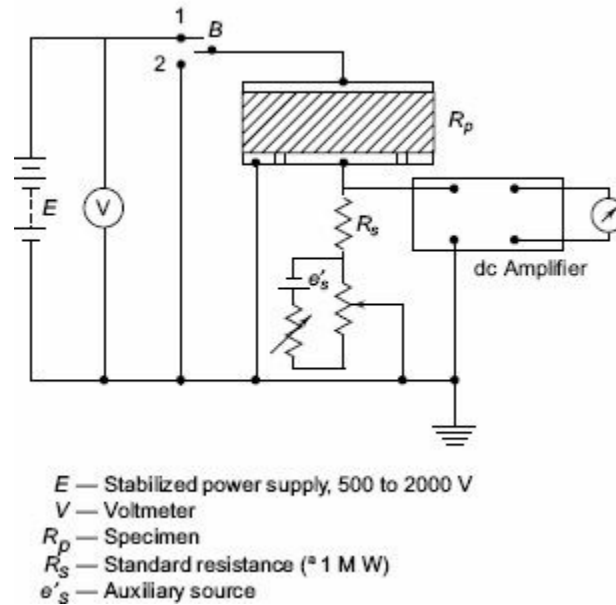


Fig. 9.7 dc amplifier circuit for resistivity measurements

Figure 9.8 gives the Wheatstone bridge network. One of the resistances (usually R_A) is made variable for balancing the bridge. At balance, R_p is given by

$$R_p = R_s \frac{R_A}{R_B} \quad (9.3)$$

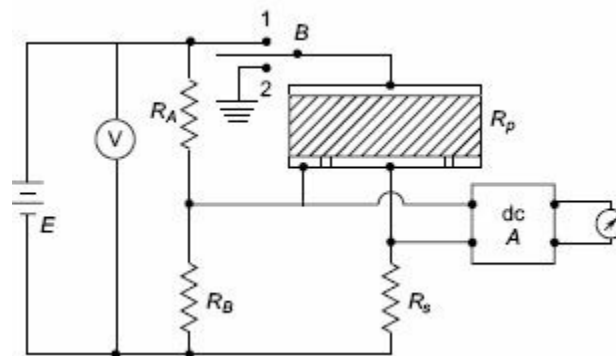


Fig. 9.8 Wheatstone bridge arrangement for resistivity measurements

With the specimen arrangement used, the volume resistivity ρ can be given as

$$\rho = \frac{R\pi r^2}{l} \Omega \text{ m} \quad (9.4)$$

where, R = measured resistance in ohms,

t = thickness of the specimen in metres, and

r = effective radius in metres.

Using this network, the volume resistivity ρ for liquid specimens with cylindrical electrodes as shown in [Fig. 9.5](#), can be expressed as

$$\rho = \frac{2\pi Rl}{\ln \frac{d_2}{d_1}} \Omega\text{m} \quad (9.5)$$

where, R = measured resistance in ohms,

l = effective length of the guarded electrode in metres,

d_2 = inner diameter of unguarded electrode, and

d_x = outer diameter of guarded electrode, both in metres.

9.2.5 Loss of Charge Method

Using the circuit shown in [Fig. 9.6](#), the current-time characteristic of the discharge current can be obtained by placing the switch B in position 2. The capacitance of the specimen is discharged through its own volume resistance. The slope of the current time characteristic gives the time constant $\tau = CR$, where C is the capacitance of the specimen. The volume resistance of the specimen R can thus be obtained from this relationship by measuring τ and C .

Alternatively, a capacitance previously charged (C_1) may be discharged through the specimen by inserting it in place of the battery E . By knowing the value of the capacitance C_1 which is very large compared to the specimen capacitance ($\approx 10 \mu\text{F}$) and knowing the current-time characteristic of the discharge current, its time constant can be calculated. Hence, the resistance of the specimen is obtained from the relationship

$$R = \frac{C_1}{\tau}$$

where C_1 is the capacitance used and τ is the time constant.

In the deflection method described, a limit is reached when the insulation resistance is so high that the galvanometer deflection is not at all adequate. This happens when the resistance is around $10^{12} \Omega$ or more. Under these conditions, the loss of charge method is convenient. It is also convenient to measure the initial voltage V_0 on the capacitor and the voltage V across it at any time τ . Then the unknown resistance R can be calculated from the relationship

$$R = \frac{t}{C_1 \ln \frac{V_0}{V}} \quad (9.6)$$

It is convenient to use an electrometer amplifier or electrostatic voltmeter for the measurement of the voltage. The measured value of R includes the resistance of the voltage measuring device in parallel.

The accuracy of this method depends on the accuracies with which the values of the capacitance and the voltage are measured.

9.3 MEASUREMENT OF DIELECTRIC CONSTANT AND LOSS FACTOR

9.3.1 Introduction

Many insulating substances have dielectric constant greater than unity and have dielectric loss when subjected to ac voltages. These two quantities, namely, the dielectric constant and the loss depend on the magnitude of the voltage stress and on the frequency of the applied voltage. When a dielectric is used in an electrical equipment such as cable or a capacitor, the variation of these quantities with frequency is of importance. The microscopic properties of the dielectric are described by combining the variation of the above two quantities into one 'complex quantity' known as 'complex permittivity' and determining them at various frequencies.

A capacitor connected to a sinusoidal voltage source $v = v_0 \exp(j\omega t)$ with an angular frequency $\omega = 2\pi f$ stores a charge $Q = C_0 v$ and draws a charging current $I_c = dQ/dt = j\omega C_0 v$. When the dielectric is vacuum, C_0 is the vacuum capacitance or geometric capacitance of the capacitor, and the current leads the voltage v_c by 90° .

If the capacitor is filled with a dielectric of permittivity ϵ' , the capacitance of the capacitor is increased to $C = C_0 \epsilon' / \epsilon_0 = C_0 K'$ where K' is the relative dielectric constant of the material with respect to vacuum.

Under these conditions, if the same voltage V is applied, there will be a charging current I_c and loss component of the current, I_l . I_l will be equal to GV where G represents the conductance of the dielectric material. The total current $I = I_c + I_l = (j\omega C + G) V$. The current leads the voltage by an angle θ which is less than 90° . The loss angle δ is equal to $(90 - \theta)^\circ$. The phasor diagrams of an ideal capacitor and a capacitor with a lossy dielectric are shown in [Figs 9.9a](#) and [b](#).

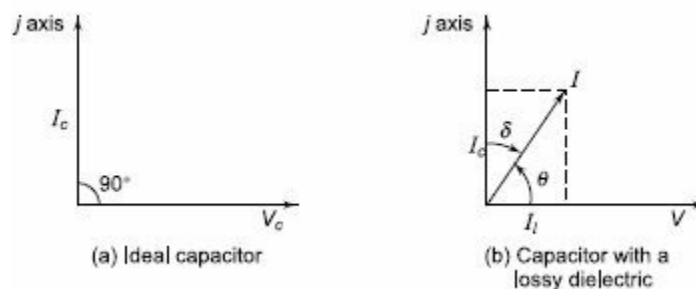


Fig. 9.9 Capacitor phasor diagrams

It would be premature to conclude that the dielectric material corresponds to an $R-C$ parallel circuit in electrical behaviour. The frequency response of this circuit which can be expressed as the ratio of the loss current to the charging current, i.e., the loss tangent

$$\tan \delta = D = \frac{I_l}{I_c} = \frac{1}{\omega CR} \quad (9.7)$$

may not at all agree with the result actually observed, because the conductance need not be due to the migration of charges or charge carriers but may represent any other energy consuming process. Hence, it is customary to refer the existence of a loss current in addition to the charging current by

introducing 'complex permittivity'

$$k^* = \epsilon' - j\epsilon'' \quad (9.8)$$

so that current I may be written as

$$I = (j\omega\epsilon' + \omega\epsilon'') \frac{C_0}{\epsilon_0} v \quad (9.9)$$

$$= j\omega C_0 K^* v$$

$$K^* = (\epsilon' - j\epsilon'')/\epsilon_0 = K' - jK'' \quad (9.10)$$

where

K^* is called the complex relative permittivity or complex dielectric constant, ϵ' and K' are called the permittivity, and relative permittivity and ϵ'' and K'' are called the loss factor and relative loss factor respectively.

The loss tangent

$$\tan \delta = \frac{\epsilon''}{\epsilon'} = \frac{K''}{K'} \quad (9.11)$$

The product of the angular frequency and ϵ'' is equivalent to the dielectric conductivity σ .

$$\sigma = \omega\epsilon'' \quad (9.12)$$

The dielectric conductivity sums up all the dissipative effects and may represent the actual conductivity as well as the energy loss associated with the frequency dependence (dispersion) of ϵ' , i.e., the orientation of dipoles in a dielectric.

In dielectric measurements, often, the geometrical capacitance and the capacitance of the system with a dielectric material are obtained. The ratio of the above two measurements gives the relative permittivity $\epsilon'/\epsilon_0 = K'$. This is sometimes referred to as the dielectric constant or ϵ_r .

Dielectric Response in Time Varying (ac) Fields In dielectric materials, the polarization P , the electric field E and the flux density D are related by the equation

$$D = \epsilon_0 E + P = \epsilon_0 [1 + \chi] E$$

where, χ is the dielectric susceptibility of the material with a varying electric fields $E(t)$, the polarization P induces current in a dielectric due to charge migration whenever an electric field is suddenly applied. With dc, if the material has a conductivity σ , then the current density obtained is $\sigma E(t)$ and the polarization displacement current will be $\delta D(t)/\delta t$. Hence, the total current density produced is

$$\begin{aligned} j(t) &= \sigma E(t) + \frac{\delta D(t)}{\delta t} = \sigma E(t) + \epsilon_0 \frac{\delta E(t)}{\delta t} + \frac{\delta P(t)}{\delta t} \\ &= \{\sigma + \epsilon_0 (1 + \chi) \delta(t) + f(t)\} E(t) \end{aligned}$$

where, $\delta(t)$ is instantaneous impulse response and $f(t)$ is the further response obtained.

Hence, the polarization current obtained in terms of the geometrical capacitance C_0 (without material) is,

$$i(t) = C_0 V \left[\frac{\sigma_0}{\epsilon_0} + (1 + \chi) \delta(t) + f(t) \right]$$

where, V is the applied voltage that produces the electric field $E(t)$

If the equations are transformed into frequency domain (ω) and with the complex frequency concept, we get

$$j(\omega) = E(\omega) [\sigma_0 + j \omega \epsilon_0 (1 + F(\omega))]$$

$$\chi(\omega) = F(\omega) = \chi'(\omega) - j \chi''(\omega)$$

where $F(\omega)$ is the complex susceptibility.

Hence, the complex permittivity $\epsilon^*(\omega)$ may be written as

$$\begin{aligned} \epsilon^*(\omega) &= \epsilon'(\omega) - j \epsilon''(\omega) \\ &= [1 + \chi(\omega)] - j \chi''(\omega) \end{aligned} \quad (9.13)$$

From this, the dissipation factor $\tan \delta$ is obtained as

$$\tan \delta(\omega) = \frac{\epsilon''(\omega) + \sigma / \epsilon_0 \omega}{\epsilon_r(\omega)} \quad (9.14)$$

where $\epsilon_r(\omega)$ is the effective dielectric constant $\epsilon(\omega) / \epsilon_0$.

The above equations clearly show that the loss factor $\tan \delta$ is a function of ω and hence is to be determined or measured over a frequency range.

9.3.2 Measurement Ranges

Lumped circuits are used in the measurements of the dielectric constant and $\tan \delta$ over the frequency range from dc (0 Hz) to about 100 MHz. Neither of these quantities are determined directly. Measurements of capacitance using either a null method or a deflection method is employed over the low frequency range (0–10 Hz), where bridge methods are difficult. Normally, the shape of the current time characteristic curve is determined from which these parameters are deduced. Sometimes, modified bridge methods are extended to this frequency range also. Over the medium frequency range (10 Hz to 10^6 Hz), bridge methods are employed. The commonly employed bridge networks are the four arm Schering-bridge to operate from power frequency (50 Hz) to about 100 kHz and the ‘High-Voltage Schering Bridge’ for power frequency (50 Hz) when the effect of voltage stress on dielectric constant and $\tan \delta$ is required. Over the high frequency range (100 kHz to 100 MHz), bridge circuits present problems in shielding and the errors measurements become excessive. Micrometer electrodes using vernier capacitors (electrode separation being controlled and measured to micrometer (μm) accuracy) have to be employed to avoid errors due to residual impedances. Using these methods, dissipation factor, $\tan \delta$, is usually obtained from the width of the resonant curve by varying either the frequency or the susceptibility of the circuit. At frequencies above 100 MHz, the lumped circuit approximation is not valid as the wavelength of the frequency approaches that of the specimen thickness. Microwave techniques like ‘the travelling wave’ or ‘the standing wave’ measurements are to be employed beyond the frequency limit of 10^8 Hz. The information obtained from the measurements of $\tan \delta$ and the complex permittivity help in assessing the quality of the dielectric and the insulation system.

- (i) Variation and sudden change in $\tan \delta$ value with applied voltage is an indication of the inception of partial discharge (PD). This is used to determine the inception level of internal discharges and losses due to PD in high-voltage equipment.
- (ii) To study the variation of the dielectric properties with frequency. Much of the interest in this study is concerned with the frequency region where dispersion occurs, i.e., where the permittivity reduces with rise in the frequency.

9.3.3 Low-Frequency Measurement Methods (0-10 Hz)

In testing equipment of large k VA ratings at high voltages and to study the properties of dielectrics at zero frequency (dc) or near to it, it is advantageous to carry out tests in the frequency range of zero to 10 Hz. Conventional Wheatstone type bridges are not suitable over this frequency range. The dc amplifier method described in [Sec. 9.2.4](#) can be used in testing the dielectrics over this frequency range. The accuracy of the measurements will depend on the stability of the supply sources and the detectors.

9.3.4 Power-Frequency-Measurement Methods—High-Voltage Schering-Bridge

In the power-Frequency range (25 to 100 Hz) Schering-bridge is a very versatile and sensitive bridge and is readily suitable for high voltage measurements. The stress dependence of K' or ϵ_r and $\tan \delta$ can be readily obtained with this bridge.

The schematic diagram of the bridge is shown in Fig. 9.10. The lossy capacitor or capacitor with the dielectric between electrodes is represented as an imperfect capacitor of capacitance C_x together with a resistance r_x . The standard capacitor is shown as C_s which will usually have a capacitance of 50 to 500 pF. The variable arms are R_4 and C_3 R_3 . Balance is obtained when

$$\frac{Z_1}{Z_2} = \frac{Z_4}{Z_3}$$

where,

$$Z_1 = r_x + \frac{1}{j\omega C_x}, \quad Z_2 = \frac{1}{j\omega C_s}$$

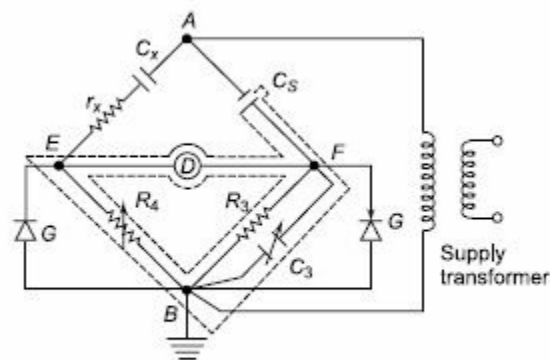
$$Z_3 = \frac{R_3}{1 + j\omega C_3 R_3}, \quad \text{and} \quad Z_4 = R_4$$

The balance equations are

$$C_x = \frac{R_3}{R_4} C_s; \quad \text{and} \quad r_x = \frac{C_3}{C_s} R_4 \quad (9.15)$$

The loss angle,

$$\tan \delta_x = \omega C_x R_x = \omega C_3 R_3 \quad (9.16)$$



... dotted line is the shielding arrangement. Shield is connected to B, the ground.
G: Protective device for Z_3 , R_4 arms.

Fig. 9.10 Schematic diagram of a Schering-bridge

Usually, δ_x will be small at power frequencies for the common dielectrics so that

$$\cos \theta_x = \sin \delta_x = \delta_x = \tan \delta_x = \omega C_3 R_3 \quad (9.17)$$

The lossy capacitor which is made as an equivalent C_x in series with r_x can be represented as a parallel combination of C_x and R_x where the parallel combination R_x is found to be

$$R_x = \frac{1}{\omega^2 C_x^2 r_x} \quad (9.18)$$

with C_x having the same value.

The normal method of balancing is by fixing the value of R_3 and adjusting C_3 and R_4 . If R_3 is chosen as $(1000/\pi)$ ohms for $\omega = 100\pi$ and if C_3 is expressed in microfarads, then $\tan \delta = 0.1 C_3$ giving a direct reading of $\tan \delta$. R_4 will be a decade box with 5 to 6 decade dials. The maximum value of R_4 is limited to $10^4 \Omega$ and the lowest value will not be less than 0.01Ω . This range adequately takes care of the errors due to contact resistances as well as the stray capacitance effects across R_4 which are usually very small. It is important to see that the resistances are pure and not reactive and the standard capacitor has negligible $\tan \delta$ (air or gas filled capacitor is used).

The arrangement shown in [Fig. 9.10](#) is suitable when the test specimen is not grounded. The standard capacitor C_s is usually a three terminal capacitor. The low-voltage arms of the bridge (R_4 and $R_3 C_3$) and the detector are enclosed in grounded shielded boxes to avoid stray capacitances during the measurements. The detector is either a vibration galvanometer or in modern bridges a tuned electronic null detector of high sensitivity. The protective gaps G are so arranged that the low-voltage arms are protected from high voltages in case the test objects fail. The values of the impedances of the low-voltage arms are such that the voltage drop across EB or FB does not exceed 10 to 20 V. The arms will be usually rated for a maximum instantaneous voltage of 100 V.

For a very accurate measurement of the dissipation factor at power frequency, the stray and grounded capacitances should be eliminated and the indirect capacitive and inductive coupling of the arms are to be minimized to a level lower than the accuracy of the bridge arms. In this bridge, the main source of error is the ground capacitance of the low-voltage terminals of high voltage arms, i.e., the stray capacitances from E and F to ground. These are eliminated by shielding the low voltage arms using doubly shielded cables for connections and using the 'Wagner earthing device'. Sometimes, compensation for the stray capacitances is given by providing a parallel $R-L$ circuit across R_4 .

(a) Schering-Bridge Arrangement for Grounded Capacitors For safety reasons and to define the shield potentials with respect to each other, one of the terminals of the bridge is earthed. This is usually the low-voltage arm connection of the supply source (Terminal B of [Fig. 9.10](#)), because a low impedance arm with respect to the detector branch gives a high signal to noise ratio in measurements.

While testing grounded test objects like underground cables or bushings with flanges grounded to the tank of a transformer, one of the detector terminals (E or F) has to be grounded. In such cases, either an inverted bridge ([Fig. 9.11](#)) or a grounded detector arrangement ([Fig. 9.12](#)) has to be adopted. In the inverted bridge operation, the self-contained bridge is located inside a Faraday cage at the high voltage terminal and a standard capacitor is mounted on insulating supports. The variable arms are operated by insulated isolating rods. Sometimes, the operator himself will be inside the Faraday cage.

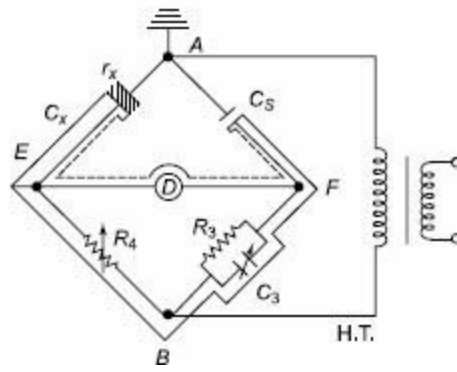


Fig. 9.11 Inverted Schering bridge for grounded capacitors

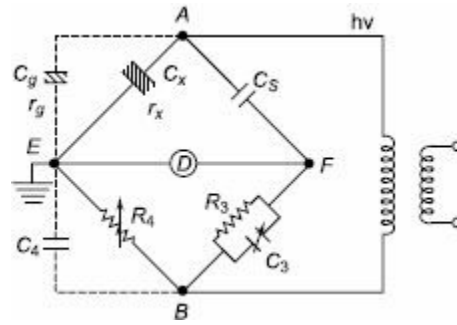


Fig. 9.12 Schering bridge for grounded objects (detector end grounded)

In the grounded detector arrangement, stray capacitances of the high voltage terminal (C_g) and of the source, leads, etc. come in parallel with the test object. Hence, the balancing is to be done in two steps. First, the test object is disconnected and the capacitance C_g and $\tan(\delta_g)$ are measured. Then the test object is connected and a new balance is obtained. The second balance gives,

$$C'_x = C_x + C_g$$

$$\text{and } \tan \delta'_x = \frac{C_x \tan \delta_x + C_g \tan \delta_g}{C_x + C_g} \quad (9.19)$$

Hence, the actual capacitance and dissipation factor of the test object are

$$C_x = C'_x - C_g$$

$$\text{and } \tan \delta_x = \frac{C'_x \tan \delta'_x - C_g \tan \delta_g}{C_x} \quad (9.20)$$

The accuracy of the measurement is poor, if the ground capacitance is large compared to the test object capacitance.

(b) Schering-Bridge for High Charging Currents High capacitance test objects, such as high-voltage power cables and power factor correction capacitors take high charging currents which may exceed the rating of the variable resistance R_4 (Fig. 9.10). Further, the value of the resistance R_4 will become so low that the contact resistances and residual inductances can no longer be neglected. For these cases, the range is increased by connecting a shunting resistor R_s in parallel across R_4 as

shown in [Fig. 9.13](#).

Hence, the balance conditions are modified as

$$C_x = C_2 R_4 \left[\frac{R_s + r + S + R_4}{R_s (R + \Delta S)} \right]$$

and

$$\tan \delta_x = \omega C_3 R_3 - \omega C_s R_3 \left[\frac{r + S - \Delta S}{R_4 + \Delta S} \right] \quad (9.21)$$

where, R_s = shunt resistance,

r = a small resistance added in the first arm,

S = slide wire resistance

R_4 = the decade variable resistor, and

ΔS = portion of the slide wire resistance.

Usually R_s , the shunt resistance is kept outside, and special arrangements are made for the correction of its inductive phase angle error, if necessary.

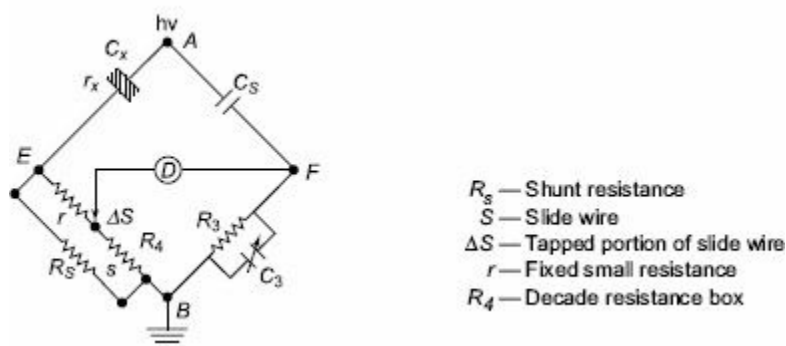


Fig. 9.13 Modified Schering-bridge for large charging currents

(c) Schering-Bridge for High Dissipation Factors Extension of range of the dissipation factor can be achieved by connecting in parallel an additional large capacitance across C_3 . But to avoid expensive and large-size decade capacitances the $C_3 R_3$ arm is modified as shown in [Fig. 9.14a](#). R_3 is made as a slide wire along with decade resistance, and C_3 is extended by connecting a single fixed capacitor. Usually, the modification is limited to $\tan \delta = 1.0$.

For $\tan \delta$ values greater than 1.0 and in the range 1 to 10 or greater, the $C_3 R_3$ arm is no longer made a parallel combination. Instead, it is made a series combination of C_3 and R_3 where R_3 is variable. This makes the test object to be an equivalent of C_x in parallel with R_x , a better approximation for the capacitors and dielectrics. With this modification, $\tan \delta$ range is made wider, from 10^{-4} to values greater than 10. The arrangement is shown in [Fig. 9.14b](#).

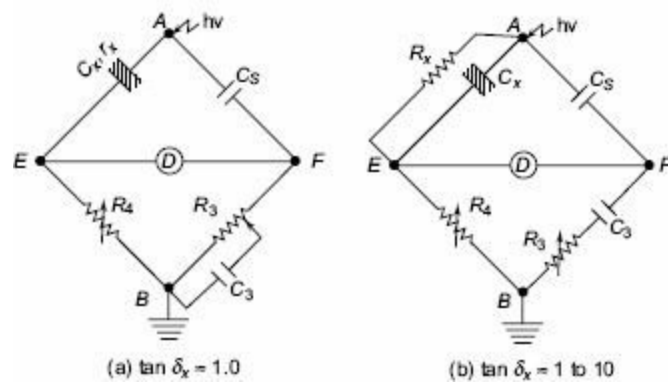


Fig. 9.14 Schering-bridge for large dissipation factors

9.3.5 Audio-Frequency Measuring Techniques

The basic Schering-Bridge discussed in [Sec. 9.3.4](#) may be used also in the audio frequency range for dielectric measurements. But it presents problems at higher frequencies, and the values of C_3 and R_3 have to be greatly altered. Sometimes, balancing also becomes difficult for low values of the test specimen capacitance, and the errors due to the stray capacitances across the arm R_4 may be appreciable. Therefore, in the case of small capacitance measurements (1 to 100 picofarads and less) substitution methods are used which, over this capacitance range may be more accurate. Also, in order to take care of all these effects modified Schering-bridge shown in [Fig. 9.15](#) is preferred.

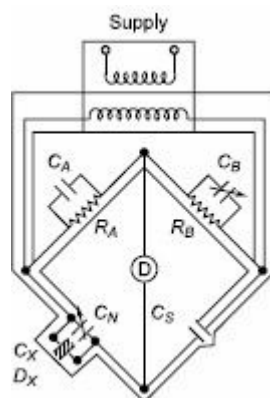


Fig. 9.15 Schering-bridge for audio frequency measurements with shields and source transformer

(a) Schering-Bridge for Audio-Frequency Range (100 Hz to 100 kHz)

The capacitance bridge used for dielectric measurements is shown in [Fig. 9.15](#), where $C_A R_A$ and $C_B R_B$ are the ratio arm capacitances. Substitution method is preferred in this range for greater accuracy. The specimen is connected across the standard variable capacitance C_N . The bridge is balanced with and without the dielectric specimen C_x . The specimen capacitance connected (C_x) is the difference of the two readings of the standard capacitor C_N .

$$C_x = \Delta C_N = C'_N - C_N \quad (9.22)$$

The balance for the loss factor (resistive component balance) may be done in any one of the following ways:

- (i) a small variable resistance in series with the standard capacitor C_N ,
- (ii) a variable resistor of high value in parallel with C_S , and
- (iii) a variable capacitor in parallel with R_B (C_B variation).

Of these three, the third method is normally used, as C_B can be made a variable air capacitor of high quality and the errors that arise within the resistances at high frequencies (skin effect, etc.) are avoided. The dissipation factor $\tan \delta$ for the third method is given as,

$$\tan \delta = \frac{C'_N}{\Delta C} \Delta D \quad (9.23)$$

where,

$$\Delta D = D - D' = \omega R_B (C_B - C'_B)$$

Usually, the total capacitance C_N in the variable arm is made small to get a large variation in ΔD .

Whenever the specimen capacitance is greater than that of the maximum value of C_N , the substitution method is not possible. In such cases, direct measurement without C_N is done. The expressions, in the case of a direct measurement for C_x and $\tan \delta$ are

$$C_x = \frac{R_B}{R_A} C_S \quad (9.24)$$

$$\tan \delta = \frac{f}{f_0} R_B C_B \quad (9.25)$$

where f_0 is the calibration frequency.

The range of this bridge extends from 1 pF to about 1000 pF when the substitution method is used, from 1000 pF to 100 nF when the direct method is used.

(b) Earthing and Shielding For two-terminal measurements, the bridge is grounded at its junction points. The supply transformer, detector, and all the components of the bridge are enclosed in earthed shields. For three-terminal measurements, it is necessary to avoid stray capacitances, for accurate measurements.

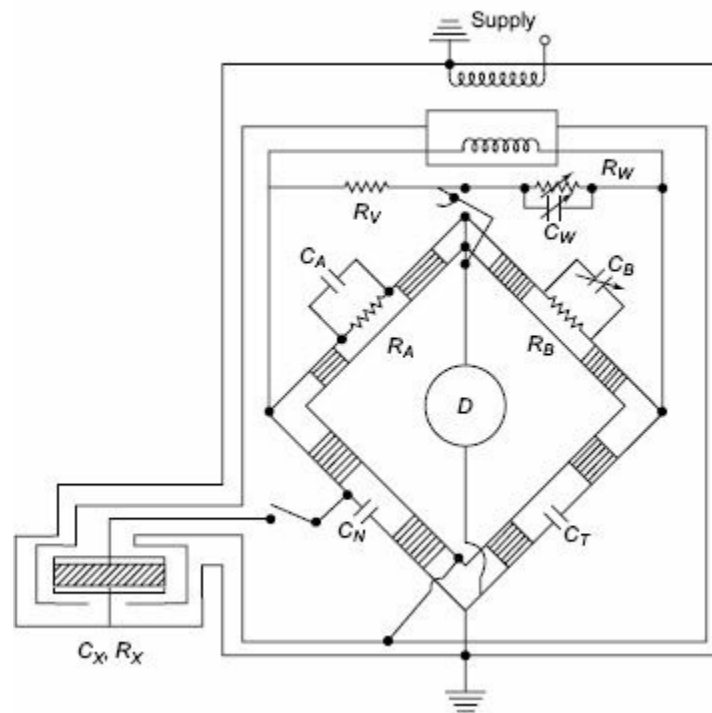


Fig. 9.16 Schering-bridge for three terminal measurements with Wagner's earthing device

Hence, a guard circuit and earthing device (known as Wagner's earthing device) are used. The bridge is balanced once with the ratio arms and again with the earthing device, alternately, so that no change in balance occurs. This ensures the elimination of stray ground capacitances and coupling. The schematic arrangement is shown in [Fig. 9.16](#). The arms, containing R_r and R_w C_w are the Wagner earthing device arms. The bridge is first balanced with R_A , R_B , C_N , and C_T and later with R_r , R_w , C_N , and C_T . The detector is alternately connected to either the earthing device or to the bridge arms A and B . The balance is achieved, when at either position the detector indicates the same null

indication.

This bridge can be extended to frequencies as high as 500 kHz beyond which the lead lengths and the residual inductances in various arms become too high to achieve proper balance. Hence, for higher frequencies other methods have to be adopted.

(c) Transformer Ratio Arm Bridges It is a common practice to use the four-arm Wheatstone bridge network for ac measurements. In high-frequency measurements, the arms with high values of resistances lead to difficulties due to their residual inductances, capacitances, and skin effect. Also, shielding and grounding becomes difficult in large arms. Hence, at high frequencies the transformer ratio arm bridge which eliminate at least two arms are preferred. These bridges are also useful for the measurement of low value of capacitances accurately.

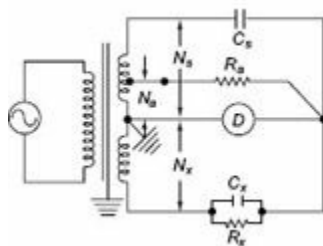


Fig. 9.17 Transformer voltage ratio arm bridge

The ratio arm bridges can be either voltage-ratio type or current-ratio type; the former being used for high frequency low voltage applications.

The schematic diagram of a ratio arm bridge (voltage ratio) is given in Fig. 9.17. Assuming ideal transformer conditions, for a null indication of the detector,

$$\frac{V_s}{V_x} = \frac{N_s}{N_x} = \frac{C_x}{C_s}; \text{ and } \frac{R_x}{R_a} = \frac{N_x}{N_a} \quad (9.26)$$

where C_x and C_s are unknown and standard capacitances respectively, R_x and R_a are unknown and standard resistances, and N_x , N_a , and N_s are the corresponding turns of the transformer ratio windings.

In practical transformers, the voltage ratio slightly differs from the turns ratio due to the no load magnetizing current and is also affected by the load current. Therefore, the balance conditions shown above involve errors. The errors are classified as the ratio and loading errors and are determined separately and compensated for in the construction. A practical bridge constructed by General Radio Company (USA) has a useful range from a fraction of one pF to about 100 μ F and covers a wide range of frequency from 100 Hz to 100 kHz, the accuracy being better than 0.5%.

For high-voltage applications where sensitive measurements at fixed frequency (at 50 Hz) are required, the current comparator or the current ratio method (Fig. 9.18a) is used. This bridge has the advantage that full voltage is applied across the test capacitor but also has the drawback that a standard conductance has to be built for high voltages. It is difficult to construct a precision conductance suitable for high-voltage operation. This disadvantage is overcome by generating a low voltage signal E_f proportional to and in phase with the supply voltage E as shown in the modified Fig. 9.18b. At balance, there is no voltage across the current comparator winding. If the gain of the amplifier (A) is high, that is,

$$E_f \approx \frac{C_s}{C_f} E$$

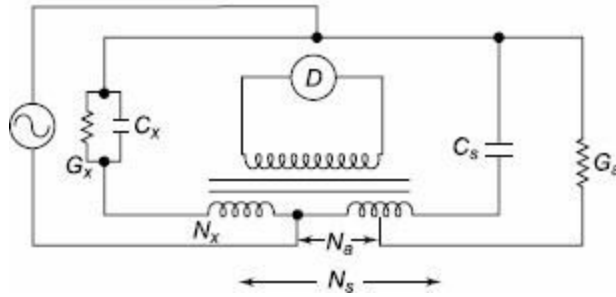
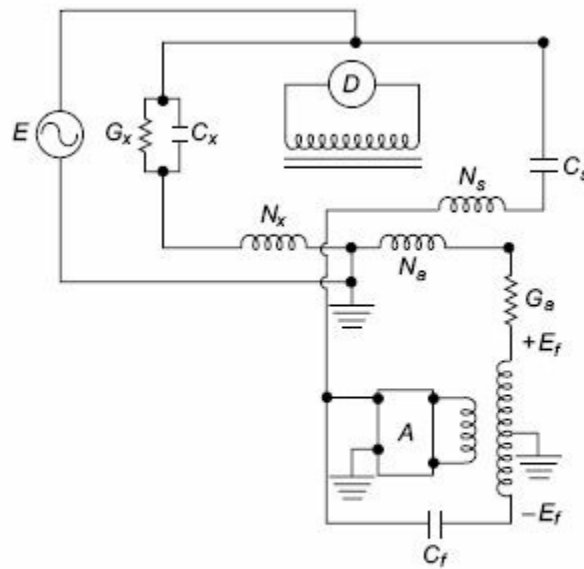


Fig. 9.18a Current comparator bridge



E_f — Proportional e.m.f
 A — Amplifier
 C_f — Balancing capacitor

Fig. 9.18b Current comparator for high voltage application

The balance equations of the bridge are

$$C_x = C_s \frac{N_s}{N_x}; G_x = \frac{C_s}{C_f} \frac{N_a}{N_x} G_a$$

and
$$\tan \delta = \frac{G_x}{\omega C_x} = \frac{1}{\omega C_f} \frac{G_a N_a}{N_x} \quad (9.27)$$

where C_x , C_s , N_s , N_a , and N_x are as defined in Eq. (9.26), G_x and G_a are unknown and standard conductances, and C_f is the balancing capacitor.

9.3.6 Detectors in Dielectric Measurements

Since the measurements cover a large range of frequency, the detectors used in various ranges differ considerably.

For dc and low frequency measurements, dc galvanometer and dc amplifiers with a microammeter are used.

In power frequency ac measurements (50 Hz/60 Hz) vibration galvanometers serve as excellent tuned detectors as their bandwidth is quite narrow (± 1 to 2 Hz). But often tuned electronic amplifier null detectors are also used.

In the audio frequency range wide band or tuned null detectors are used with a sensitivity better than $10 \mu\text{V}$. This consists of a filter, an attenuator, a multi-stage amplifier using a bridge rectifier with a microammeter. The bandwidth of the detector is from 50 Hz to 50 kHz and is protected from high input signals at off balance position.

Cathode ray oscilloscopes are also used as detectors, if too high a sensitivity is not required.

The selection of the detector depends on the type of bridge circuit used for measurement and the sensitivity required in the particular application.

9.4 PARTIAL DISCHARGE MEASUREMENTS

9.4.1 Introduction

Earlier the testing of insulators and other equipment was based on the insulation resistance measurements, dissipation factor measurements and breakdown tests. It was observed that the dissipation factor ($\tan \delta$) was voltage dependent and hence became a criterion for the monitoring of the high-voltage insulation. In further investigations it was found that weak points in an insulation like voids, cracks, and other imperfections lead to internal or intermittent discharges in the insulation. These imperfections being small were not revealed in capacitance measurements but were revealed as power loss components in contributing for an increase in the dissipation factor. In modern terminology these are designated as ‘partial discharges’ which in course of time reduce the strength of insulation leading to a total or partial failure or breakdown of the insulation.

If the sites of partial discharges can be located inside an equipment, like in a power cable or a transformer, it gives valuable information to the insulation engineer about the regions of greater stress and imperfections in the fabrication. Based on this information, the designs can be considerably improved.

Electrical insulation with imperfections or voids leading to partial discharges can be represented by an electrical equivalent circuit shown in Fig. 9.19. Consider a capacitor with a void inside the insulation (C_a). The capacitance of the void is represented by a capacitor in series with the rest of the insulation capacitance (C_b).

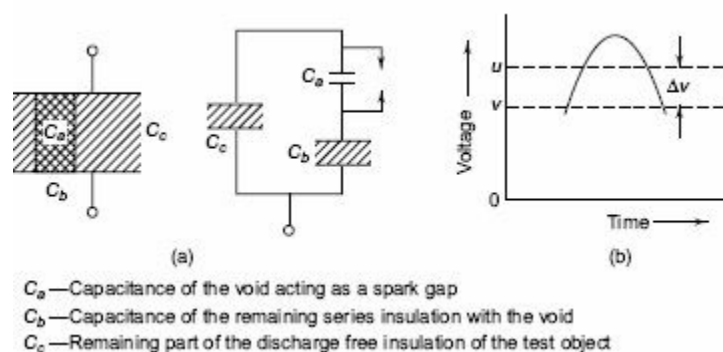


Fig. 9.19 (a) Insulating device with a void C_a and its simplified electrical equivalent circuit (b) Voltage across the void, C_a

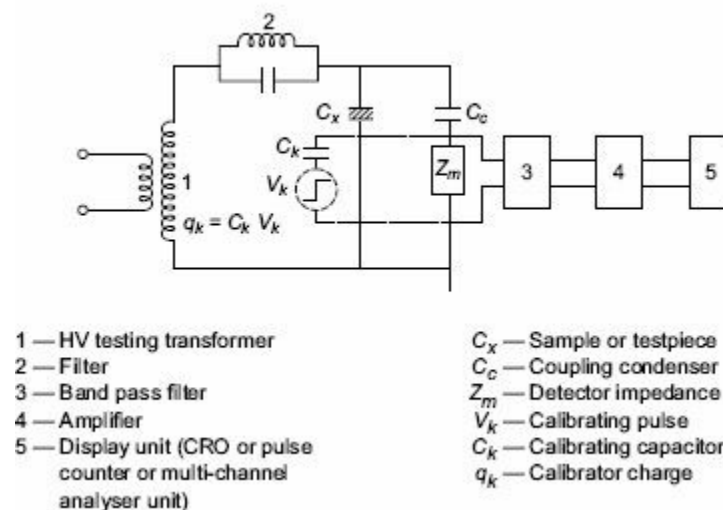


Fig. 9.20 Straight discharge detection circuit

The remaining void-free material is represented by the capacitance C_c . When the voltage across the capacitor is raised, a critical value is reached across the capacitor C_a and a discharge occurs through the capacitor, i.e. it becomes short circuited. This is represented by the closure of the switch.

Generally $C_a \ll C_b \ll C_c$. A charge Δq_a which was present in the capacitor C_a flows through C_b and C_c giving rise to a voltage pulse across the capacitor C_c . A measure of the voltage pulse across the capacitor gives the amount of discharge quality. But this measurement is difficult in practice, and an apparent charge measurement across a detecting impedance is usually made.

(a) *Partial Discharge Phenomenon: Terminology Used*

(i) *Electrical Discharge* The movement of electrical charges through an insulating (dielectric) medium, initiated by electron avalanches.

(ii) *Partial Discharge* An electrical discharge that only partially bridges the dielectric or insulating medium between two conductors. Examples are: internal discharges, surface discharges and corona discharges. Internal discharges are discharges in cavities or voids which lie inside the volume of the dielectric or at the edges of conducting inclusions in a solid or liquid insulating media.

Surface discharges are discharges from the conductor into a gas or a liquid medium and form on the surface of the solid insulation not covered by the conductor.

Corona is a discharge in a gas or a liquid insulation around the conductors that are away or remote from the solid insulation.

(iii) *Discharge Inception (Applied) Voltage* It is the lowest voltage at which discharges of specified magnitude will recur when an increasing ac voltage is applied.

(iv) *Discharge Extinction (Applied) Voltage* It is the lowest voltage at which discharges of specified magnitude will appear when an applied ac voltage, which is more than the inception voltage, is reduced.

(v) *Discharge Magnitude* It is the quantity of charge, as measured at the terminals of a sample due to a single discharge.

(vi) *Discharge Energy* It is the energy dissipated by a single discharge.

(vii) *Average Current* It is the average value of the discharge current during a cycle due to a single or multiple discharges. I_a , the average current over an interval T can be expressed as

$$I_a = \frac{1}{T} \sum_{r=1}^{r=m} |q_r|$$

when, q is the apparent charge in r th discharge.

(viii) *Quadratic Rate* It is the average value of the square of the discharge magnitudes. D , the

quadratic rate is given as

$$D = \frac{1}{T} \left| \sum q_r^2 \right|$$

(ix) *Discharge Detector* It is a device or an instrument used for either detecting and/or measuring the discharges.

(x) *Sensitivity* It is the magnitude of the smallest individual discharge that can be measured under particular test conditions.

(xi) *Resolution* It is the minimum interval between two discharges which can be measured without the magnitude of one discharge affecting the other.

(b) Energy Associated in a Single Discharge Referring to the equivalent circuit given in Fig. 9.19, a charge q will be transferred across the cavity C_a when a discharge occurs at the inception voltage u . The voltage change ΔV appears across the series combination of the rest of the capacitance C_b and C_c , i.e., $C_b C_c / (C_b + C_c)$.

The total capacitance of the combination is

$$C_a + \frac{C_b C_c}{C_b + C_c} \cong C_a + C_b \quad (C_c \gg C_b)$$

Hence the discharge magnitude,

$$q = (C_a + C_b) \Delta V \quad (9.28)$$

The charge q cannot be measured directly. The charge that can be measured is the apparent charge q_c which is the charge that has been displaced from supply source. If ΔV_a across the cavity C_a produces a voltage change ΔV across the capacitance C_c , then

$$\Delta V = \Delta V_a \cdot \frac{C_b}{C_b + C_c} \quad (9.29)$$

Hence q_c , charge across the capacitance C_c (since the total capacitance as seen across C_c is $C_c +$ series combination of C_a and C_b) is given by

$$q_c = \Delta V \left(C_c + \frac{C_a C_b}{C_a + C_b} \right) \cong \Delta V C_c \quad (\text{if } C_c \gg C_b) \quad (9.30)$$

\therefore Substituting for ΔV in terms of ΔV_a , we get

$$q_c = \Delta V_a \cdot \frac{C_b}{C_b + C_c} \cdot C_c = \Delta V_a \frac{C_b C_c}{C_b + C_c} \cong \Delta V_a C_b \quad (9.31)$$

But $\Delta V = u - v$ ([Fig. 9.19](#)), then the energy associated with the discharge is

$$W = \frac{1}{2} C_a (u^2 - v^2) = \frac{1}{2} C_a (u - v) (u + v) = \frac{1}{2} C_a \Delta V (u + v)$$

Since ΔV will be small in any discharge $(u + v) = u = V_{ip}$ = the inception voltage for the discharge (peak value), then

$$W = \frac{1}{2} C_a \Delta V \cdot V_{ip}$$

Normally v_l is expressed as r.m.s. value = $\frac{v_{ip}}{\sqrt{2}}$ so that

$$\begin{aligned} \text{the discharge energy} \quad W &= \sqrt{\frac{1}{2}} q V_{ip} / \sqrt{2} \\ &= \frac{1}{\sqrt{2}} q V_l \end{aligned} \tag{9.32}$$

where V_l is the inception voltage and q is the discharge magnitude measured at the terminals of the sample. The discharge mechanism and the discharge pattern are shown in [Fig. 4.6](#) ([Chapter 4, Sec. 4.5.3](#)). The discharge detection and measurements are given in the following section.

9.4.2 Discharge Detection using Straight Detectors

The circuit arrangement shown in [Fig. 9.20](#) gives a simplified circuit for detecting ‘partial discharges’. The high-voltage transformer shown is free from internal discharges. A resonant filter is used to prevent any pulses starting from the capacitance of the windings and bushings of the transformer. C_x is the test object, C_c is the coupling capacitor, and Z_m is a detection impedance. The signal developed across the impedance Z_m is passed through a band pass filter and amplifier and displayed on a CRO or counted by a pulse counter multi-channel analyzer unit.

In [Fig. 9.21](#), the discharge pattern displayed on the CRO screen of a partial discharge detector with an elliptical display is shown. The sinusoidal voltage and the corresponding ellipse pattern of the discharge are shown in [Fig. 9.21a](#) and a single corona pulse in a point-plane spark gap geometry is shown in [Figs 9.21b](#) and c. When the voltage applied is greater than that of the critical inception voltage, multiple pulses appear (see [Fig. 9.21c](#)), and all the pulses are of equal magnitude. A typical discharge pattern in cavities inside the insulation is shown in [Fig. 9.21d](#). This pattern of discharge appears on the quadrants of the ellipse which correspond to the test voltage rising from zero to the maximum, either positively or negatively. The discharges usually start near the peaks of the test voltage but spread towards the zero value as the test voltage is increased beyond the inception level. The number and magnitude of the discharges on both the positive and negative cycles are approximately the same. A typical discharge pattern from a void bounded on one side by the insulation and the other side by a conductor is shown in [Fig. 9.21c](#). This pattern of discharge is common in insulated cables (like polyethylene and XLPE cables) when the discharge is made up of a large number of pulses of small magnitude on the positive cycle and a much smaller number of large magnitude pulses on the negative half-cycle.

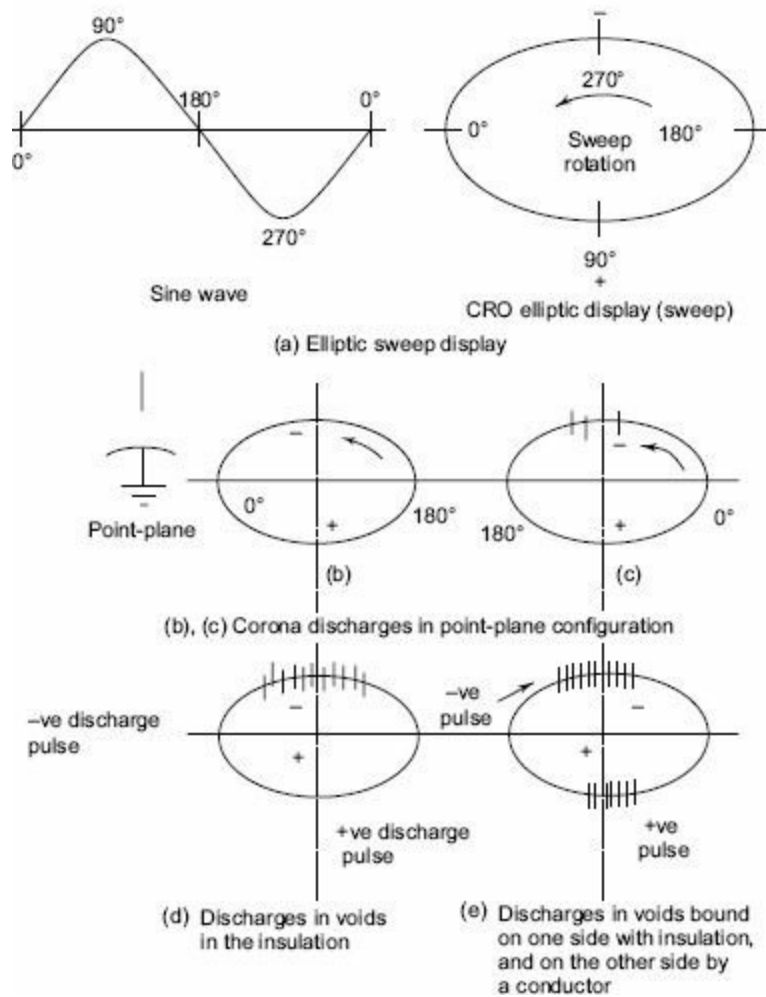


Fig. 9.21 Partial discharge patterns

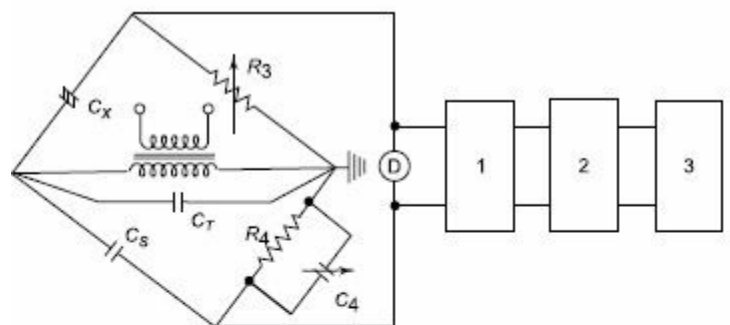
In the narrow-band detection scheme Z_m is a parallel $L-C$ circuit tuned to 500 kHz. The band pass filter has a bandwidth of about ± 10 kHz. The pulses after amplification are displayed in an elliptical time base of a CRO, and the resolution for the pulses is about 35 per quadrant.

In the wide-band detection scheme Z_m is an $R-C$ network connected to a double tuned transformer. The bandwidth is about 250 kHz with centre frequency between 150 and 200 kHz. A wide band amplifier is used, and the signal is displayed on the CRO as in the previous case. The resolution is about 200 pulses per quadrant.

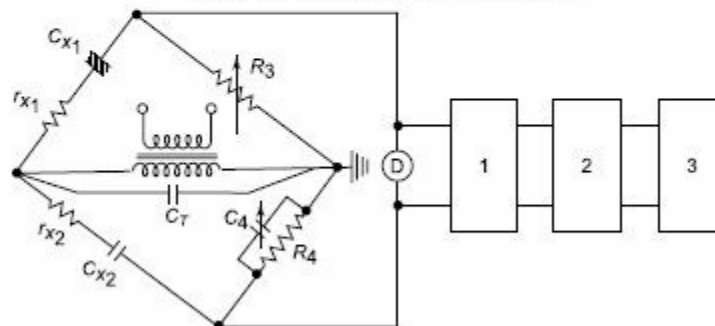
With tuned narrow-band detectors, the discharges can be detected with a sensitivity less than one pico coulomb for a test piece capacitance of 100 pF. Test pieces with capacitances in the range 100 pF to 0.1 pF can be tested. With the wide band detector samples up to 250 μ F capacitance can be tested. Sensitivity of the measurement varies from 0.005 pico coulomb at 6 pF sample capacitance to about 15 pC at a sample capacitance of 250 μ F.

9.4.3 Balanced Detection Method

In the straight detection method, the external disturbances are not fully rejected. The filter used to block the noise sources may not be effective. The Schering bridge employed for the $\tan \delta$ measurement is sometimes used. In this method, the test object is not grounded. A modification to the Schering-bridge detector is the differential discharge detector, given by Kreuger. Both the schemes are given in Fig. 9.22. The bridges are tuned and balanced at 50 Hz. A filter is used across the detector terminals to block the 50 Hz components present. Signals in the range from 5 to 50 kHz are allowed to pass through the filter and amplified. The CRO gives the display of the pulse pattern. Any external interference from outside is balanced out, and only internally (testpiece) generated pulses are detected. In the modified scheme, another test sample called dummy sample is used in the place of the standard capacitor. The capacitance and $\tan \delta$ of the dummy sample are made approximately equal, but need not be equal. The disadvantage is that if two discharges occur in both the samples simultaneously, they cancel out, but this is very rare. The main advantage of the second method is its capacity for better rejection of external noise and use of the wide frequency band with better resolution of the individual pulses.



(a) Balanced detector using Schering-bridge



(b) Differential detector

- D — Power frequency detector
- 1 — Filter (band pass)
- 2 — Amplifier
- 3 — Display unit — CRO or counter

Fig. 9.22 Balanced discharge detector schemes

9.4.4 Calibration of Discharge Detectors

Partial discharge detectors are connected across a measuring impedance Z_m as shown in [Fig. 9.20](#) and the signal measured across this impedance is read by the detector. The signal voltage developed across Z_m depends on the circuit parameters C_x and C_c and also on the internal circuitry of the instrument (blocks 3, 4, 5 shown in [Fig. 9.20](#)).

Hence, the measuring instrument or detector is calibrated by injecting a pulse having a charge of known magnitude into the detecting system. For this purpose, a square wave generator and a calibrating capacitor (C_k) are usually used. The magnitude of the charge injected is $q_k = C_k V_k$, where V_k is the magnitude of the voltage pulse. The rise time of the pulse is about $0.1 \mu\text{s}$, and the pulse width varies from 10 to 20 ms. With suitable attenuation, the output voltage of the pulse generator can be varied from a minimum output of about $10 \mu\text{V}$ to a maximum value of 100 V in steps. The value of C_k , usually used, lies between 1000 and 2500 pF. If the calibrating pulse is directly injected at the HV terminal of the test object, the magnitude of the calibration pulse will be $C_k \cdot V_k$. If the pulse is injected across the measuring impedance (as shown in [Fig. 9.20](#)), then the calibrating pulse magnitude should be multiplied by $(C_x + C_c)/C_c$.

Another method of calibration is to use a secondary standard, consisting of a point-hemisphere electrode system of specified dimensions (refer to IE publication 270, 1968 (Reference no. 8)).

This method is more accurate and is easily reproducible. With an over voltage of 10 – 20% applied above the discharge inception voltage, the arrangement gives discharges which are used for calibration purposes.

PD Measuring and Analysing System A modern PD measuring system consists of a discharge free source (transformer), filter unit, a coupling capacitance, a test sample or an object and measuring impedance, Z_m for different sample capacitances. The output from the measuring unit is fed to the measuring and analyzing system consisting of (i) the pd measuring band selector, (ii) amplifier, (iii) pulse magnitude counter, (iv) pulse pattern analyser, (v) pulse shape recorder, etc. All the above units are controlled by a microprocessor based p.c. unit that can make the pulse analysis as desired. All the pd quantities are displayed in real time mode if needed. Pulse resolution up to 100 kHz and pulse magnitude detection for less than 1 pC are possible. The software associated is available in Windows NT etc.

9.4.5 Discharge Detection in Power Cables

Power cables of long lengths may be considered to be specimens with distributed capacitance rather than a lumped capacitance. The same feature is true for windings of the transformers and rotating machines of high-voltage ratings. In such cases, the location of discharge is done using the travelling wave technique, and the circuit for the same is shown in Fig. 9.23. The breakdown or discharge in a cavity at location F causes a charge accumulation at the fault point F . This creates two travelling waves which travel in opposite directions towards the cable ends. The voltage wave is given by

$$v_i = \frac{Z_0 i(t)}{2}$$

If C_c is neglected in comparison with the detection impedance Z_d , the voltage signal across the detection impedance becomes

$$v_d(t) = \frac{Z_d}{(Z_d + Z_0)} Z_0 i(t) \quad (9.33)$$

$$\text{If } Z_d = Z_0, v_d(t) = \frac{Z_0 i(t)}{2} \quad (9.34)$$

If the partial discharge site is located exactly in the middle of the cable, the travelling wave moving to the left is reflected without any polarity change at the open end and then arrives at the detection impedance, Z_d , separated from the direct pulse by a time equal to the cable transit time τ . If the site is at any other point, the time difference between the original pulse and its reflection may be any value from 0 to 2τ . Usually, the supply transformer end is not strictly an open circuit because of the shunt capacitance of the windings of the transformer. Therefore, the travelling wave is reflected from the transformer end with the surge impedance of the transformer as its termination. To avoid this reflection an inductor is inserted at the transformer end. By knowing the transit time of the cable τ and the actual time difference between the two pulses, the fault position can be located (also see [Sec. 10.3.4](#) in [Chapter 10](#)).

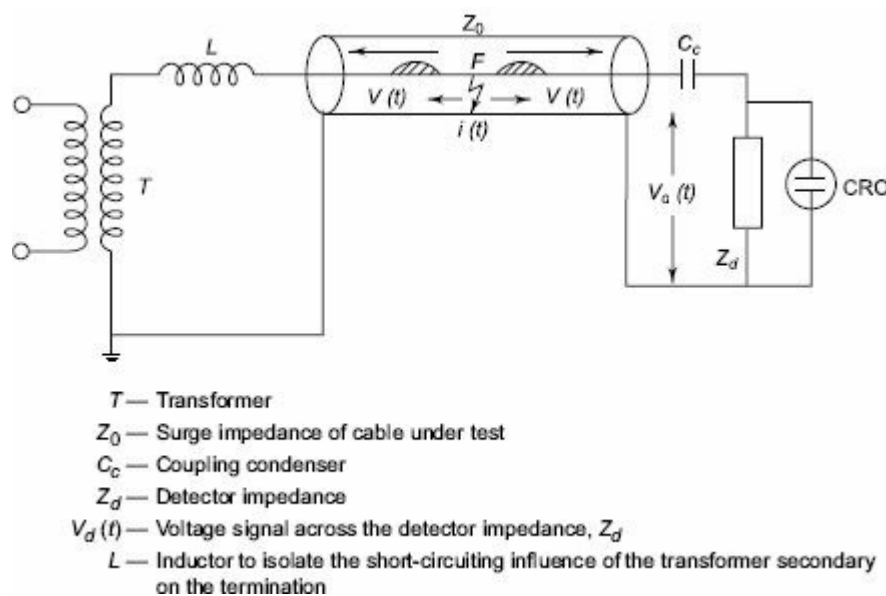


Fig. 9.23 Partial discharge testing arrangement for distributed parameter equipment (cables, transformer windings, etc.)

- Non-destructive Testing
- Dc Resistivity
- Measuring Cells
- Dielectric Constant
- Loss Factor
- Bridge Techniques
- Schering-Bridge
- Transformer Ratio Arm Bridge
- Current Comparator
- PD Measurements
- Discharge Detectors

WORKED EXAMPLES

Example 9.1 *The volume resistivity of a bakelite piece was determined by using standard circular electrodes, a sensitive galvanometer, and a stabilized power supply. When the applied voltage was 1000 V, the galvanometer deflection with the specimen was 3.2 cm. When a standard resistance of $R_s = 10M\Omega$ is used for calibration, the deflection was 33.30 cm with a universal shunt ratio of 3,000. The diameter of the electrodes is 10 cm, and the thickness of the specimen is 2 mm. Find the volume resistivity.*

Solution

Let G = galvanometer sensitivity,
 R_s = standard resistance,
 n = shunt ratio,
 D_s = deflection in cm, and
 V = applied voltage.

Then,
$$G = \frac{V}{R_s} \frac{1}{n} \frac{1}{D_s} = \frac{1000}{10^7} \frac{1}{3000} \frac{1}{33.3} \approx 10^{-9} \text{ A/cm}$$

The resistance R of the specimen =
$$\frac{V}{D \times G} = \frac{1000}{3.2 \times 10^{-9}} = 3.125 \times 10^{11} \Omega$$

Also, $R = \frac{\rho t}{\pi r^2}$ or the volume resistivity

$$\rho = \frac{\pi r^2 R}{t} = \frac{\pi (10/2)^2 3.125 \times 10^{11}}{2 \times 10^{-1}} = 1.227 \times 10^{14} \Omega \text{ cm}$$

Hence, the volume resistivity = $1.227 \times 10^{14} \Omega \text{ cm}$

Example 9.2 *The resistivity of the specimen referred to in Example 9.1 was determined using the loss of charge method. A 0.1 μF 1000 V standard condenser was charged to 1000 V and was*

discharged through the specimen. If the time taken for the voltage to fall from 1000 V to 500 V was 30 min 20 s, find the resistivity of the specimen.

Solution

$$t = 30 \text{ min } 20 \text{ s} = 1820 \text{ s}$$

$$\begin{aligned} \text{Resistance, } R &= \frac{t}{C \ln \frac{V_n}{V}} = \frac{1820}{0.1 \times 10^{-6} \times \ln \frac{1000}{500}} \\ &= 2.627 \times 10^{10} \Omega \end{aligned}$$

$$\begin{aligned} \therefore \text{ volume resistivity, } \rho &= \frac{\pi r^2 R}{\text{thickness}} = \frac{\pi \left(\frac{10}{2}\right)^2 \times 2.627 \times 10^{11}}{0.2} \\ &= 1.031 \times 10^{13} \Omega \text{ cm} \end{aligned}$$

(Note: In this method, the leakage resistance of the standard condenser insulation and the voltmeter impedance came in parallel with the specimen. Hence, the value obtained is much lower).

Example 9.3 The capacitance and loss angle of the above specimen were measured using the same electrode set-up. The capacitance and $\tan \delta$ with the specimen are 147 pF and 0.0012 respectively. The air capacitance of the electrode system was 35pF. What is the dielectric constant and complex permittivity of Bakelite?

Solution

$$\text{The dielectric constant, } \epsilon_r = \frac{147}{35} = 4.2$$

$$\begin{aligned} \text{Complex permittivity, } \epsilon^* &= \epsilon' - j\epsilon'' \\ &= \epsilon_0 (K' - jK'') \end{aligned}$$

$$\tan \delta = \frac{K''}{K'} = 0.0012, \text{ and } K' = \epsilon_r = 4.2$$

$$\therefore K'' = 0.0012 K' = 0.00504$$

$$\therefore \epsilon^* = \epsilon_0(4.2 - j0.00504)$$

Hence, the complex permittivity, $\epsilon^* = (3.71 - j0.0445) \times 10^{-11} \text{ F/m}$

Example 9.4 A Schering-bridge was used to measure the capacitance and loss angle of an hv bushing. At balance, the observations were: the value of the standard condenser = 100pF, $R_3 = 3180 \Omega$, $C_3 = 0.00125 \mu\text{F}$ and $R_4 = 636 \Omega$. What are the values of capacitance and $\tan \delta$ of the bushing?

Solution

The unknown capacitance $C_X = \frac{R_3}{R_4} C_S = \frac{3180}{636} \times 100 = 500 \text{ pF}$

$$\tan \delta = \omega C_X R_X = \omega C_3 R_3 = 314 \times 3180 \times 0.00125 \times 10^{-5} = 0.00125$$

Example 9.5 An audio frequency Schering-bridge was used to determine the dielectric constant and $\tan \delta$ of transformer oil at 1 kHz. The observations obtained were as follows.

(Method employed: Substitution method).

- (i) With standard condenser and leads, the capacitance, $C_1 = 504 \text{ pF}$ the dissipation factor, $D_1 = 0.0003$.
 - (ii) With standard condenser in parallel with the empty test cell, capacitance $C_2 = 525 \text{ pF}$, and dissipation factor $D_2 = 0.00031$.
 - (iii) With the standard condenser in parallel with the test cell and oil, capacitance $C_3 = 550 \text{ pF}$ and dissipation factor $D_3 = 0.00075$.
- Find the dielectric constant and $\tan \delta$ of the transformer oil?

Solution

$$\text{Capacitance of the test cell} = 525 - 504 = 21 \text{ pF}$$

$$\text{Capacitance of the test cell + oil} = 550 - 504 = 46 \text{ pF}$$

$$\therefore \epsilon_r = \text{dielectric constant of oil}$$

$$= \frac{46}{21} = 2.19$$

$$\Delta D \text{ of empty cell} = 0.00001$$

$$\Delta D \text{ of oil} = 0.00075 - 0.00031 = 0.00044$$

$$\therefore \tan \delta \text{ of oil} = 0.00044$$

Example 9.6 While doing studies on partial discharges in cavities of cylindrical disc of 1.0 cm diameter and 1 cm thickness, a cylindrical cavity of 1 mm dia. and 1 mm thickness is made at its centre. The discharge voltage measured across the specimen is 0.2 V with sensitivity of 1 pC/volt. What is the magnitude of charge transferred from the cavity. Take ϵ_r of the disc = 2.5.

Solution

$$1 \text{ pC} = 1 \text{ volt, (Referring to Fig. 9.20)}$$

$$\text{Since the discharge magnitude measured} = 0.2 \text{ pC}$$

$$\text{Capacitance of cavity } C_a = \frac{\epsilon_0 \times \text{area}}{\text{thickness}} = \epsilon_0 (\pi/4) \frac{(1 \times 10^{-3})^2}{1 \times 10^{-3}} = \frac{\pi \epsilon_0}{4} \times 10^{-3} \text{ F}$$

$$\text{Capacitance } C_b = \frac{\epsilon_0 \epsilon_r \text{ area}}{\text{thickness}} = \frac{\epsilon_0 \times 2 \times 5 \times \pi/4 \times (1 \times 10^{-3})^2}{9 \times 10^{-3}}$$

$$= (\epsilon_0 \times \pi/4) \times (2.5/9) \times 10^{-3} \text{ F}$$

$$\therefore q_c = \frac{C_a + C_b}{C_b} \times 0.2 = 0.92 \text{ pC}$$

Example 9.7 A Schering-bridge was used to determine the dielectric constant and loss factor of a 1 mm thick Bakelite sheet at 50 Hz using a parallel-plate electrode configuration. The electrode effective area is 100 cm². At balance, the bridge arms are AB: test object, BC: std. capacitor = 100pf.

CD: variable capacitor in parallel with resistor 50 nF and 1000/πohms.

DA: variable resistance 62.0 Ω

Determine the dielectric constant K and loss factor tan δ.

Solution

$$\text{Capacitance of parallel plate electrodes} = \frac{\epsilon_0 \epsilon_r a}{d}$$

Where a = area and ' d ' thickness.

At balance

$$C_X = \frac{R_3}{R_4} \cdot C_s$$

$$= \frac{1000}{\pi} \times \frac{1}{62.0} 100 = 513.0 \text{ pf}$$

$$C_X = \frac{\epsilon_0 \epsilon_r a}{d} = \frac{8.854 \times 10^{-12} \times \epsilon_r \times 100 \times 10^{-4}}{10^{-3}}$$

$$= 513.0$$

$$\therefore \epsilon_r = 5.79$$

$$\tan \delta = \omega C_X R_X = \omega C_3 R_3$$

$$= 2\pi \times 50 \times 50 \times 10^{-9} \times \frac{1000}{\pi} \times 10^{-3}$$

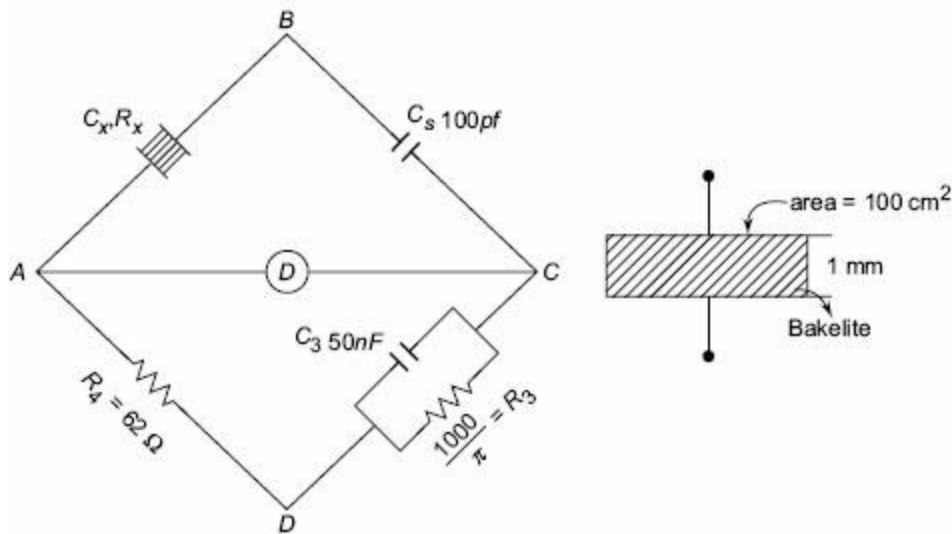
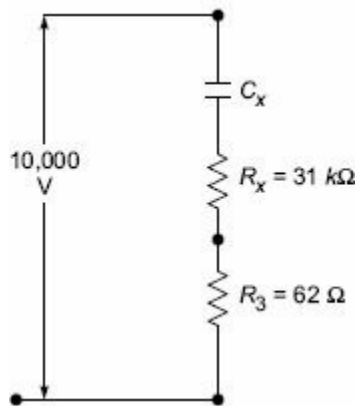


Fig. E 9.7

Example 9.8 In Example 9.7, if the voltage applied for testing is 10,000 V, what is the voltage that appears across the low voltage (AD and CD) at balance?

Solution



The test object C_X is taken as C_X in series with R_x

$$R_x = \frac{C_3}{C_s} \times R_4 = \frac{50 \times 10^{-9}}{100 \times 10^{-12}} \times 62 = 31 \text{ k}\Omega$$

Impedance of $C_X (z_X)$

$$= 31 \times 10^3 - \frac{j \times 10^{12}}{2\pi \times 50 \times 513}$$

$$= 31 \times 10^3 - j6.2 \times 10^6 \Omega$$

\therefore Voltage across

$$R_3 = \frac{R_3 \times V}{R_3 + z_X} = \frac{62 \times 10,000}{62 + 31 \times 10^3 - j6.2 \times 10^6}$$

$$= 0.1 \text{ Volts}$$

Note: The entire test voltage appears across the test object and Std. Capacitor.

Example 9.9 A high-voltage Schering-Bridge has the following arms with their component ranges. Std. Capacitor: 100pf; variable resistor R_4 : 1 to 1 k Ω (decade steps)

$$C_3: 1 \text{ nF to } 1.11 \text{ } \mu\text{F and } R_3: 100 \text{ } \Omega \text{ to } 11,100 \text{ } \Omega$$

Determine the maximum and minimum value of the capacitance and $\tan \delta$ that can be measured at 50Hz.

Solution

$$C_X(\text{Max.}) = \frac{R_3(\text{Max.}) \times C_3}{R_4(\text{Min.})} = \frac{11,100}{100} \times 100 \times 10^{-12}$$

$$= 11.1 \text{ nF}$$

$$C_X(\text{Min}) = \frac{R_3(\text{Min.}) \times C_3}{R_4(\text{Max.})} = \frac{100}{1000} \times 100 \times 10^{-12} = 10 \text{ pf}$$

$$\tan \delta(\text{max}) = \omega R_3(\text{max}) C_3(\text{max}) = 100\pi \times 11,100 \times 1.11 \times 10^{-6} = 3.83$$

$$\tan \delta(\text{min}) = \omega R_3(\text{min}) C_3(\text{min}) = 100\pi \times 100 \times 1 \times 10^{-9} = 0.0314 \times 10^{-3}$$

Note: Due to other limitations like stray couplings, uncertainties and errors in the components etc. the effective range for $\tan \delta$ in commercial bridges ($C - \tan \delta$ bridges) will be 0.1×10^{-4} to 0.5 only.

MULTIPLE-CHOICE QUESTIONS

- For resistivity and dielectric constant measurements the electrode system used is
 - two electrode
 - three electrode
 - four electrode
 - none of the above
- A sensitive dc galvanometer has a maximum sensitivity of
 - 10^{-9} A/cm
 - 10^{-8} A/cm
 - 10^{-6} A/cm
 - 10^{-12} A/cm
- The power supply used in resistivity measurements is
 - ± 110 V
 - ± 250 V
 - 500 V
 - 500 to 2000 V
- Loss of Charge Method is used to determine
 - insulation resistance
 - dielectric constant
 - loss factor – ($\tan \delta$)
 - rate of charging of a capacitor
- The equivalent circuit of a lossy capacitor or dielectric is
 - R - C series circuit
 - L - C series circuit

(c) R - C parallel circuit

(d) L - C parallel circuit

6. The type of bridge used for low frequency (≈ 50 Hz) dielectric measurement is

(a) Transformer ratio bridge

(b) Mole's-bridge

(c) shunted Schering-bridge

(d) Wagner's-bridge

7. Wagner's earth is used with Schering-bridge for

(a) grounding

(b) divert high current through the bridge when specimen fails

(c) suppress spikes and over voltages

(d) eliminating stray capacitance and coupling

8. In a transformer ratio arm bridge, unknown capacitance C_x is given by (if C_s = standard capacitor, and N_s, N_x are the number of turns used on standard capacitor and test capacitor sides)

(a) $\frac{C_s N_s}{N_x}$

(b) $\frac{C_s N_x}{N_s}$

(c) $C_s N_s C_x$

(d) $\frac{C_s}{N_x N_s}$

9. Current comparator bridge is used

(a) when test capacitance is large

(b) for high-voltage power frequency measurements

(c) for high-frequency low-voltage measurements

(d) low-voltage high-frequency measurements

10. Corona discharge is

(a) an internal discharge

(b) surface discharge

(c) a spark between conductors

(d) partial discharge around a high-voltage conductor

11. Partial discharge magnitude is

(a) quantity of charge measured at the terminals of the specimen

(b) quantity of charge inside a specimen

(c) voltage across the terminals of a specimen

(d) average current through the terminals of the specimen

12. Partial discharge detector is a device that measures of detects

(a) a partial discharge

(b) corona discharge

(c) leakage current

(d) fault current

13. A simple partial discharge detector circuit consists of a power unit and a

(a) coupling capacitor and test capacitor

(b) coupling capacitor, test capacitor, measuring impedance and detector

(c) test capacitor, measuring impedance and a detector

- (d) test capacitor, calibrating unit and detector
4. The discharge energy in a partial discharge in terms of discharge magnitude q and inception voltage v is
- q_{vi}
 - $\frac{q_{vi}}{\sqrt{2}}$
 - $0.5 q_{vi}$
 - $\sqrt{2}q_{vi}$
5. Partial discharge inception voltage is defined as
- the rms value of supply voltage at which partial discharges occur
 - the lowest value of the voltage at which discharge disappears when the voltage is reduced
 - the lowest value of the voltage at which discharge appears when voltage is increased
 - the voltage at which corona discharge starts.
6. In pd detectors partial discharges are displayed on
- any CRO
 - built in CRO with circular time base
 - built in CRO with elliptic time base
 - built in CRO with linear time base.
7. The bridge commonly used for measurement of dielectric constant and loss factor in the audio frequency range 100 Hz to 10 kHz is
- high-voltage Schering-bridge
 - transformer ratio bridge
 - Wagner's-Bridge
 - low-voltage high-frequency Schering-bridge
8. The measuring range of high-voltage Schering-bridge with Std. Capacitors of 50 or 100 pf is
- 10pfto10nF
 - 1pfto1000pf
 - 1 nF to 1 μ F
 - 1 pf to 100 μ F
9. The measuring range of a high-frequency low-voltage Schering-bridge is
- 10pfto10nF
 - 1pfto1000pf
 - 1 nF to 1 μ F
 - 1 pf to 100 μ F
10. The charge associated with partial discharges in electrical apparatus will be
- micro coulombs
 - nano coulombs
 - pico coulombs
 - coulombs

Answers to Multiple-Choice Questions

- | | | | | | |
|---------|---------|---------|---------|---------|---------|
| 1. (b) | 2. (a) | 3. (d) | 4. (a) | 5. (c) | 6. (c) |
| 7. (d) | 8. (a) | 9. (a) | 10. (d) | 11. (a) | 12. (a) |
| 13. (b) | 14. (b) | 15. (c) | 16. (c) | 17. (d) | 18. (a) |
| 19. (b) | 20. (c) | | | | |

REVIEW QUESTIONS

1. How is a lossy dielectric represented? Explain how an ideal capacitor in parallel with a resistor can represent a lossy dielectric over a wide frequency range?
2. Define 'complex permittivity'. What are the factors that govern the quantities 'relative permittivity' and 'loss factor'?
3. Explain how the volume resistivity of a solid dielectric is determined.
4. What is the three electrode arrangement used in dielectric measurements? Explain with sketches the electrode arrangements for (a) solid specimen, (b) liquid specimen.
5. Describe Mole's arrangement for measuring high dissipation factors in the low frequency range.
6. Explain the high-voltage Schering-bridge for the $\tan \delta$ and capacitance measurement of insulators or bushings.
7. Explain the modifications to be made to the Schering-bridge for the following situations:
 - (a) high dissipation factor test objects,
 - (b) high capacitance test objects, and
 - (c) one end of the test object to be grounded.
8. Why are the earthing and shielding arrangements needed in the Schering bridge measurements?
9. What is 'Wagner's earthing device' and how is it used for eliminating stray capacitances?
10. Why is the substitution method used for measuring low capacitances?
11. Explain the transformer ratio arm bridge for audio frequency range measurements. Discuss its merits and demerits over other methods.
12. Why is the micrometer electrode system needed for radio frequency ranges? Give a sketch of the micrometer electrode system for solid and liquid specimens.
13. Discuss the type of detectors used in dielectric measurements in the following cases:
 - (a) dc measurements,
 - (b) 50 Hz measurements, and
 - (c) audio frequency measurements.
14. Briefly explain how partial discharges in an insulation system or equipment can be detected and displayed.
15. Briefly explain the methods used for calibrating the partial discharge detectors.
16. What are partial discharges and how are they detected under power frequency operating conditions?
17. Discuss the method of balanced detection for locating partial discharges in electrical equipment.
18. Describe how a fault in a long cable can be detected and located using partial discharge technique.
19. What are 'broad band' and 'narrow band' detectors? What is the sensitivity in each of the above detectors?
20. A high-voltage Schering-bridge has the following arms
 - (i) standard capacitors: 500 pF and 100 pF
 - (ii) variable resistance $R_4 = 1 \text{ ohm to } 1 \text{ k-ohm}$
 - (iii) $C_3 = 1 \text{ nF to } 2 \text{ }\mu\text{F}$, $R_3 = 100 \text{ to } 1000 \text{ ohms}$

Determine (a) the maximum and minimum values of C_x , unknown capacitance that can be measured (b) the loss angle of the specimen if balance is obtained with $C_x = 200 \text{ pF}$, $C_3 = 10 \text{ nF}$ and $R_4 = 1 \text{ k-ohm}$ with a standard capacitor having a capacitance of 500 pF and (c) the value of

the shunt to be used with R_4 to measure $10 \mu\text{F}$.

Answer: (a) $0.5 \mu\text{F}$, 10 pF (b) $\tan \delta = 1.25 \times 10^{-3}$ (c) $\frac{1}{19} \approx 0.05 \Omega$

REFERENCES

1. Schwab, A., *High Voltage Measurement Technique*, M.I.T. Press (1972).
2. Harris, F.H., *Electrical Measurements*, John Wiley, New York (1966).
3. Bhimani, B.V., "Low frequency a.c. bridges", *Tr. A.I.E.E.*, **80**, Part3, 155 (1961).
4. Mole, G., "Design and performance of a portable a.c. discharge detector", *ERA Research Report*, V/T, p. 116 (1953).
5. Von Hippel, A., *Dielectrics and Applications*, M.I.T. Press (1961).
6. *ASTM Standard on "Electrical insulating materials,"* D 150-50T, 1961.
7. Kreuger, F.H., *Discharge Detection in High Voltage Equipment*, Haywood, London (1964).
8. "Partial Discharge Measurements", *I.E.C. specification No. 270* (1968).
9. CIGRE Report # 72, "Guide for the Evaluation of the Dielectric Strength of Externation Insulation", *Working group 07 of Study Committee No. 33*, CIGRE, Paris, France, (1992).
10. Kreuger, F., *Partial Discharge Detection in High Voltage Equipment*, Butterworths, London, England (1989).
11. Kreuger, F., Gulski, E. and Krivda, A., *IEEE Trans. on Elect. Insul.*, **28**, No. 6, pp. 917-931 (1993).
12. Krivda, A., "Recognition of Discharges, Discrimination and Classification", *Ph.D Thesis*, Delft University, Delft, The Netherlands (1995).
13. Peyraque, L., Boisdon, C., Berouel, A. and Buret, F., *IEEE Trans. on Dielectrics and Elec. Insul.*, **2**, No. 1, pp. 40-49 (1995).
14. Hague, B., *Alternating-Current Bridge Methods*, (5th edition), Pitman and Sons, London, England (1959).

CHAPTER

10

High-Voltage Testing of Electrical Apparatus

It is essential to ensure that the electrical equipment is capable of withstanding the overvoltages that are met with in service. The overvoltages may be either due to natural causes like lightning or system-originated ones such as switching or power frequency transient voltages. Hence, testing for overvoltages is necessary.

10.1 TESTING OF INSULATORS AND BUSHINGS

In this section, different overvoltage tests done on insulators and bushings are discussed. The overvoltage tests are classified into two groups: (i) power frequency voltage tests; and (ii) impulse voltage tests. These tests together ensure the overvoltage withstand capability of an apparatus. Before discussing the actual tests, knowledge of the general terminology of the technical terms used, is essential.

10.1.1 Definitions

In test codes and standard specifications, certain technical terms are used to specify and define conditions or procedures. Hence, commonly used technical terms are defined here before the actual testing techniques are discussed.

(a) Disruptive Discharge Voltage This is defined as the voltage which produces the loss of dielectric strength of an insulation. It is that voltage at which the electrical stress in the insulation causes a failure which includes the collapse of voltage and passage of current. In solids, this causes a permanent loss of strength, and in liquids or gases, only temporary loss may be caused. When a discharge takes place between two electrodes in a gas or a liquid or over a solid surface in air, it is called *flashover*. If the discharge occurs through a solid insulation it is called *puncture*.

(b) Withstand Voltage The voltage which has to be applied to a test object under specified conditions in a withstand test is called the withstand voltage [as per IS: 731 and IS: 2099–1963].

(c) Fifty Per Cent Flashover Voltage This is the voltage which has a probability of 50% flashover, when applied to a test object. This is normally applied in impulse test in which the loss of insulation strength is temporary.

(d) Hundred Per Cent Flashover Voltage The voltage, that causes a flashover at each of its applications under specified conditions, when applied to test objects as specified, is hundred per cent flashover voltage.

(e) Creepage Distance It is the shortest distance on the contour of the external surface of the insulator unit or between two metal fittings on the insulator.

(f) ac Test Voltages Alternating test voltages of power frequency should have a frequency range of 40 to 60 Hz and should be approximately sinusoidal. The deviation allowed from the standard sine curve is about 7%. The deviation is checked by measuring instantaneous values over specified intervals and computing the rms value, the average value, and the form factor.

(g) Impulse Voltages Impulse voltages are characterized by polarity, peak value, time to front (t_f), and time to half the peak value after the peak (t_t). The time to front is defined as 1.67 times to time between 30% and 90% of the peak value in the rising portion of the wave. According to IS: 2071 (1973), standard impulse is defined as one with $t_f = 1.2 \mu s$, $t_t = 50 \mu s$ (called 1.2/50 μs wave). The tolerances allowed are $\pm 3\%$ on the peak value, $\pm 30\%$ in the front time (t_f), and $\pm 20\%$ in the tail time (t_t).

(h) Reference Atmospheric Conditions The electrical characteristics of the insulators and other apparatus are normally referred to the reference atmospheric conditions. According to the Indian Standard Specifications, they are

Temperature : 27°C

Pressure : 1013 millibars (or 760 torr)

Absolute humidity : 17 g/m³

Since it is not always possible to do tests under these reference conditions, correction factors have to be applied. In some cases, the following test conditions are also used as reference (British Standard Specifications) conditions.

Temperature : 20°C

Pressure : 1013 millibars (or 760 torr)

Absolute humidity : 11 g/m³ (65% relative humidity at 20°C)

The flashover voltage of the test object is given by

$$V_s = V_a \times \frac{h}{d}$$

where, V_a = voltage under actual test conditions,

V_s = voltage under reference atmospheric conditions,

h = humidity correction factors, and

d = air density correction factor.

The air density correction factor is given by

$$d = \frac{0.289b}{273 + T} \text{ for } 20^\circ\text{C}$$

$$\text{or, } \frac{0.296b}{273 + T} \text{ for } 27^\circ\text{C}$$

where, b = atmospheric pressure in millibars, and

t = atmospheric temperature, °C,

Humidity correction factor h is obtained from the temperatures of a wet and dry bulb thermometer, by obtaining the absolute humidity and then computing h from the absolute humidity. These are graphically given in [Figs 10.1](#) and [10.2](#).

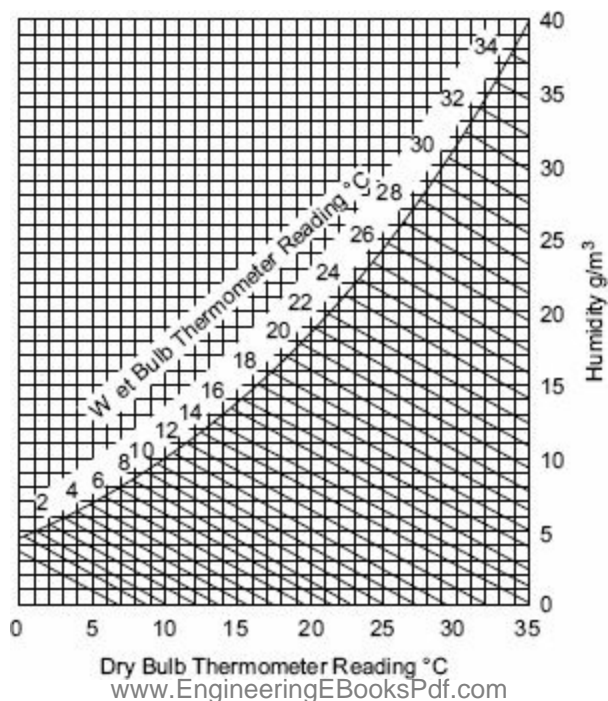
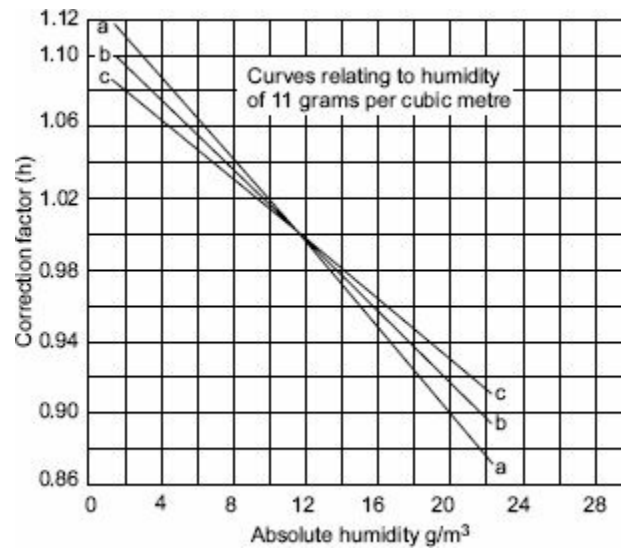


Fig. 10.1 Computation of absolute humidity from wet and dry bulb thermometer temperatures



- a* – For power frequency tests
- b* – For positive impulse tests
- c* – For negative impulse tests

Fig. 10.2 Humidity correction factor

10.1.2 Tests on Insulators

The tests that are normally conducted are usually subdivided as (i) type tests, and (ii) the routine tests. Type tests are intended to prove or check the design features and the quality. The routine tests are intended to check the quality of the individual test piece. Type tests are done on samples when new designs or design changes are introduced, whereas the routine tests are done to ensure the reliability of the individual test objects and quality and consistency of the materials used in their manufacture.

High-voltage tests include (i) the power frequency tests, and (ii) impulse tests. All the insulators are tested for both categories of test.

(a) Power Frequency Tests

(i) *Dry and Wet Flashover Tests* In these tests, the ac voltage of power frequency is applied across the insulators and increased at a uniform rate of about 2 per cent per second of 75% of the estimated test voltage, to such a value that a breakdown occurs along the surface of the insulator. If the test is conducted under normal conditions without any rain or precipitation, it is called 'dry flashover test'. If the test is done under conditions of rain, it is called 'wet flashover test'. In general, wet tests are not intended to reproduce the actual operating conditions, but only to provide a criterion based on experience that a satisfactory service operation will be obtained. The test object is subjected to a spray of water of given conductivity by means of nozzles. The spray is arranged such that the water drops fall approximately at an inclination of 45° to the vertical. The test object is sprayed for at least one minute before the voltage application, and the spray is continued during the voltage application. The characteristics of the spray are

- Precipitation rate : $3 \pm 10\%$ (mm/min)
- direction : 45° to the vertical
- conductivity of water : 100 micro Siemens $\pm 10\%$
- water temperature : ambient $\pm 15^\circ\text{C}$

The International Electrotechnical Commission (IEC) in its document (No. 42 of 1972) has revised the test procedure and precipitation conditions as follows. (Also IEC 600060 ~ 1, 1994)

Average precipitation rate:

vertical component = 1 to 1.5 mm/min

horizontal component = 1 to 1.5 mm/min

limits for individual measurements = 0.5 to 2.0 mm/min

temperature of collected water = ambient temperature $\pm 15^\circ\text{C}$

and the conductivity of water corrected to $20^\circ\text{C} = 100 \pm 15$ micro Siemens Specifications are being modified for application of 15 positive and 15 negative impulses. Two in each set are allowed to flashover. If more than two flashovers occur in each set then the insulator is deemed to have failed the test. This procedure is satisfactorily equivalent to the one mentioned above.

(ii) *Wet and Dry Withstand Tests (One Minute)* In these tests, the voltage specified in the relevant specification is applied under dry or wet conditions for a period of one minute with an insulator mounted as in service conditions. The testpiece should withstand the specified voltage.

(b) Impulse Tests

- (i) *Impulse Withstand Voltage Test* This test is done by applying standard impulse voltage of specified value under dry conditions with both positive and negative polarities of the wave. If five consecutive waves do not cause a flashover or puncture, the insulator is deemed to have passed the test. If two applications cause flashover, the object is deemed to have failed. If there is only one failure, additional ten applications of the voltage wave are made. If the test object has withstood the subsequent applications, it is said to have passed the test.
- (ii) *Impulse Flashover Test* The test is done as above with the specified voltage. Usually, the probability of failure is determined for 40% and 60% failure values or 20% and 80% failure values, since it is difficult to adjust the test voltage for the exact 50% flashover values. The average value of the upper and the lower limits is taken. The insulator surface should not be damaged by these tests, but slight marking on its surface or chipping off of the cement is allowed.
- (iii) *Pollution Testing* Because of the problem of pollution of outdoor electrical insulation and consequent problems of the maintenance of electrical power systems, pollution testing is gaining importance. The normal types of pollution are (i) dust, microorganisms, bird secretions, flies, etc., (ii) industrial pollution like smoke, petroleum vapours, dust, and other deposits, (iii) coastal pollution in which corrosive and hygroscopic salt layers are deposited on the insulator surfaces, (iv) desert pollution in which sand storms cause deposition of sand and dust layers, (v) ice and fog deposits at high altitudes and in polar countries. These pollutions cause corrosion, non-uniform gradients along the insulator strings and surface of insulators and also cause deterioration of the material. Also, pollution causes partial discharges and radio interference. Hence, pollution testing is important for extra high-voltage systems.

At present there is no standard pollution test available. The popular test that is normally done is the salt fog test. In this test, the maximum normal withstand voltage is applied on the insulator and then artificial salt fog is created around the insulator by jets of salt water and compressed air. If the flashover occurs within one hour, the test is repeated with fog of lower salinity, otherwise, with a fog to higher salinity. The maximum salinity at which the insulator withstands, three out of four tests without flashover, is taken as the representative figure. Much work is yet to be done to standardize the test procedures.

10.1.3 Testing of Bushings

(a) Power Frequency Tests

- (i) *Power Factor–Voltage Test* In this test, the bushing is set up as in service or immersed in oil. It is connected such that the line conductor goes to the high-voltage side and the tank or earth portion goes to the detector side of the high-voltage Schering-bridge. Voltage is applied up to the line value in increasing steps and then reduced. The capacitance and power factor (or $\tan \delta$) are recorded at each step. The characteristic of power factor or $\tan \delta$ versus applied voltage is drawn. This is a normal routine test but sometimes may be conducted on percentage basis.
- (ii) *Internal or Partial Discharge Test* This test is intended to find the deterioration or failure due to internal discharges caused in the composite insulation of the bushing. This is done by using internal or partial discharge arrangement (see [Sec. 9.4](#)). The voltage versus discharge magnitude as well as the quadratic rate, gives an excellent record of the performance of the bushing in service. This is now a routine test for high-voltage bushings.
- (iii) *Momentary Withstand Test at Power Frequency* This is done as per the Indian Standard Specifications, IS: 2099, applied to bushings. The test voltage is specified in the specifications. The bushing has to withstand without flashover or puncture for a minimum time (~ 30 s) to measure the voltage. At present this test is replaced by the impulse withstand test.
- (iv) *One Minute Wet Withstand Test at Power Frequency* The most common and routine tests used for all electrical apparatuses are the one minute wet, and dry voltage withstand tests. In wet test, voltage specified is applied to the bushing mounted as in service with the rain arrangement as described earlier. A properly designed bushing has to withstand the voltage without flashover for one minute. This test really does not give any information for its satisfactory performance in service, while impulse and partial discharge tests give more information.
- (v) *Visible Discharge Test at Power Frequency* This test is intended for determining whether the bushing is likely to give radio interference in service, when the voltage specified in IS: 2099 is applied. No discharge other than that from the arcing horns or grading rings should be visible to the observers in a dark room. The test arrangement is the same as that of the withstand test, but the test is conducted in a dark room.

(b) Impulse Voltage Tests

- (i) *Full Wave Withstand Test* The bushing is tested for either polarity voltages as per the specifications. Five consecutive full waves of standard waveform are applied, and, if two of them cause flashover, the bushing is said to have failed in the test. If only one flashover occurs, ten additional applications are done. The bushing is considered to have passed the test if no flashover occurs in subsequent applications.
- (ii) *Chopped Wave Withstand and Switching Surge Tests* The chopped wave test is sometimes done for high-voltage bushings (220 kV and 400 kV and above). Switching surge flashover test of specified value is nowadays included for high-voltage bushings. The tests are carried out similar to full wave withstand tests.

(c) Thermal Tests

Temperature Rise and Thermal Stability Tests The purpose of these tests is to ensure that the bushing in service for long does not have an excessive temperature rise and also does not go into the 'thermal runaway' condition of the insulation used.

Temperature rise test is carried out in free air with an ambient temperature below 40°C at a rated power frequency (50 Hz) ac. The steady temperature rise above the ambient air temperature at any part of the bushing should not exceed 45°C. The test is carried out for such a long time till the temperature is substantially constant, i.e. the increase in temperature rate is less than 1°C/h. Sometimes, the bushings have to be operated along with transformers, of which the temperature reached may exceed 80°C. This temperature is high enough to produce large dielectric losses and thermal instability. For high-voltage bushings this is particularly important, and hence the thermal stability test is done for bushings rated for 132 kV and above. The test is carried out with the bushing immersed in oil at a maximum temperature as in service, and the voltage applied is 86% of the nominal system voltage. This is approximately $\sqrt{2}$ times the working voltage of the bushing and hence the dielectric losses are about double the normal value. The additional losses account for the conductor ohmic losses. It has been considered unnecessary to specify the thermal stability test for oil-impregnated paper bushings of low ratings; but for the large high-voltage bushings (1600 A, 400 kV transformer bushings, etc.), the losses in the conductor may be high enough to outweigh the dielectric losses. It may be pointed out here, that the thermal stability tests are type tests. But in the case of large sized high-voltage bushings, it may be necessary to make them routine tests.

10.2 TESTING OF ISOLATORS AND CIRCUIT BREAKERS

10.2.1 Introduction

In this section, the testing of isolators and circuit breakers is covered, giving common characteristics for both. While these characteristics are directly relevant to the testing of circuit breakers, they are not much relevant as far as the testing of isolators are concerned since isolators are not used for interrupting high currents. At best, they interrupt small currents of the order of 0.5 A (for rated voltages of 420 kV and below) which may be the capacitive currents of bushings, busbars etc. In fact, the definition of an Isolator or a Disconnecter as per IS: 9921 (Part I)-1981 is as follows:

An isolator or a disconnecter is a mechanical switching device, which provides in the open position, an isolating distance in accordance with special requirements. An isolator is capable of opening and closing a circuit when either negligible current is broken or made or when no significant change in the voltage across the terminals of each of the poles of the isolator occurs. It is also capable of carrying currents under normal circuit conditions, and carrying for a specified time, currents under abnormal conditions such as those of a short circuit.

Thus, most of the discussion here refers to the testing of circuit breakers.

Testing of circuit breakers is intended to evaluate (a) the constructional and operational characteristics, and (b) the electrical characteristics of the circuit which the switch or the breaker has to interrupt or make. The different characteristics of a circuit breaker or a switch may be summarized as per the following groups.

- (i) (a) The electrical characteristics which determine the arcing voltage, the current chopping characteristics, the residual current, the rate of decrease of conductance of the arc space and the plasma, and the shunting effects in interruption.
- (b) Other physical characteristics including the media in which the arc is extinguished, the pressure developed or impressed at the point of interruption, the speed of the contact travel, the number of breaks, the size of the arcing chamber, and the materials and configuration of the circuit interruption.
- (ii) The characteristics of the circuit include the degree of electrical loading, the normally generated or applied voltage, the type of fault in the system which the breaker has to clear, the time of interruption, the time constant, the natural frequency and the power factor of the circuit, the rate of rise of recovery voltage, the restriking voltage, the decrease in the ac component of the short circuit current, and the degree of asymmetry and the dc component of the short circuit current.

To assess the above factors, the main tests conducted on the circuit breakers and isolator switches are

- (i) the dielectric tests or overvoltage tests,
- (ii) the temperature rise tests,
- (iii) the mechanical tests, and
- (iv) the short circuit tests

Dielectric tests consist of overvoltage withstand tests of power frequency, lightning and switching impulse voltages. Tests are done for both internal and external insulation with the switch or circuit breaker in both the open and closed positions. In the open position, the test voltage levels are 15% higher than the test voltages used when the breaker is in closed position. As such there is always the possibility of line to ground flashover. To avoid this, the circuit breaker is mounted on insulators

above the ground, and hence the insulation level of the body of the circuit breaker is raised.

The impulse tests with the lightning impulse wave of standard shape are done in a similar manner as in the case of insulators. In addition, the switching surge tests with switching overvoltages are done on circuit breakers and isolators to assess their performance under overvoltages due to switching operations.

Temperature rise and mechanical tests are type tests on circuit breakers and are done according to the specifications.

10.2.2 Short-Circuit Tests

The most important test carried out on circuit breakers are short circuit tests, since these tests assess the primary performance of these devices, i.e. their ability to safely interrupt the fault currents. These tests consist of determining the making and breaking capacities at various load currents and rated voltages. In the case of isolators, the short circuit tests are conducted only with the limited purpose to determine their capacity to carry the rated short circuit current for a given duration; and no breaking or making current tests is done.

The different methods of conducting short-circuit tests are the following:

(a) Direct Tests

- (I) Using a short circuit generator as the source
- (II) Using the power utility system or network as the source

(b) Synthetic Tests

(i) Direct Testing in the Networks or in the Fields Circuit breakers are sometimes tested for their ability to make or break the circuit under normal load conditions or under short-circuit conditions in the network itself. This is done during period of limited energy consumption or when the electrical energy is diverted to other sections of the network which are not connected to the circuit under test. The advantages of field tests are the following:

- (i) The circuit breaker is tested under actual conditions like those that occur in a given network.
- (ii) Special occasions like breaking of charging currents of long lines, very short line faults, interruption of small inductive currents, etc. can be tested by direct testing only.
- (iii) To assess the thermal and dynamic effects of short circuit currents, to study applications of safety devices, and to revise the performance test procedures, etc.

The disadvantages are the following:

- (i) The circuit breaker can be tested at only a given rated voltage and network capacity.
- (ii) The necessity to interrupt the normal services and to test only at light load conditions.
- (iii) Extra inconvenience and expenses in installation of controlling and measuring equipment in the field.

(ii) Direct Testing in Short-Circuit Test Laboratories In order to test the circuit breakers at different voltages and at different short-circuit currents, short-circuit laboratories are provided. The schematic layout of a short circuit testing laboratory is given in [Fig. 10.3](#). It consists of a short-circuit generator in association with a master circuit breaker, resistors, reactors and measuring devices. A make switch initiates the short circuit and the master circuit breaker isolates the test device from the source at the end of a predetermined time set on a test sequence controller. Also, the master circuit breaker can be tripped if the test device fails to operate properly. Short-circuit generators with induction motors as prime movers are also available.

(iii) Synthetic Testing of Circuit Breakers Due to very high interrupting capacities of circuit breakers, it is not economical to have a single source to provide the required short circuit and the

rated voltage. Hence, the effect of a short circuit is obtained as regards to the intensity of the current and the recovery voltage as a combination of the effects of two sources, one of which supplies the ac current and the other the high-voltage.

In the initial period of the short-circuit test, the ac current source supplies the heavy current at a low voltage, and then the recovery voltage is simulated by a source of comparatively high voltage of small current capacity. A schematic diagram of a synthetic testing station is shown in [Fig. 10.4](#).

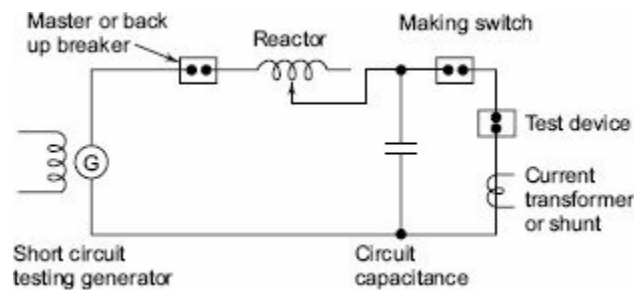
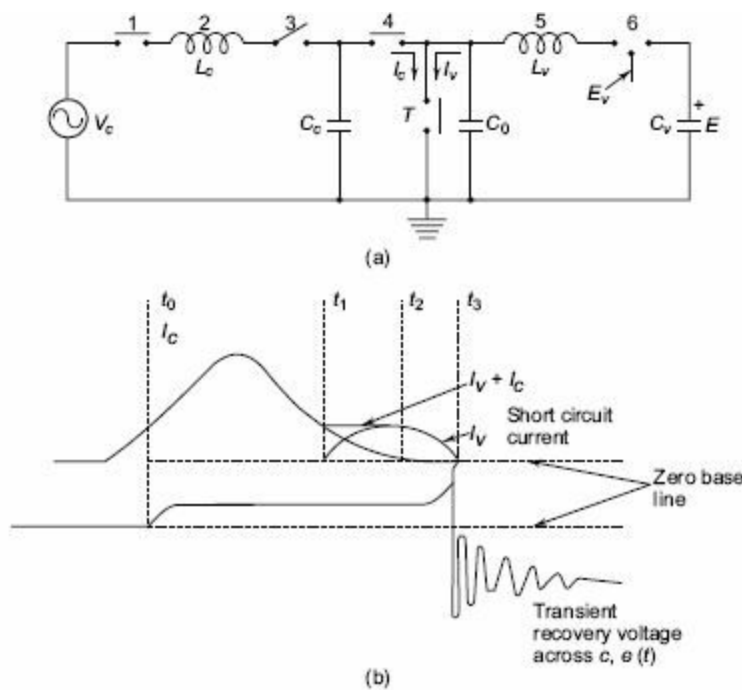


Fig. 10.3 Schematic diagram showing basic elements of a short circuit testing laboratory

With the auxiliary breaker (3) and the test breaker (T) closed, the closing of the making switch (1) causes the current to flow in the test circuit breaker. At some instant say t_0 , the test circuit breaker (T) begins to operate and the master circuit breaker (1) becomes ready to clear the generator circuit. At some time t_1 , just before the zero of the generator current, the trigger gap (6) closes and the higher frequency current from the discharging capacitor C_v also flows through the arc. At time t_2 , when the generator current is zero, the circuit breaker (1) clears that circuit, leaving only the current from C_v , which has the required rate of change of current at its zero flowing in the test circuit breaker. At the zero of this current, full test voltage will be available. The closing of gap (6) would be a little earlier in time than shown in [Fig. 10.4](#), but it has been drawn as shown, for clarity at current zeros. It is important to see that the high-current source is disconnected and a high-voltage source applied with absolute precision (by means of an auxiliary circuit breaker) at the instant of circuit breaking.



V_c – Low voltage, high current generator; L_c – Current controlling inductance (2); 1 – Master breaker; 3 – Main switch; (T – Circuit breaker) under test; 4 – Auxiliary breaker; (L_v – Voltage waveform) controlling choke (5); 6 – Trigger gap; C_v – Capacitor charged to E_v to give necessary recovery voltage; (C_0 – Capacitor to control the frequency of the transient recovery voltage;) t_0 – Opening of auxiliary circuit breaker (4); t_1 – Trigger gap 6 is fired; t_2 – Auxiliary circuit breaker clears and interrupts i_c ; t_3 – i_v becomes zero

Fig. 10.4 (a) Schematic diagram of synthetic testing of circuit breakers
(b) Current and recovery voltage waveforms across the test circuit breaker

(iv) **Composite Testing** In this method, the breaker is first tested for its rated breaking capacity at a reduced voltage and afterwards for rated voltage at a low current. This method does not give a proper estimate of the breaker performance.

(v) **Unit Testing** When large circuit breakers of very high-voltage rating (220 kV and above) are to be tested and where more than one break is provided per pole, the breaker is tested for one break at its rated current and the estimated voltage. In actual practice, the conditions of arc in each gap may not be identical and the voltage distribution along several breaks may be uneven. Hence, certain uncertainty prevails in the testing of one break.

(vi) **Testing Procedure** The circuit breakers are tested for their (i) breaking capacity B, and (ii) making capacity M. The circuit breaker, after the calibration of the short circuit generator, is tested for the following duty cycle.

- (1) B-3-B-3-B at 10% of the rated symmetrical breaking capacity
- (2) B-3-B-3-B at 30% of the rated symmetrical breaking capacity
- (3) B-3-B-3-B at 60% of the rated symmetrical breaking capacity
- (4) B-3-MB-3MB-MB at 100% breaking capacity with the recovery voltage not less than 95% of the rated service voltage.

The power factor in these tests is generally between 0.15 and 0.3. The numeral 3 in the above duty cycle indicates the time interval in minutes between the tests.

(vii) **Asymmetrical Tests** One test cycle is repeated for the asymmetrical breaking capacity in

which the dc component at the instant of contact separation is not less than 50% of the ac component.

10.3 TESTING OF CABLES

Cables are very important electrical apparatus for transmission of electrical energy by underground means. They are also very important means for transmitting voltage signals at high voltages. For power engineers, large power transmission cables are of importance, and hence testing of power cables only is considered here. Of the different electrical and other tests prescribed, the following are important to ensure that cables withstand the most severe conditions that are likely to arise in service.

Different tests on cables may be classified into

- (i) mechanical tests like bending test, dripping and drainage test, and fire resistance and corrosion tests,
- (ii) thermal duty tests,
- (iii) dielectric power factor tests,
- (iv) power frequency withstand voltage tests,
- (v) impulse withstand voltage tests,
- (vi) partial discharge tests, and
- (vii) life expectancy tests.

Here only the electrical tests are described, i.e., tests (iii) to (vii).

10.3.1 Preparation of the Cable Samples

For overvoltage and withstand tests, samples have to be carefully prepared and terminated; otherwise, excessive leakage or end flashovers may occur during testing. The normal length of the cable sample used varies from about 50 cm to 10 m. The terminations are usually made by shielding the end conductor with stress shields or terminations to relieve the ends from excessive high electrical stresses. A few terminations are shown in [Fig. 10.5](#). During power factor tests, the cable ends are provided with shields so that the surface leakage current is avoided from the measuring circuits.

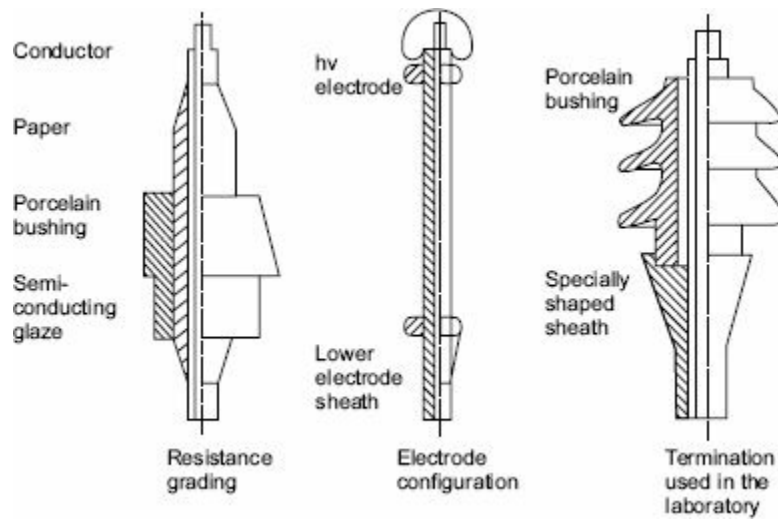


Fig. 10.5 Cable and terminals

10.3.2 Dielectric Power Factor Test

The dielectric power factor test is done using the high-voltage Schering-bridge (see [Sec. 9.3.4](#)). The power factor or dissipation factor $\tan \delta$ is measured at 0.5, 1.0, 1.66, and 2.0 times the rated voltage (phase to ground) of the cable. The maximum value of the power factor and the difference in power factor between the rated voltage and 1.66 times the rated voltage, as well as, between the rated voltage and two times the rated voltage are specified. Sometimes, difficulty is felt in supplying the charging voltamperes of the cable from the available source. In such cases, a choke is used or a suitably rated transformer winding is used in series with the cable to form a resonant circuit. This improves the power factor and raises the test voltage between the cable core and the sheath to the required value, when a source of high-voltage and high capacity is used. The Schering bridge has to be given protection against overvoltages, in case breakdown occurs in the cables.

10.3.3 High-Voltage Tests on Cables

Cables are tested for withstand voltages using the power frequency ac, dc, and impulse voltages. At the time of manufacture, the entire cable is passed through a high-voltage test at the rated voltage to check the continuity of the cable. As a routine test, the cable is tested applying an ac voltage of 2.5 times the rated value for 10 min. No damage to the cable insulation should occur. Type tests are done on cable samples using both high-voltage dc and impulse voltages. The dc test consists of applying 1.8 times the rated dc voltage of negative polarity for 30 min., and the cable system is said to be fit, if it withstands the test. For impulse tests, impulse voltage of the prescribed magnitude as per specifications is applied, and the cable has to withstand five applications without any damage. Usually, after the impulse test, the power frequency dielectric power factor test is done to ensure that no failure occurred during the impulse test.

10.3.4 Partial Discharges

(a) Discharge Measurement Partial discharge measurements and the discharge locations are important for cables, since the life of the insulation at a given voltage stress depends on the internal discharges. Also, the weakness of the insulation or faults can be detected with the help of these tests; the portion of the cable if weak may be removed, if necessary. The general arrangement for partial discharge tests is the same as described in [Sec. 9.4](#).

The equivalent circuit of the cable for discharges is shown in [Fig. 10.6](#), and the cable connection to the discharge detector through the coupling condenser is shown in [Figs 10.7a](#) and [b](#). If the detector is connected through a coupling capacitor to one end of the cable as in [Fig. 10.7a](#), it will receive the transient travelling wave directly from the cavity towards the nearer end, and after a short time, a second travelling wave pulse reflected from the far end is observed. Thus, the detected response is the combination of the above two transient pulses. But, if the connections are made as in [Fig. 10.7b](#), no severe reflection is involved except as a second-order effect of negligible magnitude. Now, two transients will arrive at both the ends of the cable, and the superposition of the two pulses is detected. This can be obtained by adding the responses of the two transients. The superpositions of the two responses may give rise to a serious error in the measurement of the discharge magnitude. The magnitude of the possible error may be determined mainly by the shape of the response of the discharge detector.

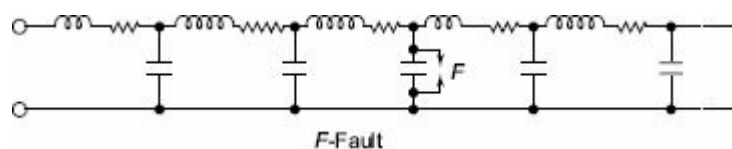


Fig. 10.6 Equivalent circuit of the cable for discharges

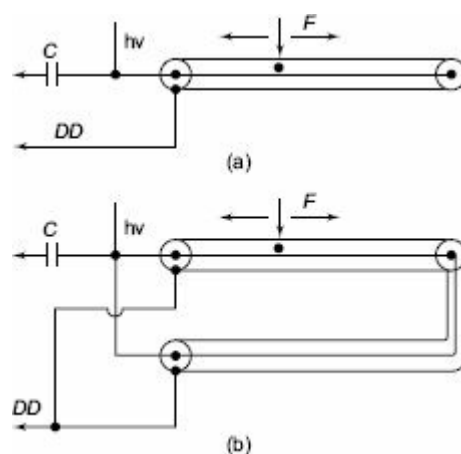


Fig. 10.7 Discharge detector connection to long length of cable DD — Discharge detector; F-Fault location

(b) Location of Discharges The voltage dip caused by a discharge at a fault or a void is propagated as a travelling wave along the cable. This wave is detected as a voltage pulse across the terminals of the cable ends. By measuring the time duration between the pulses, the distance at which the discharge is taking place from the cable end can be determined. The shapes of the voltage pulses depend on the nature of the discharges. Typical waveshapes are given in [Fig. 10.8](#). The detection circuits for the pulses are shown in [Fig. 10.9](#), and the attenuation of the travelling wave in cables is

given in Fig. 10.10. Usually, the pulses detected across the resistor are distorted after passing through the amplifier of the discharge detector.

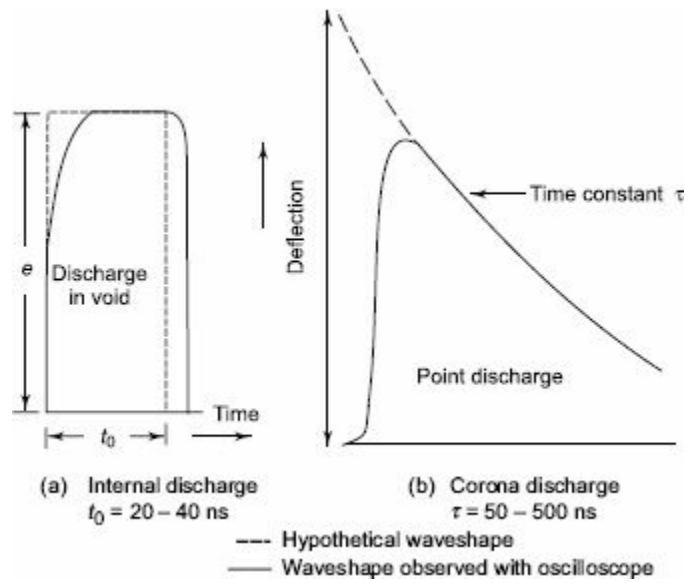


Fig. 10.8 Typical waveshapes of pulses at the cable ends

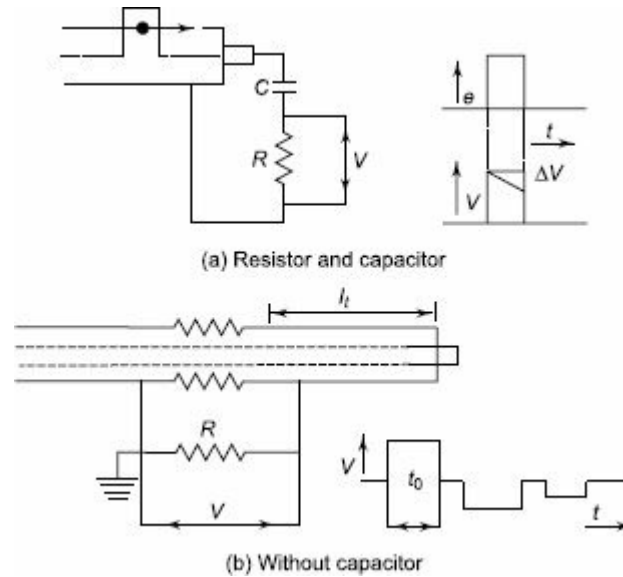


Fig. 10.9 Detection circuits for long cables

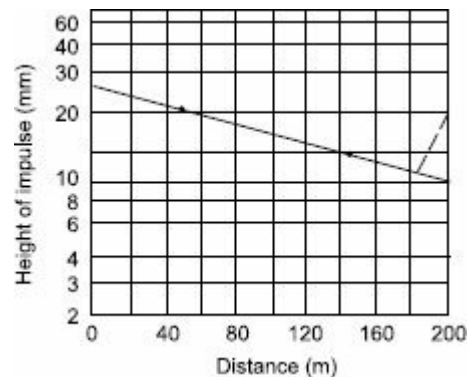


Fig. 10.10 Attenuation of travelling waves

(c) **Scanning Method** In order to scan the entire cable length for voids or imperfections in

manufacture, the bare core of the cable is passed through a high electric field and the discharge location is done. The core of the material is passed through a tube of insulating material filled with distilled water. Four electrodes in the form of rings are mounted at both ends of tube as well as at the middle, such that they have electrical contact with the water. The middle electrodes are energized with a high-voltage, and the other two electrodes and cable conductor are grounded. If a discharge occurs in the portion between the middle electrodes, as the cable is passed between the middle electrodes' portion, the discharge is detected and is located at that length of cable.

This test is very convenient for isolating the defective insulation at the factory site. The manufactured cable, before being rolled on to its former, can be conveniently passed through the test apparatus. 'The defective part' can be isolated and cut off from the cable reel before it is sent from the factory.

(d) Life Tests Life tests are intended for reliability studies in service. In order to determine the expected life to the cable under normal stress, accelerated life tests using increased voltages are performed on actual cable lengths. It is established that the relation between the maximum electrical stress E_m and the life of the cable insulation in hours t approximately follows the relationship

$$E_m = Kt^{-(1/n)}$$

where, K = constant which depends on the field conditions and the material, and
 n = life index depending on the material.

By conducting long duration life tests at increased stress (1 hr to about 1000 hr) the expected life at the rated stress may be determined.

10.4 TESTING OF TRANSFORMERS

Transformers are very important and costly apparatus in power systems. Great care has to be exercised to see that the transformers are not damaged due to transient overvoltages of either lightning or power frequency. Hence, overvoltage tests become very important in the testing of transformers. Here, only the overvoltage tests are discussed, and other routine tests like the temperature rise tests, short circuit tests, etc., are not included and can be found in the relevant specifications.

(a) Induced Overvoltage Test Transformers are tested for overvoltages by exciting the secondary of the transformer from a high frequency ac source (100 to 400 Hz) to about twice the rated voltage. This reduces the core saturation and also limits the charging current necessary in large power transformers. The insulation withstand strength can also be checked.

(b) Partial Discharge Tests Partial discharge tests on the windings are done to assess the discharge magnitudes and the radio interference levels (see also [Sec. 10.6](#)). The transformer is connected in a manner similar to any other equipment (see [Sec. 9.4](#)) and the discharge measurements are made. The location of the fault or void is sometimes done by using the travelling wave technique similar to that for cables. So far, no method has been standardized as to where the discharge is to be measured. Multi-terminal partial discharge measurements are recommended. Under the application of power frequency voltage, the discharge magnitudes greater than 10^4 pico coulomb are considered to be severe, and the transformer insulation should be such that the discharge magnitude will be far below this value.

10.4.1 Impulse Testing of Transformers

The purpose of the impulse test is to determine the ability of the insulation of the transformers to withstand the transient voltages due to lightning, etc. Since the transients are impulses of short rise time, the voltage distribution along the transformer winding will not be uniform. The equivalent circuit of a transformer winding for impulses is shown in [Fig. 10.11](#). If an impulse wave is applied to such a network (shown in [Fig. 10.11](#)) the voltage distribution along the element will be uneven, and oscillations will be set in producing voltages much higher than the applied voltage.

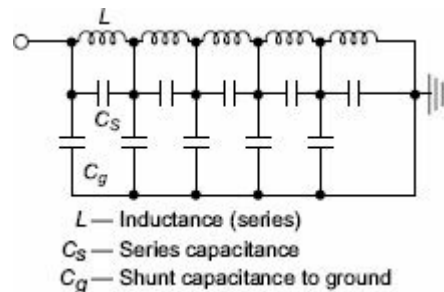


Fig. 10.11 Equivalent circuit of transformer winding for impulses

In addition to the verification of dielectric strength of transformer insulation, impulse tests indicate the quality of insulation, processing and workmanship.

Impulse testing of transformers is done using both the full wave and the chopped wave of the standard impulse, produced by a rod gap with a chopping time of 3 to 6 μs . To prevent large overvoltages being induced in the windings not under test, they are short circuited and connected to the ground. But the short circuiting reduces the impedance of the transformer and hence poses problems in adjusting the standard wave shape of the impulse generators. It also reduces the sensitivity of detection.

(a) Procedure for Impulse Testing

The schematic diagram of the transformer connection for impulse testing is shown in [Fig. 10.12a](#), and the waveshapes of the full and chopped waves are shown in [Fig. 10.13](#). In transformer testing it is essential to record the waveforms of the applied voltage and current through the windings under test. Sometimes, the transferred voltage in the secondary and the neutral current are also recorded. Measurement locations are shown in [Fig. 10.12b](#).

Impulse testing is done in the following sequence:

- (i) applying impulse voltage of magnitude 75% of the Basic Impulse Level (BIL) of the transformer under test, to establish pattern of reference waveforms,
- (ii) one full wave voltage of 100% BIL,
- (iii) two chopped waves of 100% BIL,
- (iv) one full wave of 100% BIL, and
- (v) one full wave of 75% BIL.

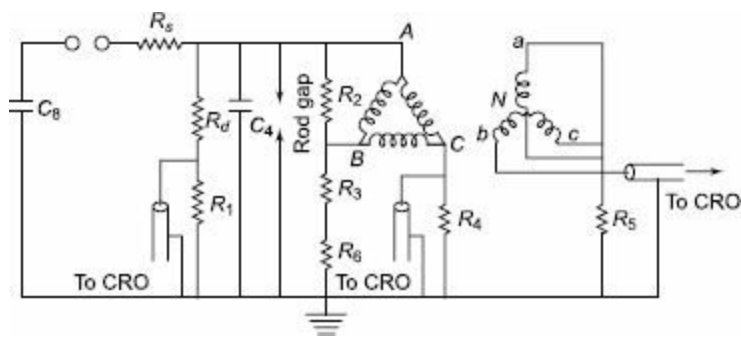


Fig. 10.12a Arrangement of transformer for impulse testing

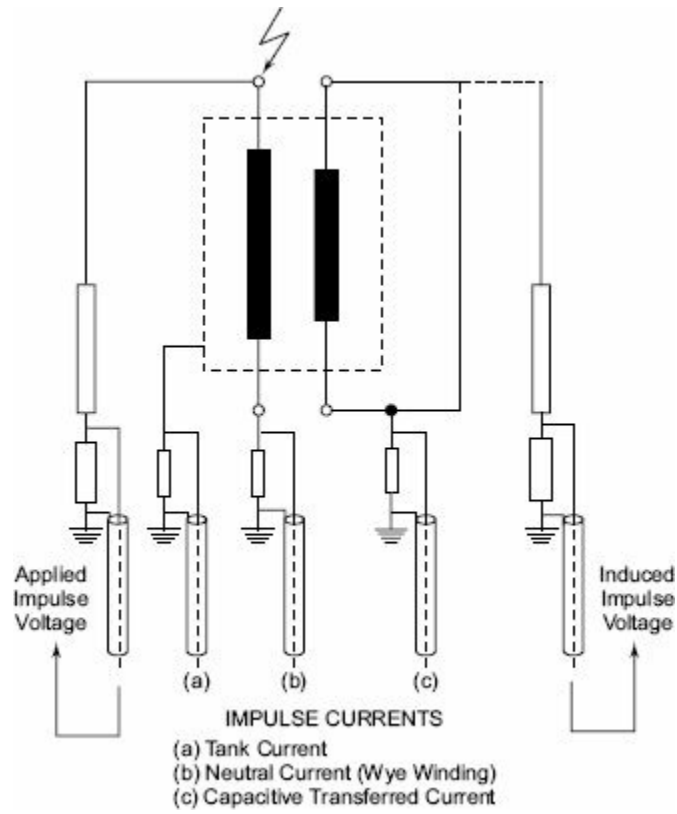


Fig. 10.12b Measurement locations for impulse testing of transformers

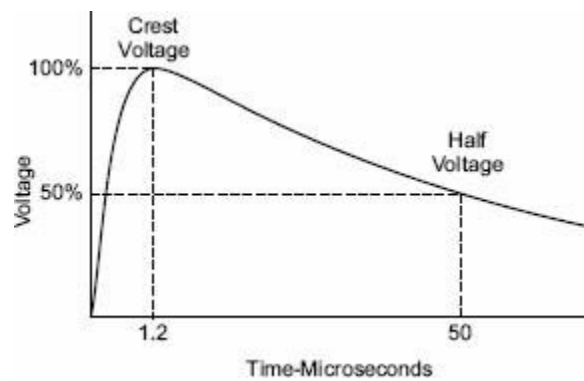


Fig. 10.13a Standard Lightning impulse full wave

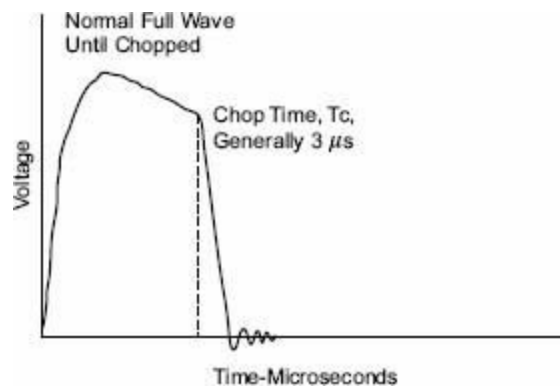


Fig. 10.13b *Standard Lightning impulse chopped wave*

It is very important to see that the grounding is proper and the windings not under test are suitably terminated.

Generally, impulse tests are made on line terminal of the winding, one terminal at a time.

Switching Impulse Tests Switching impulses or surges occur in a power system due to switching operations fault clearing, etc. (see Sec. 8.22). These are relatively long-duration impulses with rise time 0.1 to 0.3 ms and total duration more than 1 ms. Transformer windings are tested for switching impulses of suitable magnitude as given by SIL. These can induce high peak values of voltages in other windings and can drive the core into saturation. This is avoided by reversing the polarity of the applied wave between successive applications. Failure during switching impulse tests are usually clearly visible in oscillograms and also by loud noise produced and external flashovers.

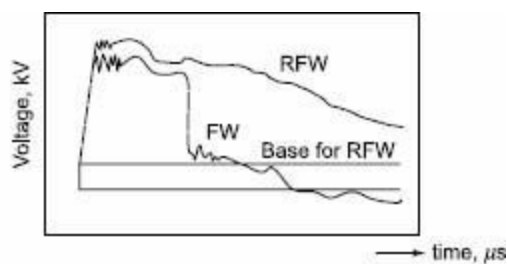
(b) Detection and Location of Fault during Impulse Testing

The fault in a transformer insulation is located in impulse tests by any one of the following methods.

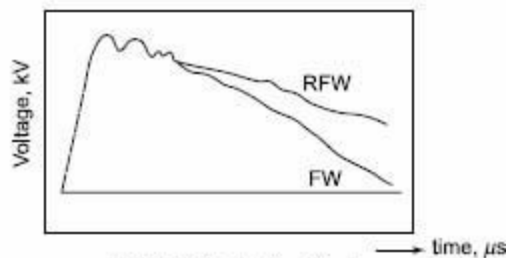
(i) **General Observations** The fault can be located by general observations like noise in the tank or smoke or bubbles in breather.

(ii) **Voltage Oscillogram Method** Fault or failure appears as a partial or complete collapse of the applied voltage wave. Figure 10.14 gives the typical waveform. The sensitivity of this method is low and does not detect faults which occur on less than 5% of the winding.

(iii) **Neutral Current Method** In the neutral current method, a record of the impulse current flowing through a resistive shunt between the neutral and ground point is used for detecting the fault. The neutral current oscillogram consists of a high-frequency oscillation, a low-frequency disturbance, and a current rise due to reflections from the ground end of the windings. When a fault occurs such as arcing between the turns or from turn to the ground, a train of high frequency pulses similar to that in the front of the impulse current wave are observed in the oscillogram and the waveshape changes. If the fault is local, like a partial discharge, only high-frequency oscillations are observed without a change of waveshape. The sensitivity of the method decreases, if other windings not under test are grounded.



(a) Failure from the line lead to ground through oil



(b) 8.5% of winding failed

RFW — Reduced full wave
FW — Full wave

Fig. 10.14 Voltage oscillograms of transformer winding with a fault

(iv) *Transferred Surge Current Method* In this method, the voltage across a resistive shunt connected between the low-voltage winding and the ground is used for fault location. A short high-frequency discharge oscillation is capacitively transferred at the event of failure and is recorded. Hence, faults at a further distance from the neutral are also clearly located. The waveshape is distorted depending on the location and type of fault, and hence can be more clearly detected.

After the location of the fault, the type of fault can be observed by dismantling the winding and looking for charred insulation or melted parts on the copper winding. This is successful in the case of major faults. Local faults or partial discharges are self healing and escape observation.

Nowadays digital recorders are used to record the waveforms and analysis is made through digital computers waveform analysis using the frequency dependance of transformer impedance known as '**Transfer function**' method.

The **transfer function** or (admittance) is the ratio of Fourier transform of the current waveform recorded to that of voltage waveform applied and is written as $\frac{I(j\omega)}{V(j\omega)}$. Each type of fault, like turn to turn, or turn to ground failure at different locations on the winding gives a different frequency spectrum and hence the fault can be easily detected.

10.5 TESTING OF SURGE ARRESTERS

10.5.1 Introduction

In modern practices, surge arrester or lightning arresters are the most reliable apparatus to protect the power system against transient voltages due to lightning and switching surges. They are invariably used from distribution voltages (400 V) to highest system transmission voltages of 765 kV or above. Hence, testing them precisely in standard laboratories with standard test procedures are of great importance in modern power system practice.

A surge arrester has to be a non-conductor for operating power frequency voltages. It should behave as a short circuit for transient overvoltages of impulse character, discharge the heavy current, and recover its insulation without allowing the follow-up of the power frequency current.

In [Table 10.1](#), the impulse current ratings of the surge arresters in relation to their voltage are given, and the testing is usually done at these current ratings.

Table 10.1 Surge diverter voltage and current ratings

<i>Diverter class</i>	<i>Diverter rating</i>	<i>Impulse current rating (8/20 μ s)</i> <i>(Amperes)</i>	<i>High current rating (4/10 μ s)</i> <i>(Amperes)</i>	<i>Long duration rating—duration is given in μ s</i> <i>(Amperes)</i>
A	Low voltage (230 V to 600 V)	1500 2500	10,000 25,000	50 (500 μ s)
B	Distribution voltages (400 V to 33 kV)	5000	65,000	75 (1000 μ s)
C	Station type lightning arresters (11 kV and above)	10,000	100,000	150 (2000 μ s)

10.5.2 Tests on Surge Arresters

(a) **Power Frequency Sparkover Test** This is routine test. This test is conducted using a series resistance to limit the current in case a sparkover occurs. The arrester has to withstand at least 1.5 times the rated value of the voltage for five successive applications. The test is generally done under dry and wet conditions also.

(b) **Hundred per cent Standard Impulse Sparkover Test** This test is conducted to ensure that the diverter operates positively when overvoltages of impulse nature occur. The impulse generator is adjusted to give the standard impulse voltage of a preset magnitude specified in the specifications. The arrester has to sparkover every time in each of the ten successive applications. The test is done with both positive and negative polarity waveforms. Sometimes, the test is done by starting at a voltage level that does not give flashover at all, and is repeated in increasing steps of voltage till hundred per cent flashover occurs. The magnitude of the voltage at which hundred per cent flashover occurs is the required sparkover voltage.

(c) **Front of Wave Sparkover Test** In order to ensure that the surge arrester flashes over for very steep fronted waves of high peaks, this test is conducted using an overvoltage having a rate of rise of 100 kV/ μ s, per 12 kV of the rating. The estimated maximum steepness of the waves are specified in standards and specifications. The test is done by conducting hundred per cent sparkover voltage test for increasing magnitudes of the standard impulse wave. The time to sparkover is measured. The volt-time characteristic of the arrester is plotted, and the intersection of the V-t characteristic and the line with slope of the virtual steepness of the front gives the front of a wave sparkover voltage.

(d) **Residual Voltage Test** This test is conducted on pro-rated diverters of ratings in the range 3 to 12 kV only. The voltage developed across the Non-Linear Resistor units (NLR) during the flow of surge currents through the arrester is called the 'residual voltage'. (A pro-rated arrester is a complete, suitably housed section of an arrester including series gaps and non-linear series resistors in the same proportion as in the complete arrester.) Standard impulse currents of the rated magnitudes are applied, and the voltage developed across the diverter is recorded using a suitable voltage divider and a CRO. The magnitudes of the currents are approximately 0.5, 1.0, and 2.0 times the rated currents. From the oscillogram, a graph is drawn between the current magnitudes and the voltage developed across the diverter prorated unit. From the graph, the residual voltage corresponding to the exact rated current is obtained.

Let V_1 = rating of the complete unit,

V_2 = rating of the pro-rated unit tested,

V_{R1} = residual voltage of the complete unit, and

V_{R2} = residual voltage of the pro-rated unit.

Then, it is assumed that

$$\frac{V_1}{V_2} = \frac{V_{R1}}{V_{R2}}$$

Let V_{RM} be the maximum permissible residual voltage for the complete unit. The ratio $V_{RM}/V_1 = r$, is defined as a multiplying factor of the rating for the residual voltage test, which depends on V_1 . The 'diverter' is said to pass the test, if

$$V_{R2} < rV_2$$

10.5.3 High-Current Impulse Test on Surge Arresters

This test is also done on pro-rated arrester units in the range of 3 to 12 kV. A high current impulse wave of $4/10 \mu s$ of peak value mentioned in the specifications is applied to a spare unit of identical characteristics. Two such applications are done on the units under test, allowing sufficient time for the cooling of the unit to the room temperature. The unit is said to pass the test, if the

- (i) power frequency sparkover voltage before and after the test does not differ by more than 10%,
- (ii) voltage and current waveforms of the diverter do not differ significantly in the two applications, and
- (iii) non-linear resistance elements in the diverter do not show any sign of puncture or external flashover.

(a) **Long Duration Impulse Current Test** This test is also done on prorated units of 3 to 12 kV. The circuit used for generating a rectangular impulse wave consists of an artificial transmission line with lumped inductances and capacitances. The duration of the current pulse t is given by $2(n - 1)\sqrt{LC}$, where n is the number of stages or sections used, and L and C are the inductance and capacitance of each unit. Rectangular wave is generated, if the surge impedance of the diverter is equal to $\sqrt{L/C}$ at the test current. As per the specifications, 20 applications are made with specified current in five groups. The interval between the successive applications is about 1 min. It is usual to record the waveforms in the first two and the last two applications of the current wave. The diverter is said to have passed the test, if

- (i) the power frequency sparkover voltage before and after the application of the current wave does not differ by 10%,
- (ii) The voltage across the arrester at the first and the last application does not differ by more than 8%, and
- (iii) there is no sign of puncture or other damage.

(b) **Operating Duty Cycle Test** This test is conducted on pro-rated units of arrester and gives better closeness to actual conditions. The arrester is kept energized at its rated power frequency supply voltage. The rated impulse current wave is applied first at a phase angle of about 30° from the ac voltage zero. If the power frequency follow-on current is not established, the angle at which current wave is applied is advanced in steps of 10° up to 90° or the peak position of the supply voltage wave till the follow-on current is established. In the course of application of the current wave, if the power frequency voltage is reduced during the flow of current, it can be compensated up to a maximum of 10% of the overvoltage. During the follow-on current period, the peak voltage across the diverter should be less than or equal to the rated peak voltage. Twenty applications of the impulse current at the selected points on the voltage wave are made in four groups. The time interval between each application is about 1 min, and between successive groups it is about half an hour. The arrester is said to have passed the test, if

- (i) the average power frequency sparkover voltage before and after the test does not differ by more than 10%,
- (ii) the residual voltage at the rated current does not vary by more than 10%,
- (iii) the follow-on power frequency current is interrupted each time, and

(iv) no significant change, signs of flashover, or puncture occurs to the prorated unit.

(c) **Other Tests** The other tests that are normally conducted on surge arresters are

- (i) mechanical tests like porosity test, temperature cycle tests, and others,
- (ii) pressure relief test,
- (iii) the voltage withstand test on the insulator housing of the diverter,
- (iv) the switching surge flashover test, and
- (v) the pollution tests.

These tests are usually done on diverters used on Extra High Voltage (EHV) systems.

10.6 RADIO INTERFERENCE MEASUREMENTS

10.6.1 Introduction

Many electrical apparatuses like transformers, line conductors, rotating machines, etc. produce unwanted electrical signals in the radio and high-frequency (television band, microwave bands, etc.) ranges. These signals arise due to corona discharges in air, internal or partial discharges in the insulation, sparking at commutators and brush gear in rotating machines, etc. It is important to see that the noise voltages generated in the radio and other transmission bands are limited to acceptable levels, and hence the radio interference voltage measurements are of importance. It has been found that the surface conditions of the overhead conductors subjected to high-voltage stresses and varying atmospheric conditions greatly influence the magnitude of the noise voltage produced. In case of solid insulators, the bonding between the porcelain and the metal pin, the binding of high voltage conductor and the insulator surface, and the surface pollution were found to be the sources of this noise.

10.6.2 Measurements of Radio Interference Voltage

The noise generated in the radio frequency band as a result of corona or partial discharges in high-voltage power apparatus may be measured

- (i) by the radio frequency line to ground voltage known as the radio influence voltage or RIV, and
- (ii) as an interfering field by means of an antenna known as the radiated radio interference voltage or RI.

Normally, the tests and measurements done in the laboratories are RIV measurements, whereas field investigations with portable radio receivers are RI measurements.

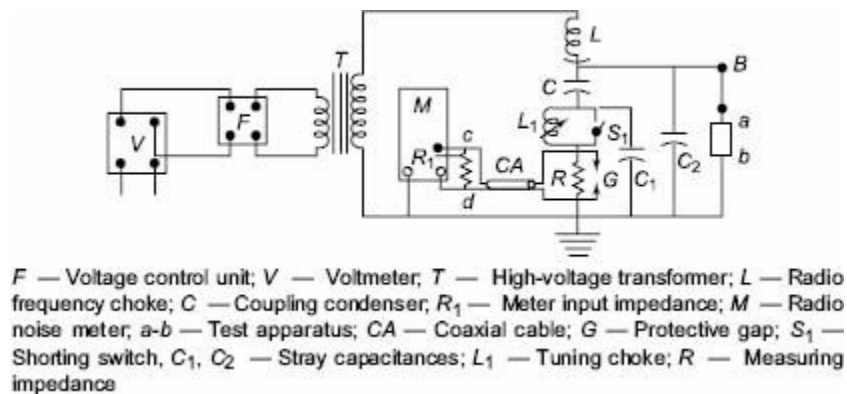


Fig. 10.15 Schematic diagram of circuit for the measurement of RIV of a high-voltage apparatus in 150 kHz to 30 MHz frequency range

A radio noise meter used in the laboratory consists of a portable radio receiver with a local oscillator, a radio frequency amplifier, a mixer, an intermediate frequency amplifier, and a detector similar to that of a standard radio receiver and operates in the frequency range 150 kHz to 30 MHz. In addition, the radio noise meter has multi-input circuits to accommodate a number of pick-up devices, attenuators, calibrators, and output circuits containing special detectors and meters. The detector circuit consists of a diode detector in series with a series resistance R_s , charging a parallel R - C circuit. The detector circuit is provided with a measuring device to measure either (a) the average value, (b) the peak value, or (c) quasi-peak value (the quasi-peak value of the impulse noise is equal to the rms value of the sine wave at the centre frequency of the passband which produces the same deflection in the meter scale as that of the impulse). The voltmeter provided at the end of the detector has an input impedance of 50 to 75 Ω .

10.6.3 Test Circuits for the Measurements

The schematic circuits used for RIV measurements are shown in [Figs 10.15](#), [10.16](#) and [10.17](#). The RIV meter is first calibrated as per standards. The important components of the circuits are the following:

- (i) The ratio frequency choke to limit the loss of the RIV voltage and to conduct energy from the sample. The choke itself should be free from noise, and its impedance should be less than 1500Ω .
- (ii) The coupling capacitor C ($< 0.001 \mu\text{F}$); it should be free from noise in the operating range and the resistance of R should be equal to 800Ω . The value indicated by the meter gives the conducted radio noise from the test sample.
- (iii) Coaxial cable (CA): A coaxial cable of characteristic impedance 185Ω shall be connected between the resistance R and the radio noise meter.

When the radio noise meter measurements are stated, the information regarding the specifications of the meter used, the frequency range of measurements, the band pass characteristics, and the open circuit and the detector characteristics have to be mentioned.

Nowadays, for transmission systems of 400 kV and above, radio noise voltages are of importance, and corrective measures are to be adopted for various apparatus and hardware to minimize the radio and television band noise.

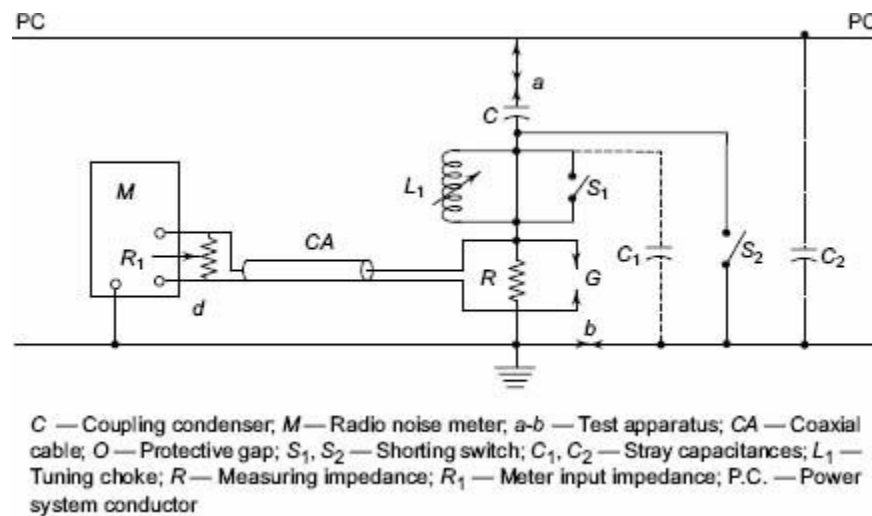


Fig. 10.16 Circuit for measurement of RIV from the conductors of an energized system

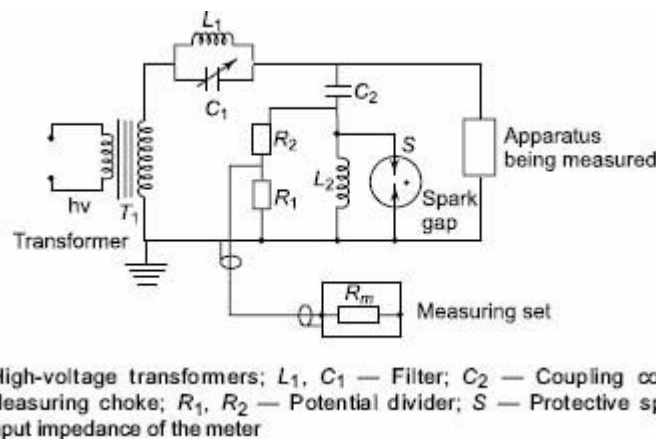


Fig. 10.17 Circuit for RIV measurement as given by British standards

10.7 TESTING OF HVDC VALVES AND EQUIPMENT

High-voltage direct-current transmission line equipment and valves require both dc, ac as well as impulse voltage testing. Since turning on and turning off of a dc valve is very fast, fast transient voltage testing is also required. Equipment is usually tested according to IEC 60700-1 or any other relevant specifications.

Testing of HVDC valves involve

- HVDC overvoltage tests of either polarity or polarity reversal tests
- Power frequency overvoltage testing
- Partial discharge measurements and testing
- Impulse testing with standard lightning impulses and short-duration fast transients (1/5 μ s waves)

Operational testing involves an in-house back-to-back testing with one six-pulse bridge acting as a rectifier and the other bridge as an inverter in a 12-pulse unit. This test ensures that appropriate test conditions are obtained. Sometimes high-angle (large firing angle $\alpha > 30^\circ$ and extinction angle $\gamma > 30^\circ$) testing also is done to ensure increase in flexibility in meeting reactive power demands.

High-voltage dielectric tests on valve structure and insulation:

- The dc corona voltage test
- Switching and lightning impulse tests

Tests on valves:

- The dc and ac withstand voltage tests
- Switching and lightning impulse voltage tests
- Fast transient, i.e. steep-front impulse voltage tests
- Non-periodic firing tests
- Back-to-back tests

All the above tests ensure and verify that sufficient and effective insulation is provided for internal over-voltages that occur and partial discharges do not occur under normal operating conditions.

10.7.1 Back-to-Back Tests on Thyristor Valves

Modern high-power thyristor valve bridges are designed for very high power (≈ 1000 MW) or more and require very large power for testing. Since the test facilities have only limited power sources available, the thyristor valve bridges are tested for their performance making one bridge the rectifier and the other, the inverter and controlling them with an auxiliary set of valves. The schematic diagram of the test circuit is shown in [Fig. 10.18](#).

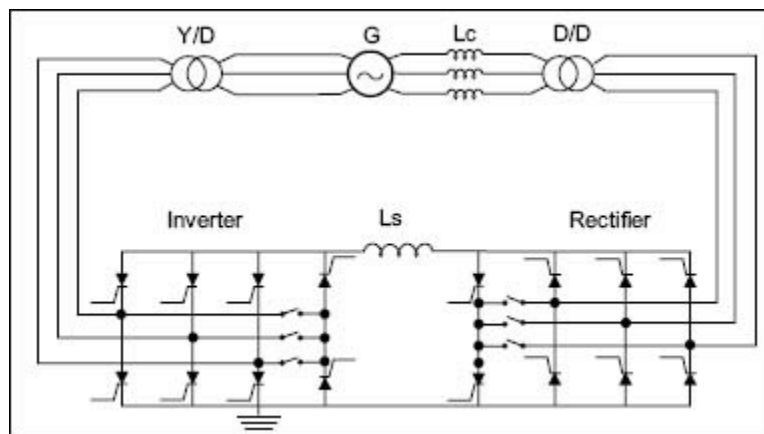


Fig. 10.18 Conventional six-pulse back-to-back test circuit

In the test set-up, the circuit naturally produces voltage and current waveforms which are almost identical with that of normal operation. The source has to only supply the losses. The circuit has the superiority that real-time interaction with valve control system is obtained. A general method is to test one section of the valve per test set-up for more accurate test stress reproduction. The voltage and current for the test section are

$$I_{\text{test}} = 1.05I_d, V_{\text{test}} = 1.1(N_{\text{test}}/N_{\text{normal}})V_d$$

where I_d and V_d are maximum steady-state current and voltage of the converter and N_{test} and N_{normal} are the number of thyristors per test section and number of thyristors per valve.

Typical line test current and voltage waveforms are shown in [Fig. 10.18a](#)

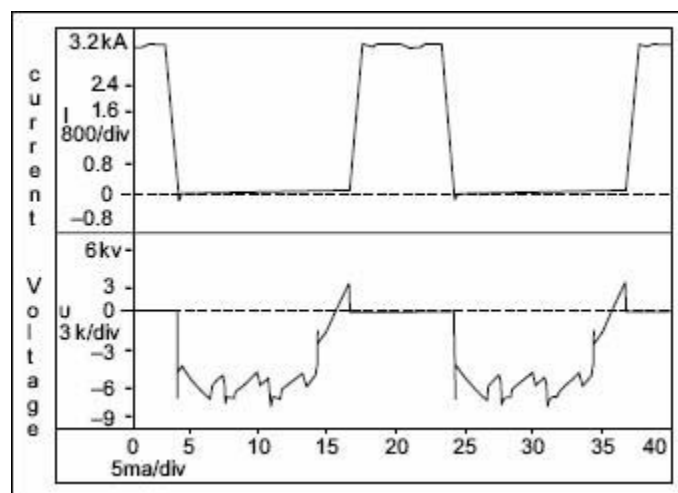


Fig. 10.18a Thyristor current and voltage in a six-pulse back-to-back test circuit

10.7.2 Synthetic Testing of HVDC Valves

In order to ensure proper operation and performance, synthetic testing is done on HVDC valves. Schematic diagram of a test circuit is shown in [Fig. 10.19](#).

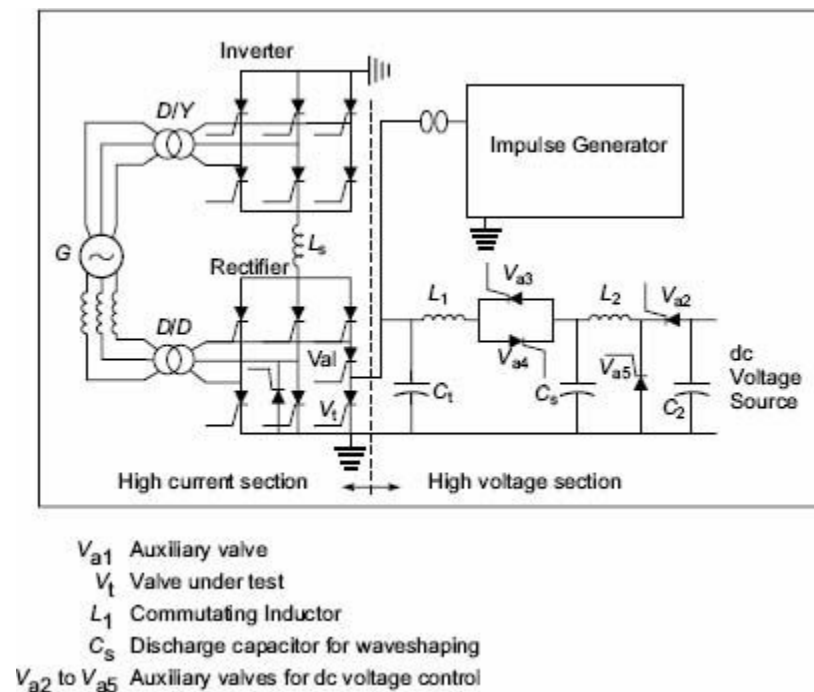


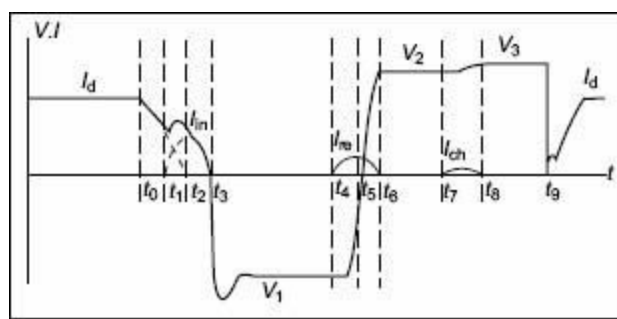
Fig. 10.19 Schematic circuit diagram of synthetic test circuit on thyristor valves

The test circuit consists of mainly two sections: (a) high-voltage, and (b) high-current sections. Out of the two sections of a 12-pulse converter, one section, i.e. one six-pulse converter, is operated as a rectifier while the other one is operated as an inverter and are connected back to back through an inductor L_s which represents the *dc* line inductance while L_1 is for commutation inductance. C_t represents that stray capacitance of the converter circuits.

(a) Test-Circuit Description The current section, i.e. the two six-pulse converter valve units operate almost at the short-circuit capacity of the unit. The auxiliary valve V_{a1} , which controls the current, and the test valve V_t are connected in one arm of the rectifier unit. A low bridge voltage is used as the current source, and hence a low commutation inductance is needed to keep the correct commutation overlap. The current source has enough rating to give the desired short-circuit current.

The voltage section consists of a *dc* rectifier unit of comparatively low current rating, a capacitor C_s , two reactors L_1 and L_2 , the auxiliary valves V_{a2} to V_{a5} . The *dc* source can be continuously varied and adjusted. Forward and reverse voltages are generated by firing the auxiliary valves V_{a3} or V_{a4} at specific instance. The impulse generator is also connected to the high-voltage test valve when transient voltage testing is done during the recovery period.

(b) Operation of the Synthetic Testing Circuit As the arm of the rectifier section of the bridge is made to conduct, both valves V_{a1} and V_t conduct representing the test or desired current. The current source has a low driving voltage. Typical operation and test cycle is shown in [Fig. 10.20](#).



I_d	Test current
V_1	Reverse voltage
V_2, V_3	Forward voltage
i_{inj}	Injected current from voltage source
i_{re}	Reverse current as V_1 changes to V_2

Fig. 10.20 Current and voltage relationship on the test object

Just before the load current I_d from the current source reaches zero value ($t_0 - t_2$ period), the residual charge from the capacitor bank C_s is released by making V_{a3} conduct at t_1 . The injected current from the high-voltage source extinguishes the valve V_{a1} at t_2 and isolates the current source until the firing of V_{a1} is done in the next cycle or period. V_1 conducts the injection current only for about $600 \mu s$ after the main current zero. The injected current is of sinusoidal nature. C_s and L_1 are selected such that the half-wave injection time $t_1 - t_3$ is equal to or higher than $600 \mu s$. V_t blocks at the injected voltage current zero. The pre-charged voltage on C_s together with L_1 will give a close representation of the normal operating current in the interval of about $200 \mu s$ before the current zero (t_3). The voltage on C_s has been reversed to a value V_1 after the half-wave injected current. The reverse voltage charges C_1 through the loop $C_s - V_{a4} - L_1 - C_t$ by firing V_{a4} to form transient recovery voltage and reverse recovery voltage. V_{a5} and V_{a3} are fired at t_4 after the transient recovery voltage is damped out to reverse the voltage on C_s . The voltage applied on C_1 and V_t change its polarity correspondingly from V_1 to V_2 during t_4 to t_6 . V_{a2} is fired at t_7 in order to allow current I_{ch} from dc voltage source to compensate for the voltage drop on C_s . V_{a2} is blocked by reversing the oscillating current after C_s is fully compensated at t_8 . V_t is fired at t_9 from forward voltage V_3 . The capacitor C_s will then discharge through V_t to produce inrush current as in normal operation. Firing of V_t will cause reduction in voltage so that current source is applied on V_{a1} . This entire cycle completes the different on and off switching operations that take place. The synthetic testing will satisfactorily test the operation performance of the following test conditions. Typical test circuit current-voltage waveforms are shown in [Fig. 10.21](#).

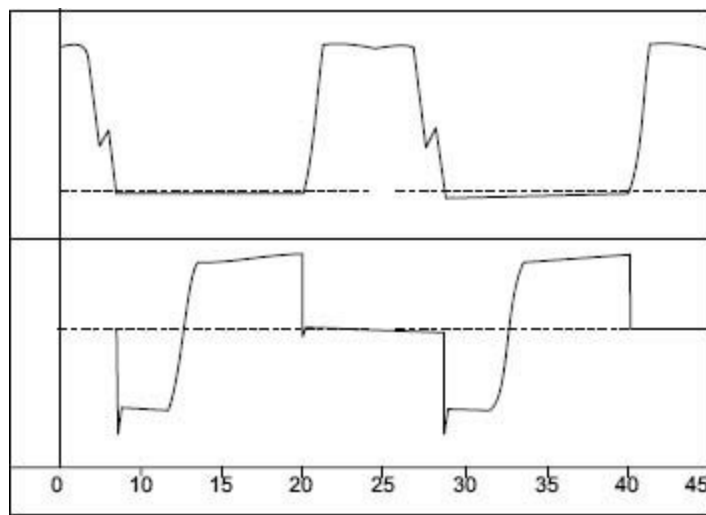


Fig. 10.21 Synthetic test circuit: current and voltage waveforms in periodic and extinction tests

Different tests done with synthetic test circuit are

- Heat run test and protective firing
- Maximum temporary operating duty test at $\alpha = 90^\circ$
- Intermittent direct current test
- Transient forward voltage during recovery period
- One-loop fault current test with reapplied forward voltage
- Three-loop fault current test with reapplied forward voltage

Synthetic tests have the advantage that both overvoltage and fault (overload) current performance can be evaluated.

Transient voltage performance for fast transients is also checked. But synthetic test produces a prolonged commutation time at turn-off due to injection current from the voltage source and also extra conduction losses.

K
T E R M S
Y

- Testing of Electrical Apparatus
- Power Frequency ac Tests
- Impulse Tests
- Testing of Insulators
- Bushings
- Cables
- Capacitors
- Short Circuit Testing of CBs
- Transformers
- Surge Arresters
- RIV Measurements

MULTIPLE-CHOICE QUESTIONS

1. Fifty per cent flashover voltage is defined as
 - (a) the voltage at which the flashover probability is 0.5

- (b) the voltage at which corona discharge appears before flashover
- (c) the voltage at which the flashover occurs alternately when applied several times
- (d) the average value of withstand voltage and flashover voltage.

2. Standard atmospheric condition as per Indian Standard Specifications are

- (a) temp = 27°C, pressure = 1013 millibans and humidity = 17 gms/m³
- (b) temp = 20°C, pressure = 1013 millibans and humidity = 11 gms/m³
- (c) temp = 27°C, pressure = 1013 millibans and humidity = 11 gms/m³
- (d) temp = 27°C, pressure = 1000 millibans and humidity = 17 gms/m³.

3. In wet flashover tests, the conductivity of water used is

- (a) 10 ± 1.5 μ Siemens
- (b) 100 ± 15 μ Siemens at ambient temperature
- (c) 45 ± 10 μ Siemens at room temperature
- (d) < 1.0 μ Siemens at 27°C.

4. Most important tests conducted on isolators and circuit breakers are

- (a) voltage withstand tests
- (b) short circuit tests
- (c) high current tests
- (d) temperature rise tests.

5. Fault location in an HV cable is done by

- (a) voltage withstand test
- (b) partial discharge scanning tests
- (c) life tests
- (d) impulse testing

6. In impulse testing of transformers fault location is usually done by

- (a) neutral current oscillogram
- (b) chopped wave oscillogram
- (c) observing for noise or smoke
- (d) scanning method

7. The most important test to assert the proper functions of a surge divertor is

- (a) 100% impulse withstand test
- (b) front of wave spark over and residual voltage tests
- (c) impulse current test
- (d) pollution tests

8. The salt-fog test done on insulators is

- (a) impulse test
- (b) power frequency pollution test
- (c) impulse current test
- (d) switching surge test

9. C- tan δ test on electric bushings is done using

- (a) impulse generator
- (b) high voltage Schering bridge
- (c) power frequency cascade transformer unit
- (d) resonant transformer

10. In C- tan δ test, a steep increase in tan δ, when the applied voltage increases from 100% to 110%

indicates.

- (a) insulation is failing
- (b) presence of an internal discharge
- (c) increase in relative permittivity
- (d) decrease in insulation resistance

1. Impulse testing of transformers indicates
 - (a) winding to ground insulation strength
 - (b) winding to winding insulation strength
 - (c) dielectric strength, quantity of insulation and processing
 - (d) induced voltages in other windings during transients
2. A better method to detect fault during impulse testing is to
 - (a) observe the windings after tests
 - (b) record more number of test oscillograms of currents and voltages
 - (c) use digital recording of waveforms
 - (d) analyse the waveforms using waveform analysis techniques such as transfer function techniques
3. Switching impulse tests on UHV and EHV transformers can result in
 - (a) failure of transformer windings
 - (b) Induce high voltages in other windings
 - (c) drive the transformer core the saturation
 - (d) both c and b
4. RIV tests on transmission line hard ware is done to
 - (a) determine the induced noise due to corona
 - (b) interfering electric field in the neighborhood of power lines.
 - (c) high frequency signals induced in power lines
 - (d) determine or measure noise generated in radio frequency range due to corona or partial discharges
5. A high-voltage dielectric test done on HVDC valves is
 - (a) dc corona test
 - (b) synthetic test
 - (c) fast transient or steep fronted impulse test
 - (d) back-to-back test

Answers to Multiple-Choice Questions

- | | | | | | |
|---------|---------|---------|---------|---------|---------|
| 1. (a) | 2. (c) | 3. (b) | 4. (b) | 5. (b) | 6. (a) |
| 7. (b) | 8. (b) | 9. (b) | 10. (b) | 11. (c) | 12. (d) |
| 13. (d) | 14. (d) | 15. (c) | | | |

REVIEW QUESTIONS

1. Explain the terms (a) withstand voltage, (b) flashover voltage, (c) 50% flashover voltage, and (d) wet and dry power frequency tests as referred to high voltage testing.
2. What are the different power frequency tests done on insulators? Mention the procedure for testing.
3. What is the significance of impulse tests? Briefly explain the impulse testing of insulators.
4. What are the significances of power factor tests and partial discharge tests on bushings? How

are they conducted in the laboratory?

5. Mention the different electrical tests done on isolators and circuit breakers.
6. Why is synthetic testing advantageous over the other testing methods for short circuit tests? Give the layout for synthetic testing.
7. Explain the partial discharge tests on high-voltage cables. How is a fault in the insulation located in this test?
8. Explain the method of impulse testing of high voltage transformers. What is the procedure adopted for locating the failure?
9. What is an operating duty cycle test on a surge arrester? Why is it more significant than other tests?
10. Explain the importance of RIV measurements for EHV power apparatus.
11. Explain, with a schematic diagram, one method of measuring RIV of transmission line hardware.
12. What are the different high-voltage tests done on HVDC power apparatus?
13. Explain briefly the different tests done on HVDC valves.
14. What is a back-to-back test on HVDC valve unit? How and why is it done?
15. Give the synthetic testing procedure on valve units in HVDC systems. What are the different tests done using synthetic test circuit?

REFERENCES

1. Kreuger, F.H., *Discharge Detection in H.V. Equipment*, Haywood London (1964).
2. Ely, C.H.A. and Lambeth, P.J., "Artificial pollution test for H.V. outdoor insulators", *Proc. I.E.E.* 111, 991 (1964).
3. Clark, C.H.W., "Radio interference from H.V. insulators", *Electrical Review*, 16, 491 (1959).
4. C.I.S.P.R. Publication 1, "R.I.V. measuring apparatus for the frequency range 150 kHz to 30 MHz" (1961).
5. Berlijn, S., Garnacho, F., Gockenbach, E. and Muhr M., *et al.* "Influence of different lighting impulse shapes on the breakdown behaviour of insulating materials-proposal for modification of IEC 60060-1", *ISH Bangalore*, paper 7-2 (2001).
6. Leibfried, T., *et al.* "On-line monitoring of power transformers-trends, new developments and first experiences" *CIGRE Pairs*, paper 12-211 (1998).
7. Lemke, E., Strehl, T. and Rubwurm, D., "New development in the field of PD detection and location in power cables under on-site condition", *ISH London*, paper 5.106.S14 (1999).
8. *IEC-76*, "Power Transformers", Part 1: General, Part 2: Temperature Rise, Part 3: Insulation and Dielectric Tests, and Part 5: Ability to Withstand Short Circuit, (1993).
9. *IEC 76-3-1*, "Power Transformers—External Clearances in Air" (1987, 1993, 1980 and 1976).
10. *IEC 55*, Paper insulated cables (1978).
11. *IEC 55-1* (1978): General-Amendment. 1 (1889).
12. *IEC 55-2* (1981): General and construction requirement-Amendment 1 (1989).
13. *IEC 141*: Tests on oil-filled and gas pressure cables and their accessories.
14. *IEC 183* (1984): Guide to the selection of HV cables-Amendment 1 (1990).
15. *IEC 203* (1966): Impulse tests on cables.
16. *IEC 383* (1983): Tests on insulator of ceramic or glass for overhead lines with voltages greater than 1 kV.
17. *IEC 506* (1975): Switching impulse tests on HV insulators.

18. *IEC 507* (1991): Artificial pollution tests on HV insulators to be used on AC system.
19. *IEC 502*: “Extruded Solid Dielectric Insulated Power Cables (1-30 kV)”, IEC, Geneva, Switzerland, (1991).
20. *IEC 56*: “High Voltage Alternating Current Circuit Breakers”, IEC, Geneva Switzerland, (1987, 1995).
21. *IEC 99-1*: “Non Linear Resistor Type Gapped Surge Arrester for AC Systems” IEC, Geneva Switzerland, (1991).
22. *IEC 694*: “Common Clauses for High Voltage Switchgear and Controlgear Standards”, IEC, Geneva Switzerland, (1980, 1993).
23. *IEC 99*: Surge arrester (SA).
24. *IEC 99-2* (1962): Expulsion type lightning arrester.
25. *IEC 99-3* (1990): Artificial pollution testing of SA.
26. *IEC 99-4* (1991): Metal-oxide SA without gap for AC system. Amendment. 1 (1993).
27. *IEC 427* (1989): Synthetic testing of HV AC circuit breakers Amendment-1 (1992) Amendment-2 (1995).
28. *IEC 137*: “Bushings for Alternating Voltages above 1000 V”, IEC, Geneva Switzerland, (1995).
29. *IEC 282*: “High-Voltage Fuses, Part 1: Current Limiting Fuse, and Part 2: Expulsion and Similar Fuses”, IEC, Geneva Switzerland, (1994 and 1995).
30. *IEEE STD 142-1972*: “IEEE Recommended Practice for Grounding”, 1972.
31. *IEC 80-1* : “Electromagnetic Compatibility for Industrial Process, Measurement and Control Equipment, Part 1: Electrostatic Discharge Requirement”, IEC, Geneva Switzerland, (1991).
32. *IEC 255-22-2*: “Current Relays, Part 22: Electrical Disturbances Tests for Measuring Relays and Protection Equipment, Section Two: Electrostatic Discharge Tests”, IEC, Geneva Switzerland (1989).
33. Ryan, H.M., H.V. Engineering and Testing I.E.T. England 2001.
34. Haddad, M., and Warne, D., (editors), *Advances in High-Voltage Engg.*
35. Sheng, B.L., et.al, *A New Test Facility for Testing HVDC Thyristor Valves*, IEEE PELS Conference, March 2001 (pp 1242–1246)
36. Sheng, B.L., et.al, *Operational Tests of Three Gorges; Chang Zhou, HVDC Thyristor Valves by using Synthetic Tests*, ICPS 2001 Conference, Sept 3rd–5th, 2001 China
37. Sheng, B.L., et.al, *Reliability Assurance of HVDC Thyristor Valves by Rigorous Type Tests*. ABB Power Systems, Ludvika, Sweden
38. *IEC 60700-1: Thyristor Valves for HVDC Power Transmission—Part I*, Electrical Testing
39. *Test Circuits for HVDC Thyristor Valves*, Cigre Technical Brochure 113 (1998)
40. *IEEE Standard 857-1996: IEEE Recommended practice for test procedures for HVDC Thyristor Valves.*

CHAPTER

11

**Design, Planning and Layout of High-Voltage
Laboratories**

11.1 INTRODUCTION

Industrial and economic development in the present world demands the use of more and more electrical energy which has to be transported over long distances in large quantities. Transportation of large amounts of power needs extra high-voltage transmission lines. Elsewhere in the world, transmission lines of 760 kV have come into operation, and transmission lines of ratings of 1200 kV or more are coming into operation in the USA and USSR. Extensive studies are being made in different countries on the possible use of complex extra high-voltage dc systems of ± 500 kV and above.

This very fast development of power systems would be followed by system studies on equipment and service conditions which they have to fulfil. These conditions will also determine the values for test voltages of ac power frequency, impulse, or dc, under specific conditions.

In the early 1970s, 400 kV transmission lines occupied a pride of place for transmission of bulk power in India and elsewhere. A national grid at this voltage having a length of 10,000 km was in operation. By 1980, in India, the situation had changed and there was need for introduction of higher transmission voltage level in the range of 700 kV–1200 kV (Ultra High-Voltage).

High-voltage laboratories are an essential requirement for making acceptance tests for the equipment that go into operation in the extra high-voltage transmission systems. In addition, Ultra High-Voltage (UHV) laboratories were also found essential to plan, design and ensure economical and reliable transmission systems at these voltage levels. They also facilitate carrying out investigations on the lightning and switching impulse voltage behaviour of apparatus designed to operate at these high voltages. Therefore, a new generation of UHV laboratories were built in Canada, USA, Italy, Japan and other countries. India also felt the imperative to develop such a laboratory and one such laboratory became functional in 1994. In the following sections a brief review of the planning and layout of high-voltage and UHV testing laboratories and some problems and limitations of the test techniques are presented.

11.2 TEST FACILITIES PROVIDED IN HIGH-VOLTAGE LABORATORIES

A high voltage laboratory is expected to carry out withstand and/or flashover tests at high-voltages on the following transmission system equipment:

- (i) Transformers
- (ii) Lightning arresters
- (iii) Isolators and circuit breakers
- (iv) Different types of insulators
- (v) Cables
- (vi) Capacitors
- (vii) Line hardware and accessories
- (viii) Other equipment like reactors, etc.

Different tests conducted on the above equipment are:

- (i) Power frequency withstand tests—wet and dry
- (ii) Impulse tests
- (iii) dc withstand tests
- (iv) Switching surge tests
- (v) Tests under polluted atmospheric conditions
- (vi) Partial discharge and RIV measurements
- (vii) High current tests.

Details of some of these tests have already been discussed in [Chapter 10](#). In addition to the above facilities, the laboratories should also have facilities for conducting research on dielectric properties of insulation and insulating materials.

An Ultra High-Voltage Laboratory should serve the long-term requirements of UHV transmission system as well the immediate short-term needs in the operation and strengthening of lower-voltage transmission lines which are presently in use or planned for the near future. In its initial phase it can be used for testing of equipment rated at 400 kV or 525 kV, i.e., insulation strings, transmission towers/lines and hardware, transformers, bushings, disconnectors and metalclad switchgear for ac/dc type testing. In addition to the above, the following test programs and research activities are carried out in an UHV laboratory.

11.3 ACTIVITIES AND STUDIES IN HIGH-VOLTAGE AND UHV LABORATORIES

High-voltage laboratories, in addition to conducting tests on equipment, are used for research and development work on the equipment. This includes determination of the safety factor for dielectrics and reliability studies under different atmospheric conditions such as rain, fog, industrial pollution, etc., at voltage higher than the test voltage required. Sometimes, it is required to study problems associated with test lines and other equipment under natural atmospheric or pollution conditions, which cannot be done indoors.

Research activities usually include the following:

- (i) breakdown phenomenon in insulating media such as gases, liquids, solids, or composite systems,
- (ii) withstand voltage on long gaps, surface flashover studies on equipment with special reference to the equipment and materials used in power systems,
- (iii) electrical interference studies due to discharges from equipment operating at high voltages,
- (iv) studies on insulation co-ordination on hv power systems, and
- (v) high current phenomenon such as electric arcs and plasma physics.

The fields of research undertaken in an UHV laboratory are generally related primarily, to the design, development and testing needs of transmission lines having ac system voltages of 765 kV and 1100 kV, and also the needs of equipment testing at this facility. The following principal research areas can be identified:

- Effect of corona and field on the performance of transmission lines
- Performance of air insulation under different voltage stresses using very long gaps
- Performance of line insulators under different weather conditions (temperature, humidity, etc.) and varying pollution conditions
- Performance of conductor bundles which are subjected to aeolian vibrations

Usually, high-voltage laboratories involve tremendous cost. Hence, planning and layout have to be carefully done so that with the testing equipment chosen, the investment is not high and the maximum utility of the laboratory is made.

11.4 CLASSIFICATION OF HIGH-VOLTAGE LABORATORIES

High-voltage laboratories, depending on the purpose for which they are intended and the resources (finances) available, can be classified into four types.

- (i) Small laboratories
- (ii) Medium size laboratories
- (iii) Large general purpose laboratories
- (iv) UHV laboratories

Some salient features of these various types of laboratories are discussed below.

(a) *Small Laboratories* A small laboratory is one that contains dc or power frequency test equipment of less than 10 kW/10 kVA rating and impulse equipment of energy rating of about 10 KJ or less. Voltage ratings can be about 300 kV for ac, single unit or 500 to 600 kV ac for cascade units, ± 200 to 400 kV dc and less than 400 kV impulse voltage. Normally the equipment is meant for housing in a room or hall of size 15 m \times 10 m \times 8 m. Sometimes the equipment ratings are limited such that they can be accommodated in a room having a height of 5 m to 6 m only. Such laboratories are meant for engineering colleges and universities who decide to build such a facility with small resources for doing high-voltage tests or research or for imparting training. In such a case, it is preferable that the engineering college or university associate with a local industry or R and D organization. It is important to device and define the responsibilities of the parties concerned as to how the test facilities and time can be shared. Another idea is to have the university to decide to own the laboratory fully but throw open the facilities of regular technical training and high-voltage testing for the clients. Here, it may be mentioned that many high-voltage problems can be solved by tests at moderate voltage levels. Such laboratories can be built with an investment of 2 to 10 million rupees (at 2000 prices).

(b) *Medium Size Laboratory—An Industrial Laboratory* In case of medium size laboratories, their main function will be for doing routine tests. The demand on future tests and test resources will be known to the same extent as that of the future production targets. Careful planning of such laboratories should include (i) ground transport, (ii) handling equipment like cranes etc., (iii) rationalization of test procedures by making instruments easily accessible, and (iv) providing room for the possibility of increasing the maximum voltage rating etc. Such a laboratory may initially contain a power frequency testing facility in the range of 200 to 600 kV depending on the ratings and the size of the equipment being manufactured and proposed to be tested, such as cables, transformers, etc., but its kVA rating will be much higher (100 to 1000 kVA). The impulse voltage generator required would have a rating of 20 to 100 kJ or more. Other test equipments like the impulse current generator for testing surge arresters and dc test facilities for testing cables and capacitors can also be made available. In industrial laboratories not much emphasis is generally given for undertaking research work and little flexibility may be available for incorporating new equipments.

(c) *Large Size Laboratories* This type of laboratories are meant to carryout testing and undertake research work as envisaged in Secs 11.2 and 11.3 and will contain almost all high voltage and high current test equipments and facilities. The basic facilities available will be

- (i) One or more hv test halls,

- (ii) Corona and pollution test chambers,
- (iii) Outdoor test area for tests on large sized equipment, transmission lines and towers, etc.,
- (iv) Controlled atmospheric test rooms/chambers,
- (v) Computer facilities, conference halls, library etc. with good office facilities, and
- (vi) Provision for overnight tests and stay.

The size and ratings of the test equipment will be quite large and are dealt with in the next Sec. 11.5. The building and equipment include the workshop, material handling equipment like cranes, ladders, air cushion platforms etc. and large control and electric supply facilities (up to few kVA or MVA). The personnel connected with such a laboratory will include a director or manager, few group leaders, and section heads separately for research, testing, measurements, electronics and computer facilities etc. In addition, there will be supporting staff comprising test engineers, technicians, librarians, office staff and skilled and semi-skilled workmen.

(d) UHV Laboratories UHV laboratories are intended for carrying out tests which help in the basic design of experimental transmission lines of voltage ratings of 765 kV and above and for full scale outdoor testing of conductors and insulation structures. In addition there should be an indoor laboratory for doing basic research. AUHV laboratory should therefore comprise:

- an outdoor experimental line for conducting corona and vibration studies,
- an outdoor corona test cage,
- an erection bay,
- a pollution test chamber, and
- indoor laboratories for basic research.

Typical high-voltage equipment and their ratings are given later, in Sec. 11.5.5 of this chapter. Ratings of equipment may vary in different laboratories depending on the requirements.

11.5 SIZE AND RATINGS OF LARGE SIZE HIGH-VOLTAGE LABORATORIES

As stated earlier, large-size laboratories contain equipment of very high ratings with enough flexibility incorporated. In the following sections, details of the ratings and size of the equipment and their layout are briefly indicated.

1.5.1 Withstand Voltages, Test Voltages and the Rating of Equipment in High-Voltage Laboratories

The ratings and size of test equipment chosen in the hv laboratories depends on the test facilities to be provided. Normally, the design of the laboratories for 230 kV system voltage and below does not pose any problems, but laboratories intended for system voltages of 400 kV and above require special attention.

In [Tables 11.1](#) and [11.2](#), various test voltages for different transmission system voltages are given.

For research and development work, the voltage levels needed are usually about 1.3 times the maximum test voltage needed. Hence, the laboratories intended for different system voltages should have the test voltages as available in [Tables 11.3](#) and [11.4](#).

Table 11.1 Test voltage for equipment (ac systems)

System nominal voltage kV (rms)	Line to ground voltage kV (peak)	Power frequency withstand voltage kV (rms)	Impulse withstand voltage kV (peak)	Switching surge withstand voltage kV (peak)	Pollution test voltage kV (rms)
400	335	530	1425	875	280
525	430	670	1800	1100	330
765	625	960	2300	1350	500
1100	900	1416	2800	1800	700
1500	1220	1920	3500	2200	950

Table 11.2 Test voltages for equipment (dc systems)

Nominal voltage kV	dc withstand voltage kV	Reverse polarity test voltage kV	Impulse withstand voltage kV (peak)	Switching surge withstand voltage kV (peak)	Pollution test voltage kV
±400	800	±600	1350	1000	440
±600	1200	±900	1900	1500	660
±800	1600	±1200	2300	2000	880

From the values given in [Tables 11.3](#) and [11.4](#), one can conclude that laboratories intended for testing and development of equipment for 1000 kV ac systems require test transformers of 1.5 to 2.0 MV, impulse generator rated for 5 to 6 MV, and hv dc rectifiers of 1.2 to 1.5 MV.

Table 11.3 Test voltage required for different system voltages (ac systems)

Nominal voltage kV (rms)	Power frequency voltage kV (rms)	Pollution test voltage kV (rms)	Impulse (voltage) kV (peak)	Switching surge voltage kV (peak)
400	800	300	2400	1150
765	1000	500	3000	1750
1100	1400	700	3700	2300
1500	1900	1000	4600	2800

Table 11.4 Test voltages required for different system voltages (dc systems)

<i>Nominal voltage kV (rms)</i>	<i>dc voltage kV (rms)</i>	<i>Pollution test voltage kV (rms)</i>	<i>Impulse voltage kV (peak)</i>	<i>Switching surge voltage kV (peak)</i>
±400	800	500	1750	1300
±600	1200	700	2500	2000
±800	1600	900	3000	2600

High-voltage laboratories intended for system voltages of 400 kV or less need not go for such super high-voltage rated equipment. The insulation levels for 400 kV system equipment are given below.

- (a) Impulse withstand voltages: Line to Earth = 1425 kV (peak)
 (standard impulse voltage) : Phase to phase = 1640 kV (peak)
- (b) Power frequency withstand One minute dry voltages = 680 kV (rms)
 Momentary dry = 800 kV (rms)
 30 sec. wet = 630 kV (rms)
- Visible corona level = 320 kV (rms)

For the above data it may be concluded that a factor of more than 3 for impulse voltages and a factor of 2 to 2.5 for power frequency voltages (highest line to ground peak voltages) are adopted for system voltages of 400 kV and less. Hence, the rating of the equipment should be at least about 900 kV (rms) for power frequency and 2000 kV (peak) for impulse voltages. The rating of the equipment will be still less, if the laboratories are intended for system voltages of 132 kV or 230 kV and may be arrived at by considering the test voltages required.

11.5.2 Voltage and Power Ratings of Test Equipment

(a) dc Testing Equipment High-voltage dc tests are performed using cascaded rectifiers. Careful consideration is necessary when tests on polluted insulation are to be performed which require currents of 50 to 200 mA, but strong predischage streamers of 0.5 to 1.0 A of milliseconds duration may occur. Hence, the generator must have adequate internal reactance in order to maintain the test voltage without too high a voltage drop. The voltage ratings are given in [Table 11.4](#), and the power rating may vary from a few kW to a few hundred kW.

(b) Power Frequency Testing Equipment It is known that the flashover voltage of an insulator in air or oil or in some fluid depends on the capacitance of the supply system, due to the fact that a voltage drop may not maintain the predischages before breakdown. Hence, a minimum of about 1000 pF or more in parallel with the energized insulator is needed to determine the real flashover or puncture voltage, and the generator has to supply at least 1 A in the case of clean and 5 A in the case of polluted insulator at test voltage on short circuit. Approximate values of the selfcapacitances of different equipments are given below:

Insulators	less than 100 pF
Bushings	100 to 400 pF
Current transformers	200 to 600 pF
Power transformers (1 MVA and above)	1000 to 8000 pF
Cables per 10 m length	1000 to 3000 pF

The output of testing transformer will be given by

$$P = (2 \pi f C) V^2 \times 10^{-9} \text{ kVA}$$

where, f = supply frequency,

C = capacitance in pF, and

V = test voltage at the transformer terminals in kV (rms).

The transformer self-capacitance and the capacitances of various high voltage leads (bushings), etc. should also be included in determining the load capacitance. From the above figures it is implied that the minimum power rating of a 1 MV testing transformer will be about 300 kVA. Usually, the power rating of a testing transformer in kVA (single unit) is approximately taken to be equal to the voltage rating in kV.

(c) Impulse Generators The maximum charging voltage of an impulse voltage generator is given by the stage voltage multiplied by the number of stages. The peak value of the impulse voltage V_s for a standard 1.2/50 μ s wave is

$$V_s = nV_{dc} \left[0.95 - \frac{C_L}{(C_L + C_g)} \right]$$

where, V_{dc} = charging voltage,

n = number of stage in the generator,

C_L = load capacitance, and

C_g = generator capacitance.

For $C_g/C_L \geq 5$, the peak value of the impulse generator output voltage will be approximately $V_s \approx 0.7 nV_{dc}$. In other words, the generator rating has to be at least 1.4 times more than the desired output voltage. The energy rating of the impulse generator at its maximum voltage rating is given by

$$W = \frac{1}{2} C_g V^2 \times 10^{-9} \text{ kJ}$$

where, W = stored energy,

C_g = capacitance of the generator in pF, and

V = total charging voltage in kV.

In order to test transformers which have large capacitance, a minimum of 30,000 to 40,000 pF of generator capacitance is needed. A simple calculation will show that a minimum of 135 kJ is required for a 3 MV impulse generator, if the IEC specification for impulse wave shape is to be maintained. The minimum energy rating of a 6 MV impulse generator will be about 600 kJ. From this it may be concluded that the energy rating in kilojoules may be approximated to be equal to 0.1 times the voltage rating in kV.

There is no problem to pile up a large size capacitance in the form of a number of capacitors and to charge them in parallel and discharge them in series to give the required peak of the standard impulse wave. But many difficulties exist in reducing the internal inductance of the circuit to a minimum to obtain a steep front and to avoid oscillations. As an example, a 4 MV impulse generator test circuit has a length equal to the height of the generator plus twice the distance between the test object and the generator. The overall inductance of such a circuit including the internal inductance of the generator will easily be more than 140 μH . With such a generator, it is impossible to test an object of capacitance of 5000 pF with a front time of 1.2 μs and with less than 5% overshoot. Hence, a very careful design and a very careful consideration of the test circuit only can give the optimum test conditions which are not far from theoretical specifications.

The necessity of rapid change of the test circuit from standard impulse to switching surges requires careful studies for placing of series and parallel resistors when producing switching surges like 100/1000 μs or 200/2000 μs waveform, in which the efficiency of the generator is very much reduced. Also, the front time and the tail time resistors have to be carefully rated, as they have to dissipate larger amounts of energy than in the case of standard impulses.

(d) Other High-Voltage Testing Equipment Usually, the other testing equipment will be available is, (i) impulse current generators for testing lightning arresters, (ii) test facilities for measuring RIV and partial discharges, (iii) sphere gaps for measurement and calibration purposes, and (iv) High-voltage Schering-bridge for dielectric testing. Usually, the impulse current generators are rated between 100 and 250 kA with an energy rating of 50 to 100 kJ. This is more than adequate for testing with lightning stroke currents. Partial discharge and RIV measurements require testing transformers free from internal discharges. The detection equipment should be capable of detecting 0.01 pico coulomb of charge in a test object capacitance of 100 pF and 2 to 3 pico coulombs at 1 μF test capacitance. Therefore, the test transformers should have internal discharges of the same order or less at the specified voltage value. Nowadays, it is possible to design ac testing transformers with necessary shielding, etc. with internal discharges less than 5 pC at 5000 kV.

Where sphere gaps are used, it is important to bestow thought regarding the proper size and space

requirements. Proper attention must be given to (i) type and magnitude of the voltage to be measured, (ii) range of operation keeping in view that the sparking distance is less than 0.5 times the diameter of the spheres, and (iii) space requirements as specified in IS: *1876–1961* and other specifications and IEC 600060 (1989).

11.5.3 Size and Dimensions of the Equipment in High-Voltage Laboratories

High-voltage laboratories may be either (a) indoor type, or (b) outdoor type. The indoor type has the advantage of protection of testing equipment against variable weather conditions, simplicity in design and control of the test equipment, and provision of observation facilities during testing. But outdoor laboratories have the advantage of less cost due to the absence of building cost and the planned facility layout cost. But outdoor test areas have limitations such as (i) absence of lifting and supporting facilities, (ii) climatic conditions which may restrict or impede testing, (iii) reproducibility of results not being guaranteed due to uncontrolled atmospheric conditions, and (iv) artificial and wet test studies which are difficult due to wind variation, etc.

When high-voltage laboratories are planned as indoor laboratories, the following figures fix the dimensions of the laboratories:

- (i) Size of the test equipment for ac, dc, or impulse generators.
- (ii) Distances or clearances between the test object and ground during test conditions and also between all the high voltage terminals and earthed or grounded surroundings such as walls, roofs of buildings, and other test equipment not energized.

In [Table 11.5](#) are given the approximate size and dimensions of the test transformers and impulse generators for different system voltages. The table also gives minimum room to be provided for the equipment.

Regarding clearances, that is, the minimum distance between the high-voltage surfaces and the ground points; they are of utmost importance in high-voltage testing. The approximate working clearances recommended are as follows:

ac power frequency voltages: 200 kV (rms)/m

dc voltages: 275 kV/m

Impulse voltages: 500 kV/m

Table 11.5 Approximate dimensions of testing apparatus and test objects

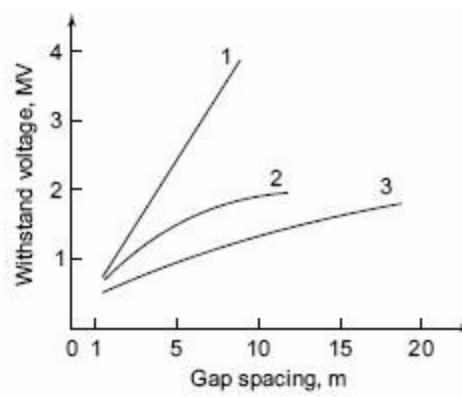
Nominal system Voltage for the equipment kV (rms)	ac test transformer height m	Impulse generator height m	Test-object dimensions (maximum)		
			length m	breadth m	height m
400	10	6	7	2	11
765	15	8	11	2	17
1100	18	12	17	2	24
1500	21	15	28	2	38

For switching surges, the clearance is worked out from the following approximate formula

$$d = (2V)^2$$

where d is in m, and V in MV.

The above clearances are safe, as long as the test voltages do not exceed 1.5 MV for ac and dc voltages and 2.5 MV for impulse and switching surge voltages. For higher voltages, clearances have to be worked out by considering the withstand voltages for rod-plane configuration. The characteristic is given in [Fig. 11.1](#). The necessary distances to the surroundings for switching surges of a long duration will be about 12 m for 760 kV and 30 m for 1500 kV system voltage equipment. Hence, from the above data and from [Fig. 11.1](#) it is evident that the hv laboratories rated for 400 kV and above are practically conditioned by the necessary clearances for switching surge tests.



1. Impulse 1.2/50 ms 50% withstand voltage, positive polarity
2. 50 Hz ac (peak) 50% withstand voltage
3. Switching surge 120/4000 ms 50% withstand voltage, positive polarity

Fig. 11.1 *Withstand voltage of rod-plane configuration (CESI-MILANO)*

11.5.4 Layout of High-Voltage Laboratories

The layout of an hv laboratory is an important aspect for providing an efficient testing facility. Laboratory arrangements differ very much from a single equipment to multi dc, ac, and impulse arrangements in different testing programmes. Each laboratory has to be designed individually considering the type of equipment to be tested, the available space, other accessories needed for the tests, the storage space required, etc. Earthing, control gear, and the safety precautions require most careful consideration.

Laboratory Building The building construction is not critical except where ionization tests are conducted. To minimize the floor loading problems and to simplify earthing arrangement, a ground level location is preferred. The floor should withstand the loading imposed by the equipment and test objects. Arrangements should be made to ensure that the laboratory is free from dust, draught, and excessive humidity. Laboratory windows may require blackout arrangement for visual corona tests, etc. The control room should be located in such a way as to include good overall view of the laboratory and test area. The main access door to the test area must accommodate the test equipment and the test object and have adequate interlocking arrangements and warning systems to ensure safety to the personnel. A typical layout of a high-voltage laboratory accommodating a 1.0 MV ac testing transformer and a 3 MV impulse generator is shown in Fig. 11.2. The dotted circles indicate the clearances necessary.

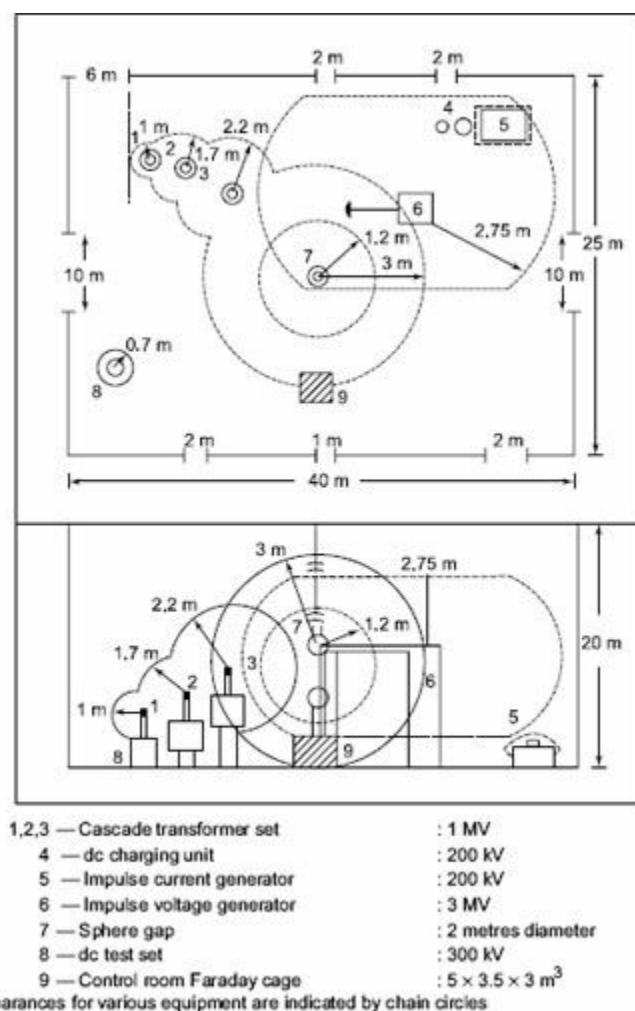


Fig. 11.2 Layout of a typical high-voltage laboratory with a 1 MV cascade transformer and 3 MV impulse generator

11.5.5 Design, Layout and Operation of UHV Laboratory of Central Power Research Institute, Bangalore

(a) Design of the UHV Laboratory UHV Laboratories are designed as indoor laboratories or outdoor laboratories depending on the specific requirements. An indoor laboratory is preferred when most of the equipment testing and associated research work is carried out indoors, whereas outdoor laboratories are preferred when the electrical and mechanical parameters of the UHV transmission lines are to be experimentally determined so that the design of future lines can be based on this data. During the 1980s when the UHV laboratory was planned in India its potential role was widely discussed—the steps involving transmission line ratings beyond 420 kV were 750-765 kV and 1100–1200 kV. There were definite indications that transmission systems at voltages greater than 420 kV would be a reality within the next 15–20 years. Further there were similar laboratories being built in Canada, USA, UK, Italy, Japan, etc. Such a facility was needed in India also to generate test data of breakdown voltages and air clearances which would be necessary to design a future transmission line. Therefore, an outdoor UHV laboratory was conceived, designed and built in India by the Central Power Research Institute to meet its future requirements. Some salient features of this laboratory are as follows:

(b) Physical Layout The laboratory is an outdoor facility except the pollution laboratory and a test hall for conducting basic research. Brief details of each of the facilities/equipment are given below.

The UHV transmission line was built in such a way that the probable incidence of winds is nearly perpendicular to its axis. From the wind data available at the site for a period of about 10 years, it was decided to construct the line in the north-south direction. This will take full advantage of the south-east winds, which are fairly abundant from November to April and the north-west winds that are frequent from May to September, the Azimuthal orientation for the test line was fixed as north, north-east, south, south-west direction. Since wind induced conductor vibrations do not pose a serious problem in India, it was decided to have only one single phase experimental line but with two bundle conductors. This type of a line permits simultaneous comparative testing, both electrical and mechanical, on two different bundles, and also allows independent electrical and mechanical studies. Further the line can be used later, if necessary, for bi-polar HVDC studies.

The line has an overall length of 720 m, of which, one section is the central suspension span of 360 m length and the other two sections are dead-end spans each having a length of 180 m. At present, a single phase line with 10 conductor bundles is strung to enable to study its corona performance including the RI, AN, and corona power loss when energized by a phase to ground voltage of 1050 kV. The mechanical vibration aspects of the line are also studied using the same line. The approximate layout of the laboratory is given in [Fig. 11.4](#).

(i) Power Frequency Testing Transformer The power frequency testing transformer is a cascade unit having two 800 kV single phase transformers with an output voltage of 1600 kV and a maximum current of 6 A at the output terminals. The input to the transformer unit is from an 11 kV, 3-phase source through a sliding-type voltage regulator whose maximum rating is 10.5 kV. The transformer winding connections can be modified to give higher short-circuit currents ranging from 17 A to 47 A. Thus, this source is best suited for conducting artificial pollution tests. The full load

current of 6 A, although is high for a normal testing transformer, is necessary for charging the experimental transmission line. The transformer is also discharge free up to the full range of voltage output making it suitable for carrying out conducted and radiated RIV measurements. It can also be used for conducting dielectric tests on the line component insulation rated up to 1050 kV. An additional feature of the transformer is that it can generate damped oscillatory waves of maximum first peak of ± 2 MV with a maximum load capacitance of 16 nF. The oscillatory frequency can be varied between 100 Hz to 250 Hz. This is useful in testing the phase to phase insulation of the transmission line conductors.

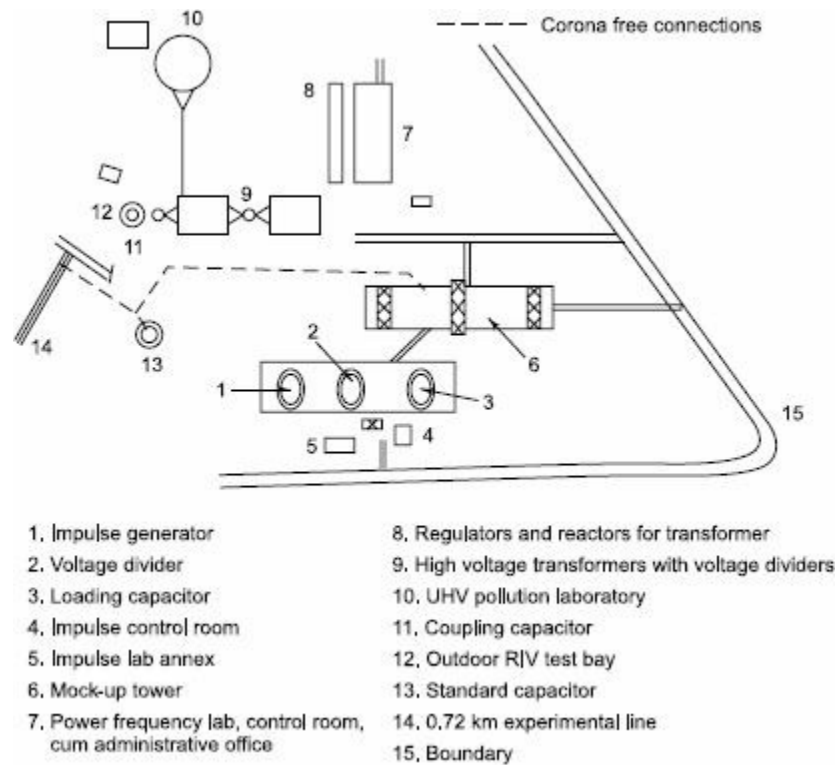


Fig. 11.3 Approximate layout of the UHV Research Laboratory of CPRI, Hyderabad.

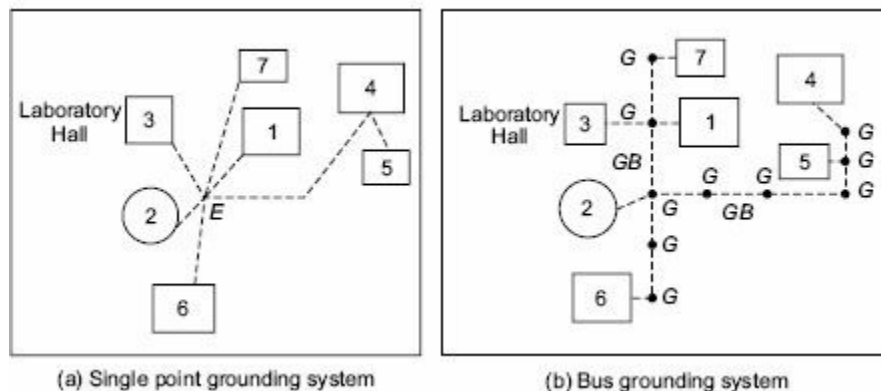


Fig. 11.4 1—Impulse voltage generator; 2—Sphere gap; 3—Position of test object for impulse testing; 4—Impulse current generator; 5—Position of test object for impulse current generator; 6—Control room and oscilloscope position; 7—Charging rectifier set; E—Single point earth position; G—Ground connection position; GB—Ground bus

The cascade transformer unit has capacitor dividers at the output of both stages I and II. In addition, the power frequency set-up has a standard capacitor having a rating of 20 pF at 1200 kV for dielectric loss measurements and a coupling capacitor of rating 2000 pF at 1200 kV for conducting RIV measurements.

(ii) Impulse Voltage Generator The impulse voltage generator consists of 25 stages with a charging voltage of 200 kV per stage, and an energy rating of 20 kJ. The overall rating of the generator is 5 MV, 500 kJ and is capable of generating standard lightning impulse voltages of up to ± 4.4 MV and standard switching impulse voltages of up to 3.4 MV (positive polarity) and 3.7 MV (negative polarity) under dry ambient conditions.

The measuring equipment along with the associated measuring cable, etc. meet the requirements of IEC 60–2 international standards for using equipment for quality assurance testing of electrical apparatus. Dielectric tests on equipment up to the rated voltage of 1100 kV can be performed using this impulse generator.

The measuring device mainly consists of 5 MV, 600 pF damped capacitor divider suitable for the measurement of the lightning impulse, switching impulse and 1500 kV (rms) power frequency voltage. The recording equipment consists of

- (i) 10 bit/60 MS/s high resolution impulse analysis system,
- (ii) 8 bit/40 MS/s digital impulse analyzer system, and
- (iii) a precision peak impulse voltmeter.

The rating of the impulse voltage generator was arrived at, based on the requirement of the insulation levels for external insulation of 800 kV and 1100 kV transmission systems. These are given below:

<i>Highest voltage rating of the equipment (kV)</i>	<i>Switching impulse withstand voltage (kV peak)</i>	<i>Lightning impulse withstand voltage (kV peak)</i>
800	1550	2400
1100	1800	2700

The generator was also intended to be used in long air gap breakdown studies for the optimization of conductor-to-tower and conductor to conductor air clearances in 800 kV and 1100 kV systems. For phase to phase air insulation clearance, considering 3 pu as the overvoltage between the phases, the switching impulse voltages required are:

System voltage 800 kv 1100 kV
 3 pu voltage 1950 kv 2720 kV

(iii) Pollution Laboratory The pollution performance of transmission line strings and other support insulators play a very important role in the determination of the adequacy of insulation for the transmission system. Salt fog test, which simulates the marine pollution and the solid layer test, which simulates the industrial pollution on the insulator are carried out in the pollution laboratory. The main test hall of this laboratory which is cylindrical in shape has an internal diameter of 24 m and a height of 27 m. The diameter of the hall was arrived at considering the maximum width of a 1100 kV transmission line V-string at the tower as 18 m. The height was decided on the consideration of a minimum ground to the bottom of the insulation chain clearance to be 12 m. All the metal structures in the laboratory were treated with anti-corrosive paint to withstand saline fog contamination. The salt fog is generated through two specially constructed nozzle systems as per the IEC 507 standard and the test voltage source is the outdoor cascade transformer having the short-circuit power as required by the standards. An 850 kV wall bushing was used to lead the test voltage into the test hall from the

outdoor transformer.

(iv) Measuring and Calibration Instruments The UHV laboratory is equipped with some of the best measuring and calibration instruments, such as the radio interference measuring system, partial discharge detector, experimental transmission line, corona loss meter, insulator surface pollution current integrator, FFT analyser, sound level meter, electric and magnetic field meters, unit step voltage and current generators, recurrent surge generator, line conductor, vibration monitor, etc.

(c) Research Programmes The research programmes undertaken at the UHV laboratory since its commissioning in 1994 are given below. These programmes were undertaken based on the specific needs of the electrical utilities and the high-voltage equipment manufacturers.

- Theoretical and experimental studies of the corona performance, namely studies of the acceptable levels RI and AN generated, and studies on the electric fields under the transmission lines, methods of reducing them and studies on the interaction between the electric fields and biological systems.
- Computational and experimental studies on the withstand capabilities and insulation coordination of long air gaps which form part of the transmission tower and equipment, when subjected to overvoltages having specified characteristics.
- Experimental studies on the performance of various types of insulators in the laboratory as well as in natural surroundings, where conditions of weather and pollution vary continuously. Advancement of laboratory test techniques to simulate the above pollution conditions and to improve the insulator design for better performance are also being studied.
- Experimental and computational studies on aeolian vibrations of conductor bundles and optimizing the conductor system. The economic impact of such studies are very significant. Further, evaluation of vibration performance of new conductor designs (self-damping, twisted, etc.) and the effectiveness of antivibration devices (dampers, spacer, spacer-dampers) are also being studied.

(d) General and Commercial High-Voltage Testing In addition to the research activities mentioned above, there has been considerable activity in the UHV laboratory in type testing, proving tests and routine production testing. 800 kV insulator strings have been successfully tested for both lightning and switching impulse voltages in recent years. Further, considerable work has been done to determine the design parameters on the experimental transmission line. Considerable laboratory time has been devoted for mechanical testing as well as for impulse and power frequency testing, especially pollution testing of insulators.

11.5.6 High-Voltage Laboratories in India and Abroad

High-voltage test facilities and large-size high-voltage laboratories are available at only a few places in the country and abroad as each of them costs several millions of dollars. It has been stated (Ref. 4) that a fully screened high-voltage laboratory with all test and research facilities will cost US \$10-50 million. In [Table 11.6](#) details of a few large size high-voltage laboratories in the world are listed along with the ratings of the equipment available. Some of the laboratories like those at the Indian Institute of Science, Bangalore, Central Power Research Institute, Bangalore, and Hyderabad have research facilities available apart from the normal test facilities ([Plate 7](#)).

11.6 GROUNDING OF IMPULSE TESTING LABORATORIES

An earth or ground system means an established stable reference potential normally taken to be zero. There are three types of grounds: (i) the ideal ground, (ii) single point ground (Fig. 11.4a), and (iii) the bus ground (Fig. 11.4b). Of all these, the best ground is the ideal ground which cannot be realized in practice. The next preferred ground is the single point ground, and the bus ground is least satisfactory. Ideal ground can be approximated by an equipotential plane realized by a finite conducting material. The laboratory is covered by a sheet of copper metal welded into a single unit. But this is very costly and is used rarely. A single point ground is commonly used. In this (see Fig. 11.4a) an earthing grid is installed within the laboratory floor, the connection from the grid is given by a large sized copper conductor to a point identified as a common ground point. The ground connections of various equipment and other components of the high-voltage test circuit are made to the common ground. High-voltage impulse tests give rise to high currents of several kiloamperes, and the rate at which the currents may change ranges between 10^7 to 10^9 A/s. If proper care is not taken, flashover or damage to control gear and risk of life to persons can occur. In order to avoid these difficulties, copper strips are used instead of round conductors to minimize the inductance in the ground circuit. Secondly, a metal grid embedded in a concrete floor gives rise to less resistance and inductance in the ground circuit. The ground is effective only when large size strips are used with close spacing. The ground system should ensure the following conditions:

Table 11.6 Ultraedit high-voltage laboratories abroad

Sl. No.	Location	Size			Power frequency test facilities		Impulse voltage test facility		Switching surge voltage (MV)	D.C (MV)
		Length (m)	Breadth (m)	Height (m)	Voltage (MV)	Current (A)	Voltage (MA)	Energy (KJ)		
1.	ABB, HVT Laden Switzerland	30	18	20.5	1.2	1	3	150	2.7	±1.0
2.	Electricite De France, France	45	25	25	1.1	1	3.0	450	2.7	0.6
3.	CEPEL, BRAZIL	44	30	27	1.1	2	3.2	—	2.8	1.0,2A
4.	Hydro Quebec, Montreal, Canada	82	67	57	3.30	2	6.4	400	6.0	—
5.	CESI, Milan, Italy	45	40	35	2.25	—	4.8	200	3.0	—
6.	U.S.S.R.	115	80	60	3.00	—	7.2	—	—	—
7.	Hemsdorf, GDR	—Outdoor—			2.25	2	7.2	—	—	—
8.	SURRY CANADA (POWER TECH LAB)	43	37	21	1.50	—	3.0	—	2.5	0.8
9.	Hitachi, Japan	60	40	31	1.65	—	4.0	600	—	—
10.	ASEA, Sweden	47	25	25	1.50	—	3.2	140	—	—
11.	CERL, U.K.	41	28	22	1.20	—	4.0	100	—	—
12.	CPRI, Hyderabad, India	Outdoor facility			1.1	6.0	4.8	500	3.7	—
13.	Test Institute GRAZ, Austria	36	26	22	1.1	1	2.9	—	1.9	1.5
14.	EPRI Massachu - sette U.S.A	Outdoor facility			1.7	—	5.6	—	5.6	1.5
15.	NIROO Inst. Tehran IRAN	20	19	20	1.2	6	2.8	—	—	—
16.	VEIKI UNL Budapest Hungery	20	40	18	1.5	2	4.0	—	2.7	0.1

- (i) imperfections of grounding system are to be avoided, as they cause excessive voltage difference between points and cause flashovers, damage, or danger to human life,
- (ii) the imperfections will cause excessive loop currents along the sheaths of measuring cables, which will introduce errors in measurements,
- (iii) the grounding system should be such that the voltage drop along the ground system, the voltage at a loop, and the circulating currents in the loops are avoided or minimized,
- (iv) metal conduits should be used for the measuring and control cables to avoid neutral inductance

effect between the ground grid and the cables.

A typical good earthing system consists of a copper network with meshes of 1 m width laid down below the ground level around the impulse test area and well connected. This network is extended over the entire area comprising all equipment such as testing transformers, charging h.v. rectifier set, test bay, etc. The grid should be electrically connected to all the metallic frames and reinforcing iron in the concrete walls and pillars of the building at their bottom points. Impulse test area must be provided with a spread, stretched, or expanded copper grid on the floor of thickness of about 2 mm with ground rods driven into the earth to a depth equal to the height of the impulse generator. The rods are welded to the inside copper grid as well as surface copper grid. Earth connection facility is to be provided for every 16 sq.m area so that the shortest lead can be used from any position inside the laboratory.

Where ionization measurements are to be made, the earthing system should keep the RIV level from external sources to the lowest value. In addition, the high frequency energy produced during impulse tests should not cause any trouble around the test area. If this is to be met the entire laboratory should be built into a Faraday cage.

The general layout of the laboratory with its conduit pipes for control and measuring cables is shown in [Fig. 7.55](#) (see [Chapter 7](#)). Such a layout will avoid all interferences.

11.6.1 Electromagnetic Shielding and Earth Return in High-Voltage Laboratories

A high-voltage laboratory, small, medium or large in size should have some type of screening against electrostatic and electromagnetic field interference. The screening is essential if partial discharge measurements are to be made in the laboratory. An attenuation of less than 40 db is needed for attenuation of electrical signals in the frequency range of 1 MHz, while a still lower attenuation is needed for electromagnetic signals. In larger test laboratories, attenuation levels due to interferences are higher and arise mostly due to imperfect screening. One way to check the screening is to tune a portable pocket-radio and walk around the laboratory tuning the radio to different frequencies between 500 kHz to 10 MHz. The signal should not be heard. However, it is often found that the signal level increases significantly when a cable or an electrical outlet is crossed. If it is possible, the same check may be carried out with the automatic volume control (gain control) disconnected. The sources of disturbance inside the laboratories are (i) switching transients due to switching-on or switching-off of loads like lifts or cranes, transformers, etc., (ii) rectifier circuits, and (iii) shielded cables acting as antennas for outside signals. Care should be taken to see that the above are avoided. The best screening is obtained if the roof, the walls and the flooring area are screened with an expanded metal wire mesh and joined together. Further, all electric conductors are fully screened in metal conduits which are run below the floor metal network.

For the purpose of measurement, one point in the test circuit such as the base of a test object or an impulse voltage generator should be made a reference ground or a zero potential point. This is usually disturbed in measurements for fault indication in transformers during impulse testing, tests with chopped waves, etc., as spikes are introduced into the test circuits due to low-voltage conductors that run into the control room from the impulse test area which carry the operating signals of large magnitude to control impulse generator, sphere gaps, etc. As such a potential difference is created momentarily during the transient period between the base of impulse voltage generator and that of the base of the measuring voltage divider and test object. These differences are carried on to the measuring device which will give erroneous results. These voltage differences can be reduced by reducing the impedance of the ground side of the test circuit. The most effective method for reducing the voltage differences is to have the return conductor in the form of a metal sheet placed on the top of the floor. Some laboratories used coarse copper nets or aluminium nets or aluminium sheets, but they are not very effective.

The high-voltage laboratory must be earthed to (i) protect the equipment against the lightning strokes, and (ii) to protect the equipment from short circuits inside the laboratory from the power supply source. If not properly earthed, these will give rise to potentials which are different at different points in the laboratory thus causing unnecessary danger to human life and damage to the equipment.

The acoustical attenuation of the building is also important. It is necessary in large laboratories to have comfortable and clear communication between persons at different locations inside the laboratory. Reverberation inside the laboratory should be avoided. To get the desired effect, the laboratory should have perforated holes and fibreglass or some such material fixed to the walls. The above aspects need careful consideration in the design of a high-voltage laboratory.

- Test facilities in hv Labs
- Activities and Studies Conducted

- Classifications of hv Labs
- Size and Rating of Test Equipment
- Layout of hv Labs
- Grounding

MULTIPLE-CHOICE QUESTIONS

- A small high-voltage laboratory usually will have
 - ac, dc test sources with ratings less than 100 kV, 10 kVA./kW and impulse of voltage 400 kV, 5 kJ
 - ac, dc test sources of 500 kV, 100 kVA/kW, and impulse of 1 MV, 10 kJ
 - ac voltage sources of 300 kV, 10 kVA, and impulse voltage of 1 MV, 15 kJ
 - ac, dc sources only
- Test sources required for testing power apparatus of 220 kV, 3-phase ac system are
 - 500 kV ac, 1 MV impulse
 - 800 kV impulse
 - 300 kV ac, 500 kV impulse
 - 250 kVA, 500 kV impulse.
- The kVA rating of a testing transformer unit intended for test voltage and test object capacitance 'C' (pF)
 - ωCV^2
 - $\omega CV^2 \times 10^{-9}$
 - $\omega C^2 V^2 \times 10^9$
 - $\omega C V^2 \times 10^{-6}$
- The rating of an impulse voltage generator with generator capacitance C_g and voltage rating V with n stages is (kJ)
 - $0.5 C_g V^2$
 - $(n/2)(C_g V^2) (C_g V^2) (C_g V^2)$
 - $\frac{(C_g V^2)}{2n}$
 - $\frac{(C_g V^2)}{2n^2}$
- The clearances normally adopted in hv laboratories for ac and impulse voltages are
 - 100 to 200 kV/m for ac and 500 kV/m for impulse
 - 300 kV/m for ac and 500 kV/m for impulse
 - 30 kV/m for ac and 50 kV/m for impulse
 - 10 kV/m for ac and 50 kV/m for impulse

Answers to Multiple-Choice Questions

1. (a) 2. (a) 3. (b) 4. (c) 5. (a)

REVIEW QUESTIONS

1. List the common test facilities available in high-voltage laboratories.
2. What are the criteria used in selecting the ratings of the testing equipment for hv laboratories?
3. Why is grounding very important in an hv laboratory? Describe a typical grounding system used.

PROBLEMS

1. Estimate the clearances required and the approximate dimensions of the test room for a high-voltage laboratory with the following equipment.

ac testing transformer	:25 kVA, 250 kV
Size	:1.2 m dia × 3 m (including bushing height)
Impulse voltage generator	:800 kV, 24 kJ
Size	:1.5 m × 1.5 m × 3 m

Charging unit requires a space of 1 m × 1 m × 1 m.

Accessories include a 75 cm sphere gap, 900 kV capacitance potential divider and a 200 kV gas-filled standard capacitor.

2. What are the extra precautions that are to be taken while grounding an impulse current generator? Give a typical grounding arrangement for a 160 kJ, 200 kA impulse-current generator.

REFERENCES

1. August F. Metraux, "Some problems and actual limits of test techniques at extra high voltages", *Haefely Publication, EIS 14* (1969).
2. August F. Metraux, "Earthing of impulse stations", *Haefely Publication, 508040'IE* (1962).
3. Hylten Cavallius, N.R. and Giao, T.N. "Floor net used as ground return in high voltage test areas", *Tr. IEEE, PAS, PAS-88*, 996, July (1969).
4. Hylten Cavallius, N., *High Voltage Laboratory Planning*, Emile Haefely and Co. Ltd., Basel, Switzerland, 1988.
5. Chinnappa, K. M., "Need for next higher voltage level in India", *National Seminar on High Voltage AC and DC Transmission*, Central Board of Irrigation and Power, New Delhi (December 1981).
6. Ryan, H. M. and Whiskard, J., "Design and operation perspective of a British UHV laboratory", *IEE Proc.* 133, pp. 501-521 (1986).
7. "Report on the Establishment of a Research Facility for UHV AC transmission" in Central Power Research Institute (CPRI), Hyderabad (1994) and subsequent reports on the R.D. activities at this laboratory.
8. *IEEE Committee Report: "Standardisation of conductor vibration measurements"*, *Trans. IEEE on Power Apparatus and Systems, PAS-85*, pp. 10-20 (1966).
9. *IEC Specification 600060-1*, "High Voltage Test Techniques—Part 1: General Specifications and Test Requirements" (1994).
10. *IEC Specification 600060-2*, "High Voltage Test Techniques—Part 2: Measuring Systems" (1989).

Appendix

Important Formulae

Field enhancement factor

$$f = \frac{E_{\max}}{E_{\text{avg}}}$$

Townsend current growth equation

$$I = I_0 \exp(\alpha d)$$

Current growth in presence of secondary processes

$$I = \frac{I_0 \exp(\alpha d)}{1 - \gamma [\exp(\alpha d) - 1]}$$

Breakdown conditions

$$\gamma \exp(\alpha d) = 1$$

$$pd_{\min} = \frac{e}{A} \ln \left[1 + \frac{1}{\gamma} \right]$$

$$V_{\min} = \frac{eB}{A} \ln \left[1 + \frac{1}{\gamma} \right]$$

Voltage gradient to corona inception for parallel wires

$$E_c = 20 md [1 + .301/\sqrt{dr}]$$

Heat generated in a dielectric in ac field

$$W = \frac{E^2 f \epsilon_r \tan \delta \times 10^{-12}}{1.8} \text{ watts/cm}^3$$

Ripple in voltage multiplier unit with 'n' capacitors included

$$\frac{I}{f_c} \frac{[n(n+1)]}{2} \quad \text{(peak ripple)}$$

$$\frac{I}{f_c} \frac{[n(n+1)]}{4} \quad \text{(average ripple)}$$

Voltage drop in n stage multiplier unit (2n capacitors included)

$$\frac{I}{f_c} [2/3n^3 + n^2/2 - n/6]$$

Optimum number of stages = $\sqrt{V_{\max} f_c / I}$

Impulse wave shape (double exponential type)

$$V = V_0 [\exp(-\alpha t) - \exp(-\beta t)]$$

Impulse current wave shape (oscillatory)

$$I = I_m \exp(-\alpha t) \sin \omega t$$

Time to front for double exponential wave

$$T_1 = 3.0 R_1 C_1 C_2 / C_1 + C_2$$

Time to front for double exponential wave

$$T_2 = 0.7(R_1 + R_2) (C_1 + C_2)$$

Impulse current wave shape (oscillatory)

$$I_m = V/\omega L [\exp(\alpha t) \sin \omega t]$$

$$\alpha = R/2L, \omega = \sqrt{1/LC - R^2/4L^2}$$

T_1 rise time from zero to max = $1/\omega \tan^{-1} \omega'/\alpha$

T_2 duration of one half cycle of oscillatory wave π/ω'

Current given by generating voltmeter = $i_{\text{rms}} = (V_m \omega) / \sqrt{2}$

Force on the plates of electrostatic voltmeter

$$F = \frac{1}{2} \epsilon_0 A (V/S)^2 Nw$$

Series capacitance required for compensation of ground capacitance in voltage dividers

$$C'_1 = nC_1 [1 - C_g/6C_1]$$

Voltage ratio of capacitance divider with ground capacitance

$$= [1 + (C_2/C_1) (1 + C_g/6C_1)]$$

Skin depth for conductor at high frequencies

$$d = 1/\sqrt{\pi f \mu \sigma}$$

Bandwidth of a coaxial shunt

$$B = \frac{1.46\rho}{\mu d^2} \text{ and rise time } T = 0.237 \mu d^2/\rho$$

For lossless transmission line

for incident wave $e_1/i_1 = Z_1$

for reflected wave $e'_1/i'_1 = -Z_1$

for transmitted wave $e''_1/i''_1 = Z_2$

$$e'' = \gamma e, \quad i' = -\gamma i$$

$$e'' = (\gamma + 1)e, \quad I'' = (1 - \gamma)I \quad \gamma = \text{reflection coefficient}$$

High resistance measurement with dc galvanometer

$$R = (V/R_s)(1/n)(1/D_s)$$

hv Schering bridge

Balance condition $C_x = (R_3/R_4)(C_s)$

$$r_x = (C_3/C_s) R_1$$

$$\tan \delta_x = \omega C_x r_x = \omega C_3 R_3$$

Transformer ratio arm bridge

Balance condition $C_r = (N_s/N_x) C_s$

$$R_x = (N_x/N_a) R_a$$

$$\tan \delta_x = (\omega(C_s R_a)) (N_s/N_a)$$

Output power rating of testing transformers

$$P(\text{kVA}) = 2\pi f V^2 \times 10^{-9} \quad [V \text{ in kV, } C \text{ in pF}]$$

Peak output voltage of impulse generator for standard impulse voltage

$$V_s = nV_{dc} [0.95 - (C_L/C_L + C_g)]$$

Energy rating of impulse generator

$$W = \frac{1}{2} C_g V^2 \times 10^{-9} \text{ kJ} \quad [V \text{ in kV, } C_g \text{ in pF}]$$

Minimum clearance required in HV laboratories for safe operation

< 1.5 MV for ac and dc ratings

< 2.5 MV for Impulse ratings

ac	200 kV (rms)/m	} Under standard atmospheric conditions
dc	275 kV (rms)/m	
Impulse	500 kV (peak)/m	

Author Index

Abdullah, M. [282](#)
Abou Seada, M.S. [24](#)
Adam, H [69](#)
Alexander, P.N. [24](#)
Allan, D.J. [141](#)
Alston, L.L. [23](#), [69](#)
Alpert, D. [69](#)
Anderson, O. W. [24](#)
Arghi, S.M. [88](#)
Arora, R. [125](#)
August, F. [457](#)

Bartnikas B. [88](#)
Bartnikas R. [126](#)
Bell, E. [359](#)
Berlijn S. [434](#)
BerouelA. [398](#)
Bewley, L. V. [359](#)
Bhimani, B. V. [398](#)
Binns K.J. [23](#)
Birks, J.B. [140](#)
Black, R.M. [140](#), [359](#)
Blalock, [283](#)
Boulder, G. W. [283](#)
Bradley,A. [125](#)
Bradwell, A. [88](#)
Brebbia C.A. [24](#)
Boisdon C. [398](#)
Brown J.D. [360](#)
Buret F. [398](#)
Cassidy, E.C. [283](#)
Chadband, W.B. [88](#)
Chari, M.V.K. [23](#)
Cherny, E.A. [126](#)
Chinnappa, K.M. [457](#)
Chowdhuri, P. [360](#)
Christophorou, L.G. [69](#)
Clark, C.H. W. [434](#)
Clark, F.M. [125](#), [140](#)
Craggs, J.D. [68](#), [204](#), [282](#)
Dale, S.J. [69](#)
De Kock, N. [25](#)
Diesendorf, W. [359](#)
Dieter Kind [204](#)
Dissado, L.D. [126](#)
Dugan, R. [360](#)

Eichhorn, R.M. [126](#)
Ely, C.H.A. [434](#)
Erickson, A.J. [360](#)

Farneti, F. [140](#)

Faser, K. [283](#)
Ferrari, R.L. [23](#)
Fisher, F.A. [360](#)
Forger, K. [24](#)
Fothergill, J.C. [126](#)

Gallager, T.J. [88](#)
Giao, T.N. [457](#)
Glaninger, P. [205](#)
Golde, R.H. [359](#)
Greenway, R. [144](#)
Greenwood, A. [88,126,141](#)
Gutfleish, F. [24](#)

Haefely [205,226](#)
Hague, B. [398](#)
Harris, F.H. [398](#)
Hawley, R. [88](#)
Heller, H. [204](#)
Henriksen, T. [360](#)
Heumann, K. [283](#)
Hogate, R.C. [126](#)
Hori, Y. [205](#)
Hylten Cavallius, N. [283, 457](#)

Iravani, M.R. [24](#)

Johns, A.J. [140](#)
Kamase, Y. [205](#)
Kannan, S.R. [205](#)
Karlsson, T. [360](#)
Kato, S. [24](#)
Kawamoto, T. [24](#)
Khalifa, M.M. [125](#)
Koritsky, Y.U. [140](#)
Koshrt, F. [283](#)
Kreuger, F.H. [398, 434](#)
Krivda, A. [398](#)
Kuffel, E. [24, 69, 88, 204, 360](#)

Lambeth, P.J. [434](#)
Lanoz, M. [360](#)
Latnam, R.V. [69](#)
Lawrenson, P.J. [23](#)
Lemke, E. [434](#)
Lewis, T.J. [88](#)
Lewis, W.W. [359](#)

Malik, N.H. [24](#)
Maller, V.N. [68](#)
Marshall, J.L. [359](#)
McGrawth, P.B. [88](#)
McKibbin, F. [283](#)
Meayats [69](#)
Meek, J.M. [68, 204, 282](#)
Miri, A.M. [24](#)
Mizuno, A. [205](#)
Mole, G. [398](#)

Mosch, W. [125](#)
Muhr, M. [434](#)
Mukherjee, P.K. [25](#)
Muller Hiller Brand [292](#), [359](#)

Nagahama, T. [205](#)
Naidu, M.S. [68](#)
Narayana Rao, Y. [205](#)
Nasser, E. [24](#), [68](#)
Nelson, J.K. [88](#)
Neugebauer, W. [360](#)
Newman, S.E. [360](#)
Norinder, J. [293](#)
Nucci, C.A. [360](#)

O'Dwyer, J.J. [125](#)

Palmer, S. [140](#)
Panek, J. [360](#)
Peyraque, L. [398](#)
Phelps [360](#)
Platts, J.R. [140](#)
Popovic, B.D. [23](#)

Quershi, M.I. [88](#)
Rabus, W. [283](#)
Rachid, F. [360](#)
Raether, H. [68](#)
Raghuveer, M.R. [24](#)
Rea, M. [205](#)
Reid, R. [205](#)
Raynolds, E.H. [359](#)
Riegel, N.A. [24](#)
Rubwurm, D. [434](#)
Ryan, H.M. [24](#), [135](#), [457](#)

Schwab, A.J. [283](#)
Seely, S. [23](#)
Sharpley, W.A. [140](#)
Shimiza, M. [205](#)
Shugg, W.T. [88](#), [125](#), [141](#)
Silvester, P.P. [23](#)
Singer, H. [23](#), [24](#)
Steinbigler, H. [24](#)
Strehl T. [434](#)
Swift, D.A. [126](#)

Takuma, T. [24](#)
Tanaka, T. [88](#), [126](#), [141](#)
Telles, J.C.F. [24](#)
Tesche, F.M. [360](#)
Thomas, R.F. [283](#)
Trinitis, C. [24](#)
Uman, M.A. [360](#)

Van De Graaff [157](#)
Veverka, A. [204](#)
Von Hippel, A. [125](#), [140](#), [398](#)

Walcher, W. [69](#)
Watson, P.K. [88](#)
Weiss, P. [23](#)
Whiskard, J. [457](#)
Witt, R. [283](#)
Wolf, J. [284](#)
Wrobel, L.C. [24](#)
Wurtz, M. [69](#)

Yan, K. [205](#)

Zaengl, W. [23](#), [69](#), [88](#), [204](#), [360](#)

Zaky, A.A. [88](#)

ZienKiewicz, O.C. [23](#)

Subject Index

Ageing, insulation [101](#)
Air [2](#)
Air Capacitor [377](#)
Air density correction factor [236](#), [401](#)
Analysis of Impulse Generator Circuits [172](#)
Arc discharge [52](#), [53](#)
Askarels [72](#)
Atmospheric conditions [278](#), [401](#)
Attachment coefficient [38](#)
Attenuation factor [238](#)
Avalanche [40](#), [42](#), [43](#), [44](#), [50](#), [58](#), [68](#), [91](#)

Boundary Element Method (BEM) [9](#), [17](#)
 gases [2](#), [21](#)
 liquids [4](#), [70](#)
 solids [70](#), [89](#), [103](#)
 vacuum [76](#)
 voltage gaseous [26](#), [38](#), [42](#), [54](#)

Bruce profile [234](#)
Bushings testing [411](#)

Cable testing [414](#), [415](#)
Capacitance voltage divider [243](#), [244](#)
Capacitance Voltage Transformer (CVT) [218](#)
Capacitor paper [94](#)
Carbon dioxide [2](#), [26](#)
Cascade transformer [161](#)
Cathode ray oscilloscope [249](#), [267](#)
Cavitation [79](#)
Cavities [97](#), [382](#)
Ceramics [103](#)
Charge formation [286](#)
Charge Simulation Method (CSM) [9](#), [14](#)
Charging resistors [180](#), [181](#), [183](#)
Chemical breakdown [89](#)
Circuit breaker testing [408](#)
Classification of liquids [72](#)
Clump Mechanism [61](#)
Coaxial cable [239](#), [258](#), [264](#)
Coefficient of reflection [309](#), [310](#)
Collision cross-section [29](#)
Collision processes [27](#)
Commercial liquids [3](#), [75](#)
Compensated resistance voltage divider [240](#)
Complex permittivity [368](#), [370](#)
Composite dielectrics [99](#), [100](#)
Composites [4](#), [21](#)
Corona discharge [47](#), [119](#)
Corona pulse [384](#)
Criterion for breakdown [34](#), [39](#), [49](#)
Current comparator bridge [380](#), [395](#)
Current shunts [263](#)

coaxial tubular [259](#)

resistive [258](#)

squirrel cage [258](#)

Current transformers [256](#)

Delay cable [237](#)

Detectors for partial discharge [396](#)

Dielectric constant [396](#)

Dielectric loss [405](#), [406](#), [450](#)

Dielectric loss factor [135](#)

Dielectric response [370](#)

Diffusion coefficient [28](#)

Digital peak voltmeter [225](#)

Discharge detection [382](#), [384](#), [388](#), [434](#)

Dissipation factor [382](#)

Divider ratio [243](#), [251](#), [273](#)

Earthing system [454](#)

Electric field [2](#), [5](#), [6](#)

 measurement [269](#)

Electric stress [5](#), [6](#)

Electrochemical deterioration [95](#)

Electromechanical breakdown [89](#), [91](#)

Electron avalanche [91](#)

Electron emission [31](#)

Electron energy [28](#)

Electronegative gases [37](#)

Electro-optical signal converter [257](#)

Electrostatic machines [157](#)

Electrostatic voltmeter [209](#), [215](#), [218](#), [225](#)

Epoxy resin [103](#)

Expulsion gap [326](#)

Faraday generator (ammeter) [265](#)

Ferranti effect [323](#)

Fibres [107](#)

Field controlled voltage divider [244](#), [245](#)

Field emission [60](#)

Field factor [8](#)

Field gradient [289](#)

Field intensity [290](#)

Field strength meters ac [213](#)

Field strength meters dc [212](#)

Finite Element Method (FEM) [9](#)

Flashover rates [324](#)

Flashover test [405](#)

Flashover voltage [328](#), [400](#)

Fluorocarbon plastics [113](#)

Galvanometer [368](#)

Gas mixtures [54](#), [55](#)

Gaseous insulation [2](#)

Generator, electrostatic [158](#)

Glass [107](#)

Glow discharge [53](#)

Ground capacitance [208](#), [217](#), [243](#)

Ground wires [330](#)

Grounding [457](#)

Guard electrode [364](#)
Guard hoops [222](#)
Guard ring [223](#)

Hall generator [255](#), [256](#), [265](#)
High temperature polymers [104](#)
Humidity [278](#), [402](#)
HV Labs—layout [455](#)
Hydrocarbons [72](#), [110](#)
Hydrogen [37](#)
Hydrolysis [95](#)

Impulse
 current [260](#), [262](#), [269](#), [279](#)
 flashover [405](#), [411](#)
 generator [175](#), [177](#)
 voltage [173](#)
 voltage divider [277](#)

Insulating materials,
 applications [131](#)
 classification [123](#)

Insulation
 bushings [137](#)
 cables [133](#)
 capacitors [135](#)
 circuit breakers [138](#)
 transformers [132](#)
 applications [131](#)
 coordination [336](#), [346](#)

Insulation-rotating machines [116](#)

Internal discharges [89](#), [98](#)

Intrinsic breakdown [90](#)

Ionization
 coefficients [34](#), [35](#), [65](#)
 electron collision [80](#)
 processes [29](#)
 secondary [30](#)

Ionization by collision [30](#)

Irradiation [231](#), [233](#)
 ultraviolet [30](#), [118](#)

Isokeraunic levels [296](#)

Isolators, testing [406](#)

Kapton film [118](#)

Lattice diagram [307](#)

Leader stroke [298](#)

Lightning
 arrester [423](#)
 discharges [295](#), [297](#), [330](#)
 phenomenon [289](#)

Lightning strokes
 characteristics [293](#), [314](#)
 mechanism [289](#)
 model [298](#)

Liquid dielectrics [3](#), [54](#), [71](#), [73](#), [97](#)
 breakdown mechanism [58](#), [79](#), [84](#)
 breakdown tests [76](#)

conduction [76](#), [77](#)
properties [73](#)
purification [71](#)
Loss angle [269](#), [272](#)
Loss tangent [369](#)

Magnetic links [207](#)
Marx circuit [180](#)
Mean free path [28](#)
Mica [130](#), [131](#)
Mobility [27](#)
Mole's bridge [395](#)
Multistage generator [181](#)
Nitrogen [3](#), [26](#)
Non-destructive testing [361](#)
Non-uniform field [40](#)
Numerical methods [5](#), [9](#)
Nylon [133](#)

Overvoltages [323](#)
 control [322](#), [328](#)
Partial discharges [95](#), [381](#), [384](#), [392](#)
Paschen's law [45](#)
Peak voltmeter [207](#), [215](#)
 series capacitance [217](#), [240](#)
PETEP-oil [71](#)
Photoelectric emission [35](#)
Photoionization [30](#), [31](#), [43](#), [67](#),
Planning of hv laboratory [436](#)
Plastics [113](#)
Polarity effect [234](#)
Pollution testing [404](#)
Polycarbonate [112](#)
Polyester [130](#)
Polyethene [112](#)
Polyimide [119](#)
Polystyrene [94](#)
Polyvinyl chloride [104](#)
Porcelain [94](#)
Positive ion [30](#), [31](#), [33](#), [34](#), [40](#), [43](#), [59](#), [65](#)
Positive ion bombardment [30](#)
Post-breakdown phenomena [53](#)
Potential divider, impulse [237](#)
Power capacitors [136](#)
Protection against overvoltages [358](#)
Protective gap [344](#)
Protector tube [326](#)

Radio interference [424](#)
 voltage [432](#)
Rectifier circuits [145](#)
Reflection coefficient [307](#)
Regulation [152](#), [153](#), [154](#), [161](#)
Relative air density [48](#)
Residual capacitance [216](#)
Residual inductance [176](#), [215](#)
Resistance potential divider [208](#), [209](#), [214](#), [220](#)
Resistivity [366](#)

Resonant transformer [166](#), [167](#)

Ripple measurement [209](#)

Ripple voltage [145](#), [149](#), [151](#)

Rod gap [227](#), [236](#)

Rogowski coil [263](#)

Rotating machines [130](#)

Rubber [95](#)

Schering bridge [376](#), [386](#)
 audio frequency [391](#)
 High voltage [374](#)
 shunted [395](#)

Secondary ionization [30](#)

Series capacitor peak voltmeter [223](#)

Shielding [323](#), [338](#), [377](#), [397](#)

Short circuit testing [408](#)

Sphere gap [41](#), [207](#), [227](#)

Sphere plane gap [49](#)

Shunt
 reactors [316](#), [323](#)
 current [299](#)

Silicone oils [72](#)

Solid dielectrics
 breakdown [89](#), [94](#)
 composites [99](#)
 electromechanical [91](#), [92](#)
 internal discharges [97](#), [98](#)
 intrinsic breakdown [90](#), [94](#)
 streamer [91](#)
 thermal [92](#)
 treeing and tracking [89](#), [95](#)

Space charge [42](#), [43](#), [59](#)

Spark gaps [181](#), [197](#)

Spark overvoltage [182](#), [353](#)

Spray point [157](#)

Stabilization ratio [159](#)

Stabilizer [159](#)

Stage capacitance [181](#)

Standard capacitor [218](#)

Stray capacitance [208](#), [215](#), [217](#), [220](#), [237](#)

Streamer breakdown [91](#)

Streamer theory [26](#), [42](#)

Sulphur hexafluoride SF₆ [2](#), [26](#), [38](#), [54](#)

Surge arrester [325](#), [327](#), [330](#), [333](#)

Surge impedance [239](#), [308](#), [309](#)

Surge voltage [20](#), [293](#)

Sustained discharge [64](#)

Switching surges [142](#), [167](#), [182](#), [314](#)

Synthetic testing [408](#), [428](#)

Teflon (P.T.F.E.) [107](#)

Terminal capacitance [237](#), [258](#)

Tesla coil [169](#)

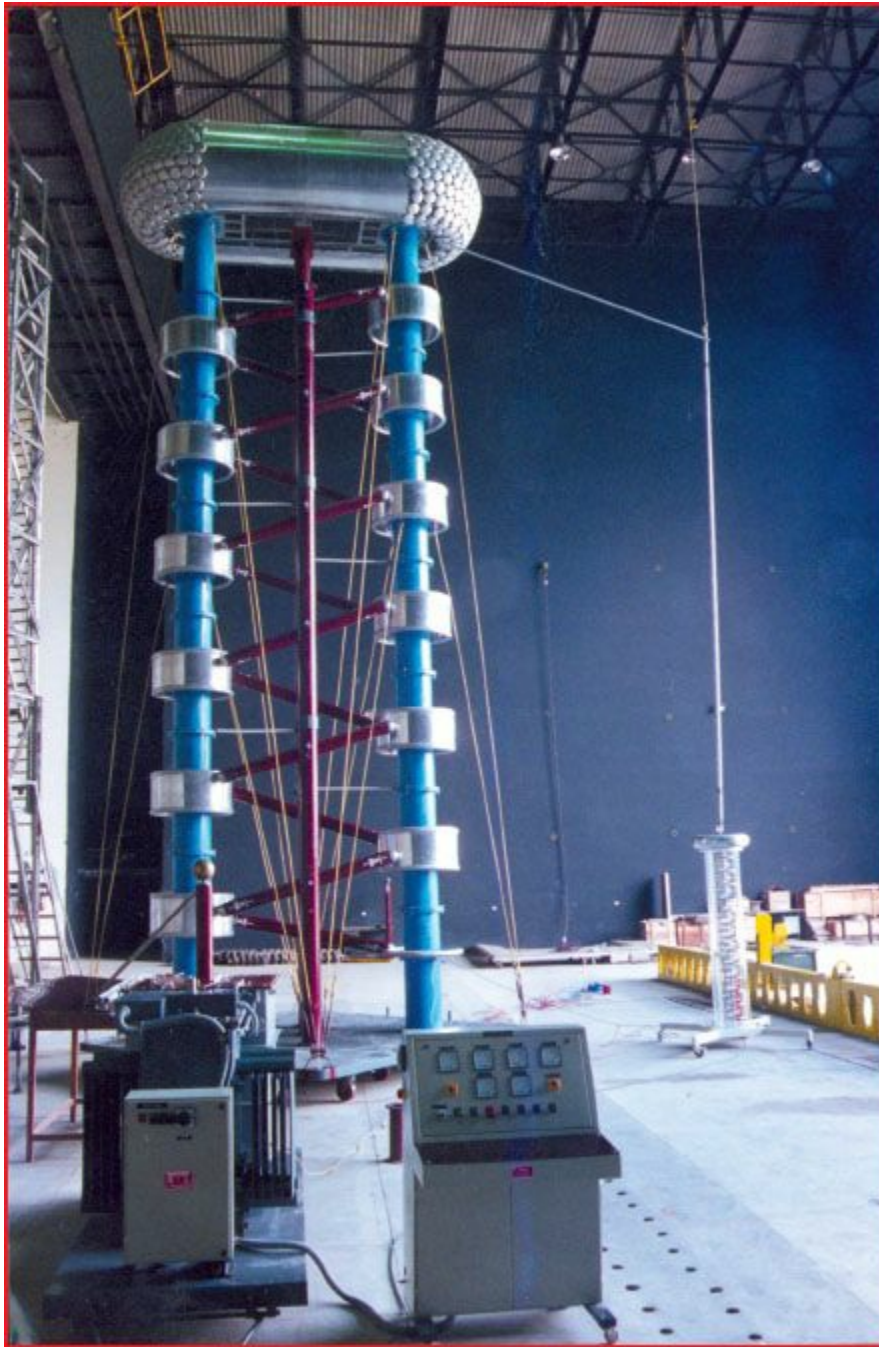
Test cells [76](#)

Test equipment [445](#)

Test facilities [439](#)

Testing transformer [184](#)
Thermal breakdown [81](#)
Thermal instability [93](#)
Thunderstorm [289](#), [296](#)
Thunderstorm Days (TD) [296](#)
Thyratron [190](#)
Time lag [40](#)
 formative [40](#), [41](#), [52](#)
 statistical [39](#), [40](#)
 total [36](#), [40](#)
Townsend breakdown [38](#), [46](#)
Townsend discharge [29](#)
Tracking [96](#), [97](#)
Transformer oil [71](#), [72](#), [105](#)
Transformer ratio arm bridge [378](#)
Transformer testing [416](#)
Transmission coefficient [307](#)
Travelling wave [268](#)
Treeing [89](#), [95](#), [97](#)
Trigatron gap [191](#)
Tripping of impulse generator [202](#)

Ultraviolet light [32](#)
Uncompensated line [321](#)
Uniform field [35](#)
 electrodes [35](#), [235](#)
 gap [238](#)
Vacuum [2](#), [55](#)
 clump mechanism [61](#)
 particle exchange [59](#)
Van de Graaff generator [157](#)
Voids [99](#), [385](#)
Voltage divider probe [241](#)
Voltage dividers—low voltage Voltage doubler [146](#)
Voltage gradient [234](#), [354](#)
Voltage multiplier [149](#), [150](#), [153](#), [154](#)
Voltage ratio arm bridge [379](#)
Voltage regulator [160](#), [164](#)
Voltmeter, series capacitance
Volt-Time characteristics [41](#)
Wagner earth [378](#)
Wave shape control [177](#), [181](#)
Wave shape, impulse [173](#)
Wave shaping network [171](#)
Wave tail [173](#), [180](#), [185](#)
Waveform [148](#), [149](#), [164](#), [167](#)
Wavefront [171](#)
Wheatstone bridge [367](#)
Withstand voltage [403](#), [410](#), [438](#)



1200 Kv. 15 mA high Voltage DC Generator. *Courtesy: Centre for Air Borne Systems, Dept. of Defence R and D, Ministry of Defence, Government of India.*



1600 Kv, 9600 kVA Outdoor Type Cascaded Power Transformers. *Courtesy: Central Power Research Institute, UHV Lab. Hyderabad, India.*

Plate 3



3 MV, 150 KJ, 15 Stages Impulse Voltage Cenerator. *Courtesy: Central Power Research Institute, Bangalore, India.*

Plate 4



100 KA, 150 KJ Impulse Current Generator. *Courtesy: Haefely Trench.*

Plate 5



5 MV, 500 KJ Outdoor Type Impulse Generator with Damped Capacitive Divider (600 pF, 400 Ohms), and Loading Capacitor (2 nF) both rated for 4.4 MV Lightning Impulse and 3.7 MV Switching Impulse. *In the picture Impulse Voltage Generator is shown on the left followed by the load capacitor and the damped capacitive divider. Courtesy: Central Power Research Institute, UHV*



Digital Impulse Analysis System (DIAS) for Impulse Voltage and Current Measurement System.
(Courtesy: Haefely Trench)



Lightning Impulse Flashover Across Bundle Conductor to Tower of an experimental transmission line. *Courtesy: Haefely Trench*

Plate A

100 kV AC/PD Test Set



Courtesy: W.S.Test Systems

Plate B

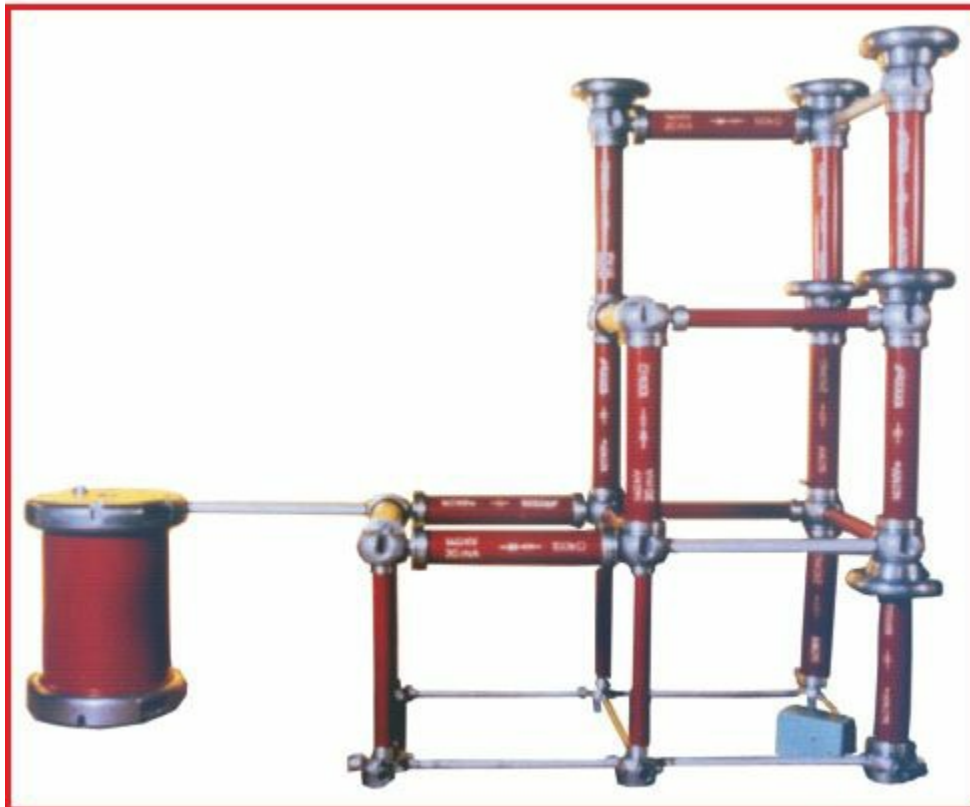
300 kV A C Test Set



Courtesy: W.S.Test Systems

Plate C

3 Stage HVDC Test Set



Courtesy: W.S.Test Systems

Plate D

280 kV 2 Stage Impulse Test Set



Courtesy: W.S.Test Systems